



Proceedings of the 14th International Congress of the International Radiation Protection Association

Cape Town, South Africa
9 – 13 May 2016

Volume 4 of 5

- 7- Environment and Natural Background
- 8- Transport / Sealed Source Management
- 9- Non-ionising Radiation

Organised in collaboration with:



The Proceedings of the 14th International Congress of the International Radiation Protection Association are divided into 5 volumes, as follows:

Volume 1 of 5

Area 1: Fundamental Science
Area 2: Policy, Standards and Culture

Volume 2 of 5

Area 3: Medical
Area 4: General Ionising Radiation Protection

Volume 3 of 5

Area 5: Optimisation and Design of New Facilities
Area 6: Radiation Detection and Dosimetry

Volume 4 of 5

Area 7: Environment and Natural Background
Area 8: Transport / Sealed Source Management
Area 9: Non-ionising Radiation

Volume 5 of 5

Area 10: Emergency Preparedness and Management
Area 11: Decommissioning, Waste Management and Remediation
Area 12: Societies

Proceedings of the 14th International Congress of the International Radiation Protection Association

EDITORIAL TEAM

Christopher Clement, Jack Valentin,
Haruyuki Ogino, Devon Foote, Julie Reyjal,
Laila Omar-Nazir

Published by
The International Radiation Protection Association



www.irpa.net

© 2017 International Radiation Protection Association

ISBN 978-0-9989666-4-9

Table of Contents

VOLUME 1

IRPA14 Membership List

Editorial

Preface


How to Protect the Public When You Can't Measure the Risk -- The Role of Radiation Epidemiology Author: John D. Boice, Jr.....	1
What Can We Learn from Studies of Nuclear Workers? Author: Ethel Gilbert.....	2
Area 1: Fundamental Science	3
Attenuation Coefficients of Some Species of Wood Authors: Chioma Nwankwo, Olatunde Oni, Folorunso Ogundare.....	4
Scoping Study of Possible Chronic Health Effects for Workers at the Rössing Uranium Mine Authors: Douglas Chambers, Gunhild von Oertzen, Paul J. Villeneuve, Ron Stager, Sylvain Saint Pierre	11
Pregnancy Outcomes in Women Exposed Along the Techa River Authors: Elena Pastukhova, Sergey Shalaginov, Alexander Akleyev.....	18
Amelioration of radiation-induced DNA damage in human and animal cells mediated by natural compounds of plant and animal origin Authors: Goran Gajski, Marko Gerić, Branka Mihaljević, Saveta Miljanić, Vera Garaj-Vrhovac	26
Ionizing Radiation and Metastasis: The Dark Side of a Keystone Treatment in Cancer Authors: Guadalupe Vedoya, Nora Mohamad, Mónica Táquez Delgado, Tamara Galarza, Rosa Bergoc, Ernesto Crescenti, Graciela Cricco, Gabriela Martín	31
Concentrations of Radiocesium and ⁹⁰Sr in Agricultural Plants Collected from Local Markets and Experimental Fields before Resuming Agriculture in Fukushima Prefecture Authors: Hirofumi Tsukada, Tomoyuki Takahashi, Satoshi Fukutani, Makoto Akashi	37
The Detriment in Radiation Protection Authors: Jonas Buermeyer, Samaneh Emami, Kaija Spruck, Joachim Breckow.....	43
Establishment of Concentration Ratios Riparian and Shrub Steppe Areas of the Eastern Washington Columbia Basin Authors: Jonathan Napier, Elizabeth Reudig, Leah Minc, David Bytwerk, Kathryn Higley	48
Development of a Standard Procedure for the Irradiation of Biomolecules Authors: Marc Benjamin Hahn, Tihomir Solomun, Susan Meyer, Hans-Jörg Kunte, Maria-Astrid Schröter, Heinz Sturm.....	56
Modelling the decrease in ambient dose rate from the Chernobyl fallout using data from the Swedish municipality measurement system Authors: Mattias Jönsson, Martin Tondel, Mats Isaksson, Robert Finck, Robert Wälinder, Afrah Mamour, Christopher Rääf	60
Reconstruction of the Montenegro territory contamination with ²³⁸Pu using ²³⁸Pu/²³⁹⁺²⁴⁰Pu activity ratio Authors: Nevenka M. Antović, Perko Vukotić, Nikola Svrkota	66
A probabilistic/stochastic model for contamination levels of Cs-137 in wild boars Authors: Philipp Hartmann, Laura Urso, Ulrich Fielitz, Martin Steiner	74
Results of proficiency test using radioactive brown rice sample contaminated by the accident at Fukushima Daiichi Nuclear Power Plant Authors: Rio Furukawa, Yasuhiro Unno, Akira Yunoki, Shioka Hamamatsu, Mayumi Hachinohe, Tsutomu Miura, Masayuki Mizui, Hidesuke Itadzu	81
The non-linear effects of low dose ionizing radiation on the eye lens and the tools needed to determine Authors: Roy A. Quinlan; Alexia Kalligeraki, Miguel Jarrin, Robert Pal.....	89
Shielding design for reducing secondary neutron doses to paediatric patients during intracranial proton therapy: Monte Carlo simulation of the neutron energy spectrum and its organ doses Authors: Shinnosuke Matsumoto, Koba Yusuke, Kohno Ryosuke, Choonsik Lee, Wesley E. Bolch, Michiaki Kai...96	96
A Study on UF₆ Transportation Accident Scenarios and Diffusion Model Authors: Shutang Sun, Guoqiang Li, Hongchao Sun, Feng Yan, Jiangang Zhang.....	102

Optimization of Sr/Y-90 measurement instrument for contaminated mixture sample without chemical separation	
<i>Authors: Yasuhiro Unno, Toshiya Sanami, Shinichi Sasaki, Masayuki Hagiwara, Akira Yunoki</i>	108
Development of Integrated Nuclear Emergency Command and Decision Support System for Nuclear Power Plant	
<i>Authors: Yang Yapeng, Zhang Jianguang, Feng Zongyang, Tang Rongyao, Jia Linsheng, Xu Xiaoxiao</i>	114
Cognitive and Cerebrovascular Effects Induced by Low Dose Ionizing Radiation 'CEREBRAD' (Grant agreement: 295552)	
<i>Author: Abderrafi Benotmane</i>	121
Evaluation of the Effect of Low and Intermediate Frequency Electromagnetic Waves on Radiosensitivity	
<i>Authors: Angela Chinhengo, Antonio Serafin, Bianca Hamman, John Akudugu</i>	122
Educational and Occupational Outcomes of Childhood Cancer Survivors 30 Years after Irradiation	
<i>Authors: Agnes Dumas, Claire Berger, Pascal Auquier, Gérard Michel, Brice Fresneau, Rodrigue Allodji, Nadia Haddy, Carole Rubino, Gilles Vassal, Dominique Valteau- Couanet, Sandrine Thouvenin-Doulet, Leonie Casagrande, H�el�ene Pacquement, Chiraz El-Fayech, Odile Oberlin, Catherine Guibout, Florent De Vathaire</i>	123
Radiation Survival Curve for Paediatrics Rhabdomyosarcoma Cells	
<i>Authors: Alexander F. Ibrahim, Siddig T. Kafi, Omer F. Idris</i>	124
How Nuclear Issues are Imagined: Social Perception in Relation to Radiation Protection	
<i>Author: Alejandro Igor Margetic</i>	125
Chromosomal Aberrations and Telomere Dysfunction Induced by Low Dose- irradiation Measured by Telomere and Centromere Staining	
<i>Authors: Akram Kaddour, Bruno Colicchio, Luc Morat, Corina Cuceu, Elie El Malouf, Monika Frenzel, Leonhard Heidingsfelder, Eric Laplagne, William Hempel, Mich�ele Elmay, Laure Sabatier, Radhia M'kacher</i>	126
Transmission of Induced Chromosomal Aberrations and Telomere Dysfunction through Successive Mitotic Divisions in Human Lymphocytes after In Vitro Exposure Measured by Telomere and Centromere Staining	
<i>Authors: Akram Kaddour, Bruno Colicchio, Diane Baron, Corina Cuceu, Monika Frenzel, Luc Morat, Eric Laplane, William Hempel, Laure Sabatier, Radhia M'kacher</i>	127
EPI-CT - European Cohort Study of Paediatric CT Risks: Challenges, Achievements and Perspectives	
<i>Authors: Ausrele Kesminiene, Sarah Baatout, Elisabeth Cardis, Michael Hauptmann, Andreas Jahnen, Magnus Kaijser, Carlo Maccia, Mark Pearce, Isabelle Thierry-Chef</i>	128
DNA Double Strand Break Formation and Repair in Human Fibroblasts Continuously Exposed to X-ray Radiation	
<i>Authors: Andreyan Osipov, Anna Grekhova, Margarita Pustovalova, Ivan Ozerov, Petr Eremin, Natalia Vorobyeva, Dmitry Klovov</i>	129
DNA Double-strand Break Repair in Mammalian Cells Exposed to Low-LET Radiation at Low Doses: The Controversy Continues	
<i>Authors: Andreyan Osipov, Aleksandr Samoylov, Andrey Bushmanov, Dmitry Klovov</i>	130
The ANDANTE Project: A Multidisciplinary Evaluation of the Risk from Neutrons Relative to Photons	
<i>Authors: Andrea Ottolenghi, Giorgio Baiocco, Vere Smyth, Klaus Trott</i>	131
Morphological and Molecular Analysis of Radiation-Induced Posterior Capsule Opacification (PCO) of the Lens	
<i>Authors: Andr�es Rossini, Severino Michelin, Marta Bouchez, Ana Julia Molinari, Diana Dubner, Marina DiGiorgio</i>	132
Muscular Pathology due to High Dose Irradiation in Human Muscle	
<i>Authors: Alhondra Solares-P�erez, Val�erie Allamand, Ga�etan Gruel, Fran�ois Trompier, Gillian Butler-Browne, Vincent Mouly, Marc Benderitter, Eric Bey, St�ephane Flamant, Radia Tamarat</i>	133
Alveolar Macrophages as a Key Target for Decorporating Agents Following Pulmonary Contamination with Moderately Soluble Actinides	
<i>Authors: Anne Van der Meeren, Olivier Gr�emy, Agn�es Moureau, David Laurent, Nina Griffiths, Pierre Laroche, Jaime F. Angulo-Mora</i>	134

Refinement of In Vitro Approaches for Radiotoxicological Studies to Predict Actinide Bioavailability In Vivo <i>Authors: Anne Van der Meeren, Olivier Grémy, Pierre Laroche, Jaime Angulo, Nina Griffiths</i>	135
Effect of Natural Chronic Low Dose Radiation on Human Population Residing in High Background Radiation Areas of Kerala Coast, in Southwest India <i>Author: Birajlaxmi Das</i>	136
Radiomodifying Effects of Medicinal Plants <i>Centella asiatica</i> and <i>Withania somnifera</i> <i>Authors: Bianca Hamman, Antonio Serafin, Angela Chinhengo, Vikash Sewram, John Akudugu</i>	137
R Highlights of the Russian Health Studies Program and Updated Research Findings <i>Author: Barrett N. Fountos</i>	138
Modifying the Cytokinesis-Block Micronucleus Assay for Triage Biodosimetry <i>Authors: Christina Beinke, Matthias Port, Armin Riecke, Christian Ruf, Michael Abend, Harry Scherthan</i>	139
Ionising Radiation Biological Markers for Health Risk Prediction <i>Author: Coretchi Liuba</i>	140
Sustainable Development and Nuclear Law in Argentina <i>Authors: Cecilia Tula, Mariana Arias</i>	141
Design, Development and Application of a Desk-Top Laser Produced Plasma X-Ray Source for Radiobiology Studies <i>Authors: Daniel Adjei, Anna Wiechec, Przemyslaw Wachulak, Mesfin Getachew Ayele, Janusz Lekki Wojciech M. Kwiatek, Marie Davidková, Andrzej Bartnik, Henryk Fiedorowicz, Ladislav Pina, Jakub Svobod</i>	142
Low Dose Effect Research at the Electric Power Research Institute <i>Author: Donald Cool</i>	143
Role of Radiation Dose in Cardiac and Cerebrovascular Disease Risk following Childhood Cancer: Results from CEREBRAD and PROCARDIO FP7-European Projects <i>Authors: Florent de Vathaire, Rodrigue Allodji, Giao Vu-Bezin, Florent Dayet, Damien Llanas, Cristina Veres, Mohamedamine Benadjaoud, Rafi Benotmane, Mike Atkinson, Mike Hawkins, Leontien Kremer, Elisabeth Cardis, David Winter, Lieke Feijen, Elisa Pasqual, Nadia Haddy, Ibrahima Diallo</i>	144
Dose-related Effects of Long-term Radiation Exposure on Aquatic Biota within the Chernobyl Exclusion Zone: 30 years after accident <i>Authors: Dmitri Gudkov, Natalia Shevtsova, Natalia Pomortseva, Elena Dzyubenko, Alexander Kaglyan, Alexander Nazarov</i>	145
R The International Nuclear Workers Study (INWORKS): a collaborative epidemiological study to improve knowledge about health effects of protracted low dose exposure <i>Authors: Dominique Laurier, David B Richardson, Elisabeth Cardis, Robert D Daniels, Michael Gillies, Jackie O'Hagan, Ghassan B Hamra, Richard Haylock, Klervi Leuraud, Monika Moissonnier, Mary K Schubauer-Berigan, Isabelle Thierry-Chef, Ausrele Kesminiene</i>	146
R Estimates of Radiation Effects on Cancer Risks in The Mayak Worker, Techa River and Atomic Bomb Survivor Studies <i>Authors: Dale L. Preston, Mikhail E. Sokolnikov, Lyudmila Yu. Krestinina, Daniel O. Stram</i>	147
Study on Cytotoxic Effects of the Auger Electron Emitter Technetium-99m in Functional Rat Thyroid Cells <i>Authors: Dominik Oskamp, Marcus Unverricht-Yeboah, Anugrah Gawai, Roshni Murali, Ekkehard Pomplun, Ralf Kriehuber</i>	148
R The Growth of Biostatistics and Estimation of Cancer Risk Estimates: Past, Current, and Future Challenges <i>Authors: Daniel O. Stram, Dale Preston</i>	149
External Irradiation of the Thyroid Results in Non-Targeted Transcriptional Response in the Kidneys and Liver <i>Authors: Eva Forssell-Aronsson, Britta Langen, Nils Rudqvist, Johan Spetz, Johan Swanpalmer, Khalil Helou</i>	150

Genome-wide Transcriptional Response in Normal Tissues are Influenced by Time of Day of I.V. Injection of ¹³¹I in Mice <i>Authors: Eva Forssell-Aronsson, Britta Langen, Nils Rudqvist, Toshima Z Parris, Khalil Helou</i>	151
R The potential impact of circadian rhythms on paediatric medical imaging and radiotherapy <i>Authors: Eva Forssell-Aronsson, Roy A Quinlan</i>	152
DS02R1: Improvements to Atomic Bomb Survivors' Input Data and Implementation of Dosimetry System 2002 (DS02) and Resulting Changes in Estimated Doses <i>Authors: Eric Grant, Kotaro Ozasa, Harry Cullings</i>	153
Solid cancer incidence among the Life Span Study of atomic bomb survivors: 1958-2009 <i>Authors: Eric J. Grant, Kotaro Ozasa</i>	154
Protein Status in Atomic Workers in Distant Period after Long-term Occupational Combined Low-dose Exposure <i>Authors: Evgeniia Kirillova, Maria Zakharova, Taisa Uryadnitskaya, Christopher Loffredo</i>	155
Cancer Incidence among Mayak Workers <i>Authors: Elena Labutina, Nezahat Hunter, Irina Kuznetsova</i>	156
Comparison of Total Antioxidant Capacity level between radiation workers in diagnostic radiology and other staffs of hospital in Zahedan <i>Authors: Fatemeh Ramrodi, Farnaz Farifteh, Amir Hossein Zarghami, AliReza Nakhaee, Dariush Askari, Jalal Ordoni, Yazdan Salimi, Mohammad Hossein Jamshidi, Hamed Dehghani</i>	157
Effects of Radon Inhalation on Biophysical Properties of Blood in Rats <i>Authors: Fayez Shahin, Omar Abdel-Salam</i>	158
Assessment of Respiratory Toxicity of ITER-like Tungsten Metal Nanoparticles using an in vitro 3D Human Airway Epithelium Model <i>Authors: George Isabelle, Hagege Agnès, Herlin Nathalie, Vrel Dominique, Rose Jérôme, Sanles Marcos, Orsiere Thierry, Uboldi Chiara, Grisolia Christian, Rousseau Bernard, Malard Véronique</i>	159
Beyond Paternalism and Strategy: Understanding Radiological Risks as a Mutual Learning Experience <i>Authors: Gaston Meskens, Tanja Perko</i>	160
Survey of the Effect of Ionizing Radiation Energy on the Blood Indices of Occupationally Exposed Staff (radiologic technologists and radiologists) <i>Authors: Hamid Behrozi, Mohammad Hossein Jamshidi, Kimia Benabbas, Marziyeh Daemolzeqr, Yazdan Salimi, Dariush Askari, Jalal Ordoni, Hamed Dehghani</i>	161
Development of Radiological Protection Powder <i>Authors: Hiroki Ohtani, Yuya Ishita</i>	162
Risk of Thyroid Cancer Incidence due to Living Close to Atomic Facility in Childhood <i>Authors: Irina Martinenko, Mikhail Sokolnikov</i>	163
Retrospective Estimation of Organ Doses for an Epidemiology Study of CT Scanning in Paediatric Patients (EPI-CT) <i>Authors: Isabelle Thierry-Chef, Jérémie Dabin, Joahannes Hermen, Tore S. Istad, Andreas Jahnen, Lucian Krille, Choonsik Lee, Carlo Maccia, Arvid Nordenskjöld, Hilde Olerud, Steven L Simon, Lara Struelens, Ausrele Kesminiene</i>	164
Biological Dosimetry after Total Body Irradiation (TBI) for Hematologic Malignancy Patients using Premature Chromosomal Condensation in Combination with Fluorescence in Situ Hybridization <i>Authors: Julien Dossou, Dominique Violot, Theodore Girinsky, Patrice Carde, Jean-Henri Bourhis, Claude Parmentier, Radhia M'kacher</i>	165
Doses and risks from radon and other internal emitters and their control <i>Author: John Harrison</i>	166

Synthesis of Novel Psammaplin A-based Radiosensitizers <i>Authors: Jin Ho Kim, Chan Woo Wee, Hak Jae Kim, Soo Youn Suh, Eun Sook Ma, Boom Soo Shin, Il Han Kim</i>	167
Responses to Radiation and Fate of Cells <i>Authors: Jin Kyu Kim, Mi Young Kang, Remigius A. Kawala, Tae Ho Ryu, Jin-Hong Kim</i>	168
Radiation-Induced p53 Level Determines Radiosensitivity of Cells <i>Authors: Jin Kyu Kim, Min Young Kang, Yun-Jong Lee, Jin-Hong Kim, Jacobus P. Slabbert</i>	169
Development and Validation of a Multivariate Calibration Strategy for Direct Analysis of Trace Elements in Soft Tissue Utilizing Chemometric Energy Dispersive X-Ray Fluorescence and Scattering (EDXRFS) Spectroscopy <i>Authors: Justus Okonda, Angeyo Kalambuka, Seth Kisia, Michael Mangala</i>	170
Radiation Shielding perfection at Design and construction Stages <i>Author: Joseph Rugut</i>	171
Application of the Spencer-Attix Cavity Theory for Determination of Conversion Coefficient for Ambient Equivalent Dose with TLD-100 Dosimeters Calibrated in Air Kerma <i>Authors: Jose T Alvarez Romero, Fernando Gonzalez Jimenez</i>	172
Evaluation of Fission Energy Deposition in the SAFARI-I Nuclear Reactor <i>Authors: Linina Jurbandam, Oscar Zamonsky</i>	173
Lung Cancer Risk from Radon and Smoking – Additive or Multiplicative Effect <i>Author: Ladislav Tomasek</i>	174
Risk of Leukemia in Uranium Miners <i>Author: Ladislav Tomasek</i>	175
Chronic Bronchitis Incidence in the Cohort of Mayak Production Association Workers Occupationally Exposed to Radiation <i>Authors: Tamara Azizova, Galina Zhuntova, Richard Haylock, Maria Moseeva, Evgenia Grigorieva, Maria Bannikova, Zinaida Belyaeva, Evgeniy Bragin</i>	176
Microdosimetric Measurements for Electron Irradiation of DNA under Physiological Conditions: Low Energy Electrons vs. Radicals <i>Authors: Marc Benjamin Hahn, Tihomir Solomun, Susan Meyer, Hans-Joerg Kunte, Heinz Sturm</i>	177
Markers of Neural Degeneration and Regeneration in Blood of Cardiac Catheterization Personals <i>Authors: Mohamed ElKhafif, Soheir Korraa, Nevine Noussier, Walid Elhammady, Eman El Gazzar, Hanan Diab</i>	178
Regulatory Culture and its Role in Radiation Protection <i>Authors: Marcela Ermacora, Chris Englefield</i>	179
The Hybrid Analytical – Voxel Head Phantom for Activity Measurement of ²⁴¹Am in Cranial Bone <i>Author: Marko Fulop</i>	180
Occupational and Medical Exposure: The Contribution to Carcinogenic Risk In Mayak Worker Cohort <i>Authors: Mikhail Osipov, Mikhail Sokolnikov</i>	181
Baseline Lifetime Mortality Risk from Circulatory Disease in Japan <i>Authors: Michiya Sasaki, Haruyuki Ogino, Takatoshi Hattori</i>	182
DNA Repair Genes XRCC1 and XRCC3 Polymorphisms and the Level of Micronuclei in Industrial Radiographers <i>Authors: Mahsa Shakeri, Farideh Zakeri, Vahid Changizi, Mohammad Reza Farshidpour, Mohammad Reza Rajabpour</i>	183
Mayak Worker Cancer Mortality <i>Authors: Mikhail Sokolnikov, Dale Preston, Dan Stram</i>	184

Repair of Ionizing Radiation-Induced DNA Damage and Risk of Second Cancer in Childhood Cancer Survivors <i>Authors: Nadia Haddy, Laurence Tartier, Serge Koscielny, Elisabeth Adjadj, Carole Rubino, Laurence Brugières, Hélène Pacquement, Ibrahima Diallo, Florent de Vathaire, Dietrich Averbeck, Janet Hall, Simone Benhamou...</i>	
The Role of the Scientific Review Group in the Russian Health Studies Programs: Key Contributions and Influence and Impact on Radiation Protection <i>Author: Nolan Hertel</i>	186
A Comprehensive Study on Tritium Release from Nuclear Accidents and Impact of Tritiated Water on Postnatal Development of Mouse Cerebellum <i>Authors: Narendra Jain, A. L. Bhati</i>	187
Current State of Pharmacologic Radioprotection for Clinical Exposure to Ionizing Radiation <i>Authors: Nivethan Vela, Joe Barfett, Kieran Murphy, David Mikulis</i>	188
Ameliorating Effects of Bone Marrow Transplantation and Zinc Supplementation on Physiological and Immunological Changes in γ-Irradiated Rats <i>Authors: Omaima Ashry, Maha Soliman, Mervat Ahmed, Yasmin Abd El Naby</i>	189
Occupational Exposure to ^7Be – A Case Study <i>Authors: Ofer Aviv, Hanan Datz, Shlomi Halfon, Zohar Yungrais, Erez Daniely</i>	190
Early and Late Alterations of Neurochemical, Behavioral, and Somatic Criteria in Rats Exposed to ^{12}C ions and γ-rays <i>Authors: Oleg Belov, Ksenia Belokopytova, Ara Bazyan, Vladimir Kudrin, Viktor Narkevich, Aleksandr Ivanov, Gennady Timoshenko, Eugene Krasavin</i>	191
Integrating Dosimetry, Radiobiology and Epidemiology to study the Effects of Occupational Exposure to Uranium in Europe: the CURE Project <i>Authors: Olivier Laurent, Maria Gomolka, Richard Haylock, Eric Blanchardon, Augusto Giussani, Will Atkinson, Derek Bingham, Sarah Baatout, Ladislav Tomasek, Elisabeth Cardis, Janet Hall, Dominique Laurier</i>	192
Investigations of radiation exposures in the aftermath of the Chernobyl accident <i>Author: Rolf Michel</i>	193
A New Tool for Genotoxic Risk Assessment: Re-evaluation of Cytokinesis-Block Micronucleus Assay using Semi-Automated Scoring following Telomere and Centromere Staining <i>Authors: Radhia M'kacher, Narjes Zaguia, Francis Finot, Luc Morat, André Essahli, Corina Cuceu, Bruno Colicchio, Leonhard Heidingsfelder, Eric Laplagne, William Hempel, Laure Sabatier</i>	194
Change in Peripheral Blood Lymphocyte Telomere Length and the Occurrence of Secondary Cancers in Hodgkin Lymphoma Patients <i>Authors: Radhia M'kacher, Theodore Girinsky, Bruno Colicchio, Michelle Ricoul, Corina Cuceu, Luc Morat, Monika Frenzel, Aude Lenain, Leonhard Heidingsfelder, William Hempel, Alain Dieterlen, Laure Sabatier, Patrice Carde</i>	195
Radiation Dose to the Eyes in the Risk of Cataract after Non-Retinoblastoma Solid Childhood Cancers <i>Authors: Rodrigue Sètchéou Allodji, Chiraz El-Fayech, Amar Kahlouche, Boris Schwartz, Odile Oberlin, Mohamed Benadjaoud, Julien Bullet, Ibrahima Diallo, Carole Rubino, Nadia Haddy, Florent de Vathaire</i>	196
Risk of Subsequent Leukaemia after a Solid Tumour in Childhood: Radiotherapy and Chemotherapy Side Effects <i>Authors: Rodrigue Sètchéou Allodji, Boris Schwartz, Cristina Veres, Nadia Haddy, Carole Rubino, Marie-Cécile Le Deley, Jérémie Vu Bezin, Jean Chavaudra, Dimitri Lefkopoulos, Eric Deutsch, Odile Oberlin, Ibrahima Diallo, Florent de Vathaire</i>	197
Simulation-extrapolation Method to Address Errors in Atomic Bomb Survivor Dosimetry on Solid Cancer and Leukaemia Mortality Risk Estimates, 1950-2003 <i>Authors: Rodrigue Sètchéou Allodji, Boris Schwartz, Ibrahima Diallo, Dominique Laurier, Florent de Vathaire</i>	198
Chernobyl, 30 Years on – Health Effects <i>Author: Richard Wakeford</i>	199
 Immunological Monitoring of the Personnel at Radiation Hazardous Facilities <i>Authors: S.M. Kiselev, M.E. Sokolnikov, L.V. Lyss, N. I. Ilyina</i>	200

Raman Spectroscopy as an Analytical Tool for Ionizing Effect Studies in Pig Lens “Ex Vivo” and “In Vitro” <i>Authors: Severino Michelin, Andres Rossini, Emilia Halac, Diana Dubner, Ana Molinari</i>	201
Current Status of the Biological Study on Low-Dose Ionizing Radiation Effects in KHNP-RHI, Korea <i>Authors: Seon Young Nam, Kwang Hee Yang</i>	202
Role of AKT and ERK Pathway in Controlling Radio-Sensitivity and Adaptive Response by Low-Dose Radiation in Human Immune Cells <i>Authors: Seon Young Nam, Hyung Sun Park, Ga Eun You, Kwang Hee Yang, Ji Young Kim</i>	203
Non-cancer Effects in the Cohort of Mayak PA Workers Occupationally Exposed to Radiation <i>Authors: Tamara Azizova, Evgeniya Grigorieva, Maria Bannikova, Richard Haylock, Nazahat Hunter</i>	204
Micro- and Mesocosms for Assessing Ecosystem Effects of Radiation – A Review <i>Authors: Tanya Hevroy, Clare Bradshaw, Hallvard Haanes, Elisabeth Hansen, Runhild Gjelsvik, Alicja Jaworska, Louise Jensen, Emmanuel Lapied, Deborah Oughton</i>	205
An Update on a Rapid Method of Biological Dosimetry to Assist in the Event of a Nuclear Emergency <i>Authors: Timothy Sebeela, JP Slabbert, V.V. Vandersickel, D. Serfontein</i>	206
Radioiodine Transfer from Seaweed to Abalone <i>Authors: Toshihiro Shibata, Yoshio Ishikawa, Yuichi Takaku, Shun-ichi Hisamatsu</i>	207
Clinical Features of Subacute Radiation Syndrome <i>Authors: Valeriy Krasnyuk, Anastasia Ustyugova</i>	208
The Frequency of Chromosome Aberrations in Peripheral Blood Lymphocyte Cultures and Risk of Disease Development after Radiation Exposure <i>Authors: Vladimir Nugis, Maria Kozlova</i>	209
Airborne I-131 detection on Internal Surface of Buildings using Common Household Products <i>Authors: Yung-Chang Lai, Ying-Fong Huang, Yu-Wen Chen, Mei-Ling Chung</i>	210
History of Ultra-Sonography Examination for Thyroid in the Residents Near Nuclear Power Plants <i>Authors: Young-Khi Lim, Kwang-Pil Ko, Keun-Young Yoo, Sue K. Park, Aesun Shin, Keon Wook Kang</i>	211
Pu isotopes in Surface Soils in China: Its Concentration and Isotopic Ratio <i>Authors: Youyi Ni, Wenting Bu, Wei Dong, Qiuju Guo</i>	212
Development and Application of High Intensity D-T Fusion Neutron Generator (HINEG) <i>Authors: Yican Wu, Song Gang, Yongfeng Wang, Taosheng Li, Xiang Ji, Chao Liu, Jieqiong Jiang</i>	213
ESR Dosimetry with Ceramic and Glass Materials from Electronic Components for Dose Assessment in Radiation Accident <i>Authors: Zhe Liu, Zhiping Luo, Jinfeng Huang, Guowen Zheng</i>	214
  Results of RELID Study 2014 - Buenos Aires, Argentina Retrospective Evaluation of Lens Injuries and Dose <i>Authors: Papp, C., Romano-Miller, M.; Descalzo, A., Michelin, S., Molinari, A., Rossini, A., Plotkin, C.; Bodino, G., Esperanza, G., Di Giorgio, M., Touzet, R.</i>	215
Area 2: Policy, Standards and Culture	216
Integration of radiation safety in management systems in Swedish health care – success or distress <i>Author: Anja Almén</i>	217
Some Suggestions to Adequate the IAEA Safety Standards Series No. 49 According to the General Safety Requirements Part 3 from IAEA <i>Authors: Adelia Sahyun, Carlos N. Ghobril, Clarice F. Perez, Gian Maria Sordi</i>	224
Restoring the “R” in ALARA <i>Author: Brant A. Ulsh</i>	228
De minimis non curat lex or endless optimization? <i>Author: Bernd Lorenz</i>	236

Ethics and radiation protection in biomedical research in the post-Fukushima era: <i>up to date</i> <i>Author: Chieko Kurihara</i>	244
e-Learning – Radiation Safety Training Course <i>Author: Carolyn Mac Kenzie</i>	253
The Romanian Society for Radiological Protection – 25 years as Associate Society to IRPA <i>Authors: Constantin Milu, Ion Chiosila, Nicolae-Mihail Mocanu</i>	256
Radiation Safety Climate in a University Setting <i>Authors: Caitlin Root, Robert Sinclair, Konstantin Povod, Nicole Martinez</i>	259
Young Scientists and Professionals (YSP) – Austria’s Young Generation as best practice example <i>Authors: Ch. Stettner, F. Kabrt, E. Langegger, N. Baumgartner</i>	267
Carbon Molecular Sieves used in the Sampling and Monitoring Technology of Krypton in the Atmosphere <i>Authors: Deng Achang, Ma Xiongnan, Zhu Jun, Xiao Xiangzhong, Zhang Aiming</i>	270
Public Acceptance of Nuclear Technology: education and communication to transform old prejudices and inspire new thoughts <i>Author: Denise S. Levy</i>	277
Enhancing communication on Radiological Protection throughout Brazil <i>Authors: Denise S. Levy, Gian M. A. A. Sordi, Demerval L. Rodrigues, Janete C. G. Carneiro</i>	284
Radiation Protection Culture in Waste Management <i>Authors: G. Hampel, J. Feinhals, H. Völkle</i>	291
Comments on the General IAEA Safety Requirements – Part 3 – and Suggestions for the Next Publications <i>Author: Gian Maria Sordi</i>	298
5th European IRPA Congress (4-8 June 2018): Encouraging Sustainability in Radiation Protection <i>Authors: Hielke Freerk Boersma, Bert Gerritsen, Gert Jonkers, Jan Kops, Lars Roobol, Carel Thijssen</i>	304
L Band EPR Tooth Dosimetry for neutron <i>Authors: Ichiro Yamaguchi, Hitoshi Sato, Hiraku Kawamura, Tuyoshi Hamano, Hiroshi Yoshii, Mituru Suda, Minoru Miyake, Naoki Kunugita</i>	309
Promoting Radiation Safety Culture in the UK: General Users Sector <i>Authors: J. R. Croft, A. MacDonald, R. Fannin, R. Hill, P. Boulton, D. Orr, A. Bannon</i>	316
Promoting Radiation Safety Culture in the UK <i>Authors: J. R. Croft, R. Coates, C. Edwards, C.-L. Chapple, K. Davies, A. MacDonald</i>	324
Radiation Protection Quantities for the Assessment of Stochastic Effects: Should we be more Papal than the Pope? <i>Authors: Jozef Sabol, Jana Hudzietzová, Bedřich Šesták</i>	331
"A North-American first: a state-of-the-art fully functional Linac for teaching to the next generations of therapists and physicists in a college" <i>Authors: Mathieu Bergeron, Louis Archambault, Luc Beaulieu</i>	336
2015 IRPA survey of professionals on the new dose limit to the lens of the eye, and wider issues associated with tissue reactions <i>Authors: Marie Claire Cantone, Merce Ginjaume, Saveta Miljanić, Colin J. Martin, Keiichi Akahane, Louisa Mpete, Severino C. Michelin, Cinthia M. Flannery, Lawrence T. Dauer, Stephen Balter</i>	342
Introducing on-line modules in the Swedish Master’s Degree Programme for Applied Radiation Protection 14 <i>Authors: Mattias Jönsson, Mats Isaksson, Robert Finck, Christopher Rääf</i>	349
Management of Radioactive Waste: Public Perceptions Versus Scientific Views <i>Author: Mogwera Khoathane</i>	355

New EU-Regulations for Radon at Workplaces and their Consequences on the Regulatory Radiation Protection in Bavaria <i>Authors: Markus Trautmannsheimer, Simone Körner</i>	364
Contributions from Women to the Radiation Sciences <i>Authors: Nicole Martinez, Elizabeth Gillenwalters</i>	370
Argentine Plan for strengthening occupational radiation protection infrastructure framed in the RLA 9075 IAEA Project <i>Authors: Nancy Puerta Yepes, Ana Rojo, Adrián Discacciatti, Marina Di Giorgio, Laura Castro, Fabio López, Analía Canoba</i>	379
Activities of EUTERP, the European Training and Education in Radiation Protection Foundation <i>Authors: Richard Paynter, Folkert Draaisma, Penelope Allisy, Michèle Coeck, Friedrich Hoyler, Marcel Schouwenburg, Joanne Stewart</i>	387
A model for determining risk constraints for potential exposures of the public and limitations of the activity of radionuclides released by accidents in nuclear facilities <i>Author: Robert R. Finck</i>	391
The Advantages of Creating a Positive Radiation Protection Safety Culture in the Higher Education and Research Sectors <i>A report from the Working Group on Culture in Research and Teaching</i> <i>Authors: T. Coldwell, P. Coleb, C. Edwards, J. Makepeace, C. Murdock, H. Odams, R. Whitcher, S. Willis, L. Yates</i>	399
Education and Training of Workers for Development of a Safety Culture in a Radioactive Facility <i>Authors: Zayda Haydeé Amador Balbona, Miguel Antonio Soria Guevara</i>	409
Assessment of radiation science studies in 4 successive years <i>Authors: Banafsheh Zeinali-Rafsanjani, Mahdi Haghghatafshar, Mahdi Saeedi-Moghadam, Mohammad-Amin Moseleh-Shirazi</i>	415
Y Gender demographics in radiation protection <i>Authors: Elizabeth Gillenwalters, Nicole Martinez</i>	419
The FORO Project on Safety Culture in Organizations, Facilities, and Activities with Sources of Ionizing Radiation <i>Authors: Rubén Ferro Fernández, Jorge Arciniegas Torres, Ana Blanes Tabernero, Ana M. Bomben, Rodolfo Cruz Suárez, Claudia Da Silva Silveira, E. Ordoñez Gutiérrez, Jorge F. Perera Meas, Renán Ramírez Quijada, Ricardo Videla Valdebenito</i>	427
The Intersection of Public Health and Radiation Protection in Radiation Emergencies <i>Author: Armin Ansari</i>	435
Assessment of the Safety Culture at Facilities Involved in Management of the Spent Nuclear Fuel and Radioactive Waste <i>Authors: Alexander Bobrov, Sergey Kiselev, Malgorzata Sneve, Victor Scheblanov</i>	436
The Decision Threshold and Other Characteristic Limits: An Approach to Re- evaluating the Current Computational Paradigm <i>Authors: Alexander Brandl, Jenelle Mann</i>	437
Lessons learned from 4th African Regional Congress of the International Radiation Protection Association (AFRIRPA04) held in Morocco <i>Authors: Abdelmajid Choukri, Oum Keltoum Hakam</i>	438
Safety Culture Issues in Nuclear Fusion Activities <i>Author: Altair de Assis</i>	439
Communication in an Organization within a Framework of Social Responsibility <i>Authors: Andrea Docters, Maria B. Lucuix</i>	440
Interdisciplinary Approach to Radiation and Nuclear Safety Education <i>Author: Andrejs Dreimanis</i>	441

Education and Training in Radiopharmacy: The INSTN Approach <i>Author: Akli Hammadi</i>	442
Experience of Belarus to the Introduction of International Radiation Safety Standards to the National System <i>Authors: Alena Nikalayenka, Sergey Sychik, Viktoia Kliaus</i>	443
R The Evaluation of the Real Alpha Value in Brazil and Its Projection until the Year 2050 <i>Authors: Adelia Sahyun, Carlos N. Ghobril, Clarice F. Perez, Gian Maria Sordi</i>	444
Radiation Protection in Medical Field in Cameroon <i>Authors: Augustin Simo, Maurice Ndontchueng Moyo, Yolande Huguette Ebele Yigbedeck, Richard Samba Ndi</i>	445
EURADOS IDEAS Guidelines Spanish Translation: A New Tool for Training Activities from the Collaboration between SEPR-SAR Radiation Protection Societies <i>Authors: Borja Bravo, Eduardo Sollet, Ana Maria Rojo, Inés Gomez</i>	446
Engaging Communities to Discuss Nuclear Power Options for the Future <i>Author: Barbara L. Hamrick</i>	447
An IRPA, WHO, IOMP Initiative on Radiation Protection Culture in Medicine <i>Authors: Bernard Le Guen, María Del Rosario Perez, Madan M. Rehani</i>	448
Regulating the Security of Radioactive Sources in South Africa and Institutionalising Nuclear Security Culture and Effective Physical Protection <i>Author: Boikanyo Ntuane</i>	449
Fraudulent Exams in the Training of Reactor Supervisors at the Laguna Verde Nuclear Power <i>Author: Bernardo Salas</i>	450
R Plenary Panel International Standards – RP in Medicine <i>Author: Claire Cousins</i>	451
R Radiation Safety Culture in the UK Medical Sector: A top to bottom strategy <i>Authors: Claire-Louise Chapple, Andy Bradley, Maria Murray, Phil Orr, Jill Reay, Peter Riley, Andy Rogers, Navneet Sandhu, Jim Thurston</i>	452
Implementation in the Republic of Moldova the Requirements of Directive 2013/59 / Euratom on Indoor Radon Concentrations <i>Authors: Coretchi Liuba, Bahnarel Ion</i>	453
Workshop on Radiopathology and Radiation Protection at the Annual Rotating Internship, School of Medicine at the University of Buenos Aires <i>Authors: Cinthia Papp, Mónica Gardey, Gerardo Rank, Roberto Agüero, Mara Scarabino, Adriana Cascón</i>	454
Implications of ICRP 103, the International and the European Basic Safety Standards on the use of Dose Constraints in the Management and Disposal of Radioactive Waste, Including Waste Containing Elevated Levels of Naturally Occurring Radionuclides in France <i>Authors: Marie-Odile Gallerand, Christophe Serres, Didier Gay, François Besnus, Jérôme Guillevic</i>	455
Dose Limits in Radioactive Waste Management: Interdisciplinary Perspectives from the German ENTRIA Project <i>Authors: Clemens Walther, Achim Brunnengräber, Peter Hocke, Karena Kalmbach, Claudia König, Sophie Kuppler, Klaus-Jürgen Röhlig, Ulrich Smeddinck</i>	456
The ICRP System of Protection for Existing Exposure Situations: The Work of Committee 4 to Elaborate the Framework for Protection <i>Author: Donald Cool</i>	457
Policy Standards and Culture <i>Author: David Crawford</i>	458
The UK Ministry of Defence Radon Safety Programme <i>Authors: Dee Emerson, Dean Williams</i>	459

R Certified Training for Nuclear and Radioactive Source Security <i>Authors: Daniel Johnson, Brunelle Battistella, Pierre Legoux</i>	460
Radiation Safety Culture at United States Nuclear Power Plants <i>Author: Ellen Anderson</i>	461
43 Years of Experience in Training in Radiation Protection <i>Author: Eduardo Medina-Gironzini</i>	462
Experience in the Use of Social Networks in Radiation Protection <i>Author: Eduardo Medina-Gironzini</i>	463
Nuclear regulators need to adopt international standards applicable to radiation measuring instruments into their national legislation <i>Author: Emma Snyman</i>	464
ICNIRP: Preliminary Thoughts on Protection Principles for Non-Ionizing Radiation <i>Author: Eric van Rongen</i>	465
Ethical Considerations on the Empowerment of People Living in Contaminated Areas after a Nuclear Accident <i>Authors: François Rollinger, Jacques Lochard, Thierry Schneider</i>	466
The Inter-Agency Committee on Radiation Safety – 25 years of Cooperation Efforts to Harmonize International Radiation Protection and Safety <i>Authors: Ferid Shannoun, Miroslav Pinak, Ted Lazo, Carl Blackburn, Stephan Mundigl, Malcolm Crick, Shengli Niu, Pablo Jimenez, María Pérez, Hans Menzel, Christopher Clement, Miroslav Voytchev, Renate Czarwinski, Alain Rannou</i>	467
Lessons Learned from the Fukushima Event: The Radiation Protection Emergency Preparedness <i>Authors: Giorgio Cucchi, Lorenzo Isolan, Federico Rocchi, Marco Sumini</i>	468
Interplay of Nuclear Power on Earth and in Space: Nuclear Energy as Sustainable Energy <i>Author: Gordana Lastovicka-Medin</i>	469
Scientific Issues, Emerging Challenges and Emerging Digital Social Innovations for Radiation and Radiological Protection <i>Author: Gordana Lastovicka-Medin</i>	470
Workers' Knowledge on Radiation Protection. A Survey at Mongi Slim Hospital <i>Author: Hager Kamoun</i>	471
R Importance to Engage in Dialogue with the Affected Population after the Acute Phase of an Accident <i>Author: Hans Vanmarcke</i>	472
Establishing Radiation Protection Culture for Local Residents Left in the outside Boundary of Fukushima and Challenges facing Mothers and Children <i>Author: Hiroko Yoshida</i>	473
Scientific, Societal, Implementation and Regulatory Challenges of Radiological Protection <i>Authors: Ingemar Lund, Ted Lazo</i>	474
Radiation Protection in a Mixed Contaminant Context, Risk Assessment Methodologies <i>Authors: Ivica Prlic, Hrvoje Mesic, Mladen Hajdinjak, Jerko Sisko, Domagoj Kosmina, Tomislav Bituh</i>	475
OPERRA-HARMONE: Harmonising Modelling Strategies of European Decision Support Systems for Nuclear Emergencies <i>Authors: Jan Christian Kaiser, Shan Bai, Johan Camps, Thomas Charnock, Damien Didier, Fabricio Fiengo, Laurent Garcia-Sanchez, Jérôme Groell, Christophe Gueibe, Kerstin Hürkamp, Olivier Isnard, Anne Nisbet, Wolfgang Raskob, Marie Simon Cornu, Christian Staudt, Lieve Sweeck, Jochen Tschiersch, Jordi Vives i Batlle, Samantha Watson, Mark Zheleznyak</i>	476
How to Develop and Maintain an Effective Training Program in Radiation Protection <i>Authors: Joe Cortese, Liz Krivososov</i>	477

Delineation of Radon Prone Areas for Mandatory Radon Measurement in Workplaces in the Czech Republic <i>Authors: Jana Davidková, Karla Petrová</i>	478
Nuclear Security Consideration for Radiation Protection Professionals <i>Authors: Jason Harris, Edward Waller</i>	479
Communicating Risk to the Public: An Important Element in Mitigating the Impact of a Radiological Terrorist Attack <i>Authors: Jozef Sabol, Bedrich Sestak, Ivo Petr</i>	480
Improvement in Radioactive Waste Management over the Past 40 Years in the U.S <i>Author: J. Scott Kirk</i>	481
Current Discussions in Japan Health Physics Society regarding Radiation Protection of the Lens of the Eye <i>Authors: Keiichi Akahane, Takeshi Iimoto, Takeshi Ichiji, Satoshi Iwai, Hiroyuki Ohguchi, Kazuko Ohno, Tadahiro Kurosawa, Chiyo Yamauchi-Kawaura, Hideo Tatsuzaki, Norio Tsujimura, Nobuyuki Hamada, Toshiyuki Hayashida, Yutaka Hotta, Tadashi Yamasaki, Sumi Yokoyama</i>	482
 The Ethical Foundations of the Radiological Protection System <i>Author: Kunwoo Cho</i>	483
Assessing and Promoting Radiation Safety Culture in the UK Nuclear Sector <i>Authors: Karl Davies, John Croft, Ellie Krukowski, John Bradshaw</i>	484
Managing Suitably Qualified and Experienced Persons (SQEP) Requirements to Meet Business Need <i>Authors: Kenneth Gibbs, Robin Wells</i>	485
The Selected Issues Related to the Development of National Legislation Based on ICRP103, IAEA BSS and EU BSS <i>Authors: Karla Petrová, Jana Davidková</i>	486
Updating the Radiation Protection Guidance for the United States <i>Authors: Kenneth Kase, Michael Boyd, John Boice, Armin Ansari</i>	487
Unification of Legal and Procedural Documentation for Emergency Response in the FMBA of Russia <i>Authors: Liudmila Bogdanova, Yuriy Salenko</i>	488
Development of Nuclear Security infrastructure in Nigeria: Achievements Challenges and prospects <i>Author: Mbet Akpanowo</i>	489
Practical Aspects of Applying Ethics to Occupational Exposures within the Nuclear Sector <i>Author: Marie Barnes</i>	490
Stakeholder Dialogue Webinar: Experience and Lessons for Young and Old Experts and Researchers <i>Authors: Mike Boyda, Ted Lazob</i>	491
Goals and Intermediate Results of the 7FP ENETRAP III Project <i>Authors: Michèle Coeck, Joanne Stewart, Annemarie Schmitt-Hannig, Paul Livolsid, Sascha Trumm, Marisa Marco</i>	492
Problems Associated with Radiation Protection Training Programs <i>Author: Mohamed Gomaa</i>	493
The INEX 5 Exercise: Notification, Communication and Interfaces for Catastrophic Radiological Events <i>Authors: Mike Griffiths, Olvido Guzman</i>	494
Mini UAS based Gamma Spectrometry Measurements in case of Emergency <i>Author: Markku Kettunen</i>	495
Radon occupancy factor for the public areas, needs for revision <i>Authors: Mohsen Shafiee, Sajad Borzoueisileh, Razieh Rashidfar</i>	496
An Insight into the Nuclear Security Science and Policy Institute at Texas A&M University <i>Author: Mani D. Shah</i>	497

Education Standards and Standards Education (ESSE) Process in Radiation Protection in a National Education Cycle <i>Author: Mehdi Sohrabi</i>	498
The URPS Hypothesis for Universal Radiation Protection Standardization <i>Author: Mehdi Sohrabi</i>	499
Lessons from Fukushima Daiichi Nuclear Accident and Efforts of Nuclear Regulation Authority <i>Author: Nobuhiko Ban</i>	500
Balancing Theory and Practicality: Engaging Non-Philosophers in Ethical Decision Making <i>Authors: Nicole Martinez, Daniel Wueste</i>	501
The 4th Workshop on Science and Values in Radiological Protection Decision Making <i>Authors: Nataliya Shandala, Aleksandr Rakhuba, Ted Lazo</i>	502
Cs-137 Contamination Incident at Scrap Yard in South Africa <i>Author: Nico van der Merwe</i>	503
Evaluation of the National Legislative & the Regulatory Framework of Security of Sealed Radioactive Sources in interim Storage <i>Authors: Oumkeltoum Hakam, Mohamed Maital, Assia Lasfar</i>	504
South African Perspective for Radon in Dwellings and the Anticipated Regulatory Control Measures <i>Author: Obusitse John Pule</i>	505
Contribution of a Master Program in Radiation Protection to Building Competencies in Morocco and Regionally <i>Authors: Oum Keltoum Hakam, Abdelmajid Choukri</i>	506
Promoting Nuclear Security Culture through the International Nuclear Security Education Network (INSEN) <i>Authors: Oum Keltoum Hakam, Guido Gluschke, Dmitriy Nikonov</i>	507
 Nuclear New Build – Integrating Cultural Differences in Radiation Protection <i>Authors: Peter A Bryant, Valentin Haemmerli, Peter Cole</i>	508
What to Say to the General Public: CT Doses are Safe or Causing Cancer? <i>Author: Pradip Deb</i>	509
The IAEA Safety Standards – Current and Future Perspectives <i>Author: Peter Johnston</i>	510
1,200 High School Students Involved in Radiation Protection Actions: Eight Years of Experience Feedback in Dissemination of Radiation Protection Culture. <i>Authors: Paul Livolsi, Thierry Schneider, Lucie D'Ascenzo, Sylvie Charron, Emmanuel Bouchot, Pascal Remond</i>	511
 Prudence in Radiation Protection - How Much? A Case Study <i>Author: Roger Coates</i>	512
Ethical Basis of Radiation Protection <i>Author: Richard Toohey</i>	513
The 1980 Sievert Lecturer: Lauriston S. Taylor <i>Author: Richard Toohey</i>	514
Management of Contaminated Goods in Post Accidental Situation: Synthesis of European Stakeholders' Panels <i>Authors: Sylvie Charron, Sandra Lafage, Jean-François Lecomte, Thierry Schneider, Pascal Crouail, Christophe Murith, Bruno Cessac, Vanessa Parache</i>	515
Establishment of a New Nuclear Regulatory Authority in Ghana <i>Authors: Stephen Inkoom, Geoffrey Emi-Reynolds, Emmanuel O. Darko, Abdel Razak Awudu, Joseph K. Amoako, Augustine Faanu, Margaret Ahiadeke, Ebenezer O. Appiah, Ann Mensah, Daniel N. Adjei, Adriana Nkansah</i>	516

Lessons learned from the Fukushima Dai-ichi accident and safety enhancements for the restart of nuclear power plants in Japan <i>Author: Shinichi Kawamura</i>	517
Accreditation Model of Courses in Radiation Protection in Medicine: One proposal to Latin America countries <i>Authors: Simone Kodlulovich Renha, Lidia Vasconcellos de Sá</i>	518
Development of Practical Guidance's for Workplace Monitoring in Nuclear and Radiation Facilities - an IAEA TECDOC Project <i>Authors: Suriya Murthy Nagamani, Jizeng Ma, Miraslov Pinak</i>	519
Management of Malaysian Nuclear Agency's License: Experiences and Challenges <i>Authors: Suzilawati Muhd Sarowi, Azimawati Ahmad, Mohd Fazlie Abdul Rashid, Noor Fadilla Ismail, Hairul Nizam Idris</i>	520
Microdistribution of Plutonium in Human Skeleton. Should we Change the ICRP Model? <i>Authors: Sergey Romanov, Ekaterina Lyovkina, Elena Labutina</i>	521
A Tool for Implementing the UNSCEAR Methodology for Estimating Human Exposures from Radioactive Discharges <i>Authors: Tracey Anderson, Kelly Jones, Helen Grogan, Ed Waller, Lynn Hubbard, Jane Simmonds</i>	522
International Standards for Managing Radionuclides in Food and Drinking Water <i>Authors: Tony Colgan, Carl Michael Blackburn, Maria Perez del Rosario, Igor Gusev</i>	523
Transition of Public Awareness and Its Factor Analysis Concerning Nuclear Energy and Radiation Application Based on Japanese Nationwide Fixed-Points Poll <i>Authors: Takeshi Iimoto, Kazuhisa Kawakami, Hiroshi Kimura, Masayuki Tomiyama, Makoto Funakoshi, Noriaki Sakai, Itaru Takahashi, Yumiko Kawasaki</i>	524
Communicating Radiological Concepts in Plain Language: The Value of International Consistency <i>Authors: Ted Lazo, Maria Perez, Shengli Niu, Miroslav Pinak, Carl Blackburn, Pablo Jimenez, Stephan Mundigl, Malcolm Crick, Chris Clement, Renate Czarwinski</i>	525
ICRP Stakeholder Dialogues: Lessons for the International Community <i>Author: Ted Lazo</i>	526
Management of Protection through Prevailing Circumstances: Interpretation of the ICRP System of Radiological Protection <i>Author: Ted Lazo</i>	527
Plain Language We Can All Understand <i>Author: Ted Lazo</i>	528
Developing Radiation Protection Culture at School: The Experience of the 2015 France-Japan High School Students Radiation Protection Workshop in Fukushima <i>Authors: Thierry Schneider, Daniel Ayrault, Sylvie Charron, Takashi Hara, Ryugo Hayano, Claire Schneider, Hiroyuki Takano</i>	529
Measurement and Data Analysis Concepts Combined with Data Assimilation Techniques for Source Term Reconstruction and Dose Assessment <i>Authors: Ulrich Stoehlker, Martin Bleher, Florian Gering</i>	530
Optimizing a Commercial Radiation Portal Monitor for Spot Traffic Controls <i>Authors: Udo Strauch, Reto Linder, Eike Hohmann, Rouven Philipp, Sabine Mayer</i>	531
Training as Awareness Factor and Dissemination of the Brazilian Nuclear Area <i>Authors: Valéria Pastura, Antonio Carlos Mol, Ana Paula Legey, Eugenio Marins</i>	532
INSTN: The Most Complete Training Centre for First Time Nuclear Plant Workers <i>Author: Vial Thierry</i>	533
Comparison between Brazilian Radiation Protection Norm and the Basic Safety Standards Published in 2014 <i>Authors: Wagner De Souza Pereira, Alphonse Kelecom, Ademir Xavier Da Silva</i>	534

Licensing of Nuclear Facilities in Brazil: Radiological Aspects <i>Authors: Wagner de Souza Pereira^{a,b}, Ana Cristina Lorençob, Alphonse Kelecomc, Ademir Xavier da Silva</i>	535
The Principle of Low Risk and Optimization and the Connection with the ALARA concept. Exemption, Exclusion and Clearance <i>Authors: Wagner De Souza Pereira, Alphonse Kelecom, Ademir Xavier Da Silva</i>	536
The State of the Art about the Radiation Protection System in the World <i>Authors: Wagner de Souza Pereira, Alphonse Kelecom, Ademir Xavier da Silva</i>	537
The Importance of Including the Human Error Factor and Decision Making in Training and Education Programs to Avoid Radiological Incidents of Accidents <i>Author: Walter Truppa</i>	538
Individual Monitoring for External Exposure of Users at Synchrotron Radiation Facilities and New Solutions <i>Authors: Xiaobin Xia, Guanghong Wang, Jianzhong Zhou, Pingan Fei, Sixin Liu</i>	539
VOLUME 2	
Area 3: Medical	540
Pediatric Head CT examination doses in two university teaching Hospitals in Tunisia <i>Authors: Bouaoun Abir, Latifa Ben Omrane, Azza Hammou</i>	541
Spanish Radiation Protection Association (SEPR) Working Groups in Radiation Protection in Medicine <i>Authors: Gil-Agudo, Antonio; Ruiz-Cruces, Rafael; Almansa-López, Julio; Torres-Cabrera, Ricardo; Martí-Climent, Josep Maria; Sanjuanbenito-Ruiz de Alda, Waldo; Prieto-Martín, Carlos; Macías-Dominguez, Maria Teresa</i>	545
Regulatory T cells (Tregs) as a possible prognostic marker in radiation skin injury <i>Authors: Ana Julia Molinari, Mercedes Portas, Andrés Rossini, Severino Michelin, Diana Dubnera</i>	549
Head and Neck Immobilization Masks: Increase in Dose Surface evaluated by EBT3, TLD-100 and PBC Method <i>Authors: Arnie Verde Nolasco, Luiz Oliveira Faria</i>	555
MCNPX versus DOSXYZnrc in patient specific voxel-based phantom calculations <i>Authors: Banafsheh Zeinali-Rafsanjani, Kamal Hadad, Mahdi Saeedi-Moghadam, Reza Jalli</i>	563
Justification of CT examinations <i>National surveys in Sweden</i> <i>Authors: Carl Bladh, Torsten Cederlund, Sven Richter</i>	566
The transposition and the practical implementation of the Council Directive 2013/59/Euratom in the medical field in Romania <i>Author: Constantin Milu</i>	569
Level 2 justification is now part of the national system for introduction of new health technologies within the specialist health service in Norway <i>Authors: Eva G. Friberg, Reidun Silkosef, Ingrid E. Heikkilä, Jan F. Unhjem</i>	576
Proposed diagnostic reference levels for coronary angiography, left ventriculography and pacemaker placement in South Africa: 3-year improvement from 2012-2015 <i>Authors: Hendrik Johannes de Vos, Christoph Jan Trauernicht</i>	583
Procedure for measurement of Intrinsic Efficiency of a High Energy Collimator Gamma camera <i>Authors: Hugo Pérez-García, Raquel Barquero, Monica Gómez-Incio</i>	592
Simulation of a High Energy Collimator Gamma camera with MCNPX <i>Authors: Hugo Pérez-García, Raquel Barquero, Monica Gómez-Incio</i>	597
Local Computed Tomography Dose Index and Dose Length Product Values Agree with Published European DRLs <i>Authors: I. Garba, A. M. Tabari, A. Dare, M. Yahuza, M. Barde, M. Abba</i>	602
A Review of Occupational Radiation Exposure among Medical Professionals in Canada (1985-2006) <i>Author: Jing Chen</i>	607

The use of the Monte Carlo simulation method for assessing the radiation burden of the hands of workers during some risky manipulations with radiopharmaceuticals <i>Authors: Jana Hudzietzová, Marko Fülöp, Pavol Ragan, Jozef Sabol, P. Povinec,</i>	613
Y Radiation dose optimization in paediatric conventional imaging using automatic dose data management software <i>Authors: Luis Alejo, Eva Corredoira, Zulima Aza, Rodrigo Plaza-Núñez, Antonio Serrada</i>	618
Practical Lessons for a Dosimetry Program <i>Authors: Michelle Baca, Chad Hopponen</i>	627
Large scale multi-national studies on radiation protection of children in CT <i>Author: Madan M. Rehani</i>	635
Extension of the IAEA-International Nuclear and Radiological Event Scale (INES) for Medical Events <i>Authors: Marc Valero, Maria Luisa Ramirez Vera, Nera Belamaric</i>	640
Control of Radiation Exposure to Pediatric Patients at Conventional Radiology and Cardiac Centers at Dubai Hospital <i>Authors: Najlaa K. Almazrouei, Jamila S. Alsuwaidi, Adel H. Hashish</i>	649
Radioprotection in Radiosynovectomy Concerning Accompanying Persons and the Public <i>Authors: Susie Medeiros Oliveira Ramos, Sylvia Thomas, Mônica Araújo Pinheiro, Mirta Bárbara Torres Berdeguez, Lidia Vasconcellos de Sá, Sergio Augusto Lopes de Souza</i>	657
Physicians' Knowledge about patient Radiation Exposure from CT Examinations: Case of Hassan II Hospital Agadir-Morocco <i>Authors: Slimane Semghouli, Bouchra Amaoui, Abdelmajid Choukri, Oum Keltoum Hakam</i>	663
Changes in patients' radiation doses during CT exams in Japan (1997-2014) <i>Authors: Shoichi Suzuki, Yuuta Matsunaga, Ai Kawaguchi, Kazuyuki Minami, Masanao Kobayashi, Yasutaka Takei, Yasuki Asada</i>	669
Estimation of response characteristics for radiophotoluminescent glass dosimeters in X-ray diagnosis by using Monte Carlo simulation method <i>Authors: Toshioh Fujibuchi, Emi Ishibashi</i>	674
Small size OSL dosimeter to measure patient exposure dose in X-ray diagnosis - Evaluation of invisibility <i>Authors: Tohru Okazaki, Hiroaki Hayashi, Kazuki Takegami, Yoshiki Mihara, Natsumi Kimoto, Yuki Kanazawa, Takuya Hashizume, Ikuo Kobayashi</i>	678
Analysis of reasons for the multiple scans of paediatric CT examinations: Finding whether there is possible confounding by indication. <i>Authors: Takayasu Yoshitake, Koji Ono, Tsuneo Ishiguchi, Michiaki Kai</i>	684
A Multi-Center Study on Eye Lens Radiation Doses for Medical Staff Performing Non-Vascular Interventional Procedures in Japan <i>Authors: Kosuke Matsubara, Yasutaka Takei, Ikuo Kobayashi, Hiroshige Mori, Kimiya Noto, Shoichi Suzuki, Takayuki Igarashi, Keiichi Akahane</i>	686
FTS (Fused Toes Homolog) can be a Target to Modulate Radiosensitivity in Uterine Cervix Cancer Cells and Normal Cells <i>Authors: Arunkumar Anandharaj, Senthilkumar Cinghu, Won-Dong Kim, Jae-Ran Yu, Woo-Yoon Park</i>	687
Standardized and Automated Risk Assessment Forms for a Dutch Radiation Organization <i>Authors: Arjanka Bandstra, Marcel Wiegman</i>	688
Bonn Conference 2012 - Implementation of Results <i>Author: Axel Böttger</i>	689
Radiological Zoning and Radiation Exposure Assessment of External Staff in the CHU-Ibn Rochd-Casablanca Nuclear Medicine Service <i>Authors: Abdelmajid Choukri, Said Ouzouh, Oum Keltoum Hakam, Rachida El Gamoussi, Amal Guensi</i>	690
Multistep Optimization Approach in Medical Radiology - The Patient Imperative <i>Author: Andrejs Dreimanis</i>	691

R Y Advanced aspects of radiation protection in the use of particle accelerators in the medical field <i>Authors: Angelo Infantino, Gianfranco Cicoria, Giulia Lucconi, Davide Pancaldi, Sara Vichi, Federico Zagni, Domiziano Mostacci, Mario Marengo</i>	692
French Recommendations on the Conditions of Implementation of “New Techniques and Practices” in Radiotherapy <i>Authors: Aurelie Isambert, Eric Lartigau, Albert Lisbona, Philippe Cadot, Sylvie Derreumaux, Olivier Dupuis, Jean-Pierre Gérard, Dominique Ledu, Marc-André Mahé, Vincent Marchesi, Jocelyne Mazurier, Aurelien De Oliveira, Olivier Pharé, Marc Valero, Bernard Aubert</i>	693
A Cross-sectional Study of Nuclear Cardiology Practices and Radiation Exposure in Africa: Results from the IAEA Nuclear Cardiology Protocols study (INCAPS) <i>Authors: Andrew J. Einstein, Salah Bouyoucef, Thomas Pascual, Mathew Mercuri, Mboyo D.T.W. Vangu, Adel Allam, Madan Rehani, Ravi Kashyap, Maurizio Dondi, Diana Paez</i>	694
Quality Control of Radiography X-ray Generators in Kerman Province, South-Eastern Iran <i>Authors: Ali Jomehzadeh, Zahra Jomehzadeh, Mohammadbagher Tavakoli</i>	695
Occupational Dose Profiles of Radiation Workers in Oman Hospitals: A 5-year Dose Analysis <i>Authors: Arun Kumar L. S., Jamal Al-Shanfari, Saeed Al-Kalbani</i>	696
Investigation of Potential Use of ¹²⁴Xe-incorporated Amorphous Si Films in Brachytherapy <i>Authors: Alexandre Leal, Telma Fonseca, Lucas Reis</i>	697
Evaluation of Patient Dose in Interventional Cardiology <i>Authors: Ayoub Momivand, Reza Zohdiaghdam, Zhaleh Behrouzkiya, Ebrahim Khayati Shal</i>	698
Review of Radiation Safety in Medical Diagnosis in Kenya <i>Author: Arthur Omondi Koteng</i>	699
Study on Incidence of Radiation Induced Cataract among Radiographers in Interventional Fluoroscopy <i>Authors: Aruna Pallewatte, Suvini Karunaratne, MPN Piyasena</i>	700
The Impact of Fluoroscopic Technique on Incidence of Radiation Injuries in Neurointervention <i>Author: Aruna Pallewatte</i>	701
Tandem KAP Meters Calibration Parameters by Monte Carlo Simulation using Reference RQR Radiation Qualities <i>Authors: Ademar Potiens Jr., Nathalia Costa, Eduardo Correa, Lucas Santos, Vitor Vivolo, Marie Da Penha Potiens</i>	702
The IAEA Latin American Working Group on Internal Dosimetry of Radionuclides in Human Body <i>Authors: Ana Rojo, Nancy Puerta, Bernardo Dantas, Arlene Reis, Mariella Teran, Rodolfo Cruz Suarez</i>	703
The Effect of Single Catheter on Patient and Operator Radiation Dose during Trans-radial Coronary Angiography <i>Authors: Ali Tarighatnia, Amirhossein Mohammadalian, Alireza Farajollahi, Morteza Ghojzade</i>	704
The Impact of Both Radial & Pelvic Lead Shields on Operator Radiation Exposure during Trans-radial Coronary Procedures <i>Authors: Ali Tarighatnia, Aida Khaleghifard, Amirhossein Mohammadalian, Alireza Farajollahi, Morteza Ghojzade</i>	705
R Establishing Diagnostic Reference Levels for Conventional X-ray Procedures in the Russian Federation <i>Author: Aleksandr Vodovatov</i>	706
Computing Calibration Factor with Visual Monte Carlo – VMC simulations of an Accident Contamination with ^{99m}Tc <i>Authors: Bruno Mendes, Fernanda Paiva, Marco Aurelio Lacerda, John Hunt, Telma Fonseca</i>	707
Establishing the Quality Management Baseline in the use of Computed Tomography Machines in Kenya <i>Authors: Bernard Ochieng, Geoffrey Korir, Jeska Wambani</i>	708
Radiation Exposure in Interventional Procedures <i>Authors: Bernard Ochieng, Geoffrey Korir, Jeska Wambani</i>	709

Study on the Effects of Gorkha Earthquake in Radiological Facilities (Nepal) <i>Authors: Buddha Ram Shah, Shanta Lal Shrestha, Kanchan Prasad Adhikary</i>	710
Evaluation of Important Physical Parameters in Micro Beam Radiotherapy of Lung Tumors <i>Authors: Banafsheh Zeinali-Rafsanjani, Mohammad-Amin Mosleh-Shirazi, Mahdi Haghatafshar, Mahdi Saeedi-Moghadam</i>	711
Dicentric Assay in DTC Patients with High Dose Radioiodine Therapy <i>Authors: Chung Mei-Ling, Huang Ying-Fong, Chen Yu-Wen, Jong Shiang-Bin, Lai Yung-Chang</i>	712
Animal Sporting Events and Radioprotection Management <i>Authors: Roy Catherine, Audigie Fabrice, Coudry Virginie, Malet Christophe, Sgro Geraldine</i>	713
Occupational Exposure Observations at Groote Schuur Hospital <i>Authors: Christoph Trauernicht, Tobie Kotzé</i>	714
R Comparison of Primary Doses Obtained in Three 6 MV Photon Beams Using a Small Attenuator <i>Author: C Trauernicht</i>	715
Detector Dependence of the Measured Spectra of the OncoSeed IMC6711 Iodine-125 Seed <i>Authors: Christoph Trauernicht, Paul Papka, Peane Maleka, Egbert Hering, Freek Du Plessis</i>	716
Measured Anisotropy of the OncoSeed IMC 6711 Iodine-125 Seed <i>Authors: Christoph Trauernicht, Paul Papka, Egbert Hering, Freek Du Plessis</i>	717
The Monte Carlo Simulation Study of Secondary Neutron Dose for Proton Therapy at Samsung Medical Center using FLUKA <i>Authors: Chae Young Lee, Jin Sung Kim, Yong Hyun Chung, Sungkoo Cho, Dae-Hyun Kim, Youngyih Han, Jongho Kim, Yunho Kim, Sangmin Lee, Chan Woo Park</i>	718
Biological Effects of Radioactive Hot Particles on the Human Lung. Assessment of the Cancer Risk <i>Authors: Diana Apostolova, Zdravko Paskalev</i>	719
Mathematical Modeling of Dose Profile of a Dental Facilities <i>Authors: Deise Diana Lava, Diogo da Silva Borges, Maria de Lourdes Moreira, Antonio Cesar Ferreira Guimaraes</i>	720
In Young Women: Justification of Breast Ultrasound Rather than Combined Breast Ultrasound and Mammography. Radiation Protection Perspective <i>Authors: Dina Salama, Hanan Gewfel</i>	721
Cone Beam CT Patient Dose in Paediatric Cardiac Catheterization Procedures <i>Authors: Eva Corredoira Silva, Luis Alejo Luque, Eliseo Vañó Carruana, Cristina Koren, Rodrigo Plaza, Antonio Serrada, Carlos Huerga Cabrerizo</i>	722
Proposal of a spreadsheet to monitor units verification for intracranial radiosurgery treatments <i>Authors: Erick Hernandez, Ricardo Contreras, Miguel Ortega</i>	723
Establishment of National Dose Reference Levels (DRLs) for Digital Mammography Practices at the UAE <i>Authors: Fatima Al Kaabi, Najla Al Mazrouei, Jamila AlSuwaidi, Jacek Janaczek, Alfani Al Ameri, Sara Booz, Wadha AlShamsi</i>	724
Risk of a Second Kidney Carcinoma Following Childhood Cancer: Role of Chemotherapy and Radiation Dose to Kidneys <i>Authors: Florent de Vathaire, Boris Schwartz, Chiraz El-Fayech, Rodrigue Allodji, Bernard Escudier, Mike Hawkins, Ibrahima Diallo, Nadia Haddy</i>	725
Developing Light Nano-Composites with Improved Mechanical Properties for Neutron Shielding <i>Authors: Fatemeh Jamali, SMJ Mortazavi, MR Kardan, Sedigheh Sina, MA Mosleh-Shirazi, Jila Rahpeyma</i>	726
Evaluation of the Scattered Radiation Field in an Interventional Radiology Room <i>Authors: Francesca Mariotti, Paolo Ferrari, Lorenzo Campani, Elena Fantuzzi, Luisa Pierotti, Pier Luca Rossi</i> ..	727
In Vivo Dosimetry for the Measurement of Doses to Breast Cancer Patients During External Beam Radiotherapy Treatment, using the Optically Stimulated Luminescence (OSL) Dosimeters at the Douala General Hospital, Cameroon <i>Authors: Fokou Mvoufo, Samba Richard</i>	728

UNSCEAR's Assessment of Medical Exposure <i>Author: Ferid Shannoun</i>	729
Radiation Dose in Childhood Cancer Management: Challenges and Recommendations for Dose Reduction <i>Author: Hamid Abdollahi</i>	730
Review and Evaluation of Imaging Methods and Analysis of Images Obtained by Magnetic Resonance Imaging to Determine the Absorbed Dose in the Phantom by Polymer Gel Dosimetry <i>Authors: Hamed Dehghani, Amin Farzadnia, Saeed Shanehsazzadeh, Yazdan Salimi, Jalal Ordoni, Dariush Askari, Mohammad Hossein Jamshidi</i>	731
Standard Calibration of Ionization Chambers Used in Radiation Therapy Dosimetry and Evaluation of Uncertainties <i>Authors: HyoJin Kim, Sung Jin Noh, Hyun Kim, Sang koo Kang, Manwoo Lee, Dong Hyeok Jeong, Kwangmo Yang, Yeong-Rok Kang</i>	732
Radiological Risk Assessment in Tunisian University Hospital <i>Authors: Hager Kamoun, Samar Kallela, Mohamed Faouzi Ben Slimane</i>	733
An Automated Mechanical Quality Assurance System for Medical Accelerators using a Smartphone <i>Authors: Hwiyoung Kim, Il Han Kim, Hyunseok Lee, Sangmin Lee, Sung-Joon Ye</i>	734
Patient Doses in a Hybrid Operating Room <i>Authors: Hugo Perez-Garcia, Carlos Andrés Rodríguez, Manuel Agulla Otero, Ricardo Torres Cabrera, Raquel Barquero Sanz</i>	735
Comparison of Patients CTDI from Two Different "Make" 16-SLICE CT Scanners in Maiduguri North Eastern Nigeria <i>Authors: Idris Garba, Aisha Abba Kato, Auwal Abubakar, Chogozie Nwobi, Mansur Yahuza, Nasiru Isha Fagge</i>	736
Hearing Radiation and its Application to in Vivo Radiation Dosimetry during Radiation Treatment <i>Authors: I.J. Kima, J.H. Kim, C.Y. Yi, C.H. Kim, J.S. Kim, E.Y. Park, Y.H. Jung</i>	737
Effectiveness of Dose Modulation Technique of CT scan on Organ Dose <i>Authors: Il Park, Seung Cheol Oh, Kwang Pyo Kim</i>	738
Application of Prospective Approaches in Preventing Accidental Exposure in Radiotherapy: A Review of Italian Experiences <i>Authors: Ivan Veronese, Marie Claire Cantone, Luisa Begnozzi</i>	739
Survey of Radiation Protection in Patients Undergoing X-ray Medical Examination <i>Authors: Justina Achuka, Mojisola Usikalu</i>	740
Long Half-Life Isotopes Europium-152 and Europium-154 Found in Hospital Waste <i>Authors: Janneke Ansems, Bunna Damink, Jelle van Riet, Corinne Valk, Ruud Hack</i>	741
Prospective Risk Assessment of the Use of Radioactive Iodine-125 Seeds for the Localisation of Impalpable Breast Lesions <i>Authors: Janneke Ansems, Bunna Damink, Jelle van Riet, Pieter Buijs, Els Vanaert</i>	742
Global Developments in DRLs and Assessment of Medical Exposures <i>Author: John Damilakis</i>	743
Persistence of Dicentric Chromosomes associated with Telomere Dysfunction: A Biomarker of Prognosis in Patients Undergoing Total Body Irradiation <i>Authors: Julien Dossou, Theodore Girinsky, Dominique Violot, Jean-Henri Bourhis, Eric Lartigaux, Luc Morat, Claude Parmentier, Radhia M'kacher</i>	744
Dosimetric Analysis with the Specifically Selected Low-Dose Threshold on Gamma Evaluation for VMAT QA <i>Authors: Ji-Hye Song, Min-Joo Kim, So-Hyun Park, Seu-Ran Lee, Min-Young Lee, Dong Soo Lee, Tae Suk Suh</i>	745

Y	The Influence of the Dose Calculation Resolution of VMAT Plans on the Calculated Dose for Eye Lens and Optic Apparatus	
	<i>Authors: Jong Min Park, So-Yeon Park, Jung-in Kim, Hong-Gyun Wu, Jin Ho Kim</i>	746
R	Monte Carlo Estimation of Effective Dose to Patients Undergoing Contrast Based X-Ray Fluoroscopy Procedures	
	<i>Authors: J. E Ngaile, P. Msaki, R. Kazema</i>	747
	An Assessment of Radiographers' Technical and Protective Performance in Hospitals Affiliated to Birjand University of Medical Sciences in 2012	
	<i>Authors: Jalal Ordoni, Saeid Ghasemi, Dariush Askari, Yazdan Salimi, Fatemeh Ramrodi, Mohammad Hossein Jamshidi, Hamed Dehghani</i>	748
	Patient Radiation Safety Control in Nuclear Medicine Practices in View of the New Basic Safety Standards (BSS)	
	<i>Authors: Jamila S AlSuwaidi, Priyank Gupta, Shabna Miyath</i>	749
	New X-ray Technology Results in 70% Dose Reduction in Pacemaker and Implantable Cardioverter Defibrillator (ICD) Implantations	
	<i>Authors: Joris van Dijk, Jan Paul Ottervanger, Peter Paul Delnoy, Martine Lagerweij, Siert Knollema, Cornelis Slump, Piet Jager</i>	750
	The Study on the Interspace Materials of Radiographic Anti-Scattering Grid with Monte Carlo Calculation	
	<i>Authors: Jun Woo Bae, Hee Reyoung Kim</i>	751
	¹³¹I Activity in the Thyroid in Members of the Nuclear Medicine Medical Personnel	
	<i>Authors: Kamil Brudecki, Aldona Kowalska, Pawel Zagrodzki, Artur Szczodry, Tomasz Mroz, Pawel Janowski, Jerzy Wojciech Mietelski</i>	752
	Impact of Earthquake on Radiological Facilities in Kathmandu Valley	
	<i>Authors: Kanchan P. Adhikari, Yaduram Panthi, Deepak Subedi</i>	753
	Radiation Dose from Whole Body F-18 FDG PET/CT: Nationwide Survey in Korea	
	<i>Authors: Keon Wook Kang, Hyun Woo Kwon, Jong Phil Kim, Jin Chul Paeng, Hong Jae Lee, Jae Sung Lee, Gi Jeong Cheon, Dong Soo Lee, June-Key Chung</i>	754
	Using I-125 Seeds for Localisation; a Retrospective Overview of Radiation Safety Issues	
	<i>Author: Linda Janssen-Pinkse</i>	755
	Activimeter Response Behaviour Analysis Related to Well Depth	
	<i>Authors: Lilian Kuahara, Eduardo Corrêa, Maria da Penha Potiens</i>	756
	Digital Breast Tomosynthesis: Preliminary Results of Patient Radiation Dose Survey in a Brazilian Facility	
	<i>Authors: Larissa Oliveira, Fernando Mecca, Simone Renha</i>	757
	Measurement of Entrance Skin Dose for Pediatric Patients during Cardiac IVR	
	<i>Authors: Lue Sun, Yusuke Mizuno, Takashi Moritake</i>	758
	New Concept: Reduction of Dose of the Lens	
	<i>Authors: Lue Sun, Yuji Matsumaru, Takashi Moritake</i>	759
	Development of a Specialization Program in Radiation Protection: Proposal to CPLP	
	<i>Authors: Lidia V. Sá, Simone K. Renha</i>	760
	Diagnostic Reference Levels in CT: First Experience in one Major Hospital in Algeria	
	<i>Authors: Merad Ahmed, Khelassi-Toutaoui Nadia, Mansouri Boudjema</i>	761
	Occupational Radiation Exposure in Nuclear Medicine	
	<i>Authors: Mashari Alnaaimi, Mohammed Alkhoryaf, Fareda Alkandri, Mousa Aldouij, Mohamed Omer, Nawaf Abughath, Talal Salhudeen</i>	762
	High Voltage Consideration to Determine the Dose Received by Patient in Conventional Radiology	
	<i>Authors: Mbolatiana Anjarasoa Luc Ralaivelo, Andriambololona Raelina, Edmond Randrianarivony, Solofonirina Ravelomanantsoa, Hery Fanja Randriantseheno, Ralainirina Dina Randriantsizafy, Tiana Harimalala Randriamora, Veroniaina Raharimboangy, Tahiry Razakarimanana, Hary Andrianarimanana Razafindramiandra</i>	763

Diagnostic Reference Levels for Fluoroscopically Guided Interventions at a Major Australian Hospital <i>Authors: Mohamed Badawy, Tegan Clark</i>	764
Image Quality and Patient Dose Assessment in Simple Radiographic Examinations in Ghana <i>Authors: Mary Boadu, Stephen Inkoom, Cyril Schandorf, Geoffrey Emi-Reynold, Emmanuel Akrobortu</i>	765
Determination of attenuation properties of lead glasses used in the catheterization laboratory <i>Authors: Marcin Brodecki, Marek Zmyslony</i>	766
Dose Reassessment Applied in Routine TL Dosimetry by using the PTTL method in LADIS Laboratory <i>Authors: Maciej Budzanowski, Renata Kopec, Anna Bieniarz-Sas</i>	767
Occupational Doses of Medical Staff in Interventional Cardiology Procedures and Correlations with Patient Dose Levels <i>Authors: Maciej Budzanowski, Agnieszka Szumska, Renata Kopec</i>	768
Out-of-field Dose and Risk of Radiogenic Second Cancer for children Treated with Craniospinal 3D-Conformal Radiotherapy or TomoTherapy <i>Authors: Marijke De Saint-Hubert, Željka Knežević, Natalia Adamek, Marija Majer, Liliana Stolarczyk, Remy Savelli, Vedran Rajevac, Saveta Miljanić, Pawel Olko, Roger M. Harrison, Filip Vanhavere, Dirk Verellen, Lara Struelens</i>	769
Evaluation of Thyroid Function after Radiotherapy for Patients with Breast Cancer <i>Authors: Masomeh Dorri Gav, Seyed Mahmood Reza Aghamiri, Mohammd Hossien Bahreini Toosi</i>	770
Preliminary Diagnostic References Levels of Audit CT at Aristide LeDantec National Hospital <i>Authors: Magatte Diagne, Fama Gning, Mamadou Moustapha Dieng, Latifatou Gueye</i>	771
Frequency of Overscan in Standard CT Protocols <i>Authors: Michael Galea, Mohamed Badawy</i>	772
Overview of the Activities on Eye Lens Dosimetry within EURADOS WG 12 (Dosimetry in medical imaging) <i>Authors: Merce Ginjaume, Isabelle Clairand, Eleftheria Carinou, Olivera Ciraj Bjelac, Paolo Ferrari, Marta Sans-Merce, Jad Farah, Frank Becker, Vadim Chumak, Josiane Daures, Joanna Domienik, Zoran Jovanovic, Renata Kopec, Dragana Krstic, Agnieszka Szumska, Denisa Nikodemova, Pedro Teles, Sara Principi, Filip Vanhavere, Željka Knežević</i>	773
Imaging for Saving Kids - Improving Radiation Safety in Paediatric Radiology <i>Authors: Donald Frush, Lawrence Lau, Maria del Rosario Perez, Michael G Kawooya</i>	774
Evaluation of Survived Neuronal Tissue Area around Brain Tumor Lesions Post Radiation Therapy by Diffusion-weighted Imaging (DWI) <i>Authors: Mohammad Hossein Jamshidi, Alireza Eftekhari Moqadam, Jafar Fatahi, Hamid Behrozi, Yavar Shahvali, Jalal Ordoni, Yazdan Salimi, Dariush Askari, Hamed Dehghani</i>	775
Surveying the Relationship between Brain CT Scan Findings in Children with a Clinical Signs and Determining the Appropriate Indications for Requesting CT Scan <i>Authors: Mohammad Hossein Jamshidi, Hamid Behrozi, Dariush Askari, Jalal Ordoni, Yazdan Salimi, Hamed Dehghani</i>	776
Radiation Emergency Medicine Preparedness: Web-Based Reporting of News and Events from SREMC to Target Expert Groups <i>Authors: Marita Lagergren Lindberg, Karin Lindberg, Rolf Lewensohn, Giuseppe V., Masucci, Jack Valentin, Leif Stenke</i>	777
Evaluation of Organ Doses and Cancer Risk from Paediatric Head CT Examination – Phantom Study <i>Authors: Marija Majer, Željka Knezevic, Saveta Miljanic, Liu Haikuan, Weihai Zhuo</i>	778
Radiation Protection Optimization in I-131 Therapy of Thyroid Cancer to Ablate Postthyroidectomy Remnants or Destroy Residual or Recurrent Tumour <i>Author: Mario Medvedec</i>	779
Operational Radiation Safety with Y-90 Microspheres <i>Authors: Mark Miller, Charles Martin III</i>	780

In-Vivo Tooth Dosimetry Using L Band EPR. The Research Involving Human Subjects Related to Fukushima Nuclear Power Plant Accident <i>Authors: Minoru Miyake, Ichiro Yamaguchi, Yasuhiro Nakai, Hiroshi Hirata, Naoki Kunugita, Harold Swartz</i>	781
Establishment of Local DRLs on Standard Radiographic Examinations and Estimation of Cancer Risk for Paediatric and Adult Patients at Two Tunisian Hospitals <i>Authors: Mohamed Mogaadi, Latifa Ben Omrane, Azza Hammou</i>	782
Audit of Clinical Image Quality in Chest Radiography using Visual Grading Analysis <i>Authors: Michael Sandborg, Jonas Nilsson Althen, Erik Tesselaar</i>	783
Radiation Protection in Medical Imaging and Radiation Oncology: A Cooperative Effort between IOMP and IRPA <i>Authors: Magdalena Stoeva, Richard Vetter, K.Y. Cheung, Renate Czarwinski, Francesca McGowan</i>	784
Monte Carlo Calculation of Neutron Doses to Organs of a Female Undergoing A Pelvic 18 MV Irradiation <i>Authors: Mansour Zabihzadeh, Seyyed Rabi Mahdavi, Mohammad Reza Ay, Zahra Shakarami</i>	785
Study of the Radiation Effect on the Biological Cellule DNA by Determination Bragg Peak Position of the Proton Beams <i>Authors: Noura Harakat, Jamal Inchaouh, Abdenbi Khouaja, Mohammed Benjelloun, Hamid Chakir, Said Boudhaim, Zouhair Housni, Mohamed Lhadi Bouhssa, Abdellatif Kartouni, Mohamed Reda Mesradi, Sara Stimade, Meriem Fiak, Mustapha Krim</i>	786
 Internal dose assessment of new ¹⁷⁷Lu-radiopharmaceuticals and its role in radiation protection of patients <i>Authors: Nancy Puerta Yepes, Ana Rojo, Sebastián Gossio, José Luis Crudo</i>	787
Design Shielding Assessment for a Nuclear Medicine Service <i>Authors: Osvaldo Brígido-Flores, José Hernández-García, Orlando Fabelo-Bonet, Adelmo Montalván-Estrada</i> 788	
Performance Study of Hybride Imaging SPECT/CT: Case of Nuclear Medicine Service - Ibn Sina Hospital in Rabat-Morocco <i>Authors: Oum Keltoum Hakam, Abdelmajid Choukri, Rajaa Sebihi, Youness Esserhir El Fassi</i>	789
Comprehensive quality audits in radiation oncology, diagnostic and interventional radiology <i>Authors: Ahmed Meghzifene, Ola Holmberg</i>	790
International Response to the Bonn Call for Action – from the Viewpoint of the Organizers of the Bonn Conference: the IAEA <i>Author: Ola Holmberg</i>	791
Assessment of the Practice of Optimizing Paediatric Doses in Conventional Radiography in Cameroon <i>Authors: Odette Ngano Samba, Jean Bernard Kamgang, Ariane Lynda Kengne Fonkam, Emmanuel Chi, Lukong Cornelius Fai, Jean Yomi</i>	792
Can Standard CT be replaced by Contrast Enhanced Ultra-low-dose CT with Iterative Reconstruction for the Screening of Patients Admitted with Acute Abdominal Pain? A Comparative Study <i>Authors: Pierre-Alexandre Poletti, Minerva Becker, Thomas Perneger, Christoph D Becker, Alexandra Platon</i>	793
Radiological and Dosimetrical Aspects of CO₂ Peripheral DSA: Optimization of X-ray Spectrum <i>Authors: Pier Luca Rossi, David Bianchini, Alessandro Lombi, Giacomo Feliciani, Manami Zanzi, Romano Zannoli, Ivan Corazza</i>	794
Establishment of National Diagnostic Reference Levels for Nuclear Medicine in Australia <i>Authors: Paul Marks, Toby Beveridge, Peter Thomas, Anna Hayton, Anthony Wallace</i>	795
Survey of Knowledge about Radiation Dose in Radiological Investigation in Kermanshah Hospitals, Iran <i>Authors: Rasool Azmoonfar, Hosein Faghirnavaz, Edalat Morovati, Hosein Younesi</i>	796
Measurement of ¹³¹I activity with a High Energy Gamma Camera <i>Authors: Raquel Barquero, Hugo Perez-Garcia, Monica Gomez-Incio</i>	797
Situation of Radiation Therapy, Cancer Diagnosis and Radiation Protection of Patients in Cameroon <i>Authors: Richard Ndi Samba, Augustin Simo, Ernest C. Nwabueze Okonkwo</i>	798

R Promoting Fluoroscopic Personal Radiation Protection Equipment: Unfamiliarity, Facts, and Fears Author: Stephen Balter	799
Traceability of the KAP-Meters Used for Patient Dosimetry in Radiodiagnostic Authors: Sorin Bercea, Constantin Cenusă, Ioan Cenusă, Aurelia Celarel, Elena Iliescu	800
Radiation Dose Assessment for Abdominal Computed Tomography Authors: Seung Cheol Oh, Il Park, Kwang Pyo Kim	801
Implementation on Methodology for the Calibration of well type chambers used in ¹⁹²Ir-Brachytherapy Sources Authors: Stefan Gutierrez Lores, Gonzalo Walwyn Salas, Jorge Luis Morales	802
Study of the ¹³¹I Thyroid Monitoring Measurements Using MCNP Simulations Authors: Sebastián Gossio, Nancy Puerta, Ana Rojo	803
Dosimetric Studies of Radionuclide Therapy of Neuroendocrine Tumors with ¹⁷⁷Lu-Dotatate Authors: Santosh Kumar Gupta, Suhas Singla, Chandrasekhar Bal	804
Managing the Gaseous Waste in Nuclear Medicine: A Novel Approach Authors: Shahed Khan, Eleonora Santos	805
Monitoring and Evaluating the Air Concentration of Radionuclides in the Vicinity of a Nuclear Medicine Facility Authors: Shahed Khan, Eleanora Santos	806
Neutron Measurement for Proton Therapy Facility at Samsung Medical Center with Wobbling and Line Scanning Mode using WENDI-2 Authors: Sangmin Lee, Jin Sung Kim, Sungkoo Cho, Dae-Hyun Kim, Jungho Kim, Yunho Kim, Youngyih Han, Sung-Joon Ye, Chae Young Lee, Yong Hyun Chang	807
Utilizing 3D Scanner/Printer for a Dummy Shield: Monte Carlo Dose Calculations on Artefact-free CT Images of a Metallic Shield for Electron Radiation Therapy Authors: Jong In Park, Il Han Kim, Jaegi Lee, Hyeonseok Lee, Sung-Joon Ye, Sangmin Lee	808
Comparison of Cadmium Zinc Telluride (CZT) with Photomultiplier Tube (PMT) Detectors in SPECT and Bismuth Germanate (BGO) in PET Authors: Seyed Mohsen Zahraei-Moghadam, Mehdi Saeedi –Moghadam, Banafsheh Zenali –Rafsenjani, Masoumeh Dorri-Gev, Fatemeh Shekoochi –Shooli	809
Nurses Knowledge of Ionizing Radiation and Radiation Protection during Mobile Radiodiagnostic Examinations Author: Samuel Opoku	810
Personal Radiation Monitoring of Occupationally Exposed Radiographers in the Biggest Tertiary Referral Hospital in Ghana Author: Samuel Opoku	811
Health Physicist Monitors Own Medical Dose from Radioiodine Thyroid Ablation Procedure Authors: Sander Perle, Kip Bennett, Chad Hopponen, Michael Lantz	812
R Evaluation of Eye Lens Doses of Interventional Cardiologists Authors: Sumi Yokoyama, Shoichi Suzuki, Hiroshi Toyama, Shinji Arakawa, Satoshi Inoue, Yutaka Kinomura, Ikuo Kobayashi	813
Development of Thermoplastic Mask set up Monitoring System using Force Sensing Resistor (FSR) Sensor Authors: Tae Ho Kim, Siyong Kim, Min-Seok Cho, Seong-Hee Kang, Dong-Su Kim, Kyeong-Hyun Kim, Dong-Seok Shin, Tae-Suk Suh	814
Measurements of Photon Spectra around IVR for the Evaluation of Eye-lens Dose Authors: Tadahiro Kurosawa, Masahiro Kato, Sumi Yokoyama	815
RADIREC: System for Mapping and Collecting Entrance Skin Dose during Neurointerventional Radiology Authors: Takashi Moritake, Lue Sun, Koichiro Futatsuya, Satoru Kawauchi, Yasuhiro Koguchi, Mikito Hayakawa, Yuji Matsumaru	816

Diagnostic Reference Levels (DRLs) for CT Examinations in Adults in Cameroon <i>Authors: Thierry Ndzana Ndah, Boniface Moifo, Mathurin Neossi Nguena</i>	817
The Dose Kernels for Pencil Beam and Differential Pencil Beam of Photons with Spectrum of Treatment Machine with ⁶⁰Co Source and their Analytical Approximations <i>Authors: Vladimir Klimanov, Alexey Moiseev, Maria Kolyvanova</i>	818
Radiation Protection of the Public and of the Immediate Family of a Patient Following the Therapy with Iodine-131 <i>Author: Youssef Ech Chaykhy</i>	819
A Study Evaluating the Dependence of the Patient Dose on the CT Dose Change in a SPECT/CT Scan <i>Authors: Young-Hwan Ryu, Ho-Sung Kim, Kyung-Rae Dong, Chang-Bok Kim, Yun-Jong Lee</i>	820
A Study on Quantitative Analysis of Exposure Dose Caused by Patient Depending on Time and Distance in Nuclear Medicine Examination <i>Authors: Young-Hwan Ryu, Ho-Sung Kim, Yun-Jong Lee, Kyung-Rae Dong, Jin-Kyu Kim, Chang- Bok Kim</i>	821
Medical Personnel Radiation Safety in Autopsies for Radiation Accidents <i>Author: Yulia Kvacheva</i>	822
Evaluating Patient Dose in Conventional Radiology for Ten Routine Projections in Tehran, Iran: Recommendation for Local Diagnostic Reference Levels <i>Authors: Yazdan Salimi, Mohammad Reza Deevband, Dariush Askari, Jalal Ordoni, Mohammad Hossein Jamshidi, Isaac Shiri, Hamed Dehghani, Hamid Behrozi</i>	823
Eye Lens Dosimetry: Measurement in Hospitals <i>Authors: Zina Cemusova, Daniela Ekendahl, Lucie Sukupova, Michael Zelizko, Martin Mates, Kamil Sedlacek, Jiri Novotny, Iva Krulova</i>	824
A National Audit Programme for Radiotherapy Centres <i>Author: Zakithi Msimang</i>	825
Calculation of Organs Doses and Secondary Cancer Risk during Mantle Field Radiotherapy for Hodgkin's Lymphoma <i>Authors: Zahra Shakarami, Mansour Zabihzadeh, Mohammad Javad Tahmasebi Birgani, MohammadAli Behrooz, Hojatollah Shahbazian</i>	826
Organ doses and associated cancer risks for CT examinations of thorax <i>Authors: Marija Majer, Željka Knežević, Jelena Popić Ramač, Hrvoje Hršak, Saveta Miljanić</i>	827
 Optimization of image quality and patient dose in radiographs of paediatric extremities using direct digital radiography <i>Authors: Jones A., Ansell C., Jerrom C., Honey Id</i>	828
Area 4: General Ionising Radiation Protection	829
Side by Side Monitoring Test for Radon Emissions from an Underground Uranium Mine <i>Authors: Douglas Chambers, David Frydenlund, Jaime Massey, Ron Stager, Kathy Weinel</i>	830
From Radiation Solutions for Engineering Problems to Engineering Solutions for Radiation Problems: the uses of industrial radiation <i>Author: Edward Waller</i>	838
 Patrimonial management of source term in French nuclear power plants <i>Authors: François Drouet, Serge Blond, Alain Rocher, Charlotte Dabat-Blondeau, François Renard, Samir Ider</i>	847
Public Dose Assessments for Atmospheric Pathways at Rössing Uranium Mine, Utilising Direct Monitoring Data <i>Author: Gunhild von Oertzen</i>	853
Health impact assessment of recovery/disposal options of sewage sludge: methodology and critical parameters <i>Authors: Hélène Caplin, Alain Thomassin</i>	862
Criticality Safety and Control System for Nuclear Fuel Fabrication Plant <i>Authors: H. A. Elsayed, M. K. Shaat, M. E. Nagy, S. A. Agamy</i>	869

Study on the transfer of Polonium-210 from soil and sediment to cattle in a catchment area influenced by gold mining <i>Author: Immanda Louw</i>	876
Release Fractions from Airborne Fluid and Slurry Spills <i>Authors: Judith Ann Bamberger, John A. Glissmeyer</i>	884
Basic Characterization of a Radioactive Facility and Evaluation of Risk Agents <i>Authors: Carneiro, J. C. G. G., Alves, A. S., Sanches, M. P., Rodrigues D. L., Levy, D. S, Sordi, G. M. A. A</i>	892
Supervision of German miners at small underground construction sites of old mining to prevent high radon exposures <i>Author: Jörg Dehnert</i>	900
Analysis of Gamma-Ray Skyshine Contribution to Dose Rates Exterior to an Above-Ground Waste Storage Facility Using Radiation Transport Models <i>Authors: Jenelle Mann, Norbert Zoeger, Roman Koppitsch, Alexander Brandl</i>	905
Use of Real-Time Radon Progeny Monitors in Uranium Mines <i>Authors: John Takala, Andre Boucher, Mikhail Ioffe, Kari Toews</i>	912
Verification of main shielding bodies at Atucha-2 during full power operation <i>Authors: Martin Brizuela, Felipe Albornoz, Elianna Cuello</i>	917
Newcomers, new build – the industry view <i>Author: Marcel Lips</i>	921
Lanthanides Patterns as a Nuclear Forensic Signature from a Uranium Mine in South Africa <i>Authors: Manny Mathuthu, Ntokozo Khumalo, Malayita M. Baloyi, Refilwe N. Maretela</i>	925
A Review of Gamma Cell 220 Research Irradiator External Dose Rates <i>Authors: Michael Shannon, Ryan Howell, Spencer Mickum, Robert Rushton</i>	931
Interpretation of Data Collected During Individual Monitoring of Uranium Dioxide Exposure: Collective Dose Assessment <i>Authors: N. Blanchin, E. Davesne, E. Blanchardon, E. Chojnacki, D. Franck, M. Ruffin</i>	936
Monte Carlo analyses for BNCT using near-threshold $^7\text{Li}(p,n)$ neutrons <i>Radiation source, shielding, activation, and external exposure</i> <i>Authors: Noriaki Nakao, Kazuaki Kosako, Noriyosu Hayashizaki, Tatsuya Katabuchi, Tooru Kobayashi</i>	943
Nuclear New Build – Disseminating Radiation Safety Culture in the Supply Chain <i>Authors: Peter A. Bryant, Peter Cole</i>	952
On the ingestion of Cs-137 at Volincy municipality in Belarus about 30 years after the Chernobyl accident <i>Authors: Peter Hill, Petro Zoriy, Herbert Dederichs, Burkhard Heuel-Fabianek, Jürgen Pillath</i>	960
In preparation for future reduction of the dose limit for the lens of the eye – an assessment at Swedish nuclear facilities <i>Author: V. Nilsson</i>	968
Findings of radiological events in the Centre of Isotopes in Cuba <i>Author: Zayda Haydeé Amador Balbona</i>	974
Occupational Exposure in Production of Radiopharmaceuticals and Labeled Compounds in Cuba <i>Authors: Zayda Haydeé Amador Balbona, Miguel Antonio Soria Guevara</i>	984
Estimation of air born radioactivity induced by 8GeV class electron LINAC accelerator <i>Author: Yoshihiro Asano</i>	993
Principles of Formation of Risk Groups for Occupational Diseases for Workers of Facilities Using Nuclear Energy during Obligatory Medical Examinations in the Russian Federation <i>Authors: Andrey Kretov, Andrey Bushmanov, Alexander Samoilov</i>	1002

PREDO – A Strengthened Dose Assessment for Routine Discharges by Swedish Nuclear Installations <i>Authors: Anna Maria Blixt Buhr, Helene Alpfjord, Rodolfo Avila, Roman Bezhenar, Robert Broed, Anna Fermvik, Eva Grusell, Kenneth Häggkvist, Vladimir Maderich, Veronika Rensfeldt, Synnöve Sundell-Bergman, Cor W.M Timmermans, Stefan Willemsen, Govert deWith</i>	1003
Y Improvement of the Dose Estimation in Case of an Occupational ²⁴¹Am Incorporation Event <i>Authors: Anna Pántya, Andor András, Tamás Pázmándi, Péter Zagyvai</i>	1004
Argentinian Intercomparison on Interpretation of Data from Internal Exposure Sceneries for Dose Assessment <i>Authors: Ana Rojo, Nancy Puerta, Sebastian Gossio, Inés Gomez Parada</i>	1005
Economic Losses of the Nuclear Industry Related to Loss of Workers Occupational Disability for Medical Reasons <i>Authors: Alexander Samoilov, Andrey Bushmanov, Andrey Kretov</i>	1006
3A vii Safety and Risk Assessment Safety Assessment for Non-Reactor Facilities <i>Author: Bethany Louise Cawood</i>	1007
RadProtect® Increases Survival Rate in Novel Murine Slow and Low (S&L) Irradiation Model <i>Authors: Chia-Hung Chen, Jen-Ling Wang, Wei-Chuan Liao, Chau-Hui Wang, Tzu-ying Hung, Alan Liss</i>	1008
Development of Mesh-Type ICRP Reference Phantoms and its Implications <i>Author: Chan Hyeong Kim</i>	1009
Devaluation of Rhinoceros Horn through Nuclear Techniques <i>Authors: Charles Kros, Jan Rijn Zeevaart, Arnaud Faanhof, Frikkie de Beer, Deon Kotze, Dave Hudson-Lamb, Frederik Botha, Gawie Nothnagel</i>	1010
The Radiological and Health Impacts to the Residents of the Tudor Shaft Informal Settlement <i>Authors: Dawid de Villiers, Gert Liebenberg, Rean Swart, Rietha Oosthuizen, Juanette John, Hanlie Liebenberg-Enslin, Didintle Modisamongwe, Grant Walters</i>	1011
Mathematical Modeling of the Aging Process of the Containment Spray Injection System using the Fault Tree Method <i>Authors: Diogo da Silva Borges, Deise Diana Lava, Maria de Lourdes Moreira, Antonio Cesar Ferreira Guimarães</i>	1012
Determination of the Detection Efficiency of ¹³¹I in Thiroid using Monte Carlo Method <i>Authors: Dayana Ramos Machado, Yoan Yera Simanca, Gladys M. López Bejerano, Nancy Acosta Rodriguez</i>	1013
Uranium Aerosols in Nuclear Fuel Manufacturing <i>Authors: Edvin Hansson, Håkan Pettersson, Christine Fortin, Mats Eriksson</i>	1014
The Future Free Electron Laser Facility SwissFEL from a Radiation Protection Point of View <i>Authors: Eike Hohmann, Roland Luescher, Elisa Musto, Albert Fuchs, Sabine Mayer</i>	1015
Assessment of Beam Dump Activation for RAON Heavy Ion Accelerator in Korea <i>Authors: Eunjoong Lee, Cheolwoo Lee, Sungchul Yang, Young-Ouk Lee, Kyeongjin Park, Gyuseong Cho</i>	1016
Area Monitoring on Nuclear Fuel Cycle Facilities <i>Authors: Elizabeth Renteria, Paula Nuñez, Analia Saavedra, Nestor Fruttero, Allan Segato</i>	1017
How Spanish Nuclear Power Plant have Implemented Lessons Learned from the Fukushima Accident in the Radiation Protection Field <i>Author: Eduardo Sollet</i>	1018
Setting up an Occupational Radiation Protection Program in NORM Industry: A Case Study in Mining Industry in the Democratic Republic of the Congo <i>Authors: Francois Kazadi Kabuya, Vincent Lukanda Mwamba, Leonard Woto Makontsh, Robert Lwamba Ilonda</i>	1019


Monitoring and Mapping of Radon Concentration within Ghana Atomic Energy Commission <i>Authors: Francis Otoo, Emmanuel Ofori Darko, Massimo Garavaglia, Concettina Giovani, Silvia Pividore, Bentil Aba Andam, Geoffrey Emi-Reynolds, Lucas Piccini</i>	1020
GIS Mapping and Background Ionizing Radiation (BIR) Assessment of Solid Mineral Mining Sites in Enugu State, Nigeria <i>Authors: Avwiri Gregory, Agbalagba Ezekiel, Osimobi Jude, Ononugbo Patience</i>	1021
Using a Portable Neutron Generator in an Open Field: The Radiation Protection Assessment <i>Authors: Gian Marco Contessa, Nadia Cherubini, Alessandro Dodaro, Luigi Lepore, Giuseppe Augusto Marzo, Sandro Sandri</i>	1022
Testing of Burn-up Calculation Method based on Chebyshev Rational Approximation with IAEA-ADS Benchmark <i>Authors: Guangyao Sun, Wending Fan, Lijuan Hao, Binhang Zhang, Jing Song, Pengcheng Long, Liqin Hu</i> ..	1023
Assessment of Occupational Exposure of ‘Conflict Mineral’ Artisanal Mine Workers via Radiogenic and Dosimetric Characterization of High Background Radiation Area (HBRA) Columbite-Tantalite (Coltan) <i>Authors: Hudson Angeyo Kalambuka, Leon Ntihakose, Jayanti Patel, David Maina</i>	1024
 Towards a Novel Modular Architecture for CERN Radiation Monitoring <i>Authors: Hamza Boukabache, Michel Pangallo, Nicola Cardines, Gael Ducos, Antonio Bellotta, Ciarán Toner, Daniel Perrin, Doris Forkel-Wirth</i>	1025
Assessment of Internal Dose due to Intake of Food for Determination of Representative Person in Normal Operation of Nuclear Power Plant <i>Authors: Hyungjoon Yu, Insu Chang, Jungil Lee, Jang-Lyul Kim, Bonghwan Kim</i>	1026
Practical use of Graph Theory to Reduce the Individual Doses of the Employees Working in Areas with High Background Radiation <i>Authors: Iliia Kudrin, Ivan Mazur, Konstantin Chizhov, Victor Kryuchkov</i>	1027
Development and Implementation Experience of Information-Analytical System of Radiation Safety of Workers <i>Authors: Ivan Mazur, Iliia Kudrin, Chizhov Konstantin, Kryuchkov Viktor</i>	1028
Recent Developments in Occupational Exposure Reduction in Nuclear Power Plants <i>Authors: Jason Harris, David Miller</i>	1029
Practical Impacts of NORM Standards on Mining and Minerals Processing <i>Author: Jim Hondros</i>	1030
Radiation Protection in the South African Mining and Minerals Extraction Industries <i>Author: James Larkin</i>	1031
Improved Approach to Estimate Fission Product Inventory using TRITON in SCALE 6.1 for a Nuclear Reactor with Gadolinium Burnable Poison <i>Authors: Jaehoon Song, Kyoyoun Kim</i>	1032
The Field Characterization Around the High Energy X-ray Cargo Screenings <i>Authors: Kamil Szewczak, Katarzyna Woloszczuk</i>	1033
Occupational Exposure during Fusion Research on PF-1000 Unit <i>Authors: Kamil Szewczak, Slawomir Jednorog</i>	1034
Room Submersion Calculations of Noble Gas Dose Rate Coefficients <i>Authors: Ken Veinot, Shaheen Dewji, Michael Bellamy, Keith Eckerman, Nolan Hertel, Mauritius Hiller</i>	1035
Residual Activity in Lead and Bismuth Materials induced by 100-40 MeV Protons <i>Authors: Leila Mokhtari Oranj, Nam-Suk Jung, Joo-Hee Oh, Hee-Seock Lee</i>	1036
Security of Radioactive Materials in Oil & Gas Industry (Compliance & Challenges) <i>Author: Mohammad Aref</i>	1037
Egypt Experience with Research Reactors Operation, Nuclear and Radiological Activities Law as a Step for Building Nuclear Power Reactors <i>Author: Mohamed Gomaa</i>	1038

Direct Measurement of Radium Levels in Waste Water Samples using Portable Medium Resolution Gamma Spectrometers <i>Authors: Michael Iwatschenko-Borho, Scott Masiella, Richard Oxford, James Williams</i>	1039
Practical Application Illustrating Excellence in Radiological Protection at the Koeberg Nuclear Power Station <i>Author: Marc Maree</i>	1040
Improvement of Underground Radon Concentrations at a South African Gold Mine <i>Author: Marc Vermeijs</i>	1041
Building Nuclear Security Culture in Morocco <i>Authors: Oumkeltoum Hakam, Abdelmajid Choukri, Taha Laghouazi</i>	1042
The Role of Radiation Protection in Nuclear Forensics: From the Crime Scene to the Laboratory <i>Authors: Philemon Magampa, Gedion Nkosi</i>	1043
EcoMine – A Software Package based on Ecolego to Assess the Radiological Impact of Mining Sites and Activities <i>Authors: Rodolfo Avila, Erik Johansson, Japie van Blerk</i>	1044
U and Th Source Term Characterisation in Selected Gold Tailings of the Witwatersrand (South Africa): A Geochemical Modelling and Reaction Network Approach <i>Authors: Robert Hansen, Japie Van Blerk</i>	1045
Radiation Protection Research <i>Author: Rebecca Tadesse</i>	1046
Radiation Protection Aspects of Uranium In Situ Recovery / In Situ Leach Facilities <i>Author: Steven Brown</i>	1047
Worker Protection Implications of the Solubility and Human Metabolism of Modern Uranium Mill Products <i>Authors: Steve Brown, Douglas Chambers</i>	1048
Dust Management on Tailings Storage Facilities at a South African Gold Mine <i>Authors: SJ van Wyk, CF Human</i>	1049
Risk of Radon Induced Health Effect: Evaluation Methods and Practical Application <i>Authors: Sergey Kiselev, Vladimir Demin</i>	1050
Comparison of the Efficacy of Neutron Shielding of Aluminum and Polyethylene Composites Containing Micro and Nano-Sized B₄C and Carbon Nanotubes <i>Authors: SMJ Mortazavi, Fatemeh Jamali, MR Kardan, Sedigheh Sina, MA Mosleh-Shirazi, Jila Rahpeyma</i>	1051
Assessment on Occupational Exposure in Malaysia: Practices and Trends <i>Authors: Suzilawati Muhd Sarowi, John Konsoh, Ahmad Bazlie Abdul Kadir</i>	1052
Advance Determination of Respiratory Protection Needs when Performing Destructive Work on Structural Materials <i>Author: Scott Schwahn</i>	1053
Reduction in Doses and Lung Cancer Risks among Canadian Uranium Miners between 1930s and 2013 <i>Authors: Tristan Barr, Pascale Reinhardt, Patsy Thompson, Douglas Chambers, Ron Stager, Occupational Cancer Research Center</i>	1054
Operational Health Physics Development Activities Related to Fast Reactor Fuel Fabrication and Pyro-Reprocessing <i>Authors: Ravi T, Akhila R, Krishnakumar D N, Rajagopal V, Jose M T, Venkatraman B, Satyamurthy S A V</i>	1055
The Information System on Occupational Exposure (ISOE): Trends and Lessons <i>Authors: Tae-Won Hwang, Olvido Guzman</i>	1056
Protecting Humans and the Environment the Next Hundred Thousands of Years <i>Authors: Ulrik Kautsky, Eva Andersson, Tobias Lindborg, Anders Löfgren, Sara Nordén, Peter Saetre</i>	1057

Assessment of Belarusian NPP for Protection of the Public <i>Author: Viktoriya Kliaus</i>	1058
Development of a Dose Assessment Code for the Radiation Protection of Representative Person in Korea <i>Authors: Won Tae Hwang, Eun Han Kim, Moon Hee Han, Hae Sun Jeong</i>	1059
Effect of Particle Size and Percentages of Boron Carbide on the Thermal Neutron Radiation Shielding Properties of HDPE/B4C Composite: Experimental and Simulation Studies <i>Authors: Zahra Soltani, Farhood Ziaie</i>	1060
VOLUME 3	
Area 5: Optimisation and Design of New Facilities	1061
Monte Carlo Modeling and Verification of the Shielding for an Ionizing Radiation Test Laboratory <i>Authors: C. Stettner, N. Baumgartner, M. Blaickner, C. Hranitzky</i>	1062
Preconcentration of cobalt metal ions onto imprinted polymer hydrogels <i>Authors: Ghada A. Mahmoud, Hegazy E. A, S. M. Elbakery</i>	1065
Dose Constraint – a Mysterious Concept of Radiation Protection <i>Author: Helena Janžekovič</i>	1072
Establishment of a Laboratory for Gamma-ray Spectrometry of Environmental Samples Collected in Fukushima <i>Authors: Jun Saegusa, Tomoyuki Yoda, Satoshi Maeda, Tsutomu Okazaki, Shuichi Otani, Toshio Yamaguchi, Yoshiyuki Kurita, Atsushi Hasumi, Chushiro Yonezawa, Minoru Takeishi</i>	1078
New Remote Controlled Experiments in Nuclear Chemistry <i>Authors: Jan-Willem Vahlbruch, Wolfgang Schulz, Claudia Fournier, Paul Hanemann, Sebastian Büchner, Clemens Walther</i>	1086
Introduction and assessment of new heavy weight concrete shields using Monte Carlo simulation <i>Authors: Mahdi Saeedi-Moghadam, Mahdi Kazempour, Sedigheh Sina, Reza Jalli, Banafsheh Zeinali-Rafsanjani</i>	1094
Exposure Rate Assessment From Selected Cathode Ray Tube Devices <i>Authors: Ife-Adediran O. O., Arogunjo A. M.</i>	1100
 Case Study: Radiation Protection measures when designing an extension of a Nuclear Medicine Department <i>Authors: Youness Esserhir El Fassi, Jean-Élie Fontaine, Mathieu Valla, Siham El Moghni, Youness Haddoudi, Paul Livolsi, Abdelmajid Choukri, Oum Keltoum Hakam</i>	1108
Optimization of occupational exposure during first operations with ¹⁸F in Cuba <i>Author: Zayda Haydeé Amador Balbona</i>	1117
The Role of the Radiological Protection Team as a Stakeholder in the Design Phase of a Nuclear Facility: the Case of Brazilian Conversion Plant <i>Authors: Ana Cristina Lourenço, Wagner de Souza Pereira</i>	1126
Design Study of ELI-NP Beam Dumps: Radioprotection Issues and Monte-Carlo Simulations <i>Authors: Adolfo Esposito, Oscar Frasciello, Maurizio Pelliccioni</i>	1127
Preliminary Thermo-mechanical Design of the Main Dump for the High Energy Electron Beam Lines in ELI-NP <i>Authors: Adolfo Esposito, Lina Quintieri</i>	1128
Radioprotection Issues for the STAR Project <i>Authors: Adolfo Esposito, Oscar Frasciello, Fiorello Martire, Maurizio Pelliccioni</i>	1129
Cyclotron Production of Sc and V Radionuclides from Natural Titanium for Medical Applications <i>Authors: Ahmed Rufai Usman, Mayeen Uddin Khandaker, Hiromitsu Haba, Naohiko Otuka</i>	1130
Design Approval and Registration for Radiation Devices <i>Authors: BokHyoung Lee, SangEun Han, KiWon Jang, JongRae Kim, WooRan Kim, KyungWha Kim, Younjin Park</i>	1131

Preliminary Analysis of Radiation Characteristic for 250 MeV Proton Accelerator Driven Sub-critical System	
<i>Authors: Bin Li, Qi Yang, Bo Chang, Chao Liu, Liqin Hu</i>	1132
New CZT (H3D) Technology Employed at Cook Nuclear Plant Achieves Immediate Individual Isotopic Identification and Verifies Adequacy of Temporary Shielding	
<i>Author: David Miller</i>	1133
Radiation Protection for NORM Industries – Results of the European Joint Research Project ‘Metrology for Processing Materials with High Natural Radioactivity (MetroNORM)	
<i>Authors: Franz Josef Maringer, Sylvie Pierre, Teresa Crespo Vazquez, Monika Mazanova, Pierino De Felice, Branko Vodenik, Mario Reis, Mikael Hult, Laszlo Szücs, Simon Jerome, Alexander Muring, Roy Pöllänen, Andreas Baumgartner, Boris Bulanek, Boguslaw Michalik, Nathalie Michielsen, Julian Dean, Philippe Cassette, Franz Kabrt, Hannah Moser</i>	1134
Effectiveness of the Shielding Mechanism in Rooms Housing X-ray Diagnostic Equipment - A Case Study of Mulago Hospital	
<i>Authors: Festo Kiragga, Rebecca Nakatudde, Akisophel Kisolo</i>	1135
KIRDI’S Role in the Project “Promoting Safety, Self-reliance and Sustainability of Non-Destructive (NDT) Testing Facilities”	
<i>Author: Humphrey Lumadede</i>	1136
Requirements for Specific Safety Issues - Fire, Earthquake, and Flooding – at Large Particle Accelerator Facilities	
<i>Authors: Hee-Seock Lee, Arim Lee, Nam-suk Jung, Joohee Oh, Leila Mokhtari Oranj</i>	1137
Modernisation of the Radiation Monitoring Systems at Research and Training Reactors in Hungary	
<i>Authors: János Petrányi, Dénes Elter, Imre Szalóki, Máté Solymosi, László Manga</i>	1138
Environmental Radiation and Meteorological Monitoring Systems of a Greenfield Nuclear Power Plant	
<i>Authors: Juho Rissanen, Jussi Huotilainen</i>	1139
Evaluation of Carbon -14 Released from Small Power Reactor	
<i>Authors: Kyo-Youn Kim, Ha-Young Kim, Jae Hoon Song</i>	1140
Development of a Methodology to Correlate Safety Classification of Components to the Maintenance Programme of a Facility	
<i>Author: Muhammad Akbar</i>	1141
Applicability of Lessons Learned from the Fukushima Accident to Radioactive Material Users	
<i>Authors: Shawn Smith, Catherine Haney</i>	1142
Local Shield Model around Beam Target Stations using Radiation Transport Code MCNPX	
<i>Authors: Tebogo Kupi, Johann van Rooyen, Raymond Njinga</i>	1143
Validation of Experimental Measurements of Activity for Radioisotopes in SAFARI-1 Reactor	
<i>Author: Tholakele Ngeleka</i>	1144
Robotic HPGe Spectrometer for Radionuclide Analysis	
<i>Authors: Vladimir Gostilo, Alexander Sokolov</i>	1145
Area 6: Radiation Detection and Dosimetry	1146
A New Approach to Worker Internal Dosimetry and its Impact on Radiation Protection	
<i>Authors: Alan Birchall, Vadim Vostrotin, Matthew Puncher, Alexander Efimov, Bruce Napier</i>	1147
Approach to uncertainties in exposure, dose and risk estimates for uranium workers within the CURE project	
<i>Authors: Augusto Giussani, Sophie Ancelet, Derek Bingham, Eric Blanchardon, Richard Bull, Estelle Davesne, James Grellier, Olivier Laurent, Dominique Laurier, Matthew Puncher, Tony Riddell</i>	1155
Joint Coordinating Committee on Radiation Effects Research Project 1.1: Techa River Population Dosimetry	
<i>Authors: Bruce A Napier, Marina O Degteva, Evgenia I Tolstykh, Natalia B Shagina, Elena A Shishkina, Marina I Vorobiova, Nickolay G Bougrov, Lynn R Anspaugh</i>	1162

Joint Coordinating Committee on Radiation Effects Research Project 2.4: Mayak Worker Dosimetry <i>Authors: Bruce Napier, Alexander Efimov, Alan Birchall, Vadim Vostrotin, Matthew Puncher, Alexandra Sokolova, Klara Suslova, Scott Miller, Alexay Zhdanov, Evgeney Vasilenko</i>	1168
Waterfowl-specific Computational Models for use in Internal Dosimetry <i>Authors: Dawn Montgomery, Jennifer Paloni, Nicole Martinez</i>	1174
Project 1.2b: Techa River Population Cancer Morbidity and Mortality <i>Authors: Daniel O. Stram, Lyudmila Krestinina, Dale Preston, Alexander Akleyev</i>	1182
Assessment of equivalent dose of the lens of the eyes and the extremities to workers under nonhomogeneous exposure situation in nuclear and accelerator facilities by means of measurements using a phantom coupled with Monte Carlo simulation <i>Authors: Hiroshi Yoshitomi, Masayuki Hagiwara, Munehiko Kowatari, Sho Nishino, Toshiya Sanami, Hiroshi Iwase</i>	1188
Implementation of Co-worker Models for the Reconstruction of Dose under an Occupational Radiation Exposure Compensation Program <i>Author: James W. Neton</i>	1196
Experience with Wound Dosimetry in Uranium Mining and Processing <i>Authors: John Takala, Kari Toews</i>	1204
Response of $^{10}\text{B}+\text{ZnS}(\text{Ag})$ as neutron detector in Radiation Portal Monitors <i>Authors: Karen A. Guzmán-García, H.R. Vega-Carrillo, Eduardo Gallego, Alfredo Lorente, Juan A. González</i>	1213
Wrist, finger, and crystalline dosimetry study with radiopharmacists and nursing technicians for various applications and tests, using various radiopharmaceuticals, for adjustment of a percentage factor between difference values obtained at the extremities to optimize the dosimetry in nuclear medicine services. <i>Authors: Maria Inês Calil Cury Guimarães, Sato, Karen A. K., Leandro F. Souza, Leia R. Santo, Elaine C. Santo, Ivani B. Melo, Heber S. Videira, Julia A. Gonzalez, Carlos A. Buchpiguel, Josefina da Silva Santos, Adélia Sahyun</i>	1221
Direct Surface Contamination Measurement of Low Energy Beta and Electron Capture Isotopes <i>Authors: Michael Iwatschenko-Borho, Reinhard Loew</i>	1224
The Facility of Radiation Standards in Japan Atomic Energy Agency, present status and its research works on dosimetry <i>Authors: Munehiko Kowatari, Hiroshi Yoshitomi, Sho Nishino, Yoshihiko Tanimura, Tetsuya Ohishi, Michio Yoshizawa</i>	1230
Evaluation of radiation detectors for a possible integration into the automated survey system TIM in the Large Hadron Collider (LHC) <i>Authors: Markus Widorski, Frédéric Aberle, Cristina Adoriso, Daniel Perrin</i>	1239
Investigations into Radiation Dose Distribution in a Computed Tomography Fluoroscopy Room: Monte Carlo Studies <i>Authors: Prince Kwabena Gyekye, Frank Becker, Geoffrey Emi-Reynolds</i>	1245
PIMAL: A GUI-Driven Software Package To Conduct Radiation Dose Assessments Using Realistic Phantom Postures <i>Authors: Shaheen Dewji, Mauritius Hiller, Nolan Hertel, Sami Sherbini, Mohammad Saba</i>	1251
Comprehensive Study on the Response of Neutron Dosimeters in Various Simulated Workplace Neutron Calibration Fields <i>Authors: Sho Nishino, Katsuya Hoshi, Norio Tsujimura, Munehiko Kowatari, Tadayoshi Yoshida</i>	1258
Estimation of basic characteristics about scintillation type survey meter using multi pixel photon counter <i>Author: Toshioh Fujibuchi</i>	1264
Comparison of dose rate measurements of commercially available hand- held gamma detectors with radiation protection dose meter <i>Authors: Theo Köble, Hermann Friedrich</i>	1268
Estimation of detective efficiency of CdZnTe semiconductor detector and NaI(Tl) scintillation detector <i>Authors: Takatoshi Toyoda, Toshioh Fujibuchi</i>	1273

A study of Energy-Compensating Metal Filter of Semiconductor Detector for Personal Dosimetry in X-ray Diagnosis <i>Authors: Kento Terasaki, Toshioh Fujibuchi, Hiroo Murazakic, Taku Kuramoto, Yoshiyuki Umezu, Yang Ishigaki, Yoshinori Matsumoto</i>	1279
Determination of fission radionuclides activities in a real fission gamma-ray field <i>Authors: Žlebčík P. , Malá H., Huml O.</i>	1285
Radiation-induced Color Bleaching of Methyl Red in Polyvinyl Alcohol (PVA) Film Dosimeter <i>Authors: Awad Alzahrany, Ahmed Basfar, Khalid Rabaeh</i>	1293
Characterization of HPGe Detectors using Computed Tomography <i>Authors: Angelica Hedman, Jalil Bahar Gogani, Micael Granström, Lennart Johansson, Jonas Andersson, Henrik Ramebäck</i>	1294
Optimized Detector for in Situ Low Energy Gamma Spectrometry in Close Geometries <i>Authors: Angelica Hedman, Göran Ågren, Lennart Johansson, Jalil Bahar Gogani, Henrik Ramebäck</i>	1295
Delineation of Radiation Dose Pattern in Radiation Workers and Dose Optimization Using Dose Reduction Methodologies <i>Authors: Ajai Kumar Shukla, Dhiraj Kumar Tewari</i>	1296
Establishment of a National Dose Register in South Africa <i>Authors: Alan Muller, Nthabiseng Mohlala</i>	1297
Public In Vivo Thyroid Monitoring for Dose Estimation after Accidental Intake of I-131. Experiences from Scandinavia <i>Authors: Asser Nyander Poulsen, Henrik Roed, Lilián del Risco Norrlid, Mats Isaksson, Bjorn Lind, Óskar Halldórson Holm, Jussi Huikari</i>	1298
Comparison of Radiation Dose Assessment Methodology used for the Public Living in the Area Contaminated with Radioactive Materials <i>Authors: A Ra Go, Min Jun Kim, Kwang Pyo Kim</i>	1299
Argentinian Intercomparison Exercise on Internal Dosimetry: ¹³¹I Thyroid Monitoring <i>Authors: Ana Rojo, Nancy Puerta, Sebastian Gossio, Ines Gomez Parada</i>	1300
Performance Comparison of OSLD (Al₂O₃:C) and TLD (LiF:Mg,Cu,P) in Accreditation Proficiency Testing <i>Authors: Alexander Romanyukha, Mathew Grypp, Anthony Williams</i>	1301
Test of Ring, Eye Lens and Whole Body Dosemeters for the Dose Quantity Hp(3) to be used in Interventional Radiology <i>Authors: Agnieszka Szumska, Renata Kopeć, Maciej Budzanowski</i>	1302
From Filter Swipe Test to Bioavailability: A Rapid Experimental Approach to Assess Actinide Behaviour Following Internal Contamination <i>Authors: Anne Van der Meeren, Agnès Moureau, Sylvie Coudert, Pierre Laroche, Jaime Angulo, Nina Griffiths</i>	1303
Microphotonics Approaches to Nuclear Forensics Analysis <i>Authors: Bobby Bhatt, Hudson Angeyo, Alix Dehayem-Massop</i>	1304
Determination of Scattering Factors Associated to the In Vivo Monitoring of Iodine-131 in the Thyroid <i>Authors: Bernardo Dantas, Fabiana Lima, Ana Leticia Dantas, Eder Lucena, Rodrigo Gontijo, Carlaine Carvalho, Clovis Hazin</i>	1305
μ-TPC: A New Recoil Nuclei Telescope for Low Energy Neutron Fields characterization <i>Authors: Benjamin Tampon, Daniel Santos, Olivier Guillaudin, Jean-François Muraz, Lena Lebreton, Thibaut Vinchon, Nadine Sauzet</i>	1306
A Passive Neutron Dosimeter for Measurement in Mixed Neutron-Photon Fields <i>Authors: Sören Mattsson, Maria Christiansson, Christian Bernhardsson</i>	1307
 The Russian Human Radiobiological Tissue Repository: A Unique Resource for Studies of Plutonium-Exposed Workers <i>Authors: Christopher Loffredo, David Goerlitz, Svetlana Sokolova, Leonidas Leondaridis, Mariya Zakharova, Valentina Revina, Evgeniya Kirillova</i>	1308

Characterization and Measurement of Dosimetry X-ray Bean on Kenya <i>Authors: Collins Omondi, David Otwoma</i>	1309
R International Standards on Radioactivity Measurement for Radiological Protection: Status and Perspectives <i>Authors: Dominique Calmet, Roselyne Ameon, Aude Bombard, Stephane Brun, Francois Byrde, Jing Chen, Jean-Marie Duda, Maurizio Forte, Marc Fournier, Ales Fronka, Thomas Haug, Margarita Herranz, Amir Husain, Simon Jerome, Martin Jiranek, Steven Judge, Sang Bog Kim, Pieter Kwakman, Jeanne Loyen, Montse LLaurado, Rolf Michel, David Porterfield, Andry Ratsirahonana, Anthony Richards, Katerina Rovenska, Tetsuya Sanada, Christoph Schuler, Laurence Thomas, Shinji Tokonami, Andrey Tsapalov, Takahiro Yamada</i>	1310
A Method for Response Time Measurement of Ionization Chamber Type Survey Meter <i>Authors: Dehong Li, Bin Guo, Jianwei Wang, Di Wu, Xingdong Li</i>	1312
The Primary Standard for Air Kerma at the NIM for the Gamma Radiation of 137Cs <i>Authors: Dehong Li, Peiwai Wang, Jianwei Huang, Bin Guo, Di Wu</i>	1313
Dosimetry for Radiological Protection at the New Research Facility, ELI-NP <i>Authors: Elena Iliescu, Sorin Bercea, Iani Mitu, Aurelia Celarel, Constantin Cenusu</i>	1314
Determination of a Urine Reference Level for an Individual Monitoring Programme for Uranium <i>Author: Frik Beeslaar</i>	1315
Data Recording Regarding the Dose Assessment due to X-ray Generator Sources and the ²⁴¹Am Calibration Curve Usefulness <i>Authors: Felicia Mihai, Ana Stochioiu, Catalina Tuca</i>	1316
R Integrated Operational Dosimetry System at CERN <i>Authors: Gérald Dumont, Fernando Baltasar Dos Santos Pedrosa, Pierre Carbonez, Doris Forkel- Wirth, Pierre Ninin, Eloy Reguero Fuentes, Stefan Roesler, Joachim Vollaire</i>	1317
Biodosimetry of in Vitro Human Lymphocytes exposed to ⁶⁰Co γ-rays and DNA Incorporated ¹²³I <i>Authors: Hein Fourie, Jacobus Slabbert, Richard Newman, Philip Beukes, Neil Rossouw</i>	1318
Development of Radiation Portal Monitoring System based on Energy Weighted Algorithm for Gamma Spectroscopy <i>Authors: Hyuncheol Lee, Wook-Geun Shin, Han Rim Lee, Chang-Il Choi, Chang-Su Park, Hong- Suk Kim, Chul Hee Min</i>	1319
Results of the EURADOS Intercomparisons IC2014 on Whole Body Dosimeters for Photons <i>Authors: Hannes Stadtmann, Tom Grimbergen, Andrew McWhan, Ana Maria Romero, Markus Figel, Christian Gärtner</i>	1320
Improving Potential in a Retrospective Dosimetry using Common Plastics by Extracting Inorganic Materials <i>Authors: Insu Chang, Jang-Lyul Kim, Jungil Lee, Tae-Hyoung Kim, Seung-Kyu Lee, Bong-Hwan Kim</i>	1321
Performance of Eye Lens Dosimeters in use in Europe <i>Authors: Isabelle Clairand, Merce Ginjaume, Filip Vanhavere, Eleftheria Carinou, Josiane Daures, Marc Denoziere, Edilaine Honorio da Silva, Maria Roig, Sara Principi, Laurent Van Rycheghem</i>	1322
Contemporary Radiation Protection Trends – Do we need a New Yype of Digital Personal Dosimeters to be used in Medicine, Homeland Security, Environmental Protection and Emergencies? <i>Authors: Ivica Prlic, Marija Suric Mihic, Mladen Hajdinjak, Tomislav Mestrovic, Zdravko Cerovac</i>	1323
Rare-earth Doped Silica Fibres for Dosimetry Applications in Medicine <i>Authors: Ivan Veronese, Mauro Fasoli, Norberto Chiodini, Eleonora Mones, Cristina De Mattia, Eduardo D'Ippolito, Marie Claire Cantone, Anna Vedda</i>	1324
DosiKit, Innovative Solution for On-site External Radiation Biodosimetry <i>Authors : Julie Bensimon, Caroline Bettencourt, Sandrine Altmeyer, Arnaud Tupinier, Nicolas Ugolin, Sylvie Chevillard</i>	1325
Analysis of Photon Energy Distribution at the Working Places in Nuclear Power Plants Using In-situ CZT Detectors <i>Authors: Jeongin Kim, Seokon Kang, Meeseon Jeong</i>	1326

Monte Carlo Approach to Accidental Dose Reconstruction Based on the EPR Measurements of Absorbed Dose to Human Teeth Authors: Jeongin Kim, Hoon Choi, Byoungil Lee.....	1327
R Development of two new single-exposure, multi-detector neutron spectrometers for radiation protection applications in workplace monitoring Authors: J.M. Gómez-Ros, R. Bedogni, D. Bortot, C. Domingo, A. Esposito, M.V. Introini, M. Lorenzoli, G. Mazzitelli, M. Moraleda, A. Pola, D. Sacco.....	1328
The Influence of the Dose Calculation Resolution of VMAT Plans on the Calculated Dose for Eye Lens and Optic Apparatus Authors: Jong Min Park, So-Yeon Park, Jung-in Kim, Hong-Gyun Wu, Jin Ho Kim.....	1329
Dosimetry Aspects for the Development of an Irradiator for Cross-linking of Cables using ⁶⁰Co Gamma Rays Authors: Jain Reji George, B K Pathak.....	1330
Development and Applications of Super Monte Carlo Simulation Program for Advanced Nuclear Energy Systems Authors: Jing Song, Liqin Hu, Pengcheng Long, Tao He, Lijuan Hao, Mengyun Cheng, Huaqing Zheng, Shengpeng Yu, Guangyao Sun, Tongqiang Dang, Qi Yang, Bin Wu, Chaobin Chen, Ling Fang, Yican Wu, FDS Team.....	1331
Study of Eye Lens Dose at the Nuclear Industries in Sweden Authors: Lisa Bäckström, Karin Andgren.....	1332
Direct Ion Storage Dosimetry Roadmap Authors: Kip Bennett, Michael Lantz, Matti Vuotilla, Jani Rakkola.....	1333
Implementation of a New BeOSL Dosimetry Platform Utilizing Lean Manufacturing Tools Authors: Kip Bennett, Mike Lantz, Joel White, Gordon Sturm, Reiner Esser, Timo Wiedenmann, Jay Thomas.....	1334
R Y Monte Carlo calibration of the whole body counting detection system for β ⁹⁰Sr measurement of people internally contaminated with ⁹⁰Sr Authors: Karin Fantinová, Pavel Fojtík, Irena Malátová.....	1335
Backscatter Response of Different Personal Dosimeter Detectors for Water Slab and Cylindrical Calibration Phantoms Authors: Kristine Marie Romallosa, Hiroshi Yoshitomi.....	1336
Dosimetric Uncertainty Analysis of the Optically Stimulated Luminescence Dosimeter System in the Philippines Authors: Kristine Marie Romallosa, Marianna Lourdes Grande, Estrella Caseria.....	1337
Development of the Electronic Personal Dosimeter Based on Scintillator for a Mobile Phone Application Authors: Kyeongjin Park, Daehee Lee, Hyunjun Yoo, Eunjoong Lee, Hyunduk Kim, Hojong Chang, Gyuseong Cho, Alexander Solodov.....	1338
Salty Nuts and Snacks for Retrospective Dosimetry Authors: Maria Christiansson, Christian Bernhardsson, Therese Geber-Bergstrand, Sören Mattsson, Christopher Rääf.....	1339
Dosimetric Evaluation of a Radiological Accident Involving a Gammagraphy Industrial Source of ¹⁹²Ir (44 Ci)-Multidisciplinary Approach Authors: Marina Di Giorgio, Analía Radl, Adrian Discacciatti, Diana Dubner, Sebastian Gossio, Francois Trompier, Ezequiel Soppe, Adriana Coppola, Mayra Deminge, Julieta Rearte, Ana Molinari, Ignacio Menchaca, Fabio Lopez, Gaston Castro, Mariana Egan, Mercedes Portas.....	1340
In Light Optically Stimulated Luminescence Dosimetry for Occupational Workers in the Philippines Authors: Marianna Grande, Kristine Romallosa, Estrella Caseria, Ahmad Bazlie.....	1341
Particle Size Distributions of Radioactive Aerosols in the Atmosphere Authors: Miroslav Hýža, Petr Rulík, Helena Malá, Vera Beckova.....	1342
Optical Stimulated luminescence from Citrine for High-Doses Dosimetry Authors: Maria Ines Teixeira, Linda V.E. Caldas.....	1343

Performance Data of a new Active Personal Dosimeter in Respect to Gamma, Beta and Pulsed X-ray Radiation	
<i>Authors: Michael Iwatschenko-Borho, Alan Laing, Ling Luo, Cassidy McKee, Greg Nelson, Ralf Pijahn, Norbert Trost</i>	1344
Calibration of Conventional Survey Meters for Soft X-ray Below 5 keV	
<i>Authors: Masahiro Kato, Tadahiro Kurosawa, Toshihiko Hino, Yoshinori Inagaki</i>	1345
Retrospective Review of Dosimeter Film Processing	
<i>Authors: Mirela Kirr, Christopher Passmore</i>	1346
Design of Long Counter Having Flat Response from Few keV up to 150 MeV	
<i>Authors: Mohamed Mazunga, Taosheng Li, Yanan Li, Jieqiong Jiang, Yican Wu</i>	1347
Measurement of Occupational Doses of Ionising Radiation to the Whole body of Diagnosis Radiologists	
<i>Author: Maryam Pourkaveh</i>	1348
Calculation of 2D Dose Distribution in an Inhomogeneous Phantom using Artificial Neural Network with Best Training Method	
<i>Authors: Mahdi Saeedi-Moghadam, Banafsheh Zeinali-Rafsanjani, Kamal Hadad, Sepideh Sefidbakht</i>	1349
Photoneutron Secondary Cancer Risk Estimation by a Novel Position-Sensitive Detection Method	
<i>Authors: Mehdi Sohrabi, Amir Hakimi</i>	1350
A New Method for Effective Dose Calculation based on the Ambient Dose Height Distribution	
<i>Authors: Niroojiny Sangarapillai, Mario Liebmann, Bjoern Poppe, Heiner von Boetticher</i>	1351
Development of a New Optical Reading Technique for Dosimetric Gels based on the Analysis of the Scattering Light	
<i>Authors: Olivier Bleuse, Régine Gschwind, Yannick Bailly</i>	1352
Performance Assessment of the Criticality Dosimetry System at The Belgian Nuclear Research Centre SCK•CEN	
<i>Authors: Olivier Van Hoey, Filip Vanhavere, Marcel Reginatto</i>	1353
PROCORAD's International Proficiency Testing for Radio-Bioassays	
<i>Authors: Robert Fottorino, Bernadette Peleau, Christian Hurtgen</i>	1354
Assessment of Dose Calibrators Performance in Nuclear Medicine Department in Sudan	
<i>Author: Suhaib Alameen</i>	1355
A Simple, Reliable and Inexpensive Microscopy-Based Method for Radiation Biodosimetry	
<i>Authors: Sudhir Chandna, Shwetanjali Nimker, Kanupriya Sharma, Vijaypal Singh</i>	1356
Secondary Neutron Dose Assessment from Proton Therapy Using Passive Scattering at The National Cancer Centre (NCC)	
<i>Authors: Sang Eun Han, Se Byeong Lee, Gyuseong Cho, Kyeongjin Park</i>	1357
Traceable Measurements for Radiation Protection Industry in South Africa	
<i>Author: Sibusiso Jozela</i>	1358
Development of the Performance Testing Procedure for the New Proposed Portable Gamma Irradiation System	
<i>Authors: Seung Kyu Lee, Hyungjoon Yu, Insu Chang, Hyoungtaek Kim, Jungil Lee, Jang-Lyul Kim, Bong-Hwan Kim</i>	1359
Development of the Probabilistic Internal Dosimetry Code	
<i>Authors: Siwan Noh, Jai-Ki Lee, Jong-Il Lee, Jang-Lyul Kim</i>	1360
Effect of Radon Progeny on Real Time Alpha-CAM Monitoring in Uranium Facility	
<i>Authors: TaeHyoungh Kim, JunBok Lee, Jong Il Lee, Bong Hwan Kim</i>	1361
PoCAMon – All in one Personal Online Continuous Air Monitor, Gamma Dose Meter and Gas warner	
<i>Author: Thomas Strel</i>	1362

R Implementation of ICRP 116 Dose Conversion Coefficients for Reconstructing Organ Dose in a Radiation Compensation Program <i>Authors: Timothy Taulbee, Keith McCartney, Richard Traub, Matthew Smith, James Neton</i>	1363
Tracking System for Radiation Works Using Passive RFID Technology to Enhance Radiation Protection <i>Authors: Yunjong Lee, Jin Kyu Kim, Jinwoo Lee, Young-Hwan Ryu, Ho-Sung Kim, Kyung-Rae Dong, Eun-Jin Choi</i>	1364
Capability Study of Multi-function Dose Rate Meter Based on Hemisphere CdZnTe Detector <i>Authors: Ying Wang, Wenjun Xiong, Zhiping Luo, Jizeng Ma, Ling Chen</i>	1365
Combination of Automated Chromatographic Separation and Off-line Cherenkov Counting in Determination of Low Level Activity of Sr-90 <i>Authors: Željko Grahek, Ivana Coha</i>	1366

VOLUME 4

Area 7: Environment and Natural Background	1367
Health Detriment Associated with Exposure to Natural Radioactivity from the Soil of Ondo and Ekiti States South Western, Nigeria. <i>Authors: A.E. Ayodele, A. M. Arogunjo, J. I. Ajisafe, O.T. Arije</i>	1368
Radioactivity Level of Drilled Well Water across Selected Cities in Ondo and Ekiti States, Southwestern Nigeria and its Radiological Implications <i>Authors: A. E. Ayodele, A. M. Arongunjo, J. I. Ajisafe, O. T. Arije</i>	1376
Dating of a sediment core from Lake Biel (Switzerland) and source characterization of fallout Pu <i>Author: Anja Pregler</i>	1382
Preliminary survey of radon population exposure in east Romanian region <i>Authors: Andreea Teodor, Irina Anca Popescu, Constantin Milu</i>	1390
Excess Lifetime Cancer Risk of Cosmetic Powders <i>Authors: Chioma Nwankwo, Damilola Folley, Olawunmi Gbolagade</i>	1397
Monitoring of ambient dose equivalent at the boundary of nuclear sites to verify compliance with the regulations <i>Authors: Cristina P. Tanzi, M. Farahmand, P. Kwakman, R.B. Tax, A.P.P.A. van Lunenburg, G.J.E Slagt, L.P. Roobol</i>	1404
Determination of the activity concentrations of natural occurring radionuclides in foodstuffs for public dose assessments <i>Authors: Deon Kotze, Immanda Louw, Charles Krös</i>	1409
Monitoring the environmental radiation by using a new gas-filled proportional counter probe as a quasi-spectroscopic system <i>Authors: Dirk Peter Schmalfuß, Uwe Hoffmann, Julia Glück, Andreas Meister</i>	1416
Radiological assessment of natural radioactivity in groundwater from Greater Accra Region of Ghana: Gross alpha and gross beta measurements and annual committed effective dose evaluation. <i>Authors: E.J.M.Nguelem, M.Ndontchueng, E.O.Darko</i>	1422
Correlations of Radon Measurements in Soil Gas and Indoor for Improving the Prediction of an Area's Radon Potential <i>Authors: Franz Kabrt, Andreas Baumgartner, Harry Friedmann, Valeria Gruber, Wolfgang Ringer, Franz Josef Maringer</i>	1429
Radiation Measurement Systems and Experiences in Japan after the Fukushima Accident <i>Author: Frazier L. Bronson</i>	1437
Environmental radiation monitoring in the gold mining region East Cameroon <i>Authors: Dallou G. B., Ngoa Engola L., Ndjana Nkoulou II, J.Emmanuel, Saïdou, Kwato Njock M. G.</i>	1446

Environmental Dosimetry of Mining Areas: Case of Abandoned Uranium Site, Vinaninkarena- Antsirabe, Madagascar	
<i>Authors: Hary A. Razafindramiandra, Tiana h. Randriamora , Elijaona H. Rakotomalala Anja, Raelina Andriambololona, R. Dina Randriantsizafy, Mbolatiana A. L. Ralaivelo , Edmond Randrianarivony, Solofonirina D. Ravelomanantsoa, Joseph L. R. Zafimanjato, H. Fanja Randriantseheno</i>	1454
The European Radioecology Alliance: Encouraging the Coordination and Integration of Research Activities in Radioecology	
<i>Authors: Hildegard Vandenhove, Jacqueline Garnier-Laplace, Almudena Real, Maarit Muikku, Catherine Lecomte-Pradines, Åste Søvik, Brenda J. Howard, Pere Masque, Rafael Tenorio</i>	1461
A cancer risk due to natural radiation on the Coast of Montenegro	
<i>Authors: Ivanka Antović, Nikola Svrkota, Danko Živković, Nevenka M. Antović</i>	1470
A Survey of Indoor Gamma Dose Rates in Selected Dwellings and Offices in Abeokuta, South Western Nigeria	
<i>Authors: Okeyode, I.C., Oladotun, I.C., Mustapha, A.O., Alatise, O.O., Bada, B.S., Makinde V., Akinboro, F.G., Al-Azmi, D.....</i>	1478
Natural radioactivity of samples from the building industry in South Africa	
<i>Authors: I. Ramathhape, D. Kotze, I. Louw.....</i>	1486
The ICRP Publication 126 on Radiological Protection against Radon Exposure	
<i>Authors: Jean-François Lecomte, Stephen Solomon, John Takala, Thomas Jung, Per Strand, Christophe Murith, Sergey Kiselev, Weihai Zhuo, Ferrid Shannoun, Augustin Janssens</i>	1492
Curies Contaminated Notebook	
<i>An analysis of a notebook and papers, originally belonging to Marie Curie, which are now retained by the Wellcome Collection, London</i>	
<i>Authors: Lindsey Simcox, Jon Taylor</i>	1497
Comparison of Federal Guidance Reports 12 and 15: External Exposure to Radionuclides in Soil, Air, and Water	
<i>Authors: M.B. Bellamy, K.G. Veinot, M.M. Hiller, S.A. Dewji, K.F. Eckerman, C.E. Easterly, N.E. Hertel, R.W. Leggett.....</i>	1504
Thoron Exhalation Rate and ²³²Th Content in Traditional Building Materials Used in the Coastal Region of Kenya	
<i>Authors: Margaret Chege, Nadir Hashim, Abdallah Merenga, Oliver Meisenberg, Jochen Tschiersch</i>	1511
A comparison of a commercial and specifically developed (CTBTO-VGSL) software packages used in high-resolution gamma-spectrometry on their applicability and accuracy in NORM analysis of environmental samples, which includes optimization of spectrum analysis parameter settings and sum-coincidence and self-absorption corrections	
<i>Authors: Monnicca M. Rapetsoa, Arnaud Faanhofa, Deon Kotze, Robert Lindsay</i>	1515
K-40 levels in the South Adriatic Sea environment (Montenegro)	
<i>Authors: N. M. Antović, I. Antović, N. Svrkota.....</i>	1520
Would Radiation Deter Space Exploration	
<i>Author: Nicholas Sion</i>	1528
Development of absolute measurement instrument for radioactivity of Radon gas	
<i>Authors: Rio Furukawa, Yasuhiro Unno, Akira Yunoki, Yasushi Sato</i>	1538
Determination of radon emission rate regarding to constructional energy- saving-measures	
<i>Authors: Thomas Neugebauer, Hans Hingmann, Jonas Buermeyer, Anna-Lisa Grund, Volker Grimm†, Joachim Breckow</i>	1543
Selection of Potassium Fertilizer Application Method to Reduce Uptake of Cs-137 in Brown Rice	
<i>Authors: Takashi Saito, Kazuhira Takahashi, Takeshi Ota, Tomoyuki Makino.....</i>	1550
Findings of the control and monitoring of liquid releases from the Centre of Isotopes of Cuba	
<i>Authors: Zayda Haydeé Amador Balbona, Pilar Oropesa Verdecia</i>	1557
Findings of the control and monitoring of airborne releases from the Centre of Isotopes of Cuba	
<i>Authors: Zayda Haydeé Amador Balbona*, Miguel Antonio Soria Guevara</i>	1564

Radiation Ecology and Human Health. Regional and Global Problems	
<i>Authors: Z.Paskalev, G.Vassilev, V.Baduline, D.Apostolova</i>	1570
Potassium-40 determination in NPK fertilizer by CZT-500s gamma spectrometry in the LPNPE Lab	
<i>Authors: A. Justinien Franck Ratovonjanahary, Hery Tiana Rakotondramanana, Haritiana L. Ralalarisoa, H. Léonce Randria-Mampianina, Solofonirina D. Ravelomanantsoa</i>	1572
Characterization of Airborne Particulates Containing Naturally Occurring Radioactive Materials in Investment Casting Facilities	
<i>Authors: Yong Gun Kim, Cheol Kyu Choi, Boncheol Goo, Kwang Pyo Kim</i>	1578
Spatial Distribution of Naturally Occurring Radioactive Materials (^{235}U, ^{238}U, ^{228}Th, ^{230}Th, ^{232}Th, ^{226}Ra, ^{228}Ra and ^{40}K) in the Marine Sediment Samples Along the Red Sea Coast of Saudi Arabia	
<i>Authors: A. A. Alzahrany, M. A. Farouk, E. I. Shabana, A. A. Al-Yousef, K. N. Alnajem, F. I. Al-Masoud</i>	1584
Radon Mass Exhalation Rates of Selected Building Materials in Tanzania	
<i>Authors: Aloyce Amasi, Kelvin Mark Mtei, Pawel Jodlowski, Chau Nguyen Dinh</i>	1585
Assessment of Natural Radionuclide Content of Some Public Well Water within Ondo and Ekiti States, South-western Nigeria	
<i>Authors: Adeolu Ayodele, Adeseye Arogunjo, Olubodun Arije</i>	1586
Study of Particular Problems Appearing in NORM Samples and Recommendations for Best Practice Gamma-ray Spectrometry	
<i>Authors: Andreas Baumgartner, Michael Stietka, Franz Kabrt, Hannah Moser, Franz Josef Maringer</i>	1587
Public Exposure due to Radon and External Radiation from Ornamental Rock Indoors	
<i>Authors: André Luiz do Carmo Leal, Dejanira da Costa Lauria</i>	1588
Outdoor Thoron and Thoron Progeny in a Thorium-rich Area in Norway	
<i>Authors: Anne Liv Rudjord, Hallvard Haanes, Trine Kolstad, Alexander Mauring, Ingvild Finne, Sven Dahlgren</i>	1589
Advanced Approach to Assessment of Potential Radon Hazard of Building Sites in Russia	
<i>Authors: Albert Marennyy, Peter Miklyaev, Andrey Tsapalov, Tatyana Petrovac, Sergey Kiselev</i>	1590
Complex Monitoring Study of Radon Field Generation in Soils under Various Geological and Climatic Conditions in Russia (2011 – 2015)	
<i>Authors: Albert Marennyy, Peter Miklyaev, Andrey Tsapalov, Andrey Penezhev, Sergey Kiselev</i>	1591
Area Monitoring of Ambient Dose rates in some parts of South Western Nigeria using a GPS integrated Dosimetric System	
<i>Authors: A.O. Mustapha, O.O. Alatise, I.C. Okeyode, V. Makinde, F.G. Akinboro, D. Al-Azmi</i>	1592
Dose Assessment from Groundwater Water Consumption in Central Portugal	
<i>Authors: Alcides Pereira, Luis Neves</i>	1593
Experimental and Numerical Studies for Understanding of Radon Emanation in Environmental Materials	
<i>Authors: Akihiro Sakoda, Yuu Ishimori</i>	1594
The Principle of Uncertainty Assessment of the Average Annual Radon Indoor based on Measurement Results of Different Duration	
<i>Authors: Andrey Tsapalov, Albert Marennyy, Peter Miklyaev, Sergey Kiselev</i>	1595
The Effect of Relative Humidity and Temperature Variability on Continuous Environmental Radon Monitoring	
<i>Author: Bashir Muhammad</i>	1596
Forecast and Analysis of Atmospheric Effluent Deposition Influenced by Buildings of Nuclear Power Plant under Normal Operation	
<i>Authors: Bo Wang, Qiong Zhang, Ruiping Guo</i>	1597
Radon and Energy Efficient Buildings	
<i>Authors: Constantin Cosma, Alexandra Cucos, Tiberius Dicu</i>	1598
Assessment of Radiological Hazards from Gold Mine Tailings in Gauteng Province, South Africa	
<i>Authors: Caspah Kamunda, Manny Mathuthu, Morgan Morgan</i>	1599

Sensitivity Study of Inhalation Dose by Airborne Particulate Properties <i>Authors: Cheol Kyu Choi, Yong Gun Kim, Jaekook Lee, Kwang Pyo Kim</i>	1600
The ICRP System for Radiation Protection of the Environment <i>Authors: Carl-Magnus Larsson, Kathryn Higley, Almudena Real, David Copplestone, Jacqueline Garnier-Laplace, Jianguo Li, Kazuo Sakai, Per Strand, Alexander Ulanovsky, Jordi Vives i Batlle</i>	1601
Spatial Distribution of Background Radiation in Kuwait Using Different Car Borne Gamma Probes <i>Author: Darwish Al-Azmi</i>	1602
Verification of Skin-Point-Source Method to Assess Annual Effective Dose by Usage of TENORM Added Consumer Products <i>Authors: Do Hyeon Yoo, Wook-Geun Shin, Jae Kook Lee, Yeon Soo Yeom, Chan Hyeong Kim, Chul Hee Min</i>	1603
A Dynamic Model to Assess Radiation Dose Rate of Biota in Freshwater Lake <i>Authors: Dong-Kwon Keum, In Jun, Kwang-Muk Lim, Byeong-Ho Kim, Yong-Ho Choi</i>	1604
Radioecological Assessments of Natural Occurring Radioactive Materials and Dose Estimation of The Public Residing Around Mt. Homa, Homabay County, Kenya <i>Authors: David Otwoma, Simon Bartilol, Jayant Patel</i>	1605
Novel Method to make a Calibrated Thoron Source <i>Authors: Elmughera Elhag, Robert Lindsay, Joash Ongori</i>	1606
Radon Gas and Other NORM Testing of Building Materials in Israel for Public Health and Safety (Category 3F) <i>Author: Ehud Ne'eman</i>	1607
Cost-Benefit Analysis Approach to Risk Assessment of Natural Radioactivity in Powdered and Liquid Milk Products Consumed in Nigeria <i>Authors: Ezekiel O. Agbalagba, Gregory O. Avwiri</i>	1608
Comparison of Efficiency of Techniques Radon Measurement (^{222}Rn) in Air and Water with Active Detectors and Passive Detectors <i>Authors: Evaldo Paulo de Oliveira, Paulo Roberto Rocha Ferreira, Mariza Ramalho Franklin</i>	1609
Organization, Some Results and Perspectives of Protection from Radon in Italy in the European Context <i>Authors: Francesco Bochicchio, Sara Antignani, Carmela Carpentieri, Gennaro Venoso</i>	1610
 The IUR FORUM : Worldwide harmonization of networks to support integration of scientific knowledge and consensus development in radioecology <i>Authors: François Bréchnignac, Rudolf Alexakhin, Andréas Bollhöfer, Kristin E. Frogg, Frank Hardeman, Kathy Higley, Thomas G. Hinton, Lawrence A. Kapustka, Wendy Kuhne, Kins Leonard, Olivier Masson, Kenji Nanba, Graham Smith, Karen Smith, Per Strand, Hildegard Vandenhove, Tamara Yankovich, Satoshi Yoshida</i>	1611
Thoron: Radon's Lesser-Known Sister – Results from a National Survey in the Netherlands <i>Authors: Fieke Dekkers, Roelf Blaauboer, Martijn vd Schaaf, Harry Slaper, Ronald Smetsers</i>	1613
^{40}K, ^{226}Ra And ^{228}Ra in Soils of Rio de Janeiro State, Brazil: A Preliminary Study <i>Authors: Fernando Ribeiro, Dejanira Lauria, Jose Ivan Silva, Fernanda Cunha</i>	1614
Gamma in Situ Survey in an Experimental Research Area <i>Authors: Fernando Ribeiro, Rocio Reis, Monique Gabriel</i>	1615
Measurement of ^{137}Cs and ^{40}K in Wild Mushrooms and their Transfer Factors <i>Authors: Fei Tuo, Qiang Zhou, Jing Zhang, Wenhong Li, Qing Zhang</i>	1616
Assessment of Natural Radioactivity and its Radiological Impact in Ortum Region in Kenya <i>Author: Felix Wanjala</i>	1617
Radiation from Building Materials in South Africa including Granite Samples with High Concentrations of Radium <i>Authors: Farrel Wentzel, Robert Lindsay</i>	1618
Ionising Radiation from the Zanzibar Coastline: Exposure to Residents and Tourists Visiting Zanzibar <i>Authors: Gharib Mohamed, Robert Lindsay, Peane Maleka, Joash Ongori</i>	1619

Results from Interlaboratory Comparison on Gross Alpha/Beta Activity Measurement in Waters <i>Authors: Gordana Pantelic, Marija Jankovic, Natasa Sarap, Dragana Todorovic</i>	1620
Source Identification of Iodine-131 in Environmental Samples around the HANARO <i>Authors: Geun-Sik Choi, Jong-Myoung Lim, Young-Gun Ko, Mee Jang, Won-Young Kim, Wannoo Lee, Young-Yong Ji, Hyuncheol Kim, Chang-Jong Kim, Young-Hyun Cho, Chung-Sup Lim, Kun-Ho Chung</i>	1621
Natural Radioactivity Systematics in a Complex Hydrothermic Environment <i>Authors: Hudson Angeyo Kalambuka, Paul Tambo, Jayanti Patel, Michael Mangala</i>	1622
Measurements of Radon Concentrations in Drinking Water in Cities, China <i>Authors: Hongxing Cui, Yunyun Wu, Bing Shang, Jianxiang Liu</i>	1623
¹⁴C Activity in Atmospheric CO₂ and Biological Samples Around the Nuclear Power Plant Krško, Slovenia <i>Authors: Ines Krajcar Bronić, Bogomil Obelić, Jadranka Barešić, Nada Horvatinčić, Borut Breznik, Aleš Volčanšek, Andreja Sironić, Damir Borković</i>	1624
Control of Emissions from a Gold and Uranium-mining Polluted Catchment in a Semi-arid Region of South Africa: The Varkenslaagte Stream <i>Authors: Isabel Weiersbye, Peter Dye, Hlanganani Tutu, Ewa Cukrowska, Christopher Curtis, Julien Lusilao, Elisee Bakatula, Bruce McLeroth, Jozua Ellis, Etienne Grond, Maxine Joubert, Salome Mthombeni, Ike Rampedi, Christopher Davies, Patricia Omo-Okoro, Henk Nel, Joel Malan, Herman Coetzee</i>	1625
The Potential for Phytoremediation of Uranium Contaminated Substrata on the Witwatersrand Basin of South Africa: Extraction and Harvesting Versus in Situ Sequestration <i>Authors: Isabel Weiersbye, Ewa Cukrowska, Jozua Ellis, Peter Dye, Bruce McLeroth, Hlanganani Tutu, Luke Chimuka, Nosipho Mntungwa, Maxine Joubert, Shakera Arendse</i>	1626
Uranium in Phosphate mining <i>Author: Jacques Bezuidenhout</i>	1627
Uranium in Wild and Cultivated Leafy Vegetables and Consumption Patterns: A Risk Assessment <i>Authors: Jenny Botha, Isabel Weiersbye, Jozua Ellis, Hlanganani Tutu</i>	1628
® Calculation of Lifetime Lung Cancer Risks Associated with Indoor Radon Exposure Based on Various Radon Risk Models <i>Author: Jing Chen</i>	1629
Measurement Results of Background Radiation Levels in Seals <i>Authors: Jing Chen, Weihua Zhang, Baki Sadi, Xiaowa Wang, Derek Muir</i>	1630
The Current Status and Plans for Safety Management of NORMs in South Korea <i>Authors: Jaekook Lee, Jaewoo Park, Zu Hee Woo, Boncheol Koo, Ki Hoon Yoon, Chang-Su Park, Byung-Uck Chang</i>	1631
Pre-assessment of Dose Rates for Marine Biota from Discharge of Nuclear Power Plants <i>Authors: Jingjing Li, Senlin Liu, Yongxing Zhang, Ling Chen, Yuan Yan, Weiya Cheng, Hailin Lou, Yongbao Zhang</i>	1632
Radon Profiles in Soil on Mine Dump <i>Authors: Joash Ongori, Robert Lindsay</i>	1633
Internal Radiation Exposure Dose From Some Commonly Consumed Food Stuff in Lagos A Commercial City in Nigeria <i>Authors: Kayode I. Ogungbemi, Moses A. Aweda, Olusola O. Oyebola, Margarent A. Adedokun, Chima E. Ireogbu</i>	1634
Seasonal and Diurnal Variation of Outdoor Radon Concentrations in Urban and Rural Area of Morocco <i>Authors: Lhoucine Oufni, Rabi Rabi</i>	1635
® Study on a step-advanced filter monitor for continuous radon progeny measurement <i>Authors: Lei Zhang, Jinming Yang, Qiuju Guo</i>	1636
Survey of the Radon Environment within Lagos State Nigeria: A Preliminary Report <i>Authors: Margret Akinloye, Oluwasayo Abodunrin</i>	1637

The Importance of Understanding Basic Concepts in Radiological Environmental Impact Assessment <i>Authors: Moon Hee Han, Hae Sun Jeong, Hyo Joon Jeong, A Reum Kil, Eun Han Kim, Won Tae Hwang</i>	1638
High Precision Gamma Dose Rate Measurements using a Spectroscopic Pager <i>Authors: Michael Iwatschenko-Borho, Erich Leder, Ralf Pijahn, Norbert Trost</i>	1639
Tritium Content in the Velika Morava River Basin: Evaluation Effective Ecological Half-Life <i>Authors: Marija Jankovic, Natasa Sarap, Gordana Pantelic, Dragana Todorovic</i>	1640
Assessing the Northern Benguela Upwelling System for Radioactivity Levels: A Baseline Study <i>Authors: Martina Rozmaric, Deon Charles Louw, Isabelle Levy, Oxana Blinova, Mai Khanh Pham, Jean Bartocci, Iolanda Osvath, David Osborn, Samorna Brian Mudumbi, Tuuovauri Kauroua Sharon Kahunda, Elena Chamizo, Ljudmila Benedik</i>	1641
Comprehensive radionuclide analysis and dose assessment of thermal and mineral waters in Croatia <i>Authors: Krmpotić Matea, Rožmarić Martina, Petrinc Branko, Bituh Tomislav, Benedik Ljudmila, Fiket Željka</i>	1642
Radioactivity values for soil replaced at some building at Tikrit University <i>Author: Mohanad Salih</i>	1643
Development of a Measurement Procedure for Radon in Waterworks <i>Author: Michael Stietka, Andreas Baumgartner, Franz Kabrt, Franz Josef Maringer</i>	1644
Natural Radionuclides in River Sediments of Poços de Caldas Plateau - Brazil: Geogenic or Anthropogenic Contribution? <i>Authors: Nivaldo Da Silva, Heber Alberti, Marcos Roberto Nascimento, Rodrigo Bonifácio, Heliana Azevedo, Raul Villegas</i>	1645
Pubic Exposure due to Indoor Radon in Three Municipalities of Poços de Caldas Plateau - Brazil <i>Authors: Nivaldo Da Silva, Berenice Navarro, Ubirani Otero, Tarcisio Cunha</i>	1646
Estimation of Terrestrial Air-Absorbed Dose Rate from the Data of Regional Geochemistry Database <i>Authors: Nan Gan, Kuang Cen, Rong Ye</i>	1647
The Study of Environmental Contamination and Public Health in the Vicinity of the Uranium Legacy Sites in the Tajik Republic <i>Authors: Natalya Shandala, Vladimir Seregin, Aleksandr Tukov, Sergey Kiselev, Vladimir Shlygin, Aleksandr Pozhidaev, Mirzoshokir Hojion</i>	1648
The Study of Environmental Contamination and the Public Health in the Vicinity of Uranium Legacy Sites in the Kyrgyz Republic <i>Authors: Natalia Shandala, Vladimir Seregin, Aleksandr Tukov, Sergey Kiselev, Aleksey Titov, Sergey Akhromeev, Aleksandr Pozhidaev, Gulnura Abasova, Aleksander Samoylov</i>	1649
Estimation of Natural Ionizing Radiation Levels Based on the Data of Gamma- Ray Spectrometry and Regional Geochemical Data in Zhuhai City Urban, China <i>Authors: Nanping Wang, Ling Zheng, Xingming Chu, Ting Li, Hongtao Liu, Xiaohong Meng</i>	1650
Evaluation of Radioactivity Concentrations in Some Bottled Drinking Water Produced in Nigeria and Associated Radiological Risk to Consumers <i>Authors: Oladele Ajayi, Ademola Abokede</i>	1651
Radiological Hazard Assessment of Natural Radionuclides in Soils of Some Oil-Producing Areas in Imo State, Nigeria <i>Authors: Oladele Ajayi, Chidiebere Dike</i>	1652
Radionuclide Concentrations in Edible Mushrooms Consumed in South- Western Nigeria and Radiation Dose Due to their Consumption <i>Authors: Oladele Ajayi, Olusola Omotoso</i>	1653
Vertical Migration of Some Natural Radionuclides in Soils of Some Oil- Producing Areas in Imo State, Nigeria <i>Authors: Oladele Ajayi, Chidiebere Dike</i>	1654
Assessment of Radionuclide Concentrations in Some Cereals and Tea Products Available in Nigeria <i>Authors: Olufunmilayo Alatise, Ireti Okeyode, Christianah Adebessin</i>	1655

Radioactivity Levels in Samples of Detergent Powder available in Local Markets of South-western Nigeria <i>Authors: Olufunmilayo Alatise, Thomas Olaniyan</i>	1656
Polonium-210 Concentration in Cuban Tobacco Products and their Contribution to the Annual Effective Dose by Inhalation of Cigarette Smoke <i>Authors: Osvaldo Brígido-Flores, Orlando Fabelo-Bonet, Adelmo Montalván-Estrada</i>	1657
Cancer Risk from Radon in Drinking Water in South-western Nigeria <i>Authors: Olatunde Michael Oni, Adetola Olive-Adelodun, Emmanuel Abiodun Oni</i>	1658
Radiological Impact Assessment within the Context of the Environmental Impact Assessment Process Associated with the Proposed South African Nuclear Power Programme; Challenges Associated with a Multiagency and Regulatory Overlap Environment <i>Authors: Paul Fitzsimons, Elisabeth Nortje</i>	1659
Integrating the Radiation Protection System for Human and Non-Human Biota: How to do it in Practice <i>Authors: Diego Telleria, Peter Johnston</i>	1660
A Map of Moscow Geogenic Radon Potential <i>Authors: Peter Miklyaev, Tatyana Petrova, Albert Marennyy, Andrey Tsapalov, Sergey Kiselev</i>	1661
Outdoor Radon Levels in China <i>Authors: Qifan WU, Ziqiang Pan, Senlin Liu</i>	1662
A Platform for Assessment of Doses to the Public from Routine Discharges of Radionuclides to the Environment from Nuclear Installations <i>Authors: Rodolfo Avila, Robert Broed, Erik Johansson, Vladimir Maderich, Roman Bezhenar</i>	1663
Radon In-Air Assessments within Selected Wine Cellars in the Western Cape (South Africa) and its Associated Effective Radiation Exposure Dose <i>Authors: Ryno Botha, Robert Lindsay, Richard Newman, Peane Maleka</i>	1664
Environmental Thoron: Monitoring, Techniques and Dose Conversion <i>Author: Rakesh Chand Ramola</i>	1665
Influence of Release Height on Radioactive Gas Effluent in Short-term for Nuclear Power Plant in China <i>Authors: Ruiping Guo, Chunlin Yang, Chunming Zhang</i>	1666
Synergistic Effect of Caffeine and Melatonin against Radiation Induced Damage in C57BL/6 Mice at Sub Lethal Radiation Dose <i>Authors: Ritu Kushwaha, Dhruv K Nishad, Aseem Bhatnagar</i>	1667
Radiation Protection Calculations for both ingestion of ²²⁶Ra and ²²⁸Ra in Reservoir and Spring Water from Central Region of Cameroon <i>Authors: Rose Lydie Marie, Oum Keltoum Hakam, Abdel Majid Choukri</i>	1668
Gamma-emitting Radionuclides Analysis in Water Samples from Two Mines in South Africa <i>Author: Raymond Njinga</i>	1669
Setting Up a Continuous Monitor for Controls the Temporal Variability of ²²²Rn in the Atmosphere and Groundwater of the Tadla Basin, Morocco <i>Authors: Radouan Saadi, Hamid Marah, Oum Keltoum Hakam</i>	1670
Radon-thoron Discriminative Measurements and Corresponding Dosimetry in the Thorium Bearing Region of Lolodorf, Cameroon <i>Authors: Saidou, Shinji Tokonami, Miroslaw Janik</i>	1671
A New Facility for Assuring the Measurements Traceability in the Environment Dosimetry <i>Authors: Sorin Bercea, Aurelia Celarel, Constantin Cenusă, Elena Iliescu, Ioan Cenusă</i>	1672
Bioaccumulation Factor of the Heavy Metal in Marine Organism from the Korean Coast <i>Authors: Seokwon Choi, Heungjun Cho, Daeji Kim, Jungseok Chae</i>	1673
In-situ Measurements of Radon Levels in Water, Soil and Exhalation Rate using Continuous Active Radon Detector <i>Author: Sanjeev Kumar</i>	1674

Exposure to External Gamma Radiation Emitted from Soil of the High Background Radiation Areas of Ramsar Reduces Bacterial Susceptibility to Antibiotics <i>Authors: SMJ Mortazavi, Samira Zerei, Mohammad Taheri, Saeed Tajbakhsh, S Ranjbar, F Momeni, Samaneh Masoumi, Leila Ansari, SAR Mortazavi, Masoud Haghani, S Taeb</i>	1675
Discharge of Gaseous Radioactive Waste in FDG Synthesis: Clearance Levels and Licensing in Italy <i>Authors: Sandro Sandri, Maurizio Guarracino, Ruggero Cifani</i>	1676
External Evaluation of the Amounts of Exposures and Intern to the Telluric Radiations Gamma, in the South-East of Gabon <i>Authors: Sylvere Yannick Loemba Mouandza, Alain-Brice Moubissi, Germain Hubert Ben-Bolie, Patrice Ele Abiama, Bouchra Ramzi, Mohammed Zaryah</i>	1677
Challenges in Managing Exposures due to Natural Radiation Sources <i>Authors: Tony Colgan, Trevor Boal</i>	1678
Radioactivity in Some Leafy Vegetables in Roodepoort South Africa <i>Authors: Thulani Dlamini, Victor Tshivhase, Manny Mathuthu</i>	1679
Determination of Natural Radioactivity in the North East Beach Sands of Madagascar <i>Author: Tiana Harimalala Randriamora</i>	1680
Availability and Reliability of Meteorological Data for Atmospheric Dispersion Models <i>Authors: Tamas Pázmándi, Sándor Deme, Lilla Hoffmann, Péter Szántó</i>	1681
A Study on Adsorption of the Radioactive Noble Gases in the Atmosphere by a Portable Sampling System <i>Authors: Wannoo Lee, Young-Yong Ji, Young-Hyun Cho, Sando Choi, Jiyoung Park, Geen-sik Choi, Hyuncheol Kim, Jong-Myong Lim</i>	1682
Animal-to-water Concentration Ratios of Various Elements in Marine Ecosystems around two Korean Nuclear Sites <i>Authors: Yong-Ho Choi, Kwang-Muk Lim, In Jun, Byung-Ho Kim, Dong-Kwon Keum</i>	1683
Review of Approaches based on ^{210}Po and other Daughters of ^{222}Rn for Retrospective Estimate of Radon Concentration <i>Authors: Yazdan Salimi, Mohammad Reza Kardan, Mohammad Reza Deevband, Dariush Askari, Jalal Ordoni, Mohammad Hossein Jamshidi, Hamed Dehghani, Fatemeh Ramrodi, Hamid Behrozi</i>	1684
A Simple Method for Measurement of Radon in Groundwater <i>Authors: Yunyun Wu, Hongxing Cui, Bing Shang, Jianxiang Liu</i>	1685
Application of Non-equilibrium Adsorption Model in the Migration of Radionuclides <i>Author: Zhu Jun</i>	1686
Environmental Impact Assessment of the NPP Krško for Period of 5 years <i>Authors: Zeljka Knezevic, Zeljko Grahek, Borut Breznik</i>	1687
Area 8: Transport / Sealed Source Management	1688
Validation Testing of Canberra-Obayashi Mobile type TruckScan Pre- production Unit <i>Authors: Atsuo Suzuki, Frazier L. Bronson, Masaru Noda, Naoya Takada, Keizo Yamasaki</i>	1689
Regulatory actions in the case of a radioactive source stuck in an oil well <i>Authors: Marcela G. Ermacora, Claudia Chiliutti, Valeria Amado, Horacio Lee Gonzáles, Hugo Vicens</i>	1700
Safety and security of sealed sources during transportation to remote area in Egypt <i>Author: M A M Gomaa</i>	1707
Orphan sources search and secure in Republic of Serbia – planning, implementation and current status <i>Authors: Milan Vujovic, Maja Eremic-Savkovic, Ivana Avramovic, Vedrana Vuletic, Slađan Velinov</i>	1710
The worldwide problem of Disused Sealed Radioactive Sources (DSRS) and what should be done to alleviate the situation. <i>Author: Robin George Heard</i>	1718

Assessment of the radiological consequences of accidents in vehicle transportation of radioactive material in the area of Bologna	
<i>Authors: Sara Vichi, Sara Baldazzi, Angelo Infantino, Gianfranco Cicoria, Giulia Lucconi, Domiziano Mostacci, Mario Marengo</i>	1725
Actions for Spent Radioactive Sources Removal	
<i>Authors: Teresa Ortiz, Elena Alcaide</i>	1732
Leak Radiation Assessment of Scanner HCV-Mobile, THSCAN Scanner And Scanner HCP-Portal	
<i>Authors: Tahiry Razakarimanana, H.A. Razafindramandra, Raelina Andriambololona, J.L.R. Zafimanjato, R.D. Randriantsizafy</i>	1738
Occupational exposure in the transport of radioactive materials in Cuba	
<i>Authors: Zayda Haydeé Amador Balbona, Miguel Antonio Soria Guevara</i>	1743
Safety Assessment for Incident-Free Pilot Transportation of Decontamination Radioactive Waste Resulting from the Fukushima Nuclear Power Plant Accident	
<i>Authors: Min Jun Kim, A Ra Go, Kwang Pyo Kim</i>	1750
Operation of Radiation Source Location Tracking System	
<i>Authors: BokHyoung Lee, CheolHong Um, KiWon Jang, DaeHyung Cho</i>	1758
Designing a Physical Protection System for the 444 TBq Co-60 Irradiation Facility at the Centre for Applied Radiation Science and Technology, Mafikeng, South Africa	
<i>Authors: Cyrus Cyril Arwui, Victor Tshivhase</i>	1759
IAEA Approach to Cradle to Grave Control and Management of Disused Sealed Radioactive Sources	
<i>Authors: Monika Kinker, Gerard Bruno, Hilaré Mansoux</i>	1760
Safety Case of The Libyan Central Radioactive Waste Storage Facility	
<i>Authors: Husam Shames, Usama Elghawi</i>	1761
Safety and Radiation Protection Requirements for Cargo and Containers Inspection Services in Brazil	
<i>Authors: Josilto Aquino, Alfredo Ferreira Filho, Marcello Nicola</i>	1762
Radiation Protection in Radioactive Material Transport	
<i>Authors: Li Guoqiang, Zhuang Dajie, Wang Xuexin, Sun Hongchao, Wang Renze, Zhang Jianguang</i>	1763
Practical Application Illustrating Excellence in the Safety and Security of Industrial Radiography Sources Employed at the Eskom, Generation Power Stations	
<i>Author: Marc Maree</i>	1764
Safe Transport of Radioactive Material in Argentina	
<i>Authors: María Soledad Rodríguez Roldán, Alejandro Fernández, Emiliano Juanena, Christian Elechosa</i>	1765
Spent fuel elements transfer between the Units I and II of the Atucha Nuclear Power Plant in Argentina	
<i>Authors: María Soledad Rodríguez Roldán, Alejandro Fernández, Emiliano Juanena, Christian Elechosa</i>	1766
Challenges in Managing Radiation Safety Program at a Biotech Facility	
<i>Author: Rao Goriparthi</i>	1767
Intermediate Nuclear Waste Return December 2015	
<i>Author: Steven Dimitrovski</i>	1768
Strategies to Improve the Safety Culture in the Field of Industrial Radiography in Peru	
<i>Author: Susana Gonzales</i>	1769
Detection of Orphan Industrial Neutron and Americium Sources in Metal Scrap Cargo	
<i>Author: Michael Iwatschenko-Borho</i>	1770
Area 9: Non-Ionising Radiation	1771
Evaluation of bone density importance in pediatric MR only treatment planning	
<i>Authors: Banafsheh Zeinali-Rafsanjani, Reza Faghihi, Mahdi Saeedi-Moghadam, Reza Jalli</i>	1772

Simulation of heat distribution in a phantom for a Philips Sonalleve MRgHIFU unit <i>Authors: Barbara Caccia, Silvia Pozzi, David Bianchini, Francesco Marcocci, Enrico Menghi, Marcello Benassi</i>	1776
Ⓜ Extrapolation techniques for evaluation of 24 hours average electromagnetic field emitted by Radio Base Station installations: spectrum analyzer measurements of LTE and UMTS signals <i>Authors: Elisa Nava, Stefano Mossetti, Daniela de Bartolo, Ivan Veronese, Marie Claire Cantone, Cristina Cosenza</i>	1777
Managing Non-Ionizing Radiation through International Basic Safety Standards <i>Authors: Jacques Abramowicz, Efthymios Karabetos, Sigurdur Magnusson, Rudiger Matthes, Mirjana Moser, Shengli Niu, John O'hagan, Rick Tinker, Emilie Van Deventer</i>	1778
Designing a Laser Lab, Errors and Solutions <i>Author: Ken Barat</i>	1779
Threshold Dose Estimation for Short Delay Onset of Cataract after In Vivo exposure to Ultraviolet Radiation, a General Strategy for Threshold Estimation for Continuous Dose Response Functions <i>Authors: Per Söderberg, Konstantin Galichanin, Nooshin Talebizadeh, Zhaohua Yu</i>	1780
Effects of Early Life Exposure to RF Fields <i>Authors: Kerry Broom, Jutta Jarvinen, Darren Addison, Zenon Sienkiewicz</i>	1781

VOLUME 5

Area 10: Emergency Preparedness and Management	1782
Study on the Protection Planning Actions and Response to Nuclear or Radiological Emergency <i>Authors: Perez, Clarice F.A., Sahyun, Adelia, Freitas, Kenia A.M.</i>	1783
The reality of the low radiation dose on population in Fukushima Daiichi 20km zone <i>Author: Jun Takada</i>	1788
🗣 Application of virtual reality technology to minimize the dose to the example of staff emergency training at the center for radioactive waste management <i>Authors: K. Chizhov, I. Kudrin, I Mazur, A. Tsovyanov, L. Bogdanova, M. Grachev, I. Tesnov, N.-K. Mark, I. Szöke, V. Kryuchkov</i>	1796
Emergency Preparedness – a continuously improving Process <i>Author: Marcel Lips</i>	1804
Medium and Long-Term Inhalation Dose Following a Major Radioactive Deposition Event <i>Author: Mauro Magnoni</i>	1812
Development and Current Status of a Carborne gamma-ray Survey System, KURAMA-II <i>Authors: Minoru Tanigaki, Ryo Okumura, Koichi Takamiya, Nobuhiro Sato, Yasuhiro Kobayashi, Hirofumi Yoshino, Hisao Yoshinaga, Akihiro Uehara</i>	1818
Socially - psychophysiological Adaptation of the Patient, who has Suffered at Failure the Chernobyl Nuclear Power Station, transferred Acute Radiation Sickness of IV Heaviest Degree and Local Radiation Injuries I-IV of Severity Level. <i>Author: N.A. Metlyaeva</i>	1826
Early measurements of members of the public after the Fukushima Daiichi NPP accident: Data made available to the EURADOS WG7 Survey <i>Authors: P. Fojtík, M.A. Lopez, D. Franck, J. Oško, U. Gerstmann, C. Scholl, A.L. Lebacqz, B. Breustedt, L. del Risco Norrild</i>	1836
Large scale monitoring of radioiodine in thyroid: equipment and preparedness in the Czech Republic <i>Authors: P. Fojtík, S. Kavan, L. Novotná, T. Svobodová, E. Čermáková, J. Baloun, J. Helebrant</i>	1845
Investigation of the radiological performances of commercial Active Personal Dosimeters for the use of the PSI fire brigade radiation protection squad <i>Authors: R. Philipp, B. Hofstetter-Boillat, E. Hohmann, S. Mayer</i>	1848
The Analytical Platform of the PREPARE project <i>Authors: W. Raskob, S. Möhrle, S. Bai, T. Müller</i>	1851

Determination of Radionuclides Surface Concentration and Radiation Level In Fukushima Prefecture, Japan: November 2014 <i>Authors: Godwin Ekong, Isa Sambo, Saiyadi Sulaiman</i>	1857
Selective Bone Marrow Shielding as an Approach to Protecting Emergency Personnel <i>Authors: Oren Milstein, Gideon Waterman, Kenneth Kase, Itzhak Orion</i>	1864
RENEB – The European Network for Emergency Preparedness and Scientific Research <i>Authors: Ulrike Kulka, Elisabeth Ainsbury, Leonard Barrios, Octavia Gil, Eric Gregoire, Alicja Jaworska, Simone Mörtl, Ursula Oestreicher, Gabriel Pantelias, Laurence Roy, Laure Sabatier, Sylwester Sommer, Georgia Terzoudi, Francois Trompier, Pedro Vaz, Anne Vral, Clemens Woda, Andrzej Wojcik</i>	1872
Absorbed Dose Measurements using Ordinary Salt on Anthropomorphic Phantoms – Novel Conversion Coefficients to Effective Dose for Various Exposure Geometries <i>Authors: Christian Bernhardsson, Therese Geber-Bergstrand, Jonas Jarneborn, Maria Christiansson</i>	1873
Monitoring and Dose Assessment for Children for Internal Radiation Contamination Following a Radiological or Nuclear Emergency <i>Authors: Chunsheng Li, Florence Ménétrier, Armin Ansari, George Etherington, Wi-Ho Ha, Jean- Rene Jourdain, Boris Kukhta, Osamu Kurihara, Maria Lopez, Arlene Alves dos Reis, Ana Rojo, Stephen Solomon, Jianfeng Zhang, Zhanat Carr</i>	1874
The Radiation Situation in the Area of Radioactive Trace Resulted From the Accident in a Nuclear Submarine at the Chazhma Bay <i>Authors: Dmitry Isaev, Alexey Titov, Sergey Kiselev, Vladimir Shlygin, Natalia Novikova, Renata Starinskaya</i>	1875
 Mass media communication of emergency issues and countermeasures in a nuclear accident. Fukushima reporting in European newspapers <i>Authors: Eduardo Gallego, Marie Claire Cantone, Deborah. H. Oughton, Tanja Perko, Iztok Prezelj, Yevgeniya Tomkiv</i>	1876
The Development of Concept of “Virtual Cytogenetic Biodosimetry Laboratory” for Radiation Emergencies in Occupational Field <i>Authors: Franz Fehring, N. Maznyk, Chr. Johannes, T. Sipko, N. Pshenichna</i>	1877
Radiological Situation at the Chernobyl Shelter Site Thirty Years after the Accident <i>Authors: Gunter Pretzsch, Viktor Krasnov</i>	1878
Assessment of Measurement Capabilities in Nuclear Accident <i>Author: Helena Janzekovic</i>	1879
Study on the Derived Response Level in Case of a Radiological Accident <i>Authors: Hyeong-Ki Shin, Juyoul Park</i>	1880
Training of RPEs for Emergency Response <i>Authors: Heleen van Elsäcker-Degenaar, Folkert Draaisma</i>	1881
Research Priorities in Emergency and Recovery Preparedness and Response: the NERIS Strategic Research Agenda <i>Authors: Johan Camps, Thierry Schneider, Wolfgang Raskob</i>	1882
Mapping of Radiation Fields in Areas with Complex 3D Source Geometries Using a Shielded Two-Detector Configuration and Data Processing <i>Authors: Jonas Jarneborn, Marcus Persson, Christopher Rääf, Robert Finck</i>	1883
Dose Re-estimation Method in Emergency Radiation Exposure Situation <i>Authors: Jungil Lee, Insu Chang, Jang Lyul Kim, Kisoo Chung</i>	1884
Introduction of Uncertainty of Atmospheric Dispersion Calculation and Improvements of Urban Countermeasure Modelling in an Operational Decision Support System <i>Authors: Steen Hoe, Kasper Andersson, Jens Havskov Sørensen, Carsten Israelson</i>	1885
Protection Actions Decision Making Support during Nuclear Emergency in China <i>Authors: Jiangang Zhang, Yapeng Yang, Zongyang Feng, Linsheng Jia, Shutang Sun</i>	1886

Capabilities of the New Mobile Laboratory of the Nuclear Forensic Laboratory <i>Author: Károly Bodor</i>	1887
Ongoing Work to Enhance Post-accident Radiation Protection at Swedish Nuclear Power Plants <i>Authors: Karin Fritioff, Staffan Hennigor, Marie Carlsson, Michael Pettersson, Ingela Svensson</i>	1888
A Spectrometry Acquisition System for UAS based on Raspberry Pi <i>Authors: Magnus Gårdestig, August Ernstsson, Håkan Pettersson</i>	1889
Comprehensive Approach to Assess Radiation Induced Individual Health Injuries and Prognostic Clinical Evaluation using Integrative "Dosimetry" Strategies <i>Authors: Matthias Port, Christina Beinke, Michael Abend</i>	1890
NEA Framework for the Post-Accident Management of Contaminated Food <i>Authors: Michael Siemann, Matt Cooper, Ted Lazo</i>	1891
Industrial Radiography Accident at the Rio Turbio Power Plant: Causes of the Event <i>Authors: Maria Teresa Alonso Jimenez, Irene Raquel Pagni, Eleazar Martin Ameal</i>	1892
 Off-site Emergency Planning at UK Nuclear Licensed Sites <i>Authors: Paul Leonard, Gareth Thomas</i>	1893
Preliminarily Integrated Simulation for Severe Accident of CLEAR-I based on Virtual Reactor Virtual4DS <i>Authors: Tao He, Jinbo Zhao, Zihui Yang, Pengcheng Long, Liqin Hu, Team FDS</i>	1894
Review on Spraying Water Soluble Resin to fix the Radioactive Material after Fukushima Accident <i>Authors: Qiong Zhang, Bo Wang, Ruiping Guo</i>	1895
Training Emergency Plan in a Nuclear Installation <i>Authors: Ruy Ferraz, Ricardo Bitelli</i>	1896
 Suitability of portable radionuclide identifiers for emergency incorporation monitoring <i>Authors: Roman Galeev, Gernot Butterweck, Markus Boschung, Bénédicte Hofstetter-Boillat, Eike Hohmann, Sabine Mayer</i>	1897
Nuclear and radiological emergencies - making early health protection decisions under uncertainty <i>Authors: Stephanie Haywood, Simon French, Matthew Hort</i>	1898
Development of Prediction Models for Ambient Dose Equivalent Rates in Inhabited Areas after the Fukushima Daiichi Nuclear Power Plant Accident <i>Authors: Sakae Kinase, Tomoyuki Takahashi, Hideaki Yamamoto, Kimiaki Saito</i>	1899
²¹⁰Po Version of the Yasser Arafat's Death. Results of the Russian investigations: Part 2. Medical research <i>Authors: Yulia Kvacheva, Vladimir Uiba, Leonid Ilyin, Alexandr Samoilov, Yuriy Abramov, Irina Galstyan, Boris Kukhta, Natalia Nadezhina, Vladimir Stebelkov, Alexandr Tsovyanov, Sergey Shinkarev, Vladimir Yatsenko</i>	1900
²¹⁰Po Version of the Yasser Arafat's death. Results of the Russian Investigations: Part 1. Physical Research <i>Authors: Sergey Shinkarev, Vladimir Uyba, Alexander Samoylov, Leonid Ilyin, Yulia Kvacheva, Yury Abramov, Irina Galstyan, Angelina Guskova, Boris Kukhta, Natalia Nadezhina, Vladimir Stebelkov, Alexander Tsovyanov, Vladimir Iatsenko</i>	1901
Health Risk Assessment of Emergency Personnel Regarding Radiation Exposures during the Aftermath of the Crash of Malaysia Airlines flight MH-17 <i>Author: Tjerk Kuipers</i>	1902
Surveillance of Radioactivity in the Atmosphere by the Deutscher Wetterdienst (DWD) – Monitoring and Prognosis <i>Authors: Thomas Steinkopff, Joachim Barth, Axel Dalheimer, Jochen Förstner, Hubert Glaab, Michael Mirsch</i>	1903
 'SUDOQU': A New Methodology for Deriving Criteria for Radiological Surface Contamination <i>Author: Teun van Dillen</i>	1904
Post-Fukushima Dai-ichi Review of Radioactive Materials Users and Panoramic Irradiators <i>Author: Vincent Holahan, William Lee, Gordon Bjorkman</i>	1905


Possible Mechanism of Realization of High Doses from Beta-Particles Exposures to the Atomic-Bomb Survivors in the Area of Wet Fallout <i>Author: Victor Kryuchkov, Sergey Shinkarev, Boris Kukhta, Evgeniya Granovskaya, Konstantin Chizhov, Masaharu Hoshi</i>	1906
Regulatory Emergency Control Centre Improvement Initiatives <i>Author: Vanessa Maree</i>	1907
Application of Backpack Radiation Detection Systems for Evaluation of External Exposure after the Chernobyl Accident <i>Authors: Valery Ramzaev, Anatoly Barkovsky, Ivan Romanovich, Jonas Jarneborn, Sören Mattsson, Christian Bernhardsson</i>	1908
R Nuclear and radiological preparedness: The achievements of the European Research Project PREPARE <i>Authors: Wolfgang Raskob, Thierry Schneider, Florian Gering, Sylvie Charron, Mark Zhelezniak, Spyros Andronopoulos, Gilles Heriard-Dubreuil, Johan Camps</i>	1909
UAV Carried Emergency Radiation Detection System for Severe Nuclear Accident <i>Authors: Yang Liu, Zhiping Luo, Luzhen Guo, Guowen Zheng, Hongchao Pang, Qin Chen</i>	1910
Area 11: Decommissioning, Waste Management and Remediation	1911
Y Analysis of radioactive inventory for radionuclide contained in liquid effluents, resulting from the decommissioning of a nuclear research reactor <i>Authors: Carmen Tuca, Ana Stochioiu, Mitica Dragusin, Daniela Gurau and Felicia Mihai</i>	1912
Discussion on practical application of radiation protection system for radioactive waste management in existing exposure situations <i>Authors: Daisuke Sugiyama, Takatoshi Hattori</i>	1918
The Role of Radiation Protection Considerations in Decommissioning A brief look at safety culture in Iraq and Ukraine <i>Authors: Eric K. Howell, Rodolfo Avila, John Rowat, David Kenagy, Ronald Chesser</i>	1924
Calculation of Dose Rates at the Surface of Storage Containers for High- Level Radioactive Waste <i>Authors: Erik Poenitz, Clemens Walther, Thomas Hassel</i>	1932
Radiological Assessment Approach for Decisions on Mining-Related Remediation Projects <i>Author: Gert de Beer</i>	1939
Application of an Artificial Neural Network for Evaluation of Activity Concentration Exemption Limits in NORM Industry by Gamma-ray Spectrometry <i>Authors: Hannah Wiedner, Virginia Peyrés, Teresa Crespo, Marcos Mejuto, Eduardo García-Toraño, Franz Josef Maringer</i>	1948
No Nuclear Power - No Disposal Facility? <i>Author: J. Feinhals</i>	1957
Radiation Protection In The Dismantling Of Nuclear Power Plants <i>Authors: Oscar González, José Campos, Teresa Ortiz</i>	1964
German Guidelines put into Practise: Inhalation or Ingestion? A study of a specific case of incorporation in an incident at a facility for dismantling nuclear installations <i>Authors: Peter Hill, Martina Froning, Burkhard Heuel-Fabianek</i>	1972
Investigation into the Pu uptake pathway in Corn (Zea mays) <i>Authors: Stephanie Hoelbling, Fred Molz, Brian Powell, Nishanth Tharayil, Nicole Martinez</i>	1978
Application of USNRC Regulatory Guide 4.21 for Decommissioning Feasibility and Life-Cycle Planning KHNP APR1400 Design Certification Project <i>Authors: Seunggi Lee, Sangho Kang, Irving Tsang, Sara Amitrani</i>	1986
The Post Fukushima Events Development and Severe Accidents Overview: Activities to Enhance Safety and Radiation Protection Regarding Academy Perspective <i>Author: Tadashi Narabayashi</i>	1994

Radioactive waste management in case of incidental melting of a Co-60 source <i>Authors: Teresa Ortiz Ramis, Elena Alcaide Trenas, Pablo Belinchon</i>	2004
Comparative Study of Radioactive Waste Management Standards in Brazil <i>Authors: Ana Cristina Lourenço, Wagner de Souza Pereira</i>	2011
Radioecological Monitoring at the Areas of the Former Military Technical Bases at the Russian Far East <i>Authors: Akhromeev Sergey, Kiselev Sergey, Titov Alexey, Isaev Dmitry, Seregin Vladimir, Gimadova Tamara</i>	2012
The Radiological Risk Assessment for Workers Involved in Liquid Waste Transfer Operations <i>Authors: Ana Stochioiu, Carmen Tuca, Mitica Dragusin, Daniela Gurau, Felicia Mihai</i>	2013
R Slaying the Dragon – The story of one FPSO, twenty odd Vietnamese and 3 concrete mixers. Decontamination and disposal of NORM <i>Authors: Annelize van Rooyen, Anthony O'Brien</i>	2014
Issues Related to Regulation, Control, and Waste Management of Natural Radioactive Scales with Low Specific Activity in Oil Producing Establishments in Libya <i>Author: Bulgasem El-Fawaris</i>	2015
R A comparison of remediation after the Chernobyl and Fukushima Daiichi accidents <i>Authors: Brenda J Howard, Sergey Fesenko, Mikhail Balonov, Gerhard Pröhl, Shinichi Nakayama</i>	2016
Radioactive Waste Management without Adherence to Standards at the Laguna Verde Nuclear Power Plant, Mexico <i>Author: Bernardo Salas</i>	2017
Statistical Learning Approaches Applied to the Calculation of Scaling Factors for Radioactive Waste Characterization <i>Authors: Biagio Zaffora, Matteo Magistris, Francesco Paolo La Torre, Gilbert Saporta, Catherine Luccioni, Jean-Pierre Chevalier</i>	2018
R The Swiss approach to deal with radium legacies from the watch industry The Radium action plan (2016-2019) <i>Authors: Christophe Murith, Sybille Estier, Martha Palacios, Sebastien Baechler</i>	2019
Post closure safety of the SFR repository for short-lived low- and intermediate level waste <i>Authors: Eva Andersson, Fredrik Vahlund, Klas Källström, Ulrik Kautsky</i>	2020
Development of a Standardised Screening Procedure for the Evaluation of Sites Potentially Contaminated with NORM in Austria <i>Authors: Eva Maria Lindner, Claudia Landstetter, Michael Tatzber, Fabian Rechberger, Michael Dauke, Christian Katzlberger</i>	2021
Critical Factors for Radiological Closure Criteria for Uranium Mine Remediation <i>Author: Frank Harris</i>	2022
The International Standards for the Safety of Radioactive Waste Management <i>Author: Gerard Bruno</i>	2023
Talking to the Future: Sustainable Solutions for Radioactive Waste <i>Author: Gordana Lastovicka-Medin</i>	2024
The Dose Calculation on Graphite Waste Samples of the Decommissioned KRR-2 <i>Authors: Heereyoung Kim, Deokjung Lee</i>	2025
Characterization of Concrete Structures to Determine the Strategy for the Decommissioning of the 250 MeV CGR Cyclotron of the Ghent University in Belgium <i>Authors: Isabelle Meirlaen, Myriam Monsieurs, Hubert Thierens, Luc Ooms, Sven Boden, Luc Noynaert</i>	2026
Waste Management at the Decommissioning of the Ghent University Research Reactor Thetis in Belgium <i>Authors: Isabelle Meirlaen, Myriam Monsieurs, Hubert Thierens, Patrick Maris, Luc Noynaert, Luc Ooms</i>	2027

R Decontamination and Recovery of a Nuclear Facility to allow Continued Operation <i>Author: Josh Cavaghan</i>	2028
General Principles for the Short and Long Term Management of Former Uranium Mining Sites in France <i>Authors: Jérôme Guillevic, Marie Odile Gallerand, Gwenaëlle Lorient, Christophe Serres</i>	2029
Safety Standards for the Management and Disposal of Radioactive Waste from Uranium Mining in France <i>Authors: Jérôme Guillevic, Marie-Odile Gallerand, Gwenaëlle Lorient, Christophe Serres</i>	2030
Enhancing Regulatory Oversight of Radioactive Sources through International Cooperation <i>Author: Jack Ramsey</i>	2031
New Measurement Systems for Clearance of Radioactive Materials from Nuclear Facilities Decommissioning <i>Authors: Jiri Suran, Jana Smoldasova, Petr Kovar, Lukas Skala, Bent Pedersen, Dirk Arnold, Daniel Zapata, Pierino de Felice, Doru Stanga, Simon Jerome</i>	2032
Development of Postulated Initiating Event's Scenarios for the Decommissioning of Korean 1400 MWe PWR <i>Authors: Kyomin Lee, Sangho Kang, Keunsung Lee</i>	2033
Impact Assessment on Rn-222 in a Radioactive Waste Disposal Facility <i>Authors: Luis Fuentes, José-Luis Pinilla, Teresa Ortiz</i>	2034
The Process of Industrialization of the Management of Radioactive Waste: The Example of High Energy Accelerators Waste at CERN <i>Authors: Luisa Ulrici, Yvon Algoet, Luca Bruno, Doris Forkel-Wirth, Francesco Paolo La Torre, Matteo Magistris, Christian Theis, Ralf Trant, Helmut Vincke, Nick Walter</i>	2035
NORM Waste in Oil & Gas Industry (Challenges & Solutions) <i>Author: Mohammad Aref</i>	2036
Disposal of Norm Waste from Oil and Gas Industry by Underground Injection (Case Study) <i>Authors: Michael Cowie, Roman Bilak, Steve Wasson, Kelly Hatch</i>	2037
Waste Management Protocols for Iridium-192 Sources Production Laboratory Used in Cancer Treatment <i>Authors: Maria Elisa C. M. Rostelato, Carla Daruich de Souza, Daiane C. Barbosa de Souza, Carlos A. Zeituni, Rodrigo Tiezzi, Osvaldo L. da Costa, Bruna Teiga Rodrigues, João A. Moura, Anselmo Feher, Anderson Sorgatti, Eduardo Santana de Moura, José Ronaldo de Oliveira Marques, Rafael Melo dos Santos, Dib Karam Jr.</i>	2038
Clearance and Declassification of Research Reactor Thetis at Ghent University, a Prime for Belgium <i>Authors: Myriam Monsieus, Isabelle Meirlaen, Hubert Thierens, Karel Strijckmans, Geert Cortenbosch, Luc Noynaert, Luc Ooms, Sven Boden</i>	2039
Methods used for Clearance of the Rooms of Former Research Reactor Thetis at Ghent University, Belgium <i>Authors: Myriam Monsieus, Isabelle Meirlaen, Hubert Thierens, Geert Cortenbosch, Luc Ooms, Sven Boden</i>	2040
Removal of Radiocesium Aqueous Solution using Activated Carbon Modified with Anionic Surfactant <i>Authors: Michael Olatunji, Mayeen Khandaker, Yusoff Amin, Ekramul Mahmud</i>	2041
R Norwegian-Russian Cooperation in Nuclear Legacy Regulation: Continuing Experience and Lessons <i>Authors: Malgorzata K. Sneve, Natalya Shandala, Alexey Titov, Vladimir Seregin, Sergey Kiselev</i>	2042
Rationale for a Comprehensive Assessment of Radio-Ecological Safety of Near Surface Radioactive Waste Storage Facilities <i>Authors: Alexander Samoylov, Nataliya Shandala, Igor Korenkov, Tatyana Lashchenova, Vladimir Romanov</i>	2043
Assessing the Environmental Impact of Man-made Radioactive Contamination at the Andreeva Bay Site for Temporary Storage of Spent Nuclear Fuel and Radioactive Waste <i>Authors: Natalia Shandala, Vladimir Seregin, Anna Filonova, Aleksey Titov, Vladimir Shlygin, Malgozhata Sneve, Graham Smyth</i>	2044

Radiation Situation around the Shipyards Involved in Decommissioning/Dismantlement of Nuclear Submarines	
<i>Authors: Nataliya Shandala, Alexey Titov, Maria Semenova, Vladimir Seregin, Anna Filonova</i>	2045
The study of the Ground Water Contamination. The Study of the Environmental Conditions of the Region during Remediation of the Andreeva Bay STS	
<i>Authors: Natalya Shandala, Vladimir Seregin, Sergey Kiselev, Stanislav Geras`kin, Malgorzhata Sneve, Graham Smith</i>	2046
The Status of Occupational Exposure Source Term Measurement with In-situ Gamma-ray Spectrometry for NPPs in China	
<i>Authors: Qinjian Cao, Xueqi Chang, Liye Liu, Wanchun Xiong, Yunshi Xiao, Sanqiang Xia</i>	2047
Study on spraying water soluble resin for Fukushima Dai-ichi nuclear power plant accident	
<i>Authors: Qiong Zhang, Ruiping Guo, Bo Wang, Liang Wang, Fudong Liu, Xiaoqiu Chen</i>	2048
Achievements by the NORM and Legacy Sites Working Group of the IAEA MODARIA Project	
<i>Author: Rodolfo Avila</i>	2049
NORMALYSA – A Tool for Risk Assessment to Support Remediation of Legacy Sites Contaminated with NORM and Artificial Radionuclides	
<i>Author: Rodolfo Avila</i>	2050
 Information Management System Supporting a Multiple Property Survey Program with Legacy Radioactive Contamination	
<i>Authors: Ron Stager, Douglas Chambers, Gerd Wiatzka, Monica Dupre, Micah Callough, John Benson, Erwin Santiago, Walter van Veen</i>	2051
Uranyl Ions Adsorption to Na-GMZ and Interactions with FA Adsorption: experiments and modelling	
<i>Authors: Yuanlv Ye, Liang Wang, Fudong Liu, Yahua Qiao</i>	2052
Occupational Dose Evaluation during Decommissioning of a Radiological Facility	
<i>Authors: Zamazizi Dlamini, Frik Beeslaar</i>	2053
Area 12: Societies	2054
Argentine Radiation Protection Society (SAR): 50 years Straightening Radiation Protection	
<i>Author: Ana María Bomben</i>	2055
The History of the South African Radiation Protection Society	
<i>Author: Christoph Trauernicht</i>	2056
Belgian Society for Radiation Protection	
<i>Authors: Tom Clarijs, Patrick Smeesters, Claire Stievenart, Andrzej Polak, Pascal Froment</i>	2057

Note:

Submissions marked with  represent entries published in a Special IRPA 14 issue of *Radiation Protection Dosimetry*.

Submissions marked with  represent entries by contestants for the Young Scientists and Professionals Award.

**The Proceedings of the 14th International Congress of the International Radiation
Protection Association
Volume 4 of 5**

Area 7: Environment and Natural Background

Health Detriment Associated with Exposure to Natural Radioactivity from the Soil of Ondo and Ekiti States South Western, Nigeria.

A.E. Ayodele^a, A. M. Arogunjo^{a,b}, J. I. Ajisafe^{a,c}, and O.T. Arije^a

^aDepartment of Physics, Federal University of Technology, Akure, Nigeria.

^bDepartment of Physics, University of Medical Sciences, Ondo, Nigeria.

^cDepartment of Industrial Safety and Environmental Engineering Technology, Petroleum Training Institute, Effurun, Warri, Nigeria.

Abstract. The health detriment associated with primordial radionuclides from the earth crust has been a major source of concern to public health observers across the globe. The level of such detriment can be mitigated by constant monitoring in order to ascertain that the safe threshold is maintained from time to time. In the light of the above, the activity concentrations of natural occurring radioactivity (i.e ^{232}Th , ^{226}Ra and ^{40}K) were determined in seventeen soil samples collected from selected cities across Ondo and Ekiti states using an n-type coaxial HPGe gamma ray detector with ORTEC multichannel analyzer (MCA) and MAESTRO-32 for spectrum analysis and processing. The measured activity concentrations ranged from 31.93 ± 1.77 to 227.50 ± 4.43 Bq Kg^{-1} ^{232}Th , 364.89 ± 6.40 to 1274.57 ± 12.48 Bq Kg^{-1} ^{40}K , 45.60 ± 2.99 to 210.36 ± 8.76 Bq Kg^{-1} ^{226}Ra and 48.64 ± 2.04 to 207.22 ± 5.50 Bq Kg^{-1} ^{232}Th , 542.26 ± 10.41 to 2348.86 ± 21.83 Bq Kg^{-1} ^{40}K and 73.52 ± 3.81 to 209.15 ± 7.45 Bq Kg^{-1} ^{226}Ra for Ondo and Ekiti states respectively. Absorbed dose was calculated using the measured activity concentrations. The mean absorbed dose rate and standard deviation in nGyh^{-1} were 140.89 ± 65.27 and 173.27 ± 85.40 respectively for the two States. Health detriment to various organs of the body resulting from the exposure scenario was evaluated.

KEYWORDS: *HPGe; absorbed dose; annual outdoor effective dose; health detriment.*

1 INTRODUCTION

The human environment is composed largely of soil, water, gases and probably microorganism. Man uses soil or otherwise called land for various purposes ranging from citing of industries, Agriculture and erecting permanent structures for dwelling purposes. Man is a product of his environment. The environmentalist has studied for decades the impact of man's activities on his environment or vice-versa. Soil is a product of weathering and contains fossils, dead organic and in-organic matter, gases and physical contaminants called radionuclides or radioisotopes. Radionuclides occur naturally in the soil in the form of the Uranium decay series (^{226}Ra and ^{232}Th) and the non-decay series ^{40}K . The presence of these Primordial radionuclides vary from one location to another and the distribution has been found to be largely dependent on geological and geographical conditions, and appear at different levels in the soils of each region of the world [1]. Hence Nuclear Scientist and or radiologist are working to characterise each environment based on the presence and distribution of these radionuclides. Human exposure to radiation is dated back to the creation of the Earth. And natural sources still contribute almost 80% of the collective radiation exposure of the World's population [1]. Despite the usefulness of radiation in the industry and Medicine (radiotherapy), exposure to radiation beyond a certain threshold value either from the primary or secondary sources pose a threat to human health.

This situation is becoming worrisome as several cases of Tumour and other deadly ailment are linked to exposure to undue radiation. Hence, it therefore becomes important to quantify human exposure to radiation for environmental monitoring [2]. Several studies performed worldwide to assess the activity concentrations of these radionuclides are reported [3, 4, 5, 6]. But data regarding the levels of natural radionuclides and the associated radiation doses are still sparse in some area of Ondo and Ekiti states

South-western Nigeria. Ondo ($5^{\circ} 48'N$, $4^{\circ} 45'E$) and Ekiti ($8^{\circ} 15'N$, $6^{\circ} 05'E$) states are underlain by crystalline rocks or basement complex. The basement complex is of Precambrian age and composed primarily of metamorphic and igneous rock such as granites, gneisses and migmatites [7].

In this work, 17 samples of soil were collected from selected cities across Ondo and Ekiti states and analysed for primordial radionuclides using gamma-ray Spectrometry to evaluate the activity concentration, absorbed dose due to exposure and the associated Health detriment to different organs of the body.

2 MATERIAL AND METHODS

2.1 Samples Collection and Preparation

At each of the designated locations, the soil samples were taken using cutlass from a depth of 10 cm. the quantity taken was about 120g; packaged in cellophane bags and labelled based on the Alphabet ascribed to each location, table 1.0 gives the Samples Code and interpretations.

The collected soil samples were transferred to the laboratory and thereby oven dried at a temperature of $110^{\circ}C$ to a constant mass, the dried samples were then pulverized and sieved using a 2 mm mesh, whilst retaining the previous labelling to indicate the city where the sample was collected. The sample was left untouched for about three or four weeks to allow the samples achieve secular equilibrium between parent and daughter nuclides prior to analysis.

2.2 Samples Analysis

The activity Concentrations of the soil samples were measured using an N-type coaxial High Purity Germanium Detector (HPGe) gamma-ray detector at the laboratory of Ghana Atomic Energy Commission Accra with ORTEC Multichannel Analyzer (MCA) and MAESTRO-32 evaluation software for spectrum acquisition and processing. The relative efficiency of the detector was 28.5 % with energy resolution of 1.8 keV at gamma ray energy of 1332 keV of ^{60}Co . The gamma lines 609.31 and 1764.49 keV of ^{214}Bi were used to determine ^{226}Ra . The gamma lines 583.19 of ^{208}Tl were used to determine ^{232}Th and that of ^{40}K was determined from the gamma line of 1460.83 keV. The samples were counted for 18,000 seconds (5 hours). The energy and efficiency calibrations were performed using mixed radionuclide calibration standard in the form of solid water, serial number NW 146 A with approximate volume 1000 mL and density 1.0 gm^{-3} in a 1.0 L Marinelli beaker. The standard was supplied by Deutscher Kalibrierdienst (DKD-3), QSA Global GmbH, Germany. Background measurements were made for the same period. Density corrections were also made where appropriate.

The specific activity concentrations (A_{sp}) of ^{226}Ra , ^{232}Th , and ^{40}K were determined in Bq kg^{-1} for the water samples using the following expression [8, 9, 10] after decay correction.

$$A_{sp} = \frac{N_{sam}}{P_E \cdot \epsilon \cdot T_c \cdot M} \quad (1)$$

where; N_{sam} is net counts of the radionuclide in the sample, P_E is gamma ray emission probability (gamma yield), ϵ is total counting efficiency of the detector system, T_c is sample counting time and M is mass or weight of the Sample.

The specific activity obtained using equation (1) coupled with appropriate dose conversion factors form the basis for the evaluation of the radiological health hazards posed by the analysed samples from the study area.

2.3 Calculation of Absorbed Dose, Dose Equivalent and Health Detriment

2.3.1 Absorbed Dose

The absorbed dose rates, in nGy h^{-1} at a height of 1m above the ground due to the ingestion or inhalation of ^{232}Th , ^{226}Ra , and ^{40}K was calculated in this work using the following relation [11]:

$$D = A_{ei} \times C_f \quad (2)$$

where A_{ei} is the activity concentration measured in Bq kg^{-1} and C_f is the dose conversion factor ($\text{nGy/h per Bqkg}^{-1}$). In this work, the dose conversion factor used for ^{232}Th , ^{226}Ra and ^{40}K where the ones determined by [12] and described by [2]. Hence equation 2 is then modified to reflect the dose conversion factor and presented as equation 3. Equation 3 is then the total absorbed dose due to gamma radiation from these radionuclides (^{232}Th & ^{226}Ra and the non series ^{40}K), thus:

$$D = 0.623A_{Th} + 0.461A_{Ra} + 0.0414A_K \quad (3)$$

Where A_{Th} = activity concentration of ^{232}Th , A_{Ra} = activity concentration of ^{226}Ra and A_K = activity concentration ^{40}K .

2.3.2 Dose Equivalent

The annual outdoor effective dose equivalent due to exposure or inhalation of these radionuclides from the soil was estimated taking into consideration the conversion coefficient from absorbed dose in air to effective dose and the outdoor occupancy factor. The former gives the equivalent human dose in Sv y^{-1} from the absorbed dose rate in air (nGy h^{-1}), while the latter gives the fraction of the time an individual is exposed. In this work, an occupancy factor of 0.3 was used (i.e. an individual is assumed to spend an average of 8 hours outdoor) and 0.7 Sv y^{-1} was used for the conversion coefficient according to [2]. Hence, the annual outdoor effective dose rate, H_E , in units of $\mu\text{Sv y}^{-1}$, is calculated using the following relation:

$$H_E = D(\gamma) \times N(h) \times O_f \times C_f \quad (4)$$

where $D(\gamma)$ is the calculated absorbed dose (nGy h^{-1}), $N(h)$ is the number of hours in a year ($0.3 \times 24\text{h} \times 365.25\text{d} = 2629.80\text{h/y}$) O_f is the occupancy factor (i.e. 0.3) and C_f is the conversion coefficient or factor (0.7Sv Gy^{-1}).

2.3.3 Collective Effective Dose Equivalent

The collective effective dose equivalent to a population is a measure of the collective detrimental effects and the percentage of people at risk of incurring radiation-induced diseases; which is calculated using the expression [13].

$$S_E = \sum N_i H_{Ei} \quad (5)$$

Where S_E = collective effective dose equivalent (person – Sv)

N_i = the numbers of individual exposed to radiation and H_{Ei} is the mean outdoor effective dose equivalent ($\mu\text{Sv y}^{-1}$). The N_i used in this work is 3441024 Persons and 2384212 Persons for Ondo and Ekiti states respectively [14].

2.3.4 Collective Health Detriment

The collective health detriment G (person), due to exposure to gamma radiation in an environment, was calculated using the relation [15].

$$G = R_T S_E \quad (6)$$

where R_T = Total risk factor

S_E = Collective effective dose equivalent (person – Sv)

2.4 Radium Equivalent Activity (Ra_{eq}): This is a radiation hazard indices used to assess the gamma radiation hazards to humans as a result of using soil for building purposes. The Ra_{eq} index is calculated using the relation of [16] as thus;

$$Ra_{eq} = A_{Ra} + 1.43A_{Th} + 0.07A_K \quad (7)$$

where A_{Ra} , A_{Th} and A_K are the activity concentrations in Bq Kg⁻¹ of ²²⁶Ra, ²³²Th and ⁴⁰K respectively. This index assumed that 370 Bq Kg⁻¹ of ²²⁶Ra or 259 Bq Kg⁻¹ of ²³²Th or 4810 Bq Kg⁻¹ ⁴⁰K produce the same gamma dose.

3 RESULTS AND DISCUSSION

The Activity concentration of the radionuclides present in the spectrum result of the gamma ray spectrometry conducted for the soil was calculated using eqn 1. Naturally occurring radionuclides ²³²Th, ⁴⁰K and ²²⁶Ra were detected in all the Seventeen (17) Soil samples. A trace quantity of ¹³⁷Cs was also detected in the soil samples of both Ondo and Ekiti states. The activity concentration of these radionuclides were found to be within the range of 31.93 ± 1.77 - 227.50 ± 4.43 Bq kg⁻¹, 364.89 ± 6.40 – 1274.57 ± 12.48 Bq kg⁻¹, 45.60 ± 2.99 - 210.36 ± 8.76 Bq kg⁻¹, and 1.85 ± 0.32 - 5.03 ± 0.56 Bqkg-1⁻¹ for ²³²Th, ⁴⁰K and ²²⁶Ra and ¹³⁷Cs respectively in Ondo state soil samples. While that of Ekiti States ranged between 48.64 ± 2.04 – 207.22 ± 5.50 Bq kg⁻¹, 542.26 ± 10.41 – 2348.86 ± 21.83 Bq kg⁻¹, 73.52 ± 3.81 – 209.15 ± 7.45 Bq kg⁻¹ and 3.09 ± 0.46 – 8.88 ± 0.82 Bq kg⁻¹ for ²³²Th, ⁴⁰K and ²²⁶Ra and ¹³⁷Cs respectively. ¹³⁷Cs was not detected in the two soil samples taken from Omuo Ekiti. A comparison of the activity concentration of these radionuclides in soil samples from different countries was done and presented in Table 2.0. The results in this work are a bit higher than findings from other parts of the world and the world average values [2]. In Ondo state soil samples, the range of activity concentrations of ²²⁶Ra (45.60 ± 2.99 - 210.36 ± 8.76 Bq kg⁻¹) measured in this work is still less than the international range of 10 Bq Kg⁻¹ to 3700 Bq Kg⁻¹ reported by [17] and comparable to the range of 9.3 ± 3.7 Bq kg⁻¹ to 198.1 ± 13.8 Bq Kg⁻¹ reported by [15] for the South-western part of Nigeria. ²³²Th had its highest activity concentration of 227.50 ± 4.43 Bq Kg⁻¹ in one of the samples taken from Ondo town and the least activity concentration of 31.93 ± 1.77 Bq Kg⁻¹ in one of the samples taken from Ikare-Akoko and ⁴⁰K had its highest concentrations of 1274.57 ± 12.48 Bq Kg⁻¹ in one of the samples taken from Akure and the least of 364.89 ± 6.40 Bq Kg⁻¹ in one of the samples taken from Owo. This is equally comparable to the range of 34.9 ± 4.4 – 1358.6 ± 28.5 Bq Kg⁻¹ reported by [15] and higher to the range of 129 ± 5.7 – 230 1.1 Bq Kg⁻¹ reported for ⁴⁰K by [18] in the soil of Saudi Arabia. The situation in Ondo town might be as a result of emerging Industries, while that of Akure might be as a result of local geology. Similarly, in Ekiti state the highest activity concentrations of (209.15 ± 7.45 Bq Kg⁻¹) and (207.22 ± 5.50 Bq Kg⁻¹) for ²²⁶Ra and ²³²Th were found in one of the samples taken from Ado-Ekiti. The highest activity concentrations of 2348.86 ± 21.83 Bq Kg⁻¹ was found for ⁴⁰K in the sample taken from Aramoko Ekiti and the least of 542.26 ± 10.41 Bq Kg⁻¹ was found in the sample taken from Ise-Ekiti. The mean activity concentrations of 118.88 ± 5.55 Bq Kg⁻¹, 105.72 ± 3.50 Bq Kg⁻¹ and 1270.74 ± 15.34 Bq Kg⁻¹ reported in this work for ²²⁶Ra, ²³²Th and ⁴⁰K are higher when compared to findings from other part of the world and the World average value of 35, 50 and 400 Bq Kg⁻¹ respectively [2]. The result is however in close range with the findings of [15]. It is important to point out that these values are not the representative values for the entire states, but for the regions where the samples were collected.

Table 1: Comparison of activity concentration of ^{40}K , ^{226}Ra and ^{232}Th in Soil measured worldwide.

Country	Activity concentration (Bqkg ⁻¹)			Reference
	⁴⁰ K	²²⁶ Ra	²³² Th	
Pakistan (Punjab)	615 ± 143	35 ± 7	41 ± 8	[20]
Cyprus	105 ± 95	7.1 ± 8.6	5.0 ± 7.1	[21]
Alexandria, Egypt	262 ± 82	16.7 ± 2.7	19.4 ± 5.0	[22]
South India	117.5	35	29.8	[23]
Spain	650	46	49	[24]
Kenya	255 ± 38.5	28.7 ± 3.6	73.3 ± 9.1	[25]
China	578 ± 164	42.7 ± 15	46.3 ± 12	[26]
Republic of Ireland	350	60	26	[3]
Saudi Arabia	225 ± 63	14.5 ± 3.9	11.2 ± 3.9	[5]
Ondo State (Nigeria)	849.03 ± 12.89	101.12 ± 5.50	91.76 ± 3.12	This study
Ekiti State (Nigeria)	1270.74 ± 15.34	118.88 ± 5.55	105.72 ± 3.50	This study
World's average	400	35	30	[2]

3.1 Absorbed Dose Rate, Health Detriment and Radium Equivalent index

The absorbed dose rate in air at a gonadal height of 1m resulting from the presence of ^{232}Th , ^{40}K and ^{226}Ra in the soil of the two states was calculated using equation 3 above. The mean absorbed dose rate in nGy h⁻¹ and the standard deviation were respectively 140.89, 65.27 and 173.27, 85.40 for Ondo & Ekiti states soils. The results in both cases is beyond the limits (30 nGy h⁻¹-70 nGy h⁻¹) recommended by [19] for area of normal background radiation. Annual outdoor effective dose equivalent ($\mu\text{Sv y}^{-1}$) was calculated using an occupancy factor of 0.3 and a conversion factor of 0.7 Sv Gy⁻¹ using the relation discussed as eqn 4. The results ranged between 0.15 - 0.70 mSv y⁻¹, mean outdoor annual effective dose equivalent and standard deviation 0.35 mSv y⁻¹ and 0.16 mSv y⁻¹ for Ondo state. For Ekiti, the range is between 0.22 - 0.79 mSv y⁻¹, mean of 0.43mSv y⁻¹ & standard deviation 0.21 mSv y⁻¹. The result exceeds the values recommended by ICRP (70 $\mu\text{Sv y}^{-1}$), but below the world's average of 1.0mSv y⁻¹. Health detriment resulting from the inhalation of these radionuclides was calculated using equation 5 and 6 and the health implication to different Organs of the body highlighted and presented in Figures 1.0 and 2.0. The calculated Ra_{eq} index for this work is presented in Table 3.0. The mean Ra_{eq} index for Ondo and Ekiti States are 295.07 Bq Kg⁻¹ and 359.01 Bq Kg⁻¹ respectively. Though an elevated concentration of Ra_{eq} index was recorded in one of the samples taken from Ondo and Okitipupa for Ondo State and in the sample taken from Ado Ekiti and Aramoko, the area under investigation is still safe for habitation since the mean value for the two states are still less than the 370 Bq Kg⁻¹ of ^{226}Ra international standard.

Figure 1: Percentage Distribution of Health Detriment From the Soil of Ondo state to different Organs of the Body

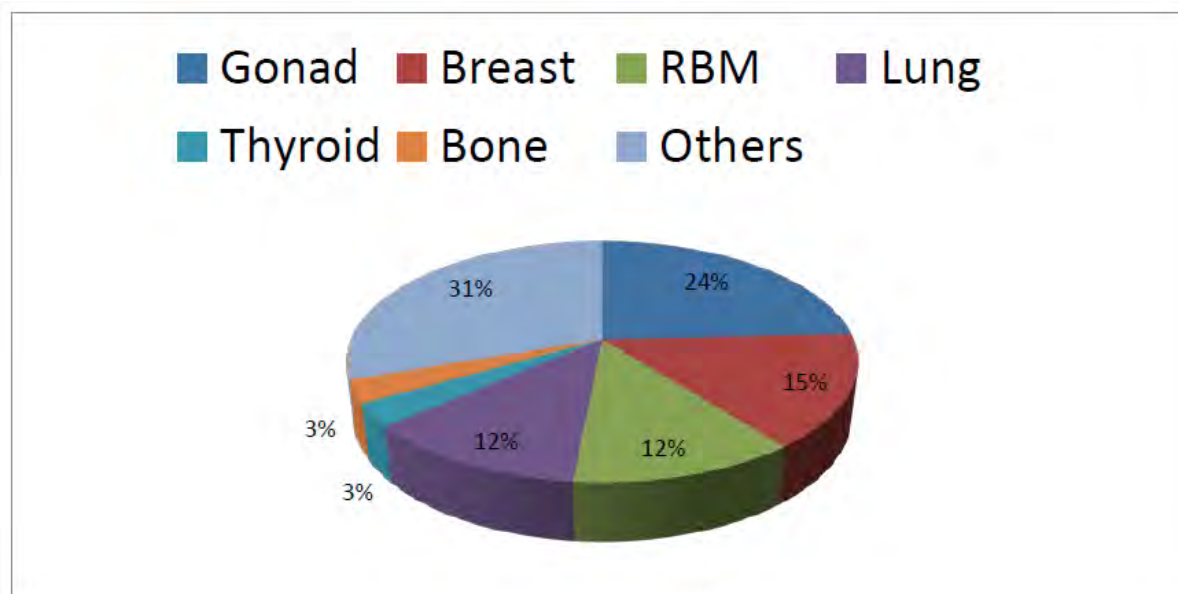
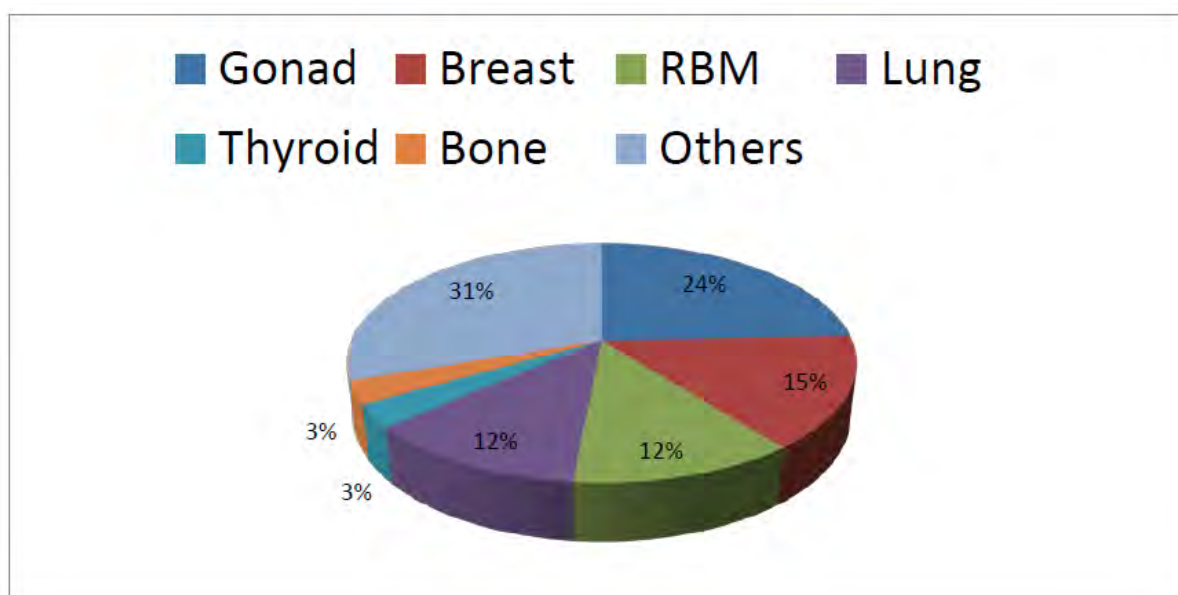


Figure 2: Percentage Distribution of Health Detriment From the Soil of Ekiti state to different Organs of the Body



RBM = Red Bone Marrow

4 CONCLUSION

This study investigated the activity concentrations of 17 soil samples taken from selected locations across Ondo and Ekiti States, the radiological health detriment resulting from exposure to different organs of the body and the Radium equivalent index was also evaluated.

Measured activity concentrations recorded in this work ranged from $31.93 \pm 1.77 - 227.50 \pm 4.43$ Bq Kg^{-1} ^{232}Th , $364.89 \pm 6.40 - 1274.57 \pm 12.48$ Bq Kg^{-1} ^{40}K , $45.60 \pm 2.99 - 210.36 \pm 8.76$ Bq Kg^{-1} ^{226}Ra and $48.64 \pm 2.04 - 207.22 \pm 5.50$ Bq Kg^{-1} ^{232}Th , $542.26 \pm 10.41 - 2348.86 \pm 21.83$ Bq Kg^{-1} ^{40}K $73.52 \pm 3.81 - 209.15 \pm 7.45$ Bq Kg^{-1} ^{226}Ra for Ondo and Ekiti states respectively. These values are found to be above those reported from other parts of the World and the World average value reported by [2]. Annual outdoor effective dose equivalent was also calculated using a dose conversion factor of 0.7 Sv Gy^{-1} for the two states. The results were found to be above the $70 \mu\text{Sv y}^{-1}$ recommended by ICRP and below the world average of 1 mSv y^{-1} . The calculated mean Radium equivalent index for Ondo and Ekiti States are $295.07 \text{ Bq Kg}^{-1}$ and $359.01 \text{ Bq Kg}^{-1}$ respectively. These values are still below the international standard of 370 Bq Kg^{-1} ^{226}Ra ; hence the area under investigation is still safe for Human habitation. Health detriment to various organs of the body resulting from exposure to these radionuclides was also evaluated.

5 REFERENCES

- [1] United Nations Scientific Committee on Effects of Atomic Radiation, "Sources and Effects of ionizing Radiation", UNSCEAR Report, New York, 1993.
- [2] United Nations Scientific Committee on Effects of Atomic Radiation, (UNSCEAR), 2000: Report to General Assembly, Report Vol 1. Sources and Effects of Ionizing Radiation, with Scientific Annexes, United Nations, New York.
- [3] McAulay, I.R. and Morgan, D., (1988): Natural Radioactivity in Soils in the republic of Ireland, Radiat. Prot. Dosimetry 24 (1/4), 47- 49.
- [4] Jibiri, N. N., Alausa, S. K. and Farai, I. P. (2009) : Radiological hazard indices due to activity concentrations of natural radionuclides in farm soils from two high background radiation areas in Nigeria. Int. J. Low Radiation, 6,(2), 79-95.
- [5] Alaamer, A.S., (2008): Assessment of Human Exposure to Natural Sources of Radiation in Soil of Riyadh, Saudi Arabia, Turkish J. Eng. Env. Sci 32, 229 – 234.
- [6] Boukhenfouf, W. and Boucenna, A. (2011): The radioactivity measurements in soils and fertilizers using gamma spectrometry technique, journal of Environmental Radioactivity,doi; 10. 1016/j.jenvrad.2011.01.006.
- [7] Rahaman, M. A., (1988); Recent advances in the study of basement complex of Nigeria. In: Proceedings of First Symposium on the Precambrian Geology of Nigeria, 11-43.
- [8] Uosif, M. A. M., El-Taher, A. and Abbady, Adel G.E. (2008): Radiological Significance of beach sand used for Climatotherapy from Safaga, Egypt, Rad. Prot Dosimetry, pg 1-9.
- [9] Darko, E. O. and Faanu, A. (2007). Baseline radioactivity measurements in the vicinity of a gold processing plant. J. Applied Science & Technology, 12(1 & 2): 18-24.
- [10] Darko, E. O., Faanu, A., Awudu, A. R., Emi-Reynolds, G., Oppon, O. C., Mensah-Brobbe, I., Quansah, T., Dapaah, K. and Addo, W. (2008). Public Exposure to hazards associated with NORMS in mining and mineral processing activities in Ghana. Final Technical Report of data, IAEA TC Project GHA 9005, Accra.
- [11] Kohshi, C., Takao, I., Hideo, S. (2001). Terrestrial gamma radiation in Koshi prefecture, Japan. Journal of Health Science, 47(4): 362-372.
- [12] Saito, K., and Jacob P.(1990): Gamma ray fields in the air due to sources in the ground. Radiat. Protect. Dosim. 58: 29-45.
- [13] International Commission on Radiological Protection ICRP (1991): 1990 recommendations of the International Commission on Radiological Protection New York: Elsevier, ICRP Publication 60, Ann ICRP 21 (1-3).
- [14] National Population Census of Nigeria (2006).
- [15] Ajayi, O. S., Ibikunle, S. B. and Ojo, T. J. (2008): An Assessment of Natural Radioactivity of Soils and its External Radiological Impact In Southwestern Nigeria. Nigerian Journal of Health Physics 94(6) 558-566.
- [16] Berekta, J. and Matthew, P. J., (1985): Natural radioactivity of Australian building materials, industrial wastes and by-products. Health Physics, 48; 87-95.
- [17] Trabidou, G., (2004): Radiological study in radioactive spring areas. Athens, Greece; University of Athens.

- [18] El-Aydarous, A. (2007): Gamma Radioactivity Levels and their Corresponding External Exposure of Some soil Samples from Taif Governorate, Saudi Arabia. *Global journal of Environmental Research*,1 (2); 49-53.
- [19] United Nations Scientific Committee on Effects of Atomic Radiation (UNSCEAR). Sources and Effects of Ionizing Radiation. New York: United Nations; 1988.
- [20] Tahir, S.N.A., Jamil, K., Zaidi, J.H., Arif, M., Ahmed, N. and Ahmad, S.A., (2005): Measurement of Activity concentrations of Naturally Occurring Radionuclides in Soil Samples from Punjab Province of Pakistan and Assessment of radiological Hazards. *Radiat. Prot. Dosimetry* 113 (4), 421- 427.
- [21] Tzortzis, M., Svoukis, E. and Tsertos, H., (2004): Comprehensive Study of Natural Gamma Radioactivity Levels and Associated Dose Rates from Surface Soils in Cyprus, *Radiat. Prot. Dosimetry* 109, 217 – 224.
- [22] Saleh, I.H., Hafez, A.F., Elanany, N.H., Motaweh, H.A., and Naim, M.A., (2007): Radiological Study on Soils, Foodstuff and Fertilizer in the Alexandria Region. *Egypt. Turkish J. Eng. Env. Sci.* 31, 9 – 17.
- [23] Narayana, Y., Somashekarappa, H.M., Karunakara, N., Avadhani, D.N., Mahesh, H.M. and K. Siddappa, (2001). Natural Radioactivity in the soil samples of coastal Karnataka of South India. *Health Physics*, 80: 24-33.
- [24] Baeza, A., Del Rio, M., Mir, C., Paniagua, J.M., (1992). “Natural Radioactivity in soils of the Province of Caceres (Spain)”, *Radiat. Prot. Dosimetry* 45, 261-263.
- [25] Mustapha, A.O., Patel, J.P. and Rathore, I.V.S., (1999): Assessment of Human Exposure to Natural Sources of Radiation in Kenya, *Radiat. Prot. Dosimetry* 82, 285 – 292.
- [26] Ziqiang, P., Yin, Y. and Mingqiang, G., (1988): Natural Radiation and Radioactivity in China, *Radiat. Prot. Dosimetry* 24 (1/4) 29 – 38.

Radioactivity Level of Drilled Well Water across Selected Cities in Ondo and Ekiti States, Southwestern Nigeria and its Radiological Implications

A. E. Ayodele^{a*}, A. M. Arogunjo^{a,b}, J. I. Ajisafe^{a,c}, O.T. Arije^a

^aDepartment of Physics, Federal University of Technology, Akure, Nigeria

^bDepartment of Physics, University of Medical Sciences, Ondo, Nigeria

^cDepartment of Industrial Safety and Environmental Engineering Technology, Petroleum Training Institute, Effurun, Warri, Nigeria

Abstract. The increasing health effects of nuclear radiation occasioned by the enhanced human activities in the environment necessitated the need for constant evaluation and assessment of radiological impact on the general populace within a confined developmental area. In response to this need, Ten (10) drilled well water samples were collected from various cities distributed across Ondo and Ekiti states and analyzed for gamma-emitting radiations using n-type coaxial High Purity Germanium Detector (HPGe) detector: with ORTEC multichannel Analyzer and Maestro-32 for spectrum analysis and processing. The measured activity concentrations ranged from 2.25 ± 0.39 to 35.61 ± 6.22 Bq l⁻¹ ²³²Th, 45.42 ± 2.98 to 467.61 ± 31.69 Bq l⁻¹ ⁴⁰K, 7.08 ± 1.71 to 56.68 ± 12.50 Bq l⁻¹ ²²⁶Ra and 1.66 ± 0.46 to 25.55 ± 5.76 Bq l⁻¹ ²³²Th, 41.50 ± 2.89 to 558.82 ± 31.69 Bq l⁻¹ ⁴⁰K, 4.90 ± 1.08 to 54.18 ± 13.34 Bq l⁻¹ ²²⁶Ra respectively for Ondo and Ekiti states. The age dependent annual effective dose and committed effective dose were calculated using the measured activity concentration and ingested dose conversion factor for three different age groups (i.e 0-1yrs, 7-12yrs and ≥ 17 yrs). The total annual effective dose was found to be above the international Commission for Radiation Protection (ICRP) and the World Health Organization (WHO) values. Hence, the drilled well are recommended for water screening to remove radionuclides.

KEYWORDS: dug well; HPGe; annual effective dose; committed effective dose.

1 INTRODUCTION

The quest for quality water supply has been a challenge to many public and private water suppliers in spite of advances in science and technology. Water purity is directly linked to the level of its contaminants i.e. physical, chemical, biological etc [1]. Diseases associated with water are also linked to the presence of these contaminants. Bottled and sachet water are usually labelled in terms of its chemical composition but no account of the level of its biological and physical contaminants. Water supply has been found to contain some physical contaminants such as ²³²Th, ²²⁶Ra, and the non-decay series ⁴⁰K which pose serious health risk for human use. ²²⁶Ra and ²²⁸Ra are known to be very hazardous [2]. When ingested into the human system, radium behaves like calcium and its accumulation over a long time can result into bone or sinus cancer [3]. Higher concentrations of radioactivity in environmental media are connected with risk of health challenges to humans such as kidney damage, mutagenicity, leukemia as well as cancer of bladder, kidney, testis and lung [4]. While many developed nations of the world have set up agencies to regulate its water supply, it is not certain whether developing nations have toed this line [5].

There is need therefore to assess the physical contaminants and or radionuclides present in various water sources and ascertain whether this is above or below the minimum permissible dose due to exposure. The World Health Organization (WHO) and the United States Environmental Protection Agency (EPA) have issued regulations and guidelines on the quality of drinking water [5]. Water supply generally whether in the form of dug or drilled well is sourced from the soil, which is the product of weathering from the parent rock. The distribution of radionuclides in any water supply is a function of the local geology of the parent rock or soil [6, 7]

*Presenting Author, e-mail: arogmuyi@yahoo.com

[8] Investigated the physical parameters and the total radioactivity concentrations in some borehole water in Zaria, Northwestern Nigeria. They noted that some of the samples met the requirements of good water supply, while some had the alpha and beta radioactive concentrations above the set values recommended by the World Health Organization and the US Environmental Protection Agency (EPA). [9] also assessed the radionuclides concentrations in some public water in Markudi Metropolis of Benue State, Nigeria using a Geiger Muller Counter. It was reported that there exist highest radiation concentration in Borehole water ranging from 2.86×10^{-1} Bq to 3.69×10^{-1} Bq and the least in bottled water in the range $0.55 \times 10^{-1} - 0.77 \times 10^{-1}$ Bq. It is evident that physical contaminant in drinking water should not be under estimated as it poses a great risk to human health.

Dug and drilled well are the major sources water available for human use in town and cities of Nigeria. Hence, this work is intend to assess the level of physical contaminants (i.e. radionuclides) present in Eleven drilled well distributed across selected cities in Ondo ($5^{\circ} 48'N, 4^{\circ} 45'E$) and Ekiti States ($8^{\circ} 15'N, 6^{\circ} 05'E$), South Western Nigeria using high resolution gamma ray Spectrometry. The age dependent annual effective dose accrued to individual due to exposure will also be calculated.

2 MATERIAL AND METHOD

2.1 Collection and Preparation of Samples

Water samples were collected from the selected well using very clean container [fetcher] whereby the usual manual procedure for collecting water from wells which involved the dipping of the containers which has been firmly tied to a rope long enough to reach the water level in the well was employed. The collected water was then emptied into a one litre keg and labeled based on the alphabet ascribed to each city. Table 2.1 gives the samples code and interpretation. Water samples collected from the various dug wells across the two states using a one liter plastic keg were acidified with 11M of HCl at the rate of 10ml per liter of samples as soon as possible, to avoid absorption of radionuclide onto the wall of container [10]. Marinelli beaker of 1L volume capacity previously washed, rinsed with a dilute sulphuric acid (H_2SO_4) and dried to avoid contamination was filled with sample from the container used for sampling. This was later sealed for at least four weeks to ensure that no loss of radon and to achieve secular equilibrium between the daughters and the parents nuclides.

2.2 Sample Analysis

The activity Concentrations of the dug well water samples were measured using an N-type coaxial HPGe gamma-ray detector at the laboratory of Ghana Atomic Energy Commission Accra with ORTEC Multichannel Analyzer (MCA) and MAESTRO-32 evaluation software for spectrum acquisition and processing. The relative efficiency of the detector was 28.5 % with energy resolution of 1.8 keV at gamma ray energy of 1332 keV of ^{60}Co . The gamma lines 609.31 and 1764.49 keV of ^{214}Bi were used to determine ^{226}Ra . The gamma lines 583.19 of ^{208}Tl were used to determine ^{232}Th and that of ^{40}K was determined from the gamma line of 1460.83 keV. The samples were counted for 18,000 seconds (5 hours). The energy and efficiency calibrations were performed using mixed radionuclide calibration standard in the form of solid water, serial number NW 146 A with approximate volume 1000 mL and density 1.0 gcm^{-3} in a 1.0 L Marinelli beaker. The standard was supplied by Deutscher Kalibrierdienst (DKD-3), QSA Global GmBH, Germany. Background measurements were made for the same period. Density corrections were also made where appropriate.

The specific activity concentrations (A_{sp}) of ^{226}Ra , ^{232}Th , and ^{40}K were determined in $Bq \text{ l}^{-1}$ for the water samples using the following expression [11, 12, 13] after decay correction.

$$A_{sp} = \frac{N_{sam}}{P_E \cdot \epsilon \cdot T_c \cdot M} \quad (1)$$

where; N_{sam} is net counts of the radionuclide in the sample, P_E is gamma ray emission probability (gamma yield), ϵ is total counting efficiency of the detector system, T_c is sample counting time and M is mass or weight of the Sample.

The specific activity obtained using equation (1) coupled with appropriate dose conversion factors form the basis for the evaluation of the radiological health hazards posed by the analysed samples from the study area.

2.3 Calculation of Annual Effective Dose and Committed Effective Dose

Estimation of annual effective dose E_d (Sv/y) to an individual due to the ingestion of the natural radionuclides present in the dug well water samples was carried out using the following relation by [14].

$$E_d = A_c A_i C_f \quad (2)$$

where A_c is the activity concentration of the radionuclide in the dug well (Bq/l), A_i is the consumption per annum or annual intake of drinking water and C_f is the ingested dose conversion factor for radionuclides (Sv/Bq). The ingested dose conversion factor and the consumption per annum vary with both radionuclides and the age of the individual ingesting the radionuclides. The ingested dose Conversion factor C_f used for ^{40}K , ^{232}Th and ^{226}Ra in this work and the corresponding consumption per annum in $l\ y^{-1}$ are $(6.2 \times 10^{-8}, 1.3 \times 10^{-8}, 6.2 \times 10^{-9})$, $(4.6 \times 10^{-6}, 2.9 \times 10^{-7}, 2.3 \times 10^{-7})$, $(4.7 \times 10^{-6}, 8.0 \times 10^{-7}, 2.8 \times 10^{-7})$ and $(2.0 \times 10^2, 3.5 \times 10^2, 7.3 \times 10^2)$ respectively for the three different age group [15, 16]. The total effective dose D (Sv/y) to an individual was established by summing contributions from all radionuclides present in the water samples, i.e.

$$D = \sum A_c A_i C_f \quad (3)$$

The annual effective dose values were calculated for three different age groups (0-1yr, 7-12yr, >17yr) i.e. babies, Children and Adult. The committed effective dose C_d , which is a measure of the total effective dose received over an average life time of 50 years was calculated for the age >17 years due to the ingestion of radionuclides using the relation

$$C_d = 50 \times D \quad (4)$$

Where D is the total effective dose to an individual

3 RESULT AND DISCUSSION

The measured activity concentration of ^{232}Th , ^{40}K and ^{226}Ra in the drilled well water samples of the two states revealed that ^{137}Cs was not detected in all the samples. The activity concentrations were found to be within the range 2.25 ± 0.39 to 35.61 ± 6.22 Bq l^{-1} ^{232}Th , 45.42 ± 2.98 to 467.61 ± 31.69 Bq l^{-1} ^{40}K , 7.08 ± 1.71 to 56.68 ± 12.50 Bq l^{-1} ^{226}Ra for Ondo state drilled well water samples. While Ekiti state drilled well water samples lie within the range 1.66 ± 0.46 to 25.55 ± 5.76 Bq l^{-1} ^{232}Th , 41.50 ± 2.89 to 558.82 ± 31.69 Bq l^{-1} ^{40}K , 4.90 ± 1.08 to 54.18 ± 13.34 Bq l^{-1} ^{226}Ra . ^{40}K had the highest concentration, followed by ^{226}Ra and the least activity was found in ^{232}Th for the two states. The highest activity concentration of the three radionuclides (^{232}Th , ^{40}K and ^{226}Ra) was recorded in the sample taken from Erinmope-Ekiti and the least was found in the sample taken from Ise-Ekiti with the exception of Ado-Ekiti that had the least activity concentration for ^{40}K . Ondo state had its highest concentration in the sample taken from Ikare-Akoko and the least concentrations, for ^{232}Th , ^{40}K and ^{226}Ra in the sample taken from Owo, Ondo and Okitipupa. The mean activity concentrations of ^{232}Th , ^{40}K and ^{226}Ra are 8.43 ± 1.47 Bq/l, 129.67 ± 8.27 Bq/l, 15.83 ± 3.39 Bq/l and 7.25 ± 1.69 Bq/l, 156.57 ± 9.05 Bq/l, 15.92 ± 3.68 Bq/l respectively for both Ondo and Ekiti drilled Well water samples. The result obtained in both cases for ^{226}Ra exceeds the recommended limits of 1.00 Bq/l [10] and 0.185 Bq/l [17]. This result corroborates the 7.15 ± 6.94 Bq l^{-1} reported for ^{226}Ra by [17] in private dug well

in Akure Southwestern Nigeria. The mean measured activity concentrations of ^{232}Th and ^{40}K for Ondo state (8.43 ± 1.47 Bq/l and 129.67 ± 8.27 Bq/l) and Ekiti state (7.25 ± 1.69 Bq/l and 156.57 ± 9.05 Bq/l) were above the values reported in other part of the world.

The age dependent annual effective dose was calculated using using equation (2) and the total annual effective dose using equation (3). The annual effective dose and the total annual effective dose were calculated. Generally, the mean total annual effective dose for each of the age groups (Babies 0-1y, Children 7-12y, and Adult >17y) resulting from the radionuclides in the drilled Well water samples of both Ondo and Ekiti States is (26.91 ± 5.11 , 6.52 ± 1.25 , 6.56 ± 1.29) mSv/y and (23.58 ± 5.12 , 5.90 ± 1.24 , 5.18 ± 1.08) mSv/y respectively. This is above the ICRP and WHO recommended limits of 1mSv/y and 0.1mSv/y respectively. Total Annual effective dose resulting from the ingestion of the three radionuclides (i.e. ^{232}Th , ^{40}K , ^{226}Ra) among the three age groups ranged from 6.65 ± 1.48 to 81.40 ± 18.20 mSv/y, 1.73 ± 0.36 to 20.30 ± 4.46 mSv/y, 1.47 ± 0.31 to 17.90 ± 3.84 mSv/y and 10.50 ± 1.77 to 91.80 ± 17.90 mSv/y, 2.68 ± 0.44 to 21.60 ± 4.28 mSv/y, 2.36 ± 0.38 to 19.70 ± 3.74 mSv/y respectively for Ekiti and Ondo states. In both states, Babies (i.e. 0-1y) are most Susceptible to radiation followed by Children (i.e. 7-12y) and the least was found in Adult (> 17y). The variation of total annual effective dose and the three age groups considered is shown in figures 1 and figure 2 for the sampled drilled well across the two states. In all the samples taken from Ondo state the annual effective dose ingested from ^{226}Ra is above the recommended limits of 1.0 mSv/y by ICRP for all ages. The annual effective dose resulting from the ingestion of ^{232}Th in the drilled well water samples of Ondo State is below the recommended limits of 1.0 mSv/y set by ICRP except for the Babies age group (0-1 y) and the adult group (>17y) only in the sample taken from Okitipupa. Annual effective dose resulting from the ingestion of ^{40}K in the dug well water samples of Ondo state is below the recommended limits of 1.0 mSv/y set by ICRP for the three age groups considered in all the samples with the exception of the one taken from Ikare-Akoko. Similarly, in Ekiti State the annual effective dose resulting from the ingestion of ^{232}Th in its dug well water samples is above the recommended limits of 1.0 mSv/y in all the drilled water samples taken for the babies age group (0-1y) and below in all the other age groups (children and Adult). The only exception is the sample taken from Erinmope for the Children and Adult groups. Annual effective dose resulting from the ingestion of ^{40}K in the drilled well of Ekiti is above the recommended limits of 1.0 mSv/y set by ICRP for the age groups considered in Erinmope Ekiti drilled well water samples and below for all the other samples. The ingestion of ^{226}Ra and its annual effective dose from the drilled well of Ekiti State is above the limits set by ICRP of 1.0 mSv/y for all the samples and for the age groups considered. It is however within the limit of 1.0 mSv/y in the sample taken from Ise-Ekiti for the adult and Children age groups. Hence the drilled well waters from Ikare –Akoko in Ondo state and that of Erinmope Ekiti should be screened for ^{226}Ra , because its accumulation in the bone of Babies and Children may result in bone or Sinus Cancer. The high activity concentrations of ^{226}Ra in Ikare-Akoko drilled well water samples from Ondo State may be as result of emerging industries coupled with local geology and that of Erinmope Ekiti may be as a result of its closeness to Guinea Savannah where the soil type (Clay-sandy) needs huge application of Potash fertilizer to grow crops and the presence of granite rock in the terrain. This result is in tandem with the findings of [18, 19, 20]. The committed effective dose which is a measure of the radiation received over a lifetime of 50y is also presented for the Adult age group.

Figure 1: Total annual Effective Dose D (Sv/yr) variation in the dug well water samples of Ekiti State

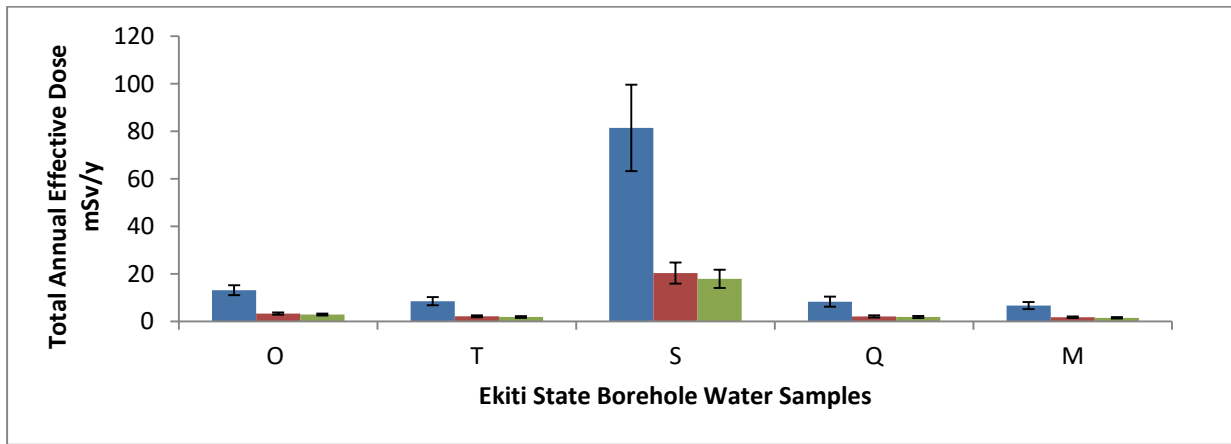
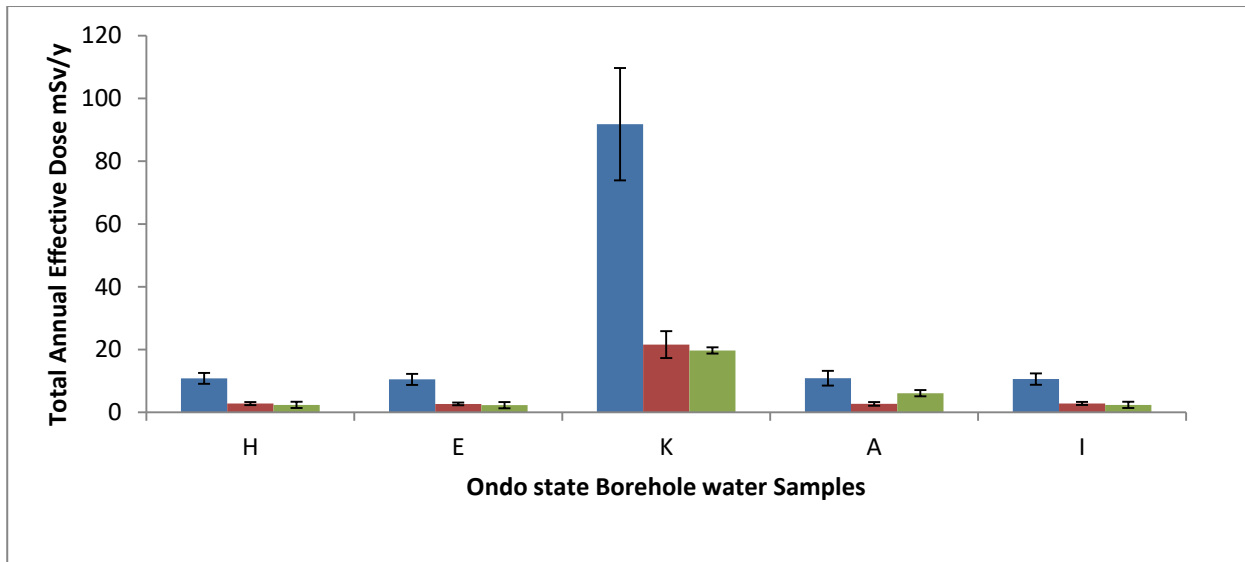


Figure 2: Total annual Effective Dose (Sv/yr) in the dug well water Samples of Ondo State



4 CONCLUSION

The activity concentrations of ^{232}Th , ^{40}K , and ^{226}Ra in the dug well water samples distributed across ten (10) notable Cities in Ondo and Ekiti States had been determined. The activity concentration of gamma emitters in the drilled well water ranged from 2.25 ± 0.39 to $35.61 \pm 6.22 \text{ Bq l}^{-1}$ ^{232}Th , 45.42 ± 2.98 to $467.61 \pm 31.69 \text{ Bq l}^{-1}$ ^{40}K , 7.08 ± 1.71 to $56.68 \pm 12.50 \text{ Bq l}^{-1}$ ^{226}Ra and 1.66 ± 0.46 to $25.55 \pm 5.76 \text{ Bq l}^{-1}$ ^{232}Th , 41.50 ± 2.89 to $558.82 \pm 31.69 \text{ Bq l}^{-1}$ ^{40}K , 4.90 ± 1.08 to $54.18 \pm 13.34 \text{ Bq l}^{-1}$ ^{226}Ra respectively for Ondo and Ekiti states. The age dependent total annual effective dose due to the ingestion of these radionuclides from the drilled well of Ondo and Ekiti States was found to be above the recommended limits of 1.0 mSv/y and 0.1 mSv y^{-1} set by ICRP and WHO respectively for the samples taken from Erinmope Ekiti and Ikare-Akoko. Hence the affected drilled are recommended for screening for radionuclides to prevent the outbreak of radiation induced diseases. In all the samples considered across the two the two states, Babies were most susceptible to radiation followed by Children and the least was Adult.

5 REFERENCES

- [1] Akinloye, M. K. (2008); Radioactivity in LAUTECH Water Supplies, Nigeria Nigerian Journal of Physics 20 (1), 29-37.
- [2] NCRPM (National Council on Radiation Protection and Measurement)., (1996): Screening Models for releases of radionuclides to atmosphere, surface water and ground. Report 123 (Bethesda, MD: NCRP Press).
- [3] Mays, C.W., Rowland, R.E. and stehney, A.E., (1985). Cancer risk from the lifetime intake of Ra and U isotopes. Health Phys. 48(5), 635 – 647
- [4] Guogang J, Giancarlo T, Leandro (2009). Concentrations of ^{238}U , ^{234}U , ^{235}U , ^{232}Th , ^{230}Th , ^{228}Th , ^{226}Ra , ^{228}Ra , ^{224}Ra , ^{210}Po , ^{210}Pb , and ^{212}Pb , in Drinking water in Italy: Reconciling Safety Standards Based on Measurements of gross α and β . J Environ. Rad., 100:941-949
- [5] WHO. Guidelines for drinking water quality, (2003). Draft, vol. 3, Chapter 9 (Geneva).
- [6] Ajayi, O.S., and Achuka, J., (2009): Radioactivity in Drilled and Dug well Drinking water of Ogun State Southwestern Nigeria and Consequent Dose Estimates. Radiat. Prot. Dosimetry 1-10.
- [7] Ajayi .O.S., Adesida G. (2009). Radioactivity in some sachet drinking water samples produced in Nigeria. Iran J. Radiat. Res., 7(3) 151-153.
- [8] Onoja R.A., Daniel J.A. and Sunday O., (2013). Physical parameters and total radioactivity concentrations in some borehole water. Archives of Applied Science Research 5(3): 211-219.
- [9] Isikwue B.C., Isikwue .M.O. and Danduwa T.F (2009): Assessment of Radionuclide Concentrations in Some Public Water in Use in Markudi Metropolis of Benue State, Nigeria. Journal of Research in Forestry, Wildlife and Environment. 1, 93-99.
- [10] International Atomic Energy Agency, Measurement of Radionuclides in food and the Environment Guide book, Technical Report series No 295, IAEA, Vienna, 1989.
- [11] Uosif, M. A. M., El-Taher, A. and Abbady, Adel G.E. (2008): Radiological Significance of beach sand used for Climatotherapy from Safaga, Egypt, Rad. Prot Dosimetry, 1-9.
- [12] Darko, E. O. and Faanu, A. (2007). Baseline radioactivity measurements in the vicinity of a gold processing plant. J. Applied Science & Technology, 12(1 & 2): 18-24.
- [13] Darko, E. O., Faanu, A., Awudu, A. R., Emi-Reynolds, G., Oppon, O. C., Mensah-Brobbe, I., Quansah, T., Dapaah, K. and Addo, W. (2008). Public Exposure to hazards associated with NORMS in mining and mineral processing activities in Ghana. Final Technical Report of data, IAEA TC Project GHA 9005, Accra.
- [14] Alam, M. N., Chowdhury, M. I., Kamal, M., Ghose, S., Islam, M. N., and Anwaruddin, M. (1999): Radiological assessment of drinking water of the Chittagong Region of Bangladesh. Radiat. Prot. Dosimetry 82, 207-214.
- [15] International Basic safety Standards for Protection against ionizing Radiation and for the safety of radiation Sources, (1996) (Safety Series Number 115).
- [16] WHO (2006): World Health Organization, Guidelines for drinking water quality 1, Recommendations; Radiological Aspects 197 - 209.
- [17] United States Environmental Protection Agency., (2000): Office of water. Setting standards for safe drinking water. Revised June 9 (US, EPA, Washington).
- [18] Ajayi, O. S. and Owolabi, T.P. (2007): Determination of natural Radioactivity in drinking water in private dug well in Akure Southwestern Nigeria. Radiation Protection Dosimetry 128, 477-484.
- [19] Rahaman, M. A., (1976); Review of basement geology of south-western Nigeria. In Geology of Nigeria. Kogbe, C. A., Ed. (Lagos, Nigeria: Elizabethan Publication). 41-58.
- [20] Oshin, I. O. and Rahaman, M. A., (1985); Uranium favorability study in Nigeria. J. Afr. Earth Sci. 5, 167-175.

Dating of a sediment core from Lake Biel (Switzerland) and source characterization of fallout Pu

Anja Pregler*

Paul Scherrer Institute, 5232 Villigen, Switzerland.

Abstract. Radionuclide dating has been a reliable and powerful tool for evaluating geological events over years. In this work, terrigenous (^{210}Pb) and anthropogenic (^{137}Cs) radionuclides were measured in a sediment core from Lake Biel by means of γ -spectrometry at the Paul Scherrer Institute as well as at the Swiss Federal Institute of Aquatic Science and Technology. Depth-related decrease of activity concentration of natural $^{210}\text{Pb}_{\text{unsupp}}$ due to radioactive decay yields a sedimentation rate of 0.7 ± 0.07 cm per year for core BIE14-67B. In comparison, the depth distribution of ^{137}Cs , revealing the basic historical fallout peaks of the Chernobyl accident in 1986 and the nuclear weapon testing period from 1945 to 1963, quantifies the sedimentation rate to 1.00 ± 0.1 cm per year. Another increased activity concentration of ^{137}Cs was dated to the middle of the 1970s when releases of the Mühleberg nuclear power station were fed into the Aare, an influent river of Lake Biel. Further slightly higher specific activities were found in depths belonging to the turn of the millennium also originating from the Mühleberg nuclear power station. Particular isotope ratios such as the $^{241}\text{Am}/^{239+240}\text{Pu}$ activity ratio (0.41 ± 0.15) and the $^{240}\text{Pu}/^{239}\text{Pu}$ atomic ratio (0.17 ± 0.04) are strong evidence of the nuclear weapon testing period between 1945 and 1963 as a source of the radionuclide fallout. Finally, an attempt to estimate how much of the total ^{137}Cs inventory originates from the different historical events apportions 55 % to the nuclear weapon testing period, 30 % to the releases of the Mühleberg nuclear power station and 15 % to the Chernobyl accident in 1986.

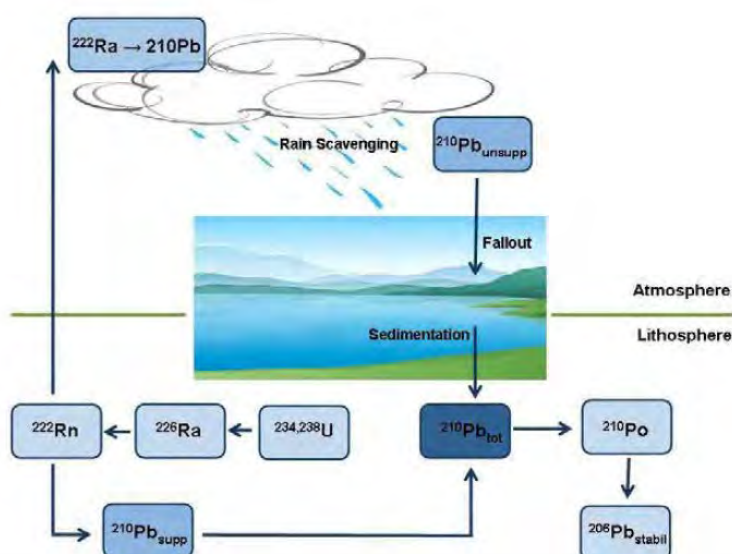
KEYWORDS: ^{210}Pb -dating; ^{137}Cs -dating; Fallout Pu.

1 INTRODUCTION

1.1 ^{210}Pb -dating

Over the last decades, radiometric dating continues to replace optical methods that focus on apparent markers like varve chronology or chronostratigraphic layers, e.g. volcanic layers or the amount of diatoms in a sediment layer. One of the most common radiometric dating methods is dating by means of the naturally occurring ^{210}Pb which was first applied to lake sediments in 1971 [1].

Figure 1: ^{210}Pb global cycle [2]



*Presenting author, e-mail: anja.pregler@psi.ch

It is based on the decay series of ^{238}U which is abundant in the form of oxides in all of the earth's crust and decays through several daughters to ^{222}Rn . This water-insoluble noble gas partially escapes from the continental crust into the atmosphere where it decays to ^{210}Pb . This distinct fraction of ^{210}Pb is fixed rapidly onto aerosols, consequently distributed by general atmospheric circulation and can either be scavenged by rain or dry fall-out onto the earth (Figure 1). Therefore, it is also called atmospheric or unsupported ^{210}Pb ($^{210}\text{Pb}_{\text{unsupp}}$). However, owed to the natural ^{226}Ra content in all geological formations, there is also a continuous production of ^{222}Rn . The part not escaping from lithosphere leads to an ingrowth of ^{210}Pb . This fraction which accumulates in the sediments is called geogenic or supported ^{210}Pb ($^{210}\text{Pb}_{\text{supp}}$) and its concentration is expected to be constant [2].

By analyzing a sediment with γ -spectrometry, both types of ^{210}Pb ($^{210}\text{Pb}_{\text{unsupp}}$ and $^{210}\text{Pb}_{\text{supp}}$) are measured simultaneously, as they release the same decay energies. Accordingly, $^{210}\text{Pb}_{\text{tot}}$ is the sum of the atmospheric and geogenic ^{210}Pb :

$$^{210}\text{Pb}_{\text{tot}} = ^{210}\text{Pb}_{\text{unsupp}} + ^{210}\text{Pb}_{\text{supp}} \quad (1)$$

By γ -spectrometry, $^{210}\text{Pb}_{\text{supp}}$ can be measured either as ^{226}Ra itself (after subtracting a distinct part which originates from ^{235}U due to overlapping photon emission energies at 186 keV) or by ^{222}Rn when it is in secular equilibrium with $^{210}\text{Pb}_{\text{supp}}$ (approximately after 3 weeks due to its half-life of 3.825 days when the sample is gas-tight closed) using the ^{222}Rn decay products ^{214}Pb and ^{214}Bi :

$$^{210}\text{Pb}_{\text{unsupp}} = ^{210}\text{Pb}_{\text{tot}} - ^{210}\text{Pb}_{\text{supp}} \quad (2)$$

$$^{210}\text{Pb}_{\text{unsupp}} = ^{210}\text{Pb}_{\text{tot}} - ^{226}\text{Ra} \text{ (or } ^{214}\text{Pb, } ^{214}\text{Bi)} \quad (3)$$

The determination of the sedimentation rate in Lake Biel is done according to the CIC model that is dimensioned for environments like deep ocean basins or large lakes where the $^{210}\text{Pb}_{\text{unsupp}}$ flux is not supplied directly by local atmospheric fallout [3]. It implies that the specific activity of $^{210}\text{Pb}_{\text{unsupp}}$ at the sediment surface is constant and that the sedimentation rate can vary [4]. The specific activity of $^{210}\text{Pb}_{\text{unsupp}}$ can then be logarithmically plotted against depth, yielding a linear relationship from which the slope and thus the sedimentation rate can be determined:

$$\text{Sedimentation rate} = \frac{\text{decay constant } ^{210}\text{Pb} (-0.03114)}{\text{slope}} = \text{cm/year} \quad (4)$$

As a result of the relatively short half-life of ^{210}Pb (22.3 years), this dating method allows a temporal resolution of about 100-150 years.

1.2 ^{137}Cs -dating

Not only naturally occurring radioactive isotopes are used for dating, but also anthropogenic radionuclides, such as ^{137}Cs that was released into the atmosphere by several historic events. Examples of such chronostratigraphic markers are for one thing the more than 500 atmospheric nuclear bomb tests that were conducted from the late 1940s to the early 1960s, especially in the northern hemisphere. For another thing, there was the Chernobyl accident in April 1986 when a nuclear power reactor exploded in consequence of a criticality experiment that was performed although the reactor operated on a non-stable basis at that time. Radionuclides released into the atmosphere during these events were tightly bound to sediment particles, distributed around the world by winds and constantly deposited onto the Earth's surface. Due to its half-life of 30 years, ^{137}Cs can still be detected in sediments and therefore helps to validate the former sedimentation rate determined by ^{210}Pb .

1.3 Fallout Pu

Activity ratios of distinct isotopes are used to characterize the source of release [5-7]. The isotopes of Pu develop e.g. in nuclear power stations using ^{235}U and ^{238}U for power generation. For instance, the generated ^{241}Pu decays with a half-life of 14.4 years to ^{241}Am which has a much longer half-life of 432 years. Each event like the Chernobyl accident or the atomic weapon testing period produced a distinct ratio of these long-lived fission products from nuclear fallout. Since ^{241}Pu is a relatively short-lived radionuclide, it already decayed to a great extent to its daughter ^{241}Am and so the ratio of $^{241}\text{Am}/^{239+240}\text{Pu}$ is constantly changing over time. By assuming no initial amount of ^{241}Am and an initial $^{241}\text{Pu}/^{239+240}\text{Pu}$ ratio of 13 at time of exposure, the activity ratio of $^{241}\text{Am}/^{239+240}\text{Pu}$ can be determined as 0.36 and 0.38 in 2003 and 2014, respectively [8].

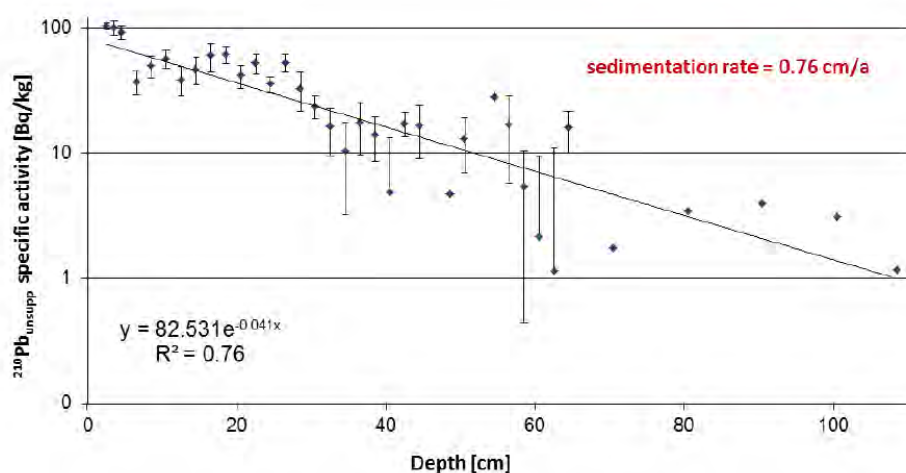
2 STUDY SITE AND SAMPLE PREPARATION

The study site is Lake Biel, a peri-alpine lake located in the canton of Berne, NW Switzerland. In April 2014, a 109 cm long core was collected in 53.1 m water depth in the middle of Lake Biel and further prepared in different laboratories. The core was cut lengthwise, dissected into 1 cm thick semicircles, freeze-dried and finally ground to a homogeneous powder. ^{210}Pb and ^{137}Cs activity concentrations can be measured directly and without any further sample preparation by means of γ -spectrometry. For α -spectrometry of the actinides, which are present only in very small amounts, Am and Pu have to be separated from all other elements. Therefore, all organic matter in the samples has to be decomposed by wet and dry ashing, then the samples are leached and the insoluble particles are filtered out. The remaining solutions have to pass several chromatographic extractions in order to separate Am and Pu amongst others from U, Th and the Lanthanides. Pure Am and Pu are then electrodeposited onto small Cr-Ni planchets which in turn can be measured by α -spectrometry. Because of the similar decay energies, ^{239}Pu and ^{240}Pu can only be detected in sum. For measuring the separated activity concentrations, the Pu has to be removed from the planchets and measured again by means of ICP-MS.

3 RESULTS

3.1 ^{210}Pb -dating

The total detected ^{210}Pb is measured by its γ -emission at 46.5 keV containing $^{210}\text{Pb}_{\text{supp}} + ^{210}\text{Pb}_{\text{unsupp}}$. In order to obtain $^{210}\text{Pb}_{\text{unsupp}}$, $^{210}\text{Pb}_{\text{supp}}$ has to be subtracted from $^{210}\text{Pb}_{\text{tot}}$. Therefore, ^{214}Bi was measured at 352 keV as substitute for $^{210}\text{Pb}_{\text{supp}}$ which can directly be subtracted from $^{210}\text{Pb}_{\text{tot}}$. This is only possible because the plastic tubes which contain the sediment were gas-tightly closed for at least 3 weeks to ensure the secular equilibrium between ^{226}Ra and its daughters. When the resulting activities of $^{210}\text{Pb}_{\text{unsupp}}$ are plotted in logarithmic scale against depth, an exponential regression curve can be fitted through these data points identifying the slope. By dividing the decay constant of ^{210}Pb (-0.03114) by the slope of the measurements (-0.041), the sedimentation rate yields 0.76 ± 0.08 cm per year (Figure 2).

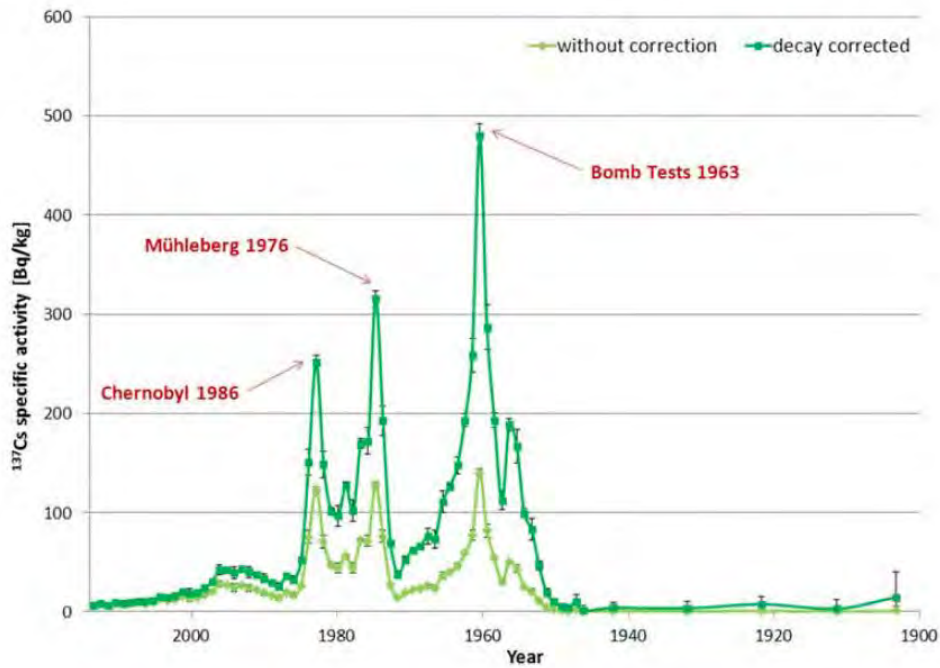
Figure 2: Specific activity plot of $^{210}\text{Pb}_{\text{unSUPP}}$ in logarithmic scale against depth

3.2 ^{137}Cs -dating

The detected ^{137}Cs activity concentrations can be plotted directly and without correction against depth revealing 3 major peaks (Figure 3). By applying the ^{210}Pb sedimentation rate of 0.76 cm per year, the peaks can be identified according to the historical events. The youngest peak at a depth of 31 cm arises from the Chernobyl accident in April 1986 whereas the oldest one at 53 cm reflects the atomic bomb testing period in the 1960s with its maximum in 1963. The smaller peak attached at a depth of 57 cm corresponds to the minor nuclear weapon testing peak in the year 1958 [9]. The intermediate peak followed by a small one in depths of 35 cm and 39 cm, respectively, correspond to the years 1976-1978 in which a release of radionuclides was caused by the Mühleberg nuclear power station nearby Lake Biel that used low-quality fuel rods during 1976-1978 [10]. The sedimentation rate is determined by relating the historical dates to the sediment depth. Four dates were chosen: the sampling date in April 2014, the Chernobyl accident in April 1986, the release from the nuclear power station Mühleberg 1976 and the Limited Test Ban Treaty coming into effect in October 1963. If these dates are plotted against the depth where their maxima are detected, a linear regression can be applied supposing a constant sedimentation. This reveals a sedimentation rate of 1.00 ± 0.1 cm per year.

The sedimentation rate is also used to calculate the age of the sediment depths. If the time scale derived by the sedimentation rate of 1.0 cm per year is then applied to the decay law using the ^{137}Cs half-life of 30.17 years, a decay correction can be made for the measured activities. As can be seen in figure 3, the highest ^{137}Cs inventory at time of deposition was approximately 500 Bq/kg. With this dating of the sediment core, the elevated range between 18 cm and 21 cm reproduces the years between 1994 and 1997. Thevenon et al. (2013) [10] were the first to reveal a ^{137}Cs peak in the year 2000 (according to their sedimentation rate) which they found to be in accordance with an emergency shutdown of the Mühleberg nuclear power station reactor due to an accidental opening of a steam-relief valve (on the 6th of June 1999. Furthermore, the slightly elevated activity in the sediment core from Lake Biel which is dated to 1994-1997 (according to the sedimentation rate of 1.0 cm per year) matches the small releases of ^{137}Cs published in 2013 [11].

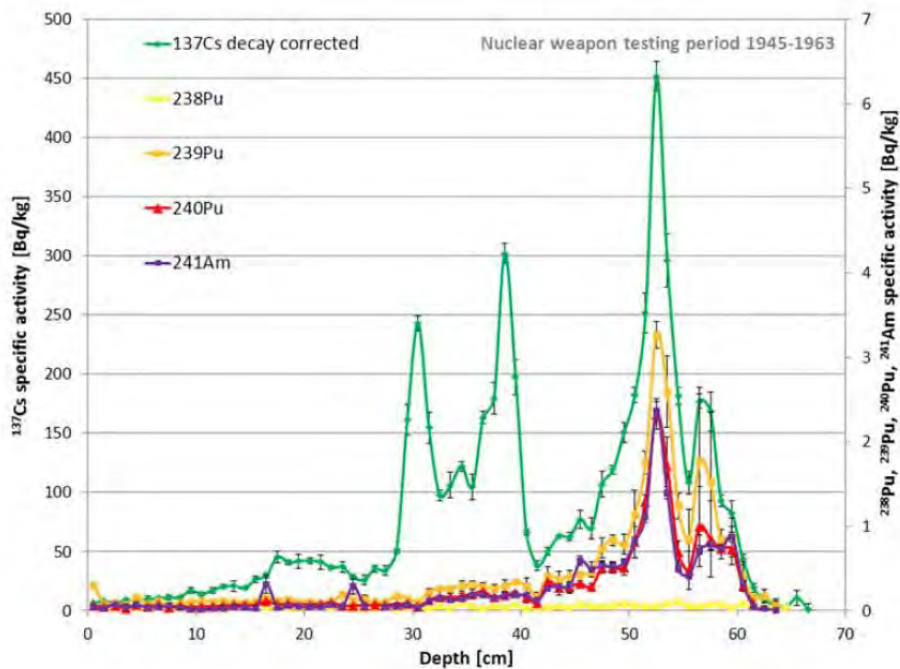
Figure 3: Specific activity plot of ^{137}Cs against calendar year indicating the detected specific activities in the sediment as well as the decay corrected values



3.3 Source Characterization of Am and Pu

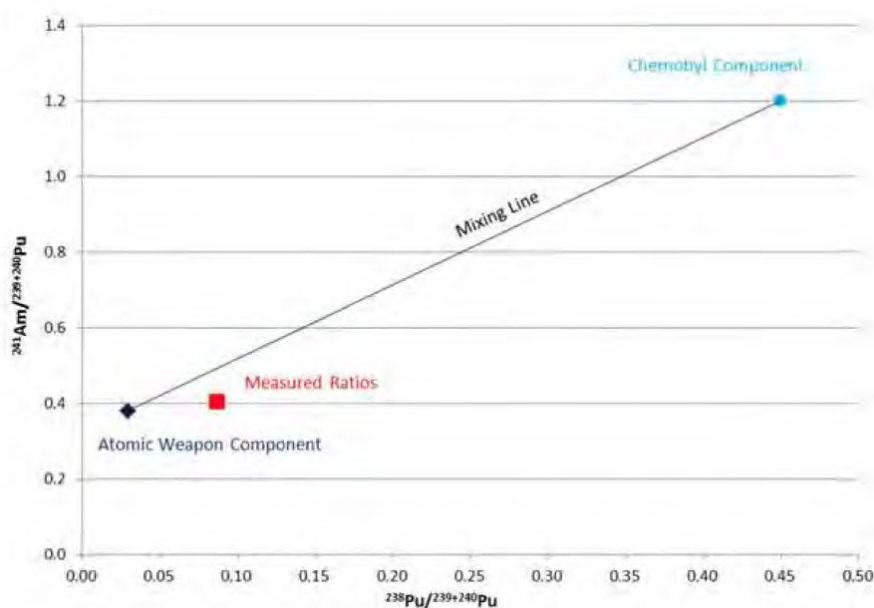
The radionuclide-releasing events such as the Chernobyl accident or the atomic weapon testing period produced a distinct ratio of certain actinides by nuclear fallout. With the help of values from literature, it is possible to assess their origin. All specific activities of the measured Pu isotopes as well as ^{241}Am and ^{137}Cs are plotted against depth in figure 4. Conspicuously, the elevated specific activities of the actinides are consistent with the nuclear weapon testing period between 1945 and 1963. This already indicates that the origin of the detected actinides is the atmospheric nuclear weapon test fallout.

Figure 4: ^{238}Pu , ^{239}Pu , ^{240}Pu , ^{241}Am (right axis) and ^{137}Cs (left axis) specific activity plotted against depth with 2σ uncertainties.



Still, this assumption has to be confirmed by determination of certain ratios. Therefore, the measured specific activities of ^{241}Am are plotted against $^{239+240}\text{Pu}$ indicating the average ratio of 0.41 ± 0.15 . Comparing this value to the literature ratios of 0.38 caused by the nuclear weapon testing period and 1.2 by the Chernobyl accident, the origin is clearly related to the first one. Moreover, this means that not only the specific activities corresponding to the peaks but also those detected in lower depths are correlatable with the atomic bombs. Reason for this is post-depositional redistribution of sediment and catchment-derived input from the surrounding area of Lake Biel [13]. The source determination is also done with ^{238}Pu which yields a $^{238}\text{Pu}/^{239+240}\text{Pu}$ ratio of 0.09 ± 0.14 . This neither perfectly fits the literature values for the nuclear weapon testing period of 0.03, nor does it fit the Chernobyl accident ratio of 0.45, but still it points towards the nuclear weapon testing period. In figure 5, these ratios are illustrated in comparison to Chernobyl and the bomb tests. The line between the two points represents the mixing line of both components. Obviously, the $^{241}\text{Am}/^{239+240}\text{Pu}$ ratio determined in the sediment from Lake Biel is quite similar to the atomic bomb ratio. The $^{238}\text{Pu}/^{239+240}\text{Pu}$ ratio does not match the atomic weapon ratio but lies within a particular uncertainty range and does not fit the Chernobyl component at all. This implicates that the actinide fallout in Lake Biel is only due to the nuclear weapon testing period and that the fallout from the Chernobyl accident is not detectable here. For this reason, the first peak detected with the ^{137}Cs dating method has to be definitely due to the Chernobyl accident. The measurements executed with ICP-MS validate this, because the measured atomic ratio of $^{239}\text{Pu}/^{240}\text{Pu}$ is 0.17 ± 0.04 which perfectly matches the values of the nuclear weapon testing period of 0.176 ± 0.014 .

Figure 5: Correlation diagram of ^{241}Am and ^{238}Pu plotted against $^{239+240}\text{Pu}$

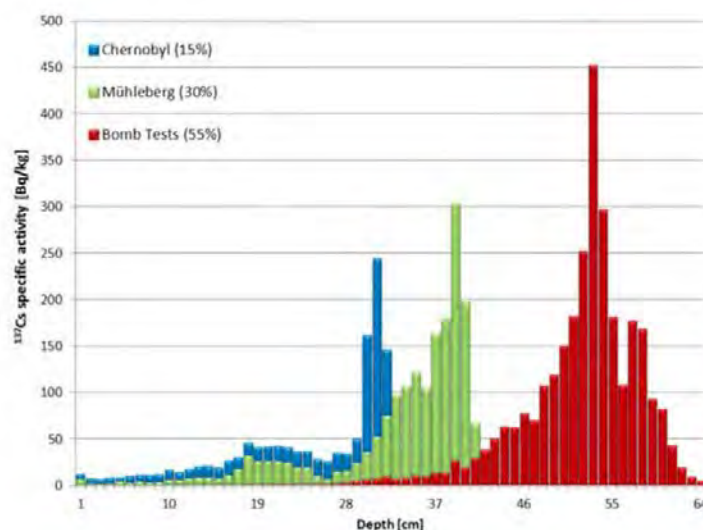


3.4 ^{137}Cs distribution

An attempt to estimate how much ^{137}Cs was released into the atmosphere differentiated by the three distinct events is shown in figure 6 (according to [7]). The input from the mid 1940s to the initial operation of the nuclear power plant Mühleberg in 1972 is completely related to the atomic weapon testing period. After 1972, the input still originating from these events has to be estimated by computing the procrastination of ^{239}Pu . In 1972, the delayed input of ^{239}Pu was approximately 10 % of the ^{239}Pu maximum during the nuclear weapon testing period. In 1986, when the Chernobyl accident happened, it was only 3%. This decreasing development was applied for the input of bomb test derived ^{137}Cs . The same tendency was assumed for the input which originates from the Chernobyl accident.

Only for the releases of the nuclear power station Mühleberg, the input was not simply decreasing but also increasing due to the identified releases in 2000. According to these estimations, 55 % of the total initial activities are due to the atomic weapon testing period, 30 % due to the releases of the Mühleberg nuclear power station and 15 % due to the Chernobyl accident in 1986. These values are in very good agreement with former supposed values [7].

Figure 6: Estimated amounts of ^{137}Cs related to the historic events



4 CONCLUSION

With the help of different dating methods, it was possible to determine the sedimentation rate for Lake Biel as well as to identify the origin of the Pu inventory. The sedimentation rate achieved by $^{210}\text{Pb}_{\text{unSUPP}}$ with the CIC model yielded 0.76 ± 0.07 cm per year. In order to validate the obtained sedimentation rate it is always necessary to compare it with an independent method. Therefore, one consistent sedimentation rate of 1.00 ± 0.1 cm per year is achieved with the ^{137}Cs dating method. The fact that the three ^{137}Cs peaks are definitely correlated to Chernobyl, Mühleberg and the atomic bombs, the sedimentation rate obtained with the ^{137}Cs dating method seems to be the more reliable one. Reason for the deviation of $^{210}\text{Pb}_{\text{unSUPP}}$ from the historical events is that the presence of $^{210}\text{Pb}_{\text{unSUPP}}$ can vary due to several independent factors. Examples for such variations can be changes in the watershed and contribution of groundwater which can carry large amounts of ^{222}Rn and ^{226}Ra into the lake [14], the presence of living organisms like phytoplankton [15], precipitation of calcium carbonate (CaCO_3) [16] or other influencing factors like changes in the surrounding area due to construction of dams [17]. There are some other independent methods that can be used for cross validation, such as the determination of ^{14}C input caused by atomic bomb proceedings or comparison with optical methods such as varve chronology, volcanic ash layers as well as historical floods or earthquakes that can cause discrepancies in the sediment layer.

5 REFERENCES

- [1] Krishnaswamy, S., Martin, J.M., Meybeck, M., 1971. Geochronology of lake sediments. *Earth and Planetary Science Letters*, 11, 407-414.
- [2] Preiss, N., Mélières, M.-A., Pourchet, M., et al., 1996. A compilation of data on lead-210 concentration in surface air and fluxes at the air-surface and water-sediment interfaces. *Journal of Geophysical Research*, 101, (D22), 28847 – 28862.
- [3] Le Roux, G., Marshall, W.A., 2001. Constructing recent peat accumulation chronologies using atmospheric fall-out radionuclides. *Mires and Peat*, 7, 1-14.
- [4] Appleby, P.G., 2000. Radiometric dating of sediment records in European mountain lakes. *Limn.* 59, 1-14.
- [5] Krey, P., 1976. Remote plutonium contamination and total inventories from rocky flats. *Health Physics*, 30, 209.
- [6] Schüttelkopf, H., 1981. Entwicklung einer Analysenmethode für Plutonium im Femtogramm/Gramm-Bereich und ihre Anwendung auf Umweltproben. Kernforschungszentrum Karlsruhe, Hauptabteilung Sicherheit, KfK 3035.
- [7] Röllin, S., Beer, J., Balsiger, B. et al., 2013. Radionuklide in Sedimenten des Bielersees. Umweltradioaktivität und Strahlendosen in der Schweiz, Bundesamt für Gesundheit, BAG.
- [8] UNSCEAR, 2000. Sources and effects of ionising radiation. Tech. rep., United Nations Scientific Committee on the Effects of Atomic Radiation, New York.
- [9] Ketterer, M.E., Hafer, K.M., Jones, V.J., et al., 2004. Rapid dating of recent sediments in Loch Ness: inductively coupled plasma mass spectrometric measurements of global fallout plutonium. *Science of the total Environment*, 322, 221-229.
- [10] Albrecht, A., Reiser, R., Lück, A. et al., 1998. Radiocesium dating of sediments from lakes and reservoirs of different hydrological regimes. *Journal of Environmental Radioactivity*, 28, 239-269.
- [11] Thevenon, F., Wirth, S.B., Fujak, M. et al., 2013. Human impact on the transport and anthropogenic elements to peri-alpine lakes (Switzerland) over the last decades. *Aquatic Sciences*, 75, 413-424.
- [12] Piller, G., 2013. Die Fakten zur Radioaktivität im Bielersee. URL: <http://ensi.ch/de/2013/07/15/die-fakten-zur-radioaktivität-im-bielersee/>
- [13] He, Q., Walling, D.E., Owens, P.N., 1996. Interpreting the ¹³⁷Cs profiles observed in several small lakes and reservoirs in southern England. *Chemical Geology including Isotope Geoscience*, 129, 115-131.
- [14] Baskaran, M., Nix, J., Kuyper, C., et al., 2014. Problems with the dating of sediment cores using excess ²¹⁰Pb in a freshwater system impacted by large scale watershed changes. *Journal of Environmental Radioactivity*, 138, 355-363.
- [15] Struminska-Paurulska. D.I., Skwarzeg, B., 2010. Plutonium isotopes ²³⁸Pu, ²³⁹⁺²⁴⁰Pu, ²⁴¹Pu and ²⁴⁰Pu/²³⁹Pu atomic ratios in the southern Baltic Sea ecosystem. *Oceanologia*, 52, 280-283.
- [16] Wright, R.F., Matter, A., Schweingruber, M., et al., 1980. Sedimentation in Lake Biel, an eutrophic, hard-water lake in northwestern Switzerland. *Schweiz. Z. Hydrol.* 42, 101-126.
- [17] Anselmetti, F.S., Bühler, R., Finger, D., et al., 2007. Effects of alpine hydropower dams on particle transport and lacustrine sedimentation. *Aquatic Sciences*, 69, 179-198.

Preliminary survey of radon population exposure in east Romanian region

Andreea Teodor^a, Irina Anca Popescu^a, Constantin Milu^b

^aNational Institute of Public Health, Regional Center of Public Health Iasi, Radiation Laboratory.

^bExpert Pro-Rad, Bucharest.

Abstract. In this recent 36 months survey we measured the population's exposure due to inhaled airborne Radon (^{222}Rn) and Radium (^{226}Ra) water ingestion by indoor air (598) and water (151) measurements together with effective dose estimations. All the measurements for this region of seven counties from east Romania (18.9% of total national territory), were performed only by four radiation laboratories with specific techniques, registered in our statistics as Bacau (Bc) and Iasi (Is) for one county, Suceava (Sv) for a territory of two counties and Galati (Gl) for three counties area. The maximum concentration value was recorded in very old buildings (from 1905s) in the rural Gl detached houses from adobe and clay bricks (622.0 Bq/m^3), the second highest value was measured in urban area (561.0 Bq/m^3). The values of ^{222}Rn performed in typical urban and rural dwellings and public institutions (schools, nursery schools) were significant higher in cold months compared to warm season. We noticed that for public institutions the maximum annual effective dose - MAED (1.55 mSv/year) was received by population in rural Sv kindergartens. There were some health status changes (respiratory pathologies) and one death possible in relation to this specific exposure only in Sv territory. The maximum value for effective dose at ingestion from water samples (ground, spring, drinking water and well) was identified for well water in rural Sv location (0.224 mSv/year) over admitted Indicative Dose. In this study phase for Radon assessment the results emphasis that further surveillance should be continued for risk evaluation and mapping of the region. To reduce the population exposure from areas with increased radon levels it is important to provide information for corrective actions.

KEYWORDS: Radon; population exposure; water ingestion; effective dose.

1 INTRODUCTION

The main goal in public health prevention of lung cancer related to radon (^{222}Rn) exposure is to identify the regions susceptible of high concentrations levels.

In the last years Romania joined the efforts of the other European Union member states in order to establish a comprehensive mapping of radon levels, especially in homes and public buildings. [1, 2].

Previous national campaigns performed (1987-1990, 1990-1994, 2000) in 567 dwellings from different regions (south and north-east) reported high level of ^{222}Rn concentrations in North-East region [1].

2 MEASUREMENTS AND METHODS

In the present study we intended to determine the general distributions of ^{222}Rn concentrations in buildings and Radium (^{226}Ra) and ^{222}Rn from water ingestion, to estimate the individual exposures and to identify the public health pathologies related to natural radiation exposure.

The survey was conducted over three years (2012-2014) in a territory of eight counties from the east region, representing 18.9% from national territory with approximately 4 million inhabitants (20% from total population). The measurements were performed only by four radiation laboratories with specific techniques, registered in our statistics as Bacau (Bc) for one county area, Iasi (Is) and Suceava (Sv) for a territory of two counties each, and Galati (Gl) for three counties.

For each location we measured samples of airborne ^{222}Rn concentration in randomly selected season months, from 226 urban buildings (96 block of flats, 54 detached houses, 39 kindergartens, 37 schools) and 99 rural locations (69 dwellings, 21 schools, 9 kindergartens) at the same time with outdoor determinations (273), using different alpha detectors (Durrige RAD 7 and SARAD RTM), the ^{222}Rn concentrations were counted for a certain period of time (30 to 60 minutes). The measurements were

registered in ground floors, bedrooms and living rooms in buildings constructed from various materials (woods, bricks, adobe, hollow masonry blocks, concrete blocks). In water samples (151) there were measured ^{222}Rn and ^{226}Ra concentrations and were estimated the effective doses from drinking water ingestion [3].

The data were analyzed in respect of EC statistics [1, 2]. For effective dose estimations specific adult conversion coefficients have been used: mean exposure time of indoor air inhalation (7000 h/year), respiratory flow ($0.9 \text{ m}^3/\text{h}$), radon equilibrium factor (0.4), and the dose conversion coefficient ($6.3 \times 10^{-6} \text{ Sv/Bq}$). Also, for outdoor air estimations were needed the equilibrium factor (0.8) and the mean exposure time (2000 h/year) For annual collective effective dose estimation were taking into account the nominal fatality and detriment coefficient ($7.3 \times 10^{-2} \text{ Sv}^{-1}$) for risk assessment. As an estimate, 1102 life-time radio-induced lung cancers each year might be attributed to inhalation of radon for east Romanian population. [4-7].

From an estimated region population of 3.86 mil (18.9%), a number of 23204 persons (0.6%) which were working in public institutions –schools and kindergartens were monitored as being at risk for developing health disorders related to radon exposure. Analytical methods used in this study were the descriptive statistics by SPSS 18.0 functions.

3 RESULTS

3.1 Indoor radon and dose estimates

The mean levels of ^{222}Rn concentrations and 95% Confidence Interval (95% CI) for urban and rural locations during the surveyed period are summarized in Table 1.

Table 1: Distribution of mean radon concentration levels by locations during 2012 -2014.

Location	N	Mean Bq/m ³	S.D.	Std. Error	95% CI		Min	Max
					-95%CI	+95%CI		
2012								
Public	6	46.54	16.39	6.69	29.34	63.75	30.12	69.40
Urban	4	38.60	12.77	6.38	18.28	58.91	30.12	57.36
Rural	2	62.44	9.85	6.97	-26.06	150.93	55.47	69.4
Dwellings ^{a)}	7	80.67	106.46	40.24	-17.79	179.12	20.17	318.0
Urban	5	41.06	23.91	10.69	11.37	70.74	20.17	81.9
Rural	2	179.7	195.60	138.3	-1577.7	1937.09	41.38	318.0
2013								
Public	6	49.52	19.11	7.80	29.46	69.58	29.50	80.95
Urban	4	51.47	24.06	12.03	13.19	89.75	29.50	80.95
Rural	2	45.62	6.72	4.75	-14.73	105.97	40.87	50.37
Dwellings ^{b)}	8	96.98	116.46	41.17	-0.38	194.34	24.75	367.0
Urban	6	43.5	21.66	8.84	20.82	66.28	24.75	82.50
Rural	2	257.3	155.21	109.7	-1137.3	1651.76	147.5	367.0
2014								
Public	12	83.39	86.02	24.83	28.73	138.05	18.91	320.0
Urban	7	56.01	30.49	11.52	27.81	84.20	18.91	93.41
Rural	5	121.7	125.72	56.22	-34.37	277.84	22.64	320.0
Dwellings	9	59.34	37.39	12.46	30.59	88.08	17.20	112.3
Urban	6	49.73	27.78	11.34	20.58	78.88	26.37	100.0
Rural	3	78.56	53.22	30.73	-53.66	210.77	17.20	112.3

^{a)} $p < 0.05$

^{b)} $p < 0.01$

For the measurements performed in 2012 and 2013 there were a strong positive correlation between the concentrations of radon in public institutions and the houses from rural locations ($p < 0.05$).

The single maximum value (622.0 Bq/m^3) was recorded in a very old building (from 1905s) in the rural GI detached house from adobe and clay bricks, the second highest concentration was measured in urban detached houses from concrete and bricks (561.0 Bq/m^3). The mean distribution and median values concentrations for each counties area are presented in figure 1.

Figure 1: The mean distribution and median values concentrations by counties

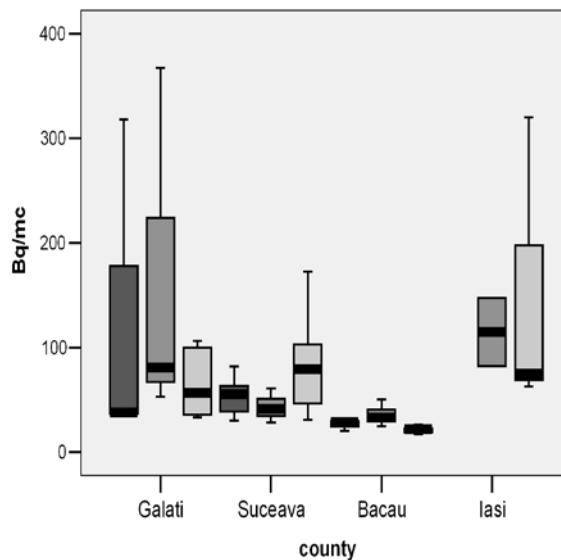
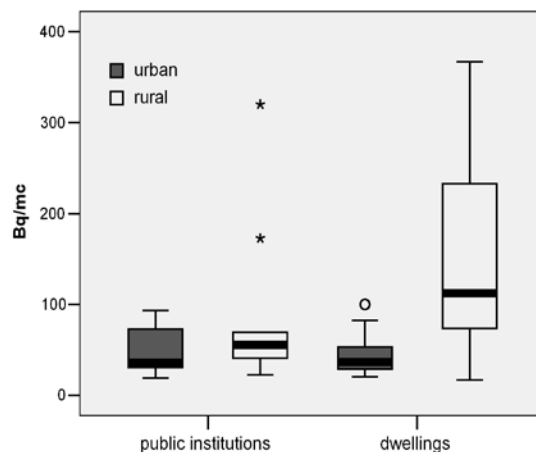


Figure 2 illustrates the mean and median levels concentrations for public institution and dwellings from urban and rural territory, the highest levels being recorded in rural dwellings.

Figure 2: The mean and median levels concentrations by urban and rural locations



The measurements performed in typical urban and rural dwellings and public locations were significant higher in cold months compared to warm season, knowing that during winter the exposure is enhanced due to lesser degree of ventilation. [1, 8].

We noticed that for public institutions MAED (1.55 mSv/year) was received by population in urban schools from Sv area, the value being slightly over the admitted limit of 1 mSv/year [9, 10]. Table 2 shows the mean annual effective doses distribution and their 95% CI.

Table 2: The distribution of mean effective doses by location and year of survey

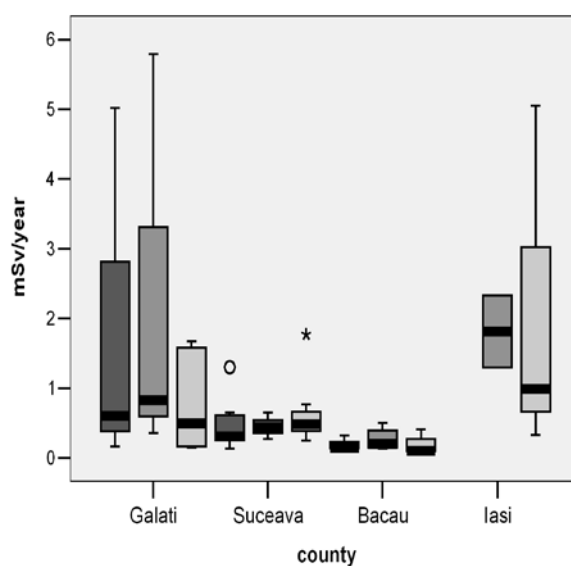
Location	N	Mean	S.D.	Std. Error	95% CI		Min	Max
					-95%CI	+95%CI		
2012								
Public	6	0.209	0.073	0.030	0.132	0.286	0.135	0.310
Urban	4	0.174	0.057	0.029	0.082	0.265	0.135	0.258
Rural	2	0.280	0.043	0.031	-0.108	0.667	0.249	0.310
Dwellings ^{c)}	7	1.230	1.107	0.646	0.351	2.111	0.140	5.020
Urban	5	0.588	0.442	0.197	0.040	10.136	0.140	1.300
Rural	2	2.835	2.090	1.185	1.928	3.598	0.650	5.020
2013								
Public	6	0.218	0.086	0.035	0.128	0.308	0.130	0.360
Urban	4	0.228	0.108	0.054	0.056	0.399	0.130	0.360
Rural	2	0.200	0.028	0.020	-0.054	0.454	0.180	0.220
Dwellings ^{b)}	8	1.529	1.838	0.650	-0.008	3.066	0.390	5.790
Urban	6	0.685	0.341	0.139	0.327	10.043	0.390	1.300
Rural	2	4.060	2.447	1.730	-17.922	26.042	2.330	5.790
2014								
Public ^{a)}	12	0.673	10.392	0.402	-0.212	1.557	0.085	5.050
Urban	7	0.249	0.135	0.051	0.124	0.374	0.085	0.420
Rural	5	1.266	2.132	0.953	-1.381	3.913	0.101	5.050
Dwellings	9	0.933	0.591	0.197	0.479	1.387	0.270	1.770
Urban	6	0.782	0.441	0.180	0.319	1.244	0.410	1.580
Rural	3	1.237	0.839	0.484	-0.847	3.320	0.270	1.770

^{a)} $p < 0.05$

^{b)} $p < 0.01$

^{c)} $p < 0.001$

Figure 3 shows the distribution of mean and median annual effective doses estimations by county area

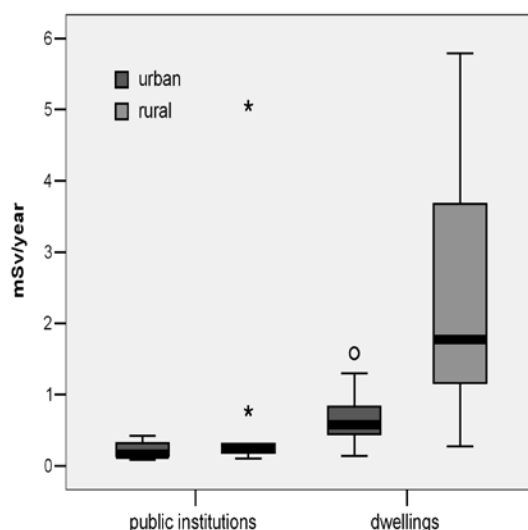
Figure 3: The mean distribution and median annual effective doses estimations by county area

The highest value for MAED (8.86 mSv/year) was estimated for living rural detached house in GI area in warm season corresponding to the single maximum level recorded. The distribution of estimated annual individual effective doses by indoor locations measured in cold and warm season are presented in table 3.

Table 3: The estimated annual per capita effective doses and range by location and season.

Indoors locations		Warm season (April-September)		Cold season (October-March)	
		Mean annual per capita effective dose (mSv)	Range (mSv)	Mean annual per capita effective dose (mSv)	Range (mSv)
Schools,	Urban	0.20	0.03-1.26	0.33	0.08-1.47
kindergartens	Rural	0.40	0.02-1.55	0.41	0.10-0.87
Block of flats,	Urban	1.63	0.07-8.86	0.79	0.13-2.24
houses	Rural	1.68	0.11-9.82	2.16	0.13-7.63

For rural houses locations, the annual mean and median effective doses were increased, in correlation with radon high concentrations levels. Figure 4 shows the estimated effective doses for urban and rural locations.

Figure 4: The annual mean and median effective doses by locations

3.2 Outdoor radon and dose estimation

In all the counties the outdoor ^{222}Rn mean concentrations varied in the range of 12.5 Bq/m^3 both for urban and rural locations and seasons. The mean values for outdoors measurements were of 12.41 Bq/m^3 with a corresponding annual per capita effective dose of 0.11 mSv .

3.3 Radon and Radium concentrations in water samples and dose estimates

In GI counties the annual mean effective dose due to ingestion of ^{226}Ra was below the reference level of 0.5 Bq/l . [3]. In Sv counties were measured samples from surface water, mine, spring, drinking water and fountain water and the maximum effective dose at ingestion (0.224 mSv) was identified for well water in Mestecanis location over admitted 0.1 mSv Indicative Dose [3]. In the other two counties territory the annual effective dose due to water ^{222}Rn ingestion did not exceed the reference value. Table 4 shows the ^{226}Ra and ^{222}Rn concentrations and effective dose estimations by type of water samples and county.

Table 4: The distribution of mean concentrations (Bq/l) and annual effective doses (mSv) by county.

County	Samples type	Mean concentrations (Bq/l)	Variation interval (Bq/l)	Mean annual effective doses at ingestion (mSv)
Galati ^{a)}	Drinking water	0.034	0.010-0.070	0.006
Suceava	Drinking water	2.911	0.130-7.590	0.021
	Fountain water	5.153	0.049-32	0.036
	Mine water	17.18	1.95-32.4	-
	Surface water	4.50	0.71-8.29	-
	Spring water	3.695	2.09-5.3	0.026
Bacau	Drinking water	6.895	5.64-8.15	0.045
	Surface water	8.905	8.35-9.46	-
	Spring water	16.88	16.53-17.22	0.118
Iasi	Drinking water	1.024	0.353-2.13	0.0075

^{a)}Radium concentrations (Bq/l)

3.4 The impact of inhaled radon to the public health

The possible impact of inhaled ²²²Rn to the public health status were reported only for a number of 23204 at risk persons in public institutions (16773 in urban, 6431 in rural) and 514 in dwellings (369 in urban, 145 in rural), being reported 22 cases (8.1%) with respiratory diseases, 7.8 % from exposed population living in rural dwellings near the uranium mine area. In the same Sv counties it was registered one death from pulmonary cancer in rural houses possible related to natural radiation exposure. The relative risk (RR) for health status disorders by locations with high levels of radon concentrations are presented in table 5.

Table 5: Estimates of relative risks for health status disorders by locations (2012-2014)

Locations	2012		2013		2014		2012-2014	
	High levels %	RR	High levels %	RR	High levels %	RR	High levels %	RR
Public								
Urban	-	-	-	-	-	-	-	-
Rural	-	-	-	-	20,0	2.75	11.1	2.88
						1.26-6.01		1.64-5.03
Dwellings								
Urban	20.0	0.63	16.7	0.33	16.7	0.40	17.6	0.43
		0.15-2.67		0.07-1.65		0.08-2.06		0.17-1.07
Rural	50.0	2.50	100.0	-	66.7	4.00	71.4	5.00
		0.27-23.4				0.56-28.4		1.29-20.4
All measurements								
Urban	11.1	0.69	10.0	0.41	7.7	0.35	9.4	0.45
		0.16-2.88		0.08-2.07		0.06-1.99		0.18-1.16
Rural	25.0	1.83	50.0	3.67	37.5	2.55	37.5	2.60
		0.34-9.92		0.83-16.2		1.01-6.45		1.28-5.27

The RRs for health modifications related to radon exposure showed a statistically significant excess for rural dwellings locations, RR=2.60, for the surveyed period.

The overall annual per capita effective dose arising from internal exposure to inhaled radon was estimated at 3.912 mSv with an associated annual collective effective dose of 15100 manSv and for water ingestion at 0.08 mSv with 308.8 manSv respectively.

4 CONCLUSION

The present study showed statistically increased levels in rural locations and to reduce the population exposure it is important to provide information for corrective actions.

There were reported health status changes possible in relation to ^{222}Rn exposure from the areas reported as having high concentrations levels.

The results emphasize that further surveillance should be continued for surveilling the population at risk concomitant with region radon mapping.

5 REFERENCES

- [1] European Commission, Joint Research Center, 2005. An overview of Radon Surveys in Europe, Luxembourg, Office for Official Publications of the European Communities, pp 3-9, 129.
- [2] T. Tollefsen, V. Gruber, P. Bossew, et al, 2009. Status of the European Indoor Radon Map”, Radiat. Prot. Dosimetry, vol. 145, no. 2-3, pp 110-116.
- [3] Directive 2013/51/ Euratom, 2013. Laying down the requirements for the protection of the health of the general public with regard to radioactive substances in water intended for human consumption.
- [4] ICRP, 1993. Publication 65, Annals of ICRP Protection Against ^{222}Rn at home and at work, Pergamon Press, Oxford.
- [5] UNSCEAR, 2010. United Nations Scientific Committee on the Effects of Atomic Radiation, Sources and effects of ionizing radiation, 2008 Report, volume I: Sources, Report to the General Assembly with Scientific Annexes A and B, ed. United Nations, New York, pp. 327.
- [6] CNCAN, 2000. National Commission of Nuclear Activities, President Order No. 207: NMR 03 Radiological Protection Norms in Uranium and Thorium Mining (in romanian).
- [7] ICRP, 2012. Publication 119, Compendium of dose coefficients based on Publication 60, Ann.ICRP 41(Suppl.), Elsevier Ltd.
- [8] O. Burke, P. Murphy, 2011. Regional variation of seasonal correction factors for indoor radon levels, Radiation Measurements, Elsevier, pp 1168-1172.
- [9] Directive 2013/59/ Euratom, 2013. Laying down basic safety standards for protection against the dangers arising from exposure to ionizing radiation and repealing Directives 89/618/ Euratom, 90/641/ Euratom, 96/29 Euratom, 97/43/ Euratom and 2003/122/ Euratom.
- [10] CNCAN, 2000. National Commission of Nuclear Activities, President Order No. 14: Fundamental Norms for Radiological Safety, chapter VII: The significant increase in exposure due to natural sources, Chapter VIII Implementation of radiation protection in the general population, (in romanian).

Excess Lifetime Cancer Risk of Cosmetic Powders

Chioma Nwankwo^{a,b*}, Damilola Folley^c, Olawunmi Gbolagade^b

^aNational Institute of Radiation Protection and Research, Ibadan, Nigeria.

^bUniversity of Ibadan, Ibadan, Nigeria.

^cAugustine University, Ilara-Epe, Lagos State, Nigeria.

Abstract. Talc powders are often commonly used for facial makeup and to prevent rashes. There have been strong indications of connection between talc and some cancers. Most studies have tried to find the chemical compounds that could cause these cancers. However, since talc is a mined material, there are strong reasons to examine the concentrations of naturally occurring radionuclides in some of these powders. This study examines the activity concentration of radionuclide in thirty powder samples that are commonly sold in Nigerian markets, using sodium iodide detector (NaI) well type. The activity concentrations of ²³⁸U, ²³²Th and ⁴⁰K in cosmetics powders samples ranged from 4.28±0.66-130.10±5.84 Bq/kg, 4.46±0.34-65.85±4.97 Bq/kg and 108.95±6.47-1938.73±116.85 Bq/kg, respectively. Some of the results obtained for the corresponding radionuclides are higher than the worldwide average values of 33, 45, and 412 Bq/kg for ²³⁸U, ²³²Th and ⁴⁰K respectively. The absorbed dose and the annual effective dose rates observed ranges from 14.59-43.15 nGy/h and 0.09-0.26mSv, respectively. Excess life cancer risk rates due to ²³⁸U, ²³²Th and ⁴⁰K were observed to be between 0.31 and 0.93 which are above the average values (0.29 x 10⁻³) for each samples. Hence, it is evident that the probability of contacting cancer from some of the sampled powders is high. It is advised that the use of such powders should be restricted due to the harmful health hazards it might cause.

1 INTRODUCTION

Cosmetic powder is an important aspect of women beauty. Women are mostly conscious of their appearances, especially facial appearance. Consequently, women often frequently use different cosmetic powder to enhance their beauty. Nash, *et al.* [1] posits cosmetics play a significant part in increasing attractiveness because they may, in part, enhance facial symmetry. Women therefore employ cosmetics to manipulate their appearance and in so doing, may also benefit from a boost in positive self-perception and well-being. Furthermore, the use of cosmetic powders by women is believed to influence how they are perceived by others, and how at ease they feel in different situations. However, the mineral components of most cosmetic powders vary. Most cosmetic powders consist of components that are naturally occurring such as thin sheet-like mica flake, sericite, talc, etc. Large percentage of cosmetic powders is produced from talc.

Talc is a magnesium trisilicate mineral, it absorbs moisture well and helps cut down on friction, making it useful for keeping skin dry and helping to prevent rashes. It is widely used in cosmetic products such as baby powder and adult body and facial powders, as well as in a number of other consumer products. It is also used by the pharmaceutical industry to manufacture medications and is a listed ingredient of some antacids. Talc is used in smaller quantities in deodorants, chalk, crayons, textiles, soap, insulating materials, paints, asphalt filler, paper, and in food processing [2]. Talc is made up of finely ground particles of stone, since it originates from the ground, and is a mined product, it can be contaminated with NORM because the three (²³⁸U, ²³²Th and ⁴⁰K) primordial radionuclides have long half live that they survived since their creation and decay to attain stable state producing ionizing radiation [3]. Also, in its raw state, talc contains asbestos, which is known to be a carcinogen, a substance that causes cancer.

Numerous studies have shown a strong link between frequent use of talc in the female genital area and cervix/ovarian cancer. Talc particles are able to move through the reproductive system and become imbedded in the lining of the ovary [4]. Researchers have found talc particles in ovarian tumours and have found that women with ovarian cancer have used talcum powder in their genital area more frequently than healthy women [5]. Talc poses a health risk when exposed to the lungs [6]. Talc miners have shown higher rates of lung cancer and other respiratory illnesses from exposure to

industrial grade talc. The common household hazard posed by talc is inhalation of baby powder by infants [7].

Findings have established that there is a link between talc and cancer. Most of these findings have considered that the link is because of asbestos [8]. Though asbestos containing powder has been banned in the market, there is still a link between powder and cancer. Is it possible that there is a link between cancer cases and the NORM in the talc of powder? This study intends to examine the presence and concentration of radioactive element in cosmetic powders made from talc and its contribution to cancer risk. The empirical results of the study may provide a basis for the establishment and confirmation of the relationship between usage of cosmetic powder and cancer, especially among women.

This study will also go a long way to help policy makers on cosmetic product to regulate the NORM contained in cosmetic product.

2 MATERIALS AND METHODS

2.1 Sample Collection and Preparation

A total number of thirty different samples of cosmetic powders including baby powders were purchased directly from the market and marked by the sample numbers 1 to 30. About 50 grams of each sample was packed and sealed separately, with each in a container of about 7cm in diameter and height, respectively. Each container was tightly sealed with an insulating tape around the opening of the containers and stored for twenty-eight days, in order to attain secular radioactive equilibrium. The Sodium Iodide Detector (Well type) was used for the analysis.

2.2 Determination of Activity concentration

The activity concentrations were calculated using the detected photopeaks at 911.07 and 968.90 keV for ^{232}Th , 609.32 and 1764.51 keV for ^{238}U and 1460.75 keV for ^{40}K and the 185.99 keV gamma ray of ^{226}Ra . In the present study, the activity concentration of the ^{226}Ra radionuclide in the ^{238}U decay series was not used for the activity concentration of ^{238}U radionuclide because it may have slightly different concentration than the ^{238}U radionuclide. This is due to the separation that may occur between its parent ^{230}Th and ^{238}U and also due to the fact that ^{226}Ra has greater mobility in the environment [9]. Hence, the activity concentration (A_i) in Bqkg^{-1} , for a radionuclide i with a detected photopeak at energy ε , is obtained from the following equation:

$$A_i = \frac{NC_i}{\varepsilon \times y_i \times M \times T} \quad (1)$$

Where

A_i is the activity concentration of the i^{th} radionuclide in Bqkg^{-1} . NC_i = net counts of the i^{th} radionuclide
 ε = NaI detector efficiency. y_i = probability of emission. M = mass of the sampled cosmetic powder (kg)

T = counting time (3600 seconds)

2.3 Radium equivalent activity

The radium equivalent activity (R_{aeq}) in Bqkg^{-1} was introduced to define uniformity in respect to radiation exposure. The radium equivalent index compares the activity concentration of powders containing different amounts of these radionuclides. It is the weighted sum of ^{234}U , ^{232}Th and ^{40}K activity concentrations, based on the assumption that 10 Bqkg^{-1} of ^{234}U , 7 Bqkg^{-1} of ^{232}Th and 130 Bqkg^{-1} of ^{40}K produce the same gamma dose rate. It is calculated as follows:

$$Ra_{eq} = A_u + 1.423A_{Th} + 0.077A_K \quad (2)$$

where A_u , A_{Th} and A_K are the mean activity concentrations of ^{234}U , ^{232}Th and ^{40}K in Bq/kg, respectively.

2.4 Dose Rate Estimation

Dose Rate from Activity Concentration

The absorbed dose rate (D) in nGy/h from the ^{40}K isotope and the radionuclides from ^{232}Th and ^{238}U decay series, was calculated as follows:

$$DR \text{ (nGy/h)} = K * A_c \quad (3)$$

where A_c is the mean activity concentrations of ^{238}U , ^{232}Th and ^{40}K in Bqkg⁻¹. The activity concentrations of the three radionuclides were multiplied by the corresponding values of K for each of the radionuclides. (^{238}U (K=0.16), ^{232}Th (K=0.19) and ^{40}K (K=0.014))

2.5 Annual effective dose rates (AEDE)

The annual effective dose rate was calculated from the absorbed dose rate taking into account the conversion factor (CF) of the absorbed dose to the corresponding effective dose and the occupancy factor (OF). It is equal to:

$$E = [DR \times CF \times OF] / 10^6 \quad (4)$$

where E (mSv/y), DR(Gy/h), CF = 0.7 Sv/Gy, and OF = 24 hrs × 365.25 days= 8766h_{yr}⁻¹ [9].

2.6 External Hazard Index

The model of the external hazard index (H_{ex}) places an upper limit to the external gamma radiation dose, which corresponds to a radium equivalent activity of 370 Bq/kg. It is defined as:

$$H_{ex} = \frac{A_u}{370 \text{ Bq/kg}} + \frac{A_{Th}}{259 \text{ Bq/kg}} + \frac{A_K}{4810 \text{ Bq/kg}} \quad (5)$$

where A_U , A_{Th} and A_K are the mean activity concentrations of ^{234}U , ^{232}Th and ^{40}K in Bq/kg, respectively. The value of this index should be less than unity to keep the radiation hazard negligible. This is defined by [10].

2.7 Internal Hazard Index (H_{in})

The internal exposures are also hazardous which leads to diseases like cancer and other respiratory sickness. This is defined by the equation below used by Avwiri *et al* and Jibiri *et al* [11-12].

$$H_{in} = \frac{A_U}{185 \text{ Bq/kg}} + \frac{A_{Th}}{259 \text{ Bq/kg}} + \frac{A_K}{4810 \text{ Bq/kg}} \quad (6)$$

Where A_u , A_{Th} , A_K are the activity concentrations of ^{234}U , ^{232}Th and ^{40}K , respectively.

2.8 Excess Life Cancer Risk (ELCR)

There is a potential carcinogenic effects that is characterized by estimating the probability of cancer incidence in a population of individuals for a specific lifetime from projected intakes (and exposures) and chemical-specific dose-response data. ELCR result is a probability. The additional or extra risk of

developing cancer due to exposure to a toxic substance incurred over the lifetime of an individual. It is calculated as follows:

$$ELCR = AEDE \times DL \times RF \quad (7)$$

Where DL= average duration of life (estimated to be 70 years)

RF= Risk factor (s/v) i.e. fatal cancer risk per sievert. For stochastic effects, ICRP uses RF as 0.05 for the public.

2.9 Gamma Activity Index (I_{yr})

This is used to estimate the γ – radiation hazard associated with the natural radionuclide in the powder samples. It is also used to correlate the annual dose rate due to excess external gamma radiation. Values of $I_{yr} \leq 1$ corresponds to an annual effective dose of less than or equal to 1mSv, while $I_{yr} \leq 0.5$ corresponds to annual effective dose less or equal to 0.3mSv [13]. The representative gamma index is expressed as

$$I_{yr} = \frac{A_u}{150} + \frac{A_{Th}}{100} + \frac{A_k}{1500} \quad (8)$$

Where A_U , A_{Th} and A_K are the activity concentration of ^{238}U , ^{232}Th and ^{40}K , respectively.

3 RESULTS AND DISCUSSION

3.1 Activity concentration of radionuclides detected in the samples

The measured activity concentrations of naturally occurring radionuclides for the 30 cosmetics powders samples collected as shown in Table 1 ranging between 108.95 ± 6.47 and 1938.73 ± 116.85 Bqkg⁻¹ for ^{40}K , ^{238}U ranges between 4.28 ± 0.66 and 130.10 ± 5.84 Bqkg⁻¹ while ^{232}Th ranges between 4.46 ± 0.34 and 65.85 ± 4.97 Bqkg⁻¹ on Table 4.1.

In this research work, sample 8 (1938.73 ± 116.85 Bqkg⁻¹) has the highest activity concentration for ^{40}K , sample 4 has the highest activity concentration for ^{238}U (130.10 ± 5.84 Bqkg⁻¹) while sample 24 has the highest for ^{232}Th (65.85 ± 4.97 Bqkg⁻¹). In general, the activity concentrations in ^{40}K are higher than in ^{238}U and ^{232}Th activity concentrations.

Table 1: Activity Concentration of the radionuclides

Sample No	K-40 (Bq/Kg)	U-238 (Bq/Kg)	Th-232 (Bq/Kg)	Raeq (Bq/Kg)
1.	931.12±57.89	21.14±5.03	31.60±2.55	137.80
2.	1064.94±63.26	44.55±7.10	31.07±2.42	170.76
3.	108.95±6.47	4.28±0.66	4.46±0.34	19.01
4.	1013.61±62.52	130.10±5.84	15.88±1.58	130.75
5.	1327.78±80.03	Not Detected	29.77±2.52	144.60
6.	1388.24±82.47	52.37±8.07	52.13±3.95	233.44
7.	1129.73±66.64	50.53±7.39	28.47±2.23	178.03
8.	1938.73±116.85	Not Detected	39.77±3.24	205.87
9.	1104.96±65.18	46.47±6.90	43.19±32.88	193.02
10.	1075.02±64.79	42.16±6.56	41.78±3.17	184.38
11.	1085.00±64.92	33.61±4.71	26.36±1.95	151.82
12.	861.01±53.10	37.46±5.81	16.59±1.56	127.57

13.	1109.05±66.36	48.04±7.37	29.43±2.30	127.57
14.	1067.398±64.34	32.29±4.72	42.82±3.25	175.41
15.	1462.09±86.85	52.91±8.51	59.95±4.51	250.79
16.	1398.31±83.07	60.21±7.34	32.49±2.59	214.12
17.	1065.40±63.29	31.99±5.60	24.57±1.94	148.99
18.	1386.20±84.18	Not Detected	24.68±2.15	141.86
19.	1063.05±62.71	33.84±5.37	42.14±3.18	175.67
20.	1493.76±88.74	52.52±8.66	58.60±4.42	250.93
21.	1276.388±78.11	Not Detected	33.37±2.66	145.77
22.	1788.373±112.08	64.76±11.34	40.80±3.4	260.52
23.	1305.62±77.56	56.44±8.46	37.34±2.90	210.10
24.	1593.06±95.32	44.44±8.2	65.85±4.97	260.81
25.	1143.35±71.66	Not Detected	21.15±2.08	118.14
26.	719.65±42.45	Not Detected	23.74±1.91	89.19
27.	1087.05± 64.56	24.06± 5.44	19.43 ±1.61	111.39
28.	1041.756± 63.26	18.07± 4.04	16.74 ±1.49	104.04
29.	1076.81± 63.97	43.86± 6.89	42.15± 3.18	142.89
30.	1067.91± 62.99	Not Detected	32.16± 2.53	127.99

According to UNSCEAR (2008) [14], the reported worldwide average values for ^{238}U , ^{232}Th , and ^{40}K are 33, 45 and 412 Bqkg^{-1} respectively. All the samples except sample 3 were found to have higher ^{40}K activity concentration than the worldwide average value; Samples 1,3,14,17,27 and 28 have lesser values while the rest samples have higher ^{238}U activity concentration than the worldwide average value and samples 6,15,20 and 24 have higher ^{232}Th activity concentration than the average values. The activity concentration of ^{238}U was not detected in some powders.

The calculated radium equivalent activity in Table 4.2 for the samples also ranges from 19.01-260.81(Bqkg^{-1}) and the average value is 370 Bqkg^{-1} where all the samples are lower than the average value indicating no radiation hazards.

3.2 Radiation Hazards

In order to access the health effect, the radiation hazards such as radium equivalent, external and internal hazards, gamma activity index and excess life cancer risks have been calculated from the activity concentration of the radionuclides.

Table 2 lists the calculated absorbed dose rates, the annual effective dose rates values for the corresponding measured samples in Table 1 for each of the radionuclides. The total absorbed dose rates of the measured samples range between 14.59 and 43.15 nGy/h . The corresponding worldwide average value is between 50 and 59 nGy/h . Sample 22 has the highest absorbed dose rate and all the samples are lower than the average value.

However, the results of the annual effective dose rates of the measured samples ranges between 0.09 and 0.26 mSv/yr in Table 4.1 and sample 22 and 24 have the highest annual effective dose rates; while all the samples are lower than the corresponding average value (0.3-0.6 mSv); the total effective dose is 0.48 mSv (outdoor plus indoor = 0.07+0.41). This also shows that the results are higher than the outdoor and indoor effective doses.

Table 2: Radiation Hazards Indices for the samples

Sample No	DR (nGy/h)	AEDE (mSv/yr)	H_{in}	H_{ex}	I _{yr}	ELCR	ELCR X 10 ³
1	22.42	0.14	0.43	0.37	1.08	0.48	0.00048
2	27.94	0.17	0.58	0.46	1.32	0.60	0.0006
3	30.57	0.19	0.06	0.05	0.15	0.66	0.00066
4	22.03	0.14	0.43	0.35	1.04	0.47	0.00047
5	24.24	0.15	0.39	0.39	1.18	0.52	0.00052
6	37.72	0.23	0.77	0.63	1.80	0.81	0.00081
7	29.31	0.18	0.62	0.48	1.37	0.63	0.00063
8	34.70	0.21	0.56	0.56	1.70	0.75	0.00075
9	31.11	0.19	0.65	0.52	1.48	0.67	0.00067
10	29.73	0.18	0.61	0.50	1.42	0.64	0.00064
11	25.20	0.15	0.50	0.41	1.19	0.54	0.00054
12	21.23	0.13	0.45	0.34	0.99	0.45	0.00045
13	21.23	0.13	0.60	0.47	1.35	0.45	0.00045
14	28.25	0.17	0.56	0.47	1.34	0.61	0.00061
15	40.32	0.25	0.82	0.68	1.93	0.87	0.00087
16	35.38	0.22	0.74	0.58	1.66	0.76	0.00076
17	24.70	0.15	0.49	0.40	1.17	0.53	0.00053
18	24.09	0.15	0.38	0.38	1.17	0.52	0.00052
19	28.30	0.17	0.57	0.48	1.36	0.61	0.00061
20	40.45	0.25	0.82	0.68	1.93	0.87	0.00087
21	24.21	0.15	0.39	0.39	1.18	0.52	0.00052
22	43.15	0.26	0.88	0.70	2.03	0.93	0.00093
23	34.40	0.21	0.72	0.57	1.62	0.74	0.00074
24	41.93	0.26	0.83	0.71	2.02	0.90	0.00090
25	20.03	0.12	0.32	0.32	0.97	0.43	0.00043
26	14.59	0.09	0.24	0.24	0.72	0.31	0.00031
27	18.91	0.12	0.43	0.37	1.08	0.41	0.00041
28	17.77	0.11	0.38	0.33	0.98	0.38	0.00038
29	23.08	0.14	0.62	0.51	1.43	0.50	0.00050
30	21.06	0.13	0.35	0.35	1.03	0.45	0.00045

External hazards index (H_{ex}) range between 0.05 and 0.71. Similarly, the results calculated from the internal hazards index (H_{in}) ranges between (0.06 and 0.88), and the results shows that all the samples are also lesser than the unity. The calculated gamma activity index ranges from 0.97 to 2.03, the

results obtained shows that all most of the samples indices are greater than unity which correspond to 1mSv/yr, while sample 3, 12, 25, 26 and 28 gamma indices are less than unity.

The excess life cancer risk calculated and summarized in Table 2 ranges between (0.31-0.93) and sample 22 (0.93) has the highest excess life cancer risk. The corresponding world average value is 0.29×10^{-3} [14], all the samples are high compared to the world average value which means that women who use these powder for long duration have the probability of having cancer.

4 CONCLUSION

Based on the findings from this study and all the reviewed literatures, it is recommended that Government agencies that are in charge of standardization of locally produced cosmetic products should conduct extensive study on the radionuclide content of raw materials used in the manufacturing of locally made cosmetic products. Women should avoid application of talc powders on their genital to avoid ovarian cancer. Also, Nursing mothers should avoid the use of talc baby powders on infant

5 REFERENCES

- [1] Nash, R., Fieldman, G., Hussey, T., et al, 2006. Cosmetics: they influence more than caucasian female facial attractiveness. *Journal of Applied Social Psychology*, 36(2):493-504.
- [2] Neill, A.S., Nagle, C.M., Spurdle, A.B., 2012. Webb PM. Use of talcum powder and endometrial cancer risk. *Cancer Causes Control*, 2:513–519.
- [3] Mohanty, A.K., Sengupta, D., Das, S.K., et al, 2004. Natural radioactivity in the newly discovered high background radiation area on the eastern coast of Orissa, India. *Radiation Measurement*, 38:153–165.
- [4] Henderson, W.J., Joslin, C.A.F., Turnbull, A.C., et al 2001. Talc and carcinoma of the ovary and cervix. *Journal ObstetGynaecol Br Commonw*, 78: 266-272.
- [5] Gertig, D.M., Hunter, D.J., Cramer, D.W., et al, 2000. Prospective study of talc use and ovarian cancer. *Journal Natl Cancer Inst*, 92(3):249-252.
- [6] Mostafa, S.A.M., Bargeron, C.B., Flower, R.W., et al, 2001. Foreign body granulomas in normal ovaries. *ObstetGynecol*, 66(5):701-702.
- [7] Terry, K.L., Karageorgi, S., Shvetsov, Y.B., 2013. Genital powder use and risk of ovarian cancer: A pooled analysis of 8,525 cases and 9,859 controls. *Cancer Prev Res (Phila)*, 6:811–821.
- [8] Heller, D.S., Westhoff, C., Gordon, R.E., et al, 2002. The relationship between perineal cosmetic talc usage and ovarian talc particle burden. *America Journal ObstetGynecol*, 174:1507-1510.
- [9] UNSCEAR, 2000. Sources and Effects of Ionizing Radiation. Report to General Assembly, Vol. 1, Annex B, United Nations, New York.
- [10] Beretka, J., Mathew, P. J., 1985. Natural radioactivity of Australia Building materials industrial wastes and by-products. *Health physics*, 48:87-95.
- [11] Avwiri, G.O., Osimobi, J.C., Agbalagba, E.O., 2013. Evaluation of Natural Occurring Radionuclide Variation With Lithology Depth Profile of Udi and Ezeagu Local Government Areas of Enugu State, Nigeria. *International Journal of Engineering and Applied Sciences*, 4(3).
- [12] Jibiri, N.N., Temagee, S.T., 2013. Radionuclide contents in raw minerals and soil samples and the associated radiological risk from some mining sites in Benue State North-Central Nigeria. *International Journal of Scientific and Engineering Research*, 4(7).
- [13] Turhan, S., Gunduz, L., 2008. Determination of specific activity of ^{226}Ra , ^{232}Th and ^{40}K for assessment of radiation hazards from Turkish plumice samples. *Journal of Environmental Radioactivity*.
- [14] UNSCEAR, 2008. Exposures from Natural Sources United Nation Scientific Committee on Effect of Atomic Radiation Report to General Assembly, Annex B, New York.

Monitoring of ambient dose equivalent at the boundary of nuclear sites to verify compliance with the regulations

Cristina P. Tanzi*, M. Farahmand, P. Kwakman, R.B. Tax, A.P.P.A. van Lunenburg, G.J.E Slagt, L.P. Roobol

National Institute for Public Health and the Environment (RIVM), the Netherlands.

Abstract. The gamma ambient dose equivalent is measured by a group of monitoring posts (the local network) placed along the boundary of two facilities in the Netherlands, in order to verify compliance with the dose limit granted in the permit. The two facilities are the nuclear power plant Borssele and a facility for storage of radioactive waste.

These measurements are analysed in conjunction with the ambient dose equivalent data from a national network of over 150 gamma monitoring posts distributed all over the country, over a surface area of 40,000 km².

The data from the national network are used to compute a common background gamma dose equivalent rate and an offset for each of the monitors of the local network. This method distinguishes an additional gamma dose due to the operations of the nuclear facilities from changes caused by cosmic radiation. Also changes due to the presence of radon progeny in air can, to a certain extent, be determined.

This approach yields the variance of the offset which is calculated for each of the monitors of the local network. The influence of transient phenomena can be filtered out, for example of Non-Destructive Testing activities carried out in the vicinity of the facilities. We provide an example of how changes in the local background, have been identified. The method presented makes it possible to estimate, for the measured ambient dose equivalent, the contribution due to normal operations of the nuclear facilities, together with a confidence limit.

KEYWORDS: *Environmental Radiation, Nuclear Power Plant, Radiation Protection, Ambient Dose Equivalent.*

1 INTRODUCTION

The gamma ambient dose equivalent is measured by a set of monitoring posts (the local network MONET) placed along the boundary of two facilities in the Netherlands, in order to independently verify compliance with the dose limit granted in the permit. The two facilities are the only nuclear power plant and a facility for storage of radioactive waste. The detectors used are proportional counters placed at fixed positions along the (fenced) boundary, complemented by portable Geiger-Müller detectors, which also include a rain sensor. The network is operated by the National Institute for Public Health and the Environment (RIVM).

2 MEASUREMENTS OF AMBIENT DOSE EQUIVALENT

2.1 The local MONET network

RIVM operates a network of 8 and 16 monitoring posts located along the (fenced) boundary of the Nuclear Power Plant in Borssele and the Central Organisation for Radioactive Waste in Vlissingen, both in the South-West of the Netherlands. Figure 1 shows the positions of the monitors around the Nuclear Power Plant in Borssele. The ambient dose equivalent rate of such a monitoring post for the year 2013 varies between 82 and 112 nSv/h and is shown in Fig. 2 (data from [1]).

* Presenting author, e-mail: cristina.tanzi@rivm.nl

Figure 1: The nuclear power plant in Borssele and the locations of the monitors of the proportional counters of the MONET network.

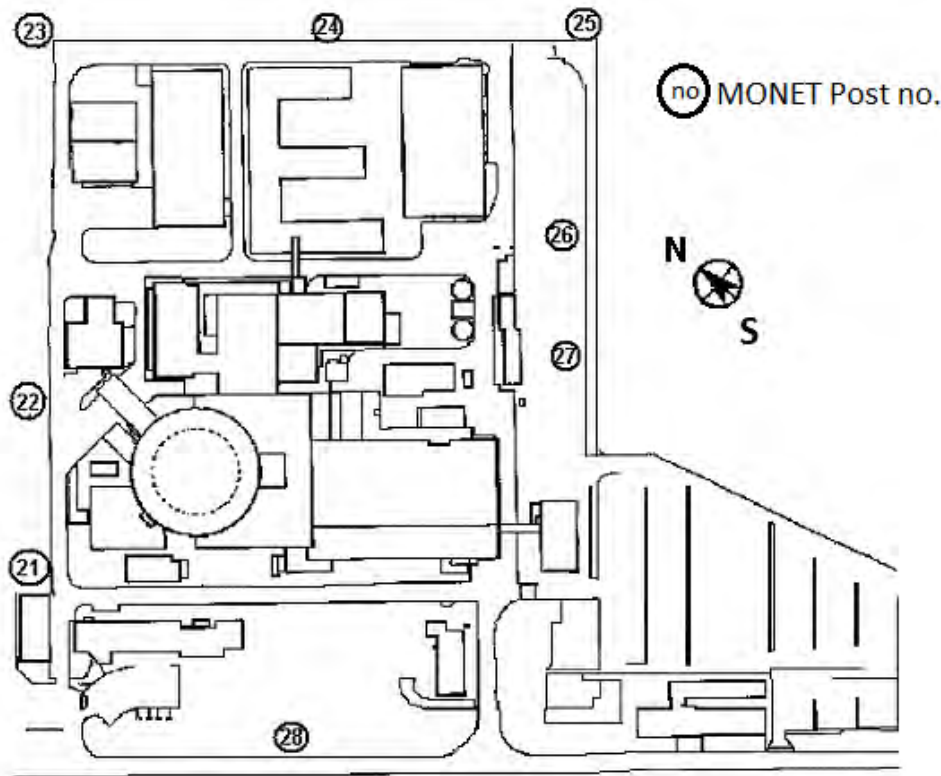
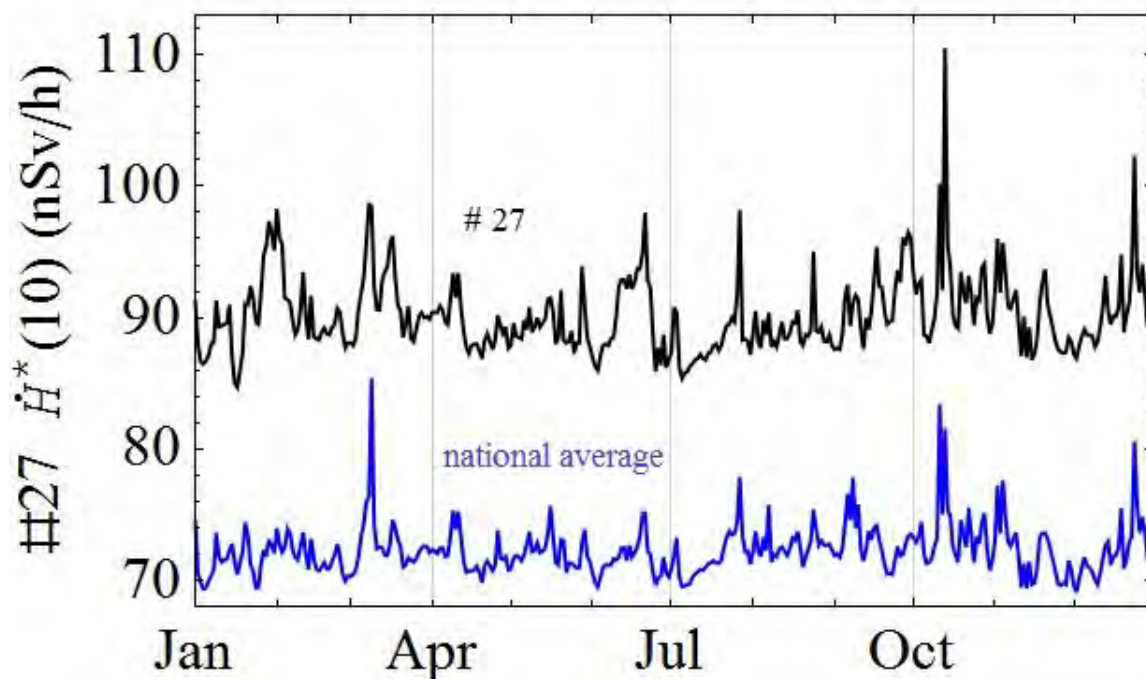


Figure 2: Daily averaged measurement of $\dot{H}^*(10)$ in 2013 for Monitoring Post 27 of the dedicated MONET Network (in black, above), and the national average value of $\dot{H}^*(10)$ (in blue, below) calculated from the National Measuring Radiation Network in 2013. The days where the daily national average rate exceeds 80 nSv/h coincide with periods of increased precipitation (see Figure 4).



2.2 The national network

The measurements of the local network MONET are analysed in conjunction with the data from a national network (NMR) of over 150 gamma monitoring posts distributed over a 40,000 km² area [3]. Figure 3 shows the hourly averages of $\dot{H}^*(10)$ for April 8, 2016 at 15:00.

In the course of 2014 and 2015 the Bitt RS03/X proportional counters have been progressively substituted by Geiger-Müller detectors, and the monitoring posts are also outfitted with a rain sensor.

Figure 3: The gamma ambient dose equivalent rate $\dot{H}^*(10)$ measured by the national network of the Netherlands on April 8, 2016. The data are made available as hourly averages, not validated, at http://www.rivm.nl/Onderwerpen/N/Nationaal_Meetnet_Radioactiviteit/Resultaten, and through EURDEP, the European Radiological Data Exchange Platform, <http://eurdepweb.jrc.ec.europa.eu/EurdepMap>.

The grey background shows differences in the yearly averaged ambient dose equivalent, which vary between 55 and 100 nSv/h, calculated from the geological characteristics of the soil [4].

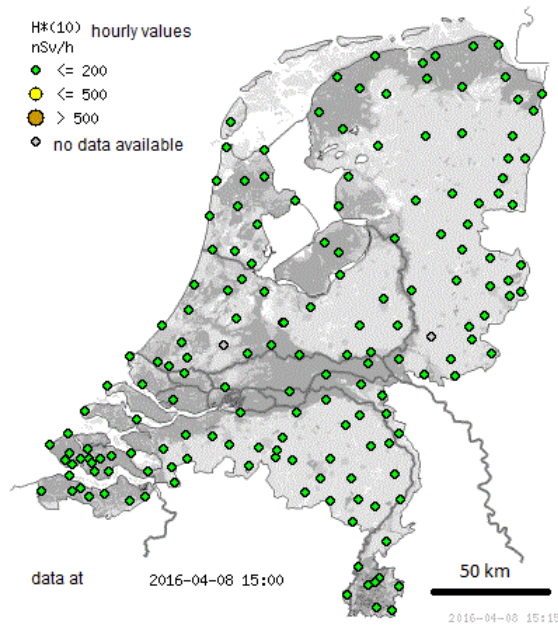


Figure 4: Daily precipitation at the weather station closest to the dedicated MONET Network (Vlissingen, station nr.310, data: KNMI).

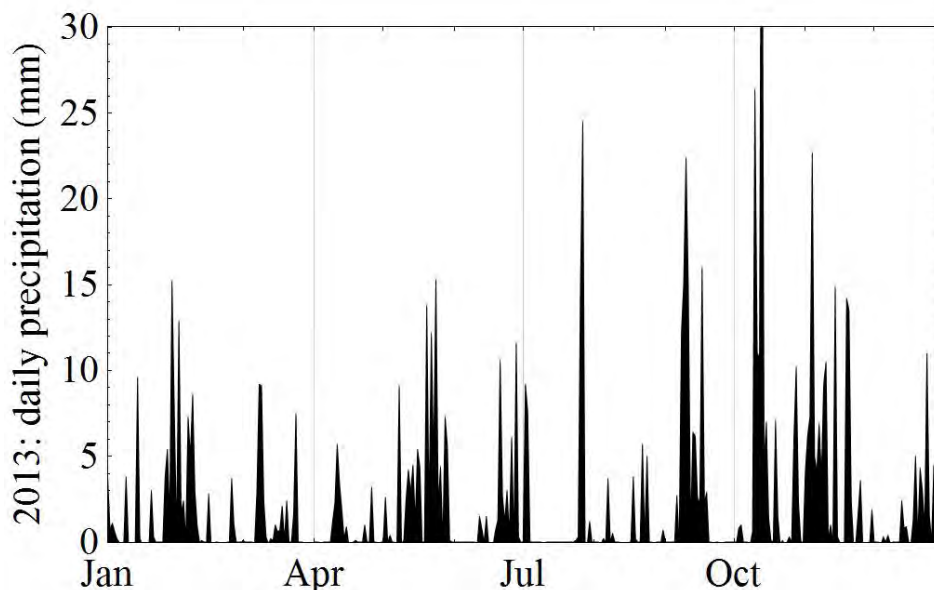
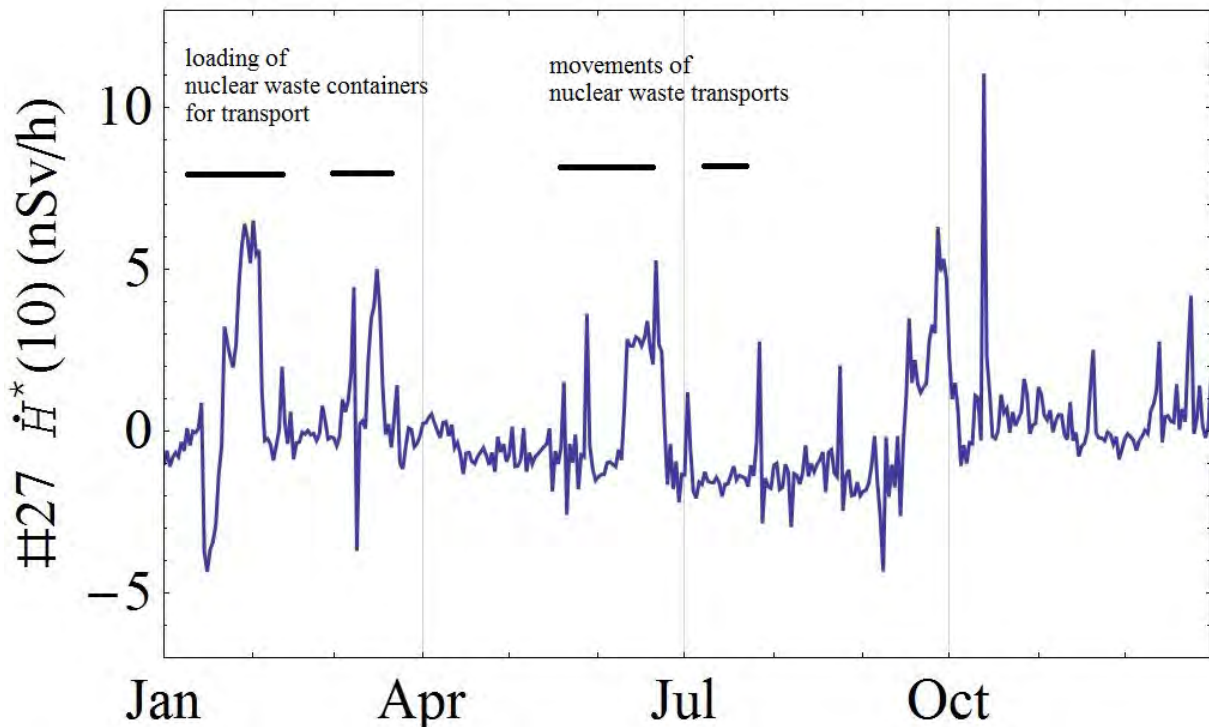


Figure 5: Daily averaged measurement of $\dot{H}^*(10)$ in 2013 for Monitoring Post 27 of the dedicated MONET Network, with the subtraction of the background (see Fig. 2) and the calculated offset of 17.8 ± 1.6 nSv/h.



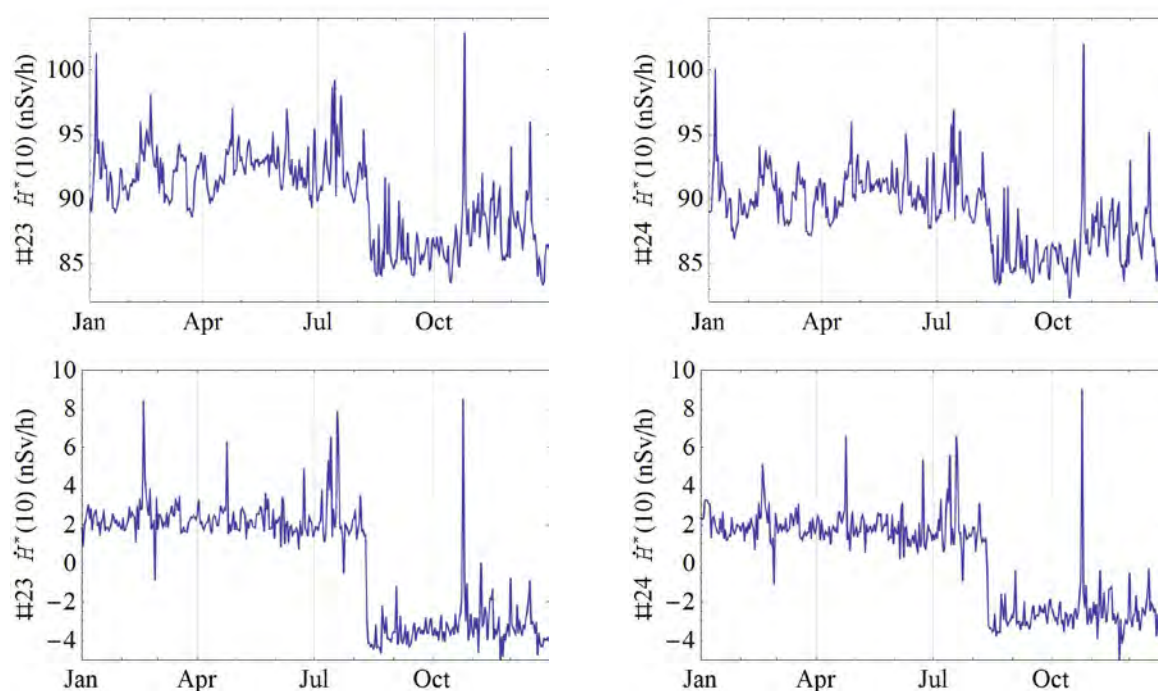
3 THE ANALYSIS METHOD AND RESULTS

The measurements of the gamma ambient dose equivalent rate from the national network, at the positions shown in Fig. 3, are selected and averaged in order to obtain a reference value for the local network, gamma ambient dose equivalent rate, following the method given in Ref. [2]. Figure 2 shows the daily averages of the gamma ambient dose equivalent for the year 2013: the days where the daily average rate exceeds 80 nSv/h coincide with periods of increased precipitation (see Fig. 4). This leads to a wash-out of Rn-222 progeny and hence an increase in ambient dose equivalent rate [5].

Subsequently, an offset for each monitoring post of the local network MONET is determined over the whole calendar year with respect to the reference value: this is visible in Fig. 2. This offset, and its standard deviation σ , is determined using days where no particular events cause an increase of the ambient dose equivalent rate, and it is different for each detector, as described in [2]. For the monitoring post shown in Fig. 2 the offset in 2013 is 17.8 ± 1.6 nSv/h. This value is used to determine a net change of the ambient dose equivalent rate that might be attributed to the nuclear installation (see Fig. 5). The increase is considered significant when it is larger than 3σ of the calculated offset, and it amounts to $1,9 \mu\text{Sv}$ over 2013 for this detector. This is the value which is compared to effective dose which has been granted in the permit by the regulatory authority. The assumption is made that gamma ambient dose equivalent is used as proxy for the effective dose [1].

In Fig. 5 activities that lead to an increase of the ambient dose have been identified: the loading of nuclear waste containers for transport and movements of nuclear waste transport. Figure 6 shows two monitoring posts in 2011, where the decrease in the ambient dose equivalent rate in the middle of August coincides with the substitution of soil or grass with gravel.

Figure 6: Daily averaged measurement of $\dot{H}^*(10)$ in 2011 for Monitoring Post 23 and 24 of the dedicated MONET Network: the decrease in the ambient dose equivalent rate in the middle of August coincides with the substitution of soil or grass with gravel.



4 CONCLUSION

The gamma ambient dose equivalent rate is measured at the boundary of two nuclear installations in the Netherlands in order to verify the compliance with the permit. In order to identify the excess of the ambient dose equivalent due to the nuclear installations, the background is determined by analysing the measurements at 150 locations, and by determining an offset and a confidence level for each of the monitors placed at the boundary.

5 REFERENCES

- [1] RIVM reports, various authors, in Dutch, see www.rivm.nl, RIVM rapport 610330059, RIVM Rapport 610330131, RIVM Rapport 610330087, RIVM Rapport 610330082, RIVM Rapport 2014-0139, RIVM Rapport 2014-0140, RIVM Rapport 2015-0093.
- [2] Reinen, H.A.J.M., Slaper, H., Overwater, R.M.W. and Stoop, P., 2000, Comparing Environmental Dose Rate Meters: A Method to Determine Natural and Non-natural Variations in External Radiation Levels, *Radiat Prot Dosimetry* (2000) 92 (1-3): 123-126.
- [3] Twenhöfel, C.J.W., de Hoog van Beynen, C., van Lunenburg, A.P.P.A., Slagt, G.J.E., Tax, R.B., van Westerlaak, P.J.M., Aldenkamp, F.J., (2005). Operation of the Dutch 3rd generation National Radioactivity Monitoring network. In: Dubois, G. (Ed.), *Spatial interpolation comparison 2004 report, 2005*, EUR 21595 EN, pp. 19–31.
- [4] Smetsers, R., Blaauboer, R., 1996. Variations in outdoor radiation levels in the Netherlands, ISBN 90-367-0621-1, Ph.D. dissertation, Rijksuniversiteit Groningen.
- [5] Greenfield, M. B., Domondon, A. T., Okamoto, N., and Watanabe, I.: Variation in γ -ray count rates as a monitor of precipitation rates, radon concentrations, and tectonic activity, *J. Appl. Phys.*, 91(3), 1628–1633, 2002.

Determination of the activity concentrations of natural occurring radionuclides in foodstuffs for public dose assessments

Deon Kotze^a, Immanda Louw^a, Charles Krös^a

^aSouth African Nuclear Energy Corporation (Necsa), P O Box 582, Pretoria 0001, Republic of South Africa

Abstract. The capability of an analytical methodology to screen food products for dose assessments is evaluated. The methodology is based on a combination of instrumental and radiochemical methods to determine radionuclides in a range of food samples. The evaluation is based on a minimum measurable dose derived from the minimum detectable activities for various radionuclides required for the dose calculation. Screening at a dose level of 100 $\mu\text{S/a}$ is attainable. Lower screening levels will require more sensitive methods especially for the determination of Ra-228 and Pb-210.

KEYWORDS: *NORMs; dose; food; analysis; gamma spectrometry; alpha spectrometry; neutron activation analysis; delayed neutron counting.*

1 INTRODUCTION

Mining and other operations in South Africa involving natural occurring radioactive materials (NORMS) are authorized by the National Nuclear Regulator (NNR). Applicants must perform a safety assessment to determine impact of operations on the environment and health of the public [1]. An ongoing safety assessment and maintenance program is required for authorized operations. Part of such an assessment is to identify pathways through which the public may be exposed to potential release of NORMs. Possible pathways include (i) external exposure by gamma radiation (ii) internal exposure by dust inhalation (iii) internal exposure by ingestion (food and water) and (iv) external exposure by contamination of the skin.

Screening limits for public safety dose assessments are set by the regulator that defines the degree of monitoring releases. The accuracy of dose assessment from ingestion will depend to a large degree on the capability of the analytical methodology employed to determine radionuclide concentrations in food stuffs. A conservative approach is assumed; if the concentration of a radionuclide is below detection limits, a value higher or equal than the detection limit is used. An overestimate of the true dose may result in more stringent monitoring actions or even engineering modification of the operations to be authorised. The sensitivity of the analytical methods in determining radionuclide activity concentrations becomes crucial to make a fair assessment of dose by ingestion.

Radiometric techniques such as gamma spectrometry, alpha spectrometry and liquid scintillation analysis are commonly used for determination of NORMs in foodstuffs. A high efficiency and broad energy gamma with good background shielding would be beneficial for the simultaneous measurement of several radionuclides at low levels typically encountered in foods. Alpha spectrometry offers higher sensitivity but requires dissolution of the sample matrix and extraction of radionuclides of interest using expensive resins and tracers required for yield determinations. Photon Ejection Alpha Rejection Liquid Scintillation (PERALS) offers alpha spectrometry capability but also requires extraction and purification of the radionuclides of interest [2]. Liquid scintillation analysis in combination with extraction techniques can be applied for the determination of NORM beta emitters such as radium-228 and lead-210 [3]. In the last 10 to 15 years, mass spectrometric techniques for the determination long live NORM nuclides have become available. The technique offers multi isotopic analysis and can be performed directly on solid samples or on extracted nuclides [4,5].

The analytical methods apply were Delayed Neutron Counting (DNC) and Neutron Activation Analysis (NAA), gamma spectrometry and alpha spectrometry. DNC and NAA as well as gammas spectrometry were chosen to reduce costs associated with radiochemical analysis. Alpha spectrometry is applied only for analysis of polonium-210, a technique commonly applied for this nuclide [6].

In this study four different food types were used that are typically encountered in dose assessments: potato (root vegetables), cabbage (leafy vegetables), fish (meat) and milk. These samples were taken as part of routine monitoring at mines associated with potential uranium releases. The objective is to determine the detection limits for the suit of radionuclides analysed for and use it in the calculation of ingested dose to obtain a 'minimum measurable dose'. Although the same analytical methodology is applied, different minimum measurable doses can be expected due to dissimilarities of the sample types and consumption rates. The results will indicate if the methodologies apply is adequate for proper dose assessment or if it requires alterations to obtain appropriate sensitivities.

2 DOSE RATE CALCULATIONS

Dose rate calculations were performed according to the formulae supplied in reference [1]:

$$\text{Dose rate (Sv/year)} = [\sum (A_i \cdot DCF_i)] \cdot CR \quad \text{for a particular population age group}$$

where A_i is the activity concentration (Bq/kg or Bq/L) of a selected nuclide in the uranium-235, -238 and thorium-232 decay series;
 DCF_i is the associated Dose Conversion Factor (Sv/Bq) for the selected nuclide
 CR is the age dependent consumption rate (kg/year) for the particular food

The sum is taken over 25 nuclides listed in table 2 below. 12 of these nuclides have short half-lives (< 1 month) and can be regarded as in equilibrium with parent nuclides. The Remaining 13 nuclides need various analytical techniques, some will require expensive radiochemical analysis. The analytical methodology apply measures only 9 of the 13 nuclides. Long live nuclides not covered are: U-234, Th-230, Pa-231 and Ac-227. For the purpose of this study, the activity concentrations were set equal to parents: Th-230 and U-234 activities equal to U-238 activity; Ac-227 and Pa-231 activities equal to U-235. These assumptions can be justified to some extent.

- Uranium-234 may be enriched due to its higher mobility (as a result of recoil) in geological structures leading to preferential leaching into ground water. However, where releases of uranium due to mining activities occurred, the natural abundance ratio or equilibrium activities is re-established.
- Thorium uptake from soil into plants (root and leafy vegetables) is also greater for uranium [7]
- The uptake of Ac, Pa and Th from soil into leafy and root vegetables is less than for U [7].
- Transfer factors [7] from feed to cow's milk for U are higher than the factors for Ac, Pa and Th
- Bioaccumulation factor for U is however lower than the factors for Ac, Pa and Th [7]

Table 1: Application of analytical methods on selected nuclides for dose rate calculations

U-238 series			U-235 series			Th-232 series		
Nuclide	Half-life	Method	Nuclide	Half-life	Method	Nuclide	Half-life	Method
U-238	4.468E9 y	DNC (a)	U-235	7.04E8 y	DNC	Th-232	1.4E10 y	NAA (b)
Th-234	24.10 d	=U-238	Th-231	1.06 d	=U-235	Ra-228	5.75 y	=Ac-228
Pa-234	6.70 h	=U-238	Pa-231	3.27E4 y	=U-235	Ac-228	6.13 h	GS
U-234	2.445E5 y	=U-238	Ac-227	21.8 y	=U-235	Th-228	1.91 y	=Pb-212
Th-230	7.7E4 y	=U-238	Th-227	18.7 d	=U-235	Ra-224	3.66 d	=Pb-212
Ra-226	1600 y	=Pb/Bi-214	Ra-223	11.4 d	=U-235	Pb-212	10.6 h	GS
Pb-214	26.8 m	GS (c)	Pb-211	0.601 h	=U-235	Bi-212	1.01 h	=Pb-212
Bi-214	19.9 m	GS						
Pb-210	22.3 y	GS						
Bi-210	5.012 d	=Pb-210						
Po-210	138.38 d	AS (d)						

(a) Delayed Neutron Counting

(b) Neutron Activation Analysis

(c) Gamma Spectrometry

(d) Alpha Spectrometry

For milk, leafy and root vegetables, transfer and factors support the notion that activity concentrations of Th-230, Pa-231 and Ac-227 would be equal or less than the relevant uranium parent nuclide. In the case of fish, it cannot be ruled out that U-234 and U-235 may be at a lower concentration than their progeny. For the purpose of this study, equilibrium was assumed between U-234 and Th-230 and between U-235 and Pa-231/Ac-227.

3 DETERMINATION OF MINIMUM DETECTABLE ACTIVITY CONCENTRATIONS

3.1 Sample preparation

Drying and ashing of materials is performed to preconcentrate radionuclides for analysis. Because biological material contain a high amount of combustible compounds, ashing of the material can result in a high preconcentration factor that will greatly improve the sensitivity of gamma spectrometry and neutron activation analysis.

The edible parts of the fish and vegetables were prepared for analysis. Vegetables were first rinsed with deionised water to remove dirt and soil particles. Fish was dissected to recover fleshy parts for analysis.

The prepared solid material were dried overnight at 80 °C. About two-third of the dried material was ashed at 600 °C to further preconcentrate radionuclides. Due to vitality of polonium-210, the ashed material cannot be used for analysis of this nuclide. The remaining dried material is therefore reserved for polonium-210.

Milk (1 L) was added to a large porcelain dish and the material was placed in a cold muffle furnace. The oven was switched on the material allowed to dried overnight at a set temperature of 100 °C. A 100 mL portion of the liquid milk was reserved for polonium-210 analysis.

Masses of the fresh or wet weight of the sample material and the dried and ashed parts were recorded. Table 2 summarises the results obtained. Milk, potato and cabbage has an ash content close to 1% and fish an ash content of 4%. The preconcentration factors obtained are indicated in brackets.

Table 2: Dry and ash content of tested food types

Food	Fresh weight (kg)	% Dried weight		% Ash	
Potato	1.62	18	(5.59)	1.1	(87)
Fish	0.315	30	(3.33)	4	(25)
Milk	1.00	-		0.8	(125)
Cabbage	1.47	8	(12.5)	0.9	(111)

3.2 Analysis

3.2.1 Delayed Neutron Counting for determination of uranium isotopes

A 200 mg portion of the sample material was transferred to high purity polyethylene irradiation vial. Standards were prepared from certified uranium and thorium solutions traceable to National Institute of Science and Technology (NIST). Appropriate aliquots of the solutions were transferred into irradiation vials and evaporated to dryness.

Vials (samples, standards and blanks) were transported pneumatically for irradiation in the SAFARA-1 reactor core and subsequently for measurement of the delayed neutrons on a BF₃ gas proportional counter. An irradiation time of 10 seconds, a delay period of 15 seconds and counting period of 45

seconds were used. U-235 concentration was obtained by comparing blank corrected count rates of the standards and samples. U-238 concentrations was calculated by applying the fix 238U:235U ratio that exists for natural uranium [8]. U-234 was also derived by assuming equilibrium with U-238 as explained previously.

3.2.2 Neutron activation analysis for determination of thorium-232

Th-232 was determined by measurement of its activation products Pa-233. After a cooling period of 3 days, the irradiated vials were measured in a well type germanium detector. The waiting period was introduced to allow other short lived activation products to decay to negligible levels so that it did not interfere in the detection of Pa-233. Th-232 activity concentrations were obtained by comparing Pa-232 activities of the samples and standards.

3.2.3 Gamma spectrometry

A portion of the sample material was transferred to a cylindrical container (5 cm diameter, 1 cm height). The container is placed in a special aluminium pouch and vacuum sealed. After a 3 week waiting period, the gamma spectrum of the samples collected on a Canberra model BEGE5030 gamma detector housed in a low background lead shield. A spectrum acquisition time of 24 hours is used. The 3 week waiting period is introduced to allow Rn-222 (3.8 day half-life) and its shorter live progeny, Pb-214 and Bi-214 (half-lives < 30 min) to become in secular equilibrium with Ra-226.

Analysis of the spectrum is performed with Genie2000 gamma spectroscopy software. The detector has been characterized by Canberra for efficiency calibration modeling using LabSOCs software. Ra-226 was determined from the measured activities of Pb-214 and Bi-214, Ra-228 from Ac-228 and Th-228 from Pb-212. Pb-210 was measured directly.

3.2.4 Polonium-210 analysis

A portion of the dried sample material (1 gram, accurately weighed) was transferred to a dissolution vessel. A known amount of Po-209 tracer was added for activity measurement. An appropriate amount of concentrated nitric acid was added to the material. Heat was applied and small portions of hydrogen peroxide were added as required to aid in the complete dissolution of the material. The solution was evaporated to near dryness. Diluted hydrochloric acid was added to the sample to a specified volume. A silver disk (one side coated with plastic film) was added and the solution, heated to below boiling point, is stirred for an allocated time to allow the auto electroplating of polonium on the disk. A reducing agent is added to prevent iron that may be present from plating. The disk was removed after the allocated stirring period, rinsed with deionized water and allowed to air dried.

No preparation on the milk was performed and Po-210 was plated directly on a silver disk from a 100 mL portion [9].

Alpha activities collected on the disc was measured on a calibrated alpha spectrometer (Canberra Alpha Apex system with passivated ion implanted silicon detectors) for an acquisition time of 24 hours. Activities were calculated by comparing the peak areas of Po-210 and Po-209. Chemical yield was obtained by comparing measured Po-209 activity against the known added activity.

3.2.5 Detection limits

The formulae of LA Curry [10] was used for the calculation of detection limits using a confidence level of 95%. The detection limit is automatically calculated by the Genie200 gamma spectroscopy software using the background continuum at the peak position. In case of Delayed Neutron Counting and alpha spectrometry, detection limits were calculated from the respective blank readings.

4 RESULTS

Table 3 lists the minimum detectable activity concentrations expressed in Bq per unit mass (kg or L) fresh weight as well as reference activity concentrations in foodstuffs as published in an UNSCEAR Report on exposure of the public to natural radiation [11].

Table 3: Minimum detectable activity concentrations and reference values for radionuclides in foodstuffs. All values expressed in mBq/kg

Nuclide	Potato		Fish		Milk		Cabbage	
	MDA	Ref	MDA	Ref	MDA	Ref	MDA	Ref
U-238	8.2	3	22	30	3.5	1	4.9	20
Ra-226	150	30	450	100	52	5	120	50
Pb-210	550	30	1200	200	220	15	970	89
Po-210	250	40	200	2000	3.4	15	30	100
U-235	0.38	0.1	1.0		0.16	0.05	0.23	1
Th-232	130	0.5	280	10	740	0.3	270	15
Ra-228	320	20	720		120	5	270	40
Th-228	480	0.5	220	100	3.1	0.3	100	15

The following can be observed:

- Most of the reference values are lower than the MDA results. The methods generally lack the required sensitivities to measure radionuclides at the reference values. Exceptions are the analyses for Po-210 in fish, milk and cabbage, and uranium in fish and cabbage.
- Minimum detectable activities for fish is higher compared to the other sample matrices due to the lower preconcentration factor obtained for this material
- Although the preconcentration factors for potato, milk and cabbage were similar (about factor 100), the results for a nuclide are spread over one order of magnitude. This may be attributed to differences in sample sizes analyzed, chemical yields and activation interferences.

Table 4 lists the minimum measurable dose rates per radionuclide that were calculated based on MDA concentrations (Table 3) and criteria set out in paragraph 2.

The minimum measurable dose consists mainly of contributions of the calculated values for Ra-228 (70% - 80%), Pb-210 (10% - 25%) and to lesser extent, Po-210 (0% -10%). The dominant contributions for Ra-228 and Pb-210 can be ascribed to their relatively high detection limits in combination with their high dose conversion factors.

Table 4: Calculated doses of individual nuclides in potato and fish

Sample type	Potato		Fish		Milk		Cabbage		
Consumption rate (kg/a)	115		25		120		55		
Nuclide	DCF (Sv/Bq)	Dose (μ Sv/a)	% of total	Dose (μ Sv/a)	% of total	Dose (μ Sv/a)	% of total	Dose (μ Sv/a)	% of total
U-238	4.5E-08	4.3E-02	< 0.1	2.5E-02	< 0.1	1.9E-02	< 0.1	1.2E-02	< 0.1
Th-234	3.4E-09	3.2E-03	< 0.1	1.9E-03	< 0.1	1.4E-03	< 0.1	9.1E-04	< 0.1
Pa-234	5.1E-10	4.8E-04	< 0.1	2.9E-04	< 0.1	2.1E-04	< 0.1	1.4E-04	< 0.1
U-234	4.9E-08	4.7E-02	< 0.1	2.8E-02	< 0.1	2.1E-02	< 0.1	1.3E-02	< 0.1
Th-230	2.1E-07	2.0E-01	< 0.1	1.2E-01	< 0.1	8.8E-02	< 0.1	5.7E-02	< 0.1
Ra-226	2.8E-07	4.9E+00	1.4	1.4E+01	8.5	1.7E+00	1.4	1.8E+00	1.2
Pb-214	1.4E-10	2.5E-03	< 0.1	7.2E-03	< 0.1	8.7E-04	< 0.1	9.1E-04	< 0.1
Bi-214	1.1E-10	1.9E-03	< 0.1	5.6E-03	< 0.1	6.8E-04	< 0.1	7.1E-04	< 0.1

Pb-210	6.9E-07	4.4E+01	12	2.1E+01	12	1.9E+01	15	3.7E+01	25
Bi-210	1.3E-09	3.8E-02	< 0.1	6.4E-03	< 0.1	5.4E-04	< 0.1	2.1E-03	< 0.1
Po-210	1.2E-06	3.5E+01	10.2	5.9E+00	3.5	4.9E-01	0.41	2.0E+00	1.4
U-235	4.7E-08	2.0E-03	< 0.1	1.2E-03	< 0.1	9.0E-04	< 0.1	5.8E-04	< 0.1
Th-231	3.4E-10	1.5E-05	< 0.1	8.8E-06	< 0.1	6.5E-06	< 0.1	4.2E-06	< 0.1
Pa-231	1.1E-06	4.8E-02	< 0.1	2.8E-02	< 0.1	2.1E-02	< 0.1	1.4E-02	< 0.1
Ac-227	7.1E-07	3.1E-02	< 0.1	1.8E-02	< 0.1	1.4E-02	< 0.1	8.8E-03	< 0.1
Th-227	8.8E-09	3.8E-04	< 0.1	2.3E-04	< 0.1	1.7E-04	< 0.1	1.1E-04	< 0.1
Ra-223	1.0E-07	4.3E-03	< 0.1	2.6E-03	< 0.1	1.9E-03	< 0.1	1.2E-03	< 0.1
Pb-211	1.8E-10	7.8E-06	< 0.1	4.7E-06	< 0.1	3.5E-06	< 0.1	2.2E-06	< 0.1
Th-232	2.3E-07	3.5E+00	1.0	1.6E+00	0.96	2.0E+00	1.7	3.5E-01	0.24
Ra-228	6.9E-06	2.5E+02	74	1.2E+02	74	9.6E+01	80	1.0E+02	71
Ac-228	4.3E-10	1.6E-02	< 0.1	7.8E-03	< 0.1	6.0E-03	< 0.1	6.4E-03	< 0.1
Th-228	7.2E-08	4.0E-01	0.12	3.9E-01	0.23	2.6E-01	< 0.1	4.0E-01	0.27
Ra-224	6.5E-08	3.6E-01	0.11	3.5E-01	0.21	2.4E-01	< 0.1	3.6E-01	0.25
Pb-212	6.0E-09	3.3E-02	< 0.1	3.2E-02	< 0.1	2.2E-02	< 0.1	3.3E-02	< 0.1
Bi-212	2.6E-10	1.4E-03	< 0.1	1.4E-03	< 0.1	9.6E-04	< 0.1	1.4E-03	< 0.1
Total dose (uSv/a):		3.4E+02		1.7E+02		1.2E+02		1.4E+02	

It seems that the analytical methodology is able to allow screening at the 250 uSv/a level for most foodstuffs. In the case of potatoes, less than 20 grams ash were obtained from the fresh amount of 1.62 kg used. Using a much larger sample size will result in lower detection limits for Pb-210 and Ra-228. A sample size of 5 kg for potatoes (still manageable for drying and ashing) will result in a gain in sensitivity by a factor 3 to 4 allowing screening at the 100 uSv/a level.

5 CONCLUSION

An analytical methodology was evaluated for its performance to screen foodstuffs for dose by ingestion. The methodology is based on preconcentration of radionuclides by drying and ashing and utilizing a combination of instrumental techniques for direct analysis of the ash (less costly) and a single radiochemical method (more expensive) for analysis of polonium-210 in dried material. The methodology has the capability to screen foodstuffs for dose at 100 uSv/a using appropriate sample sizes. The relatively high MDA's of Ra-228 and Pb-210 will not allow screening at lower dose levels. Expensive radiochemical separation and concentration of the nuclides will be required. This will probably also be applicable to the isotopes of thorium and uranium.

6 ACKNOWLEDGEMENTS

This work was made possible through the kind assistance of the radioanalytical laboratory of the South African Nuclear Energy Corporation.

7 REFERENCES

- [1] South African National Nuclear Regulatory Guide RG-002: Safety Assessments of Radiation Hazards to Members of the Public from NORM Activities.
- [2] Handbook of Radioactivity Analysis, 3rd Edition, 2008, Michael F. L'Annunziata (Editor).
- [3] S. Moebiusa, et al., 2009, Liquid scintillation for NORMs in the Oil and Gas industry, http://www.iaea.org/inis/collection/NCLCollectionStore/_Public/42/070/42070487.pdf
- [4] J.S. Becker, 2003. Mass spectrometry of long-lived nuclides. Spectrochimica Acta Part B Vol. 58, p. 1757–1784.

- [5] X. Hou, P. Roos, 2009. Critical comparison of radiometric and mass spectrometric methods for the determination of radionuclides in environmental, biological and nuclear waste samples. *Analytical Chimica Acta* Vol. 608 (2), p. 105 -139.
- [6] K.M. Mathes, C. Kim, P. Martin, 2007. Determination of ²¹⁰Po in environmental materials: A review of analytical methodology. *Applied Radiation and Isotopes*, Vol. 65, p. 267-279.
- [7] Y.Y. Wang, B.M. Biwer, C. Yu. ANL/EAIS/TM-103, August 1993. Compilation of Radionuclide Transfer Factors for the Plant, Meat, Milk and Aquatic Food Pathways and the Suggested Default Values for the RESRAD Code.
- [8] A.N. Hamer, E.J. Robbins, 1956. The natural abundances of uranium isotopes. *Can. J. Phys.*, Vol 34, p. 259.
- [9] Z. Lin, Z. Who, 2009. Analysis of polonium-210 in food products and bioassay samples by isotope dilution alpha spectrometry. *Applied Radiation and Isotopes*, Vol.67, p. 907 – 912.
- [10] Currie, L.A.,1968. Limits for qualitative detection and quantitative determination: application to radiochemistry. *Analytical Chemistry* Vol. 40 (3), p. 586–593.
- [11] UNSCEAR 2000 Report Vol. 1. Sources and effects of ionizing radiation. Appendix B: Exposures from natural radiation sources.

Monitoring the environmental radiation by using a new gas-filled proportional counter probe as a quasi-spectroscopic system

Dirk Peter Schmalfuß¹, Uwe Hoffmann, Julia Glück, Andreas Meister

VacuTec Meßtechnik GmbH, Dornblüthstraße 14, 01277 Dresden, Germany

Abstract. The “VacuTec Meßtechnik GmbH”, specialised in manufacturing radiation detectors since 1956, provides an economic, innovative quasi-spectroscopic proportional counter probe (hereinafter referred as to PCP) that combines a conventional Geiger-Mueller probe (hereinafter referred as to GMP) with a gas-filled proportional detector of high efficiency towards photon radiation. By means of a sophisticated deconvolution algorithm, the continuously updated pulse height spectra are reconstructed into a natural and a non-natural part. To be more precisely, the PCP evaluates the local background by comparing a current spectrum with a set of response vectors containing the radiometric fingerprint of the location where the PCP is installed stationarily, whereby a reliable differentiation is obtained between the local background and non-local spectral contributions of artificial origin. Additionally, is calculated as well being extremely sensitive to deviations from the general spectrum shape, for example due to present contamination. Natural background radiation may vary in intensity, for example as a result of precipitation regardless of whether rain or snow, however without the spectrum shape changing. Accordingly, a natural increase of intensity can be well-distinguished from a non-natural increase following a contingent nuclear incident. To obtain additional dose rate data, two Geiger-Mueller tubes are attached. They are operated in an innovative dead-time independent measuring mode. Neutron detection using ³He proportional counters is available optionally. In this paper, we present results of on-going measurements under real environmental and “non-natural” conditions.

KEYWORDS: *natural radiation; monitoring network; spectroscopy; gas-filled proportional counter.*

1 INTRODUCTION

To evaluate the composition of complex gamma-fields, spectroscopic systems are increasingly gaining in significance in environmental monitoring especially triggered by the Fukushima incident in 2011. Nowadays, commercial solutions that provide accurate and valid information concerning the potential nuclide vector are based upon scintillators and semiconductors. However, the cost of acquisition and maintenance of such systems are high-priced aside from general stability problems if operated under ambient conditions. Therefore, it is illusory to implement a continuous and comprehensive monitoring network solely equipped with such spectroscopic systems. To mention an example, the German monitoring network is currently operated by using conventional GMP's measuring dose rates only, and on a limited scale, the application of scintillator-based spectrometers is taken into consideration exclusively for selected locations being exposed to a higher nuclear risk. In this context, the “VacuTec Meßtechnik GmbH” has developed a quasi-spectroscopic probe based upon a large volume gas-filled proportional detector to meet the demand of low-cost spectroscopic devices providing at least basic information about the composition of the local radiation registered. The PCP allows a rough analysis of spectra as to the contingent presence of non-natural radiation components. Naturally occurring events such as rainfall can cause a temporary increase of the radiation level. In this case, the increase would be identified as natural variation of the local background, whereas a GMP at best would register merely an unspecific gain of the dose rate not being distinguishable from a possible increase caused by a nuclear incident. Additionally, due to the comparable high efficiency of the PCP towards photon radiation, the data to be obtained are much less interfered by statistical effects. The PCP is thought to be a potential substitute for commonly used GMP's for the comprehensive application under ambient conditions.

¹ Dirk Peter Schmalfuß: Dirk.Schmalfuss@vacutec-gmbh.de

2 FORMALISM

The proportional detector response to photon radiation of different energy constitutes the system matrix A , where the number of rows is given by the number of channels m . Consequently, each column of matrix A represents a certain energy. The number of columns n corresponds to the number of different energies taken into account. Generally, the number of rows is greater than or equal to the number of columns: $m \geq n$. Alternatively, the system matrix A may also be defined in such a way that each column represents the specific photon radiation emitted by a certain nuclide. Thus, each column represents a certain nuclide. Within our approach the natural background radiation is considered as one of these nuclides reflecting the contamination-free situation locally. The choice of the other nuclides depends on which nuclide one would expect to be released in the event of a nuclear incident. Mathematically, the detector response defines a set of basis vectors. Each basis vector can be understood as a discrete probability distribution. In its simplest version applied here, A is composed of $n=2$ basis vectors only, i.e., the natural component and a pre-set non-natural component. The natural component must be measured on-site initially. Considering the non-natural component, we have chosen the response to 30 keV X-ray photons representing a typical radiation to be expected if ^{137}Cs is accidentally released. To photon energies lower than 100 keV the PCP responds very sensitively. Taking into account the natural constraint $x \geq 0$, the following equation has to be solved:

$$\nabla_{x,\lambda}[(y - Ax)^T(y - Ax) + 2\lambda v^T(y - Ax)] = 0 \quad (1)$$

That way the measured spectrum y is approximately reconstructed as linear combination Ax of the underlying basis set. The Lagrange multiplier λ ensures pulse number conservation. This means that the number of pulses in the measured spectrum is exactly the same as in the reconstructed spectrum. To express the conservation of pulse numbers compactly, an auxiliary vector v is introduced. Its m entries are set to be 1 to sum up the contents of all m channels according to $N = v^T y$. Eliminating λ the solution of (1) reads as follows:

$$Ax = P \left(1 + \frac{v v^T (1-P)}{v^T P v} \right) y \quad (2)$$

with $P = P^2$ being the corresponding projection matrix given by

$$P = (A(A^T A)^{-1} A^T). \quad (3)$$

Obviously, the invertibility of $A^T A$ must be assumed. To obtain count rates, the solution has to be divided by the acquisition time. The conservation of pulse numbers can be easily shown. Right multiplying the transpose of v by (2) yields first $v^T Ax = v^T y = N$. Because of the probabilistic character of the basis set, summing up the entries of A generates the transpose of a new vector u , whose n entries are equal to 1. Accordingly, the conservation of pulse numbers is evident: $N = v^T y = u^T x$. Basically, (2) implies an interesting geometric aspect. Neglecting the pulse conserving term, (2) can be rewritten as follows:

$$A^T Ax = = A^T P y \quad (4)$$

Furthermore, y may be understood as being composed of two contributions, i.e., the parallel part y_{\parallel} and the perpendicular part y_{\perp} . The projection matrix acts on both parts differently: $P y_{\parallel} = y_{\parallel}$ and $P y_{\perp} = 0$. Accordingly, one obtains $A^T Ax = A^T y_{\parallel}$. The right-hand side of this equation represents a vector, whose entries are identifiable with the projections of y_{\parallel} onto each basis vector, by definition the covariant components of y_{\parallel} . The matrix product $A^T A$ on the left-hand side defines the metric, more precisely, the covariant components $g_{\mu\nu}$ of the metric tensor. Consequently, the solution x represents the set of contravariant components of y_{\parallel} . It is evident that the co- and contravariant components of y_{\perp} vanish identically. For that reason, they may be reintroduced formally with the result that (4) can be reformulated according to

$$g_{\mu\nu}y^\nu = y_\mu \text{ or inverse } y^\nu = g^{\nu\mu}y_\mu \text{ with } g^{\mu\eta}g_{\eta\nu} = \delta_\nu^\mu \quad (5)$$

In summary one obtains the known transformation rules between co- and contravariant vector components within a space characterised by a given metric. This means that basically deconvolution may be considered as transforming the covariant components of into the corresponding contravariant components.

The relation between both the covariance matrix of x and the covariance matrix of y is given simply by following equation

$$AC(x)A^T = P \left(1 + \frac{vv^T(1-P)}{v^T P v} \right) C(y) \left(1 + \frac{(1-P)vv^T}{v^T P v} \right) P \quad (6)$$

with $C(y) = y_i \delta_{ij}$ being diagonal due to the Poisson statistics that governs the buildup of spectra. Differentiating of $N = v^T y = u^T x$ yields first $\Delta N = v^T \Delta = u^T \Delta x$. By averaging the square of this expression one finds $\langle \Delta N \Delta N \rangle = v^T C(y) v = u^T C(x) u$ with $C(y) = \langle \Delta y \Delta y^T \rangle$ and $C(x) = \langle \Delta x \Delta x^T \rangle$. Apparently, the sum of all matrix entries of $C(y)$ equals to the sum of all matrix entries of $C(x)$. This sum is nothing but the total number of pulses what agrees with the variance $\langle \Delta N \Delta N \rangle = N$.

The quantity x^2 tests the hypothesis that both the reconstructed spectrum Ax and the measured spectrum match as to shape. To illustrate the basic properties of x^2 clearly, we consider a simplified A composed of one basis vector only, where the quantity to be studied actually is the mean $\langle x^2 \rangle$. As usual $\langle x^2 \rangle$ is defined as a sum covering all m channels according to

$$\langle x^2 \rangle = \sum_k \frac{\langle (y_k - NA_k)^2 \rangle}{NA_k} = \sum_k \frac{\langle y_k^2 \rangle - \langle y_k \rangle^2 + \langle (y_k - NA_k)^2 \rangle}{NA_k} \quad (7)$$

Due to Poisson statistics the variance of y_k is equal to $\langle y_k \rangle$. Introducing $\langle y_k \rangle = NB_k$ one obtains

$$\langle x^2 \rangle = \sum_k \frac{B_k + N(B_k - A_k)^2}{A_k} \quad (8)$$

Equation (8) allows a simple interpretation. If B_k equals A_k for each channel both spectra match and $\langle x^2 \rangle = m$ complies with the number of channels, namely independent of N . Then, the variance of x^2 is given by $2m$ in the limit of large N . Otherwise, $\langle x^2 \rangle$ is growing linearly with the number of pulses registered. For a fixed count rate it becomes a linear function of acquisition time indicating that there are existing spectral contributions not being consistent as to the basis. The growing is controlled by the squared difference $B_k - A_k$. The smaller these difference the longer the acquisition time to be needed to reveal residual spectral discrepancies. Without any restriction, all the results apply to the general case of a multicomponent basis.

As mentioned above, the attached low and high dose Geiger-Mueller tubes are operated in a dead-time independent measuring mode based upon the idea of measuring time intervals between consecutive pulses instead of counting pulse numbers per time which would be interfered by dead-time effects. After every single pulse the tubes are quenched and restarted automatically with a defined recovering time much larger than the intrinsic dead-time. This method results in a linear count rate-dose rate relationship, which expands the usable measuring range by one to two decades. As is known, the time up to the next pulse obeys an Exponential distribution with a mean being the inverse pulse rate

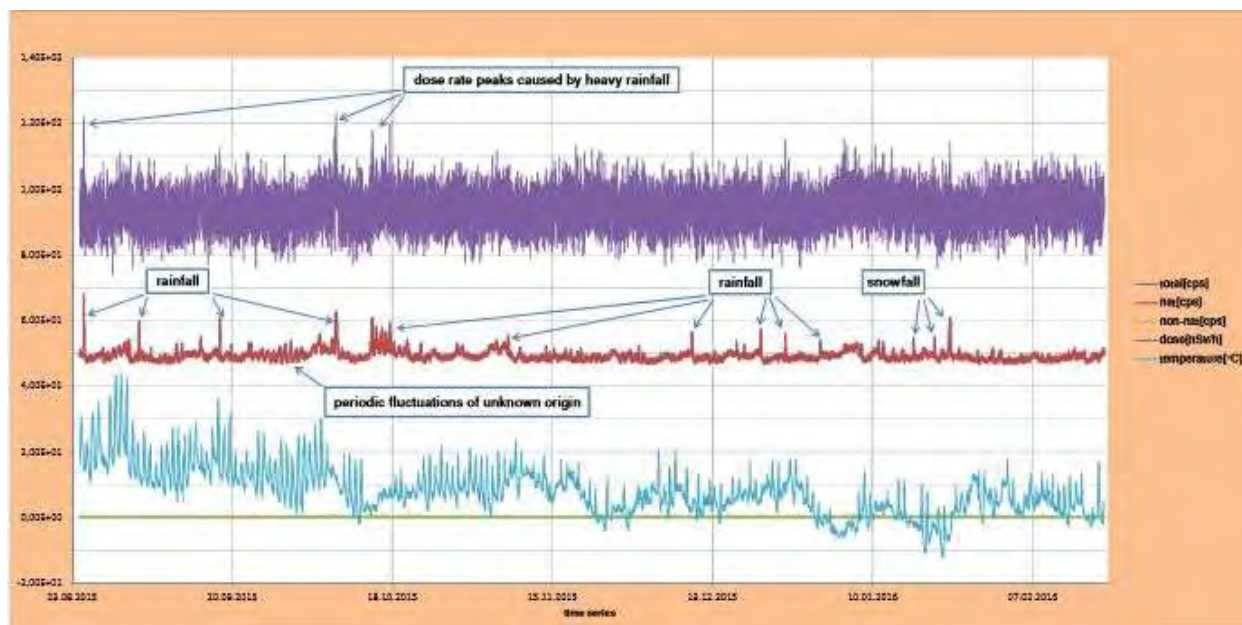
$$\langle \Delta t \rangle = \int_0^\infty R \Delta t e^{-R \Delta t} d \Delta t = R^{-1} \quad (9)$$

Both tubes are energy-compensated. Knowing the pulse rates, the corresponding ambient dose rates \dot{H}^* (10) can be calculated. The dose rate values of both tubes are used to deduce an overall dose rate taking the statistical precision of the measurements into account.

3 RESULTS

One PCP was installed outdoors on the rooftop of our company building. Dresden, localised in the proximity of known uranium deposits, is characterised by a comparative high natural radiation level. Since August 2015 the PCP has been exposed to various weather conditions with temperatures ranging from +40 °C in late summer down to nearly -20 °C in winter.

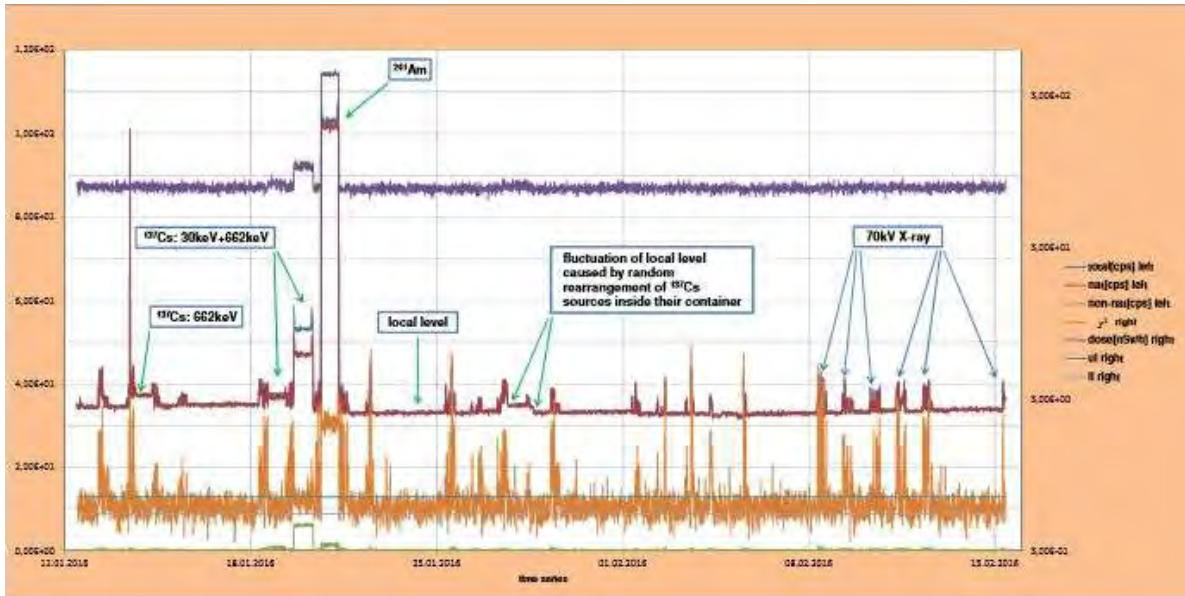
Figure 1: Selection of ambient data recorded during a period from August 2015 to February 2016.



In Figure 1 recorded data are shown, i.e., the dose rate “dose”, all rate components and the temperature. Due to pulse conservation, the natural component “nat” and the non-natural component “non-nat” provide the overall count rate “total” exactly. The overall count rate displays distinct peak structures. These structures definitely may be attributed to precipitation events regardless of whether rain or snow. During a heavy thunderstorm in late August 2015 the overall count rate increased by nearly 40 % temporarily, however without any effect on the associated non-natural component. Generally, the non-natural component did never exceed its own statistical noise level. Hence, the natural count rate equals the overall count rate approximately. Any increase of the overall count rate is clearly allocated to the natural component so far. In parallel, the associated χ^2 remained within its statistical limits, emphasising that the observed fluctuations were not caused by present contaminations. Another remarkable event occurred in early October 2015 related to a heavy downpour after a longer period of dry weather. The individual characteristic of a precipitation induced radiometric event results from the interplay of various factors such as duration, intensity and frequency of precipitations. Thanks to its extreme sensitivity, the PCP allows a fairly precise insight into the dynamics of a radiation field. The fact that not only precipitation influences the intensity of natural radiation is illustrated in Figure 1 as well. During a period in September 2015 a cyclical, nightly increase of the background intensity in connection with a recurrent decrease back to the initial level during the daytime was observable. At that time rain could be excluded. Without being able to allocate the concrete causes for the observed fluctuations occurring that time, the data emphasise the sensitivity of the PCP in the face of numerous factors such as geologic, topographic and meteorological conditions along with the omnipresent cosmic background of variable intensity, which influence the natural radiation level directly or indirectly. However, eye-catching dose rate peaks are only to be ascertained in connection with exceptional precipitation events. Otherwise, the course of dose rate is dominated by statistical noise and at best indicates general trends. To simulate the “worst case scenario”, the PCP was tested next to our calibration facility which is used regularly for development and manufacturing purposes. It provides various photon irradiation devices including

^{137}Cs and ^{60}Co sources of different activity as well as an X-ray system. The measuring setup was installed in an adjoining room ensuring, if any, the PCP would register just a small amount of additional radiation. Prior to the actual test, the natural basis component being typical for the local conditions was recorded during a weekend when the facility usually is not in use.

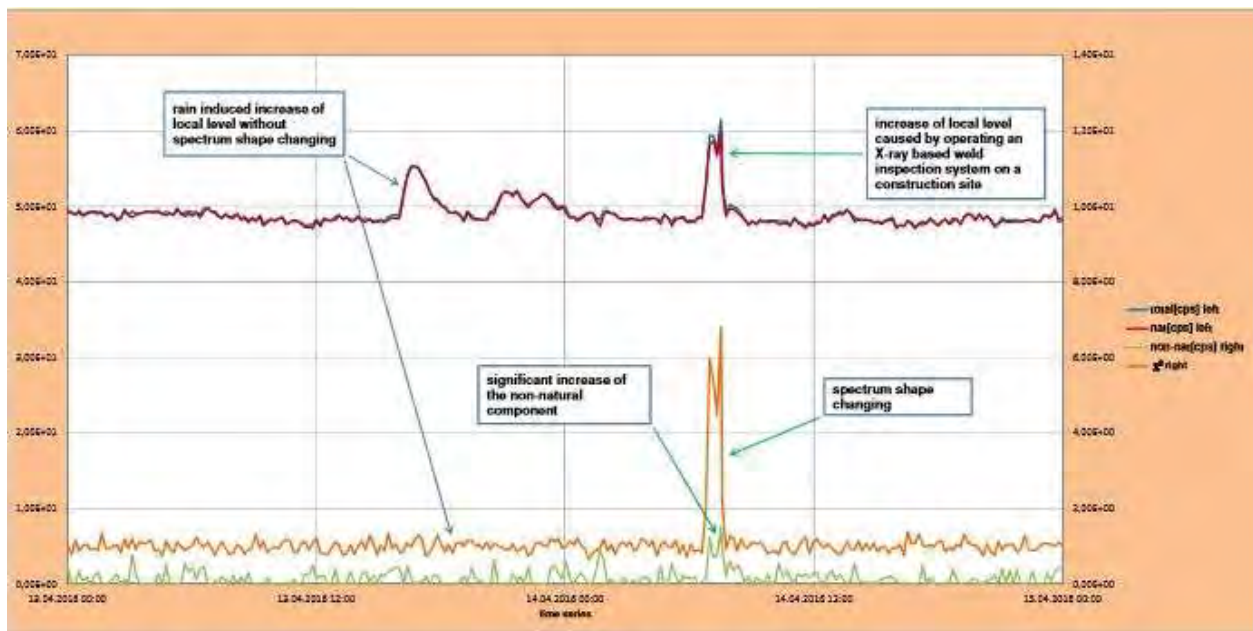
Figure 2: Selection of data recorded next to our calibration laboratory: count rates (left axis); dose rate, normalised χ^2 including its statistical limits (right axis).



The data shown in Figure 2 comprise the dose rate “dose”, both rate components “nat” and “non-nat”, the overall count rate “total” as well as χ^2 divided by m , measured during four weeks of normal business. Both horizontal lines “ul” and “ll” denote the upper and lower limit respectively, within χ^2 may fluctuate provided the spectra are consistent with the basis set. Obviously, distinctive effects were observed when the X-ray system was operating. Depending on the applied tube current, both the overall and the natural count rate increased considerably while the non-natural count rate responded in a rather modest way. However, the concurrent risen χ^2 indicates the presence of spectral contributions being different from the contamination-free local background. The radiation of a ^{137}Cs source emitting 662 keV photons only has induced a slight gain of pulses registered. Neither the non-natural component nor χ^2 has been affected noteworthy, which presumably is due to low additional intensity connected with the fact that the detector responds to photons of higher energy in a rather uniform way. Equation (8) would provide an explanation that therefore χ^2 seems to be widely unaffected. Nevertheless, considering the distance, the separating wall and the source being used inside a massive lead shielding, it is astonishing that there has been a measurable effect at all. Even the random rearrangement of ^{137}Cs sources inside their storage container has raised the overall count rate significantly. Free ^{137}Cs emits 662 keV photons along with 30 keV photons. To reproduce an accidental release of ^{137}Cs on the laboratory scale, the PCP was irradiated additionally using small ^{137}Cs sources of different activity. These sources have thin windows allowing low energy photons to escape. According to Figure 2, as expected both the natural as well as the non-natural component increased obviously depending on the additional intensity provided. Evidently, the gain of χ^2 has been a matter of intensity as well. Because of the spectral similarities mentioned above, it would take a longer acquisition time to indicate the presence of free ^{137}Cs solely by the increase of χ^2 . Furthermore, the PCP has been exposed to the radiation of a fairly strong ^{241}Am source emitting 60 keV photons. Apparently, this radiation did not fit to the underlying basis set which is clearly visible regarding χ^2 . Except for radiation originating from those sources, the corresponding dose rate has proved widely to be much less sensitive to fluctuations of the radiation level. In April 2016 the PCP on the rooftop registered the concurrence of two radiometric events of different origin within a 24-hour period, which

is well-illustrated in Figure 3. The first radiometric event was induced by a thunderstorm in the evening of April 13th. Due to heavy rainfall the overall count rate and its natural component increased temporarily, however without having any effect being visible neither on the non-natural component nor on χ^2 , whereby the observed increase of radiation may be considered as natural variation of the normal background level. As opposed to this, the increase of radiation the next morning was accompanied by a significant gain of both χ^2 and the non-natural component suggesting the temporary presence of artificial spectral contributions. The further investigation revealed that the additional radiation arose from an operating X-ray based weld inspection system on a construction site nearby.

Figure 3: Concurrence of a natural and a non-natural radiometric event within a 24-hour period: the data shown comprise the overall count rate and its natural component (left axis), its non-natural component and normalised χ^2 (right axis).



4 CONCLUSIONS

Applied to monitor environmental radiation, the introduced PCP enhances the extent of available information. By deconvoluting continuously updated pulse height spectra, the PCP is capable of differentiating between natural and non-natural radiation components. The PCP may be integrated into monitoring networks as a substitute for conventional counting probes based upon Geiger-Mueller tubes. In addition to dose rate data, it provides basic evidence of the spectral constitution of the radiation being detected. Where ordinary GMP's at best would register just unspecific fluctuations of the background level, the PCP allows a rough spectroscopic classification. For example, a temporary increase of radiation, typically induced by naturally occurring events such as precipitation, will be identified as a non-hazardous variation of the natural background, whereby man-made causes may be excluded. Being very sensitive to any deviation from the local background, the PCP indicates the presence of air or surface contaminations, however without analysing the hypothetical nuclide vector itself.

Radiological assessment of natural radioactivity in groundwater from Greater Accra Region of Ghana: Gross alpha and gross beta measurements and annual committed effective dose evaluation.

E.J.M.Nguelem^{a,b}, M.Ndontchueng^a, E.O.Darko^b

^aNational Radiation Protection Agency, P.O.Box 33732, Yaounde.

^bGraduate School of Nuclear and Allied Sciences, University of Ghana, Atomic Campus, P.O.Box AE1, Atomic Energy.

Abstract. This present work is aimed to determine the gross alpha and gross beta in twenty six (26) groundwater samples from Adentan and Abokobi areas in the Greater Accra Region of Ghana and evaluate the gross average annual committed effective dose due to intake. The radiometric nuclear technique used was low background automatic Alpha/Beta counting system (Canberra *iMatic*TM). According to the procedure selected during counting time, each water sample was counted twice to obtain good statistical results. The average activity concentrations of gross alpha and gross beta were 0.03 and 0.50 Bq/L for Adentan, and 0.07 and 0.43 Bq/L for Abokobi, respectively. The results obtained are below the guideline levels of gross alpha (0.5 Bq/L) and gross beta (1.0 Bq/L) in drinking water established by the World Health Organisation. The estimated gross average committed effective dose for each member group of the public resulting from those activity concentrations of gross alpha and gross beta was 0.33 mSv/y for infants, 0.25 mSv/y for children and 0.20 mSv/y for adult member of the public in Adentan, and 0.27 mSv/y for infants, 0.22 mSv/y for children and 0.10 mSv/y for an adult member of the public in Abokobi, respectively. These results are compared be relatively high that the worldwide safe limits except to values of infants and adult member of the public in Adentan areas. Since no significant health risk as a result of intake of radiation in water has been observed or not studied, consumption of groundwater for the study areas may not pose any significant radiological health hazards through ingestion to the population.

KEYWORDS: *Canberra iMatic*TM; *gross alpha/beta activity; radiological health; groundwater.*

1 INTRODUCTION

The measurement of natural radioactivity in our physical environment allows the determination and assessment of population exposure to radiation. The occurrence of natural radionuclides in water depends on the waters origin as well as humans activities in the area, such as fertilisers used in agriculture, where the water is located. These are known as such products products which usually contain some trace elements like uranium and thorium decay series and non-series of potassium (40K) which may increase the amounts of natural radionuclides in soil. Industrial activities (the extraction and processing of earth materials or their industrial products) may increase the incorporation of radionuclides into the hydrosphere through surface or/and ground water (Pujol et al. 2000). For groundwater (boreholes and wells), it depends on their presence and contents in lithologic of solids aquifers or surrounding rocks where groundwater is stored (Nour Khalifa, 2004). These solids aquifers or rocks known as geological materials usually contain some trace amounts of radioactive elements such as uranium, thorium decay series and non-series of potassium (40K), which may dissolve into groundwater system during water/rocks-soils interaction mechanism (Bonotto et al., 2009).

Considering the presence of these natural radionuclides in the groundwater system and the radiotoxicity to human, consumption of groundwater with high amounts of natural radionuclides may rise to internal exposure caused by the decay of natural radionuclides taken into body through ingestion as well as inhalation (UNSCEAR,2000). During the decay process, they release several alpha and beta particles which are also responsible for a significant portion of the total radiation dose received from natural radioactivity, particularly through ingestion (UNSCEAR,1993; Gürsel Karahan et al. 2000). Gross alpha in water is usually presented by ²³⁸U series while gross beta is presented by non-series of ⁴⁰K as well as ²³²Th series (Yuce et al., 2009). Determination of gross alpha and gross

beta activity concentration levels in groundwater are of particular interest for routine monitoring of radioactivity levels in groundwater resources and to ascertain the radiological risk associated.

According to the World Health Organisation (WHO, 2004), the recommendations apply to routine operational limits of gross alpha and gross beta in existing or new water supplies below which no further action is required are 0.5 Bq.L^{-1} and 1.0 Bq.L^{-1} respectively. These guidelines levels of gross alpha and gross beta established by the WHO have been adopted by many countries in the world in order to avoid high dose to radiation and enhance radiological health hazards due to consumption of groundwater. These are also been used by other developed and under developed countries to develop their own nation water quality standards on natural radioactivity level in drinking and domestic water.

In Ghana, there is no guideline for gross alpha and gross beta activity concentrations levels in drinking water. Most of the rural communities as well as urban areas in the Greater Accra Region of Ghana who do not receive public water supply used groundwater (boreholes and wells) for domestic purposes particularly and drinking water as well. According to literature of natural radioactivity in groundwater by gross alpha and gross beta measurement, only few studies have been done on radiological quality of drinking water in Ghana (Faanu et al. 2011); and sufficient information is not available. Estimation of gross alpha and gross beta activity concentration in groundwater resources is an important route for assessment of the radiological health hazards to ionizing radiation due to ingestion. Particular attention is focused on the major alpha and beta emitting radionuclides in the Uranium and Thorium Series. Bonotto et al. (2009) recognizes ^{238}U , ^{234}U , ^{232}Th , ^{226}Ra , ^{210}Pb and ^{210}Po for the Uranium series and ^{232}Th , ^{228}Ra and ^{228}Th for the Thorium series as the major alpha and beta emitting radionuclides which are of importance to internal irradiation.

The present work is aimed to evaluate the radiation dose intake in water (boreholes and wells) in the Greater Accra Region of Ghana by gross alpha and gross beta measurement using low background gross Alpha/Beta counting system. The investigations were performed in selected communities, namely; Adentan and Abokobi, and the population in the both areas were estimated to be 1 to 2 million, respectively since we could not have any information reliable information. Both study areas have relatively different geological structure. The geological structure of the investigated communities is grouped into two major geological formations found in abundance in the study areas, mainly Dahomeyan formations (with undifferentiated rocks mainly schists and gneisses) found in abundance in the area where Adentan is located, Togo formations (with undifferentiated mainly siliciclastics, high or low metamorphosed) as well as Dahomeyan are major rocks found in a zone where Abokobi is located. Each of these dominant geological formations found in the study areas consist of different lithologic of solids aquifers or rocks (Martin et al., 2005; Darko et al., 2010; Ahmed et al., 1977; Bonoeng-Yakubo et al. 2010). Figure1 below shows the geology of the study areas. Groundwater available in both areas is boreholes and wells. The hydrogeology of groundwater system in both areas is relatively different since this is governed by the geological settings of the areas (Darko et al. 2010).

2 EXPERIMENTAL

The nuclear analytical technique used to carry out this study was a low background Gass-less Automatic gross Alpha/ Beta counting system (Canberra *iMaticTM*) set-up at the Radiation Protection Institute (RPI) of Ghana Atomic Energy Commission (GAEC). The equipment is a firmware based instrument and does not require a computer to set up. The entire program of the instrument is stored in flash memory. It consists of solid state Passivated Implanted Planar Silicon (PIPS) detector position facing down for alpha and beta detection; can be operated continually for over six hours with internal batteries and is totally self contained.

2.1 Sampling

In order to cover the study areas, a pre-field survey was done to know the number of boreholes and hand dug wells available in the areas and frequently used by the population at the time of sampling for domestic use, in particular and drinking water as well. The sampling campaigns were carried out between November 2011 and January 2012 and the weather conditions at the time of sampling were fairly stable. The places where samples were collected were marked by using a Global Positioning System (GPS). These are depicted in Figure1 with their sample ID (ADW and ABW for Adentan and Abokobi samples, respectively). A total of (26) groundwater samples were collected from boreholes and wells covering some communities in Adentan and Abokobi. In this way, (10) groundwater samples from Adentan site and (16) groundwater samples were from Abokobi site. The pH, salinity and total dissolved solids (TDS) of the water samples were measured on field using Metrohm model 691 pH-meter for the pH and a portable HACH conductivity for salinity and TDS of water samples.

Samples were obtained after allowing water to run fully at least 10 minutes before in order to remove stagnant water from the pump. Samples were then collected into 2 liters of polyethylene gallons tightly sealed and labelled. A few drops of ultra-pure nitric acid (60%) were added to prevent adherence of radionuclides to the walls of the containers. The samples were then stored in the laboratory for preparation and analysis. The sample containers were carefully watched and rinsed three times with the distilled water before sampling.

2.2 Sample preparation and measurement

One litre of each collected groundwater sample was first filtered through filter paper of 47 millimetres of diameter and transferred into 1 liter beaker. Two millimetre of ultra-pure acid were added into one litre of filtered sample in order to maintain the radionuclides in the sample and to liberate dissolved metals from exchange sites on dissolved organic particles (Gürsel Karahan et al. 2000) and let stay overnight. Each of filtered water sample (300 ml) was transferred into 400 ml glass beaker and evaporated slowly to near dryness on the electrical hot plate placed in a fume chamber. The remaining water sample was transferred quantitatively in 47 mm stainless steel counting planchets. These were then heated to near dryness, stored into desiccators to allow them to cool into room temperature and to prevent them from absorbing moisture reading for counting in Canberra iMatic™ low background Gas-less Automatic counting system with a solid state silicon PIPS detector for gross Alpha/Beta detection system.

The samples were counted according to the procedure selected during calibration of the equipment. The calibration was done using two standards sources: ^{241}Am source (with alpha particle energy $E=5485.60\text{KeV}$ and activity at the calibration time 666 Bq) for Alpha and ^{90}Sr (with beta particle energy $E=1492\text{KeV}$ and activity at the calibration time 666 Bq) for beta, respectively. The counting efficiencies of alpha and beta were then $36.25\pm 2.18\%$ and $73.16\pm 4.39\%$, respectively. The selected procedure was to allow the samples to be counted for 100 minutes each. This was done twice for each water sample.

The background reading of the detector (the minimum detection activity) for alpha and beta after counting three blank stainless steel planchets according to the selected procedure was 0.00148 Bq and 0.0026 Bq, respectively.

2.3 Annual equivalent dose due to intake

In order to control radiological risk associated with the use of groundwater and avoid high dose to radiations via intake, the average annual alpha or beta committed effective dose for a particular sample was determined by averaging the individual annual committed effective doses contributed by the major alpha or beta emitters in the ^{238}U and ^{232}Th series of the naturally occurring radionuclides as shown in equation below:

$$E_{avg}(\alpha/\beta) = \frac{I_w}{N(\alpha/\beta)} \sum_{i=1}^{n(\alpha/\beta)} A_{\alpha/\beta} * DCF_{ing}(\alpha/\beta) \quad (1)$$

where, $E_{ing}(\alpha/\beta)$ is the average gross annual alpha or beta committed effective dose in the water sample, $A_{\alpha/\beta}$ is the gross alpha or beta activity concentration, I_w is the consumption rate for the intake of water, $N(\alpha/\beta)$ is the number of radionuclides considered as major alpha or major beta emitters in the ^{232}Th and ^{238}U series of naturally occurring radionuclides and $DCF_{ing}(\alpha/\beta)$ is the dose conversion factor for ingestion of radionuclides for each age category from UNSCEAR (2000).

3 RESULTS AND DISCUSSIONS

Tables 1.a and 1.b show the locations, pH, total dissolved solids (TDS), and salinity of water samples from Adentan and Abokobi areas recorded during sampling campaign. The calculated activity concentrations of gross alpha and gross beta in the groundwater samples in Adentan and Abokobi are given in Tables 2.

The activity concentrations of gross alpha in water samples from Adentan and Abokobi varied from <0.01 (alpha detection limit value) to 0.09 Bq/L with an average value of 0.03 Bq/L and between <0.01(alpha detection limit value) and 0.16 Bq/L with an average value of 0.07 Bq/L, respectively. The gross beta radioactivity concentrations in water samples ranged from 0.03 to 1.87 Bq/L with an average value of 0.50 Bq/L for Adentan and between 0.05 and 2.72 Bq/L with an average value of 0.47 Bq/L for Abokobi. The highest values of the gross beta radioactivity concentrations were recorded in Abokobi in the sample referenced as ABW13 located at Oyarifa followed by the sample referenced as ADW3 at Ashiyie in Adentan site (see Table 2 and Figure 1a and b).

Since both study areas have slightly different geological formations, this slight variation in the activity concentrations of gross alpha and gross beta could be a result of the geological characteristics of the soils, the irregular distribution of the minerals in the surfaces of rocks or solids aquifers from which each groundwater has been in contact, the residence time of groundwater in contact with soil and bedrock system, their inhomogeneous distribution in multi-grain aggregates (Bonotto et al., 2009; Lopes et al., 2010) as well as the pH of each groundwater sample. This variation could also be as a result of radionuclides content in soil and bedrock system. As it is known, the gross alpha activity is presented by ^{238}U series and gross beta activity is presented by ^{40}K as well as ^{232}Th series (Yuce et al., 2009). The main aquifers or rocks in Adentan are Dahomeyan Formations (with undifferentiated mainly schists and gneisses) and those in Abokobi are Togo Formations (with also undifferentiated mainly siliciclastics, un- or low metamorphosed) and some Dahomeyan rock types, and consist of different lithology of solid aquifers or rocks (Figure 1.a and 1.b).

The activity concentrations of gross alpha and gross beta obtained in the present study were compared with those values recorded in various groundwaters in different parts of the world collected from the literature and presented in Table 3. The recorded activity concentrations of the gross alpha and gross beta in water samples from both Adentan and Abokobi areas varied within the validated results observed in other countries. This statistical variation of the gross alpha and gross beta activity concentrations in the water samples of the present study compared to those obtained in other countries could be a result of the different geological characteristics of the soils and rocks in Adentan and Abokobi areas and the geographical locations of the groundwater system.

Considering the guidelines values of the average activity concentrations of 0.5 BqL^{-1} for gross alpha and 1.0 BqL^{-1} for gross beta in drinking water established by the World Health Organisation (WHO, 2004), the calculated average gross alpha and gross beta radioactivity concentrations in both Adentan and Abokobi areas are below that established guidelines values. However, the activity concentrations of gross alpha and gross beta in all the samples from various locations in Adentan and Abokobi are below the guidelines values established by the WHO with the exception of the samples referenced ADW3 located at Ashiyie in Adentan with gross beta activity concentration of 1.87 BqL^{-1} followed by a sample referenced ABW13 located at Oyarifa in Abokobi with gross beta value of 2.72 BqL^{-1} .

(Figure 1.a and 1.b). This higher value of gross beta activity concentration can be related to the higher abundance of potassium (^{40}K) in soil and feldspar minerals of the bedrock system as well as ^{232}Th and its daughter's radionuclides contents.

The activity concentrations of the gross alpha and gross beta obtained in the present study was also compared with the salinity and the total dissolved solids (TDS) as shown in Figure 2. These parameters are given in Tables 1.a and 1.b. Each of the parameters such as the salinity, the total dissolved solid, and the gross alpha and gross beta radioactivity were normalized to unity and expressed as percentage index, $P_{ind}(\%)$. The total dissolved solids known as water quality parameters are assumed to have some effects on the gross alpha and gross beta concentrations and hence radiological quality of the water (Bonotto et al., 2009). Comparing the trends in the TDS and the salinity with the gross alpha and gross beta activity concentrations, neither gross alpha nor gross beta related to both TDS and salinity. This indicated that the radionuclide released to the liquid phase is dependent on parameters that are difficult or impossible to properly evaluate. These parameters include the extent of large minerals surfaces and irregular distribution of large minerals in the surfaces of the rocks.

The estimated values of the annual average committed effective dose due to ingestion of alpha and beta particles in water received by members of the public living in Adentan and Abokobi areas are given in Table 3, respectively. It was noted that the annual average committed effective dose received by member group varied from 0.02 to 0.56 mSv/y with an average of 0.33 mSv/y for infants, from 0.02 to 0.47 mSv/y with an average of 0.25 mSv/y for children and from 0.19 to 0.20 mSv/y with an average value of 0.20 mSv/y for adult member of the public, respectively. The obtained annual effective dose for each age group in samples from Abokobi varied from 0.03 to 1.55 mSv/y with a mean of 0.27 mSv/y for infants, from 0.02 to 1.33 mSv/y with an average of 0.22 mSv/y for children and from 0.01 to 0.56 mSv/y with an average value of 0.10 mSv/y for an adult member of the public (see Figure 3.a and 3.b).

Following the WHO, IAEA and UNSCEAR^[8,4,16] recommendations, the recommended reference levels of the average committed effective dose for infants, children and adults corresponding to one year consumption of drinking water are 0.26 (for infants), 0.2 (for Children) and 0.1mSv/year (adult), respectively. The average committed doses due to intake of alpha and beta particles in water for each member group obtained in the present study are relatively high than the recommended reference level with the exception of those of adult and infant member group average value in Abokobi site (see Figure 4). The obtained mean values for infants and children member of the public in samples from both studies areas are comparably lower that the worldwide limits set by WHO, IAEA.

Considering the recommended value of the annual effective dose due to ingestion of radionuclides through drinking water and food estimated by the United Nations Scientific Committee on the Effects of Atomic Radiation (UNSCEAR), the estimated worldwide average annual effective dose for adult is 0.29mSv/y (290 μ Sv/y) with a typical range of 0.2 to 0.8mSv/y (200 to 800 μ Sv/y) [UNSCEAR, 2000]. All the values obtained in this work are observed to be within the typical range of 0.2 to 0.8mSv/y (200 to 800 μ Sv/y) established by the UNSCEAR. Hence, the calculated average values in both study areas are lower than the average value set by the UNSCEAR.

4 CONCLUSION

Natural radioactivity by gross alpha and gross beta measurements in twenty six (26) groundwater samples (borehole and wells) from Adentan and Abokobi in the Greater Accra Region of Ghana have been investigated using a low background gas-less Automatic Alpha/Beta counting system (Canberra *iMaticTM*). To control radiological risk associated with the use of groundwater and avoid high dose to radiations via intake, the average annual alpha and beta committed effective dose for a particular sample was determined by averaging the individual annual committed effective doses contributed by the major alpha or beta emitters in the ^{238}U and ^{232}Th series.

The average activity concentrations of gross alpha and gross beta recorded in groundwater samples were 0.03 and 0.5 BqL⁻¹ for Adentan and 0.07 and 0.43 BqL⁻¹ for Abokobi, respectively. The observed variation in the results from this work compared with those from different origins may be attributed to geological factors including the geochemical characteristic of each groundwater. A long time study is necessary to investigate the dependence of gross alpha and gross beta activity concentrations on these parameters. Some particular groundwater samples referenced as ADW3 from Adentan and ABW13 from Abokobi recorded higher values of gross beta than the World Health Organisation guideline value. This higher value of gross beta can be attributed to the higher content of ⁴⁰K as well as ²³²Th and its daughter's nuclides in both groundwater samples. The average activity concentrations of gross alpha and gross beta in the groundwater samples are below the guidelines values of 0.5 BqL⁻¹ for gross alpha and 1.0 BqL⁻¹ for gross beta activity concentrations in drinking water established by the World Health Organisation (WHO).

The estimated gross average annual committed effective dose for each member group of the public as a result of intake of both alpha and beta particles in water are comparably be high that the save limits values recommended by WHO, UNSCEAR and IAEA except those observed values for Adult and Infants in Adentan. Since no significant of health risk due to ingestion of radiation in water have been observed or studied, consumption of water from boreholes and wells in the study Areas may not cause any radiological health hazards to human due to ingestion and any action to reduce radioactivity might not be necessary.

The study covers only a limited area of the country. It is recommended that further studies should be extended to cover the whole country in order to obtain the national global picture of gross alpha and gross beta activity concentration in water, which should include the epidemiological survey of incidences of radiation-related health effects as well as the effects of geological factors and the geochemical characteristics of groundwater on the gross alpha and gross beta values.

5 ACKNOWLEDGMENT

The authors are very grateful to the Radiation Protection Institute of the Ghana Atomic Energy Commission is for the use of laboratory facilities.

6 REFERENCES

- [1] Ahmed, Blay P. K, Castor S. B., Coakley G. J. Ghana geological survey: the geology of ¼ field sheets: Nos. 33 winneba, NE 59, 61 and 62 Accra SW, NW and NE, 1977.
- [2] Banoeng-Yakubo Bruce, Sandow Mark Yidana, Joseph O. Ajayi, Yvonne Loh, Daniel Aseidu. Hydrogeology and groundwater resources of Ghana: A review of the hydrogeological zonation in Ghana. Portable Water and Sanitation, 2010.
- [3] Bonotto D. M., Bueno T. O., Tessari B. W., Silva A. The natural radioactivity in water by gross alpha and gross beta measurement. Radiation measurements 2009; 44(1): 92-101.
- [4] Darko E.O., Adukpo O.K., Fletcher J.J., Awudu A.R., Otoo F. Preliminary studies on Rn-222 concentration in ground water from selected areas of the Accra metropolis in Ghana. Journal Radioanal. Nucl. Chem 2010; 283(2): 507-512.
- [5] Faanu A., Ephraim J. H, Darko E.O., Kpeglo D. O., Lawluvi H., and Adukpo O.K. Determination of the content of physicochemical parameters in water and soil from a Gold Mining Area In, Ghana. Research Journal of Environmental and Earth Sciences 2011; 3(2): 177-186.
- [6] Gürsel Karahan, Neset Öztürk and Ahmet Baylügen. Natural radioactivity in various surface waters in Istanbul, Turkey. Wat. Res. 2000; 34(18):4367-4370.
- [7] IAEA (International Atomic Energy Agency), Specification of Radionuclide Content in Commodities Requiring Regulation for Purposes of Radiation Protection Safety. Guide (Draft), Vienna, 2002.
- [8] KLeinschmidt Ross I. Gross alpha and beta activity analysis in water –a routine laboratory method using liquid scintillation analysis. Applied Radiation and isotopes 2004; vol. 61(2&3):333-338.

- [9] Lopes I., Madruga M. J, Ferrador G. O., Sequeira M. M., Oliveira E. J., Gomes A. R., Rodrigues F. D, F., Carvalho F. P. Monitoring of gross alpha, gross beta and tritium activities in Portuguese drinking waters. Estrada National 10, Apartado 21, 2686-953 Sacavem, Portugal, 2010.
- [10] Martin N., Somuah D., Efa E., Muff R. Environmental and Engineering geology map of Greater Accra Metropolitan Area ; hydrogeological map for urban planning, scale 1:100,000. Geological Survey Department Accra, Ghana, 2005.
- [11] Nour Khalifa Ahmed. Natural radioactivity of ground and drinking water in some Areas of Upper Egypt. Turkish J. Eng. Env. Sci. 2004; 28 (6):345-354.
- [12] Pujol Li, Sanchez-Cebeza J. A. Natural and artificial radioactivity in surface waters of the Ebro river basin (Northeast Spain). Journal of Environmental Radioactivity 2000; 51(2):181-210.
- [13] United Nations Scientific Committee on the Effects of Atomic Radiation (UNSCEAR). Report to the general assembly. Annex B: exposure from natural radiation sources. ISBN: 92-1-142238-8; 2000.
- [14] United Nations Scientific Committee on the Effects of Atomic Radiation (UNSCEAR). Report to the General Assembly, with Scientific Annexes: Ionizing Radiation: Sources and Effects of Ionizing Radiation. United Nations Sales Publication E.94.IX.2. (1993).
- [15] World Health Organisation (WHO) guidelines for drinking water quality, 3rd edn, vol 1 recommendations. Geneva. ISBN: 92 45 154638 7, 2004.
- [16] Yuce Galip, Didem Ugurluoglu, Alime T. Dilaver, Turgay Eser, Muset Sayin, Mert Donmez, Sakir Ozcelik Funda Aydin. The effects of lithology on water pollution: Natural radioactivity and trace elements in water resources of Eskisehir Region (Turkey). Water Air Soil Pollution 2009; 202:69-89.

Correlations of Radon Measurements in Soil Gas and Indoor for Improving the Prediction of an Area's Radon Potential

Franz Kabrt^{a,b*}, Andreas Baumgartner^b, Harry Friedmann^c, Valeria Gruber^d, Wolfgang Ringer^d, Franz Josef Maringer^{a,b,e}

^aBEV - Federal Office of Metrology and Surveying, Arltgasse 35, 1160 Vienna, Austria.

^bUniversity of Natural Resources and Life Sciences, Vienna, Low-Level Counting Laboratory Arsenal, Faradaygasse 3, Arsenal 214, 1030 Vienna, Austria.

^cUniversity of Vienna, Nuclear Physics, Währinger Straße 17, 1090 Vienna, Austria.

^dAustrian Agency for Health and Food Safety, National Radon Centre of Austria, Wieningerstrasse 8, A-4020 Linz, Austria.

^eVienna University of Technology, Karlsplatz 13, 1040 Vienna, Austria.

Abstract. The radon potential of a certain area represents the expected ²²²Rn indoor activity concentration of the air in a ground floor living room. To improve the existing radon potential map of Austria a geologically versatile region was chosen for investigation. At 100 sites the ²²²Rn soil gas activity concentration, soil gas permeability and local gamma dose rate were measured and soil samples, for gamma spectrometric analysis of ²²⁶Ra and ²³⁸U, were taken. In the same area ²²²Rn indoor activity concentration measurements were conducted, too. The different measurement results are compared and their correlations are investigated. Thereby, the main focus is on the comparison between the radon activity concentration in soil and indoors. The investigation of the correlation between these two parameters is important for the prediction of an area's radon potential. The aim of the study is the improvement of the prediction of the radon potential by soil gas measurements and consequently the radon potential map. As in the new EU BSS the identification of areas, where the radon concentration above the national reference level in a significant number of buildings is expected, is demanded, it is important to further develop the methods for the prediction to guarantee a meaningful implementation in the radiation protection of the general public.

KEYWORDS: radon map; geogenic radon potential.

1 INTRODUCTION

Radon is a radioactive noble gas which originates everywhere in the ground as it occurs in the natural decay chains. From the ground it can diffuse into dwellings followed by the possibility of causing high activity concentration. After inhalation radon and its progeny can directly harm the lung, which increases the lung cancer risk. Radon is identified as greatest cause for lung cancer after smoking by the WHO. (1) For that reason, action plans against radon were established by different countries and are demanded by the EU Safety Basic Standards. (2) In this directive 300 Bq/m³ is given as the maximum reference level for the yearly mean radon activity concentration in indoor air in private accommodations and work places was introduced. Furthermore, areas shall be identified where this threshold is exceeded by a significant number of dwellings, which is implemented by most countries in establishing radon maps. The radon potential represents the expected radon activity concentration, but the definition, calculation and measurement procedure is not consistently assessed.

There are different methods to derive the radon potential from: direct measurements of indoor radon concentrations, geological aspects or multi-factor scoring systems are used. For example a method is based on indoor measurements with 20 data points within a 10 x 10 km grid (Canada) or on 5 measurements within a 5 x 5 km (UK) to predict an indoor value. (3) Another approach is to set up a classification by a matrix, using soil gas and permeability measurements. (4)

*Corresponding author: franz.kabrt@mailz.at

In Austria within the ÖNRAP, the Austrian national radon project, a radon potential map was established on the basis of indoor measurements. (5) New data is implemented in this map. 2011 a further project followed in which three municipalities in Upper Austria were investigated in more detail including soil gas measurement. Following that project, a new one was executed to carry out soil gas and indoor measurements in a Styrian region. The aim was focused on the geological characteristic and correlation. Now the measurement values of the soil gas measurement are analysed with use of the indoor measurements. For establishing a meaningful radon potential map, the correlation between soil gas measurements and indoor values are of utmost importance.

2 MATERIAL AND METHOD

2.1 Soil gas radon measurements

The described measurements were carried out at 100 sites. One series was set in autumn 2012 with 40 sites and the other series in spring 2013 with 60 sites. Only the measurements which provided the results used in the analysis of this paper are presented.

At each site three probes with a length of 1.6 m and a diameter of 12 mm were hammered up to 1.4 m into the ground. At their ends pointy tips were attached and were lowered by rod 5 cm further into the ground. Afterwards an adapter was put on the end above the ground to seal the probe from the ambient air, but to enable an extraction of the gas from the rod by syringes. Soil gas was extracted by 200 ml syringes. The first volume was discarded as mixed with outdoor air. Then 100 ml volumes of gas were extracted from each of the three probes and were injected each in an AlphaGUARD (Saphymo GmbH) measuring device with attached plug on the backside (usually, done in diffusion mode, but the injected air should be prevented from escaping). The AlphaGUARDS were operated in 10 min flow mode. The radon activity concentration displayed the moment of the injection was documented as blank value of the measurements, which was subtracted from the resulting measuring value. The first actualization of the displayed value was not considered as result, as the injected soil gas was not inside the device over the whole measuring cycle. The mean of the second and third value of the radon activity concentration was taken as measuring result, from which the first value was subtracted. A possible influence of thoron was eliminated, as the soil gas has been at least ten minutes inside the AlphaGUARD when the second value was displayed. Furthermore, the resulting measurement values were multiplied with a calibration factor, because the injected 100 ml soil gas did not fill the 620 ml of measuring chamber of the AlphaGUARD completely. This factor was determined in a former project by Gruber. (6) When it was not possible to hammer the probes the whole 1.4 m into the ground, the result of that probe was multiplied with a correction factor. To calculate that factor the depth distribution of the radon activity concentration in the ground was used. For analysing the data beside the mean value of the radon activity concentration at a site the maximum of the three measured values is taken into account too.

The soil permeability was estimated for each probe by measuring the flow rate and the pressure while pumping gas out of the probe. Following Damkjaer and Korsbech beside these measured values the geometry factor (considering the 5 cm hole in the grounded end of the probe) and the gas' viscosity (approximation) was used. (7)

Additionally, the ambient dose equivalent rate was measured 1 m above the ground at each site. Therefore, a 6150 AD 6/E with a connected scintillator 6150AD-b by Automess was used, measuring the mean value of five minutes.

Soil samples were taken from up to 1 m depth at each site. Afterwards these samples were used to determine the ^{226}Ra and ^{238}U mass activity concentration by gamma ray spectroscopy in the Low-Level Counting Laboratory Arsenal.

2.2 Indoor radon measurements

Indoor radon measurements were organized by the Austrian Agency for Health and Food Safety (AGES) in the investigated region. Thereby SSNTD detectors were used, which were set up over a period of six months in 963 dwellings. The detectors, two per dwelling, were mainly placed in the ground floor; the detailed distribution is listed in Table 1. Furthermore, construction characteristics of the dwellings were documented. Only the categories which are supposed to have a high impact on the indoor radon activity concentration were taken into account for the analysis.

Table 1: Number of measurements on different floor levels.

Floor	Cellar	Ground floor	First floor	Second floor
Number of measurements	30	1208	646	38

2.3 Analysis methods

For the analysis of the soil gas measurements together with the indoor measurements, the values of the soil gas measurements were interpolated at the points of the indoor measurements. The inverse distance weighting method (shown in equation 1) was used, which includes a power parameter for weighing. A higher power parameter lays the weight more on nearer situated points, whereas a low parameter includes the points, which are further away, more into the interpolation.

$$u(x) = \frac{\sum_{i=1}^N u_i / d(x, x_i)^p}{\sum_{i=1}^N 1 / d(x, x_i)^p} \quad (1)$$

$u(x)$... interpolated value at x

u_i ... measurement value at x_i

$d(x, x_i)$... Distance between x and x_i

p ... power parameter for distance weighting

The Neznal potential (RP_N), which calculates a potential value using the radon activity concentration in soil gas (c) and the permeability (k) is shown in equation 2. (8)

$$RP_N = \frac{c_a^{-1}}{-\log_{10}(k) - 10} \quad (2)$$

For analysing the data own python routines were written. Functions of the numpy, scipy, math and matplotlib libraries were accessed therefore.

For determining the correlation between parameters the pearson and spearman correlation were used. The correlation is 1 at a high correlation, -1 at a high negative correlation and zero if there is no correlation. The pearson correlation (numpy.corrcoef) analyses a linear relationship between two parameters. However the spearman correlation (scipy.stats.spearmanr) determines a relationship, where the parameters do not change together at a constant rate.

3 RESULTS

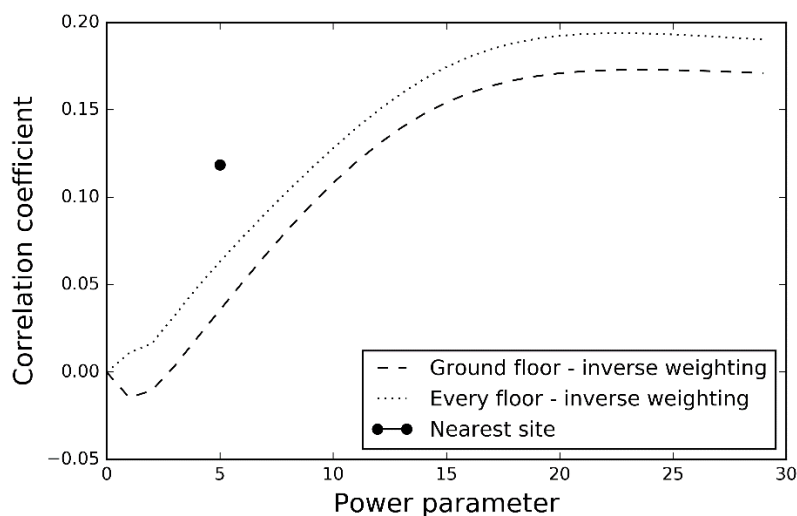
3.1 Excerpt of former analysis of the soil gas measurements

The radon activity concentration in the soil gas showed a logarithmic distribution. In the dolomite, lime category the lowest values were observed from 0.9 up to 79.5 kBq/m³ and in the gneiss the highest values within a range from 23 up to 953 kBq/m³. The distributions of the remaining geologies overlapped in large parts. Among others the results showed no correlation between the radon activity concentration and the permeability, a very low correlation between radon and the radium massic activity, and a medium correlation between radon and the ambient equivalent dose rate.

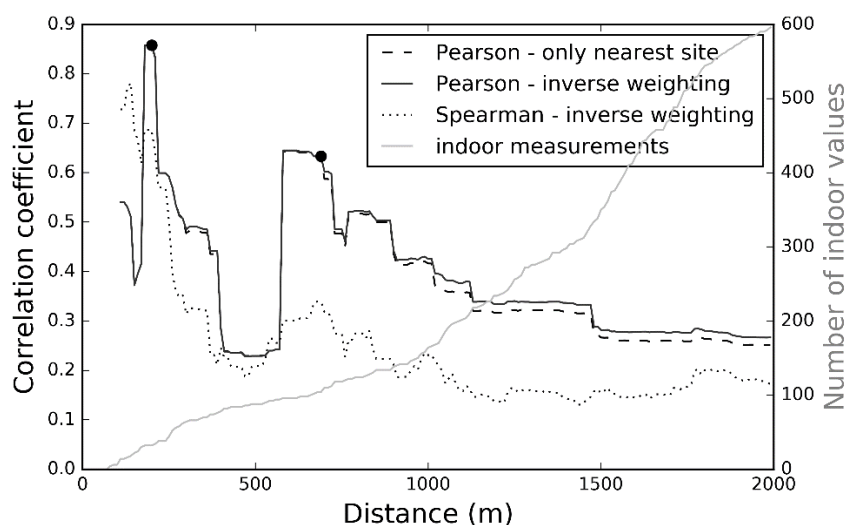
3.2 Proper power parameter and dependence from nearest site

First of all, a proper power parameter for interpolating the measured soil gas values using the inverse distance weighting method has to be obtained. Therefore, the Pearson coefficient between the indoor radon activity concentration and the interpolated radon activity concentration of the soil gas was calculated as function of the power parameter. The resulting curve is shown in Figure 1. The correlation was observed for every measurement and only taking into account the indoor measurements on the ground floor. The correlation is supposed to be higher only analysing the measurements at the ground floor, as the impact of the radon in soil gas is higher than on the floor levels. However, the resulting values show, that the correlation including all values is higher than only including the ground floor values. The correlation for the case that just the nearest site measurement is taken for comparison with a certain indoor value is shown as black dot in the diagram, the position of the dot on the x-scale has no meaning, as there is no power parameter in that case.

Figure 1: Pearson correlation depending on the power parameter and nearest site



The correlation has its maximum at a power parameter of 23, which means that weighting lays more on the nearer points. Due to the fact, that there can be big distances between sites of soil for measurements and dwellings with indoor measurements, the impact of the distance is analysed. Additionally to the interpolated values of the soil gas by inverse distance weighting method the values were interpolated by just using the nearest measuring point. The resulting dependencies are shown in Figure 2. It can be seen that there is nearly no difference between the inverse weighing and only regarding the nearest site, as the continuous line and the dashed line overlap for the most part.

Figure 2: The correlation depending on the distance to the nearest site.**Table 2:** Detailed values for the points from Figure 2.

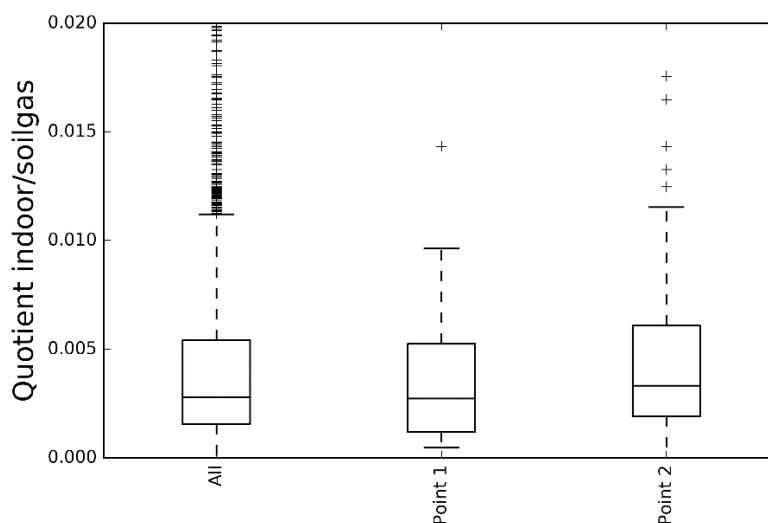
	Dwellings		Pearson correlation with indoor values					Neznal
	Number	Max. distance to nearest site	Radon	Max.	Dose rate	Permeability	Ra ²²⁶	
First point	32	200 m	0.86	0.86	0.24	-0.57	0.32	0.66
Second point	104	690 m	0.63	0.65	0.02	-0.27	0.1	0.49
All	1926	4913 m	0.19	0.20	0.08	-0.09	0.02	0.09

The Pearson correlation shows much higher values than the Spearman correlation. After a first maximum with nearly 0.9 as correlation coefficient, it decreases to 0.2. The second maximum lies around 0.6 and sinks afterwards without these high fluctuations from the first part. In Table 2 the values for the correlations at the marked points in the diagram and for the whole number of indoor values are shown. Compared to the correlation of radon in soil gas, the other parameters show a significant lower correlation with the indoor radon.

The primary aim of the project was to carry out the measurements in different geologic areas and secondary to comply with the distribution of the population. So the distances between the sites and dwellings are not optimal for that approach of analysis, especially as more dwellings nearer to the sites would lead to more significant results.

3.3 Quotients between indoor and soil gas radon activity concentration

Now the quotient between the radon activity concentration indoor and in the soil gas is analysed. Therefore the indoor value is divided by the interpolated soil gas value. Dwellings with a high sealing from soil gas radon have a quotient nearly zero, whereas a comparatively high quotient stands for an easy transport from radon into the building. In Figure 3 the boxplots of these quotients are shown for all measurements, and again only for the dwellings at point one and two from Figure 2.

Figure 3: Boxplots of the quotient of indoor / soil gas values at the points from Figure 2.

It can be seen that the distributions are nearly the same with the median around 0.003. The boxplot with all distances and with the values of lower correlation has a high amount of outliers. It can be suggested that these outliers cause the low correlation and that a reasonable quotient goes up to 0.01. This can be an important clue to estimate the radon potential from soil gas measurements. For example, if these quotient values are used to calculate a possible indoor radon activity concentration from soil gas, for exceeding the limit of 300 Bq/m^3 a soil gas activity concentration of $100\,000 \text{ Bq/m}^3$ would be sufficient. Using the quotient of the lowest whisker (of point 1) as worst case, even $30\,000 \text{ Bq/m}^3$ would be enough. 76 % of the soil gas values measured were over $30\,000 \text{ Bq/m}^3$ and 21 % over $100\,000 \text{ Bq/m}^3$. Beside geological characteristics, the quotient is supposed to depend mainly on the construction characteristics and living habits. As these constructional types and building material are as well as the weather influenced behaviour of ventilation representative for a region, the quotient is supposed to vary for different areas.

3.4 Observation of construction characteristics

To investigate the impact of the construction characteristics, the ones with the highest supposed impact were chosen. It was tried to assign different factors for different characteristics and compare the thereby occurring correlation coefficients. These factors should be identified by iteration. So looking at one category, for every factor a quotient between 0.1 and 1 in steps of 0.1 was tried and used for calculating the correlation. Finally, the factors, where the highest correlation occurred, were saved and are listed in Table 3. Due to computing effort the factors were investigated only within one category at once. But the factors were applied to all interpolated radon activity concentrations in soil gas and again analysed for correlation with the indoor values, which lead to a coefficient of 0.31 and for the dwellings within point two in Figure 2 to a coefficient of 0.74. These are enhancements of 63 % and 18 % respectively. For a more meaningful analysis all factors should be computed during one calculation, which was not possible because of the high processing effort.

Table 3: Limiting factors for construction characteristics leading to a higher correlation.

Cellar	Entirely		Partial		No				Corr.
	Number	Factor	Number	Factor	Number	Factor			
	1290	0.3	392	1	220	0.7			0.32
Fundament	Stripes		Board		Partial board		None		Corr.
	Number	Factor	Number	Factor	Number	Factor	Number	Factor	
	632	1	806	0.5	154	0.9	94	1	0.26
Composition	Screed		Sand		Brick		Concrete		Corr.
	Number	Factor	Number	Factor	Number	Factor	Number	Factor	
	1420	0.5	222	0.9	380	1	104	0.7	0.23
Walls	Building stone		Concrete		Formwork		Brick		Corr.
	Number	Factor	Number	Factor	Number	Factor	Number	Factor	
	286	1	938	0.7	207	0.5	206	0.7	0.25

The application of parameters is able to slightly increase the correlation values. As the factors lower the resulting radon activity concentration, they represent a difficulty for radon to reach indoor rooms. So it is sensible that dwellings with a cellar, have a limiting factor, as it is more difficult for radon to get into the ground floor, where most of the measurements were carried out. But following the calculation, also dwellings without a cellar have a slightly limiting factor. This could be caused by a better fundament of the house if there is no cellar underneath. Generally looking at these results, the amount of dwellings with a certain characteristic have to be taken into account to. As there are more numbers the change in the factor has a higher weight than another factor, which could lead to a results that rather goes back to statistical causes than to constructional ones.

4 DISCUSSION

The results show the importance to combine the results of soil gas and indoor measurements. Indoor measurements imply high effort, a long duration (3 months minimum) and the need of the collaboration of the inhabitants. Therefore, soil gas measurements represent a good alternative, as they could be carried out more flexible and deliver results more quickly. However, for a meaningful evaluation of the results a reliable correlation with the indoor activity concentration is of utmost importance. The observed dependency of the correlation between indoor and soil gas activity concentration is a factor which raises the effort for these measurements. In turn the measurement of other parameters can be skipped, as they show such low correlation coefficients, which lowers the effort. Also the need of three measurements at one site could be discussed. Only a slight difference between the maximum and mean value at the site is observable calculating the correlation with indoor radon. Maybe more measurements over an area are more important than a more detailed assessment at one site, which could be an issue for further investigation. The consideration of construction characteristics is another important factor. By assigning a certain factor to a characteristic the correlation coefficients were increased. Thereby the importance of correlating the indoor values with the soil gas values is reflected. Without that knowledge the soil gas measurements cannot be evaluated sensibly; just because a soil gas value is lower compared to others, does not mean that it cannot lead to high indoor activity concentrations, which is shown by the calculation of the quotient distribution between the radon activity concentration in soil gas and indoor.

5 OUTLOOK

The shown correlation between indoor and soil gas radon activity concentration has to be investigated in other areas, too. Constructional characteristics and living styles influence the indoor concentration in a high degree, but differ for different regions. The consequential quotient between indoor and soil gas radon activity concentration and the density of the measuring sites are important aspects regarding the evaluation of the radon potential by soil gas measurements, which require further investigations.

6 FUNDING

The author's participation at the IRPA14 was financially supported by the *Austrian Association for Radiation Protection*. The project was funded by the *Austrian Federal Ministry of Agriculture, Forestry, Environment and Water Management* project number BMLFUW-UW 1.1.8/0208-V/7/2012.

7 REFERENCES

- [1] World Health Organization. WHO Handbook on Indoor Radon - A Public Health Perspective. World Health Organization, Geneva, Switzerland, ISBN-978-9-241-54767-3, (2009).
- [2] Council Directive 2013/59/Euratom of 5 December 2013 laying down basic safety standards for protection against the dangers arising from exposure to ionising radiation, Official Journal L 57, 1-73.
- [3] Chen, J., 2016. A preliminary design of a radon potential map for Canada: a multi-tier approach. *Environmental Earth Sciences* 2016 59:775-782 Doi 10.1007/s12665-009-0073-x.
- [4] Kemski, J., Klingel, R., Siehl, A. Das geogene Radon-Potential. In: Siehl, A. (Hrsg.) *Umweltradioaktivität*. S. 179-222. Reihe Geologie und Ökologie im Kontext, Ernst & Sohn, Berlin, (in German), (1996).
- [5] Friedmann, H., 2005. Final results of the Austrian Radon Project. *Health Phys.* 89(4), 339-348.
- [6] Gruber V., 2004. *Untersuchung und Evaluierung der geogenen Radon-Aktivitätskonzentration in eiszeitlich-glazialen Ablagerungen in Oberösterreich*, Diplomarbeit ausgeführt am Atominstitut der Österreichischen Universitäten.
- [7] Damkjaer, A., Korsbech, U., 1992. A Small-Diameter Probe for in Situ Measurements of Gas Permeability of Soils, *Rad. Prot. Dos.*, Vol. 45, p. 85 89.
- [8] Neznal, M., Neznal, M., Matolin, M., Barnet, I., Miksova, J., 2004. The new method for assessing the radon risk of building sites. *Czech Geol. Survey Special Papers*, 16, Czech Geol. Survey, Prague, p.7-13, <https://www.radon-vos.cz/pdf/metodika.pdf>

Radiation Measurement Systems and Experiences in Japan after the Fukushima Accident

Frazier L. Bronson

Canberra Industries, 800 Research Parkway, Meriden CT USA.

Abstract. In the approximately 5 years since the March 2011 earthquake and subsequent Tsunami damaged the three Dai-Ichi nuclear power plants, the AREVA and Canberra team have deployed a variety of different radiation measurement machines in Japan. These measurement projects or instruments include: Dose-rate mapping of the close-in areas on the damaged reactor site; Spectroscopic nuclide-specific on-line measurements of the first water processing unit on the site; General purpose food measurement units, both high precision HPGe systems and low cost NaI systems; In-vivo measurement systems, both fixed and mobile whole body counting units, that were used on at least 500,000 people; In-vivo measurements with special high-sensitivity system for babies and children; Automatic systems for high throughput assay of bags of rice from Fukushima Prefecture; High sensitivity automatic system to assay boxes of special semi-dry persimmons; System to assay soil on a conveyor belt and sort the output according to level of radioactivity; System to assay a truck loaded with 1 cubic meter sacks of soil and vegetation and report the activity of each sack separately; On-line water measurement system for SrY90 at levels suitable for release to the environment; and a Mobile system to prove that rolls of grass to feed animals meet the regulatory requirements. This document briefly describes the purpose of each measurement project, the instruments and assay method that used, and discusses some of the operational experiences from each of these projects.

KEYWORDS: *Fukushima; Canberra; food; in-vivo; HPGe; NaI; rice; persimmons; gamma spectroscopy; radiation measurements.*

1 INTRODUCTION

The March 2011 earthquake and tsunami off the coast of Japan caused about 16,000 people to lose their lives, and about 750,000 buildings to be lost or damaged. The tsunami also caused 3 of the 6 Nuclear Power Plants [NPP] at the TEPCO Daiichi site to fail, and release large quantities of radioactivity. The combination of these two events resulted in about 400,000 people without homes, including about 100,000 due to the forced evacuation of the population around the failed Daiichi NPPs.

Radiation measurements were very important in the early phases of the accident to predict what might happen, and to evaluate the mitigation measurements. AREVA had a large taskforce assembled in Tokyo to provide support to the early phases of the accident recovery. Canberra was a part of that team. Radiation measurements continue to be important today, more than 5 years after the accident. Measurements are currently being taken to evaluate the status of the off-site cleanup efforts, to demonstrate the safety of the food products from the Fukushima region, to demonstrate the low levels of dose to the population from eating that food, and to measure the very low levels of radioactivity being released to the environment from current operations.

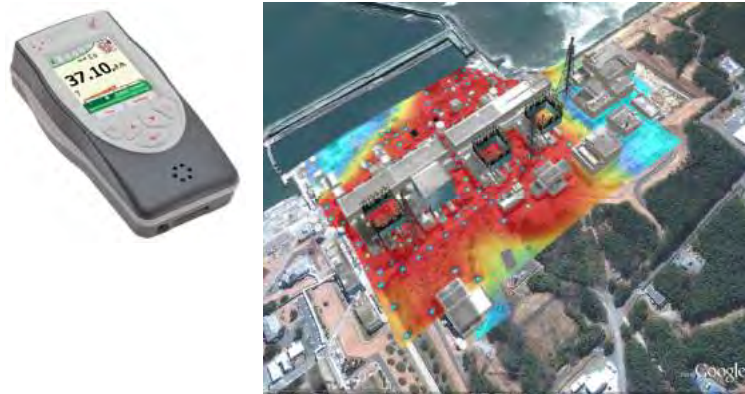
2 EXAMPLES OF RADIATION MEASUREMENT PROJECTS

Most of the examples here are from items provided by Canberra, the AREVA Nuclear Measurements Business Unit.

2.1 Radiation dose-rate mapping

One of the earliest maps of on-site radiation dose rates was gathered as an incidental effort from the AREVA workers planning the installation of the water processing unit. The on-site workers had the Canberra Colibri instrument with them, which records the dose-rate and the GPS coordinates every few seconds. After a few days the readings were consolidated and incorporated into a dose-rate map [Fig.1] of the site. This map was used to plan the movement of the AREVA personnel to minimize their total dose during the planning and installation of the water processing system.

Figure 1: Radiation intensity map and the Colibri instrument.



2.2 Water processing

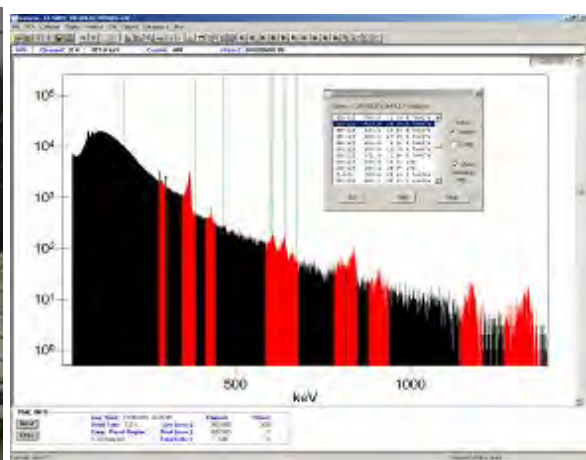
Large quantities of water were used to cool the reactor to prevent further deterioration. This water quickly threatened to fill up all available holding facilities. AREVA was part of the team that constructed the first water processing unit on site to meet these extreme emergency conditions [Fig. 2]. The unit was designed, transported, assembled, and operational in 75 days – a tremendous achievement under these very difficult conditions.

Canberra supplied the radiation sensors that were used to provide remote indication to the operators about the status and the efficiency of the unit. Five heavily shielded and collimated CZT detectors were used for on-line nuclide identification and quantification [Fig. 3] and 6 wide dynamic range dual GM probes used for dose-rate measurements. The devices were networked to off-site monitoring and control locations and to the Canberra offices in France.

Figure 2: AREVA water processing unit.



Figure 3: CZT detector spectrum.



2.3 Food Monitoring

Due to the widespread release of radioactivity into the air, the ground in most of Northern Japan was contaminated to varying degrees. Much of that land is used for growing food, therefore the radioactivity in that food must be measured, and if above limits, that food must be prevented from entering the distribution channels. Based upon the previous Chernobyl experience, Canberra immediately increased the production capacity of our Germanium detectors, which are commonly used for this application. [Fig. 4].

Figure 4: Ge food assay system.



We also designed a completely new lower-cost NaI detector product for this application. About 300 of the Germanium units and about 700 of the low-cost NaI units [Fig. 5] were sold in Japan. Both types are capable of <10 Bq/kg MDAs in a few minutes counting time. These were very effective at showing that most of the food in distribution had quite low levels of radioactivity.

Figure 5: Transportable NaI food assay system.



2.4 Radioactivity measurements on people

The accident put the Whole Body Counters [WBC] at the site out of commission. The first WBC measurements were ~ 2 weeks after the accident by JAEA using a mobile FastScan WBC that they purchased from Canberra many years ago. They used these measurements to prioritize the order of workers that were sent to the JAEA-Tokai facility which has multiple Canberra Germanium detectors in a large shielded room. The US military moved 3 Canberra WBCs to Japan for use by the large

number of US military personnel supporting the accident and their dependents. The first one, a Canberra Accuscan-II scanning Ge system, arrived and was operational April 15, 2011 [1]. The next two FastScans [2] arrived a month later. Over the next several months ~8000 US DoD personnel and dependents were measured. Limited population measurements using locally available chair-type WBCs was started but these had difficulties due to the lack of shielding and the elevated background [3]. Large scale low level [MDA ~ 3Bq/kg Cs] population measurements started about 6 months after the accident when the first Canberra FastScan arrived. Eventually there were about 60 FastScan WBC units in use for population counting, including 20 new mobile units. [Fig. 6] This large scale measurement campaign was very important to assure the public that the food measurement program was effective and that there was very little internal contamination in the people. A simple 2-minute measurement with the results presented immediately to the person can greatly reduce their anxiety about radioactivity they might have eaten or breathed.

Figure 6: Various WBC systems: left is the JAEA-Tokai facility; middle is the Canberra FastScan; right is one of the trucks containing a FastScan.



2.5 Radioactivity measurements on babies

Measurements on small children and babies are much more difficult than for adults. Their small size moves them outside of the sensitive region of the FastScan and most other WBCs that were designed for adults. It was previously shown following the Chernobyl accident that when children stood on a small stool, the adult calibrations were adequate; that technique was also used here. When adults are measured in the FastScan, the naturally occurring K40 is reported, and if it is at the expected value this gives confidence in the ability to correctly report the Cs-134/137 results. But the low mass of children also means low levels of K-40, which was too low to be measured. Their low mass also means lower levels of Cs-134/137 for a similar dose in adults. And finally, small children are not very cooperative about standing still for the required amount of time in the Fastscan.

Consequently a new design was created specifically for this population group, with the help of Tokyo University [4]. The BabyScan [Figs. 7 & 8] has more shielding and more detectors than the FastScan, for better detection limits despite the lower mass (2-3 Bq/kg) with a 4 minute counting time. And to keep the mothers of the babies happy, a lot of care was taken by the Tokyo University design team to make the unit look “soft and warm”. Three of these units are installed and operating now with excellent results – no radioactivity from the accident has been detected in any of the babies, and they all have “normal” K-40.

Figure 7: BabyScan with large child.**Figure 8:** BabyScan and small child.

2.6 Rice Bag Counter

The Fukushima Prefecture and surrounding prefectures grow very high quality rice. This is an important part of this largely rural economy. Extensive statistical testing of small samples of rice in the normal food counters as shown in section 2.3, showed statistically that the rice met the stringent Japanese 100 Bq/kg total Cs requirement, and therefore was OK to eat. But the combination of a very worried public, sensational news reports, and plenty of adequate rice from other parts of Japan resulted in a dramatic reduction in consumer purchases of Fukushima rice. To counter this, the Prefecture government declared that statistical sampling isn't adequate, and that 100% of the rice from the prefecture would be assayed. Canberra 30 units, and 4 other Japanese companies supplied the rest of the ~200 automatic rice bag counters. Our design is shown here [Fig. 9] and can measure each bag in 10 seconds. The MDA is ~10 Bq/kg in a background of 1 μ Sv/hr. The results from each bag of rice are stored in a cloud database. A QR sticker on each bag of rice allows the consumer with a smart phone to view the assay results on that bag of rice.

Figure 9: Automatic Rice Bag Counter.

2.7 Persimmon or “Gaki” Counter

An important specialty crop that is grown in the Fukushima Prefecture is semi-dried persimmons [Fig. 10]. These are prized by consumers and especially important as a ceremonial gift to the host when visiting.

These food items are also required to comply with the 100 Bq/kg requirement. The problem is that gaki are normally sold in small trays of 1-5 gaki each, with small mass and therefore a very few Bq. The Canberra Persimmon counter [Fig. 11] has 32 separate tightly packed NaI detectors and MCAs, 16 above and 16 below. When a box containing 8 trays is measured, the software automatically corrects for cross-talk from the adjacent trays and reports the radioactivity for each individual tray. The typical assay time is only 1 minute for the entire box. Fourteen such units have been installed and are operating.

Figure 10: A single Gaki.



Figure 11: The Persimmon Counter.



2.8 Conveyor Sorting of Contaminated Soil

The process for remediation of the contaminated land involves surveying the ground surface to see if it is OK or not. If above the dose-rate limits, the top 5-10 cm is removed and placed in 1 cubic meter bags and taken to a temporary storage facility, awaiting the construction of the disposal facility. But much of this soil removed is actually below the 8000 Bq/kg residual soil contamination limits and doesn't need to be treated as radiological contamination. The AREVA Back-End group has designed a conveyor soil sorting unit [Fig. 12] and is currently demonstrating it in Japan. This device is easily transported close to the excavation area, and will assay the excavated soil and separate out the clean material to avoid the expense of treating it as radioactive waste. This unit can process up to 100 tons per hour.

Figure 12: The AREVA Soil Sorting unit in operation.



2.9 Contaminated soil measurement in 1 cubic meter bags

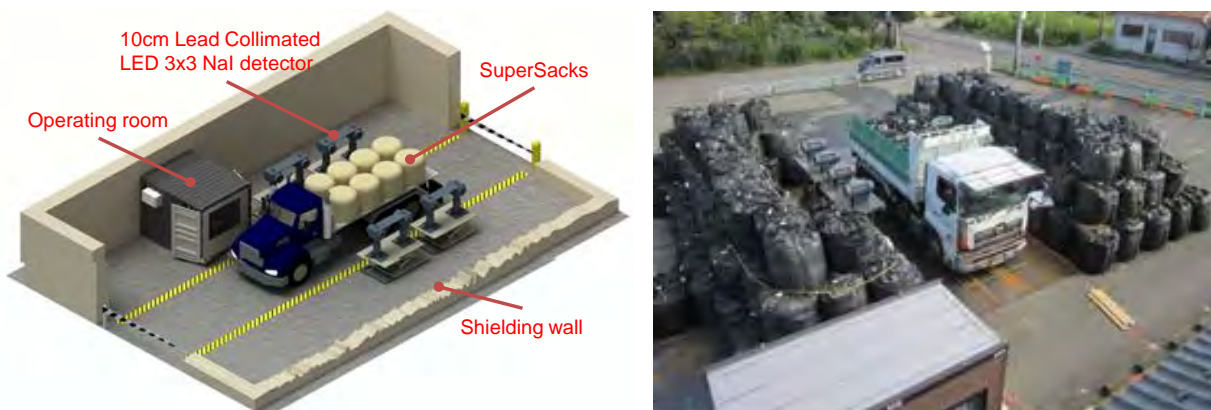
There are now 10s of millions of 1 cubic meter bags around the countryside waiting for the opening of the 4 Interim Storage Facilities. [Fig. 13] Canberra has designed a system called TruckScan that can quickly measure these bags while on the truck. This measurement can be done at the truck loading site or at the storage facility. This allows separation of the bags categories appropriate for each type of disposal option at the facility. A prototype of the unit was constructed and tested in 2014. A full size unit with a pre-production version of the software was built and tested in 2015. A performance report was submitted to the Japan MOE documenting the accuracy of the unit, and the significant cost and dose savings as compared to alternate technologies [5].

Figure 13: 1m³ bags of soil in the field, and temporary storage.



The TruckScan [Fig. 14] has 8 shielded and collimated NaI detectors, 4 on each side of the truck. The automatic software accounts for the cross-talk from the multiple bags in the field of view of each detector, and properly reports the activity of each individual bag. The typical measurement time is 10-20 seconds which then allows a truck to be counted every 45 seconds.

Figure. 14: Left: Graphic of TruckScan; Right: the pre-production TruckScan at the demonstration.



The sorting levels for various disposal options are 3000, 8000, and 100,000 Bq/kg total Cesium. The removal of all bags that are less than 8000 Bq/kg eliminates the un-necessary expense of further processing. Those bags above this level will be undergo some form of volume reduction, perhaps in the soil sorter shown above, or in an incinerator for combustible material like vegetation.

2.10 Sr/Y90 measurements of the output from water cleanup systems

The water processing unit in section 2.2 is now in standby, having been replaced by several other larger and more efficient units. There are still a very large number of tanks of water, waiting for final cleanup. Canberra has supplied 5 on-line monitors to determine if the output from these systems meets the criteria for Sr90. Sr90 is an important nuclide to measure since it has a long physical half-life [30y] and since it can become incorporated in the bones of animals and people and stay there a long time. It is also a very difficult nuclide to measure, as it is only a beta emitter. The device [Fig. 15] uses two large area beta detectors from our Whole Body Contamination monitors that are used inside NPPs to show that workers clothing is not contaminated. These two detectors are inside a thick lead shield and surround a thin-walled water chamber. They measure the high energy betas from Y90 to infer an equilibrium quantity of Sr90. Two of these units operate in parallel measuring the output of the water processing system, and will stop it if the radioactivity is above the release limits. The MDA is 8 Bq/kg Y-90 in a 60min count time; alternate mechanically interchangeable detectors are available with an MDA of 3 Bq/kg.

Figure 15: Y90 Water Measurement System.



2.11 Feed for cattle

Many cows are raised in the Fukushima region for both milk, and the very special [and expensive] Japanese beef. Since feeding them hay raised in the region is prohibited because of unknown levels of radioactivity, the hay must be imported from other regions. A mobile system [Fig. 16] has been designed, tested, and is now starting service to measure the rolls of hay at the farm where they are used.

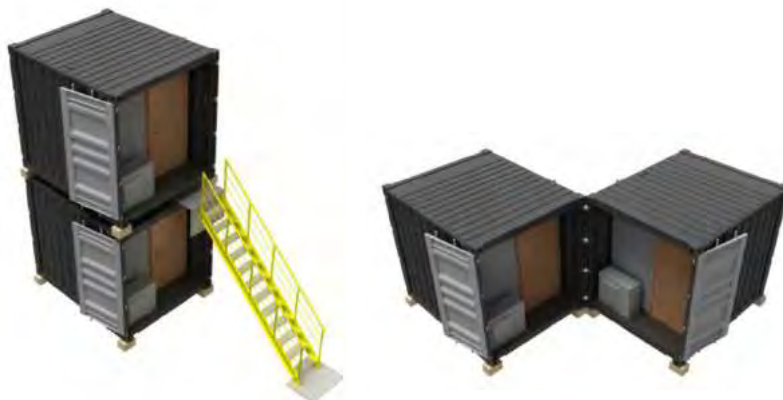
Figure 16: Mobile Feed Roll counter. The white bags are feed rolls.



2.12 Other systems

There many other systems that are in the design and proposal phase. One project would supply transportable units to monitor radioactivity in the sea water adjacent to the Daiichi site, and in canals which channel water from the site into the sea. These modules [Fig. 17] would be constructed at the Canberra factory and transported to the site with the instrumentation fully installed. Inside the modules would be a Sr/Y-90 unit like above, a very sensitive Ge detector for continuous gamma spectroscopy for Cs134 and Cs137 [MDA 0.05 Bq/kg with 1 hour count time], and a monitor for continuous measurements of Tritium.

Figure 17: Transportable modules housing various radiation detection systems.



Discussions have also been held about systems to measure radioactivity in logs from the forest used for timber, small logs used to grow mushrooms, live or freshly caught fish from the sea, soil at the bottom of lakes and canals, mushrooms, live cows, and many other items.

3 CONCLUSION

The Fukushima accident has created the need for many different and innovative instruments to measure radioactivity. Canberra is proud to have been a part of the very broad international response to support the needs of the country and its people.

4 REFERENCES

- [1] Cassata, J, et al., 2013. Radiation Internal Monitoring by In Vivo Scanning in Operation Tomodachi, DTRA-TR-12-004.
- [2] Bronson, F.L., (1984). FastScan - A Computerized, Anthropometrically Designed, High Throughput, Whole Body Counter for the Nuclear Industry, Canberra Industries from www.canberra.com/literature/invivo_counting/tech_papers/fastscan.pdf on May 2, 2016.
- [3] Hayano, R. S., 2014. Whole-body counter survey results 4 months after the Fukushima Dai-ichi NPP accident in Minamisoma City, Fukushima. *J. Radiol. Prot.* 34 787–799 <http://dx.doi:10.1088/0952-4746/34/4/787>.
- [4] Bronson, F. L. et al., (2014). Design, Development, and Initial Operation of BabyScan: An In-vivo Counter for Children around Fukushima. *Nuclear Instruments & Methods in Physics Research (A)*, <http://dx.doi.org/10.1016/j.nima.2014.09.028>.
- [5] Suzuki, A, et al., 2016. Validation Testing of Canberra-Obayashi Mobile type TruckScan Pre-production Unit, Proceedings of the International Radiation Protection Association 2016, Cape Town, South Africa, May 8-13, 2016.

Environmental radiation monitoring in the gold mining region East Cameroon

Dallou G. B.^a, Ngoa Engola L.^a, Ndjana Nkoulou II, J. Emmanuel^{b*}, Saïdou^{b,c}, Kwato Njock M. G.^a

^aCentre for Atomic Molecular Physics and Quantum Optics, University of Douala, P.O. Box 8580 Douala, Cameroon.

^bNuclear Technology Section, Institute of Geological and Mining Research, P.O. Box 4110 Yaounde, Cameroon.

^cFaculty of Science, University of Yaounde I, P.O. Box 812 Yaounde, Cameroon.

Abstract. The aim of the study is to assess radiological exposure of the public and level of heavy metals pollution in the gold mining areas of Eastern Cameroon. For this purpose sodium iodide (NaI) detector and Quant'X EDXRF spectrometer were used respectively to determine activity concentrations of natural radionuclides and heavy metals concentrations in soil samples collected from the mining areas. The activities concentration mean values of ²²⁶Ra, ²³²Th, and ⁴⁰K were 39.4 Bq.kg⁻¹, 28.7 Bq.kg⁻¹ and 257.9 Bq.kg⁻¹ to Betaré-Oya. While in Batouri, ²²⁶Ra, ²³²Th, and ⁴⁰K has activity mean value 46.3 Bq.kg⁻¹, 31.7 Bq.kg⁻¹ and 75.5 Bq.kg⁻¹ respectively. ²²⁶Ra is identified as major natural radionuclide with the activity concentrations slightly higher than the world average value given by UNSCEAR. The averaged External annual effective dose were 0.356 mSv/yr for Betaré-Oya and 0.31 mSv/yr for Batouri. Beside radiological exposure, study of heavy metals level shows predominance of iron (33528.3 ± 188.5ppm), for Betaré-Oya and (28677.9 ± 188.5ppm) for Batouri. Due to enrichment factor, Pb and As appear as the major elements of anthropogenic loading. Finally there is an exposure to potential threat for humans and environmental media such as food chain, dust and water. Some recommendations are drawn to strengthen the environmental protection of mining areas.

KEYWORDS: *gold mine; soil; heavy metals; enrichment factor; natural radioactivity; external hazard index.*

1 INTRODUCTION

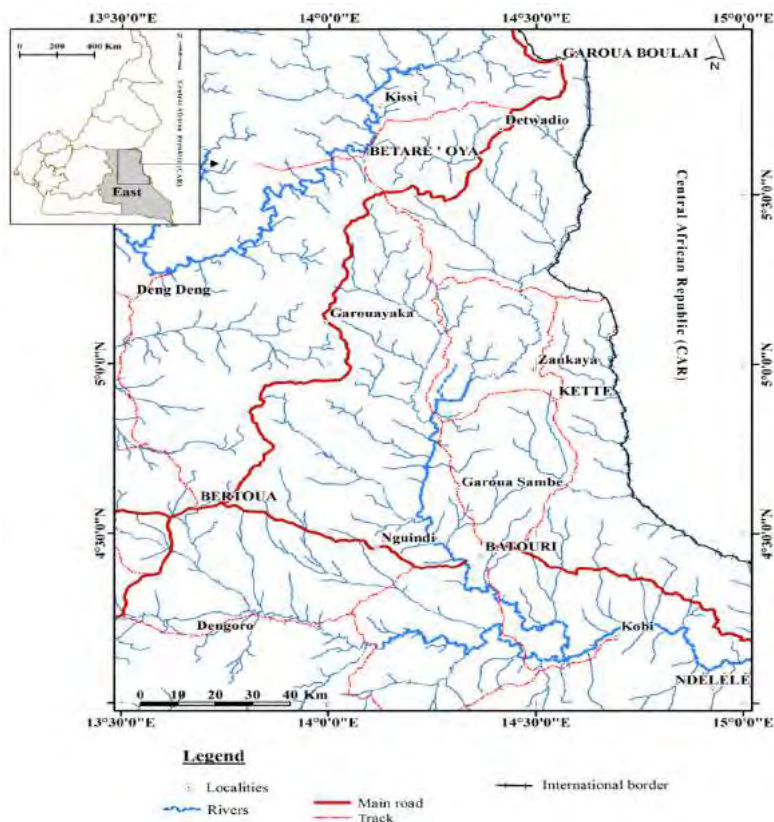
Several gold mining sites are registered in Eastern Cameroon located at Bétaré Oya, Batouri, Kette, etc. including artisanal and semi-industrial mining. In some of these sites, gold is still being nowadays collected by panning soils in rivers. The levels of heavy metals and naturally occurring radioactive materials (NORM) resulting from industrial activities such as mining and mineral processing has not been evaluated in almost all the mines in Cameroon. Although studies on the environmental pollution by heavy metals are still at their beginning, several works were carried out on natural radiological exposure in Cameroon. The works known until then are those of [1, 2] concerning the study of heavy metals (mercury and cadmium) in the fish of Douala and Limbé; and the study of heavy metals in waters and sediments of the Municipal lake of Yaounde and its main tributary Mingo, carried out by [3, 4]. We note also study of [5] concerning natural radiological exposure in the uranium bearing region of Poli and Lolodorf. The present work based on the monitoring of environmental pollution in the area of the Eastern Cameroon is in line with these previous studies.

2 MATERIALS AND METHODS

2.1 Study areas

The gold mining study areas are located in Bétaré-Oya and Batouri in eastern-Cameroon as shown in Figure 1. They are characterized by a monotonous landscape of undulating hill shaped domes [6]. The climate is a Sub-Equatorial Guinea, with bimodal rainfall (two rainy seasons and two dry seasons, with an average annual rainfall of over 1,500 mm).

Figure 1: Location of the gold mining areas of Batouri (Kambélé) and Bétaré Oya in Eastern Cameroon.



Betare Oya and Batouri areas belongs to the Lom Series, one volcano-sedimentary basins Neoproterozoic of Cameroon. The Lom Series consist mostly of gneisses, low-grade metasedimentary and volcanoclastic schists which gold deposits is associated with subordinate conglomeratic quartzites and intruded by granitoid plutons [7].

2.2 Sampling and conditioning

Thirty three (32) soil samples were collected within selected areas of the gold mining sites of Bétaré Oya and Batouri. For elemental analyses we press pellets soils sample of 32 mm diameter were pressed under 20T using a Manual VANEON 25t Press. For natural radioactivity analysis soil samples were conditioned in 500ml Marinelli beakers, completely sealed during at least one month to ensure secular equilibrium between radium 226 and its daughters.

2.3 Analysis

Analyses of soils samples (pellets and marinelli beakers), were carried out by EDXRF Quant'X spectrometer and Canberra NaI(Tl) detector. Spectra acquisition, quantification and analysis were performed using Wintrace 4.1 and Genie 2000 to determine heavy metal concentration and activity concentrations of natural radionuclides respectively.

2.4 Activity concentration and external effective dose

The activity concentration of a given radionuclide was calculated using the following equation:

$$A = \frac{S}{\varepsilon_{\gamma} \cdot P \cdot M \cdot T} \quad (1)$$

Where S is net peak area at energy E; ε_{γ} is Detection efficiency at energy E; P is gamma ray emission probability; M is Mass of the sample and T is counting time.

To estimate the annual effective dose we used the formula proposed by [8].

$$E_{ext} = F_c [(1 - F_{occ}) + F_{occ} F_b] \times \sum_{i=1}^3 A_i (KCF)_i \times t \quad (2)$$

Where F_c is a conversion coefficient; F_{occ} is indoor occupancy factor; F_b is a building material factor; A_i is average activity concentration; $(KCF)_i$ are air kerma conversion factors ; t number of hours in one year (8766)

2.5 Enrichment factor (EF)

EF enables to differentiate heavy metals originating from anthropogenic sources and those of natural sources. The enrichment factor was calculated using the formula originally introduced by [9] and given by the following equation (3):

$$EF = \frac{(C_n/C_{ref})_{sample}}{(B_n/B_{ref})} \quad (3)$$

Where C_n (sample) is the concentration of the examined element in the examined environment, C_{ref} (sample) is the concentration of the examined element in the reference environment, B_n is the concentration of the reference element in the examined environment and B_{ref} is the concentration of the reference element in the reference environment. Iron (Fe) was used as the reference element in the crust [10]. Five contamination categories were recognized on the basis of the enrichment factor [11]. They are given in the following Table 4:

2.6 Geoaccumulation index

The Geoaccumulation Index (Igeo), was introduced by Müller [12] to assess the level of metal accumulation in the sediments, and has been used by several researchers for various studies. It was used in the assessment of contamination by comparing the levels of heavy metal obtained to a background levels originally used with bottom sediments and can also be applied for the assessment of soil samples contamination by mining activities. Igeo is mathematically expressed as follows:

$$I_{geo} = \log_2 \left(\frac{C_n}{1.5 \times B_n} \right) \quad (4)$$

Where C_n represent the measured concentration of heavy metal in the soil, B_n is the geochemical background concentration of the heavy metal [10] with minor alterations [13, 14]. The factor 1.5 is incorporated in the relationship to account for possible variation in background data due to lithogenic effect. The geoaccumulation index (Igeo) scale consists of seven grades ranging from unpolluted to highly polluted as summarized below:

Table 1: Level of pollution following Igeo values.

Enrichment factor	Level of enrichment	Geoaccumulation index	Level of pollution
		<0	Practically unpolluted
		0-1	Unpolluted- Moderate
<2	Minimal	1-2	Moderate
2-5	Moderate	2-3	Moderately- Strongly
5-20	Significant	3-4	Strongly
20-40	Very high	4-5	Strongly- Extremely
>40	Extremely high	> 5	Extremely

3 RESULTS AND DISCUSSION

3.1 Concentration activity and external annual effective dose.

Results from soil samples show that the respective activities concentration values of ^{226}Ra , ^{232}Th , and ^{40}K range from 18.5 to 84.8 Bq.kg^{-1} with mean value 39.4 Bq.kg^{-1} , from 11.8 to 58.0 Bq.kg^{-1} with mean value 28.7 Bq.kg^{-1} and from 80.3 to 581.8 Bq.kg^{-1} with mean value 257.9 Bq.kg^{-1} to Betare-Oya as shown in Figure 1. While in Batouri, ^{226}Ra , ^{232}Th , and ^{40}K has activity range from 33.0 to 62.0 Bq.kg^{-1} with mean value 46.3 Bq.kg^{-1} , from 22.4 to 39.6 Bq.kg^{-1} with mean value 31.7 Bq.kg^{-1} and from 40.6 to 114.6 Bq.kg^{-1} with mean value 75.5 Bq.kg^{-1} respectively as presented in Figure 2.

We note also that the specific activities of radium 226 and thorium-232 are very similar in the two localities. However, a large difference was observed between the values of ^{40}K of activities between the two cities as shown in Figure 1 and 2. Using equation (2), the external annual effective dose values was assessed and is presented in Table 1. The average external annual effective dose values are less than unity as well as Betare – Oya and Batouri.

Figure 2: Distribution of the activity (Bq / kg) of ^{226}Ra , ^{232}Th , and ^{40}K in soil samples Bétaré Oya.

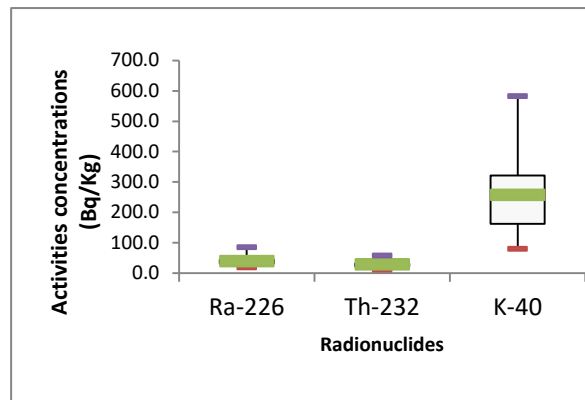


Figure 3: Distribution of the activity (Bq / kg) of ^{226}Ra , ^{232}Th , and ^{40}K in soil samples Batouri.

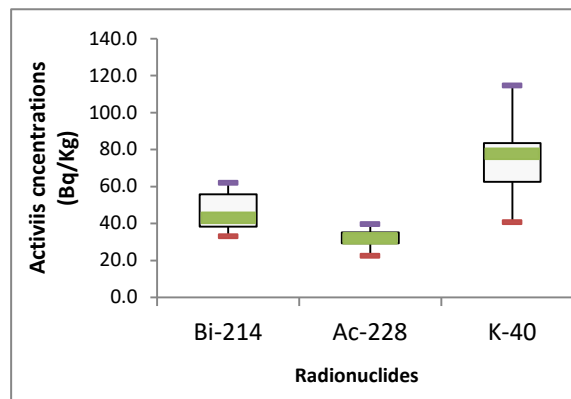


Table 2: External annual effective dose.

Statistical summary	Betaré-Oya	Batouri
	E_{ext} (mSv.yr ⁻¹)	E_{ext} (mSv.yr ⁻¹)
Range	0,17-0,75	0,25-0,42
Mean values	0,356	0,31

3.2 Concentration of heavy metal and pollution indices

The most abundant heavy metals in terms of concentration in Betare-Oya are: Iron with an average of (33528.3 ± 188.5ppm), followed by Manganese (765.2± 93.1ppm) and lead (101.2 ± 9.9 ppm). These elements have concentration values higher than their worldwide average values respectively (3500ppm, 600ppm and 20ppm). We note that, concentration of Lead is slightly upper than the permissible soil limit concentration (100 ppm) given by AFNOR. Also, Iron, Manganese and lead are the main heavy metals in Batouri. Their averages values concentration are respectively(28677.9 ppm), 801.9 ppm, 465.5 ppm, and 22.9 ppm. Compared with their worldwide average value, these elements have concentration values higher. The others measured trace element concentrations in Betaré-Oya and Batouri are presented in Figure 3 and 4 respectively. In this serie, there are five harmful metals for the environmental health. As, Pb, Ni, Zn, Cu. Table 3 shows pollution indices including the enrichment factor and the index of geoaccumulation of heavy metals in Bertero-Oya and Batouri. The results show that the level of enrichment to lead is significant in the Betare-Oya area and minimum in Batouri. As a result, the soil is moderately polluted and unpolluted to lead respectively in the two cities. Soils are moderately rich and moderately polluted by arsenic.

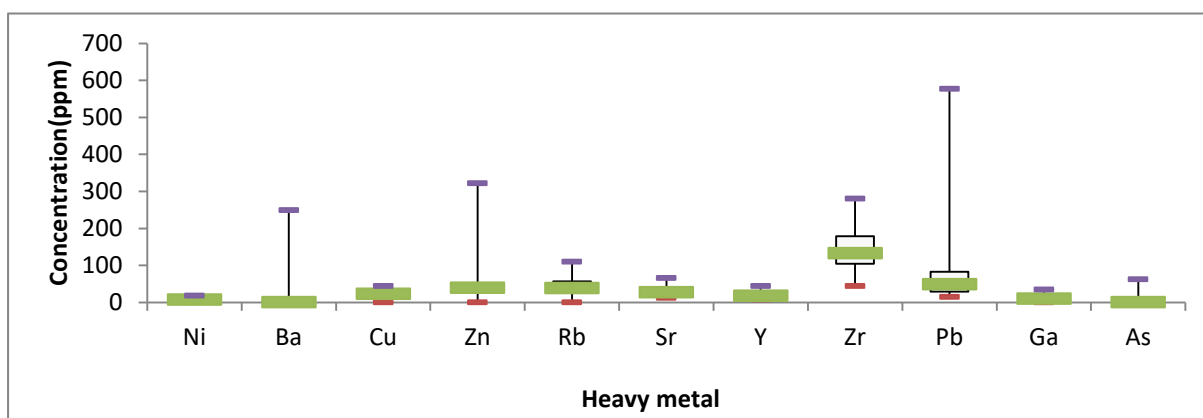
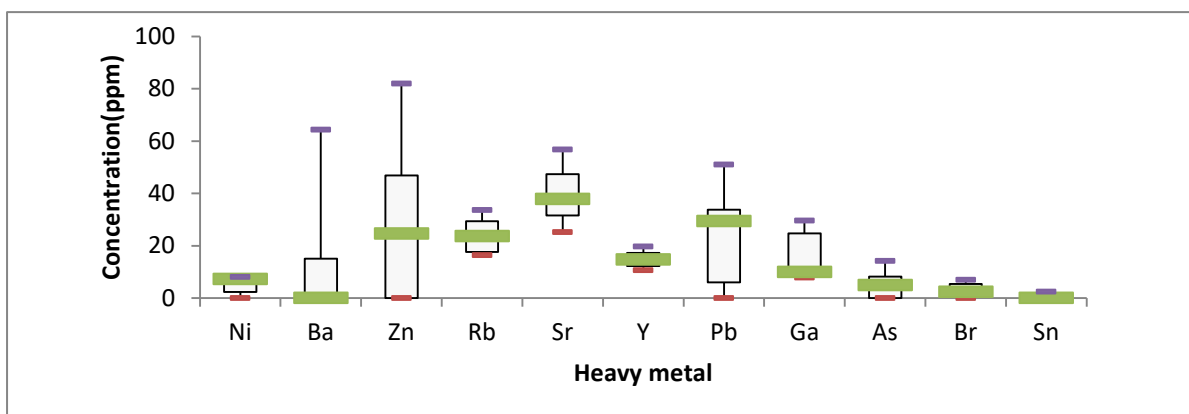
Figure 4: Concentrations distribution of heavy metals in soil samples of Betare Oya.

Figure 5: Concentrations distribution of heavy metals in soil samples of Batouri.

4 CONCLUSION

The assessment of level of pollution in soils by heavy metals and NORM in the gold mining sites of Bétaré Oya and Batouri was evaluated using enrichment factors, geoaccumulation index, activity concentration and external annual effective dose. The study revealed that there were high concentrations of certain metals (As, Pb, Mn, Zr, and Fe) in terms of enrichment of the soil from some sites. For instance, the enrichment factor of lead (Pb) and zirconium (Zr) found respectively for the site in Bétaré Oya and Batouri indicates a significant enrichment and geoaccumulation index shows that these sites are moderately polluted. Activities concentration mean values of ^{226}Ra , ^{232}Th , and ^{40}K were 39.4 Bq.kg^{-1} , 28.7 Bq.kg^{-1} and 257.9 Bq.kg^{-1} to Bétaré-Oya . While in Batouri, ^{226}Ra , ^{232}Th , and ^{40}K has activity mean value 46.3 Bq.kg^{-1} , 31.7 Bq.kg^{-1} and 75.5 Bq.kg^{-1} respectively. External annual effective dose were 0.356 mSv/yr for Bétaré-Oya and 0.31 mSv/yr for Batouri. With regard to the overall pollution of soils at the studied sites, the analysis indicates that pollution by metals and NORM originated from anthropogenic sources. Based on the findings of this study, it is urgent to regulate mining activities in Cameroon to prevent environmental pollution, protecting people against harmful effects of toxic elements.

Table 3: Index of soil pollution in Betare-Oya and Batouri.

Element	Betaré-Oya					Batouri				
	E.F	Level of Enrichment [A]	Igeo	Level of Pollution [B]	E.F	Level of Enrichment [A]	Igeo	Level of Pollution [B]		
Fe	1,0	Minimal	-0,6	Pratically unpoluted	1,0	Minimal	-0,9	Pratically unpoluted		
Mn	1,3	Minimal	-0,2	Pratically unpoluted	0,9	Minimal	-1,0	Pratically unpoluted		
Ni	0,4	Minimal	-2,0	Pratically unpoluted	0,3	Minimal	-2,6	Pratically unpoluted		
Ba	0,0	Minimal	-5,1	Pratically unpoluted	0,0	Minimal	-5,9	Pratically unpoluted		
Cu	0,8	Minimal	-0,9	Pratically unpoluted	0,0	Minimal	-	Pratically unpoluted		
Zn	0,7	Minimal	-1,1	Pratically unpoluted	0,5	Minimal	-1,9	Pratically unpoluted		
Rb	0,4	Minimal	-1,8	Pratically unpoluted	0,3	Minimal	-2,8	Pratically unpoluted		
Sr	0,1	Minimal	-4,0	Pratically unpoluted	0,1	Minimal	-3,7	Pratically unpoluted		
Y	1,0	Minimal	-0,7	Pratically unpoluted	0,8	Minimal	-1,2	Pratically unpoluted		
Zr	0,8	Minimal	-0,9	Pratically unpoluted	5,2	Significant	1,5	Moderate		
Pb	5,3	Significant	1,8	Moderate	1,4	Minimal	-0,4	Pratically unpoluted		
Ga	0,6	Minimal	-1,3	Pratically unpoluted	1,2	Minimal	-0,7	Pratically unpoluted		
As	4,8	Moderate	1,6	Moderate	4,1	Moderate	1,2	Moderate		
Br	-	-	-0,8	Pratically unpoluted	-	-	1,1	Moderate		
Sb	-	-	-3,3	Pratically unpoluted	-	-	-	Pratically unpoluted		
Se	-	-	-2,8	Pratically unpoluted	-	-	-	Pratically unpoluted		
Sn	0,0	Minimal	-5,8	Pratically unpoluted	0,2	Minimal	-3,6	Pratically unpoluted		

5 REFERENCES

- [1] Mbome, I. L., Agbor, E. T., Martin, G. E., Njock, C., Ikome, F., Mbi, C., 1985. Preliminary survey on mercury and cadmium levels in some marine fishery products: IOC Workshop Report, Cameroon. 7p, 2.
- [2] Mbome, I. L., 1988. Project on pollution in the marine environment of the west and central African region (WACAF/2-First Phase): Report presented to Second Workshop of participants in the Joint FAO/IOC/WHO/IAEA/UNEP, Accra, Ghana, 13–17 June 1988. Paris, IOC of Unesco, Mesres/Orstom, 733 p,9.
- [3] Demanou, J., Brumett, R. E., 2003. Heavy metal and faecal bacterial contamination of urban lakes in Yaoundé: African Journal of Aquatic Science, Cameroon. 49-56.
- [4] Ekenguele, N. L., Jung, M. C., Ombolo, A., Ngacha, N., Ekodeck, G., Mbome, L., 2008. Metals pollution in freshly deposited sediments from river Mingoa, main tributary to the Municipal lake of Yaounde: Geosciences Journal, Cameroon. 12 (4), 337-347.
- [5] Saidou., Bochud, F. O., Beachler, S., Kwato Njock, M. G., Ngachin, M., Froidevaux, P., 2011. Natural radioactivity measurements and dose calculations to public: case of uranium bearing region of poli in Cameroon : Radiat. Meas. 46, 254-260
- [6] Emmanuel, A.,Cobbina, S. J., Adomako, D., Duwiejuah, A. B., Asare, W., 2014. Assessment of heavy metals concentration in soils around oil filling and service stations in the Tamale Metropolis: African Journal of Environmental Science and Technology. 8(4), 256-266.
- [7] Pahimi, H., Panda, C. R., Ngassoum, M. B., Tchameni, R., 2015. Environmental Impact of mining in the volcano-sedimentary basins of Cameroon : case study of artisanal gold mine tailing (Betare Oya, East-Cameroon): International Journal of Energy, Sustainability and Environmental Engineering,2 (1), pp. 5-15.
- [8] Saidou., Abdourahimi, Tchuenta Siaka, Y.F., Kwato Njock, M. G., 2011. Natural radiation exposure to the public in oil bearing Bakassi Peninsula: Radioprotection 50(1), 35-41
- [9] Buat-Menard, P., Chesselet. R., 1979. Variable influence of atmospheric flux on the trace metal chemistry of oceanic suspended matter: Earth and Planetary Science Letters, 42, 398–411.
- [10] Taylor, S. R., McLennan, S. M., 1985. The continental crust: its composition and evolution. Blackwell Scientific Publications: Oxford.
- [11] Yongming, H., Peixuan, D., Junji, C., Posmentier, E. S., 2006. Multivariate analysis of heavy metal contamination in urban dusts of Xi'an, Central China: Sci. Total Environ., 355, 176-186.
- [12] Muller, G., 1969 Index of geoaccumulation in sediments of the Rhine River: Geojournal, 2, 108-118.
- [13] Esser, B. K., Turekian, K. K., 1993.The Osmium isotopic composition of the continental crust: Geochimica and Cosmochimica Acta, 57, 3093-3104.
- [14] JOCHUM, K. P.,HOFMANN,W. H., SEUFERT, M., 1993.: Tin in mantle-derived rocks: constraints on Earth evolution: Geochimica and Cosmochimica Acta,57, 3585-3595.

Environmental Dosimetry of Mining Areas: Case of Abandoned Uranium Site, Vinaninkarena- Antsirabe, Madagascar

Hary A. Razafindramiandra^a, Tiana h. Randriamora^a, Elijaona H. Rakotomalala Anja^a, Raelina Andriambololona^a, R. Dina Randriantsizafy^a, Mbolatiana A. L. Ralaivelo^a, Edmond Randrianarivony^b, Solofonirina D. Ravelomanantsoa^b, Joseph L. R. Zafimanjato^a, H. Fanja Randriantseho^a

^aInstitut National des Sciences et Techniques Nucléaires (INSTN- Madagascar), PO Box 4279, Antananarivo, Madagascar

^bFaculté des Sciences, Université d'Antananarivo

Abstract. Madagascar is in a zone of high natural radioactivity. Several sites in exploration, extraction phases, and abandoned uranium mining sites are existing. The human exposure to the natural radiation sources is unavoidable either through external or internal pathways. The protection of the environment and the public living around the mine site is not insured if the radiation protection program in the mine is not available. The mining in the Vinaninkarena, Vakinankaratra Region (Antsirabe) [19° 57' 16''; 47° 2' 3''] was carried out in the past and then abandoned. The damage of the environment and the harmful effects on the public remain in the old uranium site. The work was performed to study the ambient dose levels and the measurements of radon-222 in situ and around the abandoned uranium sites. The estimated annual effective dose to the public was done by using the calculation method of the "UNSCEAR 2000", for external exposure with a GRAETZ X5 DE dosimeter and the average values of radon-222, concentration indoor and outdoor with an Alpoguard detector. The results were compared to the reference levels given by the IAEA - GSR part-3.

KEYWORDS: *radioactive ores; mining; abandoned uranium site; exposure.*

1 INTRODUCTION

Since the discovery of ionizing radiation, particularly after the discovery of harmful effects, the scientists are moving on causality of these effects, the reduction of internal and external exposures due to the source of ionizing radiation. In this case, the natural radioactivity is the primary source of human exposure due to ionizing radiation. The origin of this natural radiation is twofold: either by cosmic radiation from the space, or by radioactive elements in the earth's crust.

The cosmic origin exposure is relatively constant at ground level and varies with altitude while land-based exposure depends on the soil geology and, to a lesser degree, the nature of building materials.

Radionuclides responsible for radioactivity in the Earth's crust are mostly uranium-238 and thorium-232, and their descendants such radon which contributes approximately to the population at about half of exposures from all natural radiation sources.

Madagascar is rich in radioactive minerals. Some sites are in exploration phase, other extraction, and even abandoned mining sites. In this case, the radiological impact study of the environment is very useful. This work was carried out on the abandoned uranium mining sites of Vinaninkarena- Antsirabe i.e. Fitatahana [19° 57' 19'' ; 47° 3' 30''], Ambohitrinimasina [19° 57' 37'' ; 47° 3' 27''], Vatovory [19° 57' 46'' ; 47° 3' 43''] and Village des Jeunesse [19° 57' 27'' ; 47° 3' 16'']. The assessment of the doses received by the public and measurements of radon-222 was carried out on the villages in the vicinity (Ambohitraivo [19° 57' 37''; 47° 4' 7''], Vatovory, and Village des Jeunesse) of these abandoned sites to protect against the harmful effects of ionizing radiation sources.

The discovery of the uranium occurrences in the basin "Pliocene-Pleistocene" of region of Antsirabe by the French Atomic Energy Commission (CEA) was dated on 1910. The work within the region allowed the mining of uranocircite oxide ores deposits that would have provided about forty tons of exported concentrates before 1940 for the uranium and radium mining.

After 1945, research has been taken up by the CEA by surface prospecting work (geological and scintillometer surveying) and subsurface (poll) until 1954. Since 1976, the development of Uranium resources in the region in framework of the « Office des Mines Nationales et des Industries Stratégiques » (OMNIS) with the assistance of the International Atomic Energy Agency (IAEA 1976-1977) and the United Nations Development Program (UNDP 1979-1982). The indices are located on either side of the river of Manandona.

From the Municipality of Vinaninkarena to the Village de Jeunesse, the old mining of CEA was operated under ground and in open pit. The uranium in the form of autunite and uranocircite was recognized there. The autunite comes from the alteration of pitchblende, often associated with chalcocite, uranium in pegmatites and granites of the oxidation zone [5].

2 MATERIALS AND METHODS

Two measurement equipments (Alphaguard [8] and GRAETZ X5 DE [9]) were used for internal and external exposure assessment within the abandoned sites and surrounding the villages. The points of measurement were identified by GPS (Global Positioning System) [10].

2.1 Ambient dose rate in the study area

The work focuses on the assessment of doses rates from gamma radiation and radon-222 inhalations in old abandoned uranium sites represented in Figure 1 and in the villages in the vicinity. The ambient dose rate measurements in the environment were carried out using a survey meter "GRAETZ X5DE". All points of the measurements are identified using GPS.

Figure 1: Old site of Vinaninkarena- Antsirabe



2.2 Indoor and Outdoor Radon concentrations

The presence of uranium and radium-bearing waste in the soil and the subsoil causes the existence of radioactive gas (radon-222) on the sites and surrounding. The radioactive gas is generated by the decay of radium-226, with period of 1600 years. At the human level, there will be a permanent production of radon-222 for several thousands of years [2].

The emanation of radon into the atmosphere causes internal exposures. It can be enriched intensively in confined spaces such as home, for example. However, the probability of radon effects increases with their concentration. To protect the public, we realized measurements of radon levels in the environment in the villages around these old sites using the Alphaguard.

3 RESULTS AND DISCUSSION

3.1 Ambient doses due to gamma rays

3.1.1 Outdoor

96 measurement points distributed over five (05) sites were performed and shown in Table 1. The external exposure was evaluated by mean dose rate at each site.

The annual effective dose is calculated using a conversion factor of 0.7 Sv.Gy^{-1} to convert from the absorbed dose to human effective dose with an outdoor occupancy factor of 20% and 80% for indoors [6].

The annual effective doses are determined as follows:

$$\text{Indoor (nSv)} = (\text{absorbed dose}) \text{ nGy}^{-1} \times 8760\text{h} \times 0,8 \times 0,7 \text{ Sv.Gy}^{-1} \quad (1)$$

$$\text{Outdoor (nSv)} = (\text{absorbed dose}) \text{ nGy}^{-1} \times 8760\text{h} \times 0,2 \times 0,7 \text{ Sv.Gy}^{-1} \quad (2)$$

Table 1: Annual and average outdoor dose rate

Location	Measurement number	Average dose rate ($\mu\text{Sv.h}^{-1}$)	Annual dose rate (mSv)
Ambohitraivo	9	0.21	0.26
Vatovory	32	1.02	1.25
Village de jeunesse	10	0.28	0.34
Ambohitrinimasina	32	0.31	0.38
Fitatahana	13	0.35	0.43

3.1.2 Indoor

18 measuring points distributed in the three villages (Table 2) have been considered, the average dose rates were calculated for each village. The populations are assumed to stay inside their house during the night.

Table 2: Annual and average indoor dose rate

Location	Measurement Number	Average dose rate ($\mu\text{Sv.h}^{-1}$)	Annual dose rate (mSv)
Village of Ambohitraivo	9	0.31	1.52
Village of Vatovory	4	0.34	1.67
Village de jeunesse	5	0.22	1.08

Case of Ambohitraivo village: the mean value of indoors dose rate is higher than to outdoor dose rate. Indeed, the used building materials increased the indoor ambient dose rates.

Case of Vatovory village: the outdoor mean dose rate is higher than indoors dose rate. Even if, contributions dose facilitated by the building materials, the outdoor ambient dose level also increases because of high dose rates in the old site of Vatovory.

Case of village de Jeunesse: the outdoor mean dose rate increases as a result of the existence galleries at east of this village.

The table 3 shows the total annual dose due the sum of annual outdoor and indoor dose.

Table 3: Representation of doses from ambient gamma irradiation

Location	Indoor annual dose (mSv)	Outdoor annual dose (mSv)	Total annual effective dose (mSv)
Ambohitraivo	1.52	0.26	1.78
Vatovory	1.67	1.25	2.92
Village de jeunesse	1.08	0.34	1.42
Ambohitrinimasina	-	0.38	0.38
Fitatahana	-	0.43	0.43

In the village of Vatovory, the total annual effective dose due to external exposure is 2.92 mSv. Compared to other villages, this is the highest dose.

For the case of Ambohitraivo, Vatovory, and village de Jeunesse, the effective doses were estimated from indoor and outdoor exposure. For the case of Ambohitrinimasina, and Fitatahana, there is no dwelling. Hence, the doses due to external radiation are estimated from outdoor exposure.

3.2 Contributions of dose rate from radon

The assessment of dose rate from radon exposure was calculated with the indoor and outdoor average radon concentration. Indeed, the most of the population in the village are farmers, thus their workplaces are outdoor.

For this case, during the night, Alphaguard was placed indoor for radon concentration measurement. While, during the journey, it was placed outdoor

The table 4 summarizes the range of Outdoor and indoor radon concentrations.

Table 4: Range of outdoor and indoor radon concentrations

Location	radon concentrations (Bq.m ⁻³)		Average radon concentrations (Bq.m ⁻³)	
	indoor	Outdoor	Indoor	Outdoor
	Range	Range		
Ambohitraivo	51 - 372	19- 175	217.77	45.06
Vatovory	99 - 1120	17- 167	726.63	87.82
Village de jeunesse	22 - 216	16- 126	94.82	72.76
Ambohitrinimasina (site)	-	25- 208	-	91.27

Ambohitraivo Village

The outdoor and indoor average radon concentration values are less than the reference level published in the «GSR-part3 » [3]. Thus, it is necessary to improve the indoor ventilation of such public building (School, church...) by opening the windows and the door for few minutes before entering in these areas.

Vatovory Village

The indoor mean radon concentration in this village is higher than the reference level of 300 Bq.m⁻³ [3]. To diminish the exposure hazard, the quantity of radon must be reduced as soon as possible. Thereby, it is useful to aerate the dwelling. On the other hand, the outdoor mean radon concentration is less than the reference level for the public.

Ambohitrinimasina

The Alpaguard was placed outdoor because, there are no dwellings. The radon concentration is less than to the reference level for the public [3]. For the population to build the new house at Ambohitrinimasina, it is recommended to:

To minimize the indoor radon entry (use of higher strength concrete to prevent cracking of walls, building materials must be prepared outside of this site, paving the habitat should recover by cement).

To facilitate radon removal after building (increase the size of doors and windows, put windows in each side of the room).

Village de Jeunesse

Indoor radon-222 concentration measurement was done during the night. The next morning, the Radon concentration was done outdoor. The indoor and outdoor average concentrations are less than the public reference level [3].

3.2.1 Dose from inhalation of radon

The effective dose assessment from radon exposure [11] is as follows:

$$E = C_{Rn} (\text{Bq.m}^{-3}) \times F \times T(\text{h}) \times 9 \text{ nSv } (\text{Bq.h.m}^{-3})^{-1}$$

E : effective dose

C_{Rn} : concentration of radon-222.

F: equilibrium factor

T: exposure time

DCF: dose conversion factor for radon: 9 nSv (Bq.h.m⁻³)⁻¹

The exposure time is the product of occupancy factor with the annual time. The outdoor occupancy factor is assumed 0.2 and 0.8 for indoor.

The outdoor and indoor equilibrium factors are respectively 0.6 and 0.4[7].

Following the average radon concentration given by table 4, the annual indoor and outdoor effective doses of Radon were calculated in the table 5:

Table 5 : Annual Effective Doses from radon inhalation

Location	Annual dose (mSv)		Annual effective dose (mSv)
	Indoor	Outdoor	
Ambohitraivo Village	5.49	0.43	5.92
Vatovory Village	18.33	0.83	19.16
Village de Jeunesse	2.39	0.68	3.07
Ancien site Ambohitrinimasina	-	0.86	0.86

3.3 Annual doses

The annual effective dose received by the population in the villages from ambient gamma radiation and the radon are estimated from indoor and outdoor exposure. They are represented as follows:

7.70 mSv in the Ambohitraivo Village;

22.08 mSv in the Vatovory Village;

4.49 mSv in the Village de jeunesse ;

1.24 mSv in Ambohitrinimasina (only, for outdoor)

0.43 mSv à Fitatahana: for outdoor (only for the dose from ambient gamma radiation)

According to the above result, all values of the annual dose to the public are included in the reference level range [1-20 mSv] published by the "GSR part-3", except, the Vatovory Village. Even, this value exceeds the reference level [3] because; the indoor radon concentration value causes the increasing of annual effective dose. Particular safety measures should be taken.

4 CONCLUSION

The protection against ionizing radiation is always linked to dosimetry [1]. The ambient gamma dosimetry in the environment and radon concentration measurements is one of the effective ways to study the impact of ionizing radiation in the environment.

For the old sites Vinaninkarena- Antsirabe, the measured dose rates are low in the following locations: Fitatahana old site, Ambohitrinimasina old site, Ambohitraivo Village and village de Jeunesse. The external exposure hazard of public is minimal. While, in the old site of Vatovory, the dose rates are higher than the above other old sites. Special safety measures must be taken to that site. In the village of Vatovory, the indoor average radon-222 concentration is double in comparison with the reference level published by the "GSR-part3".

The estimated annual effective dose becomes important because of high levels radon-222 concentrations. To minimize these doses, it is necessary to reduce as low as achievable reasonably [4], the radon concentration by ventilation. In the other study areas, the mean concentrations were less than the reference level for the public published by the « GSR-part3».

There is a strong probability to increase the public and workers exposure hazards due to the mining, which may contaminate the skin through contact. There will also exposure hazard associated with the inhalation of dust or the exposure in close proximity to workers against the radioactive ores. Nevertheless, it can reduce the risk of exposure and the public and workers contaminations, if we adopt the appropriate security measures.

5 REFERENCES

- [1] International Atomic Energy Agency, 1999, Assessment of Occupational Exposure Due to External Sources of Radiation, Safety Guide, No. RS-G-1.3.
- [2] Commission de Recherche et d'Information Indépendante sur la Radioactivité, 1998, Risque liée à l'inhalation de radon-222 et de poussières radioactives sur le groupe scolaire Marie Curie à Nogent sur Marne, CRII-RAD.
- [3] International Atomic Energy Agency, 2011, Radiation Protection and Safety of Radiation Sources: International Basic Safety Standards, Safety Standards, N° GSR. Part3.
- [4] International Atomic Energy Agency, 2007, Terminology used in Nuclear Safety and Radiation Protection, Safety Glossary.
- [5] J.L.R. ZAFIMANJATO, 2007, Etude du comportement et détection du radon dans les échantillons de l'environnement par la technique des scintillations. Application au radium, Thèse Doctorat de Physique.
- [6] United Nations Scientific Committee on the Effect of Atomic Radiation, 1988, Effect and risk of ionizing radiation, Report of the general Assembly, New York.
- [7] United Nations Scientific Committee on the Effect of Atomic Radiation, 2000, Effect and risk of ionizing radiation, Report of the general Assembly, New York.
- [8] User Manual Portable Radon Monitor « AlphaGUARD ».
- [9] User Manual Dose Rate Measuring System « GRAETZ X5 DE ».
- [10] Global Positioning System, standard positioning service signal specification, 2nd Edition.
- [11] United Nations Scientific Committee on the Effect of Atomic Radiation, 1993, Source and Effects of Ionizing Radiation, United Nations, New York.

The European Radioecology Alliance: Encouraging the Coordination and Integration of Research Activities in Radioecology

Hildegard Vandenhove^{a*}, Jacqueline Garnier-Laplace^b, Almudena Real^c, Maarit Muikku^d, Catherine Lecomte-Pradines^b, Åste Søvik^e, Brenda J. Howard^f, Pere Masque^g, Rafael Tenorio^h

^aBelgian Nuclear Research Centre, SCK-CEN, Mol, Belgium.

^bInstitut De Radioprotection Et De Surete Nucleaire, IRSN, Cadarache, France.

^cCentro de Investigaciones Energeticas, Medioambientales y Tecnologicas, CIEMAT, Madrid, Spain.

^dSateilyturvakeskus, STUK, Helsinki, Finland.

^eNorwegian Radiation Protection Authority, NRPA, Østerås, Norway.

^fCentre of Ecology and Hydrology, Lancaster, UK.

^gUniversitat Autònoma de Barcelona, Barcelona Spain.

^hUniversidad de Seville, Seville, Spain.

Abstract. The European Radioecology Alliance (ALLIANCE) was established in 2009 by eight founding European organizations with the main objective to progressively strengthen the coordination and integration of research in the field of radioecology at national, European and international level. In 2012, the Radioecology Alliance was officially constituted as an Association, and in 2016 it grew to 25 members from 14 different countries. Within the framework of the ALLIANCE, an EC-Network of Excellence in Radioecology STAR (Strategy for Allied Radioecology) was created in 2011. In 2013, the EC-project COMET (COordination and iMplementation of a pan-European instrumenT for radioecology) was funded to strengthen the pan-European research initiative on the radiation impact on man and the environment by facilitating the integration of the Research and Development activities in radioecology. The ALLIANCE in close collaboration with STAR and COMET, has developed a Strategic Research Agenda (SRA) for Radioecology. The SRA identifies three challenges: (1) To predict human and wildlife exposure more robustly by quantifying the key processes that most influence radionuclide transfers; (2) To determine ecological consequences under realistic exposure conditions and (3) To improve human and environmental protection by integrating radioecology. Within these 3 challenges, 15 research lines have been identified. After a consultation process an updated version of the SRA was launched. Recently, a first proposal for a 5-year roadmap of the radioecology SRA has been developed within the COMET project in collaboration with the ALLIANCE. This shorter-term roadmap will be the basis of an implementation plan for the priority research activities that have been identified in the SRA.

KEYWORDS: *radioecology; strategic research agenda; roadmap; Europe.*

1 INTRODUCTION

Radioecology is a branch of environmental sciences concerned with radionuclides as contaminants and radiation as a stressor. Radioecological studies form the basis for estimating exposures, doses and the consequences of radioactive pollution in the environment, including risks to humans. The study of environmental radioactivity includes aspects common with other groups of pollutants (i.e., environmental transport, fate, and effects to humans and environment), as well as aspects specific to radionuclides (i.e., specialised source terms, external irradiation pathway, radiation dosimetry, radioactive decay). Radioecological expertise is needed whenever radiation within the environment is of potential concern and an evaluation of potential risks is needed. For example, radioecology is important when evaluating the risks from the nuclear fuel cycle including waste disposal and the NORM industry; in the debate on effects from chronic, low level exposures to humans and wildlife; in response to emergencies such as nuclear accidents or terrorist events.

To address emerging issues in radioecology within Europe, eight organisations signed a Memorandum of Understanding (MoU) in 2009 to create the European Radioecology Alliance¹. The Radioecology

* Presenting author, e-mail: hvandenh@sckcen.be

Alliance is an association open to other organisations throughout the world with similar interests in promoting radioecology and already 17 additional European organisations have joined. The MoU states the intentions of the Radioecology Alliance members to integrate a portion of their respective research efforts into a trans-national programme that will enhance radioecology. The Radioecology Alliance members recognise that their shared radioecological research can be strengthened by efficiently pooling resources among its partner organisations and prioritising group efforts along common themes of mutual interest. A major step in the prioritisation process was to develop a Strategic Research Agenda (SRA) for radioecology. An EC-funded Network of Excellence in Radioecology, called STAR (Strategy for Allied Radioecology²), was formed to, among other tasks, develop the SRA. The SRA outlines a prioritisation of research topics in radioecology, with a goal of improving research efficiency and more rapidly advancing the science [1]. The SRA responds to the question: “What topics, if critically addressed over the next 20 years, would significantly advance radioecology?” The SRA developed by ALLIANCE/STAR needs to respond to society needs and to be supported by the radioecological community and other stakeholders. A large-scale invitation for contributions to the SRA from interested stakeholders was realised through the development of an online survey on the proposed content of the SRA. The survey, attracted a large amount of interest within the wider radioecology community, eliciting 110 responses. At a Stakeholders’ workshop organised in 2012 by STAR and ALLIANCE the key research areas identified by the respondents to the survey and their major comments to the SRA were highlighted. Interest groups (regulators, international organisations, research networks, industry, NGOs) gave their perspective on the importance of, and expectations for, radioecology and views on the SRA. A second version of the research part of the SRA for radioecology which incorporates updates addressing the recommendations from stakeholders was released³.

2 THE STRATEGIC RESEARCH AGENDA PRIORITISES THREE MAJOR SCIENTIFIC CHALLENGES

The SRA prioritises three major Scientific Challenges facing radioecology [1]. Addressing these challenges is important both for the future of radioecology and to provide adequate scientific knowledge to decision makers and the public.

2.1 Challenge one: Predict human and wildlife exposure more robustly by quantifying key processes that influence radionuclide transfers, and incorporate the knowledge into new dynamic models

One of the fundamental goals of radioecology is to predict the environmental transfers of radionuclides and consequent exposure of humans and wildlife. The problem is that the key processes that govern radionuclide behaviour are not always well understood, leading to models that incompletely (or even inaccurately) represent these processes. The challenge faced by radioecologists is to identify key processes, improve our understanding of them and incorporate this knowledge into models such that they more realistically predict the behaviour of radionuclides. By making the models more process-based, we expect: (i) a significant reduction in model uncertainty, (ii) a better quantification of environmental variability, (iii) identification of the most influential parameters, and (iv) improved modelling tools capable of predicting radionuclide exposure to humans and wildlife under a variety of conditions, thereby enhancing the robustness of both human and wildlife assessments of exposure to ionising radiation.

¹ <http://www.er-alliance.eu/>

² www.star-radioecology.org.

³ SRA available at www.radioecology-exchange.org

Our strategic vision for research on transfer and exposure is that: *over the next 20 years radioecology will have achieved a thorough mechanistic conceptualisation of radionuclide transfer processes within major ecosystems (terrestrial, aquatic, urban), and be able to accurately predict exposure to humans and wildlife by incorporating a more profound understanding of environmental processes.* Four lines of research will need to be addressed to achieve this vision:

- Identify and mathematically represent key processes that make significant contributions to the environmental transfers of radionuclides and resultant exposures of humans and wildlife.
- Acquire the data necessary for parameterisation of the key processes controlling the transfer of radionuclides.
- Develop transfer and exposure models that incorporate physical, chemical and biological interactions, and enable predictions to be made spatially and temporally.
- Represent radionuclide transfer and exposure at a landscape or global environmental level with an indication of the associated uncertainty.

2.2 Challenge two: Determine ecological consequences under realistic conditions of exposure

Over the last 15 years, international efforts have focused on new strategies for protecting the environment from radioactive substances. For example, in Europe considerable work has been done on collecting relevant information on effects of ionising radiation in non-human species to create the FREDERICA database [2] and on producing the screening ecological benchmarks needed to implement a tiered Ecological Risk Assessment approach (ERA) [(FASSET [3], ERICA [4], PROTECT [5]). While the ERA-type approach is a substantial advancement in radioecology, a lack of sufficient data prevents current ERA analyses from fully accounting for the realistic environmental conditions to which organisms are actually exposed. For example, data are still insufficient to take into account low dose effects, variable dose rate regime, multi-contaminant scenarios, species variation in radiation sensitivity due to life-history traits, or ecosystem level effects. Such knowledge gaps are accounted for *via* extrapolation and the use of assessment factors (or safety factors) that add conservatism and increase uncertainties in risk assessments. New approaches to understand and assess the effects of radiation on wildlife are emerging; mainly due to the similarities that radioecology has with ecotoxicology of chemical substances, stress ecology and human radiation biology. These approaches emphasise that to properly determine the effects from any contaminant we must address the realistic environmental conditions in which organisms are actually exposed. We must link exposure to effects under realistic conditions that incorporate natural abiotic (e.g., climate change, temperature, flooding events, snow and ice) and biotic factors (e.g., physiological and life-history status of organisms; ecological processes such as competition, predation).

Our strategic vision for research on environmental effects is that: *over the next 20 years radioecology will have gained a thorough mechanistic understanding of the processes inducing radiation effects at different levels of biological organisation, including the consequences on ecosystem integrity, and be able to accurately predict effects under the realistic exposure conditions.* Five lines of research will need to be addressed to achieve this vision:

- Establish how processes link radiation induced effects in wildlife from molecular to individual levels of biological complexity.
- Determine what causes intra- and inter-species differences in radiosensitivity (e.g. among cell types, tissues, life stages, life histories, ecological characteristics).
- Understand the interactions between ionising radiation effects and other co-stressors.
- Understand the mechanisms underlying multi-generational responses to long-term ecologically relevant exposures (e.g. maternal effects, hereditary effects, adaptive responses, genomic instability, and epigenetic processes).
- Understand how radiation effects combine in a broader ecological context at higher levels of biological organisation (population dynamics, trophic interactions, indirect effects at the community level, and consequences for ecosystem functioning).

2.3 Challenge three: Improve human and environmental protection by integrating radioecology

In the wider sciences of environmental pollution and risk assessment the individual contaminant-medium-pathway paradigm is changing towards a more holistic, integrated view of the environment as a whole. Radioecology's position relative to this paradigm shift can be best maintained by embracing the concept of integration – integration of the underlying systems and methods of human and environmental protection, and integration of radioecology with other scientific disciplines.

Our strategic vision for research on the integration of radioecology is that: *over the next 20 years radioecological research will develop this scientific foundation for the holistic integration of human and environmental protection, as well as their associated management systems.* Six tasks will need to be addressed to achieve the vision:

- Integrate uncertainty and variability from transfer modelling, exposure assessment, and effects characterisation into risk characterisation.
- Integrate human and environmental protection frameworks.
- Integrate the risk assessment frameworks for ionising radiation and chemicals.
- Provide a multi-criteria perspective in support of optimised decision-making.
- Integrate ecosystem approaches, such as ecosystem services and ecological economics, within radioecology.
- Integrate decision support systems.

2.4 From strategic research agenda to roadmap

To provide rapid and efficient solutions to the difficult problems highlighted within the SRA, a focused, hypothesis-driven research program with clear common goals and resources shared among the international radioecology community is needed. Furthermore, such a long-term, multidisciplinary approach, that goes beyond national boundaries, will better ensure that radioecology will make a significant contribution to the wider society. The development of a roadmap for radioecology research in Europe by the ALLIANCE was partially facilitated through the EC- COMET consortium⁴.

3 COMET - COORDINATION AND IMPLEMENTATION OF A PAN-EUROPEAN INSTRUMENT FOR RADIOECOLOGY

COMET aims to strengthen the pan-European research initiative on the impact of radiation on man and the environment by facilitating the integration of radioecological research, including both the human food chain and the protection of wildlife. The project builds upon and compliments the foundations laid by ALLIANCE and STAR. COMET contributes to the realisation of the ambitions of the ALLIANCE on a larger pan-European scale and prepare for *Horizon 2020*, by collaborating with the European platforms on nuclear and radiological emergency response and recovery (NERIS⁵), low dose radiation risk (MELODI⁶), to some extent with the dosimetry platform (EURADOS⁷) and with relevant training networks (e.g. EUTERP, ENEN⁸). In the context of the *Horizon 2020* approach, the European Commission (EC) looked for umbrella structures (legal entities/associations) to delegate some of the tasks related to the management of Community research programmes to third parties.

⁴ COMET– FP7 Euratom Fission-2013- project number: 604974, Start June 1, 2013, duration 48 months- www.comet-radioecology.org

⁵ NERIS: European Platform on Preparedness for Nuclear and Radiological Emergency Response and Recovery, <http://www.eu-neris.net>

⁶ MELODI: Multidisciplinary European Low Dose Initiative, <http://www.melodi-online.eu>

⁷ EURADOS: European Dosimetry Group, <http://www.eurados.org>

⁸ EUTERP; <http://www.euterp.eu>; ENEN: <http://www.enen-assoc.org>

Such an umbrella structure for Radiation Protection has been prepared by OPERRA⁹ and in the recently started H2020 EC-project CONCERT-EJP¹⁰ with which ALLIANCE and COMET collaborates.

The COMET consortium has 20 partners of which seven are from outside the EU (Norway, Switzerland, Ukraine, Japan, USA, Australia), fostering links with countries which have experienced major nuclear accidents (i.e. former Soviet Union states and Japan). COMET is structured around four work packages (WP) besides the co-ordination WP.

3.1 WP2: Joint Programming and Implementation – Expanding the ALLIANCE

WP2 aims to strengthen the pan-European research initiative on the impact of radiation on environment and man. To achieve this objective we are further developing the SRA in light of advances in knowledge, identification of new priority needs and to better align it with the SRAs of other radiation protection platforms. COMET will form the nucleus to bring together European radioecology and begin to work towards achieving the goals of the SRA in collaboration with those of allied European platforms (in low dose effects and post-accident management) which rely upon radioecology for their underpinning science. COMET will encourage organisations from the European radioecological research community to join the ALLIANCE to help realise the identified priorities for radioecological research; these can only be accomplished by an enlarged and committed network.

In close collaboration with the ALLIANCE, COMET is further developing innovative mechanisms for joint programming and implementation of radioecological research as well as a roadmap and implementation plan for radioecology. A limited number of key research priorities have been identified around which working groups have been established and where partners of COMET and members of the ALLIANCE are involved.

To work towards increased sustainability, COMET is working to identify and integrate national radioecology programmes in order to create a framework for future research. The aim is to get an overview of national programmes, funding schemes and requirements for radioecological research in Europe and begin the integration of national radioecology programmes to create a common framework for future research. This will give a first indication in the extent to which nationally funded projects could assist in reaching the overall goals of the SRA at the European level. The national funding bodies will be encouraged to take into account the research lines indicated in the SRA.

State of the art and optimized use of research infrastructure is key for sustainable radioecology in Europe. A prominent task is the creation of Observatories for Radioecological Research. It is the intention to establish long-term research programmes connected to the priority research domains identified by the roadmaps at the Observatory Sites. These sites are being established in the Chernobyl and Fukushima affected areas and a number of NORM legacy sites (i.e. in Poland and Belgium) are being screened. Research programmes will be established at these sites.

3.2 WP3: Improving and validating radioecological models for risk assessment and for emergency and post-accident situations

Under WP3 COMET is undertaking joint research activities to improve and validate radioecological models for improved protection of humans and the environment in existing, planned and emergency exposure situations.

⁹ OPERRA: Open Project for the European Radiation Research Area, <http://www.melodi-online.eu/operra.html>

¹⁰ CONCERT: European Joint Programme for the Integration of Radiation Protection Research, <http://www.concert-h2020.eu>

Initial Research Activities (IRA) are currently addressing priority needs highlighted by the SRA, with an emphasis on challenge 1. The IRA focus on improved parameterisation of key processes controlling the transfer of radionuclides, with an emphasis on process based, dynamic modelling approaches. The IRA topics are presented in D3.1¹¹ and their objectives can be summarised as follows:

1. *Marine modelling* – improving predictions of concentrations in, and exposures of, marine biota and humans through sophisticated modelling, e.g. dynamic modelling, trophic transfer modelling and by combining transfer modelling with sediment modelling.
2. *Forest modelling* - reducing the uncertainties in assessments of short and long term impacts of radioactive contamination in forested areas through model development and parameterization of key processes controlling the transfer of radionuclides.
3. *Human food chain modelling* - improving human food chain modelling through regional customization of parameter values, using Bayesian methods and studying the long-term dynamics of soil-to-plant transfers for specific soil types and for long-lived radionuclides.
4. *NORM modelling* - acquiring data necessary for the parameterization of key processes, and improving existing models or developing parametric models linking observed accumulation, mobility, and transfer with environmental parameters and processes for Naturally Occurring Radioactive Materials.
5. *Particle behaviour* - improving our ability to describe the processes of hot particle transformation in the environment and radionuclide leaching in various media.
6. *ICRP reference sites* - providing the data to derive a taxonomically based model of radionuclide transfer for wildlife independent of site-specific factors.

The IRA related research and development (R&D) is for a large part realised by internal resources of the participating institutes. Where possible, and appropriate, the research is being conducted at the Observatory Sites.

Further R&D on improved transfer and exposure assessment and reducing uncertainties is being carried out under two projects joining COMET after an open call, FRAME and RATE.

FRAME (The impact of recent releases from the Fukushima nuclear Accident on the Marine Environment) aims to better understand the sources, fate, transport, bioaccumulation and associated impact of radionuclides from the Fukushima Dai-ichi NPP accident in Japan. The investigation encompasses the main compartments of a complex marine environment. Two oceanographic cruises were performed to investigate coastal and offshore sites. The concentrations of a suite of radionuclides (¹³⁷Cs, ¹³⁴Cs, ⁹⁰Sr, plutonium isotopes, ²³⁶U and ¹²⁹I) were measured in water, suspended matter and bottom sediments; these data will help in assessing the transfer to marine biota.

RATE (Radioactive particle Transformation procEsses) intends to fill knowledge gaps related to transformation processes influencing weathering of radioactive particles released to different ecosystems and the subsequent release of associated radionuclides to reduce the uncertainties in environmental impact assessments of particle contaminated sites. The project focuses on particle characteristics, weathering rates, remobilization and prediction of ecosystem transfer of radionuclides associated with U and/or Pu containing particles originating from selected key sources (nuclear weapons tests, safety tests, conventional detonation of nuclear or DU weapons, nuclear reactor accident, NORM).

¹¹ https://wiki.ceb.ac.uk/download/attachments/197986961/D3%201__Final%20PU.pdf?api=v2

3.3 WP4: Shared challenges in chronic low dose effects and risk assessment, and beyond

The research developed under WP4 is related to Challenge 2 of the Radioecology SRA - Chronic low dose effects and risk assessment. The IRA is focused on a specific topic of common interest to radioecology and radiobiology: the possible contribution to long-term or transgenerational effects of mechanisms governing the activation or the repression of the epigenome of organisms exposed chronically to ionising radiation. To streamline the research, deliverable D4.1¹² describes the state-of-art on epigenetic pathways, their relevance for radioecology and the up-to-date methods to characterize them. Based on this state-of-the art, DNA methylation was chosen as the focus of the studies. A description of the initial research activity for the chosen biological models (zebrafish, frogs, earthworms, plants – *A. thaliana*, *C. bursoa-pastoris*) is also included. After optimization of required protocols for global DNA methylation measurement, transgenerational irradiation experiments on vertebrates and plant under controlled laboratory conditions are carried out. Field work campaigns in the Chernobyl exclusion zone and the Fukushima affected area are ongoing to confirm DNA methylation in local species (e.g. frogs, plants, earthworms) and relate these changes to species phenotype/fitness.

3.4 WP5: Knowledge exchange

The objective of WP5 is to enhance and maintain European capacity and skills in radioecology by establishing a dynamic interaction promoting effective collaboration between researchers, tool developers, regulators and industry. This will ensure (i) more effective ‘take-up’ of scientific advances by the user community and (ii) that radioecological research is better focused to address the needs of users. Key to this are effective links between other networks, projects and platforms (e.g. OPERRA, CONCERT, ALLIANCE, MELODI, NERIS). An interactive website for COMET¹³ has been established including supporting materials for the user community providing informed and regular updates of developments.

COMET facilitates discussion of topical radioecological issues between researchers and users to support radiation protection in Europe and beyond. Two workshops have already been organised – one on 'Effects uncertainty' took place in UK in late 2014 and the other on 'Potential environmental impact of the accident in the NPP of Fukushima-Daiichi' was organised in Japan in connection with the ICOBTE conference (July 2015). Two other workshops are planned : “Fit for Purpose Modelling” (June 2016, Seville) and “Is the environment of the CEZ affected?” (August 2016).

As a third mechanism, COMET develops training packages to maintain and enhance professional competence, including field based training courses. The first of these courses was organised at the Polish Observatory Site (September 2015) and the second will take place in the Chernobyl Exclusion Zone (September 2016).

4 A ROADMAP FOR RADIOECOLOGY

Based on the revised SRA, a first phase (5-year) roadmap to achieve and realize a limited number of priority lines of research is being developed. The roadmap, developed by the COMET consortium in close collaboration with the ALLIANCE, deals with focused research areas and intends to have strong interactions with the two other key areas of radiation protection (post-emergency management and low dose research).

¹²

<https://wiki.ceh.ac.uk/download/attachments/197986961/COMET%20Deliverable%20D4%201%20final%2013%2009%2013.pdf?api=v2>

¹³ www.comet-radioecology.org

The overall strategy/objective of the roadmap development was highlighted as ‘Underpinning science for an enhanced basis for fit-for-purpose human and environmental impact assessment by mechanistic modelling, improved parametrization, improved databases’. The scoping should extend from basic science (mechanistic understanding) to application to improve radiation protection and communication with society. R&D should interlink the different Challenges presented in the SRA. Additionally, research topics of radioecology within the roadmap should extend also to areas relevant for post-emergency management, low-dose effect and dosimetry research, to provide a powerful catalyst to further develop collaboration between the four existing radiation protection platforms in Europe.

The overall strategy was translated into a Challenge-related approach and an expected outcome.

For Challenge 1, the approach is to “Improve human and environmental dose and impact assessment by mechanistic/process-based modelling of environmental transfer and exposure in the biosphere”. The expected outcome is to have fit-for-purpose environmental models to support human and wildlife impact assessment and risk management.

For Challenge 2, the approach is to “Unravel causes and mechanisms of radiation induced effects in wildlife from molecular to individual levels up to populations”. The expected outcome will be knowing causes of biological effects to detect early damages and to protect populations.

For Challenge 3, the approach is to “Improve risk characterisation by better quantification of uncertainty and variability of exposure and effects”. The expected outcome is an integrated approach to enhanced risk characterisation and communication (connecting science, economy & society).

The criteria considered to prioritize the research lines included: Impact, Achievable, Relevance and Public perception, Good science. As such, 5 domains were identified where R&D was considered of highest importance, impact and relevance: *marine radioecology* since Fukushima demonstrated our community did not have appropriate marine radioecological models; *human food chain modelling* since the current models include a Germany-based Terrestrial Food Chain and Dose Module (FDMT) which needs to be adapted to other regions of Europe and the underlying radioecological models need to be improved; *Atmospheric radionuclides in transfer processes*: since the Fukushima accident has highlighted several deficiencies in air transport and inhalation dose assessment, deposition stage from atmospheric releases or long-lasting secondary emissions; *NORM radioecology* since NORM legacy sites and facilities are often located close to human settlements requiring close follow up and appropriate remediation and the waste products of this industries are an economic burden unless they can be recycled which requires additional assessments; *Transgenerational effects and species sensitivity*: there is major concern of the biological effects of low doses of ionising radiation along with the potential hereditary effects for both humans and wildlife. To answer this we need to improve our knowledge on long-term and transgenerational effects and on inter-species differences of radiation sensitivity which has important implications for understanding the overall effects of radiation.

For these five priority areas, the scope and objectives have been defined and participants identified. The intended activities are highlighted and an implementation plan to attain the set-objectives and expected outcome is being developed. External funding is being sought. The roadmap and continued SRA update are also integrated into the CONCERT-EJP project.

5 ACKNOWLEDGEMENTS

Funds for producing SRA and roadmap were provided, in part, by the European Commission, under Contract Numbers Fission-2010-269672 and Fission-2013-604974. The authors acknowledge the contributions of the Scientific Committees of STAR and COMET to respectively the SRA and roadmap, as well as the contributions of STAR, COMET and ALLIANCE members.

6 REFERENCES

- [1] Hinton, T. G., Garnier-Laplace, J., Vandenhove H. et al. 2013. An invitation to contribute to a strategic research agenda in radioecology. *J. Environ. Rad.* 115:73-82.
- [2] Copplestone, D., Hingston, J., Real, A., 2008. The Development and Purpose of the FREDERICA Radiation Effects Database, *J. Environ. Rad.*, 99: 1456-1463.
- [3] Williams C., (Ed), 2004. Framework for Assessment of Environmental Impact (FASSET) of Ionising Radiation in European Ecosystems, *J. Rad. Prot.*, 24 (4A).
- [4] Larsson, C.M. 2008. An Overview of the ERICA Integrated Approach to the Assessment and Management of Environmental Risks from Ionising Contaminants, *J. Environ. Rad.* 99, 1364-1370.
- [5] Howard, B.J., Beresford, N.A., Andersson, P. et al., 2010. Protection of the Environment from Ionising Radiation in a Regulatory Context - an Overview of the PROTECT Coordinated Action Project, *J. Rad. Prot.*, 30, 195-214.

A cancer risk due to natural radiation on the Coast of Montenegro

Ivanka Antović^c, Nikola Svrkota^d, Danko Živković^e, Nevenka M. Antović^{f*}

^cDepartment for Biomedical Sciences, State University of Novi Pazar, Novi Pazar, Serbia.

^dCentre for Ecotoxicological Research, Podgorica, Montenegro.

^eFaculty of Medicine, University of Montenegro, Podgorica, Montenegro.

^fFaculty of Natural Sciences and Mathematics, University of Montenegro, Podgorica, Montenegro.

Abstract. The Coastal region of Montenegro includes six municipalities and has an area of 1591 km² (~11.5 % of the total country area of 13 812 km²) and total population of 148 683 (~24 % of the total in Montenegro). Terrestrial gamma radiation could be considered as one of the major contributors to natural radiation exposure of the population living there, and excess lifetime cancer risk due to this radiation – *outdoors* and *indoors* was assessed on the basis of radioisotope activity concentrations in uncultivated soil samples, as well as on the basis of directly measured *outdoor* absorbed dose rates in air at 1 m above the ground. With lifetime expectancy taken as 70 years, in a consideration of natural radioisotopes only (²²⁶Ra, ²³²Th, ⁴⁰K), an average excess lifetime cancer risk was found to be 0.26·10⁻³ (*outdoors*) and 1.94·10⁻³ (*indoors*). If ¹³⁷Cs activity concentration is included, it is 0.27·10⁻³ (*outdoors*), whilst from direct *outdoor* dose rate measurements – 0.18·10⁻³. Having in mind that *indoor* radon is the main contributor to the exposure of humans from natural sources of ionizing radiation, annual *indoor* radon concentrations previously measured in 107 homes in six towns were used to estimate exposure to radon daughters (ranged from 0.006 to 0.61 WLM/y, with an average of 0.1 WLM/y) and assess the risk factor due to radon which is found to be between 0.02 and 2.13 %. Lung cancers at the Coast of Montenegro in 2009 were also analyzed (23.3 % of the total in the country, the incidence rate of 38.2 per hundred thousand) – to establish baselines for further research. Total number of patients from the Coastal area was 48, and regarding histology cancer types were: small cell lung cancers – 7, non-small cell lung cancers, i.e., epidermoid – 16, adenocarcinoma – 14, mixed (adeno- and epidermoid) – 9 and large cell – 2.

KEYWORDS: cancer risk; terrestrial radiation; indoor radon.

1 INTRODUCTION

The Coastal region of Montenegro includes an area of 1591 km² (in six municipalities: Ulcinj – 255 km², Bar – 598 km², Budva – 122 km², Tivat – 46 km², Kotor – 335 km², Herceg Novi – 235 km²) and total population of 148 683 – based on the Census in 2011 [1]. This region makes around 11.5% of the total Montenegro area (13 812 km²) and around 24% of the total Montenegro population (~620 000 in 2011 [1]).

Since *indoor* radon is the main contributor to the exposure of humans from natural sources of ionizing radiation, the data on its annual concentrations on the Coast of Montenegro obtained in the earlier work [2] were used to evaluate the risk factor for lung cancer due to radon.

Some radiological impacts of natural radioactivity from soil in Montenegro (including points from the Coast), such as annual gonadal dose equivalent, radium equivalent activity etc., have been previously analyzed [3]. Assuming that terrestrial radiation is the second major contributor to natural radiation exposure of the population living in this sea level area, uncultivated soil was considered in the present study – to evaluate excess lifetime cancer risk due to terrestrial gamma radiation, and to compare it with the risk from *indoor* radon.

So, in this work we couple previously published results with the results of new analyses, and evaluate a cancer risk due to ionizing radiation from its two main sources in the region, with an objective to

* Presenting author, e-mail: nena@rc.pmf.ac.me

establish initial data for a further research and understanding potential role of radioactivity in initiating cancer, particularly lung cancer – in the study area, for which the biomedical data were also analysed.

2 MATERIALS AND METHODS

2.1 Terrestrial gamma radiation

As a part of a wider research [3] the top 5 cm of uncultivated soil had been sampled on the Coast of Montenegro at the locations shown in Fig. 1. After drying at room temperature, passing through 2 mm sieves, the samples in mass from 0.877 to 1.299 kg were sealed in 1L Marinelli beakers and measured after equilibrium ^{226}Ra and its decay products was established (~40 days). Measurements were performed using the HPGe spectrometer ORTEC – GEM-40190 (40% of relative efficiency) for different measuring times (up to 71 240 s), and natural radioisotope activity concentrations were determined from the photopeaks – 295 keV, 352 keV, 609 keV, 1120 keV, 1765 keV (^{226}Ra); 338 keV, 911 keV ($^{232}\text{Th}/^{228}\text{Ac}$); 1461 keV (^{40}K). Activity concentrations of artificial ^{137}Cs were additionally determined using the 662 keV photopeak.

Figure 1: Measuring points – terrestrial radiation



Measured radioisotope activity concentrations, and the dose coefficients/factors (in nGy/h per Bq/kg) found in literature [4, 5], were used to evaluate the external terrestrial gamma absorbed dose rate in air (*outdoor* and *indoor*) at 1 m above the ground, using

$$D_{\text{out}} = A_c(^{226}\text{Ra}) \cdot 0.462 + A_c(^{232}\text{Th}) \cdot 0.604 + A_c(^{40}\text{K}) \cdot 0.0417, \quad (1)$$

$$D_{\text{in}} = A_c(^{226}\text{Ra}) \cdot 0.92 + A_c(^{232}\text{Th}) \cdot 1.1 + A_c(^{40}\text{K}) \cdot 0.08. \quad (2)$$

It is important to point out the last one, D_{in} , is given just to illustrate dose rate if the level of radioisotopes in building materials is the same as in here studied soil samples.

For *outdoor* dose rate, a contribution of ^{137}Cs is also taken into account with the dose coefficient from [6],

$$D_{\text{out}2} = A_c(^{226}\text{Ra}) \cdot 0.462 + A_c(^{232}\text{Th}) \cdot 0.604 + A_c(^{40}\text{K}) \cdot 0.0417 + A_c(^{137}\text{Cs}) \cdot 0.1243, \quad (3)$$

and this dose rate was also directly measured at the same locations ($D_{\text{dm,out}}$), in standard procedures of the Thermo Scientific RadEye PRD and CANBERRA Inspector 1000.

Corresponding annual effective dose rates for adults were calculated applying the conversion coefficient from absorbed dose in air to effective dose (0.7 Sv/Gy), *outdoor* occupancy factor (0.2) and *indoor* occupancy factor (0.8) from the UNSCEAR report [4], i.e.,

$$E_{\text{out}} = D_{\text{out}} (\text{nGy/h}) \cdot 8760 \text{ h/y} \cdot 0.2 \cdot 0.7 \text{ Sv/Gy}, \quad (4)$$

$$E_{\text{in}} = D_{\text{in}} (\text{nGy/h}) \cdot 8760 \text{ h/y} \cdot 0.8 \cdot 0.7 \text{ Sv/Gy}. \quad (5)$$

The effective dose rates have also been calculated using D_{out2} and $D_{dm,out}$ (E_{out2} and $E_{dm,out}$, respectively), for a comparison. Excess lifetime cancer risks (ELCRs) from these dose rates were then evaluated applying [7]

$$ELCR = E \cdot T_e \cdot CR, \quad (6)$$

where T_e is average life time expectancy taken to be 70 years, and CR is cancer risk – taken to be 0.05 per Sv [8].

2.2 Indoor radon

In regard to annual *indoor* radon concentrations, 107 randomly selected homes in urban areas on the Coast of Montenegro (Ulcinj – 19, Bar – 27, Budva – 17, Tivat – 6, Kotor – 6, Herceg Novi – 32) were previously surveyed, and results were reported in [2]. A lung cancer risk due to lifetime exposure to radon is estimated applying these results and an equation based on the U.S. EPA methodology [9]

$$CR_{Rn} = ERD \cdot T_e \cdot RC, \quad (7)$$

where RC is the risk coefficient for exposure to radon and its daughters in equilibrium ($5 \cdot 10^{-4}$ 1/WLM [10]); T_e is lifetime (taken as 70 years); ERD (in WLM/y) is exposure to radon daughters, evaluated using $ERD = C_{Rn} \cdot (2.7 \cdot 10^{-4}) \cdot F \cdot n \cdot 51.6$, where C_{Rn} is annual radon concentration (Bq/m^3), $2.7 \cdot 10^{-4}$ – conversion factor of radon concentration to the WL per Bq/m^3 , F – equilibrium factor (0.4 [11]), n – occupancy time equal to 0.5 (taken from the annual exposure of 4380 h/y, which means 12 hours daily spent *indoor*), and 51.6 WLM/y per WL is ratio of 8766 h (total, taking into account the leap years) and 170 (total working hours/month). For a comparison, occupancy time of 0.54 taken from 13 hours daily spent *indoor* (the annual exposure of 4745 h/y) was also evaluated.

Lung cancer is the most common cancer in males of Montenegro [12], and an analysis of this cancer type diagnosed in 2009 was performed – from the data of the Special hospital for lung diseases, as well as the data of the Oncology Consilium for all lung cancer diseased in Montenegro.

3 RESULTS AND DISCUSSION

3.1 Terrestrial gamma radiation

As abovementioned, soil samples from the Coast of Montenegro (Table 1), were previously analyzed for radioactivity from natural radioisotopes [3] and measurements carried out by the HPGe spectrometry showed average ^{226}Ra activity of 38.3 Bq/kg, $^{232}\text{Th}/^{228}\text{Ac}$ – 38.5 Bq/kg and ^{40}K – 445 Bq/kg. These values are in a good accordance with the world median of mean activity concentrations for ^{226}Ra , ^{232}Th and ^{40}K – 35, 30 and 400 Bq/kg, respectively [4]. The same samples are also analyzed by the same spectrometer for the ^{137}Cs activity (Table 1), and its activity concentration has minimum, maximum, average, standard deviation and median – 1.90, 85.5, 36.4, 30.1 and 26.8 Bq/kg, respectively. The estimated dose rates (eqs. 1-5) are also given in Table 1. Table 2 contains statistics of all the assessments related to terrestrial radiation.

The external terrestrial gamma absorbed dose rate in air at 1 m above the ground at the Coast of Montenegro due to natural radionuclides (^{226}Ra , ^{228}Th and ^{40}K), *outdoor* and *indoor*, is shown in Fig. 2a, while corresponding excess lifetime cancer risk – in Fig. 2b. Absorbed dose rates – calculated from ^{226}Ra , ^{232}Th , ^{40}K and ^{137}Cs activity concentrations in soil (D_{out2}), and directly measured at the same locations ($D_{dm,out}$), are presented in Fig. 3a, and corresponding ELCRs – in Fig. 3b.

Table 1: Dose rates at the Coast of Montenegro – terrestrial radiation.

Location	D_{out} , nGy/h [3]	E_{out} , μ Sv/y [3]	D_{in} , nGy/h	E_{in} , μ Sv/y	$A_c(^{137}\text{Cs})$, Bq/kg	D_{out2} , nGy/h	E_{out2} , μ Sv/y	$E_{dm,out}$, μ Sv/y
Ulcinj	27.9	34.2	52.8	259	1.90±0.12	28.1	34.5	49.1
Bar	43.6	53.4	82.3	404	19.7±0.7	46	56.4	42.9
Sutomore	56.2	69	107	523	5.74±0.23	57	69.9	36.8
Petrovac	48.2	59.2	91.3	448	48.6±1.6	54.3	66.6	55.2
Budva (town)	34.3	42.1	64.8	318	33.9±1.1	38.5	47.2	24.5
Jaz (Budva)	61.3	75.2	116	569	17.6±0.6	63.5	77.9	55.2
Plavi Horizonti (Tivat)	185	227	356	1745	82.4±2.7	195	239	147
Kotor	66.2	81.1	125	612	15.9±0.6	68.1	83.51	42.9
Risan	39.1	47.9	74.6	366	52.6±1.8	45.7	56	36.8
Herceg Novi	33.2	40.7	62.7	308	85.5±2.8	43.8	53.7	36.8

Figure 2: Absorbed dose rates due to natural radioisotopes (D_{out} and D_{in}) (a), and excess lifetime cancer risk (b)

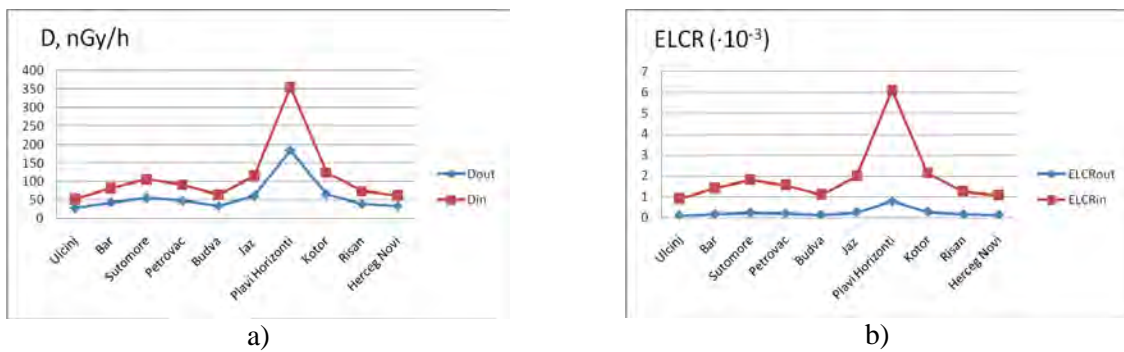
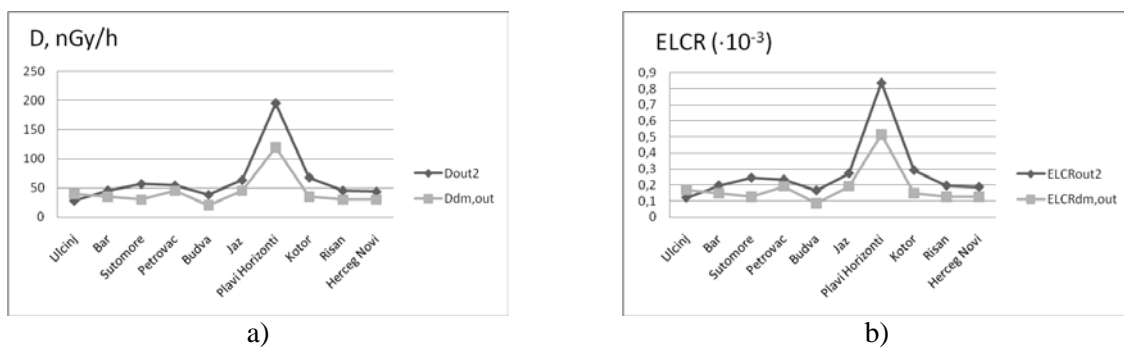


Figure 3: Outdoor absorbed dose rates due to natural radioisotopes and ^{137}Cs – calculated (D_{out2}) and measured ($D_{dm,out}$) (a), and excess lifetime cancer risk (b)



The worldwide average annual effective dose due to external terrestrial radiation (natural sources) was found to be 0.48 mSv (0.07 mSv – outdoors, and 0.41 mSv – indoors) [4], which means an average ELCR of $0.245 \cdot 10^{-3}$ outdoors and $1.44 \cdot 10^{-3}$ indoors. Slightly higher (average) effective doses and ELCRs at the Coastal Montenegro are mainly due to one location (Plavi Horizonti, Tivat) showing higher natural radioisotope (^{226}Ra and ^{232}Th) activity concentrations [3]. The same location also showed the second highest ^{137}Cs concentration.

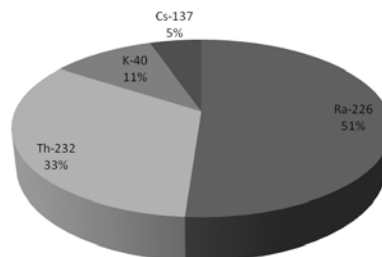
The dose rates inferred from concentrations of radioisotopes in soil and from direct measurements at the locations showed ratios from 0.7 (Ulcinj) to 1.95 (Kotor). It is important to point out that direct measurements gave the instant dose rate at the measuring points, while calculated values included ^{226}Ra , ^{232}Th , ^{40}K and ^{137}Cs , assuming that a contribution of the other possible present isotopes is negligible.

The highest absorbed dose rate $D_{\text{out}2}$ has been found for the location Plavi Horizonti – Tivat (where the highest dose rate $D_{\text{dm,out}}$ was also measured), and it is dominantly caused by radium (216 Bq/kg of ^{226}Ra , 107 Bq/kg of $^{232}\text{Th}/^{228}\text{Ac}$, 491 Bq/kg of ^{40}K [3], and 82.4 Bq/kg of ^{137}Cs – Table 1). A relative contribution of ^{226}Ra , ^{232}Th , ^{40}K and ^{137}Cs to this, the highest dose rate, is shown in Fig. 4. The lowest $D_{\text{out}2}$ was found for the Ulcinj soil, with a relative contribution of ^{226}Ra , ^{232}Th , ^{40}K and ^{137}Cs – 18, 39, 42 and 1%, respectively. On the other hand, the lowest $D_{\text{dm,out}}$ was found for the location Budva (town) (20 nGy/h), showing the second lowest $D_{\text{out}2}$, as well.

Table 2: Statistics of the assessments (terrestrial radiation).

	Minimum	Maximum	Average	Standard deviation	Median
<i>Natural radioisotopes (^{226}Ra, ^{232}Th, ^{40}K)</i>					
D_{out} , nGy/h	27.9	185	59.5	45.8	45.9
D_{in} , nGy/h	52.8	356	113	88.5	86.8
E_{out} , $\mu\text{Sv/y}$	34.2	227	73	56.2	56.3
E_{in} , $\mu\text{Sv/y}$	259	1745	555	434	426
$\text{ELCR}_{\text{out}} (\cdot 10^{-3})$	0.12	0.79	0.26	0.2	0.2
$\text{ELCR}_{\text{in}} (\cdot 10^{-3})$	0.91	6.11	1.94	1.52	1.49
<i>Natural radioisotopes and ^{137}Cs</i>					
$D_{\text{out}2}$, nGy/h	28.1	195	64	47.6	50.2
$D_{\text{dm,out}}$, nGy/h	20	120	43	28.1	35
$E_{\text{out}2}$, $\mu\text{Sv/y}$	34.5	239	78.5	58.3	61.5
$E_{\text{dm,out}}$, $\mu\text{Sv/y}$	24.5	147	52.7	34.5	42.9
$\text{ELCR}_{\text{out}2} (\cdot 10^{-3})$	0.12	0.84	0.27	0.20	0.22
$\text{ELCR}_{\text{dm,out}} (\cdot 10^{-3})$	0.09	0.52	0.18	0.12	0.15

Figure 4: A relative contribution of particular radioisotope to the highest determined absorbed dose rate (Plavi Horizonti – Tivat)



3.2 Indoor radon

As abovementioned, *indoor* radon was previously measured in 107 randomly selected dwellings at the Coast of Montenegro, and annual radon concentrations were found to range up to 202 Bq/m³, with arithmetic mean (AM) of 31.8 Bq/m³, and median of 25.1 Bq/m³ (as well as with geometric mean (GM) of 25.5 Bq/m³, and geometric standard deviation (GSD) of 2.1). Statistics for the annual concentrations of *indoor* radon by town/municipality, is reported in Table 3 [2].

Table 3: Indoor radon on the Montenegrin Coast [2].

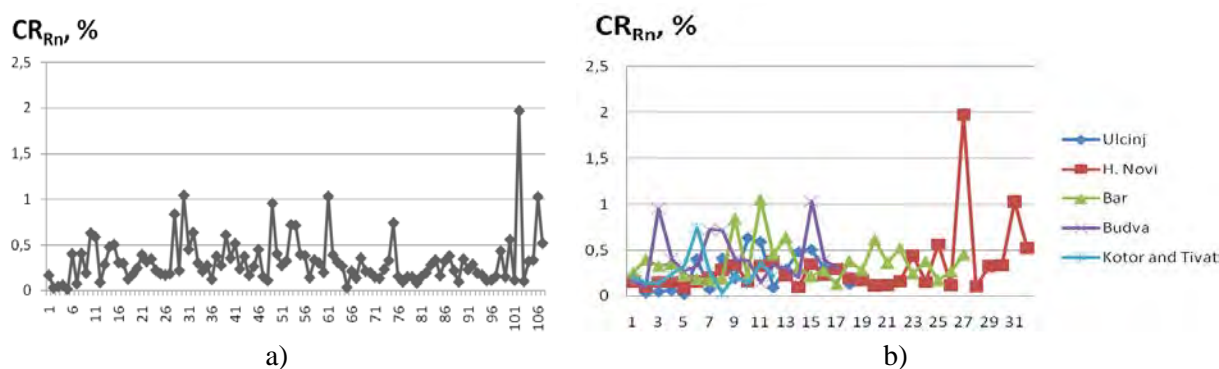
Bq/m ³	Ulcinj	Bar	Budva	Tivat	Kotor	Herceg Novi
AM	26.5	37.4	43.3	21.1	30.8	32.0
SD	20.1	21.8	27.9	11.2	23.3	36.4
GM	17.9	32.7	35.9	17.3	25.6	23.5
GSD [-]	2.8	1.6	1.9	2.2	1.8	2.0
Median	19.9	31.2	34.8	22.1	22.4	20

Thus, taking occupancy time of 0.54 (13 hours daily spent *indoor*), ERD for the studied area is found to be with maximum, average, standard deviation and median of 0.61, 0.1, 0.08 and 0.09 WLM/y, respectively; while a risk of a fatal lung cancer due to lifetime exposure to radon (CR_{Rn}) – with maximum, average, standard deviation and median of 2.13, 0.35, 0.29 and 0.3%, respectively.

If occupancy time is 0.5 (12 hours daily spent *indoor*), the ERD and CR_{Rn} show minimum, maximum, average, standard deviation and median of 0.06, 0.56, 0.09, 0.08 and 0.08 WLM/y, respectively (ERD), and 0.02, 1.97, 0.33, 0.27 and 0.28%, respectively (CR_{Rn} – shown in Fig. 5).

The risk estimated for workers in Khewra Salt Mines (Pakistan), for example, was found to range from 0.24 to 0.43% [13], i.e., with an average (0.33%) comparable with one found for the Montenegrin Coast.

Figure 5: Cancer risk due to exposure to radon – 107 dwellings in the Coastal area of Montenegro (a), by towns (b)



As previously mentioned, lung cancer is the most common in males in Montenegro, and generally appeared as one with the greatest frequency. According to available data for the period from 1978 to 2005, the lung cancer incidence rate increased ~6% annually, and an average (standardized) incidence rate for that period was found to be 20.8 per hundred thousand [12].

The number of diagnosed and treated lung cancers in Montenegro in 2009 was 206, with the incidence rate of 33 per hundred thousand. The patients' age was mostly between 60 and 70 years, with a median of 66 years. Among all the patients, 171 (i.e., 83%) were males; 167 (i.e., 81%) were smokers, and among them 75% were heavy smokers (29 cigarettes daily, during ~29 years).

Diagnosed lung cancers in people from the Coastal area (Table 4) were 48, i.e., 23.3% of the total in Montenegro, with the incidence rate of 38.2/100 000 (somewhat higher than the Montenegro average in 2009). Among these diseased, 8 were from Ulcinj (the incidence rate of 39.42/100 000), 12 from Bar (29.97/100 000), 4 from Budva (25.14/100 000), 3 from Tivat (22.01/100 000), 9 from Kotor (39.16/100 000) and 12 from Herceg Novi (36.32/100 000); i.e., Ulcinj, Kotor and Herceg Novi showed an incidence rate higher than the country average. In regard to histology, these lung cancers were: SCLC (small cell lung cancer) – 7, NSCLC (non-small cell lung cancer, i.e., epidermoid) – 16, adenocarcinoma – 14, mixed (adeno- and epidermoid) – 9, and large cell – 2.

Table 4: Lung cancers diagnosed and treated in 2009.

Town	N	M	F	S	NS	IR
Ulcinj	8	6	2	7	1	39.42
Bar	12	11	1	9	3	29.97
Budva	4	4	0	3	1	25.14
Tivat	3	2	1	3	0	22.01
Kotor	9	7	2	8	1	39.16
H. Novi	12	9	3	10	2	36.32
Total	48	39	9	41	7	38.23

N – number of patients, M – male, F – female, S – smoker, NS – never smoker, IR – incidence rate

Looking at all these findings, although average annual radon concentrations were found to be relatively low, the risk factor for lung cancer due to *indoor* radon exposure with an average of 0.33% is for one or more order of magnitude higher than excess cancer risk due to terrestrial radiation *outdoors* with an average of $0.27 \cdot 10^{-3}$ – obtained from laboratory measurements, and $0.18 \cdot 10^{-3}$ – obtained from direct dose rate measurements at the selected locations.

From a consideration of risk factor for lung cancer due to *indoor* radon exposure in Ulcinj, Kotor and Herceg Novi (19, 6 and 32 measuring points, respectively), minimum, maximum, average, standard deviation and median were found to be around – 0.02, 0.63, 0.26, 0.2, 0.19%, respectively (Ulcinj); 0.14, 0.74, 0.3, 0.23, 0.22%, respectively (Kotor); 0.09, 1.97, 0.31, 0.36, 0.2%, respectively (Herceg Novi).

On the other hand, in Tivat (where, in Plavi Horizonti, the highest excess lifetime cancer risk due to terrestrial radiation was observed), they were – 0.04, 0.36, 0.21, 0.11, 0.22%, respectively.

4 CONCLUSIONS

Among 10 locations on the Coast of Montenegro, the highest excess lifetime cancer risk due to terrestrial radiation *outdoor* was found for Plavi Horizonti (Tivat area), with $ELCR_{out} = 0.79 \cdot 10^{-3}$ (natural radioisotopes only) and $ELCR_{out2} = 0.84 \cdot 10^{-3}$ (natural radioisotopes and ^{137}Cs) – in 51% caused by ^{226}Ra . At the same time, the risk factor for lung cancer due to *indoor* radon exposure was estimated to be from 0.04 to 0.36%, with an average of 0.21% (i.e., lower than the region average), but it should be noted that the total number of *indoor* radon measurements in Tivat was only 6 (and none on the location Plavi Horizonti).

In regard to the risk factor for lung cancer due to *indoor* radon, the highest value was found for Herceg Novi (1.97%). By considering 32 radon measurements, CR_{Rn} is found to be within the range from 0.09

to 1.97%, with an average of 0.31% (slightly lower than for the studied area), while estimated cancer risk due to terrestrial gamma radiation *outdoors* was $ELCR_{out2} = 0.19 \cdot 10^{-3}$.

The areas of Herceg Novi, Kotor and Ulcinj showed the lung cancer incidence rate higher than an average in Montenegro in 2009, and it is important to note that in Kotor, based on 6 radon measurements only, CR_{Rn} is within the range from 0.14 to 0.74%, with an average of 0.3%, as $ELCR_{out2} = 0.29 \cdot 10^{-3}$. In Ulcinj, from 19 radon measurements, CR_{Rn} is in the range from 0.02 to 0.63 %, with an average of 0.26%, and estimated cancer risk due to terrestrial gamma radiation *outdoors* of $ELCR_{out2} = 0.12 \cdot 10^{-3}$.

Therefore, a further research should include the results of additional *indoor* radon measurements in dwellings in Kotor and Tivat, together with considering integrated risk from – radon and terrestrial radiation (*indoor* and *outdoor*). Having in mind epidemiological importance of a situation when mortality and incidence can be considered as approximately equal, mortality studies should also be included in a further comprehensive research.

5 ACKNOWLEDGEMENTS

Funded (project 01-683/2013) by the Ministry of Science of Montenegro.

6 REFERENCES

- [1] MONSTAT, 2012. Statistical Yearbook of Montenegro. Statistical Office of Montenegro (MONSTAT), Podgorica.
- [2] Antovic, N., Vukotic, P., Zekic, R., et al., 2007. Indoor radon concentrations in urban settlements on the Montenegrin Coast. *Radiat. Meas.* 42(9), 1573-1579.
- [3] Antovic, N.M., Svrkota, N., Antovic, I., 2012. Radiological impacts of natural radioactivity from soil in Montenegro. *Radiat. Prot. Dosim.* 148(3), 310-317.
- [4] UNSCEAR, 2000. Sources and Effects of Ionizing Radiation. Annex B: Exposure from natural radiation sources. United Nations Scientific Committee on the Effects of Atomic Radiation, Report to the General Assembly of the United Nations with Scientific Annexes, United Nations, New York.
- [5] Senthilkumar, G., Raghu, Y., Sivakumar, S., et al., 2014. Natural radioactivity measurement and evaluation of radiological hazards in some commercial flooring materials used in Thiruvannamalai, Tamilnadu, India. *J. Radiat. Res. Appl. Sci.* 7(1), 116-122.
- [6] Kapdan, E., Varinlioglu, A., Karahan, G., 2011. Radioactivity levels and health risks due to radionuclides in the soil of Yalova, northwestern Turkey. *Int. J. Environ. Res.* 5(4), 837-846.
- [7] Taskin, H., Karavus, M., Ay, P., et al., 2009. Radionuclide concentrations in soil and lifetime cancer risk due to gamma radioactivity in Kirklareli, Turkey. *J. Environ. Radioact.* 100(1), 49-53.
- [8] ICRP, 1991. The 1990 Recommendations of the International Commission on Radiological Protection. ICRP Publication 60. Ann. ICRP 21(1-3).
- [9] EPA, 2003. EPA Assessment of Risk from Radon in Homes, Washington, DC: Environmental Protection Agency; EPA 402-R03-003, USA;
<http://www.epa.gov/radiation/docs/assessment/402-r-03-003.pdf>
- [10] ICRP, 2009. Recommendations of the International Commission on Radiological Protection. Press Release, ref: 00/902/09.
- [11] UNSCEAR, 2006. Sources and Effects of Ionizing Radiation. Annex E: Sources-to-effects assessment for radon in homes and workplaces. United Nations Scientific Committee on the Effects of Atomic Radiation, Report to the General Assembly of the United Nations with Scientific Annexes, United Nations, New York.
- [12] Živković, D., 2009. Effect of delays on surviving patients with lung carcinoma. *PhD thesis*, Faculty of Medicine, University of Belgrade (in Serbian).
- [13] Baloch, M.A., Qureshi, A.A., Waheed, A., et al., 2012. A study on natural radioactivity in Khewra Salt Mines, Pakistan. *J. Radiat. Res.* 53, 411-421.

A Survey of Indoor Gamma Dose Rates in Selected Dwellings and Offices in Abeokuta, South Western Nigeria

Okeyode, I.C.^{a*}, Oladotun, I.C.^a, Mustapha, A.O.^a, Alatise, O.O.^a, Bada, B.S.^b, Makinde V.^a, Akinboro, F.G.^a, Al-Azmi, D.^c

^aDepartment of Physics, Federal University of Agriculture, Abeokuta, P.M.B. 2240 Abeokuta, Nigeria

^bDepartment of Environmental Management and Toxicology, Federal University of Agriculture, Abeokuta, P.M.B. 2240 Abeokuta, Nigeria

^cDepartment of Applied Sciences, College of Technological Studies, Public Authority for Applied Education and Training, Shuwaikh, P. O. Box: 42325, Code 70654, Kuwait

Abstract. An indoor gamma dose rate survey was conducted in selected dwellings and offices around Abeokuta, South Western Nigeria. Absorbed dose rates were measured using Gamma RAE II R (RAE Systems) a CsI-based dosimeter. At each location six measurements were taken every five minutes with the dosimeter held at one meter above the floor and the mean (over 30 minutes) was considered to be the indoor gamma dose rate in that part of the building. The absorbed dose rates in the surveyed buildings varied from $0.077 \pm 0.008 \mu\text{Sv/h}$ to $0.397 \pm 0.019 \mu\text{Sv/h}$ and the overall mean was $0.201 \pm 0.014 \mu\text{Sv/h}$, which is more than twice the world population-weighted average indoor absorbed dose rate ($0.059 \mu\text{Sv/h}$). The absorbed dose rates in mud buildings were higher than in cement-block buildings, and higher absorbed dose rates were encountered inside houses built on rock outcrops compared to those erected/built on soil. The calculated annual effective dose in the study area (assuming 0.8 indoor occupancy factor) ranges from 0.540 to 2.782 mSv with an average value of $1.406 \pm 0.521 \text{mSv}$ which is 3.4 times the world population-weighted average value (0.41mSv) and also higher than the recommended dose limit (1.0mSv/yr) for the general public.

KEYWORDS: *indoor gamma; houses and offices.*

1 INTRODUCTION

Exposure of human beings to ionizing radiation arises from natural and artificial sources. Exposure to natural source of ionizing radiation is a continuing and inescapable feature of life on earth since they have always been part of the human's natural environment. The main components of human exposure to natural sources of radiation include external irradiation from cosmic rays and terrestrial gamma rays, internal irradiation from radionuclides ingested, and from the decay products of radon isotopes inhaled (Quindos *et al*, 1991). External exposure to gamma ray can occur outdoors as well as indoors. Indoor exposures depend on concentrations of the radionuclides in the soil under and outside the building as well as the building materials (UNSCEAR, 2000). Many comprehensive studies of indoor and outdoor gamma exposures have been carried out in many parts of the world (UNSCEAR, 2000; Boucher, 2008). Measurements of the outdoor gamma radiation doses have also been carried out in Abeokuta, Nigeria (Farai and Vincent, 2006; Okeyode *et al*, 2012). Farai and Vincent (2006) used Thermoluminescent Dosimetry and reported effective doses due to outdoor exposure in the city range between 0.19 to 1.64 mSv/yr with a mean of 0.45 mSv/yr. However, no report has been found on the indoor gamma dose rates in Abeokuta.

In the present study, the indoor gamma doses received by the population of Abeokuta were determined considering the types of dwellings/houses, ventilation and geology. The radiological consequences of indoor gamma doses to dwellers and office workers were also estimated.

2 MATERIALS AND METHODS

2.1 Location and Geology of Study Area

The study area Abeokuta is located in the sub-humid tropical region of Southwestern Nigeria situated between coordinates: 7°9'39"N, 3°16'54"E latitude and longitude and 7°13'N, 3°25'E. The city has tropical climate with distinct wet and dry seasons. The city is underlain by crystalline pre-Cambrian basement complex rock of igneous and metamorphic origin noted for their rather poor ground-water bearing properties and high contents of natural radioactive elements. The undulating terrain is known for scattered mass of grey granite with its geology being underlain by migmatitic gneiss and granitic gneiss and coarse porphyritic granite. Migmatitic gneiss rocks cover only very limited areas while granitic gneiss cover the most extensive terrain of the area, at the center of which we have Olumo rock, a famous tourist center.

2.1.1 Selection of Location/Measurement Sites

The selection of houses was random (Sivakumar *et al.*, 2002) and at most 4 rooms in each location – (houses and offices) were chosen for the measurement. The types of dwellings where the measurement took place include bungalow, storey buildings, and semi-detached houses. The buildings were made from mud (bricks) and cement blocks, and they were either built on soil or rock outcrops. A total of 79 living rooms, 2 dining rooms, 32 bedrooms, 58 kitchens and 56 office rooms were considered in the survey. The detector used is a sensitive Cesium Iodide (CsI) scintillation based dosimeter - Gamma RAE II R. It is a portable instrument that has a gamma-ray detector and dosimeter in a single unit.

2.1.2 Absorbed Dose Rate Measurements

The survey meter (GAMMARAE II R) was held on a tripod stand (Hazrati *et al.*, 2010) one meter above the floor (Mahmoud *et al.*, 2014; Gholami *et al.*, 2011). The detector on the tripod stand was placed at the center of the rooms and at distances of at least 1 meter from the side walls where the rooms had large space (Hong Kong Observatory, 1999). Readings of absorbed dose rates were taken every 5 minutes for 30 minutes at each location. A total exposure time of 30 minutes was considered in each measurement (Gholami *et al.*, 2011; Saghatchi *et al.*, 2009). The mean of all recorded data in each building were computed and considered as indoor absorbed dose value of the location (Mahmoud *et al.*, 2014; Jibiri and Obarhua, 2013; Bahreyni *et al.*, 2008) and the dose rates acquired were statistically tested (Bahreyni *et al.*, 2008).

2.1.3 Effective dose Calculation

The measured gamma radiation absorbed dose in $\mu\text{Sv}/h$ was converted to effective dose equivalent ($m\text{Sv}/y$) to assess the radiological consequence of the indoor exposure using the following equations (Sadiq and Agba, 2012):

$$H_E (m\text{Sv}/y) = D_{in} \times T \times OF_{in} \times 10^{-3} \quad (1)$$

and

$$H_E (m\text{Sv}/y) = D(\mu\text{Sv}/h) \times (24 \times 365) \text{ hr}/\text{yr} \times 0.8 \times 10^{-3} \quad (2)$$

where $D(\mu\text{Sv}/h)$ is the dose rate in the indoor air, T is the time in hours for a year, OF_{in} is the occupancy factor indoor; 0.8 for indoor and 0.2 for outdoor (UNSCEAR, 2000), and H_E effective dose equivalent (Hazrati *et al.*, 2012; Jibiri and Okeyode, 2011; Mahmoud *et al.*, 2014).

2.1.4 Analysis of Data

Data obtained were subjected to descriptive (mean and standard deviation) and Inferential Statistics (ANOVA). Means were separated using Duncan Multiple Range Test.

2.2 RESULTS

The average absorbed dose rates, the calculated corresponding human effective dose and the number of people per dwelling and offices for each of the study area are shown in table 1 below

Table 1: Average absorbed dose, Human Effective dose equivalent and number of people per dwelling and offices.

DWELLINGS	LATITUDE	LONGITUDE	Din ($\mu\text{Sv/h}$)	He (mSv/y)	N
HOKEM1	7°7'16.57"	3°23'23.97"	0.195±0.033	1.367	4
HONI1	7°7'6.78"	3°20'20.32"	0.1±0.014	0.701	6
HIBA1	7°7'39.78"	3°20'56.27"	0.137± 0.005	0.96	4
HADI1	7°7'54.51"	3°19'2.92"	0.119±0.007	0.834	3
HLEM1	7°8'13.52"	3°22'8.96"	0.294±0.017	2.06	2
HOJE1	7°6'33.09"	3°20'4.28"	0.153±0.014	1.072	3
HADI2	7°7'36.07"	3°19'13.41"	0.108± 0.004	0.757	5
HITA1	7°11'14.64"	3°21'31.48"	0.259±0.024	1.815	3
HADI3	7°7'2.68"	3°18'43.13"	0.166±0.008	1.163	5
HKOT1	7°10'58.42"	3°25'26.23"	0.302±0.023	2.116	6
HIBA2	7°7'25.06"	3°20'48.95"	0.148±0.013	1.037	3
HLEM2	7°7'40.43"	3°22'13.31"	0.153±0.008	1.072	2
HADI4	7°7'5.69"	3°19'15.93"	0.123±0.007	0.862	4
HOBA1	7°10'55.9"	3°23'47.76"	0.288±0.021	2.018	1
HOKEM2	7°7'36.36"	3°22'53.79"	0.259±0.057	1.815	5
HONI2	7°7'4.67"	3°20'9.03"	0.112±0.005	0.785	3
HITA2	7°11'57.98"	3°21'3.64"	0.241±0.005	1.689	4
HADI5	7°6'37.04"	3°19'8.47"	0.104±0.006	0.729	5
HIBA3	7°7'15.31"	3°20'28.11"	0.195±0.019	1.367	3
HOLOK	7°7'12.63"	3°20'44.12"	0.276±0.029	1.934	2
HOBA2	7°10'31.3"	3°24'11.87"	0.331±0.016	2.32	3
OLAF	7°9'45.63"	3°18'53.18"	0.094±0.005	0.659	3
HITAK	7°8'28.06"	3°19'34.54"	0.118±0.01	0.827	1
OOKEI1	7°8'3.35"	3°20'18.86"	0.269±0.005	1.885	6
HKOT2	7°10'51.27"	3°25'52.05"	0.237±0.005	1.661	2
HOBA3	7°10'35.37	3°24'7.66"	0.211±0.024	1.479	3
HISO	7°12'36.17"	3°26'41.42	0.237±0.005	1.661	1
HELE	7°11'7.71"	3°25'20.5"	0.291±0.028	2.039	3
HCAM1	7°11'15.28"	3°26'9.29"	0.263±0.005	1.843	1
HCAM2	7°11'4.73"	3°26'14.33"	0.237±0.005	1.661	1
HIBA4	7°7'37.14"	3°20'15.97"	0.143±0.035	1.002	4
HAKI	7°8'45.42"	3°19'35.98"	0.178±0.007	1.247	5
HOKEM3	7°7'14.1"	3°23'18.88"	0.146±0.015	1.023	6

Table 1 (contd): Average absorbed dose, Human Effective dose equivalent for the dwellings and number of people per dwelling.

DWELLINGS	LATITUDE	LONGITUDE	Din ($\mu\text{Sv/h}$)	He (mSv/y)	N
HLEM3	7°8'4.13"	3°21'44.08"	0.276±0.033	1.934	3
OALA1	7°13'41.69"	3°26'14.84"	0.257±0.005	1.801	3
OALA2	7°13'39.41"	3°26'12.98"	0.214±0.007	1.5	1
OALA3	7°13'55.05"	3°26'30.54"	0.155±0.005	1.086	1
HASE1	7°10'47.59"	3°22'39.38"	0.237±0.015	1.661	1
HASE2	7°10'39.6"	3°22'52.54"	0.144±0.015	1.009	5
HLEAF	7°9'43.79	3°18'30.03"	0.083±0.014	0.582	3
HOLO1	7°8'27.04"	3°18'27.57"	0.087±0.008	0.61	5
OALA4	7°13'57.09"	3°26'11.04"	0.197±0.005	1.381	2
OITAK	7°8'24.73"	3°19'51.98"	0.163±0.707	1.142	4
HIDI	7°8'22.12"	3°22'6.95"	0.284±0.032	1.99	8
OIDI1	7°8'39.64"	3°22'8.89"	0.29±0.024	2.032	6
HOLO2	7°8'51.82"	3°18'28.11"	0.082±0.014	0.575	3
HOLO3	7°8'50.32"	3°18'28.92"	0.077±0.008	0.54	4
HOLO4	7°9'4.2"	3°18'10.05"	0.126±0.005	0.883	4
HOLO5	7°9'4.81"	3°18'27.76"	0.092±0.004	0.644	5
HIYA1	7°8'35.59"	3°21'41.73"	0.185±0.013	1.296	6
HIYA2	7°8'35.49"	3°21'42.48"	0.289±0.039	2.025	3
HOBA4	7°10'47.21"	3°23'50.33"	0.268±0.027	1.878	4
HOJE2	7°5'23.27"	3°19'25.11"	0.145±0.005	1.016	4
HOJE3	7°5'23.95"	3°19'26.26"	0.14±0.006	0.981	1
HIJE1	7°9'47.34"	3°20'49.52"	0.192±0.024	1.346	11
HIJE2	7°9'59.13"	3°20'48.65"	0.395±0.039	2.768	1
OOKEM1	7°7'5.07"	3°22'5.98"	0.193±0.028	1.353	6
OARO	7°7'46.04"	3°17'40.2"	0.098±0.004	0.687	5
HAIDI1	7°8'15.74"	3°22'39.78"	0.196±0.005	1.374	6
HAIDI2	7°8'15.97"	3°22'38.57"	0.299±0.014	2.095	4
OOKEI2	7°8'10.19"	3°20'10.45"	0.136±0.005	0.953	3
HOKE1	7°10'59.03"	3°21'10.21	0.397±0.019	2.782	1
HOKE2	7°11'0.72"	3°21'11.71"	0.261±0.013	1.829	7
HOKE3	7°11'9.02"	3°21'14.72"	0.18±0.006	1.261	4
HOKE4	7°11'2.45"	3°21'5.91"	0.257±0.022	1.801	4
HTIDI1	7°9'0.15"	3°22'20.18"	0.136±0.007	0.953	3
HELI	7°9'7.33"	3°22'40.8"	0.121±0.012	0.848	4
HOKE5	7°11'0.72"	3°21'11.71"	0.248±0.012	1.738	3
HOKE6	7°10'59.71"	3°21'11.55"	0.298±0.034	2.088	2
HOKE7	7°11'0.69"	3°21'11.58"	0.261±0.011	1.829	4
HOKE8	7°10'54.08"	3°21'10.6"	0.217±0.025	1.52	4
HISA1	7°9'53.07"	3°22'6.4"	0.363±0.018	2.544	1
HALA1	7°14'30.09"	3°26'37.39"	0.248±0.01	1.738	5

Table 1 (contd): Average absorbed dose, Human Effective dose equivalent for the dwellings and number of people per dwelling contd.

DWELLINGS	LATITUDE	LONGITUDE	Din ($\mu\text{Sv/h}$)	He (mSv/y)	N
HALA2	7°14'30.28"	3°26'37.39"	0.257±0.008	1.801	1
HOSI1	7°10'38.51"	3°27'58.28"	0.3±0.006	2.102	4
HOSI2	7°10'37.11"	3°28'0.14"	0.263±0.005	1.843	5
HOSI3	7°10'38.77"	3°27'59.46"	0.212±0.008	1.486	4
HOSI4	7°10'40.13"	3°28'3.79"	0.25±0.006	1.752	1
HALA3	7°14'30.32"	3°26'37.26"	0.182±0.008	1.275	1
HALA4	7°14'30.35"	3°26'36.77"	0.243±0.005	1.703	3
HALA5	7°14'12.92"	3°26'12.62"	0.208±0.008	1.458	2
HALA6	7°14'12.82"	3°26'12.2"	0.212±0.004	1.486	1
HALA7	7°14'12.66"	3°26'11.97"	0.223±0.005	1.563	1
HALA8	7°14'12.46"	3°26'11.77"	0.235±0.01	1.647	1
HTIDI2	7°9'7.02"	3°22'16.15"	0.257±0.003	1.801	3
OITO	7°9'26.47"	3°20'42.59"	0.178±0.012	1.247	16
OOKEJ	7°9'44.02"	3°20'48.28"	0.276±0.078	1.934	20
OITOK	7°10'9.22"	3°20'49.79"	0.251±0.062	1.759	30
OOKEM2	7°7'3.09"	3°22'8.68"	0.182±0.022	1.275	7
HISA2	7°9'52.55"	3°22'6.17"	0.224±0.006	1.57	3
OIBA1	7°7'15.53"	3°20'43.47"	0.149±0.009	1.044	3
OIDI2	7°8'39.36"	3°22'35.69"	0.192±0.033	1.346	1
OPAN	7°7'58.74"	3°19'51.96"	0.145±0.008	1.016	3
OIBB	7°8'20.46"	3°20'44.01"	0.086±0.006	0.603	10
OIBA2	7°7'21.11"	3°20'22.67"	0.107±0.005	0.75	5
OIDI3	7°8'28.82"	3°22'12.89"	0.241±0.008	1.689	4
OONI	7°7'56.49"	3°20'0.33"	0.109±0.01	0.764	3
OQUA	7°8'16.37"	3°19'40.56"	0.162±0.017	1.135	9
OAKI	7°8'34.42"	3°19'25.48"	0.104±0.007	0.729	2
OOLO	7°8'45.35"	3°18'50.83"	0.093±0.014	0.652	5
OIJE	7°8'39.63"	3°20'8.42"	0.142±0.004	0.995	3

3 DISCUSSION

A total number of 75 houses were studied and the average minimum and maximum indoor dose rates were obtained to be $0.077\pm 0.008\mu\text{Sv/h}$ and $0.397\pm 0.019\mu\text{Sv/h}$ with an average value of $0.210\pm 0.014\mu\text{Sv/h}$. A total number of 26 offices were studied and the average minimum and maximum indoor dose rates in offices were obtained to be $0.094\pm 0.005\mu\text{Sv/h}$ and $0.290\pm 0.024\mu\text{Sv/h}$ with an average value of $0.172\pm 0.042\mu\text{Sv/h}$. The average absorbed dose rate in indoor air of the study areas in Abeokuta for all 101 dwellings was $0.210\mu\text{Sv/h}$ which was higher than the value for the worldwide average indoor absorbed dose rate in air of $0.059\mu\text{Sv/h}$ (UNSCEAR, 2000).

The human effective dose equivalent in Abeokuta ranges from 0.540 to 2.782 with the average value of 1.406 which was 3.4 times the worldwide average reported value of 0.41 for indoor human effective dose equivalent (UNSCEAR, 2000), also higher than the ICRP (1999) recommended value of 1 for exposure to members of the public.

The locations with lowest values of indoor absorbed dose *for offices* included Lafenwa (OLAF), Aro (OARO), Olomore (OOLo), Housing Ibara (OIBA2), Akin Olugbade (OAKI), IBB Boulevard (OIBB), and locations with highest values were Idi- Aba (OIDI), some parts of OkeIlewo (OOKEI1) and Alabata (OALA).

For houses, locations with lowest values were Onikolobo (HONI), Olomore (HOLO), Lafenwa (HLAF), Adigbe (HADI), Idi- Aba (HIDI), Housing Ibara (HIBA), Akin Olugbade (HAKI), and locations having highest values were Idi- Aba, Abule Nla (HAIDI), Oloke (HOLOK), Eleweran (HELE), Obantoko (HOBA), some parts of OkeMosan (HOKEM) and Leme (HLEM1).

From the Duncan Multiple Range Test, levels of gamma ray as affected by:

3.1 Types of house building materials

(Block and Mud) types of house building materials (Block and Mud) at time intervals from the 5th minute to the 30th minute shows no significant difference in gamma radiation values at all-time intervals. It was observed that there was no particular increase or decrease in the gamma ray values for the Block or the mud houses with time.

Although, the mean values of the mud houses are slightly higher than the block houses. The building construction type influences the total background gamma radiation: either by absorbing radiation coming from outdoors and/or by contributing from the radionuclides contained in the construction materials (Boucher, 2008). This was observed in two houses located at Abule-Nla, Idi-Ababa, the bungalows were built side by side, but had different gamma values, HAIDI2 (0.28-0.33 μ Sv/h) had higher gamma reading than HAIDI1 (0.19-0.20 μ Sv/h).

Also for levels of gamma ray as affected by types of houses (bungalow and storey houses), ($P > 0.05$), but mean values of the storey houses are slightly higher than the bungalow houses.

3.2 Terrain/Geology

The terrain of Abeokuta is characterized by two types of landforms: sparsely distributed low hills and knolls of granite, other rocks of the basement complex and nearly flat topography (Adekunle *et al.*, 2013). Major parts of Abeokuta lies within the Basement Complex rocks. The rocks are Coarse-porphyrific biotite and biotite, Biotite garnet gneiss and schist, sandstone and limestone, Porphyroblastic gneiss and Migmatite. Places like Obantoko (HOBA), Camp (HCAM), Isolu (HISO), Eleeweran (HELE), Alabata (HALA/OALA) fall within the Migmatite rock formation and since the radiation content of migmatite (metamorphosed igneous) rock is high, indoor gamma readings were seen to be high (from 0.23-0.35 μ Sv/h) as expected and reported (Jibiri and Famodimu, 2013; Farai and Vincent, 2006). Sandstone and Limestone rock formation have low level of radiation and hence places like Lafenwa (OLAF/HLAF), Olomore (HOLO/OLOO), Aro (OARO), Onikolobo (0.06-0.13 μ Sv/h) have low level of radiation. When type of house/office, building materials and terrain were compared, it was observed that there was no particular pattern of increase or decrease in the gamma radiation values for the block or the mud houses with time. For example, HIJE2, the house was directly built on the rock and the gamma readings were high (0.35-0.44 μ Sv/h) and it was observed that some buildings built on the rock and with block didn't give high gamma readings; places like Ijemo, HIJE1 (0.16-0.20 μ Sv/h), OITO, Itoku (0.16-0.19 μ Sv/h). This may be due to the fact that the block reduced the amount of indoor gamma radiation as the outdoor values were higher, over 0.30 μ Sv/h. At Itoko, OITOK a block of office (0.16-0.17 μ Sv/h) had a lower gamma value than the other offices that were also built on rock outcrops but were mud buildings with cement plastering (0.26-0.32 μ Sv/h); a set of offices at Oke Ijemo (OOKEJ), mud building with cement plastering, also had a high gamma reading (0.31-0.35 μ Sv/h).

3.3: Ventilation

In rooms of poor ventilation, the dose rate was very high. This was observed in Office rooms that have smaller spaces and also in houses, mostly in the kitchen. Ventilation and accumulated higher levels of radiation in indoor environments and larger ventilators provided in a building may reduce the levels of gamma radiation in the air.

Since exposures to natural radiation sources are more significant to the world's population than most exposures to man-made sources, the natural background baseline indoor gamma radiation in Abeokuta dwellings is worth evaluating in details.

4 CONCLUSION

The average absorbed dose rate in the indoor air of the study areas of Abeokuta is 0.210 $\mu\text{Sv/h}$ which is higher than 0.059 $\mu\text{Sv/h}$ of the worldwide average indoor absorbed dose rate in air. The human effective dose equivalent of the study areas ranges from 0.540 to 2.782 with the average value as 1.406, which is 3.4 times the worldwide average reported value of 0.41 for indoor human effective dose equivalent (UNSCEAR, 2000). The human effective dose equivalent of the study areas is also higher than the ICRP, 1999 recommended value of 1 for exposure to the public. The highest values of gamma radiation in Abeokuta were detected in areas where the dwellings were built on rock outcrops, some mud type constructions, some particular building materials, poor ventilated dwellings, and areas of elevated radiation level.

Statistical analysis confirms higher gamma values in buildings on rock outcrops than those on leveled soil, storey or built with block. The areas of elevated radiation level were observed in Obantoko (HOBA), Elewera (HELE), Kotopo (HKOT) which agree with previous work and low areas included Olomore (HOLO/OOLO), Onikolobo (HONI), Akin Olugbade (OAKI/HAKI), and Lafenwa (HLAF/OLAF). From the gamma radiation values obtained, Abeokuta is an area of high natural radiation background due to its igneous rocks such as granitic rocks and sands (UNSCEAR 2000). The obtained results of the study could serve as an important baseline radiometric data for future epidemiological studies and monitoring initiatives in the study area.

5 REFERENCES

- [1] Adekunle A., Badejo A. and Oyerinde A. 2013. Pollution Studies on Ground Water Contamination: Water Quality of Abeokuta, Ogun State, South West Nigeria. *Journal of Environment and Earth Science*, 3(5): 161-166.
- [2] Bahreyni T. M. T., Bayani S., Abdolrahimi M. R. and Sazgarnia A. 2008. First Report of Environmental Gamma Radiation Levels in Twenty Four Towns and Cities of Khorasan Region-Iran. *Journal of Nuclear Science and Technology*, 5:602-605.
- [3] Bajwa B.S., Singh H., Singh J., Singh S. and Vivek W. 2008. A Combination study of indoor Radon and Gamma Radiation levels in Tusham Ring Complex. *Radiation Measurements* 43: 475-478, Elsevier BV.
- [4] Boucher, M. 2008. External background radiation in the Fribourg (Switzerland) urban area. A PhD Thesis 1599, l'Université de Fribourg (Suisse), Canada. 225pp.
- [5] Farai I.P. and Vincent U.E. 2006. Outdoor Radiation Level Measurement in Abeokuta, Nigeria by Thermoluminescent Dosimetry. *Nigerian Journal of Physics*, 18(1): 121-126
- [6] Frittelli L. 1988. Difficulties in using the objective health detriment as an indicator of the radiation harm in a population, International Radiation Protection Association, Sydney, Australia, 1: 32-35. ENEA - ROMA - Italy.
- [7] Gholami M., Mirzaei S. and Jomehzadeh A. 2011. Gamma background radiation measurement in Lorestan province, Iran. *Iran Journal Radiation Res.*, 9(2): 89-93.

- [8] Hazrati S., Sadeghi H., Amanim M., Alizadeh B., Fakhimi H. and Rahimzadeh S. 2010. Assessment of Gamma dose rate in indoor environments in selected districts of Ardabil Province, Northwestern Iran. *International Journal of Occupational Hygiene*, 2(1): 42-45.
- [9] Hazrati S., Baghi A. N., Sadeghi H., Barak M., Zivari S. and Rahimzadeh S. 2012. Investigation of natural effective gamma dose rates case study: Ardebil Province in Iran. *Iranian Journal of Environmental Health Sciences & Engineering*, 9:1.
- [10] Hong Kong Observatory, 1999. Environmental gamma absorbed dose rate in air in Hong Kong. Environmental radiation monitoring in Hong Kong, Technical Report No.17. 32pp.
- [11] ICRP (International Commission on Radiological Protection), 1999. Recommendations of the International Commission on Radiological Protection, Publication 82. <http://www.icrp.org/publication>.
- [12] Jibiri N. N. and Famodimu J. B. 2013. Natural background radiation dose rate levels and incidences of reproductive abnormalities in high radiation area in Abeokuta, Southwestern Nigeria. *Journal of Natural Science*, 5(11): 1145-1153.
- [13] Jibiri N. N. and Obarhua S. T. U. 2013. Indoor and Outdoor Gamma dose rate exposure levels in major Commercial building material distribution outlets and their Radiological Implications to Occupants in Ibadan. *Journal of Natural Sciences Research*, 3(3): 25-32.
- [14] Jibiri, N.N. and Okeyode I.C. 2011. Activity concentrations of natural radionuclides in the sediments of Ogun River, Southwestern Nigeria. *Rad. Protection Dosimetry*, 147(4):555-564.
- [15] Mahmoud P.A., Aghajani M., Nabipour I. and Assadi M. 2014. Annual Effective Dose from Environmental Gamma Radiation in Bushehr City. *Journal of Environmental Health Sciences & Engineering*, 12:4.
- [16] Okeyode I.C., Akinboro F.G., Makinde V., Towolawi G.B and Mustapha A.O (2012). Absorbed Dose Rates Above Soils and Rock Outcrops in Selected Areas of Abeokuta, Nigeria. *Journal of Natural Sciences, Engineering and Technology*, Vol.11(2), pp 66-72.
- [17] Quindos L. S., Fernandez P. L., Soto J. and Rodenas C. 1991. Terrestrial Gamma Radiation levels Outdoors in Cantabria, Spain. *Journal Radiological Protection*, 11(2): 127-130.
- [18] Reddy M. S., Reddy C. G., Reddy P. Y. and Reddy K. R. 2010. Study of Natural background Gamma radiation levels in Hyderabad and its surroundings, Andhra Pradesh, India. *Indian Journal of Pure and Applied Physics*, 48: 778-781.
- [19] Sadiq A. A. and Agba E. H. 2012. Indoor and Outdoor Ambient Radiation levels in Keffi, Nigeria. *Facta Universitatis Series: Working and Living Environmental Protection*, 9(1): 19-26.
- [20] Saghatchi F., Eslami A. and Salouti M. 2009. Assessment of Indoor Gamma radiation and related Annual Effective dose in Zanjan, Iran. *Iran. Journal Health & Environment*, 2(2): 88-93.
- [21] Sivakumar R., Selvasekarapandian S., Mugunthamanikandan N. and Raghunath V.M. 2002. Indoor gamma dose measurements in Gudalore (India) using TLD. *Applied Radiation and Isotopes*, 56: 883-889.
- [22] UNSCEAR (United Nations Scientific Committee on the Effects of Atomic Radiation), 2000. Annex- B, Exposure from natural radiation sources, New York. pp83-156.

Natural radioactivity of samples from the building industry in South Africa

I. Ramathape^{*}, D. Kotze, I. Louw

NECSA, P.O. Box 582, Pretoria 0001, Republic of South Africa.

Abstract. Knowledge of radioactivity levels of materials used in the building industry is important in the assessment of possible radiological hazards to human health. This knowledge is essential for the development of standards and guidelines for the use and management of these materials. The radioactivity of building material has been assessed by many authors in different countries and usually involves the measurement of the activity concentration of ^{232}Th , ^{226}Ra and ^{40}K by gamma spectrometry. Almost no data on the levels of natural radioactivity of building material in South Africa have been published. Standards and guidelines with regard to acceptable levels of natural radioactivity in building material are also not specifically defined by the regulatory authority in South Africa. The radio-analytical laboratory of the South African Nuclear Energy Corporation (RadioAnalysis) routinely performs analysis of naturally occurring radioactive materials (NORMs) in a variety of matrices. Several samples from various role players in the building industry have been analyzed over the last decade, including cement, fly-ash, slag, gypsum, phosphogypsum, industrial wastes, bricks and clay. These results will be presented here with the specific aim to evaluate whether the building industry, and more specific the cement manufacturing industry in South Africa, falls within the scope of regulatory control. The results were evaluated against the provisions of the South African National Nuclear Regulator Act, which applies for nuclide activity values above the 500 Bq/kg level, as well as the European radioactivity index. Use of radiochemical methods create the opportunity to analyze for and evaluate the exposure due to high radiotoxic nuclides like ^{210}Po otherwise overlooked by the instrumental techniques. Use of the results for ^{232}Th obtained by Instrumental Neutron Activation Analysis (INAA) in the radioactivity index may result in an underestimation of the risk in samples enriched in ^{228}Ra as was found for South African gypsum samples.

KEYWORDS: NORMs; radiochemical methods; INAA; Activity Concentration Index (ACI).

1 INTRODUCTION

In order to assess the possible radiological risks to human health due to living in buildings, it is required to measure the radioactivity levels in building materials. The strategy for reducing radiological risk to humans is through careful pre-selection of low-background building materials. This implies that material used in the building industry should be analyzed for radioactivity before being used for building purposes.

The major concern currently in South Africa is that data on levels of natural radioactivity of building materials are not freely available because standards and guidelines with regard to acceptable levels are not specifically defined by the regulatory authorities. On the contrary, a European working group of experts examined the issue of regulatory control of building materials and developed guidance documents which were published by the European Commission [5], and countries such as China, Poland, Austria, Israel, the Czech Republic, Russia and Finland formulated their own standards for regulatory purposes [7].

The South African Government, released notice R849 specifying that any person dealing with materials that contain radioactivity should apply to the National Nuclear Regulator (NNR) for a nuclear license [1]. In terms of regulation R388 any material with a radioactivity content of less than 500 Bq/kg per individual nuclide are exempted from legislation [2]. Solid materials from various origins, including building material, are evaluated using these criteria. At a recent meeting of the South African Radiation Protection Association (SARPA) the NNR recommended that the control of building materials and radon emanation be investigated [3].

Cement is widely used in the building industry for construction purposes and the radioactivity in cement may contribute to external exposure in buildings. A selection of cement and their raw materials from the main cement manufacturers in South Africa were analysed for NORMs to assess whether the cement manufacturing industry falls within the scope of regulatory control. The data in this paper was obtained from analysis, of various samples of material often used in the building industry submitted to RadioAnalysis over a period of 10 years. Samples were analyzed for ^{226}Ra , ^{232}Th , ^{40}K in materials such as cement, concrete, gypsum, phosphogypsum, fly-ash and slag. Results for other natural radionuclides in selected samples from the cement industry in South Africa were previously reported [4].

Methods such as gross alpha and beta screening, elemental techniques, radiochemical, INAA and instrumentation techniques can be used to determine the activity concentrations in building materials. RadioAnalysis has the capability of applying most of these methods. A South African standard on building materials should clearly indicate the analysis approach, assessment of radiation and dose criterion.

The use of radiochemical methods creates the opportunity to analyse and evaluate dose due to high radiotoxic nuclides like ^{210}Po , ^{231}Pa and ^{227}Ac . To investigate the possibility of using a radiochemical method for analyses of samples from the building industry, selected samples were digested by using microwave dissolution and analysed ^{232}Th and ^{228}Th using a suitable radiochemical method. Results obtained with closed vessel microwave dissolution and subsequent radiochemical analyses were compared with results from instrumental techniques such as Instrumental Neutron Activation Analysis (INAA) and gamma spectrometry. No screening for gross alpha/beta activities in building materials was done.

1.1 Radiological hazard calculations

A number of studies have been conducted over the years on building materials such as cement, tiles and other types of building material, to analyze their radioactivity content for probable hazard exposure to public. There are two concepts which are evaluated in order to assess the radiological hazards of radioactivity in building materials based on activities of ^{226}Ra , ^{232}Th and ^{40}K , namely; activity concentration index or gamma index (ACI or I) and radium equivalent concentration index (Raeq). Of course, the indexes can be expressed further and manipulated to deduce the internal and external hazard indexes for doses below 1 mSv per annum.

1.1.1 Activity concentration index (ACI) or gamma index (I)

The activity concentration of ^{226}Ra (^CRa), ^{232}Th (^CTh) and ^{40}K (^CK) measured results in Bq/kg can be used to calculate indexes for specific building material which are evaluated against the acceptable dose criterion. Equation (1) derives the activity concentration index [5]. Table 1 below shows the dose criterions acceptable for calculated activity concentration indexes.

$$ACI = \frac{C_{Ra}}{300\text{Bq / kg}} + \frac{C_{Th}}{200\text{Bq / kg}} + \frac{C_K}{3000\text{Bq / kg}} \quad (1)$$

Table 1: Dose criterion

Dose Criterion	0.3 mSv/a	1 mSv/a
Materials used in bulk amounts, e.g. concrete, cement	$ACI \leq 0.5$	$ACI \leq 1$
Superficial and other materials with restricted use: tiles, boards, etc.	$ACI \leq 2$	$ACI \leq 6$

Countries apply this dose criterion to establish indexes and limits for indoor and outdoor exposures as recommended by the European Commission [5]. For instance, many countries have established standards which apply totally the same activity concentration indexes to comply with the 0.3 – 1 mSv/a dose criterion [7]. Likewise, South Africa should establish regulatory control for materials that give rise to doses of between 0.3 mSv and 1 mSv per annum, and those above 1 mSv per annum should be regulated. If the upper dose of 1 mSv per annum was exceeded by a particular building material authorities should make appropriate decision or provision on measurement controls to take.

1.1.2 Radium equivalent (Ra_{eq}) activity

The radium equivalent (Ra_{eq}) activity, shown as equation 2 below, is used to assess radiation hazards by taking into consideration the specific radioactivity concentration of ^{226}Ra , ^{232}Th and ^{40}K in a common index:

$$Ra_{eq} = C_{Ra} + 1.43 \cdot C_{Th} + 0.077 \cdot C_K \quad (2)$$

Where C_{Ra} , C_{Th} , and C_K are specific activity concentrations of ^{226}Ra , ^{232}Th and ^{40}K , respectively in Bq/kg. This expression is based on the assumption that 10 Bq/kg of ^{226}Ra , 7 Bq/kg of ^{232}Th and 130 Bq/kg of ^{40}K produce the same gamma-ray dose rate and must be less than the upper limit of 370 Bq/kg [9].

2 MATERIALS AND METHODS

2.1 Sample preparation

Samples were dried overnight at 105°C in an oven to remove large percentage of sample weights and then homogenized by using the grinding vessel to micron particle size to be fine powder. Digestion of samples was carried out for 20 minutes at 200°C in a mixture of known concentrations of HCl, HNO₃ and HF for, using a two-step program. After digestion, the samples were evaporated on a hot plate and dissolved in the suitable acid medium for radiochemical analysis.

2.2 Radiochemical method

Thorium was separated from interfering nuclides on a reversed-phase extraction column (EiChrom TruResin) followed by a cation exchange separation. ^{229}Th tracer was added as a tracer for chemical yield determination. The final elute was deposited onto a filter paper using LiF_3 precipitation, and counted with alpha spectrometry.

2.3 Instrumentation techniques

Subsamples of about 200 mg were prepared in specially designed irradiation capsules and irradiated in the SAFARI research reactor for determination of the U and Th element concentrations. The uranium concentration ($\mu\text{g/g}$) was determined by Delayed Neutron Counting (DNC). Samples are counted again after a cooling-off period of approximately 7 days on a well-type HPGe gamma detector for determination of the thorium concentration ($\mu\text{g/g}$).

A sub-sample of approximately 20 grams was weighed in a specific sample container for analysis using the low-background high energy HPGe detector system with 20% relative efficiency. The acquired samples spectra are analysed for the radionuclides ^{226}Ra , ^{228}Ra , ^{228}Th and ^{40}K . Samples were sealed and stored for 3 weeks before counting to allow for radium and its short-lived progeny to be in equilibrium.

3 RESULTS AND DISCUSSION

Radiochemical method results compared well with those obtained by instrumental techniques for ^{232}Th and ^{228}Th as can be seen from the good correlation coefficients (see Figure 1 and Figure 2). Non-destructive instrumental techniques have been used for sample analysis by Msila et.al 2016 and Louw et.al. 2008, where measured activity concentrations results were used to calculate the radiation indexes for building materials.

The ACI and Raeq values were calculated from reported activity concentrations of ^{226}Ra , ^{232}Th and ^{40}K as in equations 1 and 2, respectively. ^{232}Th was measured by INAA while in most published reports ^{232}Th is determined by measuring ^{228}Ac (911 keV) by gamma spectrometry and assuming equilibrium between ^{232}Th , ^{228}Ra and ^{228}Ac . ^{226}Ra , from the ^{238}U decay series, activity concentration was determined from its daughter nuclides ^{214}Bi (609.31 keV) and ^{214}Pb (351.9 keV) energies and ^{40}K from its 1460.8 keV gamma energy line.

Figure 1: Correlation plot for ^{232}Th .

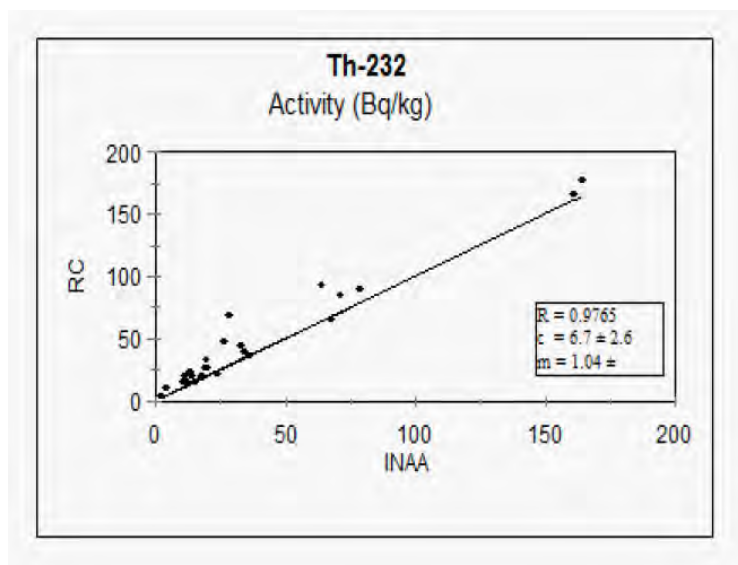
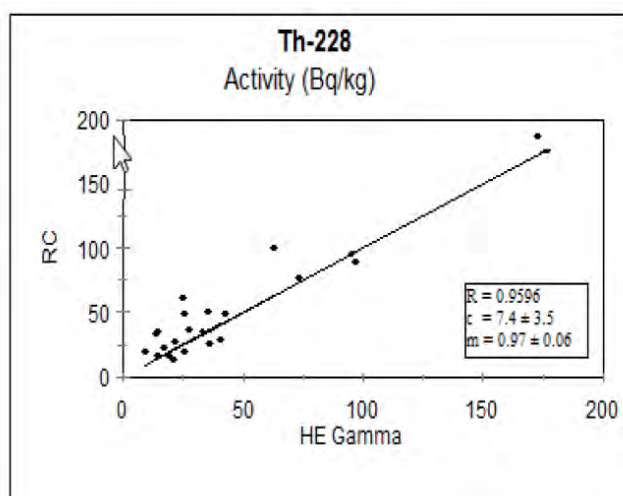


Figure 2: Correlation plot for ^{228}Th .

The ACI values for brick, cement, concrete, sand and silica fume samples were less than 0.5, which implied an exposure level of less than 0.3 mSv per annum. In the case of gypsum, phosphogypsum and plasterboard the ACI value was greater than 0.5 but less than 1 and implied that if these materials were used in bulk in building works, occupiers of such buildings were unlikely to receive radiation doses in excess of 1 mSv per annum. Slag and fly-ash materials exceed the recommended exemption level ($\text{ACI} > 1$), these raw materials were used in restricted amounts ($< 30\%$) and the final cement product is therefore expected to be exempted. In terms of cement the reason is that it usually contains only 5% of minor additional constituents but even in a cement mixture containing a high percentage of constituents with higher radioactivity concentrations, for example fly-ash 35%, is unlikely to have a nuclide concentration exceeding 500 Bq/kg. The use of ceramics will probably be exempted based on the dose criterion of $\text{ACI} < 6$, which applies for superficial materials with restricted use such as tiles [7].

The radium equivalent activity (Ra_{eq}) values for cement, concrete, gypsum, phosphogypsum and slag samples were below the maximum limit of 370 Bq/kg, and as such do not pose a radiological hazard when used for construction of buildings. The materials which may be of concern according to this index were ceramic and fly-ash; however both has only restricted use in the building industry (see Table 2). In this case since the dose levels were limited to the dose received of 1.5 mSv/yr, it was generally clear that even if the fly-ash may be acceptable according to South African legislation, it could exceed the maximum radium equivalent index.

Table 2: Summary of results from the building industry

Sample	n	ACI (or D)	Ra_{eq}
Brick	5	0.41 ± 0.09	117 ± 26
Cement	10	0.24 ± 0.1	67 ± 27
Ceramic	1	3.4	996
Concrete	6	0.43 ± 0.12	125 ± 25
Fly-ash	30	1.3 ± 0.4	370 ± 114
Gypsum	60	0.73 ± 0.42	214 ± 123
Phosphogypsum	55	0.52 ± 0.14	151 ± 39
Plasterboard	3	0.68 ± 0.1	197 ± 27
Sand	1	0.39	115
Slag	4	0.9 ± 0.1	256 ± 34
Silica fume	1	0.37	97

4 CONCLUSION

It is clear that radiation hazardous indexes and dose limits are based on radiochemical methods and instrumental techniques in many world studies. If cement or other building material was to be imported or exported from South Africa to countries of the Asian, European, Russian, Australian and Americas communities the activity concentration index and/or radium equivalent activity index should be used as a screening tool and criterion for regulatory purposes considering the radiochemical methods and gamma spectrometric methods.

Although some of the raw materials (such as slag, fly-ash) exceed the recommended exemption levels for exposure, the final cement product is expected to be exempted since these materials constitute a small portion of the final product. Activity limits used by South Africa for regulatory control do not automatically mean that the materials are acceptable according to international standards and could result in trade restrictions. In South Africa currently there are no regulations specific for building material and no limits for such materials.

5 ACKNOWLEDGMENTS

The authors would like to acknowledge NECSA management including RadioAnalysis staff for making this work possible.

6 REFERENCES

- [1] National Nuclear Energy Act, Act No. 131 of 1993. Regulation 849 on Regulations in respect of nuclear licenses. South African Government Gazette, Vol. 15670, 23 April 1994. [Online] Available at: <http://www.enviroleg.co.za/acts/Nuclear%20Energy/REGS/849-94%20Regs%20re%20nuclear%20licences.pdf>. Accessed 20 November 2015.
- [2] Regulation No. 388 (2006), Regulations in terms of section 36 read with section 47 of the National Nuclear Regulator Act, 1999 (Act No. 47 of 1999), on Safety Standards and Regulatory Practices (SSRP).
- [3] Pule, O.J. (2015). South African perspective for radon in dwellings and the anticipated regulatory control measures. Paper presented at SARPA conference, 10-12 June 2015, Villa Paradiso, South Africa.
- [4] Louw, I., Faanhof, A. (2008). Natural radioactivity of building material in South Africa. Proceedings series: Naturally occurring radioactivity material (NORM V). Proceedings of the fifth international symposium on naturally occurring material organized by the University of Seville in cooperation with IAEA, the Spanish nuclear safety council and the University of Huelva held in Seville, 19 -22 March 2007.
- [5] European Commission, (1999). Radiation Protection 112: Radiological protection principles concerning the natural radioactivity of building materials.
- [6] Msila, X., Labuschagne, F., Barnard, W., Billing, D.G., (2016). Radioactive nuclides in phosphogypsum from the lowveld region of South Africa. S. Afr. J. Sci. 2016; 112(1/2), # Art. 2015-0102, 5 pages. <http://dx.doi.org/10.17159/sajs.2016/20150102>.
- [7] Ortiz, J., Ballesteros, L., Serradell, V. Radioactivity reference levels in ceramics tiles as building materials from different countries. Universidad Politécna de Valencia, Environmental radioactivity laboratory, Camino de Vera, s/n, E-46022, Valencia, Spain.
- [8] Department of Energy. National Nuclear Regulator Act 47 of 1999 [document on the internet]. C1999 [cited 2015 December 04]. Available from: <http://www.energy.gov.za/files/resources/nuclear/act47.pdf>
- [9] Berekta, J., Matthew, P.J., (1985). Natural radioactivity of Australian building materials. Industrial wastes and by-products, Health Phys. 48, 87-95.

The ICRP Publication 126 on Radiological Protection against Radon Exposure

Jean-François Lecomte^a, Stephen Solomon^b, John Takala^c, Thomas Jung^d, Per Strand^e, Christophe Murith^f, Sergey Kiselev^g, Weihai Zhuo^h, Ferrid Shannounⁱ, Augustin Janssens^j

^aInstitut de Radioprotection et de Sûreté Nucléaire BP 17 F-92262 Fontenay-aux-Roses, France.

^bAustralian Radiation Protection and Nuclear Safety Agency (ARPANSA), Yallambie VIC 3085, Australia.

^cCAMECO Corporation, Saskatoon, Saskatchewan, S7K 0C6, Canada.

^dBundesamt für Strahlenschutz (BfS), Willy-Brandt-Straße 5 D-38226 Salzgitter, Germany.

^eNorway Radiation Protection Association (NRPA), Grini næringspark 13 1332 Østerås Norway.

^fSwiss Federal Office of Public Health, Schwarzenburgstrasse 157 CH – 3003 Bern, Switzerland.

^gBurnasyan Federal Medical Biophysical Centre (BFMBC), Moscow, Russia.

^hInstitute of Radiation Medicine, Fudan University, Shanghai, 20032, P.R. China.

ⁱWorld Health Organization, 1211 Geneva 27, Switzerland.

^jEuropean Commission L-2920 Luxembourg.

Abstract. In 2009, the Main Commission of the International Commission on Radiological Protection (ICRP) approved the development by the Committee 4 of updated guidance on radiological protection against radon exposure. The draft report was posted on the ICRP website for public consultation in 2012. It was published as Publication 126 (ICRP 126) late 2014. The objective of the new publication is to describe and clarify the application of the Commission's system to the protection of members of the public and workers against radon exposures in dwellings, workplace and other types of locations. ICRP 126 is considering the recently consolidated ICRP general recommendations, the new scientific knowledge about the radon risk and the experience gained by many organizations and countries in the control of radon exposure. It is mainly focused on radon 222. In summary, in the previous recommendations on the same subject (ICRP 65, ICRP 103), the Commission recommended a strategy based on the distinction between a protection approach for dwellings and a protection approach for workplaces. Now, the Commission recommends an integrated approach for the protection against radon exposure in all buildings in which radon exposure occurs whatever the purpose of the building and the types of its occupants. The strategy of protection in buildings, implemented through a national action plan, is based on the application of the optimization principle below a derived reference level in concentration, chosen as low as reasonably achievable. When the concentration reference level cannot be met, additional considerations can be made on the basis of a reference level in effective dose of the order of 10 mSv per year. A graded approach is recommended, according to the degree of responsibilities, notably in workplaces, and the priorities determined at national level.

1 INTRODUCTION

In 2009, the Main Commission of the International Commission on Radiological Protection (ICRP) approved the development by the Committee 4 of updated guidance on radiological protection against radon exposure. The draft report has been posted on the ICRP website for public consultation in 2012. It has been approved by the Main Commission in early 2014 and published as Publication 126 (ICRP 126) late 2014. The objective of the new publication is to describe and clarify the application of the Commission's system to the protection of members of the public and workers against radon exposures in dwellings, workplace and other types of locations. ICRP 126 is mainly focused on radon 222.

2 CHARACTERISTICS OF RADON EXPOSURE

The Commission made recently a thorough review and analysis of the epidemiology of radon for both underground miners and the general population (Publication 115). There is compelling evidence that radon and its progeny can cause lung cancer. For solid tumors other than lung cancer, and also for leukemia, there is currently no convincing or consistent evidence of any excesses associated with radon and radon progeny exposures.

Radon exposure situations have the characteristics of existing exposure situations since the source is unmodified concentrations of ubiquitous natural activity in the earth's crust. Human activities (e.g. construction of buildings, operation of mines...) may create or modify pathways increasing indoor exposure to radon compared with outdoor background. These pathways can be controlled by preventive and mitigating actions. The source itself, however, cannot be deleted or modified and then already exists when a decision on control has to be taken. In some workplace, however, the radon exposure situation may be deemed to be a planned exposure situation from the outset by regulatory authorities. Such workplace includes uranium mines associated with the nuclear fuel cycle.

Radon is not likely to give rise to an emergency exposure situation even though the discovery of very high concentrations in a place may require the prompt implementation of protective actions. The philosophy of Publication 103 compared with Publication 60 is to recommend a consistent approach for the management of all types of exposure situations. This approach is based on the application of the optimization principle implemented below appropriate individual dose restrictions: dose constraints or reference levels.

Several characteristics of radon exposure in dwellings (and in many other locations) are similar to those of exposures arising from other existing exposure situations such as exposures to NORM or exposures in long-term contaminated areas. Radon exposure may affect nearly all places of living. The variability of radon concentration results in a very heterogeneous distribution of individual exposures. Day to day life at home and at work inevitably leads to some exposure to radon. The level of the risk is highly depending on individual choices and behavior. The characterization of the exposure situation is a pre-requisite to its control. Domestic radon exposure management should address several considerations such as environmental, health, economic, architectural, educational etc. A large spectrum of stakeholders is concerned.

Control of indoor radon exposure poses many challenges. As a given individual can move from place to place in the same area, the radon protection strategy should be implemented in a consistent and integrated approach in the various locations. As the radon risk is mainly due to domestic exposure, the radon protection strategy should address primarily exposure in dwellings in a public health perspective. Radon in many buildings is well above the concentrations at which the risk has been demonstrated by epidemiology and efforts should be made to reduce both the overall risk for the general population and the highest individual exposures. Radon protection strategy should not be in contradiction with the raising role of energy saving policies. It should be as simple as possible, properly scaled with other health hazards, supported and implemented on a long-term basis and involving all the concerned parties.

A national radon protection strategy has also to address many challenges in terms of legal responsibilities, notably the responsibility of the individual householder towards her/his family, of the builder or the seller of a house or a building towards the buyer, of the landlord towards the tenant, of the employer towards the employee, and generally speaking, of the responsible person for any building towards its users. The degree of enforcement of the actions that are warranted is very much related to the degree of legal responsibility for the situation.

The responsibility dimension calls clearly for the need of a graded approach in defining and implementing a radon protection strategy. Such a graded approach should be based on realism, effectiveness and ambition. Any radon protection strategy should thus aim to maintain and/or reduce radon concentrations as low as reasonably achievable in an effective way keeping in mind that it is not feasible to totally eliminate indoor radon concentration.

3 THE SYSTEM RECOMMENDED FOR RADON EXPOSURE

The Commission considers that a national radon protection strategy appears to be justified since radon is a significant source of radiation exposure (second leading cause of lung cancer after smoking) and radon exposure can be controlled. The characterization of the situation (i.e. assessment of radon concentrations, identification of radon prone areas...) as well as considerations about public health priorities and social and economic factors are necessary for regulatory authority to determine whether a radon protection strategy is justified or not in the country. The Commission considers that radon strategies should address together both smokers and non-smokers and that specific requirements for children are not warranted.

The characterization of the exposure situation is also a pre-requisite of the application of the optimization principle. This principle is the driver for controlling radon exposure in order to maintain or reduce exposure as low as reasonably achievable taking into account the prevailing economic and societal circumstances. It is the responsibility of the appropriate regulatory authorities, as with other radiation sources, to establish their own national reference level and then to apply the process of optimization of protection in their country. The objective is both to reduce the overall risk of the general population and, for the sake of equity, the individual risk of the most exposed individuals. In both cases, the process is implemented through the management of buildings rather than individual exposures and should result in radon concentrations in ambient indoor air as low as reasonably achievable below the national derived reference level.

Taking into account the degree of control by actions on pathways, the benefit for individuals due to the use of buildings as well as the support provided to individuals to reduce their doses, the Commission considers that a value in the order of 10 mSv as set in Publication 65 should remain dosimetric reference level for radon exposure. In practice reference levels for radon are derived in concentration which is a measurable quantity, expressed in Becquerel per cubic meters (Bq m^3). ICRP 126 does not provide does coefficients for radon. It will be the purpose of the future Occupational Intakes of Radionuclides (OIR) Part 3 related, notably, to radon. An annual dose of 10 mSv would correspond to a radon concentration in dwellings in the range of a few hundreds of Bq m^3 . For the practical implementation of the radon protection strategy, the Commission continues to recommend an upper value of the derived reference level for radon 222 in dwellings of the order of 300 Bq m^3 . The Commission strongly encourages regulatory authorities to set a national derived reference level as low as reasonably achievable in the range of $100\text{--}300 \text{ Bq m}^3$ taking into account the prevailing economic and societal circumstances (see ICRP Statement from Porto meeting and the Handbook of WHO). The measurement should be representative of the annual mean concentration of radon in a building or location.

For the sake of simplicity, considering that individuals going from place to place in the same area in their daily life should be protected on the same basis whatever is the location, the Commission recommends to use a priori the same upper value of 300 Bq m^3 in mixed-use buildings (with access for both members of the public and workers).

In a graded approach perspective, the radon protection strategy should start with a programme aiming at encouraging relevant decision makers to enter in a process of self-help protective actions such as measurement and, if needed, remediation. This process may be implemented with more or less incentive and helping provisions and, if judged necessary, with requirements. The degree of enforcement of these various actions should be increased depending on the degree of legal responsibility for the situation and the ambition of the national radon protection strategy.

A specific graded approach should be implemented for workplace. Where workers' exposure to radon is not considered as occupational exposure, i.e. when the radon exposure situation cannot reasonably be regarded as being the responsibility of the operating management (typically office buildings), the first step is to reduce concentration of radon as low as reasonably achievable below the same derived reference level as set for dwellings (even though the corresponding level in dose is usually lower than that in dwellings because the conditions of exposure in workplace are different). If difficulties are met in the first step, a more realistic approach is recommended as the second step consisting in optimizing exposure on the basis of a dose reference level in the order of 10 mSv per year taking into account the actual parameters of the exposure situation.

If despite all reasonable efforts to reduce radon exposure at workplace, the exposure remains durably above the dose reference level in the order of 10 mSv per year (quantitative criterion), and/or where workers' exposure to radon can reasonably be regarded as being the responsibility of the operating management, e.g. some underground workplace, spas etc. (qualitative criterion), the workers should be considered as occupationally exposed. In such cases, the Commission recommends to apply the optimization principle and the relevant requirements for occupational exposure.

The dose limit should apply when the regulatory authorities consider that the radon exposure situation should be managed like a planned exposure situation. In any case using, either the occupational dose limit or a reference level, an annual dose on the order of 20 mSv per year, possibly averaged over 5 years, should not be exceeded for the exposure of workers.

4 IMPLEMENTATION OF PROTECTION STRATEGIES

A national radon action plan should be established by regulatory authorities, with the involvement of relevant stakeholders, in order to frame the implementation of the national radon protection strategy in dwellings, places open to the public and workplace. The action plan should establish a framework with a clear infrastructure, determine priorities and responsibilities, describe the successive steps to deal with radon in the country and in a given location, identify concerned parties (who is exposed, who should take actions, who could provide support?), address ethical issues (notably in link with the responsibilities) and provide information, guidance, support as well as conditions for sustainability.

To be efficient, the national radon protection strategy should be established on a long-term perspective. The process to reduce significantly the radon risk of the general population is rather a matter of several decades than several years. The national action plan should be periodically evaluated and reviewed, including the value of the derived reference level.

The Commission considers that, for the sake of clarification, when dealing with existing exposure situations, the distinction should be made between prevention aiming at maintaining exposure as low as reasonably achievable under the prevailing circumstances and mitigation aiming at reducing exposure as low as reasonably achievable.

As a consequence, a radon protection strategy should include a prevention part. Whatever the indoor location is, the category of individuals inside and the type of exposure situation, it is possible to optimize radon exposure by taking into account the issue of radon exposure during the planning, design and construction phase of a building. Preventive actions mean land-planning and building codes for new buildings and for renovation of old buildings. They also mean the integration of the radon protection strategy consistently with other strategies concerning buildings such as indoor air quality or energy saving in order to develop synergies and avoid contradictions.

The mitigation part of a national radon protection strategy concerns mainly existing buildings or locations. In such case, the control of exposure should be ensured as far as possible through the management of the building (or location) and the conditions of its use, whatever the category of individuals inside. The main steps are measurements and, when needed, corrective actions. The action plan should also deal with radon measurement techniques and protocols, national radon surveys to identify radon prone areas, methods for mitigating the radon exposure and their applicability in different situations, support policy including information, training and involvement of concerned parties, as well as assessment of effectiveness. The issues of buildings with public access and workplace should also be addressed with a specific graded approach for the latest.

The future Publication provides also guidance for the management of specific radon exposure situations in which workers are considered as occupationally exposed. It covers exposure situations when the compliance with the reference level cannot be achieved (quantitative criterion) or they are included in the national list of activities or facilities established by the regulatory authorities (qualitative criterion). The strategy of protection is then based on the application of the optimization principle and the relevant requirements for occupational exposure. If the regulatory authorities decided to, notably when the radon exposure situation is managed as a planned exposure situation, the protection may also be based on the application of dose limits.

5 CONCLUSION

In summary, in the previous recommendations on the same subject (ICRP 65, ICRP 103), the Commission recommended a strategy based on the distinction between a protection approach for dwellings and a protection approach for workplaces. Now, the Commission recommends an integrated approach for the protection against radon exposure in all buildings whatever their purpose and the status of their occupants. The strategy of protection in buildings, implemented through a national action plan, is based on the application of the optimization principle below a derived reference level in concentration, chosen as low as reasonably achievable on the basis of a reference level in effective dose of the order of 10 mSv per year. By the integrated, graded and straightforward approach now recommended for most of the radon exposure situations, the Commission expects a real improvement in the reduction of exposure due to radon, which is by far the main source of public exposure worldwide.

Curies Contaminated Notebook

An analysis of a notebook and papers, originally belonging to Marie Curie, which are now retained by the Wellcome Collection, London

Lindsey Simcox*, Jon Taylor#

Aurora Health Physics Services Ltd, Harwell Oxford, UK.

Abstract. This paper describes the radiological analysis of a notebook and papers originally belonging to Marie Curie, which were identified as contaminated. The analysis used direct monitoring techniques, wipe samples and gamma spectrometry to identify the type and extent of contamination. The subsequent work to ensure the safe keeping and handling of the notebook illustrated that the UK's legislation for radiation protection and keeping of radioactive materials does not easily cover such items.

KEYWORDS: *Curie; radium; legacy; contamination; gamma spectrometry; radium-226; thorium-232.*

1 INTRODUCTION

In September 2014 Aurora Health Physics Services Ltd (Aurora) was approached by Health and Safety Advisers at the Wellcome Trust concerning a notebook kept within the Trusts library collection in London. The notebook had originally belonged to the scientist Marie Curie, who had used the notebook to record laboratory results of her experiments on radioactivity. Preliminary monitoring with hand-held contamination instruments had indicated that the item was contaminated with radioactive material; however, the isotopes and activity of the material were unknown. The Wellcome Trust was keen to ensure that staff and visitors were adequately protected from exposure to the notebook, but still wanted to allow public access to view the item if possible. The Trust were also required to have demonstrable evidence of compliance with the relevant regulatory requirements for keeping and using the notebook.

2 BACKGROUND OF THE CURIE NOTEBOOK

2.1 Curies work with Radium

Marie Curie and her husband Pierre Curie are well known for their experiments with radioactive material in the early 20th Century. The Curies are credited with the discovery of both Radium and Polonium in addition to coining the word "radioactivity". Their method to isolate Radium-226 from pitchblende required considerable manual labour to grind and chemically process the mineral in very large quantities. It is now known that the Curies were exposed to significant radiation during this work at their laboratory in Paris.

* Presenting author, e-mail: lindsey.simcox@aurorahp.co.uk

#Co-author, e-mail: jon.taylor@aurorahp.co.uk

2.2 The Wellcome Trust and the Wellcome Collection

The Wellcome Trust was established in 1936 after the death of Sir Henry Wellcome. Throughout his life Sir Henry Wellcome amassed an extensive collection of books, journals, manuscripts, prints and drawings on the broad topic of medical history. After his death he also left substantial sums of money to be invested in progressing medical advancements. Since 1936 the Wellcome Trust has financed a number of major biomedical research initiatives. The Wellcome Collection in London has now grown into a library of over 750,000 items, the majority of which can be viewed and handled directly by the general public.

2.3 ‘Discovery’ of the Curie notebook at the Wellcome Collection

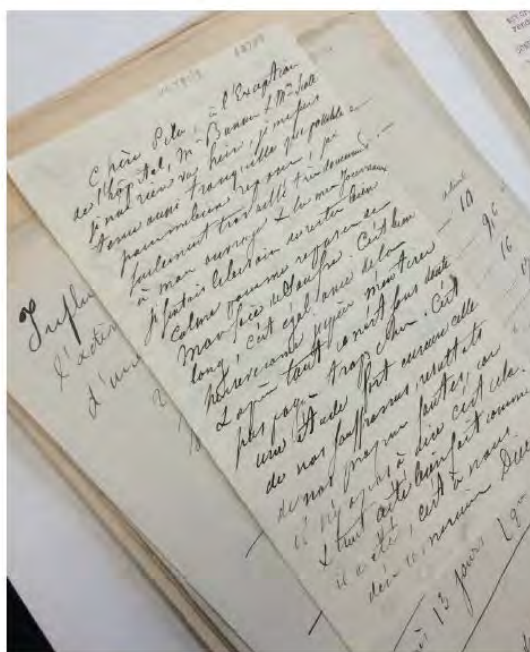
In August 2014 it came to the attention of the Health and Safety Team at the Wellcome Collection that a library user had flagged that workbooks and possessions of Marie Curie, similar to that of the notebook held in the London Collection, were kept at the Bibliotheque Nationale in France. The user mentioned that in France, those who want to view and touch the items must ‘sign a waiver and wear protective clothing’. Unsure as to whether their Curie notebook may also be contaminated, the Health and Safety Team in London quickly withdrew the item from the Collection catalogue and sought help from radiation safety professionals.

2.4 The notebook, associated notecards and papers

The notebook is approximately 15cm x10cm in size with a hardbound front and back cover. The label on the front (see Figure 1) has Marie Curie’s name and the date, 1920, and is somewhat damaged, but otherwise the notebook is in good condition. The book is handwritten in French and contains experimental method details, results and sketches. Within the notebook were five loose notecards, also with experimental records. Also tested were three sheets of paper: two letters/ notes (see Figure 2) and the other a certificate. Records show that the notebook was originally purchased by the Collection in the early 1960’s.

Figure 1: Front cover of the Marie Curie notebook



Figure 2: Marie Curie's writing on separate sheets of paper

3 RELEVANT LEGISLATION IN THE UNITED KINGDOM

3.1 Ionising Radiations Regulations 1999 (IRR99)

IRR99 are enforced by the Health and Safety Executive. The aim of IRR99 is to ensure that doses to radiation workers and members of the public are kept as low as reasonably practicable and that dose limits are not exceeded.

3.2 Environmental Permitting (England and Wales) Regulations 2010 (EPR10)

EPR10 are enforced by the Environment Agency (EA). These regulations aim to establish and maintain control over the keeping, use and security of radioactive materials and also to ensure that the accumulation and disposal of radioactive wastes are managed effectively to limit radiological impact on the general public and the environment.

3.3 Environmental Permitting (England and Wales) Regulations (Amendment) 2011 (EPR11)

EPR11 outline the conditions under which radioactive materials should be managed in circumstances where EPR10 does not apply. This essentially exempts minor practices; however, a number of conditions must still be met for exempt items.

4 SEARCH FOR OTHER POTENTIALLY CONTAMINATED LIBRARY ITEMS

Before the initial survey of the notebook, library curators were also asked to consider if the Collection included any other items on the theme of 'radioactivity' or 'radium', or work from other scientists of the time (such as William Crookes), which may also be contaminated with radioactive material. This search resulted in fifteen bulk boxes of books and documents which were taken from storage for analysis by Aurora, in addition to the Curie notebook.

5 ANALYSIS

Analysis of the identified items was carried out using a range of methods. Direct monitoring was initially used to search for items contaminated with beta-gamma emitters, where the contaminated items were found. Wipe tests were used to test for loose contamination. Finally, gamma spectrometry analysis was carried out on all bulk boxes of items and on the Curie notebook in isolation.

5.1 Direct Monitoring

The notebook and other items were monitored using an Electra Ratemeter with a DP6 dual phosphor probe (Figure 3). The highest levels of contamination were found on the outside cover of the notebook up to 2,500 cps alpha and up to 3,500 cps beta corresponding to an estimated 200 Bq/cm² Radium-226 for a porous surface. The inside pages of the notebook were less contaminated with count rates up to 60 cps alpha and 2,000 cps beta. The other items in the collection had much lower levels typically less than 10 cps alpha.

Figure 3: Direct monitoring of the Marie Curie notebook using DP6 probe



5.2 Wipe Tests

Items, where the presence of radioactive material was confirmed by direct monitoring, were also subject to wipe testing. This consisted of a filter paper being wiped across the surface of the item in order to pick up any loose contamination. The wipe samples were screened initially with a hand held probe and then were later analysed in Aurora's laboratory using two high sensitivity alpha and beta drawer counters. The results of the wipe tests are provided below in Table 1. Loose contamination was present but was found to be below the typical action levels for establishing a contamination controlled area (0.4 Bq/cm² for loose alpha contamination and 4 Bq/cm² for loose beta contamination).

Table 1: Wipe test results

Description	Loose Alpha (Bq/cm ²)	Loose Beta (Bq/cm ²)
Letter 1	0.024	0.000
Letter 2	0.018	0.108
Certificate	0.003	0.051
Notebook Front Cover	0.033	0.379
Notebook Back Cover	0.042	0.740

5.3 Gamma Spectrometry

The Aurora High Resolution Gamma Spectroscopy (HRGS) system uses an Ortec trans-Spec-DX-100 detector with a 67 mm × 52 mm high purity germanium P-type crystal. The detector is electrically cooled meaning that liquid nitrogen is not required. Although the detector takes 12 hours to cool from room temperature, Aurora routinely maintains the detector in a constantly cooled state so that it can be deployed for immediate measurement.

The trans-Spec-DX-100 was set up in within a location which was chosen with consideration to minimising background radiation readings. A background spectra was collected in order to subtract the background from measurements of items in the collection.

Each item was weighed and analysed for five or fifteen minutes. The collected spectra were post processed using software to provide spectral analysis and nuclide identification and this information, together with the data from the calibration model, provided quantification of the radioactivity present. By carrying out background subtraction and using a geometry calibration file it is possible to calculate the total activity in the measurement volume.

The minimum detectable activity is dependent on the counting geometry, the density of the package and the count time. Typically, the minimum detectable activity during this work varied from 1kBq to 5kBq of Radium or Thorium activity in a box or package.

Table 2: Gamma spectrometry results

Item	Radium-226 Activity (kBq)	Thorium-232 Activity (kBq)
Notebook	120	1
Letters (Combined)	3	1

6 RECOMMENDATIONS TO THE COLLECTION FOLLOWING ANALYSIS

6.1 Public handling of the notebook and papers

The survey and sample analysis results were used to provide a radiation dose assessment for handling and inspection of the items containing radioactivity. Conservators and members of the public could be exposed to contact dose rates of up to 3.5 μ Sv/h although whole body dose rates are only marginally above the background of 0.1 μ Sv/h. Even regular exposure to the identified items is likely to result in annual whole body doses of less than 10 μ Sv (or 0.010mSv) and hand doses of less than 35 μ Sv (0.035mSv). The dose limit to members of the public from an employer's activity is 1,000 μ Sv (1mSv) whole body and 50,000 μ Sv (50mSv) to the hands.

Loose activity could be removed from handling the notebooks at levels similar to those removed during the wipe test; if the handling of items was not carefully supervised some of this activity could be ingested by hand to mouth contact. Up to 10Bq of activity was removed from the items during the wipe tests. Ingestion of this level of activity would result in a Committed Effective Dose of 22 μ Sv which is again well below the above limits.

6.2 Complying with IRR99

A prior radiological risk assessment was carried for handling of the notebook by staff and members of the public. Many of the existing controls for physical protection of valuable historical documents such as wrapping, gloves and supervision also provided a high degree of protection from the radiological hazard. Additional recommendations on storage and supervision procedures were made.

6.3 Environmental Permit

The Environmental Permitting (England and Wales) Regulations 2010 apply to naturally occurring radioactive materials (NORM) but only to specific industrial practices. The notebook could not be classified in any of the specified practices and after consultation with the Environment Agency the Wellcome Trust applied for and received an Environmental Permit for the keeping and use of open radioactive sources, but with no allowance for radioactive waste to be generated.

7 WIDER CONTEXT

The discovery of the contamination present in the Curie notebook and papers presents a number of questions about other items of a similar nature that could be unknowingly kept across the globe. However, it's difficult to estimate the number of items, their level of possible contamination, or their location. Considering the likely public perception of the discovery of such items in the public domain, the radiation protection community would be wise to be ready to respond to these situations quickly in order to ensure that dose implications are understood and misinformation is prevented from spreading.

It could be argued that the radiation protection community should have some responsibility in helping finding these items, though who provides the resource to search for and then keep such items securely would depend on each individual situation. In some cases, it may transpire that such an item cannot be kept or used safely, in which case those responsible will have to ask themselves at what point is safety more important than preserving historical artefacts.

8 CONCLUSION

Analysis confirmed that the Collections notebook from Marie Curie contains approximately 120kBq of Tadium-226 and 1kBq of Thorium-232. Additional notecards and papers from Marie Curie also contain 3kBq of Radium-226 and 1kBq of Thorium-232, with some evidence that this contamination is loose.

The documents present a very low external radiation hazard, but contamination when touching or the items is possible. The Collection have now implemented a number of controls to ensure compliance with the relevant legislation within the UK.

9 ACKNOWLEDGEMENTS

The author would like to acknowledge the efforts of the Wellcome Collection Conservation team for their work to ensure compliance with all the necessary requirements to keep the contaminated items on site.

Thanks to staff at Imperial College London for their initial help to the Wellcome Trust to identify the notebook as containing radioactive material.

Thanks are also extended to Amber Bannon and Phil Fahey who carried out the site inspection at the Wellcome Collection on behalf of the Environment Agency, shortly after the initial analysis. Their help to understand legal requirements for keeping of the items is much appreciated.

Comparison of Federal Guidance Reports 12 and 15: External Exposure to Radionuclides in Soil, Air, and Water

M.B. Bellamy^{a,*}, K.G. Veinot^{b,c}, M.M. Hiller^a, S.A. Dewji^a, K.F. Eckerman^b, C.E. Easterly^b, N.E. Hertel^{a,d,**}, R.W. Leggett^a.

^aOak Ridge National Laboratory, Center for Radiation Protection Knowledge, P.O. Box 2008 MS 6335, Oak Ridge, TN 37831-6335

^bEasterly Scientific, 6412 Westminster Rd., Knoxville, TN, 37919

^cY-12 National Security Complex, P.O. Box 2009 MS-8206 Oak Ridge, TN 37831-8206

^dGeorgia Institute of Technology, 770 State Street, Atlanta, GA 30332-0745

Abstract. The U.S. Environmental Protection Agency publishes Federal Guidance Reports (FGR) to provide federal agencies with technical information needed to implement radiation protection programs for workers and the public. Federal Guidance Report 15, an update of Federal Guidance Report 12 entitled “External Exposure to Radionuclides in Air, Water, and Soil” (EPA-402-R-93-08), is currently under review by federal agencies. FGR 12 and 15 provide dose rate coefficients for external exposure to radionuclides distributed in the environment. Its precursor, FGR 12, addresses only adults and tabulated coefficients for 825 radionuclides using the radiation protection guidance of the 1980s. FGR 15 provides age-specific dose rate coefficients for six ages and the 1252 radionuclides of ICRP Publication 107 using the latest radiation protection recommendations of ICRP Publication 103.

KEYWORDS: *environmental exposures; air and water dose coefficients.*

Notice: This manuscript has been authored by UT-Battelle, LLC, under Contract No. DE-AC0500OR22725 with the U.S. Department of Energy. The United States Government retains and the publisher, by accepting the article for publication, acknowledges that the United States Government retains a non-exclusive, paid-up, irrevocable, world-wide license to publish or reproduce the published form of this manuscript, or allow others to do so, for the United States Government purposes. The Department of Energy will provide public access to these results of federally sponsored research in accordance with the DOE Public Access Plan (<http://energy.gov/downloads/doe-public-access-plan>).

1 INTRODUCTION

In environmental settings such as submersion in contaminated air or immersion in contaminated water, dose rate coefficients for such external exposures relate the dose rate to organs and tissues of the body to the concentrations of radionuclides. For external exposures, of primary concern are the types of radiation of concern sufficiently penetrating the body to deposit ionizing energy in radiosensitive organs and tissues. The less penetrating radiations are also of interest, primarily delivering dose to the skin and other outlying organs and tissues such as photons, electrons (including bremsstrahlung), and positrons. The dose rate coefficient accounts for the deposition of ionizing energy in the tissues of the body due to the transport of emitted radiations in the environment. In this work, organs specified in the ICRP 103 [1] recommendations for determining effective dose are scored for source energies ranging from 0.01 to 5 MeV. By interpolation of their emissions using the discrete source energies, dose rate coefficients for specific radionuclides were derived. In the case of photon emitters, this endpoint is sufficient to determine organ equivalent dose and effective dose rate coefficients since the emission spectra can be folded with the dose rate coefficients and summed over each photon emission weighted by the photon yield. For electron emitters, however, additional steps were required since beta emissions are not monoenergetic and bremsstrahlung production has to be considered. Bremsstrahlung contributions can be significant since these photons can contribute to organs located at relatively deep depth within the body where electrons are not able to penetrate. A broader effort to update the dose coefficients reported in FGR 12 supported the calculation of dose rate coefficients for radionuclides addressed in ICRP Publication 107 [2]. Dose contributions from neutrons were not included in the coefficients because detailed information has not been assembled on the radiation field resulting from distributed sources of neutrons in the environment; prompt and delayed emissions for photons and electrons following spontaneous fission were included in the decay data tabulations of ICRP 107.

Yoo et al. [3] and Petoussi-Henss et al. [4] show recent calculations of dose rate coefficients for external irradiation of the body from radionuclides distributed in the environment. Irradiation from bremsstrahlung has been ignored in some cases in these works, even though for pure beta emitters it is the only source of radiation that is sufficiently penetrating resulting in doses to tissues below the surface of the body.

The computational approach of Federal Guidance Report (FGR) 12 [5] was a combination of deterministic and Monte Carlo methods. The calculations in the current work employed MCNP6 [7] in conjunction with ENDF/B-VI.8 [8] cross sections. External dose rate coefficients for radionuclides in soil, air, or water were derived using an adult hermaphrodite phantom [6]. The present report incorporates six age-specific phantoms from newborn through adult while FGR 12 only considered an adult. Nuclear decay data was updated from ICRP Publication 38 [9] to ICRP Publication 107 that includes a larger number of isotopes and refinements to the decay data.

2 MATERIALS AND METHODS

2.1 Computational Phantoms

A series of stylized computational phantoms were used representing a newborn, 1 year old, 5 year old, 10 year old, 15 year old, and adult. These phantoms were developed at Oak Ridge National Laboratory (ORNL) [6] and later modified by the University of Florida and ORNL [10]. The update of the phantoms included changes to the head, brain, extrathoracic airways, kidneys and rectosigmoid colon and the addition of explicit representations of the salivary glands, alimentary track mucosa, respiratory tract airways, and the urinary bladder. Tissue compositions and densities were simulated according to ICRP Publication 89 [11] and ICRU Report 46 [12] and prepared for use with the MCNP6 radiation transport code [7]. For additional information on the stylized computational phantoms, the reader is directed to Han et al. [10] and Bellamy et al. [13].

Voxel phantoms are typically limited in resolution such that precise calculations at the 0.007 cm thickness of the skin as recommended by the ICRP are not possible. Using the stylized phantoms, whose advantage lies in the determination of dose to thin tissues like the skin, can solve this issue. This is of notable interest for radionuclides with significant fractions of beta and/or low energy photon emissions during decay. The stylized phantoms include the organs and tissues in the ICRP 103 [1] tissue weighting factors. The soft tissue and the lung were used as surrogates for the lymphatic nodes and ET region, respectively, which are not included in the stylized phantom.

2.2 Comparison Studies

The results were compared to those of Yoo et al. [3] and Petoussi-Henss et al. [4]; as well as the values reported in FGR 12. FGR 12 used ICRP Publication 26 [14] and ICRP 60 [15] weighting factors to calculate the effective dose, while ICRP Publication 103 [1] weighting factors are used in this publication.

2.3 Computational Methods

In this work for all transport calculations, the MCNP code version 6 [7] was used. To determine the energy deposition within organs the kerma was scored using the MCNP F6 tally. The average track-length estimator folded with energy-dependent kerma factors within the MCNP6 code is used to calculate this tally. The contribution of secondary electrons to the kerma was considered using the thick target bremsstrahlung approximation. The detailed physics treatment by MCNP was used including bremsstrahlung production. The calculation of the effective dose E was based on the tissue weighting factors of ICRP Publication 103 [1].

2.4 Air Submersion Calculations

Dose rate coefficients in the air submersion scenarios were calculated assuming an individual standing on the ground and exposed to a uniform airborne contamination of a monoenergetic photon emitter. Source photons were uniformly sampled within the cloud volume. The computational method involved two steps to improve transport calculation efficiency. First, a calculation of photons incident on a closed surface surrounding a phantom was performed for 12 monoenergetic photons ranging in energy from 10 keV to 5 MeV. A cylinder of height 200 cm and radius 30 cm was used to represent the closed surface. The energy, fluence, and angular dependence of the particles incident upon the coupling surface was tallied for use in the second calculation step. Next, the computation of organ equivalent dose rate coefficients due to photons transported from the coupling cylinder into the phantom was performed.

2.5 Water Immersion Calculations

Dose rate coefficients for water immersion were calculated under the assumption of complete immersion in an infinite volume of uniformly contaminated water. In contrast to air submersion, with Monte Carlo methods it is possible to simulate an effectively infinite pool using relatively small dimensions since the linear attenuation coefficients of water are much greater than those for air. The water density was taken to be 1 g cm^{-3} and the composition by mass fraction was 0.112 for H and 0.888 for O.

2.6 Generation of Radionuclide Dose Coefficients

Radionuclide specific dose rate coefficients, \dot{h}_T^S , for tissue T and exposure mode, S, were computed as:

$$\dot{h}_T^S = \sum_{j=e,\gamma} [\sum_i Y_j(E_i) \widehat{h}_{T,j}^S(E_i) + \int_0^\infty Y_j(E) \widehat{h}_{T,j}^S(E) dE] \quad (1)$$

where the outer summation extends over electron, positron, and photon radiations emitted by the radionuclide. The first term within the major bracket sums over all radiation i of type j emitted with yield $Y_j(E_i)$ and energy E_i . The integral of the second term is over the continuous beta and bremsstrahlung spectra. The quantity $\widehat{h}_{T,j}^S$ is the monoenergetic dose rate coefficients discussed above for radiation type j and tissue T . The yield of the various radiation types and the beta spectrum, if applicable, of the radionuclide were those tabulated in ICRP 107.

3 RESULTS AND DISCUSSION

Dose rate coefficients for submersion in air and immersion in water were generated for 1252 radionuclides. Tables 1 and 2 list the effective dose rate coefficients for selected radionuclides by phantom age for air and water immersion, respectively.

Table 1: Air submersion effective dose rate coefficients for age-specific phantoms computed in this work

Nuclide	Effective Dose Rate for Submersion in Air ($\text{Sv m}^3 \text{Bq}^{-1} \text{s}^{-1}$)					
	Adult	15-yr. old	10-yr. old	5-yr. old	1-yr. old	Newborn
Ag-110m	1.27E-13	1.29E-13	1.40E-13	1.46E-13	1.58E-13	1.70E-13
Ar-41	6.16E-14	6.23E-14	6.68E-14	6.96E-14	7.53E-14	8.03E-14
Ba-137m	2.67E-14	2.71E-14	2.96E-14	3.09E-14	3.36E-14	3.62E-14
Co-58	4.43E-14	4.48E-14	4.88E-14	5.09E-14	5.55E-14	5.96E-14
Co-60	1.19E-13	1.21E-13	1.29E-13	1.35E-13	1.46E-13	1.56E-13
Cs-134	7.04E-14	7.13E-14	7.76E-14	8.11E-14	8.82E-14	9.49E-14
Cs-136	9.79E-14	9.91E-14	1.07E-13	1.12E-13	1.22E-13	1.31E-13
Cs-138	1.15E-13	1.16E-13	1.24E-13	1.30E-13	1.39E-13	1.49E-13
I-131	1.67E-14	1.69E-14	1.87E-14	1.95E-14	2.10E-14	2.30E-14
I-132	1.04E-13	1.05E-13	1.14E-13	1.19E-13	1.30E-13	1.39E-13
I-133	2.76E-14	2.80E-14	3.05E-14	3.20E-14	3.46E-14	3.73E-14
I-134	1.21E-13	1.22E-13	1.32E-13	1.38E-13	1.50E-13	1.60E-13
I-135	7.57E-14	7.66E-14	8.21E-14	8.57E-14	9.24E-14	9.87E-14
Kr-85	2.40E-16	2.41E-16	2.53E-16	2.59E-16	2.70E-16	2.82E-16
Kr-85m	6.72E-15	6.82E-15	7.56E-15	7.93E-15	8.70E-15	9.53E-15
Kr-87	3.96E-14	4.00E-14	4.28E-14	4.45E-14	4.76E-14	5.08E-14
Kr-88	9.71E-14	9.82E-14	1.04E-13	1.09E-13	1.16E-13	1.23E-13
Mn-54	3.83E-14	3.87E-14	4.20E-14	4.38E-14	4.79E-14	5.14E-14
Mo-99	6.88E-15	6.97E-15	7.59E-15	7.92E-15	8.62E-15	9.28E-15
Na-24	2.08E-13	2.10E-13	2.23E-13	2.31E-13	2.47E-13	2.62E-13
Nb-95	3.48E-14	3.52E-14	3.83E-14	4.00E-14	4.36E-14	4.68E-14
Np-239	7.15E-15	7.27E-15	8.09E-15	8.52E-15	9.29E-15	1.04E-14
Rb-88	3.37E-14	3.41E-14	3.62E-14	3.77E-14	4.03E-14	4.28E-14
Rb-89	1.09E-13	1.11E-13	1.18E-13	1.23E-13	1.33E-13	1.41E-13
Ru-103	2.18E-14	2.22E-14	2.43E-14	2.54E-14	2.75E-14	2.98E-14
Ru-105	3.37E-14	3.41E-14	3.73E-14	3.89E-14	4.23E-14	4.56E-14
Sr-90	9.81E-17	9.82E-17	9.92E-17	9.97E-17	1.01E-16	1.02E-16
Xe-133	1.27E-15	1.30E-15	1.52E-15	1.63E-15	1.83E-15	2.17E-15
Xe-135	1.08E-14	1.09E-14	1.21E-14	1.26E-14	1.36E-14	1.51E-14
Xe-135m	1.87E-14	1.89E-14	2.07E-14	2.17E-14	2.35E-14	2.54E-14
Y-90	7.88E-16	7.90E-16	8.10E-16	8.20E-16	8.40E-16	8.64E-16

Table 2: Water immersion effective dose rate coefficients for age-specific phantoms computed in this work.

Nuclide	Effective Dose Rate for Submersion in Air ($\text{Sv m}^3 \text{Bq}^{-1} \text{s}^{-1}$)					
	Adult	15-yr. old	10-yr. old	5-yr. old	1-yr. old	Newborn
Ag-110m	2.67E-16	2.71E-16	3.01E-16	3.08E-16	3.32E-16	3.60E-16
Ar-41	1.30E-16	1.32E-16	1.45E-16	1.48E-16	1.59E-16	1.73E-16
Ba-137m	5.54E-17	5.62E-17	6.27E-17	6.45E-17	6.98E-17	7.58E-17
Co-58	9.23E-17	9.37E-17	1.04E-16	1.07E-16	1.16E-16	1.25E-16
Co-60	2.52E-16	2.56E-16	2.82E-16	2.87E-16	3.09E-16	3.35E-16
Cs-134	1.46E-16	1.48E-16	1.65E-16	1.70E-16	1.84E-16	1.99E-16
Cs-136	2.05E-16	2.08E-16	2.31E-16	2.36E-16	2.55E-16	2.78E-16
Cs-138	2.42E-16	2.46E-16	2.69E-16	2.74E-16	2.94E-16	3.20E-16
I-131	3.36E-17	3.41E-17	3.83E-17	3.98E-17	4.35E-17	4.82E-17
I-132	2.17E-16	2.20E-16	2.44E-16	2.50E-16	2.70E-16	2.93E-16
I-133	5.67E-17	5.76E-17	6.41E-17	6.62E-17	7.16E-17	7.81E-17
I-134	2.52E-16	2.56E-16	2.84E-16	2.91E-16	3.13E-16	3.40E-16
I-135	1.60E-16	1.62E-16	1.78E-16	1.82E-16	1.95E-16	2.13E-16
Kr-85	3.57E-19	3.61E-19	3.89E-19	3.97E-19	4.20E-19	4.48E-19
Kr-85m	1.29E-17	1.31E-17	1.49E-17	1.58E-17	1.74E-17	1.98E-17
Kr-87	8.24E-17	8.34E-17	9.10E-17	9.29E-17	9.99E-17	1.09E-16
Kr-88	2.06E-16	2.09E-16	2.27E-16	2.31E-16	2.47E-16	2.69E-16
Mn-54	8.01E-17	8.13E-17	9.05E-17	9.27E-17	9.99E-17	1.08E-16
Mo-99	1.40E-17	1.42E-17	1.58E-17	1.63E-17	1.76E-17	1.92E-17
Na-24	4.45E-16	4.50E-16	4.86E-16	4.94E-16	5.29E-16	5.71E-16
Nb-95	7.26E-17	7.36E-17	8.20E-17	8.41E-17	9.08E-17	9.85E-17
Np-239	1.38E-17	1.41E-17	1.60E-17	1.69E-17	1.88E-17	2.14E-17
Rb-88	6.99E-17	7.08E-17	7.69E-17	7.83E-17	8.40E-17	9.13E-17
Rb-89	2.31E-16	2.34E-16	2.56E-16	2.61E-16	2.81E-16	3.04E-16
Ru-103	4.47E-17	4.54E-17	5.07E-17	5.25E-17	5.70E-17	6.23E-17
Ru-105	6.93E-17	7.04E-17	7.85E-17	8.09E-17	8.76E-17	9.56E-17
Sr-90	1.07E-19	1.07E-19	1.10E-19	1.10E-19	1.11E-19	1.14E-19
Xe-133	2.52E-18	2.51E-18	2.96E-18	3.10E-18	3.59E-18	4.39E-18
Xe-135	2.11E-17	2.14E-17	2.43E-17	2.54E-17	2.79E-17	3.16E-17
Xe-135m	3.82E-17	3.88E-17	4.33E-17	4.48E-17	4.87E-17	5.31E-17
Y-90	9.47E-19	9.52E-19	1.00E-18	1.01E-18	1.04E-18	1.10E-18

Figure 1: Comparison of adult effective dose rate coefficient under FGR 12 (ICRP 60 tissue weighting factors and ICRP 38 decay data) and this work (ICRP 103 tissue weighting factors and ICRP 107 decay data) for 825 radionuclides for air submersion.

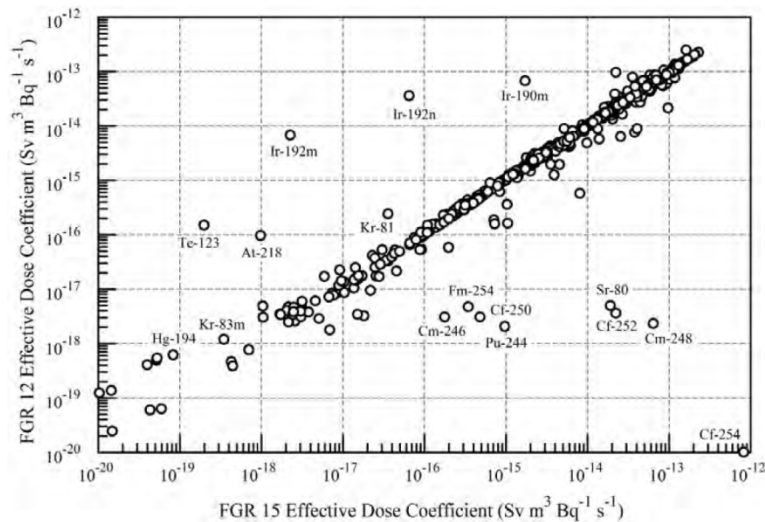
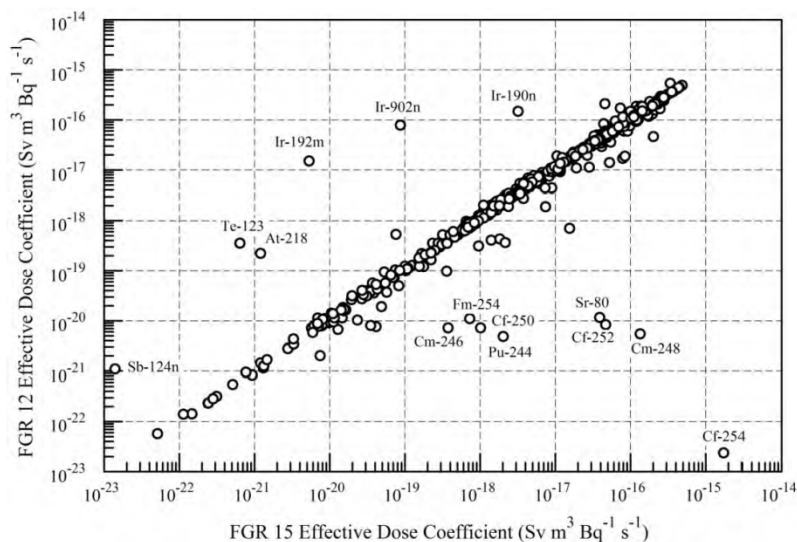


Figure 2: Comparison of adult effective dose rate coefficient under FGR 12 (ICRP 60 tissue weighting factors and ICRP 38 decay data) and this work (ICRP 103 tissue weighting factors and ICRP 107 decay data) for 825 radionuclides for water immersion.



The difference in calculated effective dose rates, using the ICRP-103 recommendations and those reported by Yoo et al. and Petoussi et al. were minimal for most radionuclides, indicating that the stylized phantoms provide an adequate substitute for the voxel models. The advantage of the stylized phantoms, as noted earlier, is the more representative skin model allowing for dose computation at the appropriate depth. The skin dose rate has a high impact on the nuclide coefficient this advantage can be significant. The inclusion of source electron emissions and bremsstrahlung production results in insignificant differences for radionuclides such as ^{85}Kr .

Plots showing the differences between the adult effective dose rate coefficients in FGR 12 and the adult effective dose rate coefficients in this work for 825 radionuclides are shown in Fig.1 for the case of air submersion and in Fig. 2 for water immersion.

4 CONCLUSION

The effective dose rate coefficients for immersion in contaminated air and water have been reported. These results compare favorably with previously published values and the main differences are due to the inclusion of electron emissions and bremsstrahlung radiations. The effective dose rate coefficients for the fourteen radionuclides shown within this work give an indication of the impact of the methods used compared to other studies. The coefficients are similar to those computed under the auspices of ICRP 60. The difference in the values provided by others are mainly due to differences in transport calculation methods, updated decay data, and other assumptions. The complete compilation of 1252 radionuclides will be released by the US EPA in its upcoming FGR 15 report.

5 ACKNOWLEDGEMENTS

This work was supported by the U.S. Environmental Protection Agency Office of Radiation and Indoor Air under Interagency Agreement number DOE 1886-T249-06/1886-T233-06 and was prepared by Oak Ridge National Laboratory, managed by UT Battelle, LLC, for the U.S. Department of Energy under contract DEAC05-00OR22725.

6 REFERENCES

- [1] INTERNATIONAL COMMISSION ON RADIOLOGICAL PROTECTION (ICRP), “The 2007 Recommendations of the International Commission on Radiological Protection,” ICRP Publication 103. Ann. ICRP 37 (2-4). Elsevier, 2007.
- [2] INTERNATIONAL COMMISSION ON RADIOLOGICAL PROTECTION (ICRP), “Nuclear Decay Data for Dosimetric Calculations,” ICRP Publication 107. Ann. ICRP 38 (3). Elsevier, 2008.
- [3] S.J. Yoo, H-K Jang, J-K Lee, S. Noh, and G. Cho. External Dose-Rate Conversion Factors of Radionuclides for Air Submersion, Ground Surface Contamination, and Water Immersion Based on the New ICRP Dosimetric Setting. *Radiation Protection Dosimetry*, 156, No. 1, pp. 7-24, 2013.
- [4] N. Petoussi-Henss, H. Schlattl, M. Zankl, A. Endo, and K. Saito. Organ Doses from Environmental Exposures Calculated Using Voxel Phantoms of Adults and Children. *Phys. Med. Biol.*, 57, pp. 5679-5713, 2012.
- [5] K. F. Eckerman, and J. C. Ryman. External Exposure to Radionuclides in Air, Water, and Soil, Federal Guidance Report No. 12, EPA 402-R-93-081. Oak Ridge National Laboratory, Oak Ridge, TN, 1987.
- [6] M. Cristy and K.F. Eckerman. Specific Absorbed Fractions of Energy at Various Ages from Internal Photon Sources Parts I-VII, ORNL/TM 8381/V1-V7. Oak Ridge National Laboratory, Oak Ridge, TN; U.S. Environmental Protection Agency, Washington, DC, 1987.
- [7] D.B. Pelowicz, Ed. MCNP6 User’s Manual, LA-CP-13-00634, Rev. 0. Los Alamos National Security, LLC, Los Alamos, NM, 2013.
- [8] ENDF- 6 Formats Manual, M. Herman, Ed. ENDF/B-VI Release 8, BNL-NCS-44945-05-Rev., National Nuclear Data Center Brookhaven National Laboratory, Upton, N.Y. 11973-5000, 2005.
- [9] INTERNATIONAL COMMISSION ON RADIOLOGICAL PROTECTION (ICRP), “Radionuclide Transformations: Energy and Intensity of Emissions,” ICRP Publication 38. Ann. ICRP Vols. 11-13, 1983.
- [10] E. Y. Han, W. E. Bolch and K. F. Eckerman. Revisions to the ORNL Series of Adult and Pediatric Computational Phantoms for use with the MIRD Schema. *Health Physics*, 90(4), pp. 337-356, 2006.
- [11] INTERNATIONAL COMMISSION ON RADIOLOGICAL PROTECTION (ICRP), “Basic Anatomical and Physiological Data for Use in Radiological Protection Reference Values,” ICRP Publication 89. Ann. ICRP 32 (3-4). Pergamon Press, 2002.
- [12] INTERNATIONAL COMMISSION ON RADIATION UNITS AND MEASUREMENTS (ICRU), “Photon, Electron, Proton and Neutron Interaction Data for Body Tissues,” ICRU Publication 46, Bethesda, MD; ICRU, 1992.
- [13] M. B. Bellamy, S. A. Dewji, M. M. Hiller, K.G. Veinot, R. W. Leggett, K. F. Eckerman, C. E. Easterly, N. E. Hertel. Comparison Of Monoenergetic Photon Organ Doses For Stylized And Voxel Phantoms Submerged In Air. *Radiation Protection Dosimetry*, Advance Access, Feb. 8, 2016.
- [14] INTERNATIONAL COMMISSION ON RADIOLOGICAL PROTECTION (ICRP), “Recommendations of the ICRP,” ICRP Publication 26. Oxford, Pergamon Press, 1977.
- [15] INTERNATIONAL COMMISSION ON RADIOLOGICAL PROTECTION (ICRP), “1990 Recommendations of the International Commission for Radiological Protection,” ICRP Publication 60. Oxford, Pergamon Press, 1991.

Thoron Exhalation Rate and ^{232}Th Content in Traditional Building Materials Used in the Coastal Region of Kenya

Margaret Chege^{a*}, Nadir Hashim^b, Abdallah Merenga^b, Oliver Meisenberg^{c#},
Jochen Tschiersch^c

^aKenyatta University, Mombasa Campus, Department of Physics, P.O. Box 16778-80100, Mombasa, Kenya.

^bKenyatta University, Department of Physics, P.O. Box 43844-00100, Nairobi, Kenya.

^cHelmholtz Zentrum München – German Research Center for Environmental Health (GmbH), Institute of Radiation Protection, P.O. Box 11 29, 85758 Neuherberg, Germany.

Abstract. This paper presents thoron exhalation rate and specific concentration of ^{232}Th in samples of dried-up mud lumps from the walls of selected dwellings in the coastal region of Kenya. Exhalation measurement was done using RAD7 alpha detection system while that of ^{232}Th was done using a high purity germanium detector. The exhalation rate ranged from below detection limit to $35.7 \pm 5.2 \text{ Bq m}^{-2} \text{ s}^{-1}$ with an arithmetic mean of $10.3 \pm 1.6 \text{ Bq m}^{-2} \text{ s}^{-1}$. ^{232}Th concentration averaged $227 \pm 10 \text{ Bq kg}^{-1}$ with a minimum of $17 \pm 1 \text{ Bq kg}^{-1}$ and a maximum of $804 \pm 34 \text{ Bq kg}^{-1}$. A strong positive correlation ($R^2=0.99$) was observed between thoron exhalation rate and ^{232}Th content in the building material samples studied.

KEYWORDS: Thoron; ^{232}Th ; soil; building materials; exhalation rate; dwellings; Mrima hill.

1 INTRODUCTION

Radioactivity in indoor air is mainly attributed to the radon isotopes. The most common radon isotopes are ^{222}Rn (generally referred to as radon) and ^{220}Rn (thoron) in the decay chains of ^{238}U and ^{232}Th respectively. ^{238}U and ^{232}Th are terrestrial radionuclides that are ubiquitously present in trace amounts in rock and soil, with concentration varying from one region to another depending on the geological setting. Rock and soil constitute the main building materials in most parts of the world. Unlike the parent radionuclides, the radon isotopes are gases and subject to the nature of the building material, they may exhale from the solid matrix where they are formed and into indoor air. Radon is a known carcinogen and is considered responsible for the largest fraction of lung cancer cases among non-smokers and the second leading cause of lung cancer after cigarette smoking [1].

Until recently, little attention was paid to thoron in the context of radiation protection. With a half-life of 55.6 s it was assumed to largely decay before leaving the solid matrix. Recent studies have however shown that thoron can considerably add to the inhaled dose particularly in dwellings where the main building material is soil [2-5]. In China, residential dwellings constructed using soil were found with thoron concentration of up to 1860 Bq m^{-3} [4] while in some cave dwellings thoron concentration was as high as 865 Bq m^{-3} [6]. Thoron exhalation from building materials is increasingly being acknowledged as a potential source of radiation exposure [7] and is therefore an important aspect in the characterization of building materials.

This study was conducted in the region around Mrima hill in the south coast of Mombasa, Kenya. This is one of the regions with high levels of natural background radiation in the country. The background radiation is mainly attributed to ^{232}Th given the presence of monazites and carbonatite rock formation [8-11]. Typical to rural Kenya, the dwellings in the region are constructed using soil normally dug in the backyard of the structure under construction. In this paper, thoron exhalation rate and specific concentration of ^{232}Th in samples of dried-up mud lumps from the walls of selected dwellings in the region are presented.

*Presenting author, e-mail: znimo@yahoo.com; chege.margaret@ku.ac.ke

#Present address: Bundesamt für Strahlenschutz (BfS), Ingolstädter Landstr.1, 85764 Neuherberg, Germany

2 MATERIALS AND METHODS

2.1 Measurement and Analysis of Thoron Exhalation Rate

Accumulation chamber method and continuous measurement of thoron concentration using Rad7 alpha monitor (Durrige Co., USA) were employed in the measurement of thoron exhalation rate [12]. The accumulation chamber consisted of a 3-litre stainless steel barrel fitted with an air tight lid. A small fan located near the bottom of the chamber kept the air inside well mixed. Two ports on the top of the barrel connected the accumulation chamber to the RAD7 monitor via silicon hoses. The Rad7 comprised of a hemisphere cell coated on the inside with a conducting material with silicon alpha detector implanted at the centre. The cell was equipped with a built-in pump with adjustable flow rate to draw in sample air. The hose leading to the cell was equipped with a thin filter to suppress thoron decay products while allowing free movement of air. A bias voltage of 2000 V was applied to the RAD7 monitor.

10 lumps of dried-up mud were carefully pried off the walls of randomly selected dwellings in the sampling region. To simulate their appearance on the walls of the dwellings, all but one side of each sample was thickly coated with 10 layers of lacquer which effectively suppressed thoron exhalation. Each pre-treated sample was enclosed in the accumulation chamber and after an in-growth time of about 24 h, the RAD7 monitor was connected. Thoron concentration was quantified based on the alpha particle energy 6.78 MeV. The exhalation rate (E) was evaluated using the equation [13]:

$$E = \frac{\lambda_{eff} C}{A_s} \quad (1)$$

where C is the steady state concentration of thoron in the accumulation chamber, λ_{eff} the effective decay and leakage constant, V the volume of the chamber and A_s the surface area of the exposed part of the sample.

2.2 Measurement and Analysis of Specific Concentration of ^{232}Th

A high purity germanium detector interfaced with a high voltage detector bias supply and signal processing electronics was used. Detector calibration was done using internationally accepted standards. A platform that held the sample container coaxial with the detector during counting ensured reproducibility.

Samples used for exhalation measurements were analyzed for ^{232}Th content. The resin coat on each sample was cut off. Each sample was then crushed and homogenized, weighed, sealed in standard polyethylene containers and stored for at least 21 days to allow for the in-growth of the short lived progeny and attainment of secular equilibrium with ^{232}Th . For concentration analysis, each sample was counted for 12 h. Specific concentration (C) was evaluated based on gamma-ray energies 968.97, 911.2, 727.33 and 1620.5 keV using the relation [13]:

$$C = \frac{N}{b\epsilon mt} \quad (2)$$

where N is the average net intensity of the gamma ray of interest, b the emission probability of the gamma ray of interest, ϵ the detection efficiency of the gamma ray of interest, m the mass of the sample in kg and t the measurement time in seconds.

3 RESULTS AND DISCUSSIONS

Table 1 shows the summary statistics of thoron exhalation rate in the building material samples. The exhalation rate ranged from below detection limit to $35.7 \pm 5.2 \text{ Bq m}^{-2} \text{ s}^{-1}$ with an arithmetic mean of $10.3 \pm 1.6 \text{ Bq m}^{-2} \text{ s}^{-1}$. It was observed that samples that registered higher exhalation rate coincided with those obtained from Mrima village which extends from the slopes of the hill to an approximate distance of 6 km. In this village, exhalation rate averaged $19.8 \pm 3.2 \text{ Bq m}^{-2} \text{ s}^{-1}$, nearly 20 times higher than the global average of $1 \text{ Bq m}^{-2} \text{ s}^{-1}$ in soil [14]. The lowest exhalation rate in samples from this village was $2.5 \pm 1.8 \text{ Bq m}^{-2} \text{ s}^{-1}$.

Table 1: Summary statistics of thoron exhalation rate in the building material samples.

	Thoron exhalation rate ($\text{Bq m}^{-2} \text{ s}^{-1}$)			
	Sample size	Minimum	Maximum	Average
Sampling region	10	Below detection	35.7 ± 5.2	10.3 ± 1.6
Mrima Village	5	2.5 ± 1.8	35.7 ± 5.2	19.8 ± 3.2
Kanana village	5	Below detection	1.3 ± 0.3	0.8 ± 0.2

The exhalation rate was considerably lower in samples obtained further away from the hill (7-12 km). Samples from Kanana Village in the 7-12 km radius registered average thoron exhalation rate of $0.8 \pm 0.2 \text{ Bq m}^{-2} \text{ s}^{-1}$, the highest value being $1.3 \pm 0.3 \text{ Bq m}^{-2} \text{ s}^{-1}$. This is comparable to the global average in soil.

Table 2 gives the summary statistics of specific concentration of ^{232}Th in samples of building materials analysed in this work. The concentration varied from $17 \pm 1 \text{ Bq kg}^{-1}$ to $804 \pm 34 \text{ Bq kg}^{-1}$ with an arithmetic mean $227 \pm 10 \text{ Bq kg}^{-1}$. Samples from Mrima village had the highest ^{232}Th concentration with an average 5 times higher than the world average of 40 Bq kg^{-1} in soil [14]. Samples from Kanana on the other hand had a much lower concentration, the highest being $27 \pm 2 \text{ Bq kg}^{-1}$. The results from this study further confirm that the hill soil is the source of the high background radiation level in the region.

Table 2: Summary statistics of specific concentration of ^{232}Th in the building material samples.

	^{232}Th concentration (Bq kg^{-1})			
	Sample size	Minimum	Maximum	Average
Sampling region	10	17 ± 1	804 ± 34	227 ± 10
Mrima Village	5	59 ± 3	804 ± 34	431 ± 19
Kanana village	5	17 ± 1	27 ± 2	23 ± 1

Thoron exhalation rate is not necessarily a function of the content of ^{232}Th . This is because thoron atoms may decay within the solid matrix of the building material if their mobility is hindered. In this study, a strong positive correlation ($R^2=0.99$) was observed between thoron exhalation rate and the content of ^{232}Th in the building material samples analyzed.

4 CONCLUSION

Thoron exhalation rate was significantly high in samples from Mrima village. The average specific concentration of ^{232}Th in these samples was markedly high at over a factor of 5 of the world average in soil. The exhalation rate of thoron was dependent on the content of ^{232}Th in the samples studied. The use of soil from a region of high natural background radiation as a building material may exacerbate thoron exposure in dwellings.

5 ACKNOWLEDGEMENTS

Much appreciation to the management of Helmholtz Zentrum Munchen, Institute of Radiation Protection, Germany, for facilitating the analysis of the samples used in this study, and to the National Commission for Science, Technology and Innovation (NACOSTI), Kenya, for funding this research (Grant Number: NCST/5/003/4th CALL PhD/).

6 REFERENCES

- [1] WHO, 2009. World Health Organization Handbook on Indoor Radon: A Public Health Perspective. World Health Organization, 2009.
- [2] Meisenberg O. and Tschiersch J., 2011. Thoron in indoor air: modelling for a better exposure estimate. *Indoor Air*, 21: 240–252.
- [3] Tschiersch J., Li W.B. and Meisenberg O., 2007. Increased indoor thoron concentrations and implication to inhalation dosimetry. *Radiat Prot Dosimetry*, 127: 73-78.
- [4] Shang B., Chen B., Gao Y., Wang Y., Cui H. and Li Z., 2005. Thoron levels in traditional Chinese residential dwellings. *Radiat Environ Biophys.*, 44(3): 193-199.
- [5] Sreenath R.M., Yadagiri R.P., Rama K., Eappen, K.P., Ramachandran, T.V. and Mayya Y.S., 2004. Thoron levels in the dwellings of Hyderabad city, Andhra Pradesh, India. *J Environ Radioact.*, 73: 21-28.
- [6] Tokonami S., Sun Q., Akiba S., Zhuo W., et al., 2004. Radon and thoron exposures for cave residents in Shanxi and Shaanxi provinces. *Radiat Res*, 162(4): 390-396.
- [7] With G., Jog P. and Röttger A. 2014. Measurement of thoron exhalation rates from building materials. *Health Phys.*, 107(3):206-12.
- [8] Chege, M.W., Hashim, N.O., Merenga, A.S. and Tschiersch, J., 2015. Analysis of internal exposure associated with consumption of crops and groundwater from the high background radiation area of Mrima hill, Kenya. *Radiat Prot Dosimetry*, 2015: ncv231v1-ncv231.
- [9] Chege, M.W., Hashim, N.O., Merenga, A.S., Meisenberg, O. and Tschiersch, J., 2015. Estimation of annual effective dose due to radon and thoron concentrations in mud dwellings of Mrima hill, Kenya. *Radiat Prot Dosimetry*, 2015: ncv261v1-ncv261.
- [10] Patel J.P., 1991. Environmental radiation survey of the area of high background radiation of Mrima hill, Kenya. *Discov Innov.*, 3(3): 31-35.
- [11] Kebwaro J.M., Rathore I.V.S., Hashim, N.O. and Mustapha A.O., 2011. Radiometric assessment of natural radioactivity levels around Mrima Hill, Kenya. *Int J Phys Sci.*, 6: 3105–3110.
- [12] Tuccimei, P., Moroni, M. and Norcia, D., 2006. Simultaneous determination of ^{222}Rn and ^{220}Rn exhalation rates from building materials used in Central Italy with accumulation chambers and a continuous solid state alpha detector: influence of particle size, humidity and precursors concentration, *Appl Radiat Isotopes.*, 64, 254–263.
- [13] Chege, M. W., 2014. Modelling radon and thoron exhalation and measurement of total natural radiation exposure in Mrima hill, Kenya. Ph.D. (Physics) thesis. Kenyatta University, Nairobi, Kenya. Retrieved 2016-05-12 from: <http://ir-library.ku.ac.ke/handle/123456789/12069>.
- [14] UNSCEAR, 2000. United Nations Scientific Committee on the Effects of Atomic Radiation. Sources and Effects of Ionizing Radiation. UNSCEAR 2000 Report to the General Assembly, with Scientific Annexes, (I): New York: United Nations, 2000.

A comparison of a commercial and specifically developed (CTBTO-VGSL) software packages used in high-resolution gamma-spectrometry on their applicability and accuracy in NORM analysis of environmental samples, which includes optimization of spectrum analysis parameter settings and sum-coincidence and self-absorption corrections

Monnicca M. Rapetsoa^{a*}, Arnaud Faanhof^a, Deon Kotze^a. Robert Lindsay^b

^aNECSA., P.O. Box 582, Pretoria, 0001, South Africa.

^bDepartment of Physics, UWC, P/Bag X17, Bellville, 7530, South Africa.

Abstract. In this study, a comparison has been made between an available commercial software package (Genie 2000) and Virtual Gamma Spectroscopy Laboratory (VGSL) developed by the Radionuclide Development Unit of the International Data Centre of the Comprehensive Nuclear Test-Ban Treaty Organization (CTBTO) designed to simulate gamma spectra acquired, using HPGe detectors and accordingly provide quality assessment of the data delivered by eighty (80) international monitoring stations distributed around the world to monitor nuclide emissions after an illegal nuclear test, either in the atmosphere, under water or underground. The lessons learned from the CTBTO Intercomparison studies will be applied to NORM nuclide analyses of environmental samples. Results provided are based on three (3) IAEA reference materials: stream sediments, milk powder, and soil. These samples contain decay products of uranium and thorium as well as ¹³⁷Cs, which produce multiple gamma-rays, and hence a High Purity Germanium detector (HPGe) will be used. The study has been conducted in the South African CTBTO laboratory (ZAL14) situated at the South African Nuclear Energy Corporation SOC Ltd. The laboratory is equipped with two ultra-low background gamma-spectrometry systems accredited according to world-class standards. The CTBTO reference spectra and IAEA certified samples have been analyzed looking at a variety of parameter settings including sum-coincidence effects and matrix-dependent self-absorption using both software mentioned. Optimization of various parameters has been done using the calibrated reference samples and gamma-ray spectrums used in the CTBTO proficiency tests over the past decade. The results of the study will indicate if the empirically generated efficiency calibration by the Genie 2000 software currently used at the Radioanalytical laboratories of Necsca will be adequate to perform NORM-analyses or may be complemented by the efficiency calibrations obtained from the LABSOCS and/or VGSL software, with regard to their accuracy, precision and consistency in spectra analysis.

KEYWORDS: *gamma spectrometry instrumentation; gamma spectrometry software; naturally occurring radioactive material; high resolution; ultra low background.*

1 INTRODUCTION

Gamma spectrometry is the widely known study of identifying and quantifying radionuclides by analyzing gamma-ray spectra produced by a gamma spectrometer. It is a useful tool in many fields such as environmental sciences, health physics and industrial process monitoring. Gamma spectrometry using HPGe detectors is widely used due to the excellent energy resolution of this kind of detectors. In particular, it can be used for activity determination of gamma emitting radioactive sources whenever the full-peak efficiency calibration curve is known, from which the efficiency value for single gamma ray energies is obtained by interpolation [1].

In this study, in order to evaluate the applicability to accurately analyze low-level NORM containing environmental samples, a comparison will be made between a well-known available commercial software package (Genie 2000) and a specific software package, Virtual Gamma Spectroscopy Laboratory (VGSL), developed by the Radionuclide Development Unit of the International Data Center of the Comprehensive nuclear Test-Ban Treaty Organization (CTBTO) [2]. Efficiency calibrations obtained from simulations using Canberra calibration software (LABSOCS), MCNP based Virtual Gamma Spectroscopy Laboratory software (VGSL) and from the real-time measurement of certified radionuclide sources prepared by the National Physics Laboratory in the United Kingdom will be compared. These efficiency calibrations will be used to analyze the spectra obtained in various

Proficiency Testing Exercises (PTEs) issued by the Provisional Technical Secretariat of the CTBTO to the sixteen official Nuclide Laboratories in the world-wide monitoring network. As the results of the PTEs are known the comparison of the results obtained by the application of the three individual efficiency calibrations with the “true” values should provide insight into which of the three calibrations could be used best, or even if two or more calibrations can be used best in specific energy regions.

According to these “best” findings a quantitative method will be developed for application in NORM and artificial nuclide analysis in stream sediments, soil and milk powder. These samples normally contain decay products of uranium, thorium and ^{137}Cs , which produce multiple gamma-rays.

2 METHOD

2.1 Germanium detectors

High purity germanium detectors (HPGe) are well known for their high energy resolution capabilities and for easy maintenance [3]. In this study a Broad Energy Germanium detector (BEGe) is used for spectrum collection and empirical calibration purposes. A BEGe detector has a cylindrical shape and moderate thickness; typically 80 mm in diameter and 30 mm high as shown in Table 1. It has a large detection area with an entrance window made of a composite carbon. Its efficiency is high in the low energy range and relatively low in the high energy range. The energy range of a BEGe detector typically ranges from 3 keV to 3 MeV. The BEGe detector can specifically be applied for samples containing NORM-nuclides, as most of the gamma-rays emitted are below 1, 5 MeV.

Table 1: Detector dimensions from the detector's supplier

Detector dimensions	
crystal diameter	80.5 mm
crystal length	32.5 mm
dead layer top	0.0003 μm
dead layer outside	0.5 μm
dead layer inside/bottom	0.5 μm
crystal holder thickness (copper)	0.8 mm
end cap outer diameter	102 mm
end cap thickness	1.5 mm
end cap window thickness	0.6 mm
end cap window diameter	81 mm
end cap distance to crystal	6.61 mm

2.2 CTBTO Certified materials

The PTEs organized annually by the IMS for radionuclide laboratories started in the year 2000 and is still continuing. The primary objective for the PTEs is to assess on how capable the laboratories are in identifying the radionuclides in the reference samples. In addition to this the ability to measure the radioactivity levels of radionuclides in the filter samples and to calculate the related activity concentration are also objectives of the PTEs [4].

PTE spectra from previous years were used in the study. Efficiencies for 3 different sample geometries were computed. The MANUAL3M filter sample is the most common type of air-particulate sampling method among the three major types of radionuclide monitoring systems. The MANUAL3M can be split into two, which is commonly known as ‘HALF-MOON’ geometry. The other type of filter sample is the ARAME (Automatic Radionuclide Air Monitoring Equipment) also known as CINDERELLA geometry source.

For Proficiency Test Exercises, three samples are usually provided. The blank, the calibration and the reference sample, also known as the 'unknown' sample. The blank, calibration and reference samples are counted for seven days each.

2.3 IAEA Reference materials

Three samples with certified radionuclide content were used in this study to evaluate the lessons learnt from the CTBTO Proficiency Test Samples. These samples are certified reference materials from the IAEA, i.e. stream sediment (IAEA-314), soil (IAEA-375) and milk (IAEA-152).

2.3.1 Preparation

The three samples were regarded as potentially radioactive and therefore the normal precautionary measure for handling radioactive materials were adhered to. In the study the three sample materials were prepared; two in a 7×1.5cm and one in a 5×1.5cm disc PVC containers.

2.3.2 Sealing

A prerequisite for this methodology is that the radioactive equilibrium must be established between ^{226}Ra and its direct daughter ^{222}Rn (and progeny), which is a noble-gas and accordingly may escape through the wall of the plastic sample container. The sealing method was developed to seal the sample radon tight with applicable polyethylene laminated foil, in a way that will not cause significant attenuation of low energy gamma-rays [5]. The samples were sealed for 3 weeks prior to counting to ensure radionuclide equilibrium. After three weeks the samples were counted for twenty four hours on the BEGe detector.

2.4 LABSOCs software package

The LABSOCs calibration software includes several standard geometry templates. The most commonly used templates are Beaker, Box, Cylinder, Marinelli Beaker and the Sphere. Choosing the most applicable template, which was the cylinder for the samples concerned, the necessary physical dimensions of the samples are required; i.e. the thickness, inside wall height, inside base diameter, material type and the density of the container and the source material.

2.5 VGSL software package

The VGSL software only provides for four geometry templates, MANUAL3M, ARAME, Point source and RASA geometry. The detector, shielding, source geometry and material are to be defined. Characteristics of the detector are defined by the crystal type, crystal dimension, dead-layer thickness, crystal-holder dimensions, End Cap Mantle dimensions, End Cap Window dimensions and the sample material.

All relevant parameters like the detector dimensions, the detector shield, the distance between the sample and the detector's entrance window, the dimensions of the samples and their specific mass were used to simulate/determine the efficiency calibration through the LABSOC and VGSL software.

3 RESULTS AND DISCUSSION

3.1 Efficiency calibration

Genie 2000 uses the efficiency values from the fitted efficiency curve to calculate the activity. This curve is established using algorithms entrenched in the software and efficiency values provided by the user [6]. For the empirically fitted efficiency curve, the efficiency values were calculated from measuring the calibration source. The empirical calibration is computed with the aid of the LABSOCs

software package within the Genie 2000 package. LABSOCs computes true coincidence summing with the most appropriate detector characterized by the manufacturer and the sample characteristics as discussed in 2.4.

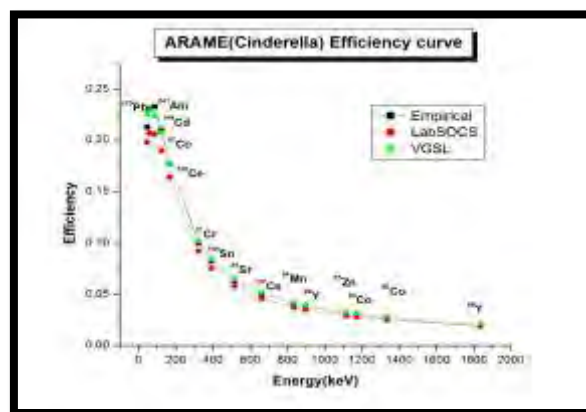
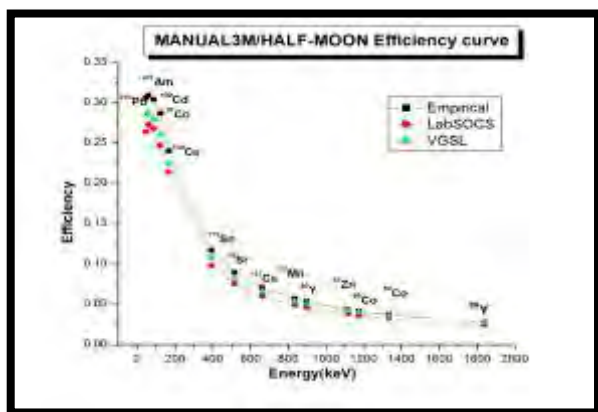
In all cases Genie 2000 was used to create a fitted dual efficiency curve comprised of a polynomial for the low energy region and the second one for the high energy region, with a common crossover point at 122 keV.

3.2 PTE analysis Results

The empirical efficiency as shown in Figures 1 and 2 of the fifth and fourth order polynomial yielded results that were in good agreement with the certified values. These were used to calibrate the reference spectra for the year 2008 (MANUAL3M), 2009(HALFMOON) and 2012(ARAME\CINDERELLA).

Figure 1: MANUAL3M/HALFMOON efficiency curves after cascade correction

Figure 2: ARAME efficiency curves after cascade correction



3.3 NORM analysis Results

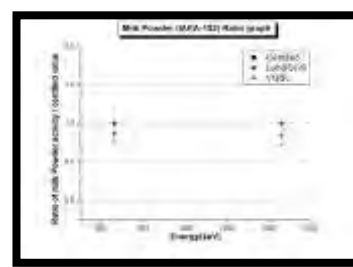
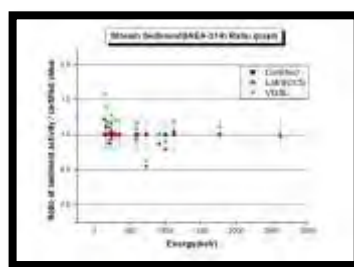
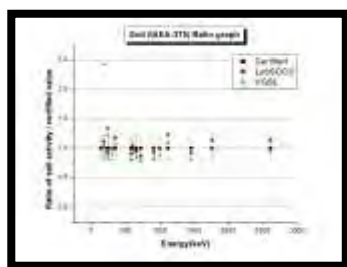
In the present study soil (IAEA-375), stream sediment (IAEA-314) and milk powder (IAEA-152) samples have been prepared from IAEA reference materials. These samples were analyzed using an ultra-low background gamma spectrometry system. The activity concentration was determined for the gamma-emitting nuclides in the ^{238}U and ^{232}Th decay series as well as ^{40}K and ^{137}Cs .

The three IAEA reference materials were analyzed with optimized spectrum analysis parameter settings resulting from the PTE analysis using the LABSOCs and VGSL software packages. The analyses results were then compared to the certified nuclide concentrations in the respective materials. The activity ratios obtained are shown in Figures 3, 4 and 5.

Figure 3: IAEA-375

Figure 4: IAEA-314

Figure 5: IAEA-152



4 CONCLUSION

In the PTE analysis the VGSL software performs slightly better compared to LABSOCs. Both VGSL and LABSOCs software can be considered reliable for gamma-ray efficiency calibration in CTBTO sample analysis. In the analysis of the IAEA reference materials LABSOCs performs slightly better than VGSL. This is somewhat contradictory to the PTE analysis. This might be due to fact that VGSL was developed specifically for PTE sample analysis; hence the geometries entrenched within the software are CTBTO samples related.

The results obtained are promising and further improvement may be expected with the development of the parameter settings for the summing effect and decay factor estimation in the final analysis. A very careful selection of detector assembly, geometry and shielding material thickness is important and should be further looked into.

5 ACKNOWLEDGEMENTS

This study was supported by the National Research Foundation, the South African Nuclear Energy Corporation SOC Ltd. and the University of the Western Cape. Special thanks to Maxie Willemse for the valuable guidance and support throughout this study as well as the Radioanalysis (RA) Laboratory team.

6 REFERENCES

- [1] Dias, M.S., Takeda, M.N. and Koskinas, M.F., (2002). Cascade summing corrections for HPGe spectrometers by the Monte Carlo method. *Appl. Radiat. Isot.*, 56(1-2), 105-109.
- [2] Plenteda, R., (2002). A Monte Carlo Based Virtual Gamma Spectroscopy Laboratory. Ph.D. Thesis. Universitaetsbibliothek der Technischen Universitat Wien, Resselgasse 4, A-1040, Vienna, Austria. Wien, Technische Universitat Wien 118 pp.
- [3] Canberra Industries Inc., (2003). Germanium detectors user's manual, Meriden, CT.
- [4] Nadalut, Duran, E.B. and Barbara, (2007). 2007 Proficiency Test Exercise for Radionuclide Laboratories Supporting the Network of IMS Radionuclide Stations, CTBT/PTS/TR, Vienna, Austria.
- [5] Willemse, M.L., (2012). Method for radon tight sealing of samples with applicable aluminium foil, RA-WIN-233 Pretoria, South Africa.
- [6] Canberra Industries Inc., (2006). Genie 2000 3.1 Customization Tools Manual, Meriden, CT. Genie 2000 3.1 Customization Tools Manual, Meriden.

K-40 levels in the South Adriatic Sea environment (Montenegro)

N. M. Antović^{a,*}, I. Antović^b, N. Svrkota^c

^aFaculty of Natural Sciences and Mathematics, University of Montenegro, Podgorica

^bDepartment for Biomedical Sciences, State University of Novi Pazar, Novi Pazar, Serbia

^cCentre for Ecotoxicological Research, Podgorica, Montenegro

Abstract. Potassium-40 in biotic (fish *Mugil cephalus*, *Chelon labrosus*, *Liza ramada*, and seagrass *Posidonia oceanica*) and abiotic (sediment and seawater) samples from the South Adriatic Sea marine environment of Montenegro, together with adjacent soils and beach sands, was analyzed for activity concentration and dose rate. In regard to soil and sand, minimum, maximum, mean, standard deviation and median were found to be – 258, 665, 442, 156 and 403 Bq/kg, respectively (soil), and 22.6, 298, 84.8, 87.8 and 42.3 Bq/kg, respectively (sand), i.e., 10.8, 27.7, 18.4, 6.5 and 16.8 nGy/h, respectively (soil), 0.94, 12.4, 3.54, 3.66 and 1.76 nGy/h, respectively (sand). In surface seawater it ranged from 3.14 to 8.84 Bq/L, while the lowest activity concentration in seawater was found for samples taken from 6.5-7 m in depth in the Boka Kotorska Bay (2.81 Bq/L). In sediment from the Boka Kotorska Bay 123 Bq/kg of ⁴⁰K was measured, and dose rate of 5.13 nGy/h has been estimated as an illustration. Real contribution of ⁴⁰K to dose rate for surface sediment will be somewhat lower, due to radiation attenuation from overlying water. Using the dose conversion coefficients for external and internal exposure to ⁴⁰K, an average dose rate for seagrass was estimated to be 190 nGy/h. Whole individuals of *M. cephalus* showed an average activity of about 97 Bq/kg, while muscles – 118 Bq/kg. In the case of *C. labrosus* it was around 96 and 90 Bq/kg, respectively, whilst in *L. ramada* – 75 and 122 Bq/kg, respectively. Since pelagic fish are internally irradiated by incorporated radionuclides and externally by the activity in water, both dose rates have been evaluated. Internal exposure of *M. cephalus* showed minimum, maximum, average and standard deviation of around 29, 49.5, 37.8 and 6.8 nGy/h, respectively, as total exposure – 30.3, 50.8, 39 and 6.8 nGy/h, respectively.

KEYWORDS: Potassium-40; seawater; seagrass; fish; Montenegro.

1 INTRODUCTION

The coastline of Montenegro adjacent to the South Adriatic Sea is 293.5 km long (6334 km² of the Sea – territorial sea and epicontinental belt [1]). The Coast (area of 1591 km²) contributes ~24 % to the total country population of 620 029 (in 2011 [2]).

A comprehensive radioecological research on this region was performed in last several years. In this paper we focus on natural radionuclide ⁴⁰K in the South Adriatic Sea environment, and soil and sand on the Coastal area of Montenegro. This radionuclide, together with those from uranium and thorium series, is responsible for the most of the external exposures to gamma radiation. Its half-life is 1.277·10⁹ yr, and decays by β⁻-decay to stable ⁴⁰Ca (89.3 %), and by electron capture and β⁺-decay to stable ⁴⁰Ar (10.7 %) with an emission of 1460.83 keV γ-ray [3]. Therefore, a standard procedure for ⁴⁰K activity measurement is gamma spectrometry. In addition to standard HPGe spectrometry, a multidetector system (as one described in [4]) can also be used for its measurements in various environmental samples. Therefore, although soils and sands from Montenegro were measured by a standard HPGe gamma spectrometry [5-6], they were also measured by a multidetector gamma spectrometer, together with the other abiotic and biotic samples from the South Adriatic Sea environment. Some of the results are presented here.

The spectrometers which were used to measure radionuclide activities are: HPGe (ORTEC – GEM-40190, relative efficiency – 40 %, FWHM – 1.80 keV at 1.33 MeV, FWHM – 840 eV at 122 keV; and ORTEC GEM – 30185-S, relative efficiency – 35 %, FWHM = 1.72 keV at 1.33 MeV, FWHM = 700 eV at 122 keV), and the six-crystal spectrometer PRIPYAT-2M [4]. The characteristics of PRIPYAT-2M allowing express ⁴⁰K measurements, are: mass of 4200 kg, outer dimension (250 x 145 x 186) cm³,

* Presenting author, e-mail: nena@rc.pmf.ac.me

six NaI(Tl) detectors (crystals of 15 cm x 10 cm), up to 15 cm of iron and lead passive shielding, measuring chamber – a cube with a side of 17.5 cm, measuring geometry close to 4π ($\sim 0.7 \times 4\pi$ sr), 40 ns resolution time for coincidences, the multiplicity of coincidences from 2 to 6, energy resolution of 10.5 % for the 662 keV γ -rays from ^{137}Cs [4]. A calibration was performed by counting the ^{137}Cs and ^{40}K γ -sources (VNIIM D.I. Mendeleev: OMASN, N.72/94-2 and OMASN, N.103/92, respectively), while in the case of the HPGe spectrometers – the Czech Metrology Institute standards. K-40 activity concentrations have been determined in standard analyses using the total net counting rate under the 1461 keV photopeak, detection efficiency, γ -ray intensity and sample weight.

2 MATERIALS AND METHODS

2.1 Sampling and measurements

Surface (0-5) cm uncultivated soil taken from a frame of 25 cm x 25 cm at ten measuring points in urban settlements on the Coast of Montenegro (Table 1) was prepared in a standard procedure [7], i.e., dried, homogenized, weighed and sealed in the Marinelli beakers, and then measured in the mentioned standard procedure. Beach sands (Table 1) sampled close to soil measuring points were also selected for the present study, had also been dried at room temperature, weighed and sealed in the Marinelli beakers.

This paper contains results obtained in measuring these samples by the PRIPYAT-2M gamma spectrometer for 2000 s real time each (live measuring times: from 1698.2 s – Tivat/Plavi Horizonti soil to 1989.7 s – Utjeha/Bar sand).

The mullet species from the genus *Mugil*, *Chelon* and *Liza* (fam. Mugilidae) have been comprehensively analyzed – with an objective to integrate radioecological picture of the South Adriatic Sea marine environment. In the present study, 10 whole fish and two muscles of the species – *Mugil cephalus* (Linnaeus, 1758), *Chelon labrosus* (Risso, 1826) and *Liza ramada* (Risso, 1826), sampled in the Boka Kotorska Bay (Kotor and Tivat), were selected to evaluate doses from natural ^{40}K . The test measurements at the PRIPYAT-2M showed that whole fish should be measured for 5000 s real measuring time, while the organs – for 10 000 s live measuring time, to assure detection of radioecologically important radionuclides. Organs were usually measured in the 50 mL and 250 mL cylindrical beakers. This paper contains results of the 5000 s real time measurements of *L. ramada* and *C. labrosus* whole individuals (live measuring times ranged from 4860.2 to 4977.1 s, and 4949.7 to 4965.8 s, respectively), as well as those for whole individuals of *M. cephalus* mostly measured over 5000 s live time.

Seagrass *Posidonia oceanica* (fam. Posidoniaceae), sampled in the Boka Kotorska Bay (Sv. Stasije – 0.1 kg and Dobrota – 0.12 kg) had been also measured by the PRIPYAT-2M, and ^{40}K activities are obtained from the spectra acquired for 4957.3 and 4951.8 s live measuring time, respectively.

Surface sediment sampled in the Boka Kotorska Bay – area of Kotor (Dobrota), was dried at room temperature, homogenized and measured in Marinelli beaker by the HPGe for 126 784 s, while seawater samples were firstly taken from Budva and Herceg Novi (30 L of surface seawater each), evaporated to 1 L, placed in Marinelli beakers and measured for 77 100 and 92 107 s, respectively. In addition, samples taken from around 6.5-7 m seawater-depth, in the Boka Kotorska Bay, in areas of Sv. Stasije and Dobrota (where seagrass had been sampled) were also analyzed in the same way – from the spectra acquired for 84 452 and 82 740 s, respectively. Finally, surface seawater from Risan, Tivat-town, Budva-Jaz, Ulcinj-Velika Plaza, were also analyzed for ^{40}K activity, from the 85 854, 91 530, 210 681 and 81 777 s spectra, respectively. Our previous research also included evaporation of different volume of water – to check results of radionuclide measurements.

2.2 Dose rate assessment

The external terrestrial gamma absorbed dose rate due to ^{40}K in soil and sand, in air at 1 m above the ground, was calculated using

$$D(^{40}\text{K}) = A_c(^{40}\text{K}) \cdot 0.0417, \quad (1)$$

where A_c is activity concentration (in Bq/kg), and 0.0417 nGy/h per Bq/kg is the dose coefficient proposed by the UNSCEAR [8]. It is important to note that the world average annual effective dose due to natural radiation sources is 2.4 mSv, with a contribution of external terrestrial radiation of 0.48 mSv (with the *outdoors* contribution of 0.07 mSv) [8].

An equation from the UNSCEAR 2008 report [9] as well as the dose conversion coefficient for exposure to ^{40}K [10] were used to evaluate doses to *P. oceanica* and mullets, i.e.,

$$D = \sum \left| \text{DCC}_{\text{ext,K-40}} \cdot A_{c,\text{water, sediment}} + \text{DCC}_{\text{int,K-40}} \cdot A_{c,\text{seagrass, fish}} \right|, \quad (2)$$

where DCC_{ext} is the dose conversion coefficient for external exposure to ^{40}K (in $\mu\text{Gy/h}$ per Bq/kg); $A_{c,\text{water, sediment}}$ is the activity concentration of ^{40}K in water or sediment (in Bq/L, i.e., Bq/kg); DCC_{int} is the dose conversion coefficient for internal exposure to ^{40}K (in $\mu\text{Gy/h}$ per Bq/kg); $A_{c,\text{seagrass, fish}}$ is the activity concentration of ^{40}K in seagrass or fish (in Bq/kg).

A value of $2.6 \cdot 10^{-6}$ Gy/yr per Bq/kg (external exposure) and $3.5 \cdot 10^{-6}$ Gy/yr per Bq/kg (internal exposure) as given in [10] was converted into $\mu\text{Gy/h}$ per Bq/kg and used in this work, as well. Since a marine environment is considered, the external dose coefficient is one half of its value for exposure in terrestrial environment [10].

As is known, fish are internally irradiated by incorporated radionuclides, and externally by the activity in water and sediment (if they are bottom dwellers). Since an external irradiation of fish from genus *Mugil*, *Chelon* and *Liza* (as pelagic fish) by the activity in water is dominant, it should be considered together with internal exposure to ^{40}K .

It is also important to note that average ^{40}K contribution to the total annual human ingestion exposure to natural radiation sources is 0.17 mSv (i.e., ~59 % of the total 0.29 mSv) [8].

3 RESULTS AND DISCUSSION

The results of gamma spectrometric measurements, i.e. ^{40}K activity concentrations in samples from the South Adriatic Sea environment, as well as corresponding dose rates, are given in Tables 1-4.

Soil from the Coast of Montenegro (Table 1) showed minimum, maximum, average, standard deviation and median of ^{40}K activity concentrations 258, 665, 442, 156 and 403 Bq/kg, respectively; while sand from the Montenegrin beaches (Table 1) around 22.6, 298, 84.8, 87.8 and 42.3 Bq/kg, respectively. The results are in a good accordance with those obtained using the HPGe spectrometry [5-6], and confirmed that an average ^{40}K activity in soils on the Coast of Montenegro is comparable with one for the soil worldwide (medians in the range from 140 to 850 Bq/kg, with a mean of 400 Bq/kg [8]).

Although soil sample from Ulcinj showed the lowest ^{40}K activity concentration, sand from its Velika Plaza exhibited the highest one (among here studied beach-sands).

A literature survey showed ^{40}K activity concentrations in sand samples from the world's beaches such as Red Sea coastline, Egypt – 930 Bq/kg [11], Rio de Janeiro, Brazil (Copacabana) – 18.9 Bq/kg

[12], Xanthos, Turkey (Patara Beach) – 54.5 Bq/kg, Tripoli, Libya (7 beaches – Tayura City Beach, Tariq City Beach, Al Masif Albalady Tower, Al Masif Albalady, Gargaresh City, Qarit City Beach, Janzour) – 27.5-82.4 Bq/kg, USA (Manhattan Beach, Los Angeles; City Beach, Santa Monica; Great Salt Desert, Utah) – 230-696 Bq/kg [13], China (Rizhao bathing beach) – 883.4-1313.6 Bq/kg [14].

Table 1: Dose rates due to ^{40}K – from soil and sand.

<i>Soil</i>				<i>Sand</i>			
Location	Coordinates	$A_c(^{40}\text{K})$, Bq/kg	$D(^{40}\text{K})$, nGy/h	Location	Coordinates	$A_c(^{40}\text{K})$, Bq/kg	$D(^{40}\text{K})$, nGy/h
Herceg Novi	N 42°27.294'	314±9	13.1±0.4	Njivice (Herceg Novi)	N 42°26.049'	37.3±1.4	1.56±0.06
	E 18°33.011'				E 18°31.033'		
Risan	N 42°30.628'	303±12	12.6±0.5	Risan	N 42°30.597'	41.6±3.6	1.73±0.15
	E 18°41.763'				E 18°41.779'		
Kotor	N 42°24.992'	665±18	27.7±0.8	Kotor	N 42°25.781'	22.6±3.4	0.94±0.14
	E 18°45.752'				E 18°46.080'		
Tivat – Plavi Horizonti	N 42°23.286'	443±22	18.5±0.9	Plavi Horizonti (Tivat)	N 42°23.152'	81.3±4.0	3.39±0.17
	E 18°40.910'				E 18°40.943'		
Budva – Jaz	N 42°16.993'	652±19	27.2±0.8	Jaz (Budva)	N 42°16.947'	43.0±6.2	1.79±0.26
	E 18°48.130'				E 18°48.153'		
Budva – town	N 42°7.149'	309±10	12.9±0.4	Mogren (Budva)	N 42°16.634'	27.1±1.1	1.13±0.05
	E 18°1.139'				E 18°49.970'		
Petrovac	N 41°54.585'	513±12	21.4±0.5	Sv. Stef. (Budva)	N 42°15.357'	40.2±3.2	1.68±0.13
	E 19°15.026'				E 18°53.669'		
Sutomore	N 41°54.585'	513±12	21.4±0.5	Petrovac	N 42°12.242'	62.5±4.2	2.61±0.18
	E 19°15.026'				E 18°56.586'		
Sutomore	N 42°08.577'	602±21	25.1±0.9	Sutomore	N 42°08.282'	96.8±4.5	4.04±0.19
	E 19°02.111'				E 19°03.003'		
Bar	N 42°06.635'	363±12	15.1±0.5	Susanj (Bar)	N 42°06.691'	231±7	9.63±0.29
	E 19°05.368'				E 19°05.086'		
Ulcinj	N 41°54.585'	258±9	10.8±0.4	Utjeha (Bar)	N 42°00.616'	36.5±3.2	1.52±0.13
	E 19°15.026'				E 19°09.052'		
Ulcinj	N 41°54.585'	258±9	10.8±0.4	Velika plaza (Ulcinj)	N 41°54.474'	298±8	12.4±0.3
	E 19°15.026'				E 19°14.987'		

The external terrestrial gamma absorbed dose rate due to ^{40}K in soil and sand, in air at 1 m above the ground, evaluated using eq. 1 are also given in Table 1.

In regard to soil, minimum, maximum, average, standard deviation and median of dose rates due to ^{40}K were found to be 10.8, 27.7, 18.4, 6.5 and 16.8 nGy/h, respectively; as those from sand – 0.94, 12.4, 3.54, 3.66 and 1.76 nGy/h, respectively.

Taking into consideration maximum absorbed dose rate (27.7 nGy/h), annual effective dose calculated using

$$E(^{40}\text{K}) = D(^{40}\text{K})(\text{nGy/h}) \cdot 8760 \text{ h/y} \cdot 0.2 \cdot 0.7 \text{ Sv/Gy}, \quad (3)$$

where 0.7 Sv/Gy is the conversion coefficient from absorbed dose in air to effective dose and 0.2 is *outdoor* occupancy factor [8], was found to be 0.03 mSv.

Potassium-40 activity concentrations in seawater samples are reported in Table 2, while in sediment and seagrass – in Table 3.

Table 2: Potassium-40 activity in the South Adriatic seawater.

Surface seawater	$A_c(^{40}\text{K})$, Bq/L
Herceg Novi	8.58±0.28
Risan	6.29±0.40
Sv. Stasije [†]	3.31±0.14
Dobrota [‡]	2.81±0.13
Tivat-town	8.84±0.46
Budva-Jaz	3.14±0.52
Budva-town	8.73±0.29
Ulcinj-Velika Plaza	4.17±0.28

Table 3: Potassium-40 activity in sediment and seagrass *P. oceanica*.

Sample	$A_c(^{40}\text{K})$, Bq/kg	D, nGy/h
Sediment – Kotor (Dobrota)	123±5	5.13±0.21
<i>P. oceanica</i> – Kotor (Sv. Stasije)	389±14	170±6
<i>P. oceanica</i> – Kotor (Dobrota)	491±26	210±11

The absorbed dose rate due to ^{40}K in sediment (Table 3) was calculated by eq. 1, i.e., for air medium and it is given as an illustration only, because the gamma radiation attenuation from overlying waters cannot be neglected in a real situation, and a contribution of ^{40}K activity concentration for surface sediment will be somewhat lower. At the same time, ^{40}K activity concentration measured in sediment from the Boka Kotorska Bay was found to be significantly lower than, for example, those in the sediments of the Irish Sea (in an amount of 560 Bq/kg [15]) or Indian Ocean (297 Bq/kg [16]).

On the other hand, doses to *P. oceanica* were calculated taking into consideration both – seawater (0.48±0.02 nGy/h – Sv. Stasije, 0.41±0.02 nGy/h – Dobrota) and sediment (17.8±0.7 nGy/h – Dobrota, which is also taken for seagrass from Sv. Stasije location), as well as internal exposures (152±5 nGy/h – Sv. Stasije, 191±10 nGy/h – Dobrota), resulting in the total doses presented in Table 3.

The results of fish measurements and dose rates evaluation are shown in Table 4. External exposure was calculated taking ^{40}K activity in the Tivat seawater sample (8.84 Bq/L), since specimens were captured in the Tivat and Kotor area.

Activity concentrations in whole individuals of *M. cephalus* (Table 4) showed minimum, maximum, average, standard deviation of 74.3, 127, 96.8, 17.3 Bq/kg, respectively; whilst the other species – 54.6, 117, 95.6, 20.6 Bq/kg, respectively (*C. labrosus*), and 49.6, 97.6, 75.4, 16.8 Bq/kg, respectively (*L. ramada*).

Internal exposure of *M. cephalus* showed minimum, maximum, average and standard deviation of around 29, 49.5, 37.8 and 6.8 nGy/h, respectively; as total exposure – 30.3, 50.8, 39, 6.8 nGy/h,

[†] Seawater – from 6.5-7 m in depth (Boka Kotorska Bay).

respectively. In the case of *C. labrosus*, they were 21.3, 45.6, 37.3 and 8.05 nGy/h, respectively (internal exposure), and 22.6, 46.9, 38.5 and 8.05 nGy/h, respectively (total exposure), while of *L. ramada* – 19.3, 38.1, 29.4 and 6.55 nGy/h, respectively (internal exposure), and 20.6, 39.3, 30.7 and 6.55 nGy/h, respectively (total exposure).

Table 4: Doses to the mullet species due to ^{40}K .

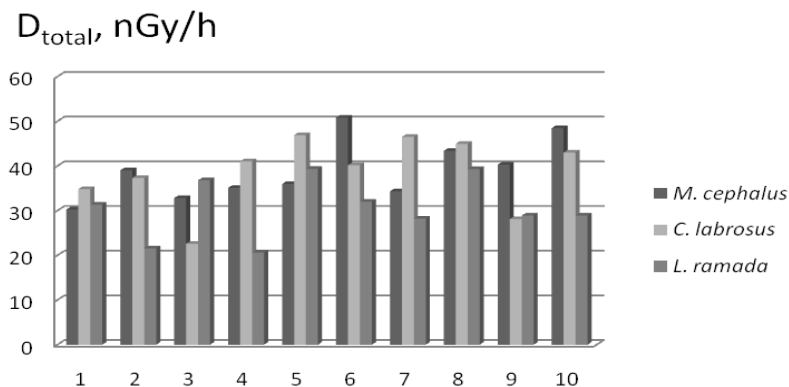
Sample	Total length, cm	Wet wt, kg	$A_c(\text{K})$, Bq/kg	D_{external} , nGy/h	D_{internal} , nGy/h	D_{total} , nGy/h
<i>M. cephalus</i>						
1	27.6	0.188	108±7	1.28±0.07	42.1±2.7	43.4±2.8
2	30.5	0.248	96.8±7.5	1.28±0.07	37.8±2.9	39.0±3.0
3	30.3	0.240	80.9±8.1	1.28±0.07	31.6±3.2	32.8±3.2
4	28.0	0.181	127±9	1.28±0.07	49.5±3.5	50.8±3.6
5	28.8	0.191	88.9±10.5	1.28±0.07	34.7±4.1	36.0±4.2
6	27.8	0.200	84.7±10.7	1.28±0.07	33.0±4.2	34.3±4.2
7	26.8	0.163	100±13	1.28±0.07	39.0±5.5	40.3±5.1
8	25.5	0.152	121±14	1.28±0.07	47.2±5.5	48.5±5.5
9	39.2	0.551	74.3±5.1	1.28±0.07	29.0±2.0	30.3±2.1
10	30.2	0.228	86.7±5.5	1.28±0.07	33.8±2.1	35.1±2.2
Muscle 9		0.053	116±11	1.28±0.07	45.2±4.3	46.5±4.3
Muscle 10		0.019	120±12	1.28±0.07	46.8±4.7	48.1±4.7
<i>C. labrosus</i>						
1	29.7	0.240	99.7±6.0	1.28±0.07	38.9±2.3	40.2±2.4
2	29.3	0.205	116±5	1.28±0.07	45.2±2.0	46.5±2.0
3	26.5	0.145	107±11	1.28±0.07	41.7±4.3	43.0±4.4
4	30.7	0.278	102±5	1.28±0.07	39.8±2.0	41.1±2.0
5	30.4	0.238	117±5	1.28±0.07	45.6±2.0	46.9±2.0
6	34.0	0.342	86.0±8.1	1.28±0.07	33.5±3.2	34.8±3.2
7	28.5	0.238	68.8±11.6	1.28±0.07	26.8±4.5	28.1±4.6
8	31.2	0.250	54.6±5.5	1.28±0.07	21.3±2.2	22.6±2.2
9	31.5	0.251	92.4±5.5	1.28±0.07	36.0±2.2	37.3±2.2
10	28.7	0.188	112±7	1.28±0.07	43.7±2.7	45.0±2.8
Muscle I		0.079	96.8±9.5	1.28±0.07	37.8±3.7	39.0±3.8
Muscle II		0.057	83.5±8.2	1.28±0.07	32.6±3.2	33.8±3.3
<i>L. ramada</i>						
1	32.0	0.195	91.1±6.0	1.28±0.07	35.5±2.3	36.8±2.4
2	32.7	0.199	77.1±8.4	1.28±0.07	30.1±3.3	31.4±3.3
3	29.8	0.182	97.6±9.6	1.28±0.07	38.1±3.7	39.3±3.8
4	29.2	0.178	69.0±6.6	1.28±0.07	26.9±2.6	28.2±2.6
5	25.3	0.130	70.9±8.5	1.28±0.07	27.7±3.3	28.9±3.4
6	29.8	0.208	78.8±9.1	1.28±0.07	30.7±3.6	32.0±3.6
7	32.1	0.184	52.0±6.9	1.28±0.07	20.3±2.7	21.6±2.8
8	28.1	0.168	97.5±6.9	1.28±0.07	38.0±2.7	39.3±2.8
9	31.8	0.220	49.6±5.7	1.28±0.07	19.3±2.2	20.6±2.3
10	26.8	0.106	70.8±8.2	1.28±0.07	27.6±3.2	28.9±3.3
Muscle I		0.059	116±10	1.28±0.07	45.2±3.9	46.5±4.0
Muscle II		0.058	127±15	1.28±0.07	49.5±5.8	50.8±5.9

^{40}K activity concentration in muscles of *M. cephalus* and *L. ramada* was higher than in whole fish, in similar proportion as it was found for cod and crucian carp (in whole individuals 86 and 96 Bq/kg, in muscles – 115 and 126 Bq/kg, respectively [17]). On the other hand, a level of ^{40}K was found to be somewhat lower in the muscles of *C. labrosus*. In the Baltic Sea fish, for example, ^{40}K measured in

2008 showed average concentration in whole individuals of sprat – 118 Bq/kg, as in the flesh of herring, plaice and cod – 121, 102 and 129 Bq/kg, respectively [18]; i.e. showed a level comparable with that in muscles of *M. cephalus* and *L. ramada*.

Total doses to the mullet whole individuals ordered by decreasing lengths are shown in Fig. 1 – for a comparison (number 1 is an individual with the highest length, whilst number 10 – one with the lowest length).

Figure 1: Total doses to whole fish



Looking at data for fish at Trombay, Mumbai, India [10], for example, where ^{40}K in seawater showed a level from 4 to 7 Bq/L (similarly as in the South Adriatic), and in fish – 150-200 Bq/kg (i.e., higher than in *L. ramada*, *C. labrosus* and *M. cephalus*), with an exposure in the range from 525 to 700 $\mu\text{Gy/y}$ [10], i.e., (60-80) nGy/h, it can be concluded that doses to three mullet species from the South Adriatic Sea (due to ^{40}K in seawater and fish themselves) are significantly lower.

Finally, as an illustration, if a total annual intake of this fish species (their muscles) by a human consumer is 15 kg (representative consumption rate for fish products [8]), taking an average ^{40}K concentration for all the muscles (110 Bq/kg), as well as the dose coefficient of 6.2 nSv/Bq for ingestion of ^{40}K for adults [19], committed effective dose is estimated to be around 0.01 mSv/yr.

4 CONCLUSIONS

Potassium-40 activity concentrations in samples from the South Adriatic Sea environment (Coast of Montenegro) were measured by standard gamma spectrometry procedures using HPGe and six-detector spectrometer PRIPYAT-2M, and its levels in surface seawater were found to have an average of 6.62 Bq/L, while in seagrass *P. oceanica* – 440 Bq/kg.

Among studied mullet species from the genus *Mugil*, *Chelon* and *Liza* (30 whole fish and 6 muscles), the highest ^{40}K activity (127 Bq/kg) was found in one *M. cephalus* whole individual and one muscle of *L. ramada*, resulting in an internal dose rate of 49.5 nGy/h, and a total – 50.8 nGy/h. Activity concentration in muscles of *M. cephalus* and *L. ramada* was higher than in whole fish, while the muscles of *C. labrosus* generally showed somewhat lower level of ^{40}K . Taking into account a reference annual intake of fish products of 15 kg, committed effective dose for adults was evaluated and found to be around 6 % of the world average ingestion exposure due to ^{40}K .

The external terrestrial gamma absorbed dose rate due to ^{40}K in soil and sand at the Coastal Montenegro, in air at 1 m above the ground, showed a maximum of 27.7 nGy/h. Corresponding annual effective dose is twice less than the world average exposure due to external terrestrial radiation outdoors (0.07 mSv annually).

5 ACKNOWLEDGEMENTS

The research was supported by the Ministry of Science of Montenegro.

6 REFERENCES

- [1] Joksimović, A., 2010. Biological research of the Adriatic Sea, status, perspectives and development trends. In: Montenegro in XXI century – in the era of competitiveness, Science and technology. Ed. J. Mirković, Montenegrin Academy of Sciences and Arts, Special editions: Monographies and Studies, 73(11), 549-558.
- [2] MONSTAT, 2012. Statistical Yearbook of Montenegro. Statistical Office of Montenegro (MONSTAT), Podgorica.
- [3] Heath, R.L., 1997. Scintillation Spectrometry – Gamma-rays spectrum catalogue, Reissue of IDO16880, 2nd Edition – Vol. 1 (Rev.), Tutorial Text, Idaho National Laboratory <http://www.inl.gov/gammaray/catalogs/pdf/naicat.pdf>
- [4] Andrukhovich, S.K., Berestov, A.V., Gutko, V.I., et al., 1995. High-sensitive multidetector gamma spectrometers PRIPYAT. Preprint of the Institute of Physics, Belarus Academy of Science, Minsk (in Russian).
- [5] Antovic, N.M., Svrkota, N., Antovic, I., 2012. Radiological impacts of natural radioactivity from soil in Montenegro. *Radiat. Prot. Dosim.* 148(3), 310-317.
- [6] Antovic, N.M., Svrkota, N., Antovic, I., et al., 2013. Radioactivity in Montenegro beach sands and assessment of the corresponding environmental risk. *Isot. Environ. Healt. S.* 49(2), 153-162.
- [7] IAEA, 1989. Technical reports series No. 295. Measurement of radionuclides in food and the environment (a guidebook).
- [8] UNSCEAR, 2000. Sources and Effects of Ionizing Radiation. Annex B: Exposure from natural radiation sources. United Nations Scientific Committee on the Effects of Atomic Radiation, Report to the General Assembly of the United Nations with Scientific Annexes, United Nations, New York.
- [9] UNSCEAR, 2008. Sources and effects of ionizing radiation, United Nations Scientific Committee on the effect of Atomic Radiation, Report to the General Assembly with Scientific Annexes. Annex E: Effects of ionizing radiation on non-human biota, United Nations, New York, 2011.
- [10] Singhal, R.K., Ajay, K., Usha, N., et al., 2009. Evaluation of doses from ionising radiation to non-human species at Trombay, Mumbai, India. *Radiat. Prot. Dosim.* 133(4), 214-222.
- [11] Harb, S., 2008. Natural radioactivity and external gamma radiation exposure at the coastal Red Sea in Egypt. *Radiat. Prot. Dosim.* 130(3), 376-384.
- [12] Veiga, R., Sanches, N., Anjos, R.M., et al., 2006. Measurement of natural radioactivity in Brazilian beach sands. *Radiat. Meas.* 41(2), 189-196.
- [13] Radenkovic, M.B., Alshikh, S.M., Andric, V.B., et al., 2009. Radioactivity of sand from several renowned public beaches and assessment of the corresponding environmental risks. *J. Serb. Chem. Soc.* 74(4), 461-470.
- [14] Lu, X., Zhang, X., 2008. Measurement of natural radioactivity in beach sands from Rizhao bathing beach, China. *Radiat. Prot. Dosim.* 130(3), 385-388.
- [15] IAEA, 1993. Report on the intercomparison run. Radionuclides in Irish Sea Sediment. IAEA/AI/063-135.
- [16] IAEA, 1996. Report on the intercomparison run. Radionuclides in Indian Ocean Sediment. IAEA/AI/065-315.
- [17] Zotina, T., Trofimova, E., Bolsunovsky, A., 2011. Artificial radionuclides in fish fauna of the Yenisei River in the vicinity of the Mining-and-Chemical Combine (Siberia, Russia). *Radioprotection* 46(6), 75-78.
- [18] Suplinska, M., Adamczyk, A., 2009. Cs-137, Ra-226 and K-40 in the southern Baltic Sea fish flesh. Helsinki Commission (HELCOM MORS-PRO 14/2009; Document 3/2).
- [19] ICRP, 2012. ICRP Publication 119. Ann. ICRP 41(Supplement 1).

Would Radiation Deter Space Exploration

Nicholas Sion*

Intercan Technologies, 140 Erskine Ave. #1702, Toronto, M4P 1Z2, ON. Canada.

Abstract. Space is considered as the final frontier and has an aura of adventure and excitement. However it is fraught with danger. Our technology has replaced the myths with the realities of space science leading to space exploration, land on the Moon, and even to consider the colonization of our nearby planet Mars; and to visit fleeting asteroids in curious endeavor. The technology of going beyond the protective layers of the Van Allen belts for prolonged durations are now available for inanimate objects but radiation protection for humans is not yet fully developed against galactic radiation that is mainly from particles. Long durations in outer space has become synonymous with radiation dose and its associated risk. This presentation enumerates the various radiation hazards in deep space, reviews the possibilities of astronaut protection, the (in)-adequacy of shielding, and the countermeasures that are currently being researched, to reduce these hazards to human tolerance levels.

KEYWORDS: *Radiation Protection for Astronauts; Space Missions; Hazards in Space.*

1 INTRODUCTION

Since the advent of modern rocketry there has been an impetus to venture into space, initially to install communication satellites, then for prolonged adaptive periods aboard the International Space Station (ISS). Though nowadays the solar system is being frequently explored robotically, only the Moon has had human visitors. Space is a hostile environment for humans, and even more so when humans explore beyond the protective layers of the Van Allen belts surrounding Earth. Radiation is mainly from particles. The environmental conditions as measured to-date in the Solar System, Table 1, show extremes in radiation, temperatures, and vast distances that make the Moon and planet Mars as realistic candidates for human exploration in the near future. Other planetary moons and asteroids may occur in the medium future; and perhaps other planets and the more distant asteroids in the far future, if ever.

Table 1: Radiation and Characteristics of the Planets

Planet	Distance from sun AU	Size	Light Intensity	Length of Day	Length of Year	Average Temp. °C	Radiation
Mercury (i)	0.39	~0.05	6.7	58d 15h 30s	88 d	-183 to +427	20 mSv/y Proton Fluence x10 at 1AU=10MeV during SPE
Venus (ii)	0.72	0.82	1.9	243d	225 d	480	7.7 mSv/y
Earth	1	1	1	23h 56m 4.1s	365 d	14	1 mSv/y
Moon (iii)	1	0.012	1	27 d	---	-153 to +123	Neutron 43.80 mSv/y 380 mSv/y (solar min.) 110 mSv/y (solar max.) [sun radiation blows counteractively against the cosmic rays during solar max.] 1 Sv during Solar Particle Event
Mars (iv)	1.52	0.11	0.43	24h 39m 35s	1.9 y	-63	85 mGy/y by Curiosity. 91mSv/y by MARIE
Jupiter (v)	5.2	317	0.037	9h 54m	12 y	-130	Electrons: 15 keV-11MeV up to 500 MeV Ions 10 keV-200MeV dipole moment of $1.55 \times 10^{20} \text{T} \cdot \text{m}^3$
Saturn (vi)	9.5	95	0.011	10h 47m 24s	29 y	-130	dipole moment of $7.91 \times 10^{13} \text{T} \cdot \text{m}^3$ Solar Electrons interact with magnetic field
Uranus (vii)	19.2	15	0.0027	17h 14m 24s	84 y	-224	Magnetic field strength $0.23 \times 10^{-4} \text{Tesla}$ [equator]
Neptune (viii)	30	17	0.0011	16h 6m 36s	165 y	-218	Magnetic field strength $0.14 \times 10^{-4} \text{Tesla}$ [equator]
Pluto (ix)	39	0.80	0.0006	6d 18m	248 y	-223 to -233	Dose Orbits from: Solar Wind [electrons, ionized helium, oxygen] $0.36 \times 10^{18} \text{eV/cm}^2$ UV less < 1500 Angstrom $7.3 \times 10^{18} \text{eV/cm}^2$ Cosmic Ray $26 \times 10^{18} \text{eV/cm}^2$ Protons $2.6 \times 10^{18} \text{eV/cm}^2$

Source of radiation measurements:
 (i) Mercury Orbiter
 (ii) Venera, and Vega probes (Russia); and Pioneer probes (USA).
 (iii) Apollo missions dosimeters. Neutron measurements from India's Chandrayaan Mission.
 (iv) MARIE = MARTian Radiation Environment Experiment; and from Curiosity
 (v) Galileo: sustained 650 kRad (2.2 gm⁻² Al shield). Also by Pioneer 10 & 11; Voyager (1980's) indicated large currents on Io.
 (vi) Cassini flyby; and by Huygens on its moon Titan.
 (vii) Voyager spacecraft flyby.
 (viii) Voyager spacecraft flyby.
 (ix) Voyager spacecraft flyby. Inferred from breaking up of methane by 60 eV protons/methane molecule on its surface.

*Presenting author, e-mail: sionn@sympatico.ca

New radiation data sent from Mars Science Laboratory (MSL) and from the Curiosity Rover, suggest that a long-term manned voyage to planet Mars is feasible both radiologically and technically. Currently, Mars is receiving the most emphasis with a progressive program of intended exploration and even colonization.

1.1 Radiation in outer space

Basic criteria in radiation protection is to minimize the exposure time, and by shielding. The governing factors are the deterministic effects where the severity is related to exposure levels; and the stochastic effects (may produce cancer where the probability of occurrence is independent of the severity), is related to the level of exposure. However, the type of radiation in outer space is primarily from particles where human data is not available, from gamma and from X-rays, and from Ultra Violet (UV).

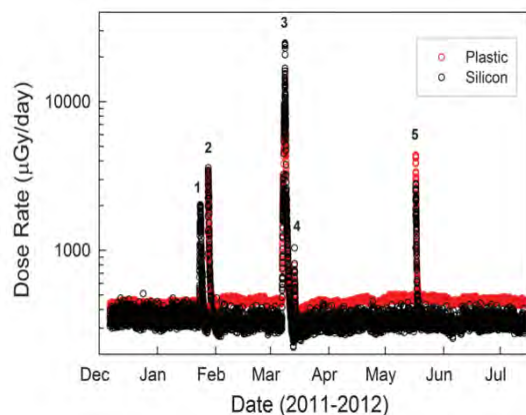
UV radiation is part of the electromagnetic spectrum that is prevalent from the Sun and is subdivided into UV-A, as found in tanning salons and may cause injury to the skin's DNA. UV-B where exposure causes sunburn and increases cellular and DNA damage. UV-C is most harmful in space, but is absorbed by the Ozone layer. An excess in UV causes premature skin aging, eye damage including cataracts and skin cancers. They also suppress the immune system giving advantage to diseases and maladies. The protection in outer space is to cover up where the visors are treated to reflect UV. The opaque layers of the space suit are adequate.

Whilst on its mission the Mars Science Laboratory took on route measurements of the Galactic Cosmic Radiation (GCR), and then continued measurements after landing for the first 300 Sols (Martian days). The data is shown in Fig. 1. It is expected that should a Solar Particle Event (SPE) occur the astronaut crew would expedite to their adequately sheltered quarters.

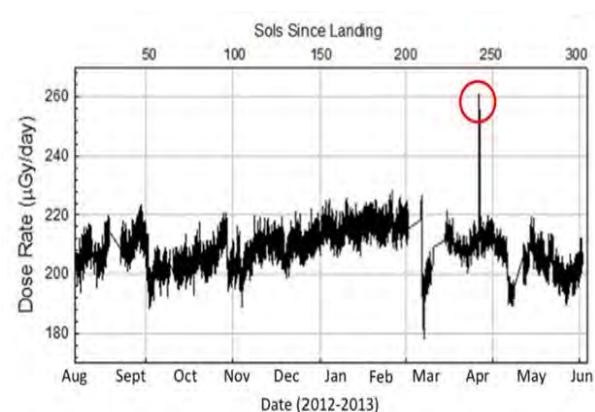
Figure 1: Radiation Dose as measured by a Radiation Assessment Dosimeter (RAD).

Credit NASA/JPL-Caltech/SWRI

On route: dose rates were concurrently about 400 $\mu\text{Gy/day}$ by RAD's silicon detector (black circles) and by a plastic scintillator (red circles). SPEs are indicated



On Mars Surface: Radiation measurements on Mars aboard MSL (Curiosity). In the first 300 Sols, RAD observed only one Solar Particle Event.



The Radiation Assessment Dosimeter (RAD) gave readings of 400 $\mu\text{Gy/day}$ whilst on route, excluding the frequent SPEs. On Mars surface, RAD's measurements were from two sources viz. from galactic cosmic rays and from solar energetic particles. The dose rate was about 210-230 $\mu\text{Gy/day}$, again assuming no SPEs during the initial 300 Sols. It is evident that these radiation levels are lower than dose rates in free space caused by some shielding that is provided even by the thin Martian atmosphere. Also evident is the wide variation in the daily radiation dose whilst on Mars surface. These are attributed to the day-night extreme variability of the air temperature causing shielding variations due to changes in atmospheric density.

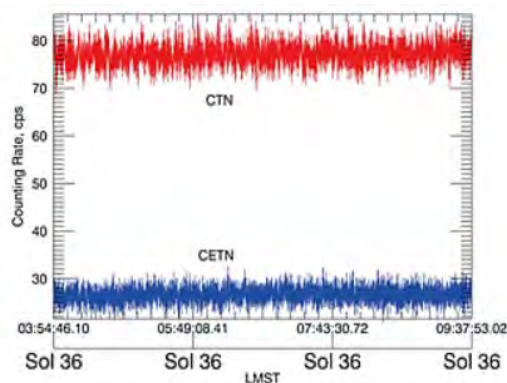
RAD dose measurements, in Sieverts whilst cruising to Mars, indicated an average daily dose rate of 1.8 mSv/d inside the space ship where only 3% are attributed to solar particles because of calm solar cycle and the protective shielding of Curiosity that housed it. On the surface of Mars the average dose rate is around 0.67 mSv/d. The accumulated dose is akin to “receiving a whole-body CT scan every five or six days” quoting Dr. Cary Zeitlin principal scientist at South West Research Institute’s (SwRI) Space Science and Engineering [1] When calculated μ A one way journey would be some 324 mSv. That is equivalent to 24 CAT scans in just getting there; equivalent to an exposure of 15 times the annual radiation limit for a US Nuclear Energy Worker in a nuclear power plant.

Noticeable are the sudden radiation drops at Sols 50, 97, 208 and 259. These are due to the Forbush² decreases and are the result of the extra shielding provided by the interplanetary coronal mass ejections from the Sun. Radiation variations around Sol 200 are mainly due to Martian seasonal effects. The dose rate on the Martian surface is also affected by constant bombardment by heavy ions every few minutes with peaks of 300-350 μ Gy/sol, but still below the 400 μ Gy/d experienced in free space.

Neutron radiation was measured by a Dynamic Albedo of Neutrons instrument (DAN) that measured the neutron background environment using two ³He proportional counters, one is unshielded, Compensated Thermal Neutron sensors (CTN), the other is shielded with Cadmium that blocks neutrons below energies \sim 0.4 eV from being counted. Operating in the passive mode, the unshielded CTN would measure the spallating neutrons through interactions with the GCR and regolith. The shielded CETN would detect neutrons emanating from the Multi-Mission Radioisotope Thermoelectric Generator [MMRTG], a ²³⁹Pu power source producing decay neutrons, on board MSL Fig. 2. Subtraction techniques are used for net counts which are in counts/second (cps). The Dynamic Albedo of Neutrons (DAN) is an active/passive neutron spectrometer and is attributed to Federal Space Agency of Russia [2]. Net neutron measurements were detected with ranges of 0.01 eV–1.0 eV thermal; 1 eV–1 keV epithermal; and 1 MeV–10 MeV high energy and soft gamma rays. In cps, the ranges were 0.01-104 cps.

Depending on where Curiosity was located to detect neutron levels, for how long it rested there, and the radiations for that Martian day (Sol), an interpretation can be obtained. Neutron measurements of energies (12–436 MeV) translated to a dose rate of 3.8 ± 1.2 μ Gy/day and a dose equivalent of 19 ± 5 μ Sv/day. Extrapolating to a range of (0.1–1000 MeV) the total neutron-induced dose rate was 6 ± 2 μ Gy/day and the dose equivalent rate was 30 ± 10 μ Sv/day [4].

Figure 2: Shielded and unshielded neutron detecting sensors. *Source [3].*



² The Forbush decrease is the rapid decrease in the galactic cosmic ray intensity following a Coronal Mass Ejection (CME). The ejections are mainly a plasma of electrons and protons and electromagnetic radiation. When a CME occurs it sweeps away some of the GCR away from a spaceship thus showing a decrease in galactic cosmic radiation. This phenomena has been observed on MIR and on the ISS. It may be possible that future astronaut explorers may benefit from this phenomena as a form of shielding during solar maxima.

1.2 Radiation risk

North American statistics indicate that some 41% of the population are likely to be diagnosed with cancer. Astronauts on missions in outer space, using the Moon and Mars as examples, may receive 1 Sv of cosmic radiation, and their incidence to cancer becomes higher at 61% [5], an increase of 20 %. Cosmic radiation results in different cancers which includes lung, breast and colorectal cancers and they tend to be more aggressive than normal. It is estimated that the lifespan of an astronaut on a trip to Mars would be reduced by some 15-24 years from the national average. About half of those cancerous tumors would result in death. Hence the current shielding methods and materials in usage cannot be considered adequate.

Table 2 tabulates the effective doses to induce cancer resulting in death. The calculations are at solar minimums where the GCR fluence is at its highest, with 5 gm/cm² aluminum shielding. The Absorbed Dose, and Effective Dose, are averaged over tissues prominent for cancer [6]. It is estimated that on a mission to Mars, every cell of the astronaut crew would be subjected to a proton and a secondary electron every few days, and would also hit by an High Atomic Number (HZE) particle about once per month.

Table 2: Effective Doses and % Risk of Death from Fatal Cancer

Exploration Mission	Absorbed Dose Gy	Effective Dose Sv	Fatal Risk %	95% CI
MALES [40 years]				
Lunar (180 days)	0.06	0.17	0.68	0.20, 2.4
Mars Swing-by (600 days)	0.37	1.03	4.0	1.0, 13.5
Mars Exploration (1000 days)	0.42	1.07	4.2	1.3, 13.6
FEMALES [40 years]				
Lunar (180 days)	0.06	0.17	0.82	0.24, 3.0
Mars Swing-by (600 days)	0.37	1.03	4.9	1.4, 16.2
Mars Exploration (1000 days)	0.42	1.07	5.1	1.6, 16.4

Source [6]

1.3 Dosimetry and instrumentation

Data on crew protection aboard the International Space Station (ISS) is plentiful but is very sparse beyond the Van Allen Belts. Four dosimeters were aboard Curiosity viz. RAD; DAN; CTN; and a High Energy Neutron Detector (HEND) that is designed to measure the flux of neutrons at different energies. HEND's dual purpose is to map out regions with subsurface water or ice. Since hydrogen atoms (water) slows neutrons, the ratio of fast to slow neutrons is an indication of the presence of subsurface water/ice, as well as provide dosimetry indications of albedo neutrons.

But these are passive dosimeters, and novel approaches are contemplated.

RaD-X: (Radiation Dosimetry Experiment) [7]: RaD-X is a microsatellite structure to provide information how cosmic rays deposit energy at the top of atmosphere. It also gives NASA the opportunity to test emerging technologies and evaluate off the shelf components for future space missions.

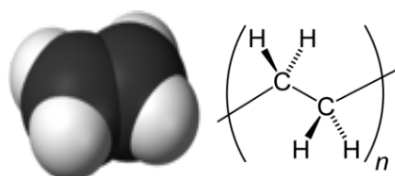
MicroDosimeter iNstrument (MIDN) [8]: This approach is to develop and test a solid state microdosimeter, measuring in real time, the dose equivalent in Sieverts and evaluate the risk and limits of radiation exposure of the astronaut in an unknown mixed radiation field. The instrument is lightweight, works on low power (<1.25 W), and uses low voltages of $\pm 5V$. Currently, it is under test.

1.4 Possible shielding and methods

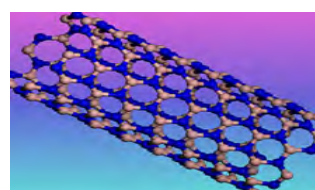
An ideal shielding material has been elusive. Appropriate radiation shielding needs to absorb the energetic GCR particles and reduce the crew exposure to acceptable levels. Research is underway at NASA's Biological and Physical Research Center on materials with large hydrogen content and/or with lighter elements. Such materials would produce less secondary radiation and are candidates for shielding. Under consideration are:

- **Liquid hydrogen:** A spacecraft could be designed where the contained liquid hydrogen surrounds the crew cabin to act as a radiation shield. The disadvantage is that as the fuel gets consumed the shielding is reduced.
- **Water on board:** can also contribute to shielding. It too, gets consumed unless it is recycled.
- **Spacecraft orientation** can provide shielding. The MSL spacecraft carrying Curiosity used its back-shell and heat shield to provide significant shielding from deep space radiation.
- **Launch timing** is aimed at solar minimum and at a time of the Forbush decreases [explained in Footnote 2]. It is hypothesized that future astronauts might benefit most from radiation shielding during a solar maxima, when Coronal Mass Ejections [CME] are most prevalent. CMEs are mainly unidirectional.
- **Plastic:** is appealing when compared to Aluminum because polyethylene offers 50% better shielding against solar flares and 15% better at shielding cosmic rays. There is no data on how human tissue is affected by deep space radiation and because of these uncertainties, the dose limits for a Mars mission have not been set.
- **RXF1:** Is a polyethylene-based material used as shielding for the sensitive parts of spacecraft. It is stronger than Al (3x tensile strength), is lighter than Al by 2.6x, offers 50% better shielding to solar flares, and 15% better at shielding cosmic rays. Fig.3. It can absorb and disperse particle radiation. It is composed of three layers compressed together and molded into desired shapes. The first layer, the outermost, is of ceramic material to protect against micro-meteoroids; a middle layer consists of Ultra High Molecular Weight polyethylene fibers in a matrix, but also provides radiation protection. The third layer, innermost, provides radiation protection and is the primary rigid support material. The main issue is flammability of the material. Pure polyethylene is very flammable and more work is needed to customize RXF1 to make it flame and temperature resistant as well.

Figure 3: Shielding possibilities with (a) RXF1 and (b) Nano Matrix



(a) - RXF shielding with chemical

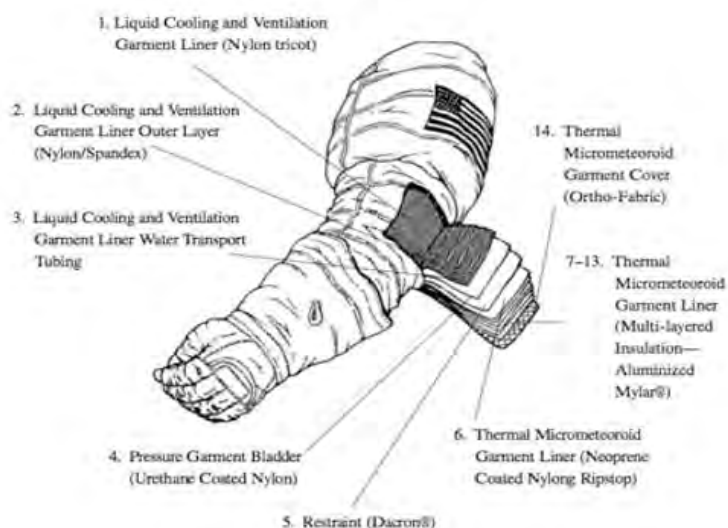


(b) - Nano Matrix of Boron and Nitrogen Tubes

- **Nanotechnology in shielding materials:** A material that combines high shielding efficiency and has high strength to carry primary loads does not exist as yet. But the NASA Langley Research Center (LaRC), Jefferson National Lab (JNL), and National Institute of Aerospace (NIA) have created a new material of highly crystalline Boron Nitride Nano-Tubes (BNNT) in a matrix Fig. 3, using a novel pressure/vapor condensation method. The BNNT have remarkable strength and are stable at high temperatures. They are made entirely of low Z (atomic number) atoms viz. boron and nitrogen, and in theory can be processed into load bearing structural items. Being nanotubes, their molecular structure is suitable for hydrogenation and research in this area is on-going.

- **Protection within Spacesuits:** The criteria in spacesuit design are its weight, its flexibility when pressurized, and its capacity for heating and cooling the astronaut within it. The intent is to keep environmental conditions inside and the radioactive particles on the outside for easier decontamination. Dose measurements are monitored by dosimeters and by hand held detectors. Not much attention was given to include radiation protection even on missions to the Moon other than customisation for UV ray protection where the visors had anti-glare coatings, same as in sunglasses. The spacesuits are still considered for short duration Extra Vehicular Activity (EVA) use.

Figure 4: Multi-layered fabrics used in arms and legs of space suits. The torso portion is of hard fiberglass.



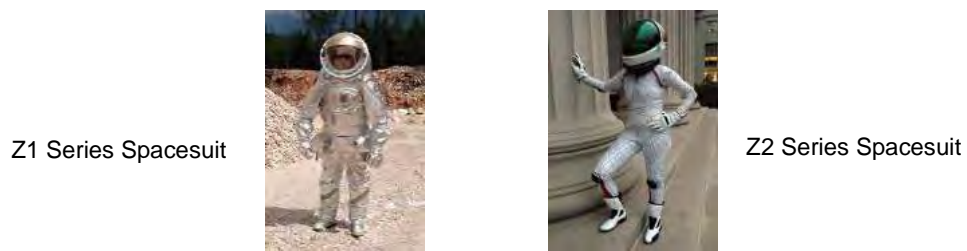
A typical spacesuit would stop alpha particles and most beta radiation but offers limited protection against particles in outer space. Adding bulk material Fig. 4 or lead shielding would cause a weight penalty on the astronaut and on the rocketry. The spacesuit comprises a hard fiberglass upper torso covered on its outside with orthofabric, aluminized Mylar and neoprene-coated nylon ripstop. The lower torso assembly and the arm assembly, including the Liquid Cooling and Ventilation Garment consist of orthofabric, aluminized Mylar, neoprene-coated ripstop, polyester, urethane-coated nylon, and water filled cooling tubes. The gloves do not include cooling tubes. Each suit has a mass of about 21kg without its life support backpack. The backpack contains the primary oxygen system, ventilation system, batteries, liquid transport system, water circuitry, secondary oxygen pack, radio unit, caution and warning system, display and control module and the electrical system. It measures 58.4x63.5x17.8 cm and weighs 64.2 kg [9 and 10], and costing some US\$12M each.

For humans to explore the moon or planets, e.g. Mars, or venture to distant asteroids or other planetary moons, new conceptual designs of space suits are contemplated where EVA would become a major activity.

1.5 Conceptual Designs and Materials

The conceptual spacesuits must incorporate shielding factors that reduce exposures to blood forming organs. They would include a soft upper torso and a reconfigured life support system, the back pack. Spacesuits suitable for a mission to Mars are the Z series Fig. 5.

Figure 5: Conceptual designs of Z spacesuits types (a) and (b) for a mission to Mars or for deep space.



New materials include low density linear polyethylene viz. Spectra³, a high density polyethylene composite. Less porous materials containing more hydrogen are under test to ascertain their shielding properties against low energy proton beams to protect the blood forming organs.

1.6 MIT BioSuit™

MIT researchers are engineering a skin tight spacesuit, a stretchy compression garment lined with muscle-like coils Fig. 6 (a). An astronaut would don this suit, plug into the spacecraft's power supply; the coils would shrink as in a shrink-wrap and provide compensating pressure in lieu of gas pressurisation. With modest force, the suit can be removed to return it to its original form and be reused. This spacesuit enhances mobility with less mass. The regular spacesuit is usually pressurised to one-third atmospheric pressure against the vacuum of space. The BioSuit uses memory alloy coils Fig. 6 (b) and (c) that provide a mechanical counter-pressure applied directly to the astronaut's body eliminating the gas pressurisation altogether.

Figure 6: The heat shrink MIT BioSuit™ and the tiny stretch memory coils.



1.7 Nanotechnology in Spacesuits

Nanotechnology can aid in making making the suits thinner, in three layers, more flexible and lighter in weight. But they become easier to rip and be damaged and likely to leave space debris. It is envisaged that a protein compound is introduced into the suit that can move freely between the layers via bio-nano robots. When a problem is detected it would rally to fix the compromised area. Even more futuristic, emergency medications can also be delivered to attend to an astronaut's body that has been hurt [11].

2 PROPULSION AND TRANSPORT

A reliable and powerful transportation system must be engineered to send a human crew and cargo efficiently and reliably on distant missions; enable productive work in space.

³ Spectra is a high density white polyethylene composite, 15x stronger than steel. For use in the Liquid Cooling and Ventilation Garment and its restraint.

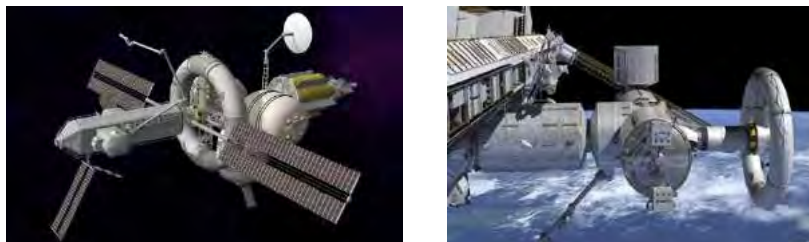
Under current development is the Space Launcher System Fig. 7 topped by the Orion crew module. It will have 20x the power of the Atlas rocket that launched Curiosity to Mars. Orion that can accommodate up to 6 astronauts, To-date Orion module has cost \$5B since 2006, with more to be spent to meet its launch date. The first crew flight is scheduled for 2021. The launcher will initially be 97.5m in height and a lift capability of 77 tons with an intended height of 122m and a lift capability of 130 tons. Orion's overall length is 8m and its liftoff weight is 21250 kg. It can sustain a brief visit to Mars.

Figure 7: The space launcher system with Orion as the crew module.



Under consideration is another space craft aptly named the NAUTILUS-X (Non Atmospheric Universal Transport Intended for Lengthy United States –Xploration), Fig. 8. It will act more like a space station for a crew of six, rather than a capsule for landing purposes. It may cost \$20B over 5 years to construct. It would be built at the ISS, able to dock with the ISS, then be used to ferry goods and astronauts to far away destinations. It will contain an area lined with liquid water and hydrogen slush to provide shielding from solar flares. The centrifuge spinning at 10 RPM can produce 50% or Earth's gravity. Designing the liquid metal seals, the counter-rotating flywheel for balance, and durable bearings would be an engineering challenge.

Figure 8: The futuristic Nautilus-X Spacecraft.

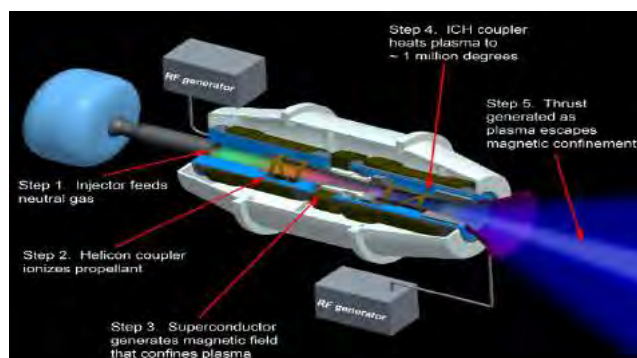


2.1 Ion Thrusters

Recent ion thrusters can deliver up to 0.5 Newtons of thrust (a force equivalent to holding 9 Canadian quarter coins) But if the thruster operates over long periods of time, this continuous force can propel a spacecraft to some 90 km/s (about 200,000 mph). This principle has already been used to propel spacecraft to distant asteroids.

Of interest is the Variable Specific Magnetoplasma Rocket (VASIMR) using Argon, is claimed to reach Mars in 39 days. Test results indicated an optimal exhaust velocity of up to 50 km/s, with a thruster efficiency of 72%. Still under test.

Figure 9: The Variable Specific Impulse Magnetoplasma Rocket (VASIMR) ion thruster.



2.2 Power

For power, the Multi Mission Radioisotope Thermoelectric Generator (MMRTG), Ref. 12, converts the heat from the natural decay of Plutonium-238 into usable electrical power. The MMRTG contains about 4.8 kg of plutonium dioxide with a total radiological activity of about 60,000 curies (Ci).

An alternate source of power is the Solar Array planned for the Mars 2020 mission to Mars. The size is constrained by its stowed volume and the diameter of the launch rocket. It may increase the weight by about 10 kg compared to the MMRTG. When deployed the panels would have an active cell surface area of 7.4 m².

3 CONCLUSIONS

- **Radiation:** still the major concern, feasible on short visits, under 6 months, but not for long duration settlement on the Moon or planets.
- **Propulsion systems** to reduce travel time are yet to be developed.
- **Enhancing the immune system** is still illusive and is futuristic.

4 REFERENCES

- [1] C. Zeitlin, D.M. Hassler, F.A. Cucinotta, et al. *Measurements of Energetic Particle Radiation in Transit to Mars on the Mars Science Laboratory*. Science, May 2013, Impact Factor 33.61, DOI: 10.1126/Science 1235989, PubMed.
- [2] V. N. Shvetsov, A.R. Krylov, Joint Institute for Nuclear Research; I.G. Mitrofanov2, G.N.Timoshenko1 et al , Russian Space Research Institute; *Neutron Derived Properties of the Martian Soil*.
- [3] I. Jun, Jet Propulsion Laboratory; I. Mitrofanov; M. L. Litvak; A. B. Sanin, et al. Space Research Institute, Moscow; *Neutron background environment measured by the Mars Science Laboratory's Dynamic Albedo of Neutrons instrument during the first 100 sols*. Journal of Geophysical Research, Vol. 118, Issue 11, Nov. 2013, pp 2400-2012.
- [4] J.Kohler, B. Ehresmann, C. Zeitlin, R.F. et al. *Measurements of the neutron spectrum in transit to Mars on the Mars Science Laboratory*. Life Sciences in Space Research, Volume 5, April 2015, Page A1.
- [5] UNSCEAR 2008; and Reports from the US National Academy of Sciences.
- [6] Francis Cucinotta, Marco Durante, *Cancer risk from exposure to galactic cosmic rays - implications for human space exploration*. Essay to Lancet Oncology. 2006 May; 7(5):431-5.
- [7] NASA Langley Research Center. *RaD-X Will Measure Radiation Levels Where Aircraft Fly*. 9Sept. 2015.
- [8] Pisacane V., Dolecek, Q., Maas, F., Nelson, M. et al., "MicroDosimeter iNstrument (MIDN) on MidSTAR-I", Published 2006-07-17 by SAE as technical paper 2006-01-2146, 2006, doi:10.4271/2006-01-2146.

- [9] J.W. Wilson, B.M. Anderson, NASA Langley Research Center, Hampton, VA 23681, F.A. Cucinotta, NASA Johnson Space Center, Houston, TX 77058, J. Ware, ILC Dover, Frederica, DE 19946, C.J. Zeitlin DOE Lawrence Berkeley. “*Design and Testing of Improved Spacesuit Shielding*”.
- [10] J. Ware, and J. Ferl ILC Dover; J.W. Wilson NASA Langley Research Center; M.S. Cloudsley NRC/NASA Langley Research Center; G. de Angelis and J. Tweed Old Dominion University; C.J. Zeitlin Lawrence Berkeley National Labs. “*Design and Testing of Improved Spacesuit Shielding Components.2002-01-330*”.
- [11] Dr. Chen, 11a Senior Fellow at Electronic Materials Engineering at the Australian National University.
- [12] NASA Mission Directorate, Washington D.C. “*Final Environmental Impact Statement For The Mars 2020 Mission*”, November 2014.

Development of absolute measurement instrument for radioactivity of Radon gas

Rio Furukawa*, Yasuhiro Unno, Akira Yunoki, Yasushi Sato

National Institute of Advanced Industrial Science and Technology, 1-1-1 Umezono, Tsukuba, Ibaraki, 305-8568 Japan.

Abstract. It has been concerned that exposure by radon gas increase the risk of lung cancer. Calibration of the measurement system is necessary to estimate radon activity accurately. We have a plan to revise calibration service for gaseous radon as a primary standard. For the purpose, we assembled a cylindrical Multi-electrode proportional counter as an absolute measurement device of radon activity directly by alpha ray spectrometry. The proportional counter had an anode wire at the center and six concentric supplemental electrodes. By calculation of electrical fields in the proportional counter, it was confirmed that the edge effect could be corrected well in the case that voltages for the supplemental electrodes were supplied. It was exhibited that we took an alpha ray pulse height distribution from radon gas successfully.

KEYWORDS: radon; primary standard; absolute measurement; proportional counter; alpha ray pulse height distribution; finite element method.

1 INTRODUCTION

Radon (Rn-222) is alpha decay nuclide, the half-life is about 3.8 day. Its descendant nuclides are ^{218}Po , ^{214}Po , ^{214}Pb , ^{214}Bi , ^{210}Pb , ^{210}Bi , ^{210}Po which are radioactive [1] and ^{206}Pb . Because Ra-226 (Half-life 1600 y), which is parent nuclide of ^{222}Rn , is distributed widely on the earth, radon gas exists in the atmosphere above the ground universally. It is concerned that radon gas exposure causes lung cancer. Radon gas concentration in workspace should be monitored accurately. For this purpose, a radon measurement device should be traceable to national standard activity. We have a plan to revise a primary standard of activity of radon gas using a Multi-electrode gas proportional counter and a calibration system in NMIJ (National Metrology Institute of Japan).

2 PRESENT STATE RELATED TO RADON MEASUREMENT IN JAPAN

2.1 Concern for exposure by radon gas

A limit of radon gas activity concentration is not regulated except for radiation controlled area in Japan. However, the industry about underground resources such as factories which handle Natural radioactive material (NORM) and the construction spot of the tunnel seem to be the high concentration of radon. About the industrial case, guidelines [2] without the legal force were set by government. If regulation is introduced to other area, users of radon gas detectors will be expanded explosively.

2.2 Measurement devices

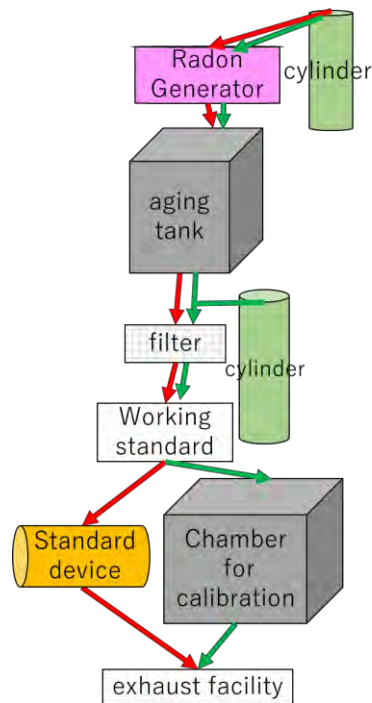
A device to measure concentration of radon gas is classified to passive type and active type. In active type detector, an ionization chamber and a scintillation detector are usually used. An alpha-track detector (ATD) is used as passive type detector. A detector which equips ATD (Raduet™) was developed in National Institute of Radiological Sciences (NIRS) [3]. The device was used for a national investigation of radon concentration in dwellings in Japan [4].

3 ESTABLISHMENT OF CALIBRATION SYSTEM IN NMIJ

We plan to carry out the calibrate client's instruments directly in our calibration system. Complicated law procedure about radiological transportation can be avoided because transport of radioactive material is not needed.

Figure 1 shows the block diagram of the calibration system. A system which is used in the calibration service is composed by a standard device, a radon gas generator, an aging tank, a filter. An activity of radon gas is measured by the standard device absolutely. Using the radon gas, we calibrate a working standard. The working standard is set between the standard device and the irradiation chamber. The working standard is used for usual calibration service.

Figure 1: Block diagram of the calibration system (Gas flow indicated by red arrows: calibration of working standard using the standard device(MEPC). Gas flow indicated by green arrows: calibration of radon monitor using calibrated radon gas.)

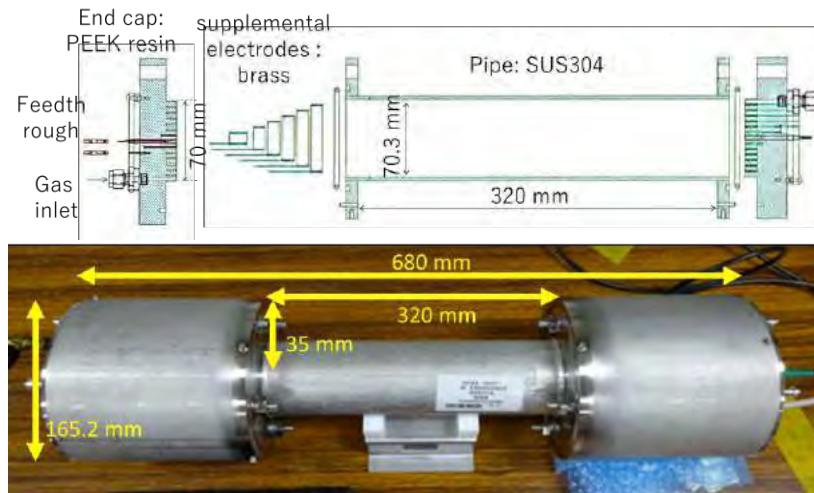


4 ABSOLUTE MEASUREMENT INSTRUMENT

We have a plan to use a Multi-electrode gas proportional counter (MEPC) as the standard device. It was originally developed by I. Busch [7]. Addition to anode wire at the centre of cylindrical proportional counter, 6 supplemental electrodes was equipped on the endcaps in MEPC. They realized parallel voltage potential in the whole lateral area of the proportional counter. Effective volume of the counter was the same as an internal volume of the proportional counter. A gas-multiplication gain was expected to be constant along the whole length of the anode. A relative expanded uncertainty of measurement of activity of radon gas is presumably evaluated as $\sim 2\%$ ($k=2$).

The manufactured MEPC is shown in Fig. 2. The whole size of the proportional counter was 68 cm in length, 16.5 cm in diameter. The sensitive area for radon gas was 32 cm in length, 7 cm in diameter. The endcap was made from PEEK (Polyether ether ketone) for insulation. The supplemental electrodes were placed circularly from the anode to wall of the proportional counter at 0.5 cm interval. The supplemental electrodes were implanted in the PEEK endcap. The anode wire was made from tungsten, and the diameter was $100 \mu\text{m} \pm 20 \mu\text{m}$

Figure 2: Manufactured proportional counter in cross-sectional view (Top) and appearance picture (Bottom)



5 CURRENT STATUS OF NMIJ AND ITS PRELIMINARY RESULTS

5.1 Calculation of Electrical field

Figure 3 shows electrical field in the proportional counter which was calculated by the finite element method using Photo-series ver. 8.3 (Photon Co. Ltd.). Model of the proportional counter was input in full scale. Supplied voltages for supplemental electrodes for the anode 1000 V were listed in Table 1. It was confirmed that the edge effect was corrected well in case that voltages for the supplemental electrodes were supplied.

Figure 3: Calculated electrical field in the proportional counter. (Top: voltage supply for the supplemental electrodes was turned on, Bottom: off. Areas of high voltage potential are coloured by red, and areas of low are by blue.)

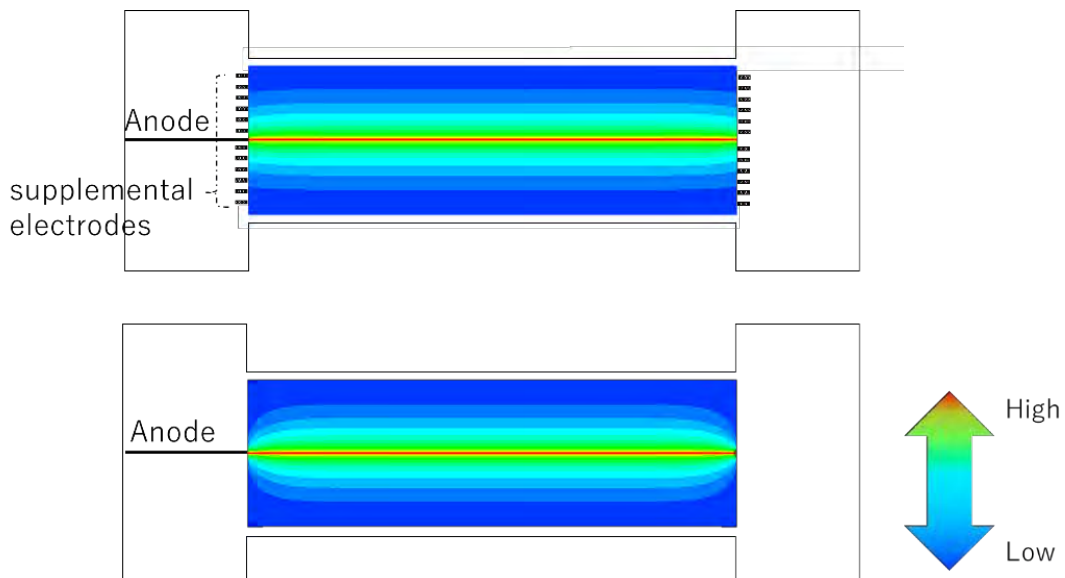


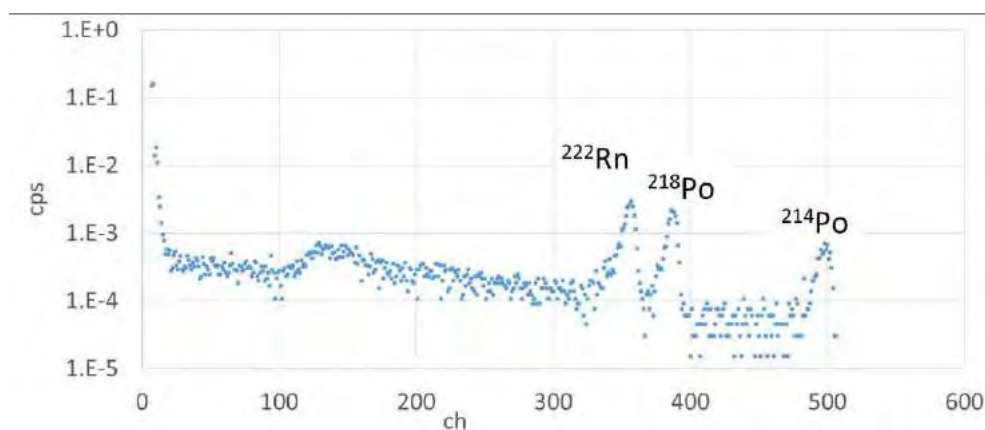
Table 1: Supplied voltages for supplemental electrodes

Distance from anode wire [cm]	Supplied voltages [V]
0.5	297.0
1	191.2
1.5	129.3
2	85.42
2.5	51.36
3	23.53

5.2 Pulse height distribution from radon gas

We took an alpha ray pulse height distribution from radon gas successfully as shown in Fig. 4. The measurement was conducted at atmospheric pressure with gas flow. Radon gas was transferred from Ra-226 by PR-gas (Ar + 10 % CH₄). Alpha ray peaks from Rn-222, Po-218, Po-214 were observed separately. The results indicated that alpha ray from radon gas can be counted by the proportional counter.

Figure 4: Obtained alpha ray pulse height distribution (Horizontal: pulse height channel (ch). Vertical: count per second (cps)).



6 CONCLUSION

We plan to establish a primary standard of activity of radon gas. We developed the proportional counter which can correct the edge effect. The successful results of alpha ray pulse height distribution were obtained.

7 ACKNOWLEDGEMENTS

The authors thanks for Dr. Yonehara in Nuclear Regulation Authority, Dr. Tokonami and Dr. Iwaoka in Hirosaki University, and Dr. Kanda and Dr. Mirosław in NIRS, Mr. Arai and Mr. Tatenuma in KAKEN Co., Ltd. Their precious comments support this work.

8 REFERENCES

- [1] M.-M. Bé, V. Chisté, C. Duiieu, E. Browne, V. Chechev, N. Kuzmenko, F. Kondev, A. Luca, M. Galán, A. Pearce, and X. Huang, 2008. Table of Radionuclides, volume 4 of Monographie BIPM-5. Bureau International des Poids et Mesures, Pavillon de Breteuil, F-92310 Sèvres, France.

- [2] Ministry of Education, Culture, Sports, Science and Technology, 2009. Guideline to safe guards for treatment of raw and manufactured product including uranium and thorium. (In Japanese).
- [3] National Institute of Radiological Sciences, 2005. "NIRSNews No. 100", http://www.nirs.go.jp/report/nirs_news/200503/hik01p.htm, (In Japanese, 29 April, 2016 confirmed).
- [4] Yongjae, K., Byung-Uck, C., Hong-Mo, P., Chang-Kyu, K. Shinji, T., 2011. National radon survey in Korea. *Radiat. Prot. Dosimetry* 146, 6–10.
- [5] Ishimori, Y., 2005. Characteristics of ^{222}Rn Measurement with a Gas filled Ionization Chamber, *Radioisotopes*, 54, 599-608 (In Japanese).
- [6] Busch, I., Greupner, H. Keyser, U., 2002. Absolute measurement of the activity of ^{222}Rn using a proportional counter. 481, 330–338.

Determination of radon emission rate regarding to constructional energy-saving-measures

Thomas Neugebauer^{*}, Hans Hingmann, Jonas Buermeyer, Anna-Lisa Grund, Volker Grimm[†], Joachim Breckow

Institute of Medical Physics and Radiation Protection (IMPS), University of Applied Sciences (THM), D-35390 Giessen, Germany

Abstract. As a consequence of constructional energy-saving measures buildings become more airtight. In frame of a project, the impact of those measures on the radon concentration was analysed. In order to determine time-dependent courses the radon concentration was measured before and after renovation for several weeks. In addition, the most relevant meteorological and indoor climate parameters were recorded. The results before and after were compared with respect to seasonal variation and the inhabitant's behaviour. By investigation of the correlation, influencing parameters on the radon concentration and the impact by the renovation was analysed. Due to the strong influence of the residents' behaviour, the radon concentration showed a large variation and made it difficult to evaluate the radon characteristic and the effect of the renovation. As a follow-up a less influenced parameter should be found. A possible quantity is the radon emission rate or radon entry rate. It describes the radon characteristics of a building and compensates the inhabitants' behaviour. The method is based on the measurement of the radon concentration and the determination of the air change rate. First results showed an improvement for the evaluation of the radon characteristics of a building. The analysis of influencing parameters of the radon emission rate is still ongoing.

KEYWORDS: *radon emission rate; radon entry rate; air change rate; tracer gas method.*

1 INTRODUCTION

Radon (Radon-222) is a radioactive noble gas. It is part of the uranium-radium-series and originates from its parent nuclide Radium-226 which is contained in the earth crust. Due to emanation, transportation processes and exhalation it reaches the atmosphere and can enter a building by different pathways (e. g. cracks in the bottom plate or leaky cable ducts) where it can be enriched to high concentrations. Many epidemiological studies showed a correlation between exposure to radon and the occurrence of lung cancer. The Council Directive 2013/59/Euratom requests EU-member states to analyse the exposition to radon for workers and the public and seize actions for reduction of this exposition.

In Germany, the legislative authority asks building owners to construct buildings energy efficient. Often this leads to a tightening of the building envelope and a reduced air exchange in those buildings. A conceivable consequence are higher radon concentration inside. The first presented project, hereinafter called project A, aimed to evaluate the impact of energy-saving measures on the radon concentration. Measurements were executed in several houses, the data underwent a statistical analysis.

The second project, called project B, was a result of the previous project. The objective was to find a parameter besides the radon concentration that is able to characterize the radon situation of a house. The quantity should compensate the user behaviour to get a lower uncertainty compared to the radon concentration. In addition, the assessment should be done by short-term- measurements, e. g. in frame of the acceptance of construction work. After preparing a concept, the method was verified using simulations and tested by measurements in an uninhabited house. The recorded data were used for a first analysis of possible influencing parameters.

* presenting author

† corresponding author, e-mail: volker.grimm@mni.thm.de

2 PROJECT A: ENERGY-SAVING MEASURES AND RADON CONCENTRATION

2.1 Methods

Five single-family houses have been chosen to analyse the impact of energy-saving measures on the radon concentration. The houses were built between 1950 and 1970. The amount of renovation varied between the objects and lasted from replacing of windows and improvements of insulation to the renewal of the roof of one of the objects. To avoid seasonal variations the measurements were executed in the same or similar time of a year and lasted over periods of six weeks.

The radon concentrations were measured using AlphaGUARDs (Saphymo GmbH, former Genitron) in two rooms of every occupied floor and the basement. Room climate parameters (temperature, humidity, CO₂-concentration) were recorded using CDL210 (Wöhler Messgeräte Kehrgeräte GmbH) while the meteorological parameters (temperature, pressure, humidity, wind direction and velocity, precipitation) outside were recorded using a weather station.

For handling and the analysis of the data, the statistics software R was used.

2.2 Results

The correlation of several parameters with the radon concentration showed no significant results. Only the temperature difference and wind velocity offered a mild correlation. A high wind velocity was the cause of a higher air change rate inside the buildings, which reduced the radon concentration. The observed correlation was higher before the renovation process, which shows the effectiveness of the energy-saving measures by tightening the building envelope.

A reason for the lack of correlation between radon and the recorded parameters is the influence of the inhabitants. Especially heating and venting are superimposing other influences and make it difficult to evaluate the radon characteristics of an occupied building.

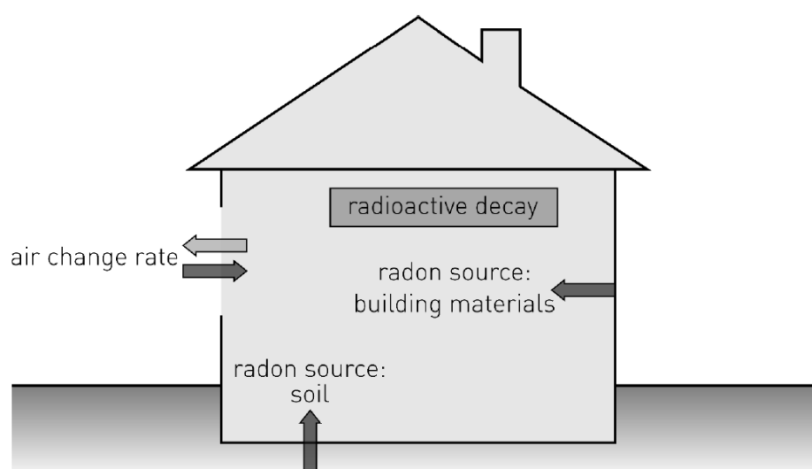
This is the reason a second project was initiated to find a parameter that is less influenced by the users behaviour and makes it easier to assess the radon situation, especially by short term measurements.

3 PROJECT B: RADON EMISSION RATE OF BUILDINGS

3.1 Methods

The radon concentration inside a room is the product of several radon sources, mainly radon from the soil entering the house via cracks in the bottom plate or leaky cable ducts. Other sources can be building materials. Since it is not possible to differentiate between the single sources all sources are summarized in one single variable QV, named radon emission rate or also known as radon entry rate.

Figure 1: Scheme representing relevant radon sources and parameters that have an influence on the radon concentration.



Apart from the sources, two other parameters are ruling the radon concentration. On the one hand the radioactive decay (λ) and on the other hand the air change rate (k). The air change rate (ACH or ACR) of a house is defined by its leakages and the users' behaviour (e. g. venting and heating) and represents the exchange of air per hour referred to the room volume. When summing up the above-mentioned circumstances in an equation the result is [1]:

$$\frac{dc_{Rn}(t)}{dt} = -\lambda \cdot c_{Rn}(t) + Qv(t) + k(t) \cdot c_{Rn,a} - k(t) \cdot c_{Rn}(t) \quad (1)$$

While $c_{Rn,a}$ is representing the radon concentration outside $c_{Rn}(t)$ is the radon concentration inside a room over the time. By assuming radon emission rate and air change rate as constant and $c_{Rn}(0)$ the result is:

$$c_{Rn}(t) = e^{-(\lambda+k) \cdot t} \cdot \left(c_{Rn}(0) - \frac{Qv(t)+c_{Rn,a} \cdot k}{\lambda+k} \right) + \frac{Qv(t)+c_{Rn,a} \cdot k}{\lambda+k} \quad (2)$$

If radon entry rate and air change rate are constant, the radon concentration will reach a point of saturation. By considering those and assuming $t = \infty$ equation 2 can be simplified to:

$$c_{Rn}(\infty) = \frac{Qv(t)+c_{Rn,a} \cdot k}{\lambda+k} \quad (3)$$

By using this equation, it is possible to determine the radon emission rate from radon concentration and air change rate. A disadvantage of this method is the required constant radon emission rate and the constant air change rate over time.

When considering time-variant air change rates and radon entry rates equation 2 has to be investigated again. By reducing the period under observation to Δt the assumption of a constant air change rate and a constant radon source persists. Every previous value [$c(n-1)$] of the radon concentration becomes the starting value $c_{Rn}(0)$ of the next step:

$$c_{Rn}(n) = e^{-(\lambda+k) \cdot \Delta t} \cdot \left(c_{Rn}(n-1) - \frac{Qv(n)+c_{Rn,a} \cdot k(n)}{\lambda+k(n)} \right) + \frac{Qv(n)+c_{Rn,a} \cdot k(n)}{\lambda+k(n)} \quad (4)$$

By solving the equation for the radon emission rate Qv the result is:

$$Qv(n) = \frac{c_{Rn}(n-1) \cdot (k(n)+\lambda) + c_{Rn}(n) \cdot (k(n)+\lambda) \cdot e^{(k(n)+\lambda) \cdot \Delta t} - c_{Rn,a} \cdot k(n) \cdot (e^{(k(n)+\lambda) \cdot \Delta t} - 1)}{e^{(k(n)+\lambda) \cdot \Delta t} - 1} \quad (5)$$

With this equation, it is possible to determine the time dependent radon emission rate based on the measurement of the radon concentration and the air change rate. The result is a released activity per time and cubic meter for the volume specific radon entry rate Qv . By multiplying this value with the volume of the analysed room, the result is the released activity per time (Q).

As stated above it is necessary to determine the air change rate. Several well-known methods, according to VDI 4300-7 [2] or DIN EN ISO 12569:2012 [3], can be used. Starting point of the favoured methods is the use of a non-radioactive tracer gas.

The mentioned regulations provide possible gases like carbon dioxide (CO_2), sulphur hexafluoride (SF_6) or nitrous oxide (N_2O). Despite several disadvantages, we used CO_2 .

During the project, two different methods for the injection of the tracer gas have been used: For the first one the gas is injected only once at one point in a room. After a short build-up the gas concentration will follow an exponential decay (concentration-decay method); the air change rate can be calculated using equation 6:

$$k = \frac{\ln\left(\frac{c_{n-1}}{c_n}\right)}{\Delta t} \quad (6)$$

c_{n-1} and c_n are representing the measured tracer gas concentration, Δt stands for the time difference between the two measured values.

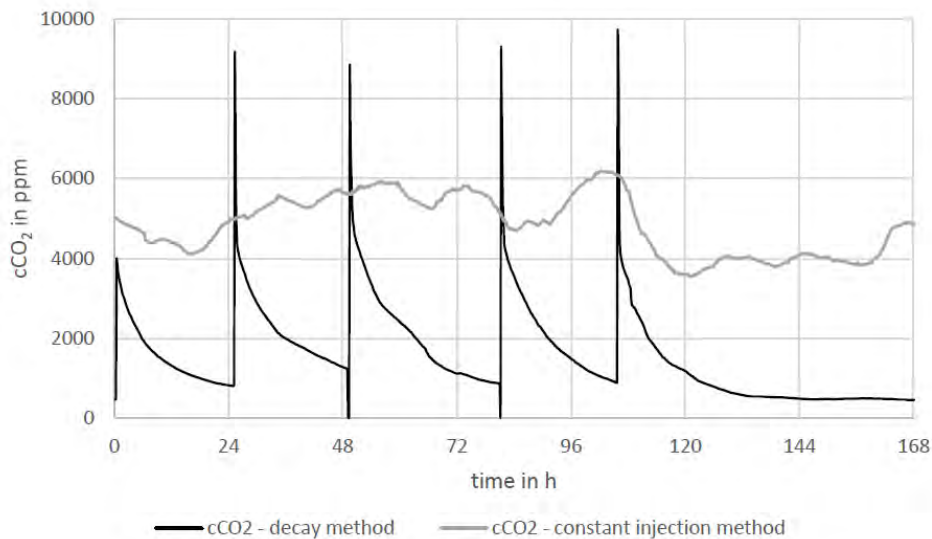
This method has several disadvantages when determining the air change rate over longer periods. After an injection, it takes some time (up to two hours) before the gas reaches a homogenous distribution in a room. During this time, it is not possible to calculate the ACH by the tracer gas concentration correctly. After the homogenization, it is possible to use one measurement point as representative for the whole room.

When using a gas that has a natural background (e. g. CO₂, underground concentration between 400 and 450 ppm) that background has to be subtracted from the measured concentrations. It is important to keep the concentration on a level above the natural background; otherwise, the air change rate cannot be determined correctly. In this project, we used a lower threshold value of twice of the underground concentration.

When determining ACR over longer periods by this method it becomes difficult to get continuous values. For this reason we used a second method: The constant-injection method. The gas is injected on a constant basis at several points of a room. This reduces the time for homogenization; the constant injection ensures a concentration above the natural background. The adjusted concentration depends on the defined injection rate and the air change rate of the object.

Figure 2 shows the comparison of both methods. The curve resulting from the decay method (black) shows the described exponential character, CO₂ was injected five times. After injection, the air change rate could not be determined and gaps of approximately two hours appeared in the course. The grey curve shows the concentration when using the constant injection of CO₂.

Figure 2: Comparison of the described tracer gas methods. When using the decay method the tracer gas has to be injected again after some time. When using the constant injection method the concentration can be maintained in a specific concentration zone.

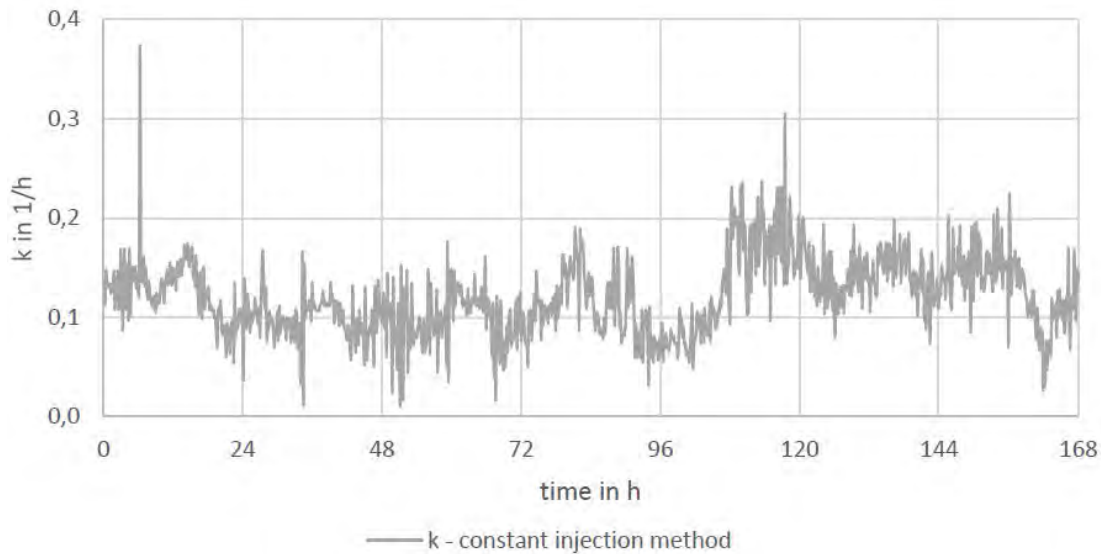


The air change rate can be calculated using an equation from [2]. This method uses the current concentration value and the injection rate of the tracer gas. A more exact technique is to use the difference between two concentration values as shown in equation 7:

$$k = \frac{\left(\frac{c_{n+1}-c_n}{\Delta t}\right) \cdot \frac{q \cdot 60}{v}}{c_a - c_n} \quad (7)$$

While c_{n+1} and c_n are the measured tracer gas concentration, q represents the injection rate of the tracer gas, V is room volume and c_a the natural background of the used tracer gas. Due to the above-mentioned advantages, the air change rate was calculated using the constant injection method, an example corresponding to the CO₂ concentration in Figure 2 (grey curve) can be seen in Figure 3.

Figure 3: Result of the calculated air change rate, based on the measured concentration of the tracer gas CO₂ (grey curve in Figure 2, constant injection method).



3.2 Verification

The described approach was verified using simulations and measurements from an older project. Via a program it is possible to simulate different radon emission rates and air change rates. In addition, the natural radon concentration, room volume and specific properties of measurement devices can be defined. The result is a radon concentration. This concentration and the defined air change rate were used to reproduce the course of the radon entry rate.

Figure 4 shows an example of a simulated radon concentration and defined air change rate. The values of both curves were used to calculate the radon emission rate via equation 5, the result can be seen in Figure 5.

Figure 4: Simulated radon concentration (grey), resulting from the air change rate (black) and the defined radon emission rate from Figure 6 (dashed).

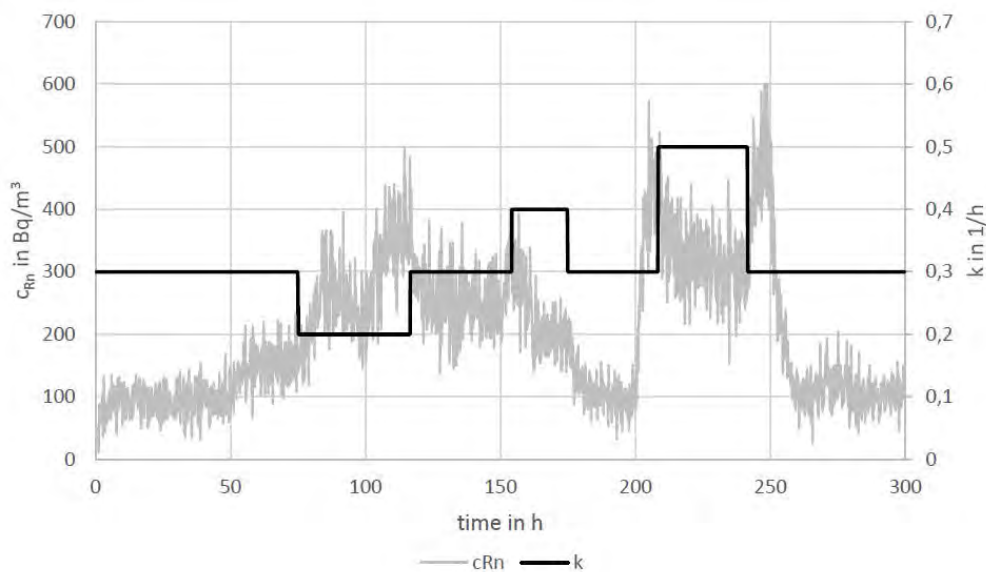
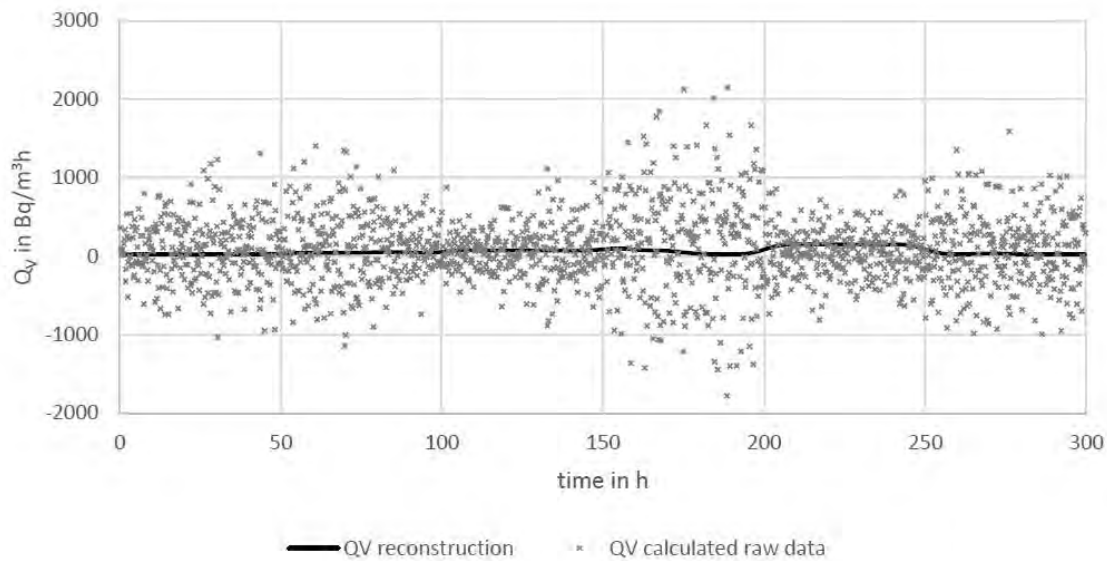


Figure 5: Result of the calculated (via equation 5) and the reconstructed radon emission rate. Input parameters have been the radon concentration and air change rate from Figure 4.

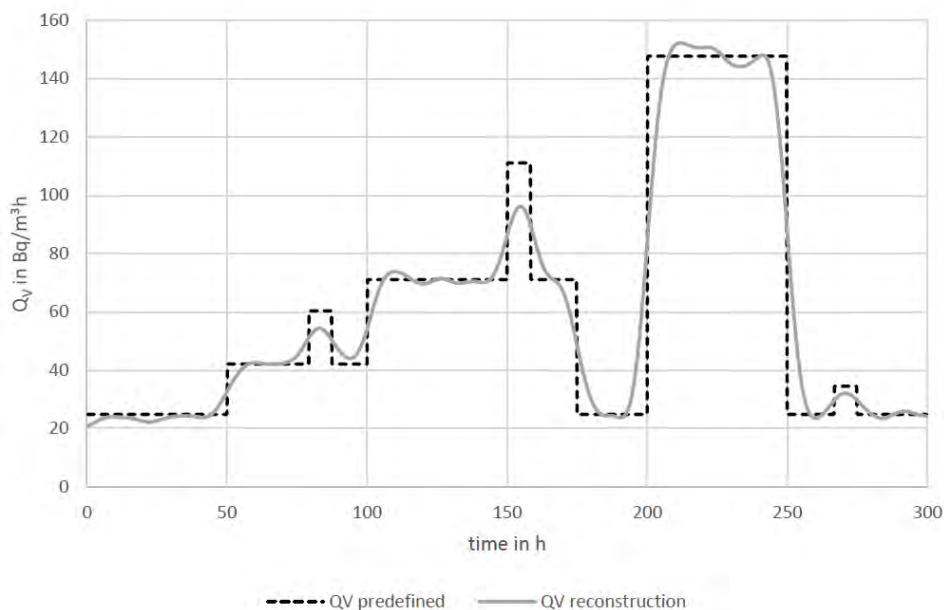


It is a very noisy signal, the original course of the radon emission rate, which was used for the simulation of the radon concentration, cannot be recognized. This problem occurred for all analysed simulations and measurements.

Due to this, we used several simple smoothing algorithms (e. g. arithmetic mean and moving average) to reproduce the original signal. The outcome showed better results but was not satisfying for jump discontinuities like the air change rate shows in Figure 4. Another approach was the application of window functions that are known from digital signal processing. Besides well-known functions like the Hamming window, we used a window, which is working as a cosine-weighted low-pass filter. This window showed the best results and is used for the reproduction of the radon entry rate.

The result of the reconstruction is also shown in Figure 5, due to the scale the actual time course is not visible. A comparison between the time course of the radon emission rate used for the simulation and the reproduced radon emission rate can be seen in Figure 6. The conformity of both curves is sufficient, larger deviations only occur at discontinuities of the radon emission rate.

Figure 6: Comparison of simulated and reconstructed radon emission rate. The outcome was produced by the application of a modified window function on the data from Figure 5. Both curves show a sufficient conformity.



3.3 Practical use

After the verification of the method by testing it via simulations and measurements from an older project, we applied the method to an uninhabited building. This building is used as a storage and consists of two connected rooms and an attic.

By using the constant injection method for determining the air change rate with CO₂ and parallel measurements of the radon concentration it was possible to calculate the radon emission rate. The results of this measurement campaign showed that the radon entry rate is not constant. Possible influencing parameters like pressure difference or temperature difference are under investigation and will be analyzed in a future project.

4 DISCUSSION

The results of the project analysing the influence of energy-saving measures on the radon concentration inside buildings were not as significant as expected. This was caused by the influence of the residents' behaviour, which superimposed many of the other possible influencing parameters. Only the temperature difference and wind velocity showed mild correlations.

In the follow-up of this project, another quantity for the characterization of the radon situation of buildings was needed. It should be less affected by inhabitants and should be able to evaluate the radon characteristics of a house via short-term measurements. The radon entry rate is to be thought to combine those requirements. Within the project, we developed a method for the continuous determination of the radon emission rate and verified it. First steps to evaluate the practicability in an uninhabited building showed satisfying results.

Nevertheless, there are several points that have to be analysed in the future to improve the outcome. At the moment the determination of the air change rate is done using CO₂ as tracer gas. This is possible in uninhabited buildings or rooms that are not in use on a regular basis. Because of the exhalation of CO₂, the use as a tracer is contradicted in the presence of humans. Other gases like SF₆ are a possible alternative but require special measurement devices.

A second point of interest is the evaluation of influencing parameters and the quantification of the benefit compared with the measurement of the radon concentration. In particular, pressure difference and temperature difference are possible quantities that have an impact on the behaviour of the radon coming from the underground of a building.

In summary, it can be stated that the presented method provides a possibility to assess the radon situation of a building. The advantage is primarily the compensation of the inhabitants' behaviour by determining the air change rate.

5 ACKNOWLEDGEMENTS

Project A was funded by the Federal Office for Radiation Protection (BfS) of Germany (BfS 3611 S 10016 Los 2), Project B was supported by the Hessian Ministry of the Environment, Climate Protection, Agriculture and Consumer Protection (HMU32206031). We would like to thank the Hessian Agency for Nature Conservation, Environment and Geology (HLNUG) for providing meteorological data.

6 REFERENCES

- [1] F. Roessler, T. Azzam Jai, V. Grimm, H. Hingmann, T. Orovvighose, N. Jach and J. Breckow, First steps in the development of a possible measurement method to estimate the radon concentration as an indicator of the indoor air quality, " *Nucl. Technol. Radiat. Vol. 29 Suppl.*, pp. 52-58, 2014.
- [2] "Measurement of the indoor air change rate (VDI 4300-7)," Association of German Engineers (VDI), Duesseldorf, 2001.
- [3] Thermal performance of buildings and materials - Determination of specific airflow rate in buildings - Tracer gas dilution method (ISO 12569:2012); German version EN ISO 12569:2012, Beuth Verlag GmbH, Berlin, 2012.

Selection of Potassium Fertilizer Application Method to Reduce Uptake of Cs-137 in Brown Rice

Takashi Saito^{a*}, Kazuhira Takahashia, Takeshi Ota^b, Tomoyuki Makino^c

^aHama Agricultural Regeneration Research Centre, Fukushima Agricultural Technology Centre, 45-169 Sukakeba, Kaibama, Haramachi-ku, Minamisoma, Fukushima 9750036, Japan.

^bNARO Tohoku Agricultural Research Centre, 50 Harajukuminami, Arai, Fukushima, Fukushima 9602156, Japan.

^cSoil Environmental Division, National Institute for Agro-Environmental Sciences, Tsukuba, Ibaraki 3058604, Japan.

Abstract. Since the March 2011 accident at the Fukushima No. 1 Nuclear Power Plant, farmers outside the exclusion zone have been adding potassium (K) fertilizer to their paddy fields with the aim of reducing the uptake of radiocesium by rice. We investigated the chemical form of K fertilizer and application method to find the most effective way of reducing Cs-137 uptake. Application of K as KCl suppressed Cs-137 uptake more effectively than application as K_2SiO_3 , a slow-release fertilizer. Application of KCl before puddling (whole-plow-layer application) reduced the Cs-137 content of brown rice more effectively than application after puddling (surface-only application). Reduction of the radiocesium content in brown rice was not appreciably improved at K application rates above 16 g m^{-2} . The hyperbolic relationship between K^+ concentration in the soil solution and Cs-137 in brown rice indicated that the optimal application of K to suppress Cs-137 uptake by rice plants is $16\text{--}32 \text{ g m}^{-2}$ as KCl. The results suggest that the K^+ concentration in the soil solution may offer a simple way to measure soil K availability. The threshold K^+ concentration in the soil solution for lowering radiocesium in brown rice to below the current health standard of 100 Bq kg^{-1} was 2.3 mg L^{-1} .

KEYWORDS: Cs-137; bioaccumulation; brown rice; potassium, soil solution, potassium chloride.

1 INTRODUCTION

The 2011 accident at the Tokyo Electric Power Company's Fukushima Dai-ichi Nuclear Power Plant in Japan released a large amount of radiocesium into the atmosphere, contaminating agricultural and forest land in and around Fukushima Prefecture. In areas where rice was planted outside the 20-km exclusion zone designated in 2011, radiocesium fallout was mixed into the plow layer during plowing and puddling. Removing radiocesium (chiefly Cs-137) from the plowed soil is difficult, but the ionic similarity of Cs and potassium (K) means that uptake by paddy rice can be reduced to below harmful levels if the soil exchangeable K concentration is high enough to displace Cs from the soil exchange complex. The uptake of Cs-137 by paddy rice has been shown to reduce with increasing soil K concentration [1]. Thus, the application of K fertilizer offers an effective and practical method of reducing radiocesium uptake by rice, and has been proven in several soil types [2].

Farmers have been adding K fertilizer to their paddy fields for crops grown since the accident, and the concentration of radiocesium in brown rice has been shown to decrease with increasing concentration of soil exchangeable K [3]. Basal application of K fertilizer, compared with application at other times, achieves the greatest reduction in uptake of Cs-137 [4]. Following the accident, the Food Sanitation Law of 2012 lowered the allowable concentration of radiocesium in food from $\leq 500 \text{ Bq kg}^{-1}$ to $\leq 100 \text{ Bq kg}^{-1}$. A soil exchangeable K concentration of $>208 \text{ mg kg}^{-1}$ dry weight was recommended for keeping the radiocesium content of brown rice within the new standard [5]. The yearly application of K fertilizer to maintain such levels of soil exchangeable K is, however, a considerable financial burden.

* Presenting author, email: saito_takashi_01@pref.fukushima.lg.jp

Here, we investigated the effectiveness of K fertilizer at reducing Cs-137 uptake by brown rice in two chemical forms, KCl and K_2SiO_3 . For KCl we also investigated four application rates and two application methods (surface or the whole plow layer). From the results, we propose a simple method for measuring soil K availability during the growing season.

2 MATERIALS AND METHODS

2.1 Experimental Field

In 2013, we grew rice in a 0.3-ha radiocesium-contaminated field in northern Fukushima Prefecture, some 50 km northwest of the Dai-ichi Power Plant. Rice had been grown in the field for many years before the accident. Brown rice produced in this field in 2011 exceeded the provisional standard at that time (500 Bq kg^{-1}); subsequently, rice planting in this area was forbidden in 2012 and 2013.

2.2 Cultivation Methods

We used a split-plot design with three replications; each plot was $3 \text{ m} \times 10 \text{ m}$. Base fertilizer was applied to the entire field at rates of 6.0 g m^{-2} of N as Ammonium sulfate and 4.4 g m^{-2} of P_2O_5 as calcium superphosphate on 17 April 2013. The field was plowed on 20 April and puddled on 4 May, and seedlings were planted out on 10 May at $17.1 \text{ hills m}^{-2}$ ($30 \text{ cm} \times 19.5 \text{ cm}$). The following experiments were conducted:

Experiment 1: K was applied at 16.0 g m^{-2} as either KCl or K_2SiO_3 before puddling. A zero K application control was included and was used as the control reference for the other two experiments.

Experiment 2: K was applied at 8.0 g m^{-2} as KCl either before puddling (whole-plow-layer application) or after puddling (surface application).

Experiment 3: K was applied at 8.0, 16.0, 32.0, or 64.0 g m^{-2} as KCl before puddling.

2.3 Sample Collection and Preparation

The soil was classified as a Fluvisol according to the World Reference for Soil Resources. After harvest, soil samples were collected from each plot on 19 September 2013 using a stainless steel auger 30 cm in length and 5 cm in diameter. The samples were air-dried for 21 days, thoroughly mixed, and passed through a 2-mm sieve before analysis. Threshed grain samples retained on a 1.8-mm sieve were used for analysis.

Soil solution samples were collected from each plot at a depth of 5 cm from May to June 2013 on a weekly basis using a DIK-8392 soil water sampler (Daiki Rika Kogyo Co., Ltd., Saitama, Japan). After the samples were passed through a $0.45\text{-}\mu\text{m}$ membrane filter, the K^+ concentrations were determined AA280FS atomic absorption spectrophotometer (Varian Technologies Japan Ltd., Tokyo, Japan).

2.4 Soil and Brown Rice Analyses

The dried soil was compressed into cylindrical polystyrene containers. The brown rice samples were compressed into 0.7-L Marinelli beakers. The concentrations of Cs-137 in each were measured with a series of Ge gamma-ray detectors measured with a germanium semiconductor detector with multichannel analyzers (GC2020, GC3020, GC3520, GC4020, Canberra USA) connected to a xxx Multiport II Multichannel analyzer for 3600–7200 s.

The chemical properties of the soils were analyzed as specified [6] (Table 1). Soil pH (H₂O) was measured at a soil-to-water ratio of 1:2.5 (w/w). The total carbon content was determined by dry combustion on a Sumigraph NC Analyzer NC-220F (Sumika Chemical Analysis Service, Ltd., Osaka, Japan). Exchangeable K, calcium, and magnesium were determined by the semi-micro Schollenberger method on an AA280FS, and cation exchange capacity was calculated as the sum of these component ions.

Table 1: Chemical properties of the experimental field soil (0–15 cm).

pH(H ₂ O)	T-C	Exchangeable Ca	Exchangeable Mg	Exchangeable K	CEC
	(g kg ⁻¹)		(mg kg ⁻¹ DW)		(cmol _c kg ⁻¹)
6.6	24	2262	416	56	42

2.5 Calculation of the Soil-to-Plant Transfer Factor

The soil-to-plant transfer factor (TF) is used to compare the tendencies of plants to bioaccumulate materials from soil. It is a simple but important parameter that can be used to estimate the concentrations of radionuclides expected in plant tissue. As the TF for a given element or compound can vary widely between sites, species, and organs of the same plant, it should be evaluated under site-specific conditions, and the particular plant organ of interest in the transfer should be specified, in this case soil to brown rice and soil to rice straw. To compare the bioaccumulation of radiocesium in brown rice and in rice straw, we calculated the TF as the ratio of radiocesium in the brown rice or rice straw (Bq kg⁻¹) to that in the soil (Bq kg⁻¹), on a dry-weight basis.

2.6 Statistical Analyses

Statistical analyses were performed in StatView 5.0 J software (SAS Institute, Berkeley, CA, USA). Analysis of variance (ANOVA) followed by *t*-test or Tukey's multiple comparison test was used to determine the significance of differences in a pairwise comparison matrix.

3 RESULTS AND DISCUSSION

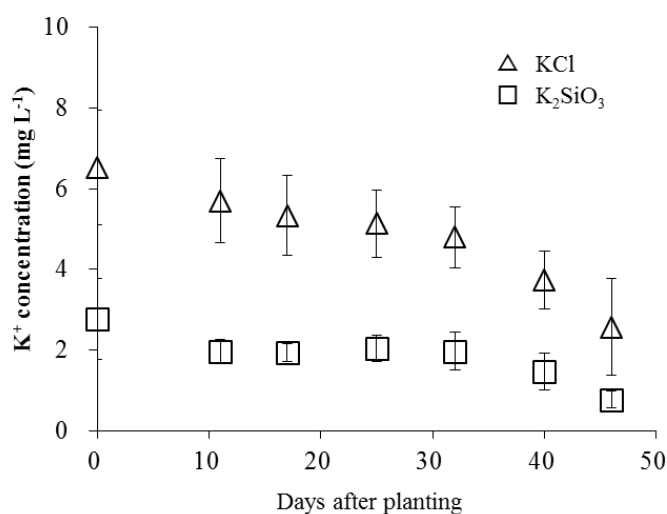
3.1 Effective of K Fertilizer Type on Cs-137 Uptake (Experiment 1)

The Cs-137 concentrations in plants were almost 3 times as high in straw and over 6 times as high in brown rice when K was applied as K₂SiO₃ as when it was applied as KCl (Table 2). Similarly, the TF values were 3 times as high in straw and 7 times as high in brown rice. The K⁺ concentration in the soil solution immediately after planting averaged 6.5 mg L⁻¹ in the plots treated with KCl and 2.8 mg L⁻¹ in the plots treated with K₂SiO₃, and the respective concentrations had decreased by 60% and 71% at 45 days after planting (Fig. 1).

Application of K as KCl clearly resulted in a higher soil K⁺ concentration and suppressed Cs-137 uptake by paddy rice more effectively than application of K₂SiO₃. The difference can be attributed to solubility: KCl is almost totally water soluble, while K₂SiO₃ has relatively low solubility, which is why it is used as a slow-release fertilizer. Water-soluble K fertilizer is obviously preferred if the aim is to reduce Cs-137 in brown rice; however, K from K₂SiO₃ might be released into the soil solution for a longer period, which, if it can reduce Cs-137 in brown rice sufficiently, may reduce the cost and labor of some subsequent K fertilizer applications. This longer-term aspect of the choice between fertilizer forms will be a subject of future investigation.

Table 2: Mean (\pm SD) concentrations of Cs-137 and transfer factors of Cs-137 from soil to straw and brown rice in paddy rice fertilized with potassium at the same application rate as either KCl or K_2SiO_3 .

Types of K fertilizer	Cs-137 in Soil (Bq kg ⁻¹ DW)	Cs-137 in Rice Straw (Bq kg ⁻¹ DW)	Cs-137 in Brown Rice (Bq kg ⁻¹)	Transfer factor of Cs-137 Soil to Rice Straw	Transfer factor of Cs-137 Soil to Brown Rice
KCl	3349 \pm 343	41 \pm 20	10 \pm 7	0.012 \pm 0.006	0.003 \pm 0.002
K_2SiO_3	2818 \pm 271	110 \pm 41	63 \pm 38	0.039 \pm 0.013	0.022 \pm 0.013

Figure 1: Mean (\pm SD) potassium ion concentrations over time in the soil solution of paddy plots treated with potassium at the same application rate as either KCl or K_2SiO_3 .

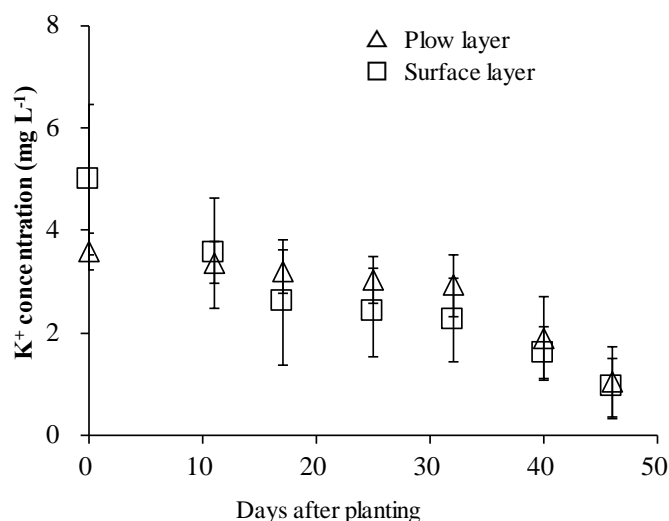
3.2 Effect of K Fertilizer Application Method on Cs-137 Uptake (Experiment 2)

The Cs-137 concentrations in rice straw and brown rice were lower when KCl was applied before puddling than when it was applied after puddling (Table 3); however, the differences were less pronounced than those between the two forms of fertilizer. As a result, the values of TF were of a similar scale when KCl was applied before or after puddling. The K^+ concentration in the soil solution immediately after planting was about 30% higher in the plots to which KCl was applied after puddling (surface application) than in those to which it was applied before puddling (plow-layer application; Fig. 2). By 10 days after planting, the concentrations were similar in both application methods and continued that way until day 45, when measurements ceased. These results favor application of K fertilizer to the whole plow layer before puddling, although the differences are not large. The soil solution monitoring indicated that surface-layer application results in greater K efflux to the paddy water and loss from the soil solution than does plow-layer application.

Table 3: Mean (\pm SD) concentrations of Cs-137 and transfer factors of Cs-137 from soil to straw and brown rice in paddy rice fertilized with potassium either before puddling (whole plow layer) or after puddling (soil surface).

Method of K fertilizer	Cs-137 in Soil (Bq kg ⁻¹ DW)	Cs-137 in Rice Straw (Bq kg ⁻¹ DW)	Cs-137 in Brown Rice (Bq kg ⁻¹)	Transfer factor of Cs-137 (Soil to Rice Straw)	Transfer factor of Cs-137 (Soil to Brown Rice)
Surface layer	3026 \pm 188	122 \pm 52	52 \pm 32	0.040 \pm 0.018	0.017 \pm 0.012
Plow layer	3359 \pm 461	95 \pm 56	41 \pm 22	0.028 \pm 0.016	0.012 \pm 0.008

Figure 2: Mean (\pm SD) potassium ion concentrations over time in the soil solution of paddy plots treated with the same amount of K applied either to the whole plow layer (before puddling) or to the surface (after puddling).



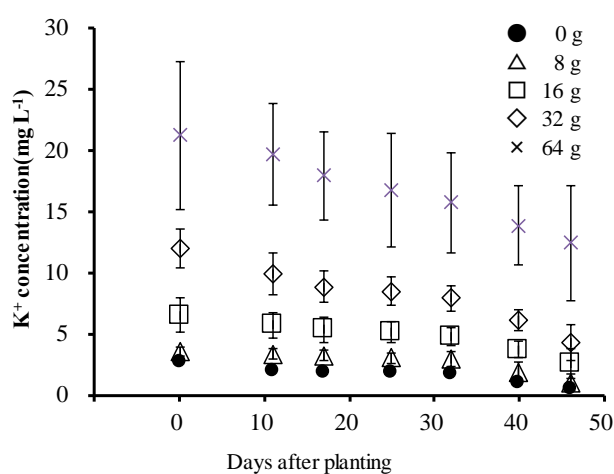
3.3 Effect of KCl Application Rate on Cs-137 Uptake (Experiment 3)

The radiocesium concentration and TF values in rice straw and brown rice declined hyperbolically with increasing rate of applied K (Table 4). Increasingly higher rates of K application had a progressively lower marginal effect on lowering the Cs-137 in rice straw and brown rice, and the optimal application rate was 16 g m⁻². The concentration of K⁺ in the soil solution was more linearly related to the amount of K applied and declined linearly over time at all application rates (Fig. 3).

We conclude that the application of KCl to the plow layer at 16 g m⁻² is the most effective way of suppressing Cs-137 uptake by rice plants at this site.

Table 4: Mean (\pm SE) Cs-137 concentrations and transfer factors in rice straw and brown rice fertilized with KCl at rates ranging from 0 to 64 g m⁻².

Amount of K fertilizer (g m ⁻²)	Radiocesium in Soil (Bq kg ⁻¹ DW)	Radiocesium in Rice Straw (Bq kg ⁻¹ DW)	Radiocesium in Brown Rice (Bq kg ⁻¹)	Transfer factor of Radiocesium (Soil to Rice Straw)	Transfer factor of Radiocesium (Soil to Brown Rice)
8	4889 \pm 691	135 \pm 77	58 \pm 30	0.027 \pm 0.014	0.012 \pm 0.008
16	4771 \pm 424	63 \pm 27	15 \pm 10	0.013 \pm 0.0054	0.0030 \pm 0.002
32	3803 \pm 283	44 \pm 28	11 \pm 6.1	0.011 \pm 0.0065	0.0028 \pm 0.002
64	5071 \pm 625	26 \pm 16	2.7 \pm 1.5	0.0050 \pm 0.0024	0.00047 \pm 0.00024
0	4353 \pm 681	226 \pm 56	112 \pm 49	0.054 \pm 0.023	0.027 \pm 0.016

Figure 3: Mean (\pm SD) potassium ion concentrations over time in the soil solution of paddy plots fertilized with KCl at rates ranging from 0 to 64 g m⁻².

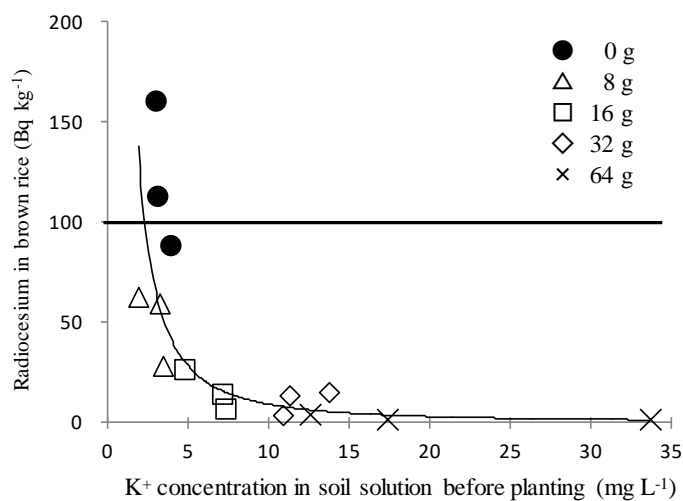
3.4 Predicting Radiocesium Concentration in Brown Rice from Soil K concentration

Following the accident at the power plant, enactment of the Food Sanitation Law 2012 lowered the standard for the allowable concentration of radiocesium in food to 100 Bq kg⁻¹, and an exchangeable soil K concentration of >208 mg kg⁻¹ dry weight was recommended to maintain the radiocesium content in brown rice below the standard (NARO 2012). However, a soil K level of >208 mg kg⁻¹ has its own safety concerns. Therefore, a method for determining the most appropriate K application rate is required. Furthermore, analysis of soil exchangeable K content takes too long after soil sampling to be practical for farmers to take remedial action if they sample close to planting time. Therefore, a simpler and quicker analytical method than soil exchangeable K content is needed.

Using the data of Experiment 3, we examined the relationship between the K⁺ concentration in the soil solution between fertilizer application and planting and the radiocesium concentration in brown rice (Fig. 4). The equation for the fitted curve was $y = 395x^{-1.6}$ ($r^2 = 0.79$).

According to the relationship, the radiocesium in brown rice was <100 Bq kg⁻¹ when K⁺ in the soil solution before planting was >2.3 mg L⁻¹. To add in a margin of error and a safety factor, we suggest a practical diagnostic value of 7.0 mg L⁻¹ for this experimental field, and conclude from Fig. 4 that a KCl application rate of 16–32 g m⁻² would reliably achieve this under the conditions of our experiment. Further work is needed to determine whether this simpler diagnostic test is reliable at other sites. In particular, soils with different types of clay mineralogy may produce different results, as the relationship between exchangeable cations and cations in soil solution depends on the dynamics of the exchange complex of clays and other soil colloids.

Figure 4: Relationship between radiocesium concentration in brown rice and K^+ concentration in soil solution before planting.



4 CONCLUSIONS

This study shows that the application of K fertilizer to reduce Cs-137 uptake by paddy rice can be optimized because additions beyond a certain level provide no additional benefit. Application of soluble KCl is more effective than a slow-release form of K, and application before puddling to ensure incorporation into the plow layer will have the greatest impact on reducing Cs-137 uptake. The penalty for applying the fertilizer after puddling is not major, so this method could be used if practical considerations prevented application before puddling. Diagnosis of the adequacy of soil K levels to reduce Cs-137 uptake may be best undertaken through analysis of K^+ concentrations in the soil solution rather than the more analytically intensive exchangeable K content in soil. Further work is required to determine whether these conclusions hold for different sites, especially those with soils containing different amounts and types of clay minerals, which influence cation exchange dynamics.

5 REFERENCES

- [1] Tsukada, H., Hasegawa, H., Hisamatsu, et al., 2002. Transfer of ¹³⁷Cs and stable Cs from paddy soil to polished rice in Aomori, Japan. *J. Environmental Radioact.*, 59, 351–363.
- [2] Naoto Kato, 2012. Countermeasures to reduce radiocaesium contamination in paddy rice, soy bean and cabbage. In: *International Science Symposium on Combating Radionuclide Contamination in Agro-soil Environment*, Fukushima, Japan, pp. 317–318.
- [3] Saito, T., Ohkoshi, S., Fujimura, S., et al., 2012. Effect of potassium application on root uptake of radiocesium in rice. In: *Proceedings of the International System on Environmental Monitoring and Dose Estimation of Residents after Accident of TEPCO's Fukushima Daiichi Nuclear Power Station*, pp. 165–169. Kyoto University Research Reactor Institute Press, Kyoto.
- [4] Saito, T., Takahashi, K., Makino, T., et al., 2015. Effect of application timing of potassium fertilizer on root uptake of ¹³⁷Cs in brown rice. *J Radioanal. Nucl. Chem.*, 303, 1585-1587.
- [5] NARO 2012. Reduction of radioactive cesium concentration in brown rice by potassium increase in various types of soil (in Japanese, April 2016; title translated by authors) <http://www.naro.affrc.go.jp/org/tarc/seika/jyouhou/H24/kankyou/H24kankyou012.html>
- [6] Editorial Boards of *Methods for Soil Environment Analysis*, 1997. *Methods for Soil Environment Analysis*. Hakubunkan Shinsha Publishers Press, Tokyo.

Findings of the control and monitoring of liquid releases from the Centre of Isotopes of Cuba

Zayda Haydeé Amador Balbona, Pilar Oropesa Verdecia

Centre of Isotopes, Radiation Protection Department, Ave. Monumental y Km. 3_{1/2}, carretera La Rada, Havana, Cuba

Abstract. The liquid effluents from the operations with the smaller levels of radioactivity in the production of radiopharmaceuticals and labelled compounds in the Centre of Isotopes (CENTIS) from Cuba, can be discharged to the environment complying with the authorized limits for the Regulatory Body. This paper summarizes the findings during more than ten years of the radiological control of the liquid effluents from CENTIS taking into account the procedures for sampling water, pH control and preparing of samples, which made covering international standards and recommendations. Moreover, the measurements of the activity concentration of gamma radionuclides in the samples are made in the spectrometric system with HPGe detector. The energy and efficiency calibrations of this system carried out with a set of punctual sources and ¹⁵²Eu solution, respectively, certificated by the Metrology Centre of Hungary. Beta emitters measured using a liquid scintillation counter and chemical separation for ⁹⁰Sr and measurement of Cherenkov radiation of ⁹⁰Y. The results show that the ¹³¹I, ³²P and ⁹⁰Sr are the most representative radionuclides. The experience indicates that the measurement methods employed allow obtain results in a week and with an uncertainty less than 10 %. In the 61% of the measurements as an average, we have to apply the reducing sources principle. The applied release limits imply not use a dilution factor with others waters. For this reason, the management costs increased, due to the very conservative character of the clearance levels of the License.

KEYWORDS: *liquid effluents; discharges; monitoring; measurement; gamma-emitters; beta-emitters.*

1 INTRODUCTION

The liquid effluents arising from radiochemical laboratories, change-rooms and showers of the Centre of Isotopes (CENTIS) in Cuba collected in a special sewage system that has 93-generation points [1]. This system provided with storage facilities so that short-lived radionuclides can decay before release in compliance with the clearance levels established by Regulatory Body [2]. In this paper, findings from about two decades of operations summarized.

2 MATERIALS AND METHODS

A quality assurance program established for control and monitoring liquid releases [2]. Requirements relating to representative samples are implemented [2]. A quality assurance program established for control and monitoring these effluents [3]. Requirements for assuring representative samples implemented and fulfilled [4-7]. Source monitoring program designed to measure the discharge rates of radionuclides [8]. The measurement of the activity concentration of gamma emitters with energy of (59 to 1500) keV carried out in a spectrometric system of high resolution with HPGe detector, according to established procedure [9] and recommendations [10]. Liquid reference materials used for quantitative analysis obtained by addition of known aliquot of both ¹⁵²Eu and ¹³³Ba solutions, provided by the National Metrological Institute of Hungary (MKEH) [11], to aqueous solutions in plastic containers, of the same type as used for performing the routine analysis. Previously, the activity concentration of ¹⁵²Eu and ¹³³Ba determined by the method described elsewhere [12]. These reference materials utilized for carrying out the efficiency calibration of the spectrometric system according the procedure [13].

For beta emitters monitoring, HiSafe 3 cocktail and the model Wallac 1409 Rackbeta are used. The uncertainties values of measurements calculated according to the

recommendations [14-15]. Detection limits (LLD) in terms of concentration minimum detectable, with a significance level of 0.05, calculated in correspondence with [10].

The traceability of samples and effluents settled down using a unique identification number for tank and the samples in the records [1] and [9]. On the other hand, for carrying out the analysis two samples with identical geometry taken from the tank, after the liquid homogenized using a proper system [4], and measured. For accepting the results of gamma activity concentration determined in both duplicated samples, requirements of established internal quality control have to be fulfilled [16-17].

Data from effluents measurements are compared with the values of unconditional clearance levels (UCL) established by Regulatory Body [2]. These values are the same for clearance and discharges limits.

The dose criterion used to derive clearance levels limits based on the Schedule I of the Basic Safety Standard (BSS) [20] of the International Atomic Energy Agency (IAEA), the use of which agreed upon by the Cuban Regulatory Authority.

This means the primary radiological basis for establishing activity concentration for radionuclides of man-made origin is that the effective doses to individuals should be of the order of 0.01 mSv or less in a year. Either the collective effective dose committed by year of performance of the discharge is no more than about 1 man-Sv or an assessment for the optimization of protection shows that clearance is the optimum option. This approach is consistent with that used in establishing the exemption levels for small amount of solid material [20].

For effluents, it has been necessary in sometimes apply dilution with clean water for reduce ^{90}Sr concentration. In all cases, we use the recommended liquid discharges pH values [7].

Handling activity by year for ^{131}I and ^{32}P calculated and compared with their respective total activity in liquid effluents. This allows determining the release fraction for both of them.

For the analysis of relationship between the annual handling activity of ^{131}I (A) and its total activity by year in the liquid effluents (AE), the correlation factor (r) is calculated bearing in mind the studied period. Besides using the software [21] the time series plot obtained.

3 RESULTS AND DISCUSSION

Results from monitoring of liquid effluents show the presence of ^{131}I , ^{90}Sr , ^{32}P , ^{125}I ^{99}Mo and ^{137}Cs . The four first radionuclides have indeed the greatest influence on the management of these effluents. This seen in the Figs. 1 and 2, where there is a prevalence of deviations between maximum and mean activity concentrations for ^{131}I , ^{32}P and ^{90}Sr and their UCL. The established UCL are $6.23\text{E}+01 \text{ Bq L}^{-1}$ and $1\text{E}+07 \text{ Bq y}^{-1}$ (^{131}I), $5.71\text{E}+02 \text{ Bq L}^{-1}$ and $1\text{E}+06 \text{ Bq y}^{-1}$ (^{32}P) and $4.89\text{E}+01 \text{ Bq L}^{-1}$ and $1\text{E}+06 \text{ Bq y}^{-1}$ (^{90}Sr) [2].

The use of UCL indicates the necessity of a specific prospective dose assessment where the concept of the representative person should be used [19] and implies an increasing of management costs.

The mean monitoring frequency is 13 days and the averaged released volume is 2 m^3 . The uncertainty obtained is about 10%. LLD for ^{131}I is 9 Bq L^{-1} and for ^{32}P is $2\text{E}+02 \text{ Bq L}^{-1}$. These values are determined with a 95% of confidence.

Chemical control of the waters reflects an averaged value of pH equal to 7; for this reason its

readjustment was not required [7].

In the Table 1 the annual handling activity and total activity for ¹³¹I by year in the effluents are presented. The percentage of effluents retained for the reduction of the source term shown.

Preliminarily, the 50% of annual effluents' volume considered as radwaste [18]. As can be seen in Table 1, there is an important reduction of generation of liquid radwastes in 2001, 2007 and 2011 and the mean value is 61.1%. Training of the staff allows obtaining this purpose. Nevertheless, additional measures implemented for decreasing the effluent generation. For instance, the close of water supply when handling radioactive materials operations are finished.

Handling activity and total activity in liquid effluents by year reflected in Table 1 (¹³¹I) and Table 2 (³²P) show the mean value of release fraction for the first is about 8.54E-07 and for the second is around 1.87E-05. Despite the higher volatility of ¹³¹I, this is an evidence of the very contaminant characteristic of Orthophosphoric Acid with ³²P, which is the radioisotopic matter for Sodium Phosphate production. A high frequency of the staff's contamination with ³²P registered and influenced this result, but the production has only two activities by month due to demand is lesser than ¹³¹I.

The correlation factor (r) obtained between A and AE for ¹³¹I, is 0.12 and this low correlation value does not mean that no relationship exists; merely that no linear relationship exists. The time series show a great variability of data. Certainly, this allows affirming that A has not relationship with AE. The total volume of liquid release is 680 m³, covering the period of 1998-2015. In the Table 3 is presented the mean activity concentration for ¹³¹I by discharge and annual release rates of this radionuclide. Certainly, these magnitudes maintained far below of UCL.

Figure 1: Averaged annual activity concentration of ¹³¹I (MAC) in the liquid effluents vs. unconditional level (UCL).

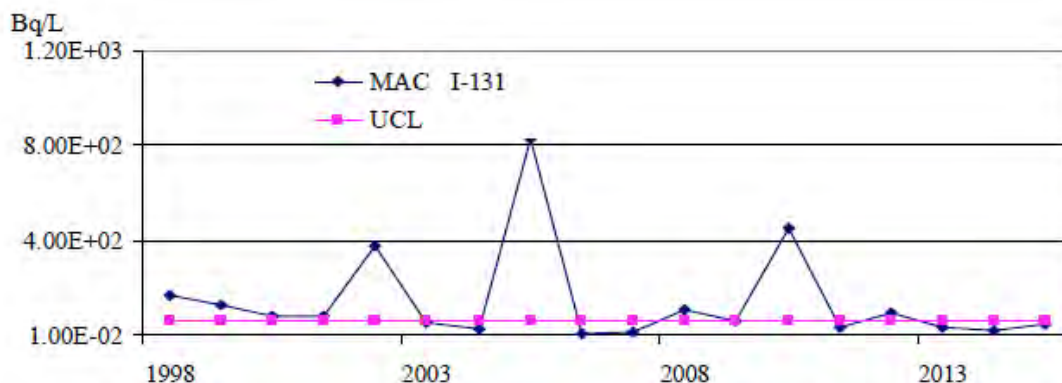


Figure 2: Maximum activity concentration radionuclides measured in liquid effluents vs. unconditional levels (UCL) for ³²P and ⁹⁰Sr.

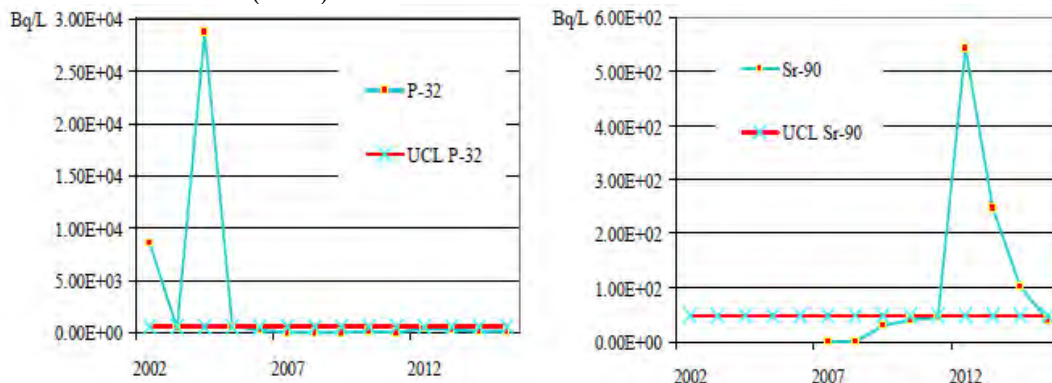


Table 1: Handling activity and total activity in the effluents for ^{131}I and the percentage of these treated as radwastes.

Year	Handling activity of ^{131}I (Bq y ⁻¹)	Total activity of ^{131}I in the effluents (Bq y ⁻¹)	Release fraction	Volume of liquid effluents (m ³ y ⁻¹)	Effluents treated as radwaste (%)
1998	4,90E+12	5.68E+06	1.16E-06	38.0	65.0
1999	4,87E+12	9.79E+06	2.01E-06	73.3	81.3
2000	4,84E+12	2.45E+06	2.38E-05	30.0	46.7
2001	4.88E+12	3.04E+06	3.05E-05	38.0	21.1
2002	4.60E+12	9.75E+06	1.25E-04	26.0	55.6
2003	3.94E+12	1.23E+06	1.50E-05	22.0	100.0
2004	4.71E+12	1.34E+06	1.19E-05	27.8	95.5
2005	4.08E+12	2.65E+07	2.92E-04	32.0	87.5
2006	3.28E+12	1.00E+05	1.39E-06	22.0	88.9
2007	4.91E+12	4.60E+05	4.42E-06	36.0	28.6
2008	4.33E+12	3.38E+06	3.72E-05	36.0	31.3
2009	5.76E+12	1.01E+06	1.75E-07	16.0	62.5
2010	7.09E+12	3.66E+06	5.16E-07	18.0	60.0
2011	1.05E+13	1.15E+06	1.10E-07	48.0	12.5
2012	1.54E+13	8.71E+05	5.65E-08	120.0	83.3
2013	1.86E+13	4.60E+05	2.47E-08	37.0	71.4
2014	2.13E+13	6.32E+05	2.97E-08	34.0	63.2
2015	2.02E+13	1.04E+06	5.14E-08	26.0	45.5

Table 2: Handling activity and total activity in the effluents for ^{32}P .

Year	Handling activity of ^{32}P (Bq y ⁻¹)	Total activity of ^{32}P in effluents (Bq y ⁻¹)	Release fraction
2002	2.35E+11	2.90E+07	1.23E-04
2003	2.35E+11	1.01E+07	4.30E-05
2004	1.93E+11	4.29E+07	2.23E-04
2005	9.75E+10	6.23E+06	6.39E-05
2006	5.45E+10	1.90E+06	3.48E-05
2010	1.51E+10	1.20E+06	7.95E-05
2011	1.30E+10	1.03E+06	7.95E-05
2012	1.68E+11	1.90E+06	1.13E-05

2013	2.65E+11	2.81E+06	1.06E-05
2014	1.16E+11	2.45E+06	2.12E-05
2015	1.58E+11	6.46E+05	4.08E-06

Figure 3: Time series plot of annual handling activity and annual activity in liquid effluents for ^{131}I .

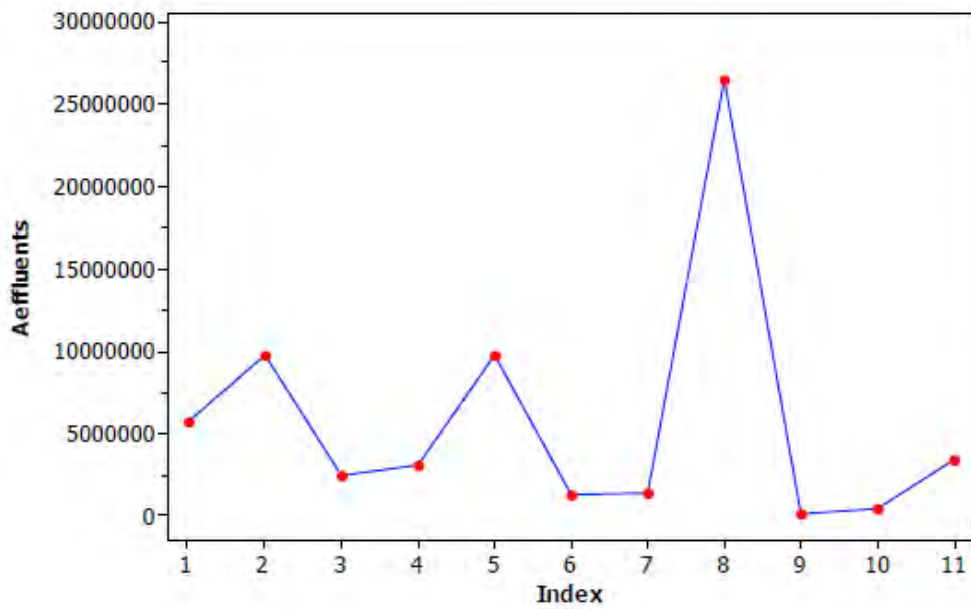
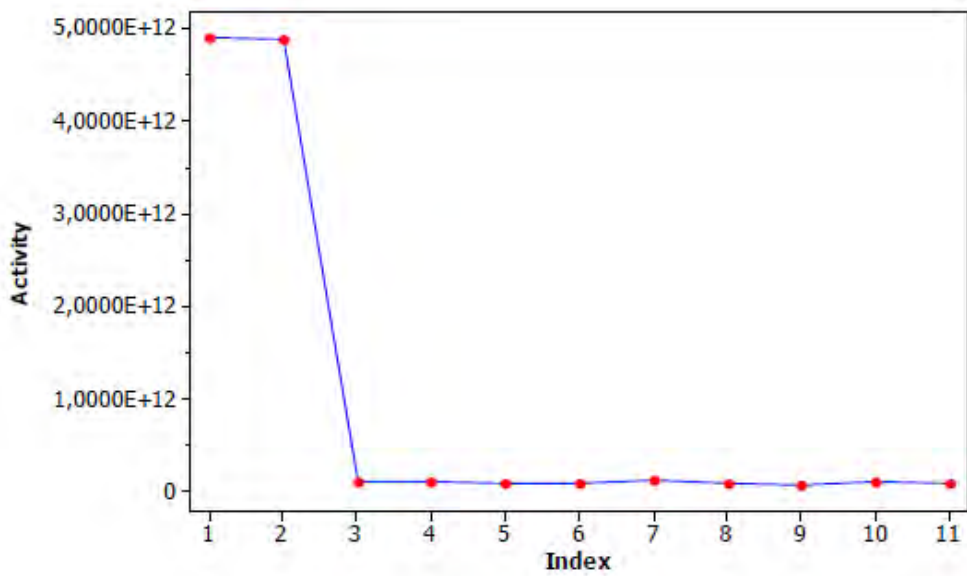


Table 3: Mean activity concentration and annual release rate of ^{131}I in liquid discharges

Year	Mean activity concentration of ^{131}I by discharge (Bq L^{-1})	Annual release rate of ^{131}I (Bq y^{-1})
1998	2.71E+01	1.04E+06
1999	1.49E+01	1.05E+06
2000	2.71E+01	8.12E+05
2001	1.77E+01	6.73E+05
2002	2.63E+01	6.84E+05
2003	4.42E-01	9.73E+03
2004	5.53E-01	3.38E+04
2005	2.18E+00	6.96E+04
2006	8.97E-01	1.61E+04
2007	3.83E+00	1.37E+05
2008	6.16E+00	2.07E+05
2009	2.50E+01	4.01E+05
2010	9.78E-01	7.96E+03
2011	1.34E+01	5.08E+05
2012	2.91E+01	7.01E+04
2013	1.64E+01	2.20E+00
2014	1.28E+01	5.20E+05
2015	2.36E+01	5.52E-01

4 CONCLUSIONS

Main operating findings from liquid effluents management in CENTIS show the radiological surveillance established and maintained complies with applicable international regulations. It is possible to detect deviations of the safety procedures and good practices in the same day of measurement of effluents and the training of personnel can have a significant effect on reducing these deviations. Nevertheless, it is necessary implementing some simple measures lead decreasing of generation of these waters.

The biggest release fraction to liquid effluents registered belongs to ^{90}Sr and this implies the necessity of reducing the frequency of the contaminations and improves the labelling procedures. Statistics allow state there is no relationship between the handling activity of ^{131}I and its total activity in liquid effluents by year. The Cuban Regulatory Body has set the same limits for clearance and discharges. These are indeed very conservatives. Clearance and discharges have not only the same limits but also the same conditions for proof of compliance. The results presented in this paper are therefore useful for clearance processes in other cases. The deriving clearance levels from specific prospective dose assessment for CENTIS is the key

step for application of the most appropriate system of protection, utilizing both compliance with quantitative constraints and optimization of protection.

5 REFERENCES

- [1] Amador Balbona, Z., Operating Manual for the Special Canalization System, CENTIS/DSR - 0533-001-0, Centre of Isotopes, Havana (1996).
- [2] International Atomic Energy Agency, Storage Tanks for Liquid Radioactive Wastes: Their Design and Uses, IAEA, Safety Guide No WS-G-2.3, Vienna (2000).
- [3] Cuban Nuclear Regulatory Authority, Unconditional levels for Clearance Radioactive Wastes, Resolution No. 1/2004, Havana (2004).
- [4] International Atomic Energy Agency, Storage Tanks for Liquid Radioactive Wastes: Their Design and Uses, IAEA, Technical Reports Series No. 135, Vienna (1972).
- [5] International Standardization Organization, Water Quality - Sampling - Parts 1 and 2: Guidance on the Design of Sampling Programmes, ISO, ISO-5667-1, and Guidance on Sampling Techniques, ISO-5667-2: 1980, Geneva (1980).
- [6] American Society for Testing and Materials, Standard Practices for Sampling Water, ASTM, D 3370-82, Philadelphia (1989).
- [7] International Atomic Energy Agency, Management of Discharge of Low Level Liquid Radioactive Waste Generated in Medical, Educational, Research and Industrial Facilities, IAEA, IAEA-TECDOC-1714, Vienna (2013).
- [8] International Atomic Energy Agency, Environmental and Source Monitoring for Purposes of Radiation Protection, IAEA, Safety Guide No. RS-G-1.8, Vienna (2005).
- [9] Department of Metrology of Radionuclides, Centre of Isotopes, DMR.PNO.006, Gamma Spectrometric Analysis of Solid and Liquids Environmental Samples and Effluents of Low Level Activity, Havana (2013).
- [10] International Atomic Energy Agency, Measurement of Radionuclides in Food and the Environment, Guidebook, IAEA, Technical Reports Series No. 295, Vienna (1989).
- [11] Department of Metrology of Radionuclides, Centre of Isotopes, ATN.R.PNO.019-1. List and Certificates of Standards and Reference Materials, Havana (2013).
- [12] Oropesa, Serra, R., Gutiérrez, S., Hernández, A.T., A Procedure for the Standardization of Gamma Reference Sources for Quality Assurance in Activity Measurements of Radiopharmaceuticals". *Appl. Radiat. Isot.* Vol.56/6, 787, (2002).
- [13] Department of Metrology of Radionuclides, Centre of Isotopes, DMR.PNO.002. Procedure for the Calibration of Gamma Spectrometric Installation Based on HPGe Detectors, Havana, 2014.
- [14] International Standardization Organization, Guide to the Expression of Uncertainty in Measurement, First Edition, ISO, ISO/TAG4/WG3, (1992).
- [15] EUROCHEM/CITAC (2000), Guide of Quantifying Uncertainty in Analytical Measurement. Eurachem, Second Edition, (2000).
- [16] International Standardization Organization, Harmonized Guidelines For Internal Quality Control in Analytical Chemistry Laboratories, ISO, ISO/REMCO N0 271 Rev., (1994).
- [17] Department of Metrology of Radionuclides, Centre of Isotopes, Procedure for the Internal Control of the Quality, ATN.PNO.007, (2000).
- [18] Gatti, A.M., Pérez, S., Preliminary Safety Report for the Centre of Isotopes, Doc. 0711-5301-OIA/OP-001-1a, INVAP S.E., Argentina, Bariloche (1989).
- [19] International Commission on Radiological Protection, Assessing Dose of the Representative Person for the Purpose of Radiation Protection of the Public, ICRP Publication 101, Part 1, (2006).
- [20] European Commission, Food and Agriculture Organization of The United Nations, International Atomic Energy Agency, International Labour Organization, OECD Nuclear Energy Agency, Pan American Health Organization, United Nations Environment Programme, World Health Organization, Radiation Protection and Safety of Radiation Sources: International Basic Safety Standards, General Safety Requirements, IAEA Safety Standards Series No, GSR Part 3, Vienna (2014).
- [21] Statistical Graphics Corporation, Statistical Software STATGRAPHICS Plus for Windows 5.1, 2000.

Findings of the control and monitoring of airborne releases from the Centre of Isotopes of Cuba

Zayda Haydeé Amador Balbona*, Miguel Antonio Soria Guevara

Centre of Isotopes, Ave. Monumental y carretera La Rada, Km 3_{1/2}, San José de Las Lajas, Mayabeque, Cuba.

Abstract. The handling of unsealed radioactive sources in the Centre of Isotopes of Cuba leads to airborne releases, which are under radiological surveillance to comply with the authorized limits of the Regulatory Body. This paper summarizes the findings in control and monitoring of these airborne discharges, covering the period of 2001-2015. The characteristic of process allow use a differed measurement method with HEPA and charcoal filters and isokinetic conditions in duct, taken into account the ISO 2889. A radiometer Berthold LB 2040 with a Geiger Müller detector is used for measurement activity concentrations of ¹³¹I, the radionuclide of the highest contribution to the public exposure. The behavior of total activity handled and airborne discharges are analyzed to look for a correlation between theses. A prospective dose assessment for these discharges is used to characterize the annual radiological impact to public. It is not identified relationship between activity and releases. The human factor is a key in the release fraction because the time of dosage and seal of vials, due to developed abilities. The MIBG process mainly contributes to the ¹³¹I releases since there is heating and dryness of the solution, but has lower frequency than production of NaI (¹³¹I). Results obtained show a good agreement with the dose constrains for public.

1 INTRODUCTION

The Centre of Isotopes (CENTIS) of the Republic of Cuba is located about 30 Km to the southeast of Havana city. During handling unsealed radioactive sources, are sampled the airborne discharges. In this paper, are summarized findings covering 14 years of their control and monitoring in accomplishment to the applicable regulations [1].

2 MATERIALS AND METHODS

For control and monitoring of airborne releases, is established a quality assurance program [2]. Requirements relating to representative samples are implemented [2]. An isokinetic sampling probe is used in the duct where is a reasonable degree of mixing in the exhaust air stream [3]. To measure the discharge rates of radionuclides, is designed source monitoring program [4]. The most volatile and frequently radionuclide used is ¹³¹I and for this reason F&J radioiodine collection cartridges (model TE2C 30x50) and 47mm glass fiber filters (FP-47) are used with a low volume air sampler (model VS 23-0523CV) from High-Quality Environmental Products Company, USA [5].

A routine exhaust air sampling and monitoring with a weekly filter exchange frequency are currently executed; using a radiometer Berthold LB 2040 with a Geiger Müller detector (model GZ-7).

The efficiency calibrations of this system are carried out with a source of ⁹⁰Sr type capsule with Aluminium as backing, from Isotopes Products Laboratories with NIST traceability. The nominal cubic flow rate from stack is 67 554 m³ h⁻¹.

The dose criterion used to derive clearance levels limits is based on [6], the use of which has been agreed upon by the Cuban Regulatory Authority [1].

*Presenting author, e-mail:zabalbona@centis.edu.cu

This means the primary radiological basis for establishing activity concentration for radionuclides of man-made origin is that the effective doses to individuals should be of the order of 0.01 mSv or less in a year. Either the collective effective dose committed by year of performance of the discharge is no more than about 1 man-Sv or an assessment for the optimization of protection shows that clearance is the optimum option. This approach is consistent with that used in establishing the exemption levels for small amount of solid material [6].

The established unconditional clearance levels (UCL) for airborne discharges of ^{131}I are $5.94\text{E}+01\text{Bq m}^{-3}$ and $1\text{E}+08\text{Bq y}^{-1}$ [1]. These values are the same for clearance and discharges limits.

The averaged activity concentration and release rate by discharge are calculated for each year. Their trends are presented and analyzed over the 8 y period from 2001 to 2008. Operations with ^{131}I in a hot cell and manufactured practices for obtaining labelled compounds in a glove box are studied.

For the analysis of relationship between the handling activity of ^{131}I by day (A) and the source term in the airborne release (ST), the correlation factor (r) is calculated bearing in mind the studied period. Besides using the software [7] are calculated standard asymmetry and kurtosis. The scatterplot is analyzed.

Preliminarily, a release fraction for radiodines was estimated as $1\text{E}-03$ in [8]. Considering our statics the release fraction distribution is determined.

The annual public exposure from airborne discharges is evaluated for the critical group and normal operation conditions considering all relevant pathways and site-specific data for CENTIS [9]. For the maximum source term is estimated an annual effective dose equal to $1\mu\text{Sv}$. The ^{131}I contribution for this exposure represents an 88.5% (belonging to $8.14\text{E}+07\text{Bq}$). The results of this study are applied in this paper, but it is assumed 100% of the dose distribution belongs to ^{131}I and 52 weeks by year. A linear relationship between annual effective dose (E) and released activity is applied in the dose assessment and plotted it.

3 RESULTS AND DISCUSSION

In the light of operating experience and as it was considered in [8], radioiodines (^{131}I and ^{125}I) have the biggest source term in airborne releases, allowing for the kind of operations with them in CENTIS. On the other hand, the first is used with biggest activity and frequency.

Table 1 lists the annual activity of ^{131}I and its maximum activity concentration by discharge and annual release rate. As can be observed in this, the maximum radioactive concentration and annual release rate of ^{131}I registered are about 30 Bq m^{-3} and $6.79\text{E}+07\text{ Bq y}^{-1}$, which are 0.5 and 0.7 times lower than their respective values of UCL.

The averaged values of activity concentration and release rate by discharge taking into account all operations with ^{131}I are shown in Table 2.

Besides the labelling of compounds has a biggest value of source term and radionuclide concentration than the practice in the hot cell. This is shown in Table 3, where data of 2008 are reflected. Only in nine occasions, this process took place in that year. The compound is concentrated by evaporation and a chemical solution is used for retention of free iodine and the discharge pass through activated charcoal filter, impregnated with triethylenediamine (TEDA).

The maximum value registered for the release fraction (RF) is $1.22\text{E}-04$ and the mean RF for the 14 y analyzed period is $4.75\text{E}-06$. The percentage contribution to RF is presented in the Table 4. As can be seen in the majority of the data, RF is about three orders lower than the estimated value ($1\text{E}-03$) in [8]. This difference is in the kind of procedure in the hot cell since radiopharmaceutical compound is not obtained from distillation, as if it firstly was projected.

On February of 2015 was necessary to change the charcoal filter of the hot cell and gloves boxes extraction. In the other hand, begging 2015 the MIBG production the contribution was eliminated.

The correlation factor (r) between A and ST obtained is 0.26. This low correlation value does not mean that no relationship exists; merely that no linear relationship exists.

The results from static's analysis are shown in the Table 5. Data for ST is bigger than cut-off level for standard asymmetry. These variables have also non-normal standard kurtosis values (out of the interval -2 to 2). This invalids tests for normally distributed populations with roughly equal variances between factor levels. On the other hand, the scatterplot of ST vs. A (Figure1) shows a great variability of data. Certainly, this allows affirm that A has not relationship with ST.

In the Figure 2 can be seen as the E distribution has values 10 times lower than individual dose constrain of $10 \mu\text{Sv y}^{-1}$. Besides, this implies for a committed collective effective dose (S) equal to 1 man-Sv y^{-1} that critical group has $1\text{E}+06$ infants. This issue is a very faraway boundary condition for CENTIS and means the deterministic approach considered requires a substitution by a specific prospective dose assessment where the concept of the representative person should be used [10].

Table 1: Annual handling activity, maximum activity concentration by discharge and annual release rate of ^{131}I in airborne releases from CENTIS.

Year	Handling activity of ^{131}I (Bq y^{-1})	Maximum activity concentration of ^{131}I by discharge (Bq m^{-3})	Annual release rate of ^{131}I (Bq y^{-1})
2001	4.88E+12	2.87E+00	1.12E+07
2002	4.60E+12	2.45E+01	6.79E+07
2003	3.94E+12	4.85E+00	1.99E+07
2004	4.71E+12	1.03E+01	6.32E+07
2005	4.08E+12	4.38E+00	4.10E+07
2006	3.28E+12	1.61E+01	2.85E+07
2007	4.91E+12	1.91E+01	6.72E+07
2008	4.33E+12	2.99E+01	2.61E+07
2009	5.76E+12	1.96E+01	3.45E+07
2010	7.09E+12	2.02E+01	3.20E+07
2011	1.05E+13	1.37E+01	3.62E+07
2012	1.54E+13	1.82E+01	4.26E+07
2013	1.86E+13	1.44E+01	6.90E+07
2014	2.13E+13	9.16E+00	3.43E+07
2015	2.02E+13	3.85E+01	3.46E+07

Table 2: Mean activity concentration and mean activity of ^{131}I by discharge.

Year	Mean activity concentration of ^{131}I (Bq m^{-3})	Mean activity of ^{131}I by discharge (Bq)
2001	5.39E+00	2.31E+05
2002	1.06E+01	5.20E+06
2003	1.27E+00	5.71E+05
2004	1.67E+01	1.35E+06
2005	7.14E+00	3.46E+06
2006	1.45E+00	6.34E+05
2007	2.66E+00	1.24E+06
2008	6.90E+00	4.66E+05
2009	2.36E+00	6.51E+05
2010	2.08E+00	5.93E+05
2011	1.61E+00	5.85E+05
2012	1.73E+00	5.46E+05
2013	1.88E+00	1.01E+06
2014	1.65E+00	4.90E+05
2015	2.27E+00	6.91E+05

Table 3: Mean activity concentration and mean activity of ^{131}I by discharge from hot cell and glove box.

Workplace	Mean activity concentration of ^{131}I (Bq m^{-3})	Mean activity of ^{131}I (Bq)
Hot cell	6.08E+00	4.54E+05
Glove box	7.73E+00	5.22E+05

Table 4: Percentage of the release fraction in the airborne discharges.

Release fraction	1.00E-04	1.00E-05	1.00E-06	1.00E-07	1.00E-08	1.00E-09
%	0.2	11.3	56.9	28.5	1.5	1.9

Table 5: Statistics for daily handling activity and release rate of ¹³¹I.

	Daily handling activity of ¹³¹ I (Bq d ⁻¹)	Daily release rate of ¹³¹ I (Bq d ⁻¹)
Frequency	235	235
Mean	9.48E10	6.54E05
Variance	1.14E21	1.49E12
Standard deviation	3.38E10	1.22E06
Minimum	1.80E09	5.11E02
Maximum	2.24E11	1.02E07
Rank	2.22E11	1.02E07
Standard asymmetry	1.10	29.51
Standard kurtosis	2.24	83.44

Figure1: Scatterplot of daily release rate vs. daily handling activity for ¹³¹I.

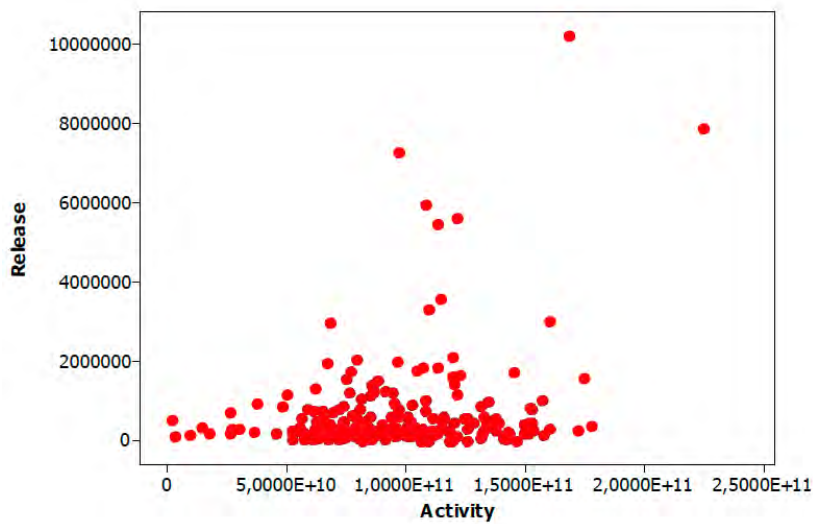
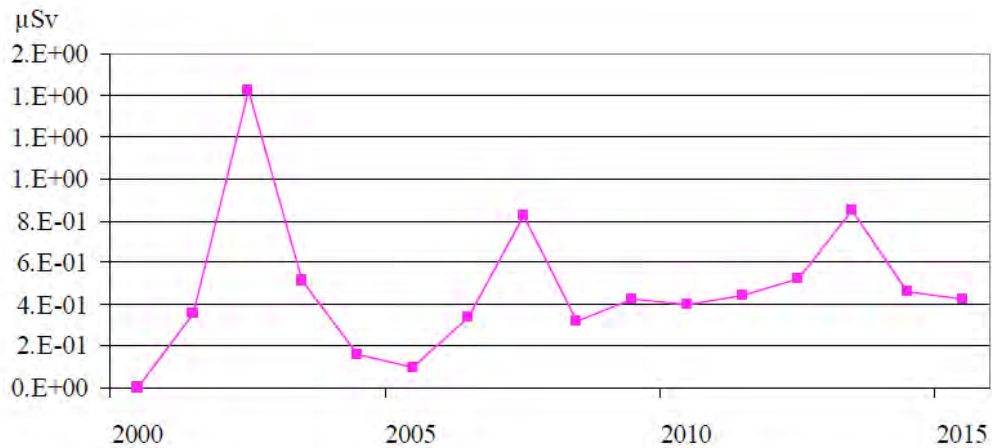


Figure 2: Plots of annual effective dose to public due to airborne releases from CENTIS



4 CONCLUSIONS

The main operating findings from airborne effluents management in CENTIS are the radiological surveillance established and maintained complies with applicable regulations and statistics allow state there is not relationship between daily handling activity of ^{131}I and its source term in the airborne release.

In the spite of low frequency of operations, the labeling of compound has a highest release fraction than the practice in the hot cell due to the concentration by evaporation. The release fraction is in the 57% of the discharges about $1\text{E}-06$, which is three orders lower than the projected value.

The Cuban Regulatory Authority has set the same limits for clearance and discharges. This is indeed very conservative. Clearance and discharges have not only the same limits but also the same conditions for proof of compliance.

The results presented in this paper are therefore useful for clearance processes in other cases. The deriving clearance levels from specific prospective dose assessment for CENTIS is the key step for application of the most appropriate system of protection, utilizing both compliance with quantitative constrains and optimization of protection.

5 REFERENCES

- [1] Cuban Nuclear Regulatory Authority, Unconditional levels for Clearance Radioactive Wastes, Resolution No. 1/2004, Havana (2004).
- [2] International Atomic Energy Agency, Regulatory Control of Radioactive Discharges to the Environment, Safety Guide No. WS-G-2.3, Vienna (2000).
- [3] International Standardization Organization, General principles for sampling airborne radioactive materials, ISO 2889, Geneva (1975).
- [4] International Atomic Energy Agency, Environmental and Source Monitoring for Purposes of Radiation Protection, IAEA, Safety Guide No. RS-G-1.8, Vienna (2005).
- [5] Department of Radiation Protection, Centre of Isotopes, Procedure for Monitoring Airborne Releases, DSR.PNO.032, Havana (2015).
- [6] European Commission, Food and Agriculture Organization of The United Nations, International Atomic Energy Agency, International Labour Organization, OECD Nuclear Energy Agency, Pan American Health Organization, United Nations Environment Programme, World Health Organization, Radiation Protection and Safety of Radiation Sources: International Basic Safety Standards, General Safety Requirements, IAEA Safety Standards Series No, GSR Part 3, Vienna (2014).
- [7] Statistical Graphics Corporation, Statistical Software STATGRAPHICS Plus for Windows 5.1 (2000).
- [8] Gatti, A.M., Pérez, S., Preliminary Safety Report for the Centre of Isotopes, Doc. 0711-5301- OIA/OP-001-1a, INVAP S.E., Argentina, Bariloche (1989).
- [9] Centre of Isotopes, Radiation Protection Department, Final Safety Report, CENTIS/DSR-144-001-C, Havana (2006).
- [10] INTERNATIONAL COMMISSION ON RADIOLOGICAL PROTECTION, Assessing Dose of the Representative Person for the Purpose of Radiation Protection of the Public, ICRP Publication 101, Part 1 (2006).

Radiation Ecology and Human Health. Regional and Global Problems

Z.Paskalev^a, G.Vassilev^a, V.Baduline^a, D.Apostolova^b

^aNational Center of Radiobiology and Radiation Protection – Sofia – Bulgaria

^bMedical University. Clinic of Occupational Diseases – Sofia – Bulgaria

1 INTRODUCTION

Radiation ecology is a multidisciplinary science that uses nuclear physics, chemistry, biology, toxicology, ecology and risk analyses to predict the effects of radioactive contaminants on humans and the environment. Radiation ecology deals with a continuum that starts with radioactive releases from a source term, continues through the dispersal and retention of the contaminants by environmental migration, and only with the determination of dose and health risks to exposed humans or other biota.

2 AIM OF THE STUDY

The this studies involve exposure to radiation of different types sources of ionizing radiation and to ingested radioactivity in organisms and assessment the radiation risk for humans and environmental biota- plants and animals.

3 MATERIALS AND METHODS

Radiation dose is radiation energy deposited in the irradiated object (human body or non-human biota) per unit mass of tissue. Exposure to ionizing radiation is measured in terms of absorbed energy – absorbed dose. The unit of absorbed dose is the gray (Gy), which is a joule per kilogram. The Sievert (Sv) is a unit of dose equivalent which takes into account the fact same absorbed dose, there is a difference in the efficiency of different type of radiation (neutrons, beta-particles, alpha-particles, gamma-rays, X-rays) to cause damage in irradiated organisms or tissues. The dose Sievert is equal to the absorbed dose in Gray multiplied by a radiation weighing factor Q. For neutrons Q = 20, for alpha-particle Q = 10, beta-particle Q=1,0, gamma-rays Q=1,0. Effective dose is equal to the equivalent dose in sivert multiplied by a tissue weighing factor.

Risk is probability of injury, diseases, or death under specific circumstances. Absolute risk is the excess risk attributed to irradiation and usually expressed as the numeric difference between irradiated and non-irradiated population (e.g.e case of cancer per million people irradiated annually for each Sv). Relative risk is the ratio between the number of cancer cases in the irradiated population to the number of cases expected in the unexposed population. The health risks from small amounts of radiation, if any, are very low in comparison with other health risk.

The aim of the Radiation and Environmental Health Program is to look for solutions to protect human health and biota from ionizing radiation hazards.

4 RESULTS

The fallout in Bulgaria of radionuclide from nuclear weapons test during the 1960-1963 has transferred to humans through different ecological pathways. Concentration (Bq/kg) of natural radionuclide (K-40, U-238, Ra-226, Th-232) in Bulgarian soils are: for K-40 is 80-800 Bq/kg, for U-238 is 8-190 Bq/kg, for Ra-226 is 12-210 Bq/kg, and for Th-232 is 7-160 Bq/kg. In region around uranium mines the annual doses were measured (Table 3)

Absorbed dose-rate D (nGy/h) in atmosphere air from earth gamma radiation in Bulgaria is min 50 nGy/h, max 110 nGy/h, average $70 \pm 21,4$ nGy/h. Mean individual effective dose per one year from natural exposure all sources in Bulgaria is 2,33 mSv per one year.

The annual average dose release of noble radioactive gas from Kozloduy NPP was 251769 GBq (0,96% of the norm); the total long lived beta aerosols released in the atmospheric air were 1186 MBq (0,14% of the norm), and the total emission of I-131 was 3260 MBq (0,62% of the norm).

The results of the analysis show that the total effective doses (from internal and external gamma-beta exposure) obtained by the population around the Kozloduy NPP were very small- 0,15% to natural background.

Heightened interests in the effects of radiation on human and environment biota is occurring because of the Chernobyl accident in April 1986, and an international interest in developing regulations that specifically protect non-human biota.

The concentrations (mBq/L) of Cs-137 and Sr-90 in water in river Danube for the years 1972-2000 are: in years 1972-1974 before starting the Kozloduy NPP for Cs-137 is $4,0 \pm 1,2$ mBq/L, for Sr-90 is $12,0 \pm 2,0$ mBq/L. For years 1975-1985 (before the Chernobyl accident): for Cs-137 is $3,2 \pm 1,8$ mBq/L, for Sr-90 is $10,0 \pm 2,0$ mBq/L. Concerning years 1988-2000 (after the Chernobyl accident): for Cs-137 is $2,8 \pm 0,7$ mBq/L, for Sr-90 is $6,2 \pm 1,8$ mBq/L.

The latter is a shift in the longstanding paradigm that if humans are adequately protected from ionizing radiation then so are all other biota, and that specific regulations for environment biota are not needed. The ICRP, the IAEA, U.S.DOE, and several National Organization in various countries, are proposing new approaches for specifically determining radiological risk to exposed biota.

5 DISCUSSION

Health risk for humans arising from low doses of ionizing radiation. Lively debate continues on the nature of the dose-response relationship for the excess risk following to ionizing radiation at low doses or low dose rates. In toxicology, hormesis is a dose response phenomenon characterized by a low dose stimulation. Risk of cancer from 1 mSv of radiation is 1 in 77000.

Amphibians are an interesting model for examining radiation exposure to biota. The incidence rates of degenerative diseases that take years or decades to develop (e.g. cancer and heart disease) are beginning to show the effects of increases in industrial poison, air pollution, use ionizing radiation in medicine and industry, nuclear reactor incidents, and behavioral changes such as exercise, diet, or the use of more drugs or radio - protectors or influencing human activity. The risk from contact with dangerous chemicals and radionuclides in soil, water, air our workplaces, and our homes are possible for health effects and cancer.

6 CONCLUSION

The outcome within a generation for this environmental quality objective should include the following:

- Radiation doses will be limited as far as reasonably possible.
- The maximum public radiation exposure (absorbed dose) due to human activities will not exceed 1 mSv per person per year.
- Serious incidents and accidents in nuclear installations will be prevented. The spread of radioactive substances is prevented or limited where accidents never occur.
- Environmental concentration of radioactive substances emitted from all human activities will be so low as not to represent a threat to human additional individual dose to men less of the public will be lower than 0,01 mSv per person per year from each individual operation.
- The radiological sciences have developed to where probabilistic risk factors can now be applied that predict specific deleterious effects to humans per unit dose. And yet, these same radiological sciences that have made such advances in human dosimetry primitive when effects to biota are concerned.

Potassium-40 determination in NPK fertilizer by CZT-500s gamma spectrometry in the LPNPE Lab

A. Justinien Franck Ratovonjanahary ^{a*}, Hery Tiana Rakotondramanana ^b, Haritiana L. Ralaiarisoa^a, H. Léonce Randria-Mampianina^a, Solofonirina D. Ravelomanantsoa^a

^aLaboratoire de Physique Nucléaire et Physique de l'Environnement (LPNPE), Madagascar

^bDepartment of physics, University of Antananarivo, Madagascar

Abstract. The isotope 40 of Potassium (⁴⁰K) is determined in NPK fertilizer by gamma spectrometry in the LPNPE Lab. For radioactive nuclide identification, the gamma spectrometry method with a CZT-500s detector is utilized and ¹³⁷Cs coupled with ¹³¹I sources are used for energy calibration. The ⁴⁰K identification is carried out by sampling of 500ml in a marinelli type beaker and based on the photopeak of 1460.8 keV. The environmental background is suppressed by applying shielding technique. The shielding is made of 8cm thick walls of lead and reduces the natural background of around 20 times. The peak position of ⁴⁰K has been precisely determined on the energy regions from 50keV to 2120keV.

KEYWORDS: ⁴⁰K; gamma spectrometry; CZT-500s.

1 INTRODUCTION

Mineral and natural resources usually contains long half-life natural radioactive nuclides (such as ²³⁸U, ²³²Th and ⁴⁰K) and had been greatly exploited for different utilizations.

In the LPNPE Lab, ⁴⁰K is determined in NPK fertilizer by gamma spectrometry. The objectives are firstly to calibrate the multichannel analyzer and secondly use it to acquire gamma-ray spectra, and to locate primary photopeaks. The spectra are measured using the CZT-500s detector coupled with the MCA-166 and lead shielding method is applied for background subtraction. Indeed, many users of gamma spectrometer are concerned with measuring low levels of radioactivity such as found in routine environmental samples. For these, the background should be as low as possible to provide lower detection limit. In the present work, a successful approach for this study is to suppress the Background by Special Detector Shielding Materials (Lead).

The ⁴⁰K determination in NPK fertilizer by CZT-500s gamma spectrometry is one method for a preliminary analysis of environmental minerals in the LPNPE Lab.

2 ENERGY CALIBRATION

The energy calibration converts the x-axis (Channel) number into energy expressed in keV. Many formula exist for energy calibration but in the present work the linear formula have been taken: $E(\text{keV})=a(\text{keV/Ch})\cdot\text{channel} + b(\text{keV})$.

As the available sources at the LPNPE Lab are only I-131 and Cs-137, the energy calibration method is based on these sources' spectra.

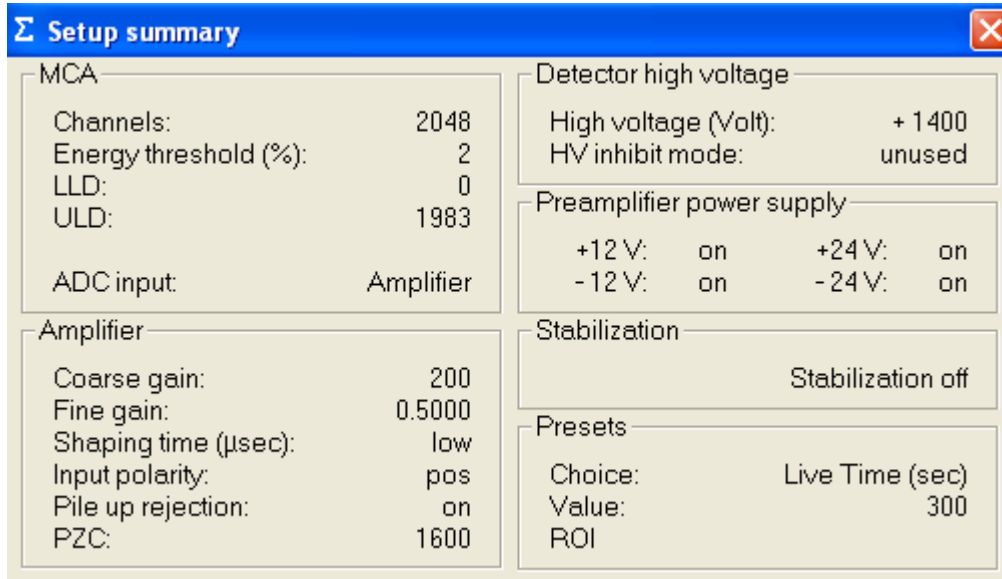
As reference for gamma energy emission, the data from the report of the French atomic energy commission "*Commissariat à l'Énergie Atomique*" (CEA) year 2008 (CEA-R-6201) have been taken. From this document, the most important gamma energies emitted by these two elements are listed below:

Cs-137:	661.657keV, emission percentage: 84.99%.
I-131:	284.305keV, emission percentage: 6.06%
	364.489keV, emission percentage: 81.2%
	636.989keV, emission percentage: 7.26%

*Presenting author, e-mail:francksylea@yahoo.fr

The following figure shows the setup relating to the energy full range of about 2MeV (energy regions from 50keV to 2120keV). 2MeV is chosen in order to be able to localise the 1.46MeV peak of 40K in a spectrum. Five spectra series are measured for each source and mean values are used for energy calibration.

Figure 1: Setup summary for energy calibration



Five spectra of I-131 are measured and the mean values as well as the standard deviations of peak centroid positions are shown in the following table.

Table 1: Identification of I-131 peaks positions for energy calibration.

	channel centroid ROI=248-278	channel centroid ROI=296-350	channel centroid ROI=586-604
Mean values	265.1	339.4	593.9
Standard deviation	0.4	0.2	0.5

The same spectra measurement process for Cs-137: Five spectra are measured and the mean values as well as the standard deviations of peak centroid positions are shown in the table below.

Table 2: Identification of Cs-137 peaks positions for energy calibration.

	channel centroid ROI=584-634
Mean values	616.6
Standard deviation	0.6

The linear fitting curve coefficients a and b as well as the R^2 (a measure of how well the fit function follows the trend in the data.) are obtained by least squares fit method (a small program written and performed at LPNPE Lab is used) and using the mean values of peak centroid positions as follows:

I-131: 284.305keV / 265.1 Ch
 364.489keV / 339.4 Ch
 636.989keV / 593.9 Ch

Cs-137: 661.657keV / 616.6 Ch

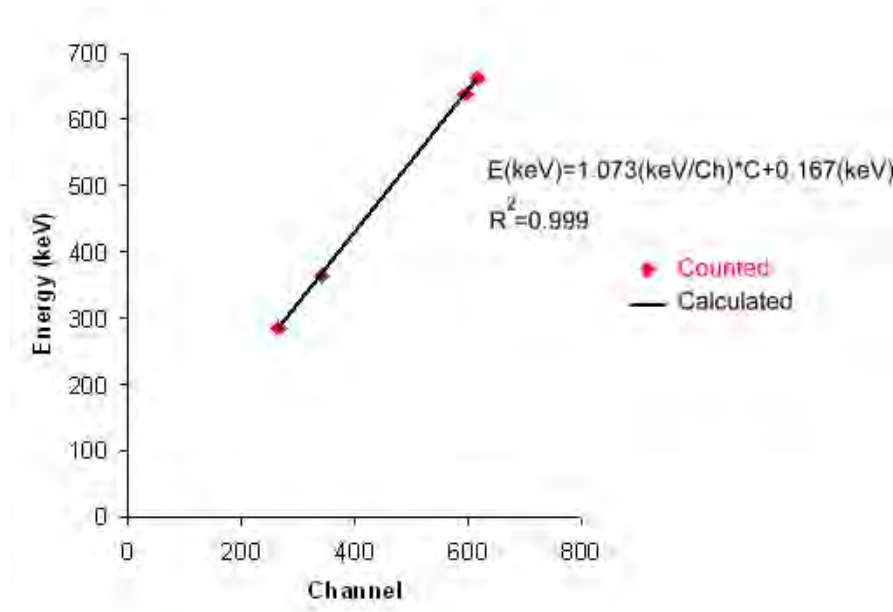
This gives:
 $a = 1.073\text{keV/Ch}$

$$b = 0.167 \text{ keV}$$

$$R^2 = 0.999$$

$R^2 \approx 1$ means that the fit function follows the trend of the data. The energy calibration curve is shown in the following figure.

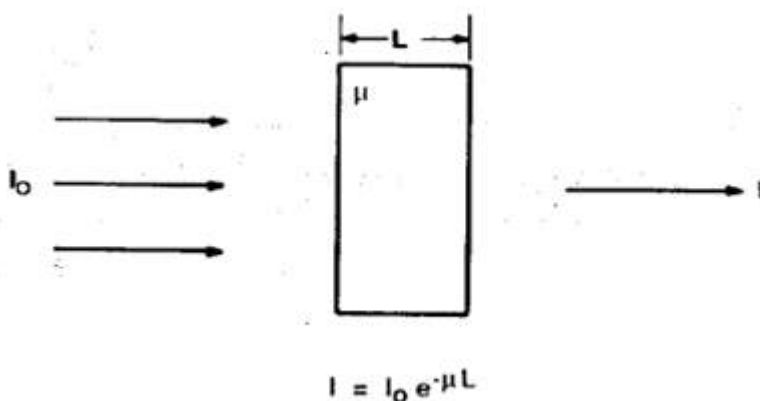
Figure 2: Energy calibration curve



3 LEAD SHIELDING FOR BACKGROUND SUBTRACTION

When gamma radiation of intensity I_0 is incident on an absorber of thickness L , the emerging intensity I transmitted by the absorber is given by the exponential expression $I = I_0 e^{-\mu L}$ where μ is the attenuation coefficient (expressed in mm^{-1}).

Figure 3: The fundamental law of gamma ray attenuation. The transmitted gamma ray intensity I is a function of gamma ray energy, absorber composition, and absorber thickness.



Gamma-ray shielding materials should be of high density and high atomic number so that they have a high total linear attenuation coefficient and a high photoelectric absorption probability. The most common shielding material is lead because it is readily available, has a density of 11.35 g/cm^3 and an atomic number of 82, and is relatively inexpensive. Lead can be moulded into many shapes.

In the LPNPE Lab, lead shielding is conceived and fabricated (Figure 4).

The optimal wall thickness is pre-determined by using the ^{137}Cs source and different thickness of lead (0mm, 5mm, 10mm and 15mm thickness) which are placed between the source and the detector. The attenuation coefficient μ (expressed in mm^{-1}) is determined by the exponential expression $I=I_0e^{-\mu L}$ and from which the optimal wall thickness is calculated.

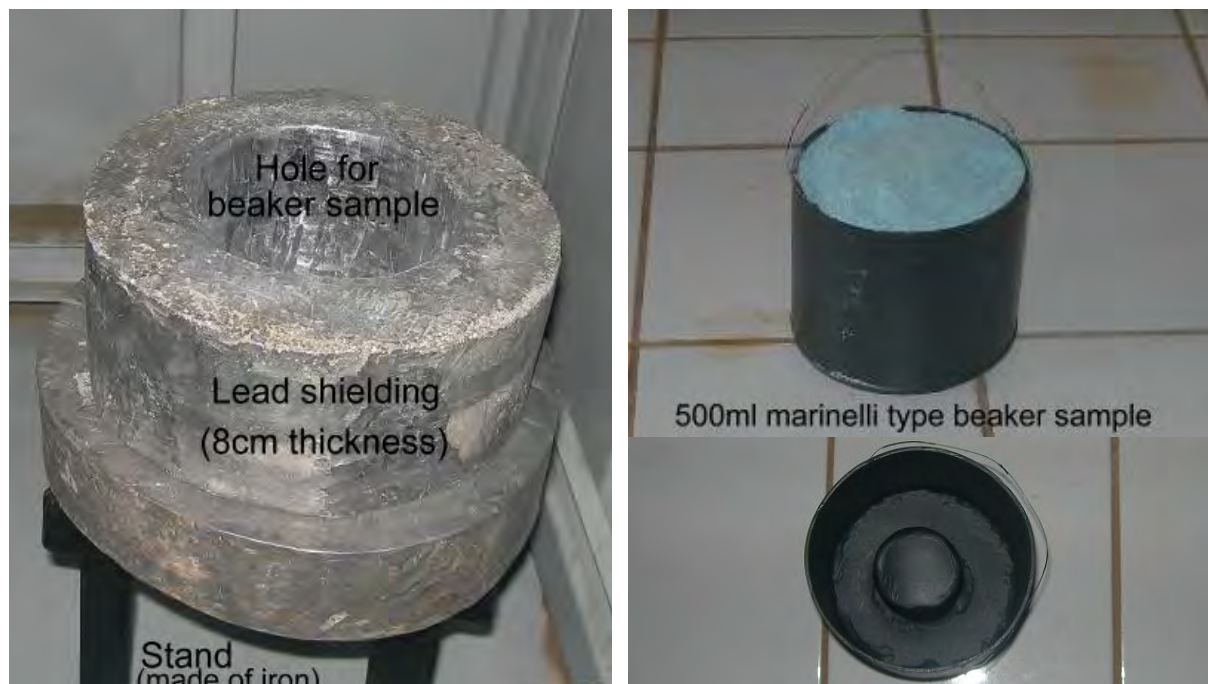
The calculation gives:

$$\mu=(0.08\pm 0.01)\text{mm}^{-1}$$

$$L_{1/10}=(2.8\pm 0.1)\text{cm} \text{ (thickness of absorber with 10\% transmission).}$$

A lead wall of 8cm thickness is fabricated. This reduces the natural background of around 20 times (of course depending on the energy of photons of gamma radiation) which is optimal for most analysis conducted in the LPNPE gamma spectrometry.

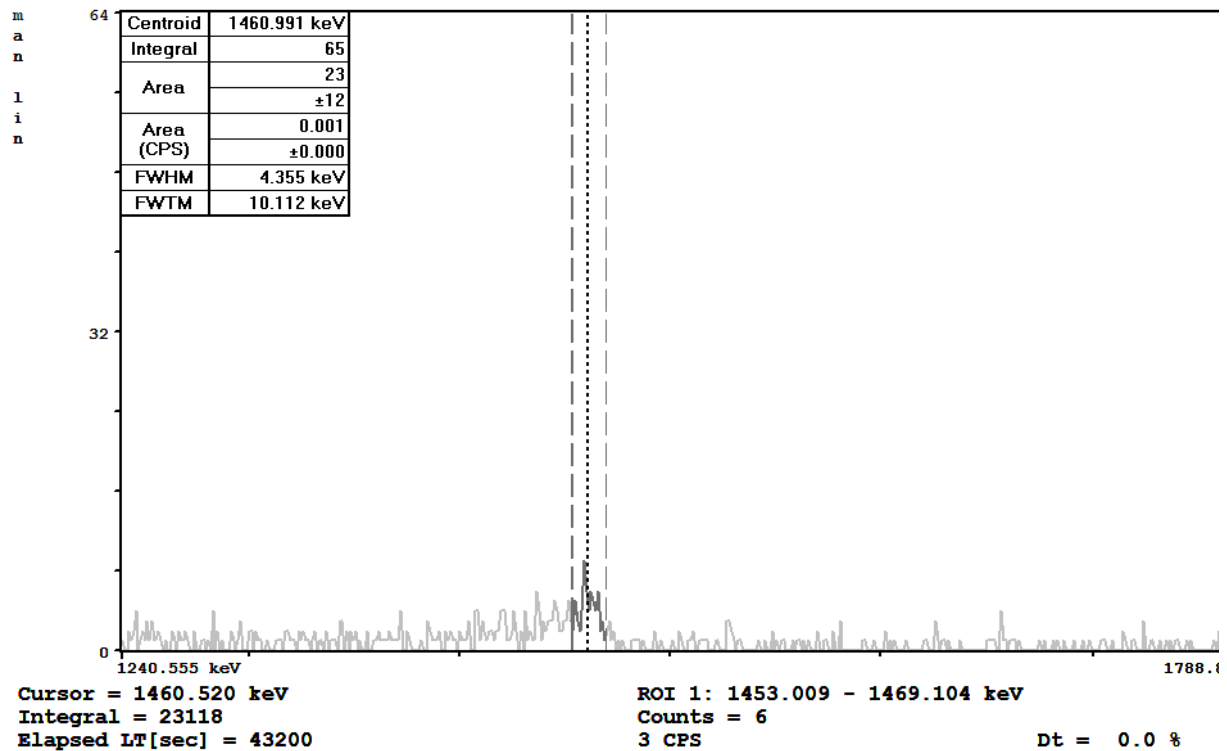
Figure 4: Lead shielding and marinelli type beaker sample



For sample measurement, the 500ml marinelli type beaker full of sample is put in the hole for beaker sample and the detector is introduced from the bottom of the lead shielding. A 2cm thickness lead cover is afterwards put on top of the beaker.

4 K-40 DETERMINATION

Data is collected for twelve hours (43200sec) because the amount of ^{40}K in the sample is relatively small. NPK fertilizer's sampling of 500ml has been performed. Five measurements are performed with the setup parameters which is the same as the one for energy calibration (*Fig.1*) except on data collection time (43200sec instead of 300sec). The following figure shows one calibrated spectrum of these series of measurements.

Figure 5: The 1460.8keV peak of ^{40}K in a NPK fertilizer spectrum

5 INTERPRETATION

All data for radionuclide determination are analyzed in the region between 1453.009keV and 1469.104keV, which encompasses the peak of gamma radiation from ^{40}K . The mean value and standard deviation of peak positions from the five spectra give the peak energy of $(1460\pm 1)\text{keV}$ which includes 1460.8keV.

The channel containing the peak centroid is used by the software WinSPECi to determine the curve for keV/channel (energy calibration). Calibration result: 1361CH \rightarrow 1460.52keV

The *Figure 5* shows one example of ^{40}K peak position: the 1460.52keV peak where the cursor is placed.

6 CONCLUSION

The gamma spectrometry method used in the measurement was found to be fairly good to detect the presence of ^{40}K in the NPK fertilizer sample. Indeed, the precision of the energy calibration method is found to be good with the R^2 value quite equal to 1 and the calculated peak energy of $(1460\pm 1)\text{keV}$ indicate that the precision of the measurement is still within the satisfactory level.

The environmental background is suppressed by applying shielding technique. The shielding is made of 8cm thick walls of lead and reduces the natural background of around 20 times which is optimal for most analysis conducted in the LPNPE gamma spectrometry.

Counting time of 12 hours (43200sec) is found to be sufficient enough to enable the spectrometry system to detect ^{40}K in the NPK fertilizer sample. Overall, this analytical technique is able to produce quality and reliable analytical result for detecting ^{40}K in a sample.

As the LPNPE Lab has not yet a standard source with known activity for efficiency calibration, the procurement of such standard is imperative for the interpretation of spectrum in terms of activity (quantify radionuclide).

7 REFERENCES

- [1] José Araújo dos Santos Júnior, Jorge João Ricardo Ferreira Cardoso, Cleomacio Miguel da Silva, Suêlto Vita Silveira and Romilton dos Santos Amaral, Department of Nuclear Energy; Federal University of Pernambuco, *Analysis of the ^{40}K Levels in Soil using Gamma Spectrometry*, Brasil.
- [2] Yii Mei Wo and Zaharudin Ahmad, Industrial Technology Division; Agensi Nuklear Malaysia, *Validation of Ra-226 and K-40 measurement in environmental samples using gamma spectrometry system*, Bangi, 43000 Kajang, Malaysia.
- [3] P. N. Yadav, P. Rajbhandari and K. K. Shrestha, Central Department of Chemistry, Tribhuvan University, Kirtipur, Kathmandu, Nepal, *Estimation of Concentration of K-40 by Gamma Spectroscopy and Atomic Emission Spectroscopy in the Environmental Samples of Northern Kathmandu Valley*, Kirtipur, Kathmandu, Nepal.
- [4] Dr. Mabrouk O. Allagi, Nuclear Engineering, University of Cambridge, UK, *Potassium-40 for the Discrimination between Honey and Dates Syrup*, UK.
- [5] Jong In Byun, Yun Ho Choi, Seung Im Kwak, Han-Yull Hwang, Kun-Ho Chung, Gun Sik Choi, Doo-Won Park, Chang Woo Lee, Nuclear Engineering, Journal of the Korean Nuclear Society, Volume 34, Number 5, December 2002, *Development of Anticomic Shielded Ultra Low Background Gamma Spectrometer for Precise Measurement of Environmental Radioactivity*, Korea.
- [6] Gerti Xhixha, Nuclear Engineering, PhD in Physics, University of Ferrara, March 2012, *Advanced gamma-ray spectrometry for environmental radioactivity monitoring*, Ferrara, Italy.
- [7] Marie-Martine Bé, Vanessa Chisté, Christophe Dulieu, Commissariat à l'Energie Atomique, CEA-R-6201, *Nucléide-LARA bibliothèque des émissions alpha, X et gamma*, France, 2008.
- [8] G. Nelson and D. Reilly, Los Alamos National Lab, *Gamma-Ray Interactions with Matter*, USA.

Characterization of Airborne Particulates Containing Naturally Occurring Radioactive Materials in Investment Casting Facilities

Yong Gun Kim^a, Cheol Kyu Choi^a, Boncheol Goo^b, Kwang Pyo Kim^{a*}

^aDepartment of Nuclear Engineering, Kyung Hee University, Gyeonggi-do, Republic of Korea

^bKorea Institute of Nuclear Safety, Daejeon, Republic of Korea.

Abstract. Investment casting facilities use zircon sand and zircon flour, which contain naturally occurred radioactive materials (NORMs). The NORM in zircon-using facilities may give rise to enhanced radiation dose to workers. The present study characterized airborne particulate properties, which influence radiation dose to workers. Airborne particulate concentrations and size distributions were measured using an eight-stage cascade impactor. Mass densities of raw materials and by-products were measured using pycnometer. Physical shapes of airborne particulates were analysed to determine shape factor. Radioactivity concentrations of the materials were measured by gamma-spectroscopy. Airborne particulate concentrations by sampling areas varied widely with more than one order of magnitude difference. The particulate concentrations were lower at shell casting separating area and the highest in coating area during fall of zircon sands. Airborne particulates were generally distributed log-normally with maximum concentrations at aerodynamic diameters of about 3.3-9.0 μm . Activity median aerodynamic diameters were about 4.5-28 μm depending on sampling area. Average mass densities were 4.7 g/cm^3 for zircon sand and zircon flour, 2.7 - 3.0 g/cm^3 for broken shell material, and 2.7 - 4.4 g/cm^3 for dusts, respectively. The airborne particulates appeared as spheroids or rough spherical fragments and thus a shape factor of unity could be assumed. The radioactivity concentrations were the highest for zircon flour, followed by zircon sand. The radioactivity concentrations were relatively low for broken shell material and dust because they were mixture of zircon materials and other constituents. The materials contained more uranium series compared with thorium series. The radioactivity concentrations of zircon flour ranged 3,177 – 3,497 Bq/kg for uranium series and 377 – 509 Bq/kg for thorium series. The database established in this study can be used for the assessment of radiation dose to workers resulting from chronic inhalation of airborne particulates containing radioactive materials.

KEYWORDS: NORM; zircon industry; particulate property; inhalation dose; dose assessment.

1 INTRODUCTION

In 2012, a law of Natural Radiation Safety Management Act (NRSMA) was enacted in Korea for protection against ionizing radiation from minerals, raw materials, by-products, etc. Investment casting process use zircon sand and zircon flour, which contain naturally occurred radioactive materials (NORMs). The zircon-using industry is one of the main industries enforced by the new law. Investment casting is an industrial process of metal forming techniques with formed pattern. Common refractory materials for the investments include zircon, silica, aluminium silicates, and alumina. Zircon based refractories are commonly used because it is less likely to react with the molten metal. The NORM in the zircon-using industry may give rise to enhanced worker radiation dose, which may need to be managed by the NRSMA regulation.

Radiation dose to workers in the zircon industry have been reported in literature [1, 2]. Righi et al. assessed radiological impacts of a zircon sand processing plant using airborne particulate concentration and radioactivity concentration [3]. Dose assessment to workers in NORM industry by characterizing airborne particulates has been reported in a NORM industry [4]. The particulate characteristics were further applied to generate site-specific inhalation dose coefficients [5]. However, such study has not been reported in investment casting process using zircon materials.

Internal radiation dose due to particulate inhalation can be estimated by Human Respiratory Tract Model (HRTM) by the International Commission on Radiological Protection (ICRP) [6]. According to the HRTM, inhalation dose depends on airborne particulate properties, including particulate

* Presenting author, e-mail: kpkim@khu.ac.kr

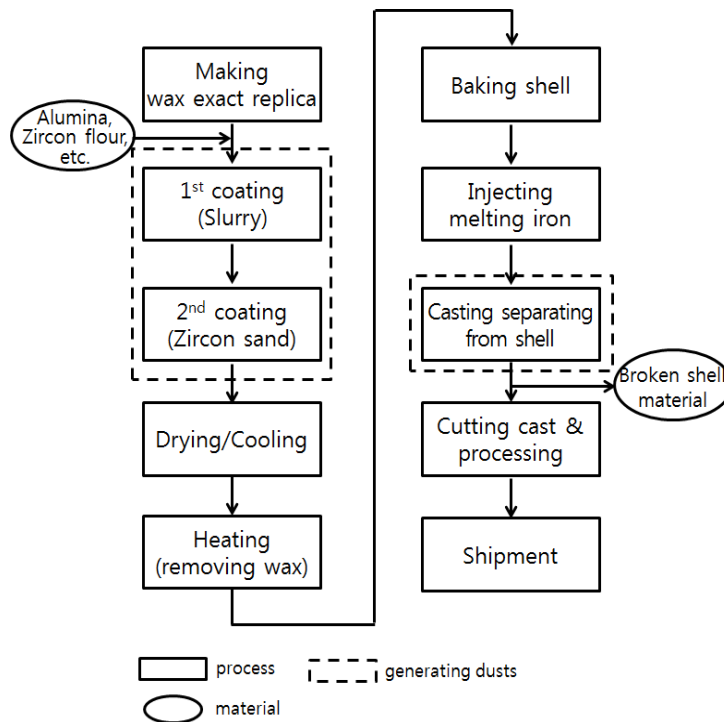
concentration, size distribution, density, shape, and radioactivity concentration. ICRP 66 HRTM suggested reference particulate parameters for the absence of the property information [6]. However, such reference data may be greatly different from site-specific real properties and skew radiation doses to unrealistic values. The ICRP 66 HRTM recommended that whenever possible, site-specific information on particulate physicochemical properties should be measured and then used for the assessment of radiation dose to workers.

The objectives of the present study were to characterize airborne particulates containing NORM in investment casting facilities, which use zircon materials. For the characterization, we directly measured concentrations and size distributions of airborne particulates, mass density, shape, and radioactivity concentrations at the zircon-using facilities in Korea.

2 MATERIALS AND METHODS

Figure 1 depicts various processes in the investment casting facility. During a series of processes, airborne particulates are generated from systems and activities, for example automated mechanical systems and operation of mobile heavy equipment. Sampling sites were selected by considering exposure duration of workers and concentrations of airborne particulates. The selected sampling sites included coating area with slurry and zircon sand, shell unloading area, and casting separating area.

Figure 1: Process schematic diagram of investment casting facility.



The Anderson cascade impactor (Anderson 1 ACFM sampler, Thermo scientific, USA) was employed for air sampling. The Anderson impactor consists of eight impactor stages followed by a final collection filter thus partitioning airborne particulates into nine different size ranges. The aerodynamic cutoff sizes were 9.00, 5.80, 4.70, 3.30, 2.10, 1.10, 0.65, and 0.40 μm for the 0th to 7th impactor stages. Upper particulate size limit of the cascade sampler was taken to be 100 μm and the lower size limit of particulates collected on the final collection filter was taken to be 0.03 μm [4]. Membrane filters were placed over the cascade impactor substrate to facilitate particle removal as needed for subsequent analyses of particle shape composition. The samplings were conducted as close as possible to current worker locations and the height of the inlet nozzle of the cascade impactor was set at a nominal breathing height of 1.5 m. The cascade impactor was operated at a flow rate of 28.3 L/min.

The mass density measurements using a pycnometer (AccuPyc 1330, Micromeritics, German) were made of raw materials and by-products. A limited number of airborne particulate samples collected by cascade impactor were further analysed for particle shape using scanning electron microscopy (SEM). Particulates of four different size ranges (0th, 3rd, 5th, and 7th impactor stages) from different sampling areas were analysed for the shape analysis.

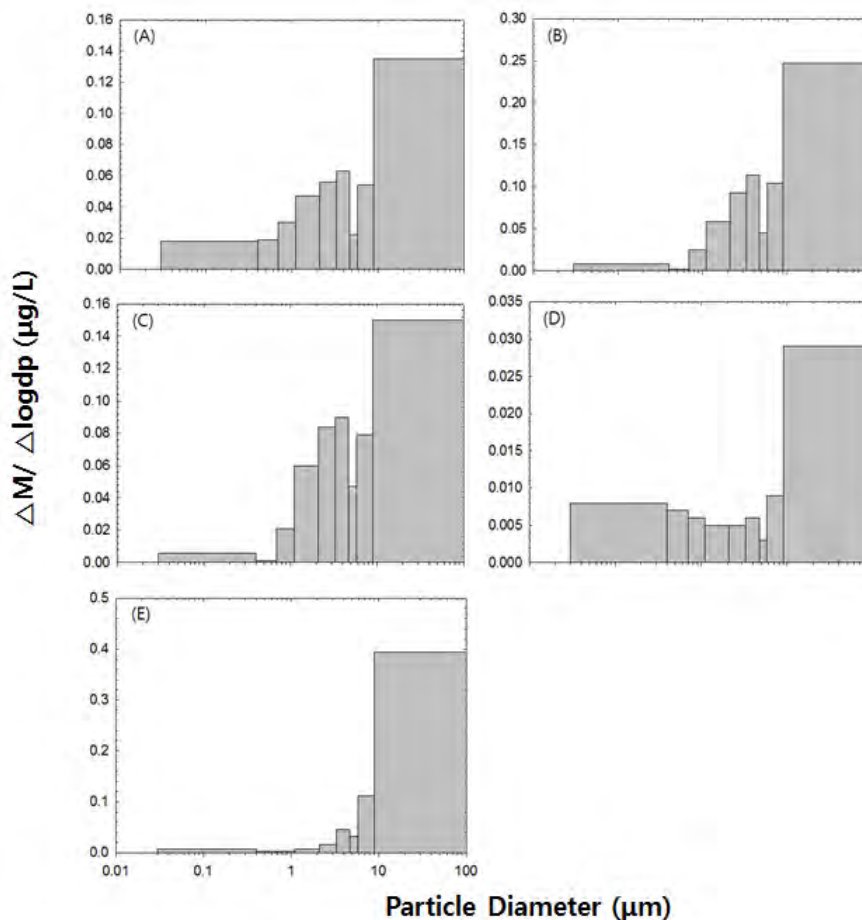
The small mass of airborne particulates collected at each cascade impactor stage resulted in radioactivity loadings that were generally below detectable limits of radiation detectors. Consequently, radioactivity measurements were carried out using bulk materials, including zircon sand, zircon flour, broken shell materials, and dusts. A High Purity Germanium (HPGe) detector was used for measurement of ^{226}Ra in uranium series and ^{228}Ra in thorium series. For gamma spectroscopy, collected samples were sealed for 30 days in Marinelli beakers to re-establish secular equilibrium between radium and radon progenies prior to measurement. For example, higher yield gamma-ray photons from ^{214}Pb and ^{214}Bi were used to directly infer the radioactivity of the ^{226}Ra .

3 RESULTS AND DISCUSSION

3.1 Particulate Concentration and Size Distribution

Figure 2 displays concentrations and size distributions of airborne particulates at each sampling area. Concentrations of airborne particulates varied widely by sampling areas with more than one order of magnitude difference.

Figure 2: Size distribution and concentration of airborne particulates. A: coating area (Facility A), B: coating area (Facility B), C: shell unloading area (Facility A), D: casting separating area (Facility A), E: casting separating area (Facility B).



Particulate concentrations depended on many factors, including operation of mechanical systems, working activities, ventilation, etc. The particulate concentrations were low at shell casting separating area and the highest in coating area during fall of zircon sands. The large variation was due to the variability of mechanical operations and building ventilations. Particulate concentrations were especially higher in coating area. Workers in coating area made an exact wax replica of the shape to be cast. The wax replica is then coated with slurry and zircon sand. Such active operation made particulates on the equipment resuspended and thus particulate concentrations were high. Shell unloading area was nearby coating area. Airborne mass concentrations of shell unloading area were lower than coating area. In casting separating area, cast parts are separated from the brittle shell by mechanical means and the part is cleaned of residual shell material. The broken shell material is placed in a container for disposal as waste. Such activity in casting separating area generated airborne particulates in the work environment.

Concentrations of airborne particulates by size were generally distributed log-normally with maximum concentrations at aerodynamic diameters of about 3.3 - 9.0 μm . Activity median aerodynamic diameters were about 4.5 - 28 μm depending on processing areas.

3.2 Particulate Density and Shape

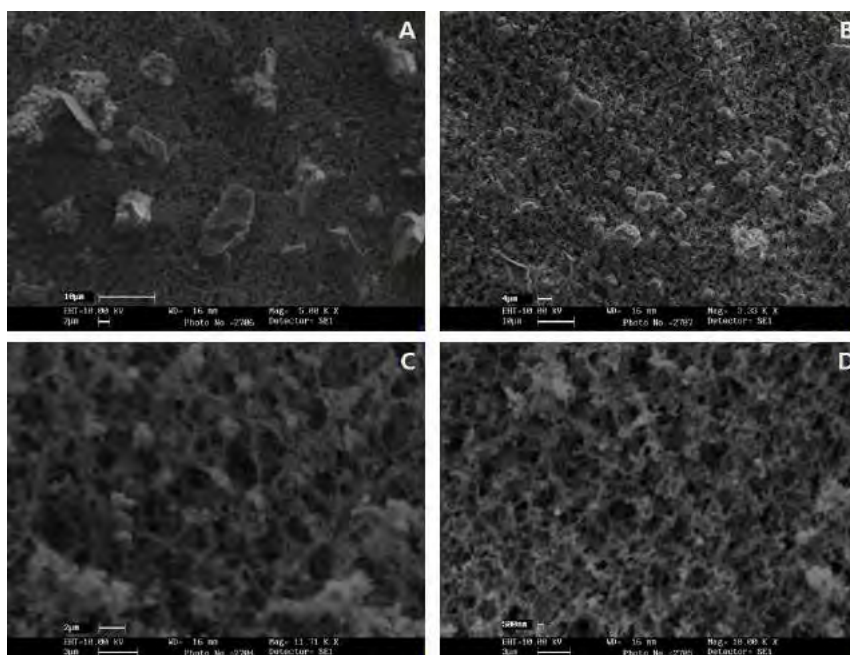
Table 1 lists the measured densities of zircon sand, zircon flour, broken shell material, and dusts. All the zircon sands and zircon flours in Korea are imported from other countries. The densities were generally higher for zircon sands, zircon flours, broken shell material, and dusts, in that sequence. The density of zircon sand was 4.7 g/cm^3 , which was similar to the density of zircon flour. Mass densities of the other materials were lower, ranging 2.7 - 4.4 g/cm^3 .

Table 1: Mass densities of zircon sand, zircon flour, broken shell material, and mixed dust.

Area	Sample	Mass density (g/cm^3)
Coating area	Zircon sand	4.7
	Zircon flour	4.7
Casting separating area	Broken shell material	2.7-3.0
	Coating area dust	2.9
Dust collector	Processing dust	2.9
	Mixed dust	4.4

Particle shape analysis was conducted on airborne particulates samples at three different areas. As an example, figure 3 shows particulates of different sizes collected at the coating area. Since the particulates were compressed during impaction on the filter, it was difficult to differentiate each individual particulate from the aggregate particulate mass. Single particulate can be found at the edges of the impactor stage, and thus images of these edge particles were used for particle shape analysis. In general, all particles collected at different impactor stages and from different sampling areas appeared as spheroids or as rough spherical fragments. No fiber-like particles were found. Particle shape influences the particle drag force, and is thus characterized by the dynamic shape factor defined as the ratio of the resistance force of the true non-spherical particle to that of a spherical particle of unit density. Johnson et al. calculated dynamic shape factors of several non-spherical particles and noted that they ranged from unity for spherical particles to values of 1.09 to 1.23 for cylindrical particles having axial ratios of 2 to 5, respectively [7]. Axial ratios of most particles observed in this study did not exceed a value of 2. Consequently, a shape factor of unity could be assumed for the airborne particulates in investment casting facilities using zircon sand and flour as needed for assessment of radiation dose due to workers due to inhalation of airborne particulates containing radioactive materials.

Figure 3: Shape of airborne particulates sampled at coating area. A: 0th impactor stage particulates, B: 3rd impactor stage particulates, C: 5th impactor stage particulates, D: 7th impactor stage particulates.



3.3 Particulate Radioactivity Concentration

Table 2 shows radioactivity concentrations of samples. The radioactivity concentrations of uranium series were higher than the radioactivity concentrations of thorium series. Radioactive concentrations of broken shell material and dust were lower than zircon sand and zircon flour. It is the same tendency with previous studies. According to an International Atomic Energy Agency (IAEA) report, most zircon currently produced contains uranium series radionuclides at activity concentrations of about 1,000 - 4,000 Bq/kg and thorium series radionuclides at activity concentrations of about 500 - 1,000 Bq/kg [2]. Radioactivity concentrations of the other samples were lower because of dilution of zircon with other constituents.

Table 2: Radioactivity concentrations of zircon sand, zircon flour, broken shell material, and dusts.

Sample	Radioactivity Concentration (Bq/kg)		
	²²⁶ Ra	²²⁸ Ra	⁴⁰ K
Zircon sand	2,839 - 3,245	351 - 634	<MDA
Zircon flour	3,177 - 3,497	377 - 509	<MDA
Broken shell material	201 - 925	89 - 258	47 - 102
Coating area dust	732	294	118
Processing dust	669	138	79
Mixed dust	377	196	106

4 CONCLUSION

An accurate assessment of radiation dose to workers due to inhalation of airborne particulates containing NORM requires detailed and site-specific knowledge of a range of airborne particulate properties. In this study, a database of site-specific airborne particulate characteristics including concentrations in the air, size distributions, mass densities, shapes, and radioactivity concentrations were established at investment casting facilities using zircon sand and flour in Korea.

Particulate concentrations in the air varied widely by processing areas. The particulate concentrations were lower at casting separating area and the highest in coating area during fall of zircon sands. Airborne particulates were generally distributed log-normally with maximum concentrations at particulate size of about 3.3 - 9.0 μm . Activity median aerodynamic diameters were about 4.5 -28 μm . Average mass densities of zircon sand, zircon flour, broken shell material, and dusts were 4.7 g/cm^3 , 4.7 g/cm^3 , 2.7 - 3.0 g/cm^3 , and 2.7 - 4.4 g/cm^3 , respectively. The airborne particulates appeared as spheroids or rough spherical fragments. Radioactive concentrations of broken shell material and dust were lower than zircon sand and zircon flour because the zircon sands were diluted with other constituents.

The database of particulate concentrations, size distribution, and physiochemical properties established in this study can be utilized for more worker-specific assessments of radiation doses devoid of potentially conservative default assumptions. In addition, the information can be used for zircon-using industry and regulators in their consideration of health protection programs and policies regarding both respiratory and radiological protection.

5 ACKNOWLEDGEMENTS

This work was supported by a grant from “Establishment of Technical Basis for Implementation on Safety Management for Radiation in the Natural Environment” carried out by Korea Institute of Nuclear Safety.

6 REFERENCES

- [1] IAEA, 2006. Assessing the Need for Radiation Protection Measures in Work Involving Minerals and Raw Materials. IAEA Safety Report Series No. 49. International Atomic Energy Agency, Vienna.
- [2] IAEA, 2007. Radiation Protection and NORM Residue Management in the Zircon and Zirconia Industries. IAEA Safety Report Series No. 51. International Atomic Energy Agency, Vienna.
- [3] Righi S, Andretta M, Bruzzi L., 2005. Assessment of the Radiological Impacts of a Zircon Sand Processing Plant. *J. Environ Radioactiv.* 82, 237–250.
- [4] Kim KP, Wu CY, Birky BK, Nall W, Bolch WE., 2006. Characterization of Radioactive Aerosols in Florida Phosphate Processing Facilities. *Aerosol Sci and Tec.* 40(6): 410-421.
- [5] Kim KP, Wu CY, Birky BK, Bolch WE., 2006. Influence of Particle Size Distribution on Inhalation Doses to Workers in the Florida Phosphate Industry. *Health Phys.* 91(1):58-67.
- [6] ICRP, 1994. Human Respiratory Tract Model for Radiological Protection. ICRP Publication 66. *Ann ICRP* 24 (1-3).
- [7] Johnson D, Leith D, Reist P., 1987. Drag on Nonspherical, Orthotropic Aerosol Particles. *J. Aerosol Sci.* 18, 87–97.

Spatial Distribution of Naturally Occurring Radioactive Materials (^{235}U , ^{238}U , ^{228}Th , ^{230}Th , ^{232}Th , ^{226}Ra , ^{228}Ra and ^{40}K) in the Marine Sediment Samples Along the Red Sea Coast of Saudi Arabia

A. A. Alzahrany^{a,b}, M. A. Farouk^b, E. I. Shabana^{b,c}, A. A. Al-Yousef^b, K. N. Alnajem^b, F. I. Al-Masoud^b

^aKing Abdullah City for Atomic and Renewable Energy (KACARE), Atomic Energy Sector, Riyadh, Saudi Arabia

^bKing Abdulaziz City for Science and Technology, Institute of Atomic Energy Research, Riyadh, Saudi Arabia

^cKing Abdul Aziz University, Nuclear Eng. Dep., Jeddah, Saudi Arabia

Abstract. Saudi Arabia has a total coastline of 2640 km and the Red Sea is representing the West Coast of the country with a length of about 1900 km. The Red Sea has a surface area of roughly 450,000 km². This paper represents the result of activity concentrations of naturally occurring radioactive materials in surface marine sediments along the Saudi Coast of the Red Sea. The activity concentrations of (^{235}U , ^{238}U , ^{228}Th , ^{230}Th , ^{232}Th , ^{226}Ra , ^{228}Ra and ^{40}K) have been determined by direct measurement of the gamma-ray spectra for more than seventy grab sediment samples using high resolution hyper-pure germanium spectrometers.

Radon Mass Exhalation Rates of Selected Building Materials in Tanzania

Aloyce Amasi^a, Kelvin Mark Mtei^b, Pawel Jodlowski^c, Chau Nguyen Dinh^c

^aDepartment of Research and Development, Tanzania Atomic Energy Commission, P.O.BOX 743, Arusha Tanzania, Arusha, Tanzania

^bDepartment of Water and Environmental Science and Engineering, The Nelson Mandela African Institution of Science and Technology, P.O.BOX 447, Tengeru, Arusha Tanzania, Arusha, Tanzania

^cFaculty of Physics and Applied Computer Science, AGH University of Science and Technology, Al. Mickiewicza 30, 30-059, Krakow, Poland, Krakow, Poland

Abstract. This study aimed at determining the mass radon exhalation rate of Tanzania Portland cements and their raw materials for assessment of the radiological hazards due to use of those materials in residential construction. The radon mass exhalation rate was measured by closed chamber coupled with the Pylon AB5™ and varied from 0.3 to 13 %. The estimated indoor radon concentrations and annual effective dose for tightly closed standard room were within the safe limits of radon potential health hazards of 600 Bq m⁻³ for dwellings and 1500 Bq m⁻³ for workplaces recommended by International Commission on Radiological Protection (ICRP).

Assessment of Natural Radionuclide Content of Some Public Well Water within Ondo and Ekiti States, South-western Nigeria

Adeolu Ayodele, Adeseye Arogunjo, Olubodun Arije

Federal University of Technology, Akure, Ondo State, Nigeria

Abstract. One of the important ways in which radiological impact assessment can be carried out within a given populace is the route via the ingestion pathway. In order to address this, sixteen (16) well water samples were collected from various cities distributed across Ondo and Ekiti states and analysed for natural radionuclides using n-type co-axial HPGe detector with ORTEC multichannel analyser (MCA) and MAESTRO-32 for spectrum analysis and processing. The measured activity concentrations ranged from 1.59 ± 0.44 to 3.75 ± 0.67 Bq l^{-1} for ^{232}Th , 35.81 ± 2.78 to 70.38 ± 3.46 Bq l^{-1} for ^{40}K , 6.43 ± 1.33 to 12.59 ± 1.50 Bq l^{-1} for ^{226}Ra and 0.45 ± 0.24 to 33.15 ± 5.99 Bq l^{-1} for ^{232}Th , 34.47 ± 2.88 to 556.9 ± 30.73 Bq l^{-1} for ^{40}K , 2.08 ± 0.53 to 78.36 ± 14.17 Bq l^{-1} for ^{226}Ra respectively for Ondo and Ekiti states. Age dependent annual effective dose and committed effective dose were calculated using the activity concentration, consumption per annum in $l\text{y}^{-1}$ and the ingested dose conversion factor in SvBq^{-1} . The total annual effective dose and committed effective dose were presented for three different age groups (0-10 years, 7-12 years and ≥ 17 years). The total annual effective dose was found to be above the recommended ICRP and WHO values.

Study of Particular Problems Appearing in NORM Samples and Recommendations for Best Practice Gamma-ray Spectrometry

Andreas Baumgartner^a, Michael Stietka^a, Franz Kabrt^{a,b}, Hannah Moser^b, Franz Josef Maringer^b

^aUniversity of Natural Resources and Life Sciences, Vienna, Prueflabor fuer Umweltradioaktivitaet und Strahlenschutz, Low-Level Counting Laboratory Arsenal, A-1030 Vienna, Austria

^bBEV - Federal Office of Metrology and Surveying, A-1160 Vienna, Austria

Abstract. The applied raw materials and processed substances within Naturally Occurring Radioactive Materials (NORM) industries have a huge diversity regarding their chemical composition and physical nature. Due to this diversity, for gamma-ray spectrometry of NORM various problems may occur. Because of overlapping gamma-lines, or X- and gamma-rays, or X-rays in coincidence, the aimed determination of specific radionuclides is challenging and requires suitable corrections for the different NORM samples. In order to perform traceable, accurate, and standardized measurements and to ensure a safe and cost optimized use of raw materials, products and by-products, improved measurement practices and procedures are required for NORM industries. Within the Joint Research Project IND57 MetroNORM in the framework of the European Metrology Research Programme (EMRP) the difficulties, which arise in the measurement of NORM samples are analyzed and new actions are proposed. This paper describes the study of spectral interferences in selected NORM key-materials. Moreover, the improvement of measurement procedures based on gamma-ray spectrometry for NORM including the definition and testing of suitable correction factors is presented. Additionally, a proposal for solutions and recommendations for best practice gamma-ray spectrometry of the NORM key-materials is given. The EMRP is jointly funded by the EMRP participating countries within EURAMET and the European Union.

Public Exposure due to Radon and External Radiation from Ornamental Rock Indoors

André Luiz do Carmo Leal^a, Dejanira da Costa Lauria^b

^aInstituto Federal do Rio de Janeiro – IFRJ, Rio de Janeiro, Brazil

^bInstituto de Radioproteção e Dosimetria-IRD, Rio de Janeiro, Brazil

Abstract. The ornamental rocks are part of those materials for which above-normal levels of natural radionuclides have been found. The dose due to its use do not only depend on the concentrations of natural radionuclides in the building material, but also on the intrinsic proprieties of the material and the characteristics of environment in which this material is used. From the radionuclide concentrations in 180 samples, the radon concentration indoor and the external and radon inhalation doses arriving from the use of Brazilian rocks as floor covering in residential buildings were assessed. The radionuclide concentrations reached a wide range of values: Ra-228 concentrations ranged from <2 to 530 Bq.kg^{-1} , Ra-226 concentrations varied between <5 and 600 Bq.kg^{-1} , while the K-40 ones varied between 190 and 2797 Bq.kg^{-1} . The contribution of rocks for indoor Rn-222 concentration falls far of the recommend investigation level of 300 Bq m^{-3} , or even the one that has been adopted by some countries of 200 Bq.m^{-3} , since the estimated concentrations of Rn-222 ranged from 0.07 to 8.6 Bq m^{-3} , (mean value of 0.77 ± 1.04 and median of 0.45 Bq m^{-3}). The mean radon inhalation dose of $0.006 \pm 0.009 \text{ mSv.year}^{-1}$ (range between 0.001 and $0.07 \text{ mSv.year}^{-1}$ and median value of $0.0004 \text{ mSv.year}^{-1}$) was far lower than the recommended level (10 mSv.year^{-1}). The value of the external dose due to use of ornamental rocks as floor covering in the residential scenario ranged between 0.01 and $0.61 \text{ mSv.year}^{-1}$, value of mean of 0.19 ± 0.10 and median of $0.16 \text{ mSv.year}^{-1}$. The sensitivity analysis highlighted the importance of the ventilation rate and the emanation rate to the Rn dose, whereas for external dose the only parameters that affect the value of dose are the density of the material and the location of the receptor.

Outdoor Thoron and Thoron Progeny in a Thorium-rich Area in Norway

Anne Liv Rudjord^a, Hallvard Haanes^a, Trine Kolstad^a, Alexander Muring^a,
Ingvild Finne^a, Sven Dahlgren^b

^aNorwegian Radiation Protection Authority, Østerås, Norway

^bBuskerud Telemark Vestfold County, Vestfold, Norway

Abstract. The Fen Complex is an ancient volcano, the remains of it is covering an area of approximately 9 km² in southern Norway, in the Telemark county. In the eastern parts of this geological complex, very high concentrations of thorium in the carbonatite rocks leads to external gamma dose rates of a few microsieverts per hour. The particular rock type found in this area is also rich in iron and rare earth minerals, and the environment has been subject to anthropogenic changes due to mining activities in the past. This area is now being used for recreational purposes by the local population. However, new road construction and mining activities are planned. It is therefore important to improve the estimates on the various contributions to radiation dose. Earlier measurements have revealed high concentrations of thoron in outdoor air, indicating a substantial thoron exhalation. In this study, measurements of radon, thoron and thoron progeny were carried out at 3 heights (20 cm, 100 cm and 170 cm) at 9 stations, both in-situ (short term) and integrating measurements with passive detectors. Extremely high thoron concentrations (> 20 000 Bq/m³) were observed near the surface of the main waste rock area. Due to both dilution and the short half-life of thoron (55.6 s), the thoron concentrations at 100 and 170 cm above ground were, as expected, considerably lower. In order to estimate inhalation dose rates in the area, measurements of thoron progeny, in particular lead-212, was performed with air filters (particle fraction) and by thoron progeny passive detectors. Although not directly comparable, the difference between these datasets were striking, the highest values were found with the passive detectors. The reason could be due to limited filter sampling efficiency, as could be expected if most of the thoron progeny were “unattached”. This seems rather likely, as it is reasonable to assume that the concentration of aerosols is low in this rural area. Based on the thoron progeny passive measurements, estimates indicate that dose rates could reach several microsieverts per hour from inhalation. This indicates that inhalation doses could be higher than the dose contribution from external gamma radiation in the area. Outdoor exposures in this high natural radiation area may have some radiation protection implications, and further studies of thoron and thoron progeny needs to be performed.

Advanced Approach to Assessment of Potential Radon Hazard of Building Sites in Russia

Albert Marennyy^a, Peter Miklyaev^{b,a}, Andrey Tsapalov^a, Tatyana Petrova^c, Sergey Kiselev^d

^aResearch and Technical Center of Radiation-Chemical Safety and Hygiene, FMBA, Moscow, Russia

^bSergeevs Institute of Environmental Geoscience, Moscow, Russia

^cMoscow State University, radiochemistry department, Moscow, Russia

^dSRC Burnasyan Federal Medical Biophysical Centre, FMBA, Moscow, Russia

Abstract. According to the Russian regulatory practice, an assessment of radon hazardous sites is based on measurement of radon flow rate from the soil surface before the beginning of building activities. The majority of the European countries use an assessment of the various integrated indicators characterizing radon-induced hazard of the site, based on measurements of radon activity concentration in soil at a depth of 0.5-1.0 m and permeability of soil. However, both approaches have significant disadvantages connected mainly with large temporal variations of measured parameters (both of radon flow rate and radon activity concentration in the soil). Moreover, the radon field changes significantly with the depth due to the depth variation of the soil permeability and radium concentration in soil. Therefore, the radon field parameters being measured both on the soil surface and at depth of 1.0 m from the soil surface specify only the upper soil layer thickness of not more than 1.5-2.0 m. The paper proposes and justifies a comprehensive approach based on direct measurement of the radon field parameters (such as radon flow rate from the surface) and the calculated assessment of annual radon flow rate from soil lying in the area to a depth of laying the foundation base of the building. We developed an empirical equation to facilitate calculations on the basis of radium activity concentration in soil, emanation fraction, soil density at a thickness of soil layer of about (1.2-1.4) m independent of soil permeability. At that, direct measurement of radon field help to identify radon anomalies at the site, because of the presence of geodynamic zones and faults on the site, while the calculation of radon flow from soil of the building base takes into account the presence of rocks characterized by elevated radon exhalation in near-surface part of the geological section.

Complex Monitoring Study of Radon Field Generation in Soils under Various Geological and Climatic Conditions in Russia (2011 – 2015)

Albert Marennyy^a, Peter Miklyaev^{a,b}, Andrey Tsapalov^a, Andrey Penezev^a, Sergey Kiselev^c

^aResearch and Technical Center of Radiation-Chemical Safety and Hygiene, FMBA, Moscow, Russia

^bSergeevs Institute of Environmental Geoscience, Moscow, Russia

^cSRC Burnasyan Federal Medical Biophysical centre, FMBA, Moscow, Russia

Abstract. To develop the theoretical foundations and improve the methodological framework of radon hazard assessment of areas, over the period 2011-2015, comprehensive monitoring studies of radon field generation have been carried out. The studies were performed at five experimental sites. The site locations (East European Plain, the South of Russia and the North Caucasus, the Urals and Siberia) characterize sufficiently the geological, geophysical and climatic features of the territories, where about 90% of Russia's population lives. The research program included: the development of a detailed description of the research, common methodological approaches to equipment and set of measurements at experimental sites; the study of the geological structure of sites to a depth of 7 - 10 m by drilling and soil sampling, and laboratory study of radiation-and-physical properties of soils (distribution of natural radionuclides by soil depth, emanation fraction and density; radon diffusion coefficient in the upper soil layer); measurement of radon flow rate on the site surfaces; measurement of radon activity concentration in soil pores at depth of 0.2-10 m; agro-meteorological observations (barometric pressure, air and soil temperature, air relative humidity, soil moisture, groundwater level, wind speed). The studies included sessions of synchronous measurements at functioning sites a once a week. The paper presents the following experimental results: spatial-temporal variations and mean values of radon field parameters, the dependence of the radon field parameters from climatic ones, the geological structure of the experimental site and radiation-and-physical properties of soils; laws of radon formation and transport in near surface soils.

Area Monitoring of Ambient Dose rates in some parts of South Western Nigeria using a GPS integrated Dosimetric System

A.O. Mustapha^a, O.O. Alatise^a, I.C. Okeyode^a, V. Makinde, F.G. Akinboro, D. Al-Azmi^b

^aDepartment of Physics, Federal University of Agriculture Abeokuta, P.M.B. 2240, Abeokuta, Nigeria

^bDepartment of Applied Sciences, College of Technological Studies, Public Authority for Applied Education and Training, Shuwaikh, P. O. Box: 42325, Code 70654, Kuwait

Abstract. A dosimetric system comprising a Geiger-Muller (GM) dosimeter connected to a smart phone via bluetooth was used for a dose rate survey in some parts of Southwestern Nigeria. The smart phone has the Geographical Positioning System (GPS), which provides the navigation information and saves it along with the dose rate data. A large number of data points was obtained that shows the dose rates distribution within the region. The results show that the ambient dose rates in the region range from 70 to 520 nSv h⁻¹ and showed the bias and influence of geology on the ambient radiation dose in the region. The geology influence was demonstrated by superimposing the dose-rates plot and the geological map of the area. The potential applications of the dosimetric system in determining pre-operational baseline background radiation dose rates, and for area monitoring (nuclear security) were discussed in the paper particularly against the background of Nigeria's declaration of intention to develop its nuclear power program.

KEYWORDS: *absorbed rate survey; background radiation; nuclear security; area radiation monitoring.*

Radiation Protection Dosimetry (2017), Vol. 173, No. 1-3, pp. 263–267

doi:10.1093/rpd/ncw336

Dose Assessment from Groundwater Water Consumption in Central Portugal

Alcides Pereira, Luis Neves

Centre for Mechanical Engineering of the University of Coimbra (CEMUC), Department of Earth Sciences, University of Coimbra, Coimbra, Portugal

Abstract. The bedrock of Central Portugal is composed by rocks of the Hercynian Massif, mostly granites and metasediments, with sedimentary meso-cenozoic rocks outcropping on its western border. A previous study in the meso-cenozoic sediments showed high variability in the U content of groundwater, with an average value of 1.5 mg.l^{-1} and a maximum of 152 mg.l^{-1} . The highest values were found spatially clustered in areas with bedrock from Triassic to Upper Jurassic and Cretaceous. To improve the existing knowledge on radionuclides contained in groundwater from Central Portugal and estimate the dose from exposure to ionizing radiation, about 200 samples were collected in selected areas where the previous studies showed the occurrence of unusual U contents, as well as in the granitic and metasedimentary areas. Samples were analysed by liquid scintillation counting techniques, and the activities of ^{222}Rn , ^{226}Ra , ^{234}U and ^{238}U were determined. The maximum ^{222}Rn activity observed in the sediments was 92 Bq.l^{-1} with an average of 15.4 Bq.l^{-1} . These values are considerably lower than those measured in water that percolates rocks from the Hercynian Massif, where values over 100 Bq.l^{-1} often occur (with a maximum of $9,784 \text{ Bq.l}^{-1}$). In the whole set ^{226}Ra activity varies from below the detection limit (0.01 Bq.l^{-1}) up to a maximum of 2.41 Bq.l^{-1} . The uranium isotopes show the highest variability in the sample set, ranging for ^{238}U from less than the detection limit (0.01 Bq.l^{-1}) up to 48.1 Bq.l^{-1} , corresponding the later to a uranium concentration of 3483 mg.l^{-1} . Around 17% of the samples from the sediments have uranium concentrations higher than 30 mg.l^{-1} (WHO action limit), a proportion higher than Hercynian rocks. Thus, we can conclude that uranium enriched water seems to be more common in the sedimentary rocks of the western border than in the Hercynian Massif. A dose assessment was carried out for different age-group of the population, assuming a daily water consumption variable between 0.7 to 2 litres and using appropriate dose-activity conversion factors. The calculated doses varies between 10 up to 50 mSv.year^{-1} , well under the national legislation limit; however, for the most enriched uranium samples, the calculated dose can be higher than that limit, with a maximum dose of $36.8 \text{ mSv.year}^{-1}$.

Experimental and Numerical Studies for Understanding of Radon Emanation in Environmental Materials

Akihiro Sakoda, Yuu Ishimori

Japan Atomic Energy Agency, Okayama, Japan

Abstract. Radon emanation (RE) can be defined as escape of a radon atom from a radium-bearing grain into pore space. Numerous studies have experimentally and numerically been made to understand this first process leading to radon exposure. We made an extensive review of previous RE measurements for more than a thousand samples, indicating representative RE fraction values of 0.03 for mineral and fly ash, 0.13 for rock, 0.2 for soil, and 0.17 for mill tailing. Through this review, an issue was also revealed that the definition of RE had not been shared well among researchers: namely, there were studies that did not necessarily measure the RE according to its definition. Thus, it is important to establish a measurement system that allows us to accurately observe the RE without interferences like adsorption of radon onto the grain surface. We have recently developed an approach to determine the emanation rates of not only radon but also thoron simultaneously from a granular sample. Depending on their parent radium activities, only a few grams of a sample can serve this measurement. The estimated detection limits may suggest that radon and thoron emanated from soil having international average activities of radium can be measured under better experimental conditions. On the other hand, we have numerically simulated the RE process to investigate the impacts of environmental factors. For example, the calculated data agreed with observed data with regard to the moisture dependence. The results of the grain-size and temperature dependences, which were basically different from the generally accepted belief or experimental results, were also obtained. We considered that this discrepancy does not necessarily mean the disadvantage of the present RE modelling, concluding that the revision of interpretation of previous experimental results could be necessary. Other aspects such as grain shape will also be presented at the meeting.

The Principle of Uncertainty Assessment of the Average Annual Radon Indoor based on Measurement Results of Different Duration

Andrey Tsapalov^b, Albert Marennyy^a, Peter Miklyaev^{a,b}, Sergey Kiselev^c

^aResearch and Technical Center of Radiation-Chemical Safety and Hygiene, FMBA, Moscow, Russia

^bSergeevs Institute of Environmental Geoscience, Moscow, Russia

^cSRC Burnasyan Federal Medical Biophysical centre, FMBA, Moscow, Russia

Abstract. Premises are reasonable to be subdivided into three types depending on the air changing nature: “A” – stable (forced ventilation), “B” - smooth variable (natural ventilation and lack of people), “C” - unstable (forced periodic ventilation or natural ventilation and the presence of people). At the “A” type premises, radon variations are negligible; therefore the variation coefficient is equal to zero. At the “B” type premises, under the certain conditions, the logical connection is revealed between radon concentration and air temperature indoors and outdoors. At the “C” type premises, the nature of radon variations is not described logically at all, so the radon variation coefficient values for this type of premises are the highest. The radon variation coefficient values depending on the duration of the measurement are determined experimentally on the basis of results of continuous annual radon monitoring at the premises of “B” and “C” types with naturally increased radon concentration. For the purpose of practical application, only the highest coefficients values are used, which were obtained following the treatment of monitoring results at least at three premises of the relevant type located in different buildings. At that, these buildings must be uniformly distributed within the area of the certain climatic belt. The paper includes the following results:- annual monitoring of radon concentration and EEC at some experimental premises of “B” and “C” types located in different buildings in Russia within the moderate climatic belt;- classification of premises and requirements for measurement terms and conditions;- coefficients of temperature dependence for the “B” type premises;- radon variation coefficients for the “B” and “C” type premises depending on the duration of the measurement.

The Effect of Relative Humidity and Temperature Variability on Continuous Environmental Radon Monitoring

Bashir Muhammad

Umaru Musa Yar'adua University Katsina, Katsina, Nigeria

Abstract. A study was conducted on the effects of temperature and relative humidity variability during continuous radon monitoring process. Rad Aqua, a continuous radon monitoring accessory of a commercial solid state, ion-implanted, planar, silicon alpha detector (Rad 7) was employed to observe the effects of temperature and relative humidity difference during continuous radon monitoring process. High radon readings of $1750 \pm 88 \text{ Bqm}^{-3}$ at moderate temperature and low relative humidity ranges of $28.9 - 33.8^\circ\text{C}$ and $4-7\%$ respectively were obtained. At lower temperatures of $24.9 - 26.8^\circ\text{C}$ and higher relative humidity values of $55-63\%$, very low activity values of $11.3 \pm 3 \text{ Bqm}^{-3}$ were recorded at the same monitoring station with same measurement parameters. The results suggested that substantial part of radon activity concentration may be lost during continuous radon monitoring due to high humidity or low temperature in the measuring environment.

KEYWORDS: *relative humidity; temperature; radon activity concentration.*

Forecast and Analysis of Atmospheric Effluent Deposition Influenced by Buildings of Nuclear Power Plant under Normal Operation

Bo Wang, Qiong Zhang, Ruiping Guo

Nuclear and Radiation Safety Center, Beijing, China

Abstract. Since the variety of meteorology and topography around the nuclear power plant, the forecast and analysis of atmospheric dispersion and deposition characteristics influenced by buildings and structures around a nuclear power plant were conducted by commercial Computational Fluid Dynamics (CFD) software, Fluidyn-PANACHE, in this paper. The simulation subjects with realizing multi-wind direction simulation in single computation was realized by constructing the database of wind fields under variable meteorological condition with higher frequency and the built-in automatic 3D mesh generator can create the computational finite- volume mesh around obstacles and body-fitting the terrain undulations. The annual average simulation results showed that the turbulent and circumferential flow around main buildings and structures in a nuclear power plant proposed in China have been presented more directly, and the maximum annual mean dispersion factors located in the front of the waste treatment plant under the combined influence of the dominant wind and the position relation of the reactor building and the waste treatment plant were more reasonable and different from the conventional Gaussian models, for the latter lack of the precision simulation in the near field, indicating that PANACHE using physical models and deterministic techniques of solution can be suitably applied in the atmospheric dispersion research and environmental evaluation around nuclear power plant.

Radon and Energy Efficient Buildings

Constantin Cosma, Alexandra Cucos, Tiberius Dicu

University Babes-Bolyai, Cluj-Napoca, Romania

Abstract. Exposure to radon and radon decay products in homes and at workplaces constitutes one of the greatest risks from ionizing radiation. Risk estimations show figures in the rank of thousands of deaths per year from cancer caused by exposure to radon and especially to its decay products. Modern trends in civil construction are based on increasing the energy efficiency of buildings in which we live. But unfortunately, efficient insulation of buildings and the introduction of high-performance windows, air conditioning systems and other architectural energy-efficient concepts reduce the air permeability of the building envelope and can cause elevated indoor radon and other pollutants levels. A significant impact of house thermal retrofitting and the air conditioning system usage on radon levels have been already reported and the conclusions of these studies prove considerable health effects caused by increasing population exposure to radon and other pollutants in modern homes. A realistic scenario envisages an increase of radon concentration in dwellings in the future due to changing lifestyles, the use of artificial materials with high content of radium and economic reasons for reducing the ventilation housing in cold seasons. Indoor radon exposure was measured by using CR-39 nuclear track detectors exposed for 6-7 months in 2 different seasons on inhabited rooms of dwellings, at 1-1.5m above floor level, in compliance with quality assurance and control programs according to the HPA-NRPB Measurements Protocol. The measuring protocol, the placement of detectors and processing of the results has already been detailed in previous works. The statistical analysis has been performed with GraphPad Prism 5.0 and the comparison between samples was made with t-test, for the natural logarithm of the radon concentration. The significance level was chosen at $\alpha = 0.05$.

Assessment of Radiological Hazards from Gold Mine Tailings in Gauteng Province, South Africa

Caspah Kamunda^a, Manny Mathuthu^a, Morgan Morgan^b

^aNorth West University (Mafikeng Campus), North West, South Africa

^biThemba LABS, Gauteng, South Africa

Abstract. Radiological hazards associated with exposure to Naturally Occurring Radionuclides Materials from gold mine tailings in Gauteng Province of South Africa were evaluated. A comparison was made with soil samples from a control area. In this study, gamma spectroscopy was used to measure the activity concentrations of these radionuclides in 56 soil samples from the mine tailings and 10 soil samples from the control area. The average activity concentrations in Bq kg⁻¹ for Uranium-238, Thorium-232, and Potassium-40 from the mine tailings were found to be 785.3±13.7, 43.9±1.0 and 427.0±13.1, respectively. On the other hand, the average activity concentrations in Bq kg⁻¹ for Uranium-238, Thorium-232, and Potassium-40 from the control area were found to be 17.0±0.4, 22.2±0.5 and 496.8±15.2, respectively. Radiological hazard parameters calculated from these activity concentrations were higher than recommended safe limits. In particular, calculated average values for the external hazard (H_{ex}) and the internal hazard (H_{in}) from the mine tailings were found to be 2.4 and 4.5. Both these values were higher than unity, posing a significant health risk to the population in the area.

Sensitivity Study of Inhalation Dose by Airborne Particulate Properties

Cheol Kyu Choi^a, Yong Gun Kim^a, Jaekook Lee^{a,b}, Kwang Pyo Kim^a

^aKyung Hee University, Yongin-Si, Gyeonggi-Do, Republic of Korea

^bKorea Institute of Nuclear Safety, Daejeon, Republic of Korea

Abstract. Radiation dose due to inhalation of NORM particulates in the air depend on particulate properties, including particulate size, shape, density, absorption type, etc. In the absence of such information, ICRP recommends using default values for routine calculations. However, these particulate parameters vary widely in reality. Consequently, use of default values rather than site-specific data can potentially skew dose estimates to unrealistic values in individual exposure. The objective of this study was to analyze inhalation dose sensitivity by particulate properties. The effective dose coefficients were calculated based on ICRP-66 human respiratory tract model for a range of particulate properties. The effective dose coefficients decreased with increasing particulate size because smaller particles were deposited in the deeper regions of respiratory tract. The particulates deposited in the deeper regions resulted in high dose due to their slower clearance rates in comparison deposited within upper regions of respiratory tract. The effective dose coefficients also decreased with increasing shape factor or decreasing density. The inhalation dose decreases with decreasing deposition ratio in respiratory. As particulate shape differs from spherical shape, deposition ratio decreased because resistance force of the particulate increased and drop velocity decreased. Lower density decreases a gravity applying for the particulate and deposition ratio was decreased. In case of the absorption type, the effective dose coefficients of uranium series radionuclides except thorium were higher in order of S, M, F type. It can be explained that slower absorption type increased absorbed dose to the lung due to increasing retention time. In contrast, the effective dose coefficients for thorium nuclides were the highest for type F because if thorium nuclides were absorbed in blood, most of thorium deposited on bone surface. Thorium nuclides deposited on bone surface remain in the body a long time and increases absorbed dose. In this study, analysis of inhalation dose sensitivity was conducted by particulate properties. Inhalation dose can be overestimated or underestimated by particulate properties. Therefore, site-specific particulate properties in industry should be used for accurate inhalation dose assessment of workers. *This study was supported by the Korea Institute of Nuclear Safety.

The ICRP System for Radiation Protection of the Environment

Carl-Magnus Larsson^a, Kathryn Higley^b, Almudena Real^c, David Copplestone^d,
Jacqueline Garnier-Laplace^e, Jianguo Li^f, Kazuo Sakai^g, Per Strand^h, Alexander
Ulanovskyⁱ, Jordi Vives i Batlle^j

^aInternational Commission on Radiological Protection Committee 5 Chair, ARPANSA,
Miranda, Australia

^bOregon State University, Corvallis, USA

^cCentro de Investigaciones Energéticas, Medioambientales y Tecnológicas (CIEMAT),
Madrid, Spain

^dUniversity of Stirling, Stirling, UK

^eInstitut de radioprotection et de sûreté nucléaire (IRSN), Saint Paul lez Durance, France

^fChina Institute for Radiation Protection, Taiyuan, China

^gNuclear Information and Research Service (NIRS), Tokyo, Japan

^hNorwegian Radiation Protection Association, Østerås, Norway

ⁱHelmholtz Zentrum, München, Germany

^jThe Belgian Nuclear Research Centre SCK·CEN, Mol, Belgium

Abstract. The 2007 Recommendations of the International Commission on Radiological Protection (ICRP) included, for the first time, specific consideration of protection of the environment. This decision was not by chance, it was the consequence of work during decades performed by ICRP and national and international organisations worldwide. Within ICRP, the foundation of the system radiation protection of the environment was laid in Publication 91, in which its ethical and philosophical basis was outlined. In 2005 the ICRP decided to establish Committee 5 (C5) on Protection of the Environment. Its task was and continues to be the establishment and further develop a system for radiation protection of the environment, which is aligned with the system for radiological protection of people and with the system for protection of the environment from all other hazardous substances. The foundations of the system were established in Publications 108 and 114, in which the concept of reference animals and plants (RAPs) was described, together with a group of 12 RAPs and their corresponding databases. These databases enable the linking of exposure scenario to dose, dose to effect, and effect to consequences in the environment. Using the available information for the RAPs, Derived Consideration Reference Levels, (DCRL; bands of environmental dose rates where potential detrimental effects may deserve attention) were established. Subsequently Task Group 99 has been established to consolidate the databases and the biological information in order to strengthen the scientific basis of the DCRLs. Significant efforts have gone in to establishing a robust dosimetric approach, including consideration of RBE for environmentally relevant endpoints. With Publication 124 a further step was taken, outlining how the system can be applied in the exposure situations considered by ICRP. Further work is under way in this area, including examination of case studies. The aim of the presentation is to outline ICRP's way forward in consolidating the system and providing guidance on its application in different scenarios.

Spatial Distribution of Background Radiation in Kuwait Using Different Car Borne Gamma Probes

Darwish Al-Azmi

Public Authority for Applied Education and Training, (PAAET), Shuwaikh, Kuwait

Abstract. Two different types of dosimeters, comprising a high sensitivity Geiger-Muller-based Gamma Tracer (GT) (Saphymo, Germany) and a NaI scintillation-based spectrometer (identiFINDER 2), were both used simultaneously in car borne measurements, and they logged the absorbed dose rates every two minutes as the car was driven around Kuwait. A total distance of about 300 km was covered on asphalt roads that passed through different areas including a residential district, desert and farm lands. The data recorded by the GT (51.9 – 98, mean= 70.7 nSv/h) were consistently higher than those recorded by the identiFINDER 2 (7 – 31, mean= 13.8 nSy/h). This distinct difference in the responses of the two devices can be attributed to the cosmic radiation component; the scintillation-based device has lower cut-off radiation energy (0-3 MeV) and therefore rejects most of the cosmic radiation compared to GT. The other main factor responsible for the difference is the detection sensitivity. The data plots from both dosimeters show almost the same information, however, the scintillation data exhibit less fluctuations compared to that of the GT.

Verification of Skin-Point-Source Method to Assess Annual Effective Dose by Usage of TENORM Added Consumer Products

Do Hyeon Yoo^a, Wook-Geun Shin^a, Jae Kook Lee^b, Yeon Soo Yeom^c, Chan Hyeong Kim^c, Chul Hee Min^a

^aYonsei University, Wonju, Republic of Korea

^bKorea Institute of Nuclear Safety, Daejeon, Republic of Korea

^cHanyang University, Seoul, Republic of Korea

Abstract. There is growing concern with the radiation exposure to the public by using products including technologically-enhanced naturally occurring radioactive material (TENORM). However, appropriate method to assess a radiation exposure with the consumer products was not developed yet. The aim of this study is to evaluate the annual effective dose due to the usage of commonly available TENORM added consumer products (pillow, mattresses, accessory etc.) using Monte Carlo (MC) simulations and a computational human phantom. Polygon-Surface Reference Korean phantom, called as PSRK-Man and PSRK-Woman composed of high resolution polygons to represent the organs was employed to evaluate the exposure dose. We also suggest a new source modelling method to effectively determine the various products shape and location by defining the point source in each skin polygon of PSRK-Man and combining the points as required to represent the product. The effective dose by each skin-point-source was compiled into database for 0-2 MeV with 0.1 MeV interval. For the various consumer products, the annual effective dose were assessed with the usage scenario for each product obtained from the Statistics Korea. To validate the skin point source method, the real shape of the product was simulated and for the same energy gammas the effective dose was compared with that by skin-point-source. Our simulation study shows that the skin-point-source shows similar organ dose compare to that by the realistic shape source of the TENORM added consumer products. For the most case, two times higher effective dose was assessed with skin-point-source, because the sources are closer to the organs than the product shape source. Finally our results demonstrate the potential that with the database obtained from skin-point-source could be used to efficiently assess the effective dose just by defining the product usage location in PSRK-Man, PSRK-Woman and its activity without additional Monte Carlo simulation. The safety regulation for the TENORM added consumer product could be easily managed with the current results.

A Dynamic Model to Assess Radiation Dose Rate of Biota in Freshwater Lake

Dong-Kwon Keum, In Jun, Kwang-Muk Lim, Byeong-Ho Kim, Yong-Ho Choi

Korean Atomic Energy Research Institute, Daejeon, Republic of Korea

Abstract. This paper describes a dynamic compartment model to assess the radiation dose for Lake Biota as a consequence of a nuclear accident. The model consists of three parts, a lake transport model, food chain model, and radiation dose rate model. The lake transport model considers three source terms: direct deposition of radionuclides from the atmosphere to the lake surface water, indirect input from the catchment area of the lake through the runoff and soil erosion, and direct discharge from the contaminated upstream. The food chain model considers a typical autotrophic food chain where primary phytoplankton is consumed by zooplankton, which in turn is eaten by prey fish that are prey for predator fish. The biota takes radionuclides from both water and food except for the phytoplankton which uptakes only from water, and loses radionuclides due to radiological as well as biological decay representing a metabolic loss and growth dilution effect. The outputs of the model are the activity concentrations of water, sediment and biota, and the radiation dose rate for biota over time. The model was applied to assess the ^{137}Cs concentration of water and fish in seven lakes of Europe contaminated as a consequence of the Chernobyl nuclear accident which was also considered in the VAMP (Validation of Environmental Model Prediction) project of IAEA/EC. A sensitivity analysis of the model parameters showed that equilibrium distribution coefficient and active surface sediment layer properties (depth and density) will result in a significant change in the water concentration. In addition to the lake transfer parameters, the water and food uptake constant, particularly of zooplankton, influences the predator fish concentration greatly as a consequence the radionuclide transfer through the food chain. A good agreement was found between the predicted and observed ^{137}Cs activity concentration of water and fish which had been measured from lakes after the Chernobyl accident. The calculated time varying radiation dose rate showed that the maximum radiation dose rate would be about $1.5\text{E}2 \mu\text{Gy/d}$ for predator fish in Ovre Heimdalsvatn, Norway, which was much lower than the UNSCEAR benchmark level of $1.5\text{E}7 \mu\text{Gy/d}$ for aquatic biota. The results indicate that the population of biota in all lakes studied will maintain its integrity without any radiological effect despite a Chernobyl type disaster.

Radioecological Assessments of Natural Occurring Radioactive Materials and Dose Estimation of The Public Residing Around Mt. Homa, Homabay County, Kenya

David Otwoma^a, Simon Bartilol^b, Jayant Patel^b

^aNational Commission for Science Technology and Innovation, Nairobi, Kenya

^bUniversity of Nairobi, Nairobi, Kenya

Abstract. External radiation from natural occurring radioactive materials (NORM) in rock and soil samples from Mt. Homa located in southwestern Kenya was measured to evaluate the concentration and distribution of NORM and the radiological hazard to the public was calculated. Absorbed dose rate in air above the ground was measured with portable Sodium Iodide survey meters giving a mean dose rate of 474 nS/h that implied an annual dose due to external radioactivity of 4.15 mSv/y. The highest values for K-40, Ra-226 and Th-232 concentrations measured with hyper pure Germanium detectors were 3017.8, 1567.5 and 1447.0 Bq/kg, respectively. A mean dose rate calculated was 383 nGy/h translating to resultant total effective dose equivalent of 5.03 mSv/y. Using RESRAD code, modeling of K, Th and U environmental pathways of exposure to external radiation, inhalation and ingestion resulted in total effective dose equivalent to exposed individuals gave an estimation of 4.93 mSv/y. Energy dispersive X-ray fluorescence enabled identification of 18 elements among them K, Th, U and rare earths. Mt. Homa study has established that radiation dose to the population qualifies the region as a high background radiation area due to carbonate rocks. The implication is that local materials used for building and human encroachment and settlements should be controlled by the Radiation Protection Board and local authorities.

Novel Method to make a Calibrated Thoron Source

Elmughera Elhag^{a,b}, Robert Lindsay^a, Joash Ongori^a

^aThe University of the Western Cape, Bellville, South Africa

^bAhfad University for Women, Omdurman, Sudan

Abstract. Researchers around the world have recognized that radon (^{222}Rn) is a hazard to human health, and more recently thoron (^{220}Rn) has been found to be a larger problem than expected. Radon is a progeny of radium in the uranium series while thoron is a member of the thorium series. The recent interest for measuring thoron activity in air and the following development of the corresponding measurement techniques, require the improvement of standards for the calibration and characterization of the measurements device which have often been optimized for radon measurements. In this work we describe a simple, cheap method that can provide a reasonably accurate flow of thoron for checking thoron detectors and to investigate thoron measurements. A novel thoron source has been developed using Thorium Nitrate crystals, $\text{Th}(\text{NO}_3)_4$, that are dissolved in water and the thoron is created by bubbling air through the solution using the continuous monitoring detector system, the RAD7. The strength of the source is found by simultaneously measuring the gamma rays from the water using a sodium iodide detector (NaI). The difference in the gamma rays that are emitted before and after the thoron in the thorium decay chain give an accurate measurement of the concentration of thoron that leaves the water. The measurement has to be taken over a few hours to allow for the decay of ^{212}Pb that has a half-life of 10.6 hours.

Radon Gas and Other NORM Testing of Building Materials in Israel for Public Health and Safety (Category 3F)

Ehud Ne'eman

System Advanced Laboratories Ltd., Yavneh, Israel

Abstract. We are the only nationally accredited laboratory in Israel that performs NORM testing on building materials according to Israeli National Standard number 5098. All building materials in Israel must be tested according to this standard and approved for use. Our testing ensures public safety and limits the amount of radioactive materials that industry can include in building materials. This mandatory testing ensures public protection from radioactive materials in doors. With your permission, we would like to present our testing process and conclusions to inform the public on the importance of restricting NORM in construction materials. After all, many of us spend most of our day in doors.

Cost-Benefit Analysis Approach to Risk Assessment of Natural Radioactivity in Powdered and Liquid Milk Products Consumed in Nigeria

Ezekiel O. Agbalagba^a, Gregory O. Avwiri^b

^aFederal University of Petroleum Resources, Dept. of Physics, Effurun, Delta State, Nigeria

^bUniversity of Port Harcourt, Dept. of Physics, Choba, Rivers State, Nigeria

Abstract. This paper presents important facts on Food safety in milks consumed in Nigeria which is in agreement with *NAFDAC* plan to reach its aims regarding the safety of food for human consumption in the area of radionuclides. The natural radioactivity concentration in powdered and liquid milk imported, produced and consumed in Nigeria has been investigated using sodium iodide (7.6cm x 7.6cm NaI(Tl)) detector. The activity concentrations of ²²⁶Ra (radium), ²³²Th (thorium) and ⁴⁰K (potassium) were measured in 10 brands of the powdered milks and 11 brands of liquid milk consumed in Nigeria. The results show that the mean activity concentration of ⁴⁰K in the powder and liquid samples was 468.0±72.7Bqkg⁻¹ and 317.6±58.5Bqkg⁻¹ respectively. The mean values for ²²⁶Ra for powder and liquid milk were 19.2±7.2Bqkg⁻¹ and 16.6±6.3Bqkg⁻¹ respectively, while for ²³²Th it is 12.1±4.8Bqkg⁻¹ and 10.6±4.3Bqkg⁻¹ respectively. The average value of ⁴⁰K in the powder milk was found to be above the standard value set by UNSCEAR for foodstuffs. The activity concentrations of imported milks samples were found to be relatively high compared to some locally produced milk brands. The values of the calculated hazard indices and the radium equivalent of all milk samples were within the permissible limit set by UNSCEAR and other international regulatory bodies. However, the consumption of powder and liquid milk by infants and children at the rate of 14 to 15kg/year will result in radiation dose to vital organs above standard values. It is there recommended that the amount of powder milk consumed per year by infant and children should not exceed 7 and 11kg/year while for liquid milk 8 and 13kg/year. The cost-benefit analysis shows a low collective effective dose equivalent with a mean radiological index ratio of 1:30,839 for infants, 1:50,909 for children and 1:247,145 for adults. The computed values of the total cost of health detriment revealed that children age group has the highest cost health detriment per-caput dose with estimated total cost of health detriment of US \$17.256 million, followed by adults with estimated cost implication of US \$11.864 million while infants is the least with estimated cost implication of US \$10.192 million. The overall results show that the powdered and liquid milks consumed in Nigeria are radiologically safe and may not cause any immediate radiation health hazard to consumers of the examined milk brands while optimizing radiation protection using cost- benefit analysis is recommended.

KEYWORDS: *gamma spectroscopy; milk samples; natural radioactivity; cost-benefit analysis.*

Comparison of Efficiency of Techniques Radon Measurement (^{222}Rn) in Air and Water with Active Detectors and Passive Detectors

Evaldo Paulo de Oliveira, Paulo Roberto Rocha Ferreira, Mariza Ramalho Franklin

Instituto de Radioproteção e Dosimetria IRD/CNEN, Rio de Janeiro, Brazil

Abstract. This study aims to evaluate the efficiency of some measurement techniques of the radioactive gas radon (^{222}Rn) in air and water, with active charcoal passive detectors and plastic Lexan polycarbonate (air) and active detectors AlphaGUARD (air and water) and RAD7 (water). Other equipment was used to compose the measuring system like: radon concentration chamber, air sampler, standard radio source (^{226}Ra), flow calibrator, flow adjuster and wire ducts. The results are presented in tables and graphs. Efficiencies and uncertainties were calculated. Considering these results we conclude that the passive detectors are very useful, each with their respective time limits in various situations that require the detection and evaluation of radon concentration in the environment. For the detection of radon in water, comparing the results with AlphaGUARD RAD7 and showed similar results, requiring smaller corrections.

Organization, Some Results and Perspectives of Protection from Radon in Italy in the European Context

Francesco Bochicchio, Sara Antignani, Carmela Carpentieri, Gennaro Venoso

Istituto Superiore di Sanità, Roma, Italy

Abstract. The protection of population and workers from the health risk due to exposure to radon and its decay products in dwellings and workplaces requires many different actions and involves many different institutions, both national and regional/local ones. Therefore, in order to optimize the protection, it is necessary to set up a national program to coordinate all the required actions, especially in countries with a federal organization. In Italy, several activities have been carried out in the framework of the Italian National Radon Action Plan of 2002, promoted by the Ministry of Health and coordinated by the Italian National Institute of Health. Information and data regarding activities carried out in Italy are collected in the National Radon Archive. In this paper a summary description of organization of radon protection in Italy and some results of the activities carried out by the Italian national and regional institutes and agency institutionally involved in protection from radon are reported. In particular: i) several national and regional surveys were carried out, involving more than 50 000 indoor environments (dwellings, schools and workplaces); ii) lung cancer rates attributable to radon exposure were estimated for each of the 21 Italian regions; iii) remedial actions were carried out in more than 300 buildings, largely in schools; iv) training activities on radon issues, mainly addressed to the public agency personnel. Moreover, the main perspectives for protection from radon exposure in Italy are presented, with particular attention to the requirements of the Directive 2013/59/Euratom and taking into account also the International Basic Safety Standards, including the development of a new national radon action plan.

The IUR FORUM : Worldwide harmonization of networks to support integration of scientific knowledge and consensus development in radioecology

François Bréchnignac^{ab}, Rudolf Alexakhin^c, Andréas Bollhöfer^d, Kristin E. Frogg^e, Frank Hardeman^f, Kathy Higley^g, Thomas G. Hinton^h, Lawrence A. Kapustkaⁱ, Wendy Kuhne^j, Kins Leonard^k, Olivier Masson^l, Kenji Nanba^h, Graham Smith^m, Karen Smithⁿ, Per Strand^e, Hildegard Vandenhove^f, Tamara Yankovich^o, Satoshi Yoshida^p

^aInstitute of Radioprotection and Nuclear Safety (IRSN), Center of Cadarache, BP 3, 13115 St Paul-lez-Durance cedex, France.

^bInternational Union of Radioecology (IUR), Secretariat at Center of Cadarache, BP 3, 13115 St Paul-lez-Durance cedex, France.

^cRIARAE, Obninsk, Russia.

^dSouth Pacific Environmental Radioactivity Association (SPERA) and Environmental Research Institute of the Supervising Scientist, Department of the Environment, Darwin, NT 0810, Australia, (present address: BfS, 79098 Freiburg, Germany).

^eNorwegian Radiation Protection Authority (NRPA), P.O. Box 55, N-1332 Østerås, Norway.

^fSCK-CEN, Belgian Nuclear Research Center, Boeretang 200, 2400 Mol, Belgium.

^gDepartment of Nuclear Engineering and Radiation Health Physics, Oregon State University, Corvallis, OR, USA 97331.

^hInstitute of Environmental Radioactivity (IER), Fukushima University, 1 Kanayagawa, Fukushima-shi, Fukushima 960-1296, Japan.

ⁱLK Consultancy, P.O. Box 373, Turner Valley, Alberta T0L 2A0 Canada.

^jSavannah River Ecology Laboratory (SREL), Drawer E, Aiken South Carolina 29802, USA.

^kCEFAS, Pakefield Road, Lowestoft, Suffolk, NR33 0HT, UK.

^lInstitute of Radioprotection and Nuclear Safety (IRSN), LEREN, Center of Cadarache, BP 3, 13115 St Paul-lez-Durance cedex, France.

^mGMS Abingdon Ltd, Oxfordshire, UK.

ⁿRadEcol Consulting Ltd, Cumbria, UK.

^oInternational Atomic Energy Agency (IAEA), Division of Radiation, Transport and Waste Safety, Vienna, Austria.

^pNational Institute of Radiological Sciences (NIRS), Fukushima Project Headquarters, Chiba-shi, Japan.

Abstract. During the past decades, many specialized networks have formed to meet specific radioecological objectives, whether regional or sectorial (purpose-oriented). Regional networks deal with an array of radioecological issues related to their territories. Examples include the south-Pacific network of radioecologists, and the European network of excellence in radioecology. The latter is now part of the European platform for radiation protection. Sectorial networks are more problem-oriented, often with wider international representativeness, but restricted to one specific issue, (e.g., radioactive waste, low-level atmospheric contamination, modelling). All such networks, whilst often working in relative isolation, contribute to a flow of scientific information which, through UNSCEAR's efforts of synthesis, feeds into the radiation protection frameworks of protecting humans and the environment. The IUR has therefore prompted a co-construction process aimed at improving worldwide harmonization of radioecology networks. An initiative based on an initial set of 15 networks, now called the IUR FORUM, was launched in June 2014. The IUR Forum agreed to build a framework for improved coordination of scientific knowledge, integration, and consensus development relative to environmental radioactivity. Three objectives have been collectively assigned to the IUR FORUM: (1) coordination, (2) global integration and construction of consensus, and (3) maintenance of expertise. One particular achievement of the FORUM was an improved description and common understanding of the respective roles and functions of the various networks within the overall scene of radioecology R&D. It clarifies how the various networks assembled within the IUR FORUM interface with UNSCEAR and other international regulatory bodies (IAEA, ICRP), and how consensus on the assessment of risk is constructed. All these agencies

interact with regional networks covering different geographical areas, and with other networks which address specific topics within radiation protection. After holding its first Consensus Symposium in 2015, examining the possible ecological impact of radiation from environmental contamination, the IUR FORUM continues its work towards improved radiation protection of humans and the environment. We welcome new members.

KEYWORDS: radioecology; environment; radiation protection; scientific networks; science harmonization; science coordination; knowledge synthesis; consensus development.

Radiation Protection Dosimetry (2017), Vol.173, No.1-3, pp. 36–42
doi:10.1093/rpd/ncw290

Thoron: Radon's Lesser-Known Sister – Results from a National Survey in the Netherlands

Fieke Dekkers, Roelf Blaauboer, Martijn vd Schaaf, Harry Slaper, Ronald Smetsers

Netherlands National Institute for Public Health and Environment (RIVM), Bilthoven, The Netherlands

Abstract. In radiation protection policies, thoron (Rn-220) receives far less attention than its sister isotope radon (Rn-222). Unexpectedly, results from a small Dutch study in 2012 suggested that in the Netherlands this was not justified: we found indications that the effects on public health of the two noble gases could be comparable. We have recently completed a national thoron survey designed to investigate if the significance of thoron for radiation protection in the Netherlands is indeed underestimated. Since thoron has a short half-life of just under one minute, there is no meaningful way to define 'the' thoron concentration in a room: a measured concentration will always depend strongly on the distance to the nearest source of thoron. Recently, passive detectors that can be used to determine the concentration of lung-damaging decay products of thoron have become available. Some of these decay products have longer half-lives, and their concentrations can meaningfully be measured. This development made it possible to determine thoron progeny concentrations in a large survey. In the largest such study conducted worldwide, we have measured thoron progeny in 3000 Dutch living rooms in dwellings built after 1930. In a smaller study conducted in parallel we measured both thoron exhalation rates and thoron progeny concentration, with the aim to determine the effects of sources of thoron on the concentrations measured. We will discuss the results of both studies, and their relevance for radiation protection policies.

^{40}K , ^{226}Ra And ^{228}Ra in Soils of Rio de Janeiro State, Brazil: A Preliminary Study

Fernando Ribeiro^a, Dejanira Lauria^a, Jose Ivan Silva^a, Fernanda Cunha^b

^aInstitute of Radiation Protection and Dosimetry, Rio de Janeiro, RJ, Brazil

^bCompanhia de Pesquisa de Recursos Minerais, Rio de Janeiro, RJ, Brazil

Abstract. The radionuclides ^{40}K , ^{226}Ra and ^{228}Ra are naturally present in soils and their concentrations vary, mainly due to the different original rock material of the soil, organic matter and landscape, among other factors. The Rio de Janeiro State, southeast of Brazil, concentrate most activities related to the nuclear power generation, including the production of nuclear fuel and also both nuclear power reactors. With the aim of mapping the distribution of these radionuclides in soils of the state, soils samples from the B horizon were collected in all state territory, the sampling points located 25 km distant from each other. The samples were oven dried, stored in polyethylene pots and sealed to reach the secular equilibrium between ^{226}Ra and its decay products, then analyzed by gamma spectrometry with a hyper pure germanium detector and associated electronic devices. The activity concentration ranged from to 55 to 1552 Bq.kg⁻¹ to ^{40}K , from 1.94 to 74.64 Bq.kg⁻¹ to ^{226}Ra and from 3.74 to 170.10 Bq.kg⁻¹ to ^{228}Ra . The software Qgis was used to produce maps showing the occurrence of the radionuclides. The obtained values will be used to establish a diagnosis of the occurrence of these radionuclides in soils of Rio de Janeiro state.

Gamma in Situ Survey in an Experimental Research Area

Fernando Ribeiro, Rocio Reis, Monique Gabriel

Institute of Radiation Protection and Dosimetry, Rio de Janeiro, RJ, Brazil

Abstract. The Institute of Radiation Protection and Dosimetry - IRD has an open sky area used for research of soil and plant transfer factor. During years many research projects were performed there and because of it a doubt about radiological contamination arises. Radiation protection is connected with a safety culture policy. Institute of Radiation Protection and Dosimetry focus in avoiding unnecessary risks or dangers to people, workers and environment. The goal of this research was to discover if the area has been contaminated with radionuclides. Gamma in situ survey was chosen as methodology because of cost and time advantages. AT6101C Spectrometric Portable Radiation Scanner was used and it produced 785 georeferenced points with a averaged dose of 0.17 $\mu\text{Sv/h}$ and a higher dose measurement of 0.27 $\mu\text{Sv/h}$. Using environmental assessment spatial decision support tools was possible to conclude that radiation activity at experimental research area is similar to the levels of the background.

Measurement of ^{137}Cs and ^{40}K in Wild Mushrooms and their Transfer Factors

Fei Tuo, Qiang Zhou, Jing Zhang, Wenhong Li, Qing Zhang

National Institute for Radiological Protection, Chinese Center for Disease Control and Prevention, Beijing, China

Abstract. Radioactivity measurements in the environment and foodstuffs have become very important to evaluate the radiation levels to which man is exposed either directly or indirectly. Environmental biomonitoring has demonstrated that organisms such as crustaceans, fish and mushrooms are useful to evaluate and monitor both ecosystem contamination and quality. Some mushroom species have a high capacity to retain radionuclides and some toxic elements, to evaluate the extent of radioactive contamination and ingestion doses to man from consumption of wild mushrooms. Samples were collected from some natural forest, China. Soil samples were collected concurrently with mushrooms at sampling site. After collection they were then placed in labelled polythene bag. After collection, the species of the mushrooms were identified at the Institute of Microbiology of the Chinese Academy of Sciences (IMCAS), soil particles were removed from the fruiting bodies by washing with water. Samples were dried at 100°C . They were then ground into powder, and homogenized in a domestic blender with Ti blades. About 140 g of each dried mushroom sample was weighed and placed in a polyethylene bottle. The bottle (75 mm of diameter and 70 mm of height) was stored for approximately 4 weeks until the respective counting. The activity concentrations of ^{137}Cs and ^{40}K were analysed by using high-purity germanium (HPGe) γ spectrometry. Except for one sample that was below the MDC, artificial radionuclides of ^{137}Cs were detected in all of the other samples, activity concentration of ^{137}Cs were in the range of 0.45 to 339.58 Bq/kg (dry weight), with an average 25.47 Bq/kg (dry weight). In regards to ^{40}K in edible mushrooms, all species presented the activity concentrations for this radionuclide and the levels varied from 453.4 to 1 882.6 Bq/kg (dry weight), with an average 815.1 Bq/kg (dry weight). There was significant difference for ^{137}Cs among 6 species of mushroom named, but no significant difference for ^{40}K . For part species of the mushrooms, soil–mushroom transfer factor (TF) was also determined, their TF values ^{137}Cs were in the range 0.08–1.94, and ^{40}K values in the range 0.95 to 2.48.

Assessment of Natural Radioactivity and its Radiological Impact in Ortum Region in Kenya

Felix Wanjala

National Commission for Science, Technology and Innovation, Nairobi, Kenya

Abstract. The earth contains natural background radiations originating from terrestrial and cosmic sources. This study aims at assessing the levels of background radiation in air, soil and water and its associated radiological impact and also determines the elemental concentration of the rocks and soils around Ortum hills and quarry. 100 points will be measured for radioactivity in the air and 40 soil and 10 water samples will be collected for laboratory analysis using both grid and purposive sampling methods. Radioactivity in the field will be determined using the hand held RedEye and Radiagem radiation survey meters. The levels of naturally occurring radionuclide Uranium-238 (^{238}U), Thorium-232 (^{232}Th) and Potassium-40 (^{40}K) in the soil and rocks will be determined using High Pure Germanium (HPGe) detector; the Liquid Scintillation Counter (LSC) will be used for analysis of water samples while the Energy Dispersive X-Ray Fluorescence Spectrometer (EDXRF) will be used to determine the elemental composition in the rocks and soil. The RESidual RADioactivity (RESRAD) program will be used to analyze and assess the doses and risks associated with radiation exposure in Ortum region.

Radiation from Building Materials in South Africa including Granite Samples with High Concentrations of Radium

Farrel Wentzel, Robert Lindsay

University of the Western Cape, Bellville, South Africa

Abstract. There is considerable public concern about radon exhalation from building materials. The purpose of this study is to address this public concern and to estimate the contribution of building materials to indoor radon levels. As in soil and rock; radon gas is formed inside the building materials by decay of the parent nuclide ^{226}Ra . It is not possible to determine the radon exhalation rate simply from the activity concentration of ^{226}Ra , instead one must measure radon exhalation rates directly from the surface of the material. ^{222}Rn has been identified as an important factor that could result in a health hazard by studies all around the world. The experiments were done at the UWC physics department, in the Nuclear Physics Lab. A RAD7 radon detector was used to measure the radon concentration via the energies of alpha particles that are emitted. The RAD 7 records the number of alpha particles with an energy of 6.11 MeV which results from the decay of ^{218}Po , the daughter of ^{222}Rn . The RAD 7 detector converts counts into Becquerel's per cubic metre (Bq/m^3). The building materials tested was the raw materials used in construction such as two different types of building sand, stones and gravel. The building materials used for composed of various raw materials to create a final product was floor-and-roof tiles and various granites from across the country. Many building materials were found to have a very low rate of radon exhalation. The only materials that had any significant radon exhalation were 2 granites and stones used in the foundations of a house that were collected at a mine prospecting site. It is safe to say that the overwhelming majority of building materials are safe to use but some granites and some materials may require further study.

Ionising Radiation from the Zanzibar Coastline: Exposure to Residents and Tourists Visiting Zanzibar

Gharib Mohamed^{a,b}, Robert Lindsay^a, Peane Maleka^c, Joash Ongori^a

^aThe University of the Western Cape, Bellville, South Africa

^bThe State University of Zanzibar, Zanzibar, Tanzania

^cDepartment of Nuclear Physics, iThemba Laboratory for Accelerator Based Sciences, Somerset West, South Africa

Abstract. Everyone on the planet is exposed to some background radiation. Human exposure to ionising radiation is one of the scientific subjects that attracts public attention, since radiation of natural origin is responsible for most of the total radiation exposure of the human exposure. Many governmental and International bodies such as the International Commission on Radiological Protection (ICRP) and the World Health Organisation (WHO) have adopted strong measures to minimize such exposure. Despite the interest of the scientific world to assess the exposure to ionising radiation, there is no data regarding natural radioactivity about Zanzibar until now. The coastline of Zanzibar is among the tourists destinations in East Africa. The coastline is also used for human settlement and other activities such as fishing and subsistence farming. The levels of natural radioactivity in Zanzibar beaches and soils were measured using a combination of in-situ and ex-situ gamma-ray spectroscopy. The in-situ gamma-ray survey was conducted using the Multi Element Sediment Detector for Underwater Sediment Activity (MEDUSA) detector. The detector was mounted on the front of a 4×4 vehicle, 60 cm off the ground. Activity concentrations of the primordial radionuclides were extracted from the MEDUSA spectra using the Full Spectrum Analysis (FSA) procedure. The collected beach sands and soil samples from the beaches and the land mapped using the MEDUSA detector were analysed using a hyper-purity germanium detector (HPGe). Both stationary and mobile measurements were made using the MEDUSA detector. Specific activity concentrations based on the emissions of ²³⁸U and ²³²Th and their progenies together with ⁴⁰K from soil and beach sands were calculated and found to be less than the world average value of a typical soil with an exception of the beach sand collected from Kukuu, in the Southern part of Pemba. The Kukuu beach consists of heavy mineral black sand which can cause the elevated level emitted from this beach. The radiological hazards indices and their effects to the population who live or use Zanzibar coasts have been evaluated. From the study, it was found that the measured dose parameters are less than the threshold values. Hence there are no radiological risks to the population living or using Zanzibar beaches for various activities.

Results from Interlaboratory Comparison on Gross Alpha/Beta Activity Measurement in Waters

Gordana Pantelic, Marija Jankovic, Natasa Sarap, Dragana Todorovic

Vinca Institute of Nuclear Sciences, Belgrade, Serbia

Abstract. The determination of radionuclides in drinking is very important in Serbia since the implementation of new regulation. It has been recommended to apply screening methods for a first cost-saving assessment of the radioactive content in drinking water. The parameters of choice are the gross-alpha and gross-beta activity concentration. If the gross-alpha activity in a tap water sample is lower than 0.5 Bq/l and the gross-beta activity does not exceed 1.0 Bq/l, it can be assumed that the annual total indicative dose of adults is less than 0.1mSv per year. Radiation and Environmental Protection Department, Vinča Institute of Nuclear Sciences is regularly participated in international proficiency tests or interlaboratory comparisons to confirm analytical performance. This is a best way to check the entire procedure and methods of the measurements and the reliability of the standard used. According to that we participated in the EC interlaboratory comparison on gross alpha/beta activity in drinking waters in 2012 (two mineral water samples and one water sample spiked with alpha and beta emitting isotopes from European Commission Joint Research) and in IAEA-TEL-2014-04 ALMERA during 2014 (two water samples). Procedure for determination of gross alpha/beta activity in waters includes evaporation of certain volume to the dry residue, under infrared lamp. The remaining was heated to dryness at 450 °C. The residues were transferred quantitatively to a stainless-steel planchete. Measurements were performed immediately after preparation. Gross alpha and beta activity in water samples were determined by α/β low level proportional counter Thermo Eberline FHT 770 T. The accuracy and reproducibility of gas proportional counter were verified on a periodic basis - every week. Total background count rate without a source is monitored to verify that the detector and shield have not been contaminated by radioactive materials. Alpha and beta efficiencies of gas proportional counter were checked with ^{241}Am and ^{90}Sr sources respectively. The counting efficiencies for the system are 23 % for alpha and 33 % for beta. The results of IAEA interlaboratory comparison showed that all results were accepted. The results of EC interlaboratory comparison showed that two of gross alpha and two of gross beta results were in acceptance limit, while one gross alpha result is much lower and one gross beta result is much higher than reference value.

Source Identification of Iodine-131 in Environmental Samples around the HANARO

Geun-Sik Choi, Jong-Myoung Lim, Young-Gun Ko, Mee Jang, Won-Young Kim, Wannoo Lee, Young-Yong Ji, Hyuncheol Kim, Chang-Jong Kim, Young-Hyun Cho, Chung-Sup Lim, Kun-Ho Chung

Korea Atomic Energy Research Institute, Daejeon, Republic of Korea

Abstract. Concern regarding the radioactivity from nuclear facilities has been more growing over the last decade due to the FDNPP accident. The main objective of the monitoring for radionuclides around nuclear facilities is to provide accurate and timely data on the level and degree of hazards from leakage accident. To determine the proper handling options, the ordinary trends and origins for the radioactivity levels in environments should be routinely monitored. Iodine-131, the fission product of nuclear facilities, is also widely used as medical isotopes for cancer diagnostic and treatment procedures. The iodine-131 is notable for causing mutation and death in cells through various pathways. Thus, it is important that all of transport media from nuclear facilities should be monitored. In this study, in order to evaluate the effect of RIPF in HANARO, radioactivity of I-131 in the environmental samples including river sediments, ground water, aquatic plants, and fishes were periodically determined from 2008 to 2015 using the gamma-spectrometer (ORTEC Co.). The samples were also collected in the Gap-cheon river, which is located by waste water treatment facility. Finally, the release amounts of the I-131 were compared between from nuclear facility and from unavoidable medical usage.

Natural Radioactivity Systematics in a Complex Hydrothermal Environment

Hudson Angeyo Kalambuka, Paul Tambo, Jayanti Patel, Michael Mangala

^aDepartment of Physics, University of Nairobi, Nairobi, Kenya

^bInstitute of Nuclear Science & Technology, University of Nairobi, Nairobi, Kenya

Abstract. The Magadi endorheic basin in Kenya, with its high heat flows and extremely saline geothermal manifestations, presents a complex hydrothermally altered environment that is challenging to radiogenically characterize and model for ecosystem quality assessment. It is at the centre and lowest point of a vast region and the confluence point for all surface and groundwater flows in the region, but with no outflows. We studied natural radioactivity levels and variability as well as its origins and distribution in geothermal spring waters, sediment and trachyte rocks associated with the Lake Magadi endorheic basin. The natural activity concentrations and spectral signatures corresponding to the radionuclides were determined and explored using multivariate chemometric techniques to characterize the radionuclide sources, model their occurrence within the basin, and interpret the systematics of their occurrence. We have discovered remarkable spatial variability in the activity concentrations of the radionuclides in the rocks and delineated three regimes of highly alkaline hydrothermal inflows that contribute to and affect the quality of trona deposits. The results also show that the Lake Magadi endorheic basin is a sink for radionuclides from the weathering of surrounding, making it a quasi-high background radiation area. (HBRA). Statistical analysis indicates an uneven spatial distribution within the basin, probably due to different radionuclide signatures of the spring recharges. It also predicts the presence of an underlying uranium-rich rock source. Pairwise analysis of the radionuclide ratios indicates that the geochemical immobilization of U-238 and Th-232 in groundwater flows are the same in the entire basin. It also shows thorium sorption capacity in sediments is strongly modulated by temperature with high temperatures enhancing it.

Measurements of Radon Concentrations in Drinking Water in Cities, China

Hongxing Cui, Yunyun Wu, Bing Shang, Jianxiang Liu

National Institute for Radiological Protection, Chinese Center for Disease Control and Prevention, Beijing, China

Abstract. Radon is believed to be the second- largest cause of lung cancer after smoking. Radon dissolved in water can be released to indoor air and contributes to the total inhalation risk of indoor radon. The aim of this study is to understanding radon levels in drinking water in Capital cities, China and to evaluate radiation doses to the population resulting from inhalation of radon from water. A total of 386 water samples from 31 Capital cities and Municipalities in China were collected. ^{222}Rn concentrations in drinking water samples in 31 Capital cities and Municipalities, China were determined using RADH20 (DurrIDGE Co., USA). A total of 386 water samples were sampled and analyzed for their ^{222}Rn content. The observed radon levels were in a range of $< \text{DL-43.15 Bq L}^{-1}$, with a mean of 5.13 Bq L^{-1} . It is found that 83.7% of all analyzed water samples gave radon values of less than 11 Bq L^{-1} recommended by the EPA, and there's no radon in drinking water exceeding the European Union recommended level of 100 Bq L^{-1} for radon in public or commercial waters. A radon dose conversion factor of $22 \times 10^{-9} [\text{Sv}/(\text{Bq h m}^{-3})]$ for radon inhalation, radon transfer from water to air which is equal to 10^{-4} , the average annual indoor occupancy of 7,000 h and equilibrium factor of 0.4 were considered. The annual effective dose for average radon content in water is $31.6 \mu\text{Sv}$ and for maximal observed radon concentration in water corresponding dose is $265.8.8 \mu\text{Sv}$. The risk of inhalation radon released from drinking water should be concerned for consumers who use water with high radon concentration in household.

¹⁴C Activity in Atmospheric CO₂ and Biological Samples Around the Nuclear Power Plant Krško, Slovenia

Ines Krajcar Bronić^a, Bogomil Obelić^a, Jadranka Barešić^a, Nada Horvatinčić^a, Borut Breznik^b, Aleš Volčanšek^b, Andreja Sironić^a, Damir Borković^a

^aRuđer Bošković Institute, Zagreb, Croatia

^bNuclear Power Plant Krško, Krško, Slovenia

Abstract. ¹⁴C activity in the atmospheric CO₂ and in biological samples in the close vicinity of the Krško Nuclear Power Plant (NPP) in Slovenia has been regularly monitored since 2006 with the aim of estimating a possible influence of the NPP on environmental ¹⁴C levels and on the effective dose of local population through food chain. Atmospheric CO₂ on two locations was collected every two months, or in shorter periods during some refuelling periods. Biological samples (apples, corn, wheat, grass, vegetables) were collected twice a year (in summer and autumn) in two circles around the NPP, inner and outer, and at the control point 12 km from the plant. Increase of ¹⁴C activity in atmospheric CO₂ was observed during and immediately after the refuelling of the power plant, performed every 18 months. Good correlation between the total ¹⁴C activity released in gaseous effluents and the ¹⁴C activity of the atmospheric CO₂ has been observed. ¹⁴C activity in plants collected close to the Krško NPP is always higher than the activities on the control point, and depends both on the distance from the exhaust of the plant ventilation system and on wind direction: it is higher on the location in the SW-NE direction that coincided with the most pronounced wind directions. Higher ¹⁴C activities have been determined in plants collected in summer after the spring refuelling than in those collected during the following vegetation period after the autumn refuelling. This can be explained by the uptake of the CO₂ of higher ¹⁴C activity for the process of photosynthesis after spring refuelling. To estimate the realistic effective dose due to ingestion to the population in the vicinity, a model of food consumption has been proposed. The calculated dose for the population at the NPP vicinity is not significantly different from the dose for the population at the control point.

Control of Emissions from a Gold and Uranium-mining Polluted Catchment in a Semi-arid Region of South Africa: The Varkenslaagte Stream

Isabel Weiersbye^a, Peter Dye^a, Hlanganani Tutu^a, Ewa Cukrowska^a, Christopher Curtis^a, Julien Lusilao^a, Elisee Bakatula^a, Bruce McLeroth^a, Jozua Ellis^b, Etienne Grond^b, Maxine Joubert^a, Salome Mthombeni^a, Ike Rampedi^a, Christopher Davies^a, Patricia Omo-Okoro^a, Henk Nel^b, Joel Malan^b, Herman Coetzee^b

^aUniversity of the Witwatersrand, Johannesburg, South Africa

^bAngloGold Ashanti Limited, Johannesburg, South Africa

Abstract. The upper Varkenslaagte stream was canalised prior to the 1930's, and, since the 1950s, formed a conduit for acid mine drainage (AMD) and NORM-contaminated seepage from gold and uranium (U) tailings facilities situated on the catchment. In order to lower the perched water-tables, woodlands with water-use ranging from 650 mm to ~1200 mm were planted on the plumes between 2003 and 2011. Soil surveys identified historical tailings spills, to which radiation in the stream was largely attributed, and +/-84,000 m³ of tailings was removed in order to eliminate this source. Re-shaping of the stream pathway onto the original wetland soils, and establishment of riparian vegetation, was facilitated by 50 metre grid surveys with detailed delineation of soil classes. Since 2013, the upper stream has flowed through a managed reed-bed system comprised of *Phragmites australis*, *Typha capensis*, *Schoenoplectus* and *Cyperus* species, with a variety of micro-algae. The reed-beds attenuate flow, evaporating and polishing contaminated water. Despite the lack of a highly functional organic layer, developing reed-beds exhibit retention of metals, including U (from 1.3 to 23 µg/g dry mass in sediments of 0-2 cm depth). Uranium concentrations decline to <1 µg/g by 5-10 cm depth. The concentration of U in trees is species-specific, from <0.01 to ~50 µg/g dry mass, in the order of root>leaves>bark> wood, whereas aquatic plants contain 2 to 33 µg/g U in rhizomes and roots, and 5 to 11 µg/g in leaves. The terrestrial mycorrhizal fungi and stream algae accumulate U to concentrations an order of magnitude greater. It is anticipated that reed-beds will require harvesting and de-sludging at intervals. Surface water-flow was logged continuously between 2004 and 2014, and has declined as a function of a cut-off trench and abstraction by woodlands and reedbeds (ET~1170 mm), with negligible surface flow by 2014. Water quality remains poor within reed-beds, but improves downstream due to the contaminant retention and dilution. The small mammals of the Varkenslaagte have been monitored since 2010 in terms of food-webs, population health and metals in hair, and monitoring will be extended to aquatic insect and amphibian larvae, which are re-colonising as stream salinity declines. This paper will focus on the sequestration and release of U by abiotic and biotic components of the woodland / wetland system, and present a seasonal budget for the Varkenslaagte.

The Potential for Phytoremediation of Uranium Contaminated Substrata on the Witwatersrand Basin of South Africa: Extraction and Harvesting Versus in Situ Sequestration

Isabel Weiersbye^a, Ewa Cukrowska^a, Jozua Ellis^b, Peter Dye^a, Bruce McLeroth^a, Hlanganani Tutu^a, Luke Chimuka^a, Nosipho Mtungwa^a, Maxine Joubert^a, Shakera Arendse^a

^aUniversity of the Witwatersrand, Johannesburg, South Africa

^bAngloGold Ashanti Limited, Johannesburg, South Africa

Abstract. Tailings facilities in the Witwatersrand Basin have covered almost 500 km² of land since the early 1900s, and contain an estimated 430,000 tons of low grade uranium. Impacts beyond facilities include dust (Van As et al. 1992) and pollution of water and soils (Funke, 1990; Hodgson et al., 2001; Sutton & Weiersbye, 2006; Tutu et al., 2008). The acid mine drainage and metal contaminated areas around facilities are zones of intense selection for tolerant flora, and thus a rich source for bioremediation. Since 1996, over seventy tailings dams on the Witwatersrand Basin and surrounding polluted soils (in combined area exceeding 100,000 hectares) have been surveyed for plants together with their substrate affinities and physiological traits, a total of 600 plant species and subspecies (Weiersbye et al., 2006). The most abundant plant taxa are those with acidophile, gypsophile, halophyte and metallophyte tendencies, i.e. acid, sulphate, salt and metal-tolerant plants, and the majority are associated with similarly tolerant mycorrhizal fungi (Straker et al., 2007, 2008; Spruyt et al., 2014). Analogous naturally saline and uraniferous environments in sub-Saharan Africa have yielded similar patterns. These findings form the basis of the phytoremediation philosophy at AngloGold Ashanti's South African operations, where gold, uranium and sulphur are products. Approaches tested include, (i) control of groundwater plumes by strategically planted woodlands (Dye et al., 2008; 2014); (ii) decontamination of water and soils using fungi, algae and plants that sequester contaminants in biomass for harvesting, including naturally occurring radioactive elements; and (iii) on tailings and NORM-contaminated footprints, two strategies, the first using flora with low translocation factors for uranium and other metals (i.e. to limit the transfer of contaminants from tailings into above-ground biomass), and the second using plants with high translocation factors, i.e. to in contrast promote extraction, resulting in a de-contaminated substrate. Whereas the objective on footprints is to meet the conditions for conditional or general release of land for other uses, on tailings facilities such a decontaminated zone could function as an in situ cap, thus reducing the need to import clean soil for cladding. This paper will report on the above approaches, focusing on translocation factors for uranium in biomass of 43 plant species, assessed throughout their life-cycles in a range of soil types and media.

Uranium in Phosphate mining

Jacques Bezuidenhout

Stellenbosch University, Saldanha, South Africa

Abstract. High concentrations of uranium are normally associated with phosphate mining, specifically when mining sedimentary phosphate reserves. This usually results in radioactive contamination of areas where phosphate mining operations are executed. The Gamma In Situ Portable Instrument (GISPI) is a transportable and robust gamma ray detection system that is ideal to survey large areas for radioactivity. The GISPI was consequently employed to measure and plot the concentrations of radium, thorium and potassium at a spend phosphate mine on the West Coast of South Africa. The measurements showed fairly high concentrations with medians of 320 Bg/kg for ^{226}Ra , 64 Bg/kg for ^{232}Th and 390 Bg/kg for ^{40}K . The highest concentrations were however confined to specific areas of the mine. Follow-up detailed surveys were conducted at these areas where high nuclide concentrations were found. The effective dose for all the areas of the mine was also estimated and the highest estimated level was 0.45 mSv/y. The paper finally draws conclusions as to the impact of the radiation and possible methods to deal with uranium when mining for phosphate.

Uranium in Wild and Cultivated Leafy Vegetables and Consumption Patterns: A Risk Assessment

Jenny Botha^a, Isabel Weiersbye^a, Jozua Ellis^b, Hlanganani Tutu^a

^aUniversity of the Witwatersrand, Johannesburg, South Africa

^bAngloGold Ashanti Limited, Johannesburg, South Africa

Abstract. Urban settlements have been established within mining zones on the Witwatersrand, where extraction of uraniferous ores has been carried out for over 120 years. Potential exposure routes include ingestion of contaminated food and water, inhalation and dermal. When grown on contaminated lands, some vegetables assimilate contaminant metals, including uranium (U), into their roots and shoots. The consumption of wild leafy vegetables depends on factors including household incomes, urbanization and seasonal availability. Vulnerability to toxicity depends on (i) concentrations of the toxin, and the quantity consumed; (ii) period of exposure; (iii) the physiology of the consumer; (iv) the age of the consumer; (v) quality of diet; (vi) body weight (vii) gender. Chronic toxicity may occur through exposure over an extended period of time. This review and studies were conducted to gain an understanding of the potential for exposure to uranium toxicity and radiation dose through the consumption of local wild and cultivated leafy vegetables in a typical settlement. Three iterative studies were conducted to determine potential risks to human health through the consumption of locally cultivated and wild harvested: (i) Consumption patterns of wild and locally cultivated leafy vegetables in Kanana, North West Province, and risks to human health, involving structured interviews to identify which species are eaten, when, and in what form and quantities (mass/day); (ii) Growth and metal content of leafy vegetables in a dose-response trial on tailings-contaminated soils, and (iii) Does cooking method affect the potential toxicity of plants from contaminated land? In the first study, interviews were conducted to determine household socioeconomic status and consumption patterns. *Amaranthus hybridus*, *Brassica oleracea*, *Spinacia oleracea* and *Chenopodium album* plants were then harvested from home gardens, growing wild adjacent to tailings facilities, and from a controlled dose-response container experiment with tailings-contaminated soils. Concentrations of U were generally between <1 and 30 µg/g dry mass of uncooked plant material. This paper reports the concentrations of elements in the raw, fried and boiled leaves, and the dietary metal intake of U per meal, based on the mass of food and average consumer body weight. The results are compared with the Provisional Tolerable Weekly Intake (PTWI) limits for toxicity and effective dose.

Calculation of Lifetime Lung Cancer Risks Associated with Indoor Radon Exposure Based on Various Radon Risk Models

Jing Chen

Radiation Protection Bureau, Health Canada, Ottawa, Ontario, Canada

Abstract. Exposure to indoor radon has been determined to be the second leading cause of lung cancer after tobacco smoking. With recent long-term radon measurements in more than 14000 homes in 121 health regions across Canada, the Canadian population risk for radon induced lung cancer was re-assessed using the risk model developed by U. S. Environmental Protection Agency (EPA) (a reasonable average of the estimates from the two BEIR VI preferred models resulting from the joint analysis of 11 cohort studies of radon exposed miners). The theoretical estimates show that about 16% of lung cancer deaths among Canadians are attributable to indoor radon exposure. This article calculates the lifetime risk of lung cancer associated with indoor radon exposure, based on several key risk models available in the literature with the same Canadian data sets as applied in previous estimates with the EPA radon risk model. Radon risk models considered in this comparative study are the joint analysis of three European cohorts of uranium miners in the Czech Republic, France and Germany; the joint analysis of 13 European residential radon studies; and the joint analysis of 7 North American residential studies. Variations in risk estimation among those models are presented and discussed. Because of rather large variations in predicted risk, the communication to the public is of very challenging. For many people, risk predicted by models is often viewed as “theoretical” or “hypothetical” risk which may not be real. The aim of this article is to make clear that various models are mathematical descriptions of epidemiologically observed real risks in different environmental settings. The risk is real and it is perfectly normal that large variations exist for observed outcomes in different environmental settings where some environmental parameters are unknown or not well known. To improve the accuracy of risk estimation/prediction, more research is needed to not only fill knowledge and data gaps but also to elaborate technical details in risk assessment. This takes time, and variations in risk prediction will be seen for a long time. While living with such large variations, we should always remember the fact that long term exposure to elevated radon concentration increases the risk of developing lung cancer.

Radiation Protection Dosimetry (2017), Vol.173, No.1-3, pp. 252–258
doi:10.1093/rpd/ncw297

Measurement Results of Background Radiation Levels in Seals

Jing Chen^a, Weihua Zhang^a, Baki Sadi^a, Xiaowa Wang^b, Derek Muir^b

^aRadiation Protection Bureau, Health Canada, Ottawa, Ontario, Canada

^bAquatic Contaminants Research Division, Environmental Canada, Burlington, Ontario, Canada

Abstract. For marine and fish products, it is well known that the top three radionuclides of interest are ^{210}Po , ^{210}Pb and ^{226}Ra with reference concentrations of 2, 0.2, and 0.1 Bqkg⁻¹, respectively. The reference values (UNSCEAR 2000) were derived with very limited data. To better understand background radiation levels in country foods, this study provides additional information on natural background radiation levels in seal. A total of 107 tissue samples (39 blubber, 39 liver, and 29 muscle samples) from 40 ringed seals were collected in Arviat area during the fall of 2014. Concentrations of naturally occurring radionuclides (such as ^{226}Ra , ^{210}Pb , ^{210}Po and ^{40}K) as well as long lived contaminants (such as ^{137}Cs) were measured. ^{210}Po was detected in all muscle and liver samples in varying concentrations. The average ^{210}Po concentrations were 25 Bq/kg fw (ranged from 13 to 39 Bq/kg fw) and 211 Bq/kg fw (ranged from 112 to 297 Bq/kg fw) for muscle and liver, respectively. No ^{210}Po was detected in blubber samples. Generally speaking, ^{210}Pb and ^{226}Ra were not detected in all samples studied here. ^{40}K was detected in all samples in varying concentrations. The average ^{40}K concentrations were 66, 9.8 and 9.6 Bq/kg fw for muscle, liver and blubber, respectively. This study confirmed that ^{210}Po is the dominant contributor to radiation doses resulting from marine food consumption. None of the seal samples analysed in this study contained any detectable levels of ^{134}Cs . In the environment, ^{137}Cs has mainly resulted from the fallout of atmospheric nuclear weapons tests in the 1950s and 1960s and accidental releases such as from the Chernobyl accident in 1986. The average ^{137}Cs levels of 0.25 and 0.017 Bq/kg fw were observed in muscle and liver samples, respectively. Our analyses indicate that the average ^{137}Cs concentration in seal is comparable to the levels observed in marine fish harvested from the Canadian west coast in 2013 and 2014. In conclusion, the resulting radiation dose for people from consumption of seal products would be a very small fraction of the annual dose from exposure to natural background radiation in Canada. Therefore, seals pose no radiological health concern.

The Current Status and Plans for Safety Management of NORMs in South Korea

Jaekook Lee, Jaewoo Park, Zu Hee Woo, Boncheol Koo, Ki Hoon Yoon, Chang-Su Park, Byung-Uck Chang

Korea Institute of Nuclear Safety, Daejeon, Republic of Korea

Abstract. The objectives of this paper are to introduce the current states, the difficulties, and future plans for NORM and NORM safety management in South Korea. There is an individual act which defines NORM safety management in South Korea, called “Act on Protective Action Guidelines against Radiation in the Natural Environment”. By following this act, the handlers, who deal with NORMs contained over 1 Bq/g and 1,000 kBq of U-series and Th-series, or 10 Bq/g and 10,000 kBq of K-40, should be registered. Therefore, 33 handlers have been registered until 2014. In addition, the field survey called, “Investigation and Analysis of the Actual State of Safety Management of Radiation in the Natural Environment” was carried out to 43 NORM workplaces until 2014. The targets for the survey were not only the registered handlers, but also unregistered handlers, manufacturers who produce the products containing natural radionuclides, or owners of suspicious materials which were detected with the Radiation Portal Monitors (RPMs). Also, there were 53 RPMs were installed and operated at the international harbors and airport until 2014. However, there were several difficulties for NORM safety management. At first, sufficient surveys and investigations were necessary to figure out the entire state of NORM industries, but not enough information has been collected. Also, NORM safety was strongly connected with the low dose exposure, so it was hard to decide the level of NORM safety management. Moreover, the handlers were not familiar with radiation and radiation safety and had no or little information. The situations made the decision hard, too. Technical difficulties existed, for example, development of NORM exposure scenarios, the enhancement about the radioactivity analysis for natural radionuclides, improvement of effectiveness of radiation monitoring with RPMs, and etc. Therefore, in conclusion, the plans will be established for continuous and professional surveys and investigation to figure out NORM status, the documents for the handlers to understand NORM and NORM safety management, and studies and researches to develop technical basis.

Pre-assessment of Dose Rates for Marine Biota from Discharge of Nuclear Power Plants

Jingjing Li, Senlin Liu, Yongxing Zhang, Ling Chen, Yuan Yan, Weiya Cheng, Hailin Lou, Yongbao Zhang

China Institute of Atomic Energy, Beijing, China

Abstract. Radiological ecological risk pre-assessment of newly-built nuclear facilities is generally required by the environmental protection authority. Conservative transfer data were used in most previous pre-assessments. Haiyang Nuclear Power Plant to be built in China was selected as a case for the dose pre-assessment for marine biota in this study. The concentrations of Cs and Co in organisms (turbot, yellow croaker, swimming crab, abalone, sea cucumber, and sea lettuce), seawater, and bottom sediment sampled on-site were measured by neutron activation analysis, and the site-specific transfer parameters (concentration ratios and distribution coefficients) of Cs and Co were calculated. ^{134}Cs , ^{137}Cs , and ^{60}Co activity concentrations in the organisms and the sediment at the site were calculated with the site-specific transfer parameters and the anticipated activity concentrations in the liquid effluent of the power plant. MCNP simulations based on the developed biological model were carried out, and then dose conversion factors of ^{134}Cs , ^{137}Cs , and ^{60}Co for the organisms were calculated in the results of the simulations. The total dose rates of ^{134}Cs , ^{137}Cs , and ^{60}Co to the six organisms were all $<0.001\mu\text{Gy h}^{-1}$.

Radon Profiles in Soil on Mine Dump

Joash Ongori, Robert Lindsay

The University of the Western Cape, Bellville, South Africa

Abstract. Radon (^{222}Rn) gas isotope with the longest half-life (3.82 days) occurs naturally by the radioactive decay of radium in the decay chain of the primordial long-lived radionuclide uranium (^{238}U). Once radon is generated within the earth's crust it migrates from the soil into the atmosphere. Radon has been recognized as a human health concern since inhalation of the short-lived decay products of radon causes irradiation of cells lining the respiratory tract. To predict radon fluxes correctly from soils to the atmosphere we must know the radium content of the soil, the soil properties and the meteorological factors such as air pressure and temperature changes at the soil surface. A study to establish the radon gas concentrations in the soil pore spaces on the mine dump was conducted. The soil is mainly made up from rocks that have been milled and processed to extract gold. In South Africa it is estimated that there are about 250 uranium bearing tailings dumps. The radon soil gas concentrations measurements were performed at 5 different spots on the non-operational Kloof mine dump using a continuous radon gas monitor, the RAD7. The RAD7 instrument is connected to a hollow stainless probe which is then inserted to different depth levels. The radon soil gas concentrations was measured in $\text{Bq}\cdot\text{m}^{-3}$ commencing at a depth of 30 cm below the air-ground interface up to a depth of 110 cm at intervals of 20cm. The range of the soil gas concentration measured was found to be between 26 ± 1 and 472 ± 23 $\text{kBq}\cdot\text{m}^{-3}$. The radium activity concentration for the mine dump soil range between 250 ± 11 and 355 ± 16 $\text{Bq}\cdot\text{kg}^{-1}$ with a weighted average of 308 ± 8 $\text{Bq}\cdot\text{kg}^{-1}$. The weighted average value of the radium content found is almost an order of 10 times higher than the average of a typical soil whose ^{238}U and ^{226}Ra content is about 40 $\text{Bq}\cdot\text{kg}^{-1}$. By using the radon soil gas concentrations measurements in the soil pore spaces utilizing the method at different depths, the diffusion coefficient of the ^{222}Rn gas in the soil air was calculated and it was found to be about 3.5×10^{-7} $\text{m}^2\cdot\text{s}^{-1}$. The diffusion coefficient was further investigated in the laboratory using an undisturbed soil sample which was collected using a PVC pipe from the mine dump. The diffusion coefficient determined in the laboratory was almost similar in magnitude to the one obtained from in-situ measurements. From the results obtained radon fluxes have been estimated from the air-ground interface.

Internal Radiation Exposure Dose From Some Commonly Consumed Food Stuff in Lagos A Commercial City in Nigeria

Kayode I Ogungbemi^a, Moses A Aweda^b, Olusola O Oyebola^a, Margaret A Adedokun^a, Chima E Ireogbu^a

^aPhysics Dept. University of Lagos, Akoka Yaba Lagos, Nigeria

^bDepartment of Radiation Biology and Radiotherapy College of Medicine/Lagos University Teaching Hospital, Idi Araba Lagos, Nigeria

Abstract. Radiation dose absorbed from commonly consumed food items have been a subject of research interest in this era of technological advancement that continually causes environmental pollution. Three locations were identified as the sources of food supply to cities with high populations in Lagos State, Nigeria. The selected food items were fish, crab, cow meat and vegetables from farms, readily available in the market and widely consumed by the general populace. The food samples were collected from the sources of supply to the Market. They were digested and analyzed to determine the radioactivity contents using Atomic Absorption Spectrometry technique. The daily estimated intakes (DEI) of the selected contaminants (Zn, Pb and Co) for an adult with average body weight of 45 kg for minimum of three days consumption period per week for the selected samples were computed. In Vegetables the DEI were 8.5977, 0.8760 and 0.0285 mg/kg/day. For the Onion that are commonly eaten in every daily meal the DEI were 1.0765, 0.7966 and 0.0020 mg/kg/day. The DEI for Beef were 5.5540, 0.3074 and 0.1170 mg/kg/day, DEI for the Cat Fish were 1.9074, 0.9995 and 0.0541 mg/kg/day, Crab were 0.6200, 0.0828, 0.0433 mg/kg/day for Zn, Pb and Co respectively. For over 50 years the DEI per pathway were 17.7556 mg/kg/day for Zn as contaminant, while for Pb and Co were 3.0623mg/kg/day and 0.2448mg/kg/day respectively. The study determined the estimate equivalent dose (ED) over 50 years to an adult for food ingested in one year expressed in mSv. Estimations for each pathway were 0.4583, 0.0034, 0.00039 mSv per contaminant. These values are within the recommended dose limits for adults of about 45kg body weight. However the daily estimated intake is fairly higher for some samples according to ICRU 19. The obtained results may serve as indication of EDI level for the studied areas, being the first attempt for the areas.

Seasonal and Diurnal Variation of Outdoor Radon Concentrations in Urban and Rural Area of Morocco

Lhoucine Oufni, Rabi Rabi

Department of Physics, Faculty of Sciences and Techniques (LPM-EIRM), University Sultan Moulay Slimane, B.P. 523, 23000 Beni-Mellal. Morocco.

Abstract. Measurement of radon (^{222}Rn) concentration is important for assessing the sources contributing to indoor and outdoor radon risks to human populations. Radon, a radioactive gas with a half-life of 3.82 days, part of the ^{238}U decay chain, is continuously produced in soil, rocks and water by natural radioactive decay of ^{226}Ra . ^{222}Rn is released from the ground into the atmosphere (exhalation), where it is transported mainly by turbulent diffusion or convection. The aim of the study was to analyze variability of ^{222}Rn concentration near the ground in urban and rural area. Continuous measurements of ^{222}Rn concentration (in 60-min intervals) were performed 1.5 m above the ground using Radon Scout Plus from January to December, 2014. The measured ^{222}Rn concentration was characterized by a diurnal cycle with an early morning maximum and a minimum in the afternoon in all seasons except winter. The urban site was characterized by a lower atmospheric ^{222}Rn concentration than the rural site, a difference that increased from winter to summer and during the nighttime periods. The present analysis indicated a positive correlation between ^{222}Rn levels and soil heat flux and a negative correlation between wind speed, air temperature, and volumetric water content in the soil. Further investigation is needed to confirm seasonal variation of ^{222}Rn concentrations in urban and rural area and to determine the long-term influence of individual meteorological parameters on radon levels in the air. The annual mean effective dose to the general public was estimated to be $0.43 \text{ mSv}\cdot\text{y}^{-1}$ based on the nationwide outdoor ^{222}Rn survey project in the studied area.

Study on a step-advanced filter monitor for continuous radon progeny measurement

Lei Zhang^a, Jinming Yang^b, Qiuju Guo^b

^aState Key Laboratory of NBC Protection for Civilian, Beijing, China

^bDepartment of Technical Physics, School of Physics, Peking University, Beijing, China

Abstract. Traditional fixed-filter (FF) radon progeny monitors are suffered from the loading of dust and couldn't be used for radon progeny continuous measurement for long period. To solve this problem, a step-advanced filter (SAF) monitor for radon progeny measurement was developed. This monitor could roll the filter and keep the filter stop during sampling and counting. Radon progeny is collected on a "fresh" filter at a follow rate of 3L/min. α/β particles emitted from filter were recorded by a PIPS detector. A newly-developed alpha-beta spectrum method was used for radon progeny concentration calculation. The ^{218}Po , ^{214}Pb , ^{214}Bi concentration as well as equilibrium equivalent concentration (EEC) could be worked out at the same time. The lower detection limit (LLD) of this monitor is 0.48 Bqm^{-3} (EEC) for one hour interval. Comparison experiments were carried out in the radon chamber at the National Institute of Metrology of China. The measurement results of this SAF monitor are consistent with EQF3220, and the uncertainty is smaller. It is suggested by measurement results that due to its high sensitivity, the periodical variety of radon progeny concentration could easily be seen the monitor is suitable for continuous measurement in both indoor and outdoor environments.

KEYWORDS: *radon progeny; fixed-filter monitor; step-advanced monitor; alpha-beta spectrum method, continuous measurement.*

Radiation Protection Dosimetry (2017), Vol. 173, No.1-3, pp. 259–262

doi:10.1093/rpd/ncw333

Survey of the Radon Environment within Lagos State Nigeria: A Preliminary Report

Margret Akinloye, Oluwasayo Abodunrin

^aLadoke Akintola University of Technology, Ogbomosho, Oyo State, Nigeria

^bBells University of Technology, Ota, Ogun State, Nigeria

Abstract. The aim of this study is to determine the radon concentration level in the residential area of Lagos State, Nigeria, evaluate the associated health risk to the residents and show the dependence of soil radon concentrations on soil moisture content. The method used is passive measurement technique which employs solid state nuclear track detectors (CR-39). A six stage on-field protocol have been employed for this study which among others, ensured proper orientation of the general public on the presence of radon, the health effects and possible ways of mitigating the concentrations of radon present in dwellings. The sampling protocol employed for this work is multi-stage sampling technique. Samples of soil were collected from different parts of Lagos at a surface soil depth of 10 cm in order to ensure adequate protection in a residential setting. A sample manually collected from each sampling point was immediately sealed with a detector attached to the cover of the measuring bottle. The other was taken to the laboratory, dried to constant weight, crushed and sieved, then packed in another bottle for measurement. In each case, the required sample-detector distance of 25 cm was applied in order to avoid the contribution from thoron to the exposure level. The moisture loss from these samples were observed to be between 7 and 19%. Each of the detectors used have been exposed for a minimum period of 90 days.

The Importance of Understanding Basic Concepts in Radiological Environmental Impact Assessment

Moon Hee Han, Hae Sun Jeong, Hyo Joon Jeong, A Reum Kil, Eun Han Kim, Won Tae Hwang

Korea Atomic Energy Research Institute, Daejeon, Republic of Korea

Abstract. Radiation safety is a crucial precondition of construction and operation of a nuclear facility. For obtaining the construction permit and operational license of a facility, radiological environmental impact assessment should be performed. Radiological environmental impact assessment is the process of estimating radiation dose and risk to human and the environment due to the radioactive materials released from a nuclear facility into the environment. The process of radiological environmental impact assessment requires a number of scientific disciplines such as meteorology, fluid dynamics, radiology, nuclear engineering, bio-dosimetry, agriculture and statistics. And the process also needs a lot of parameters which are used for describing physical and chemical phenomenon of each scientific discipline. These parameters should be site-specific as much as possible. And it is important to understand the basic concepts of the parameters and the principal of radiation protection. The principal of radiation protection provides the guideline for choosing suitable methodology for estimating radiation dose and the dose criteria which should be compared with the estimated results. Authors had experienced reviewing and finding mistakes in a radiation environmental report written for obtaining construction permit of a research reactor in Thailand. The mistakes were resulted from wrong application of a guideline due to misunderstanding of the concept of a meteorological parameter. Authors also have been involved in a project for making a radiation environmental report for obtaining construction permit and operational license of Jordan Research and Training Reactor which will be the first nuclear facility in Jordan. The report was submitted to Jordan nuclear regulatory body and it has been reviewed by Jordan regulatory body and its' technical supporting organizations. During the review processes, a lot of questions and requests have been raised. Answers have been given to almost all questions. But authors could not answer on several questions because the requests were based on misunderstanding of a concept and the principal of radiation protection. These experiences have shown us the importance of understanding basic concepts in radiological impact assessment.

High Precision Gamma Dose Rate Measurements using a Spectroscopic Pager

Michael Iwatschenko-Borho, Erich Leder, Ralf Pijahn, Norbert Trost

Thermo Fisher Scientific Messtechnik GmbH, Erlangen, Germany

Abstract. Detection of hidden radioactive material is the primary purpose of a Personal Radiation Detector (PRD) also known as a Radiation pager which is in widespread use in the Homeland Security community. In recent years, a new category of instrument, the Spectroscopic Personal Radiation Detector (SPRD) added the capability of radioactive nuclide identification to these wearable instruments. This presentation will focus on the usage of such a pocket-sized instrument as a high precision instrument for the low level measurement of the gamma dose rate. The 160 g lightweight but yet extremely rugged device incorporates a small scintillation detector, a multichannel analyzer and a microprocessor for rapid nuclide identification. For measurements of the environmental radiation level, a specific advantage of this device is given by its capability to discriminate between the contribution of gamma radiation and secondary cosmic radiation. Furthermore, the built-in spectroscopic analysis facility provides nuclide identification and enables the user to select true energy compensated readings in ambient equivalent dose rate $H^*(10)$ or Air Kerma. The built-in continuous spectral analysis of the background radiation enables the detection of small contributions originating from practically all relevant artificial radionuclides, including heavily shielded industrial gamma, beta, and neutron sources. Another interesting application is enabled by the extremely low power consumptions of the SPRD: Set into an automatic mode, e.g. up to 200 spectra with any preselected measurement and cycle time can be collected anywhere - without any interaction or infrastructure. Field application examples will be given, including the detection and analysis of Chernobyl related Cs-137 environmental ground deposition in the nSv/h range.

Tritium Content in the Velika Morava River Basin: Evaluation Effective Ecological Half-Life

Marija Jankovic, Natasa Sarap, Gordana Pantelic, Dragana Todorovic

University of Belgrade, Institute of Nuclear Sciences Vinca, Belgrade, Serbia

Abstract. The paper presents results of investigations of tritium activity concentrations in surface water samples in Velika Morava catchment, Serbia. The Velika Morava is the largest river entirely situated in Serbia (tributary of the Danube) with an average annual outflow of 220 m³/s. A purpose of this study was to apply the tritium content in local water resources investigations for a better understanding the hydrological processes. Based on the obtained results for tritium content in river, discussed in this paper, effective ecological half-life was calculated. It was applied for the first time determination of the ecological half-life of tritium in rivers that are not affected by the nuclear power plant. Because of the fact that tritium is generated in both natural and artificial processes, development of tritium activity concentration is described using a first order equation where tritium content represents the contamination from nuclear atmosphere weapons tests, generation by natural processes and discharges from nuclear facilities worldwide. Content of tritium in analyzed samples was used for assessment of radiation doses from possible use of the river water for drinking purposes. Linear correlation coefficient of the ³H activities at various pairs of studied stations was also calculated. River water samples were collected monthly at seven stream hydrological stations (one near river mouth and one more upstream) during period 2004-2006. Each sample was distilled and proceeded by an electrolytic enrichment to increase the tritium content. The activity was determined by liquid scintillation counting.

Assessing the Northern Benguela Upwelling System for Radioactivity Levels: A Baseline Study

Martina Rozmaric^a, Deon Charles Louw^b, Isabelle Levy^a, Oxana Blinova^a, Mai Khanh Pham^a, Jean Bartocci^a, Iolanda Osvath^a, David Osborn^a, Samorna Brian Mudumbi^c, Tuuovauri Kauroua Sharon Kahunda^b, Elena Chamizo^d, Ljudmila Benedik^e

^aInternational Atomic Energy Agency, Environment Laboratories (IAEA, NAEL). 4a Quai Antoine 1er, MC 98000 Monaco

^bMinistry of Fisheries and Marine Resources (MFMR), National Marine Information and Research Centre (NatMIRC), PO Box 912, Swakopmund, Namibia

^cNational Commission on Research Science and Technology (NCRST), Private bag 13253 Windhoek, Namibia

^dCentro Nacional de Aceleradores (CNA) (Universidad de Sevilla, Consejo Superior de Investigaciones Científicas, Junta de Andalucía), Thomas Alva Edison 7, 41092 Seville, Spain

^eJozef Stefan Institute, Jamova 39, SI-1000 Ljubljana, Slovenia

Abstract. IAEA and its Member States collaborate, amongst others, for capacity building in the area of marine radioactivity monitoring and for joint baseline studies. Approximately 70% of African countries have direct access to seafood and consequently population might be exposed to different pollution contaminants (including natural and anthropogenic radionuclides). Therefore it is important to encourage African countries to consider building capacity in the field of marine radioactivity monitoring and assessment. Namibia is one of the five leading countries in uranium mining. In the last decade marine mining activities (including phosphate mining, petroleum and gas mining, diamond mining), harbours and aquaculture activities and population in coastal towns have increased. Almost no data is available on the distribution of natural and anthropogenic radionuclides in the marine environment of Namibia and there was a necessity to assess the state of environment of the northern Benguela upwelling system (nBUS). Following a request for assistance from the Environmental Division of the Ministry of Fisheries and Marine Resources, the IAEA Environment Laboratories participated in a scientific sampling expedition on the R/V *Mirabilis* during its May 2014 survey along the Namibian coast. The main aim of the collaboration was to carry out a baseline study of marine radioactivity levels in the nBUS. Furthermore, to extend the existing database by including missing trace elements and to provide assistance to Namibia to set up a future marine radioactivity monitoring programme. Twenty seawater and 450 sediment samples collected at nearshore and off-shore stations along the Namibian coast, together with 45 biota samples collected at coastal towns (Swakopmund and Luderitz) are in the process of analysis at the IAEA's Environment Laboratories in Monaco and at the IAEA's Collaborating Centre the "Centro Nacional de Aceleradores" in Seville. Natural (Po-210, Pb-210, radium and uranium isotopes) and anthropogenic (H-3, Sr-90, I-129, Cs-137, U-236, Pu and Am isotopes) radionuclides are determined by using different analytical techniques and the first set of obtained results will be presented in this paper.

Comprehensive radionuclide analysis and dose assessment of thermal and mineral waters in Croatia

Krmpotić Matea^a, Rožmarić Martina^{a,b}, Petrincec Branko^c, Bituh Tomislav^c, Benedik Ljudmila^d, Fiket Željka^a

^aRudjer Boskovic Institute, Bijenicka cesta 54, 10 000 Zagreb, Croatia

^bEnvironment Laboratories, International Atomic Energy Agency, 4 Quai Antoine 1er, MC 98000, Monaco

^cInstitute for Medical Research and Occupational Health, Ksaverska cesta 2, 10 000 Zagreb, Croatia

^dJozef Stefan Institute, Jamova 39, SI-1000 Ljubljana, Slovenia

Abstract. Thermal waters are considered as natural treasures for their specific properties. They are primarily used for medical purposes (treatment of various diseases, recreation and tourism, spas, etc.), but are also being exploited for their geothermal potential (energy and heating). The northern and eastern parts of Croatia are very rich in geothermal and mineral water springs so many Croatian facilities have a long tradition of rehabilitation and tourism. However, as much as these waters are considered as cures, they can also pose a health hazard due to higher exposure to natural radioactivity since many of them are rich primarily in radium isotopes from natural uranium and thorium decay chains. Activity concentrations of ²²⁶Ra, ²²⁸Ra, ²³⁸U, ²³⁴U, ²¹⁰Po, ²¹⁰Pb, ⁴⁰K and ¹³⁷Cs for Croatian thermal and mineral waters, collected directly from springs (or wells), are presented herein with total effective doses assessed for consumption of those waters that are also used as drinking “cures”. The methods used for radionuclide determination included alpha-particle spectrometry (²²⁶Ra, ²³⁸U, ²³⁴U, ²¹⁰Po), gas-proportional counting (²¹⁰Pb) and gamma-ray spectrometry (²²⁸Ra, ⁴⁰K, ¹³⁷Cs). Activity concentrations of all radionuclides were found to be below the guidance levels set by the WHO and EC Directive, with an exception of one water sample measuring 0.26 Bq/L of ²²⁸Ra. The effective ingestion dose assessment for water “cure” consumption during one, two or four weeks time period per year showed that the maximum doses ranged between 0.004 and 0.014 mSv, which is well below the recommended 0.1 mSv for drinking water.

KEYWORDS: *thermal waters; radionuclides; alpha-particle spectrometry; gamma-ray spectrometry.*

Radioactivity values for soil replaced at some building at Tikrit University

Mohanad Salih

Tikrit Univ, Tikrit, Iraq

Abstract. In this research the idea of soil replacement is looking from the angle of the value of radioactivity that must be the lowest for the people and the environment. At Tikrit University the radioactivity values ranging between 30 and 50 counts / seconds must be for soils around the building and construction the lowest 30 c/s or mean value of 30 – 35 c/s. That doesn't mean the replacement of soils inside building but also the area around to keep the environment.

Development of a Measurement Procedure for Radon in Waterworks

Michael Stietka^a, Andreas Baumgartner^a, Franz Kabrt^{a,b}, Franz Josef Maringer^{a,b}

^aUniversity of Natural Resources and Life Sciences, Vienna, Prueflabor fuer Umweltradioaktivitaet und Strahlenschutz, Low-Level Counting Laboratory Arsenal, Vienna, Austria

^bBEV - Federal Office of Metrology and Surveying, Vienna, Austria

Abstract. Within the European Metrology Research Programme (EMRP), the IND57 MetroNORM project aims to improve the metrology for the NORM (Naturally Occurring Radioactive Materials) industries. Waterworks are among these industries, since Rn-222 can exhale in large amounts through open water surfaces and cause a significant dose contribution. For the determination of the Rn-222 activity concentration in waterworks, various procedures are applied. In order to perform accurate and standardised measurements, improved measurement practices and procedures are required. As basis for a harmonisation, a best practice measurement procedure for radon in waterworks is developed and tested on its advantages, disadvantages and its general applicability. This includes the on-site testing of active and passive, long-term and short-term measurement methods. The EMRP is jointly funded by the EMRP participating countries within EURAMET and the European Union.

Natural Radionuclides in River Sediments of Poços de Caldas Plateau - Brazil: Geogenic or Anthropogenic Contribution?

Nivaldo Da Silva, Heber Alberti, Marcos Roberto Nascimento, Rodrigo Bonifácio, Heliana Azevedo, Raul Villegas

Brazilian Commission for Nuclear Energy- Laboratory of Poços de Caldas, Poços de Caldas - MG, Brazil

Abstract. The Poços de Caldas Plateau is well known for its anomalous natural radioactivity, especially the region known as Morro do Ferro – featuring one of the highest natural external dose rates ever found on its surface (~ 0.011 mSv/h). This plateau region hosts the first Brazilian uranium mine, which was implemented in 1970s and operated from 1982 to 1995, producing approximately 1200 tons of uranium. This installation is currently under a closing process and an environmental remediation strategy is being formulated. Due to the acid mine drainage that occurs in this installation, a continuous treatment of approximately 350 m³/h of water containing natural radionuclides and other metals leached from the waste rock piles and pit mine is made necessary, generating high financial costs every year. Precisely at the point of effluent discharges of this installation, a spring of a water body – the Ribeirão das Antas River – is found. Draining 70% of the area of the Poços de Caldas plateau, the river presents strategic importance to the city of Poços de Caldas (population of approximately 150,000 inhabitants). At an altitude of over 600m higher than its surroundings, Ribeirão das Antas is a potential water source for human consumption of this city. Therefore, there is great concern arising from stakeholders in regards to the contribution of the installation discharges to the water quality of the river. This research aimed to indicate whether the radionuclides found in sediments along the Ribeirão das Antas River (~ 60 km) are of natural or anthropogenic sources. For such, sediment samples were collected in 07 stations along the river course in two campaigns carried out in 2015-2016. The radionuclides U, Th, Ra-226, Ra-228, Pb-210 were analyzed with results ranging from 168 – 53881 Bq/kg for U, 185-337 Bq/kg for Th, 138-543 Bq/kg for Ra-226, 216-777 Bq/kg for Ra-228 and 113-361 for Pb-210.

Pubic Exposure due to Indoor Radon in Three Municipalities of Poços de Caldas Plateau - Brazil

Nivaldo Da Silva^a, Berenice Navarro^b, Ubirani Otero^c, Tarcisio Cunha^c

^aBrazilian Commission for Nuclear Energy - CNEN, Poços de Caldas, Brazil

^bMinas Gerais State Health Department - SES / MG, Belo Horizonte, Brazil

^cNational Cancer Institute - INCA, Rio de Janeiro, Brazil

Abstract. The Poços de Caldas Plateau is located in the southwest region of Minas Gerais State in Brazil and it is well known by its natural radioactive anomalies. The first Brazilian uranium mine, which is now under a decommissioning process, was open in this area. The Public Health Service is assessing if there is excess in cancer cases among the population and whether there is a potential relation to the elevated natural radiation. In a collaborative effort among SES/MG (Minas Gerais State Health Department), INCA (Brazilian National Cancer Institute) and CNEN (Brazilian Commission for Nuclear Energy), the external gamma dose was already mapped and at the present time, the objective is to assess indoor radon concentrations among dwellings located in three municipalities: Poços de Caldas, Andradas and Caldas. Two campaigns- Autumn/Winter and Spring/Summer- were conducted in which 1378 dosimeters were installed in 674 dwellings (one in the living room and another in the bedroom). During the campaigns a survey was conducted in order to understand how the houses were built (e.g. building materials and foundation) as well as how they are used (e.g. ventilation). To ensure a successful project, it was decided that the local SUS health team was the one in charge of installing the dosimeters and helping people fill the questionnaire. The research produced a geo-referenced indoor radon concentration database which will allow the spatial assessment of the investigated region. In this paper the research experimental design, which uses as reference the approach used by UK's Health Protection Agency, as well as the mains results will be presented.

Estimation of Terrestrial Air-Absorbed Dose Rate from the Data of Regional Geochemistry Database

Nan Gan^{a,b}, Kuang Cen^b, Rong Ye^b

^aBeijing Research Institute of Chemical Engineering and Metallurgy, Beijing, China

^bChina University of Geosciences (Beijing), Beijing, China

Abstract. This paper presents an estimation of air-absorbed dose rate from the data of K₂O, U and Th content from Chinese regional geochemical database. A total of 421 group original data of combined samples in Zhongshan City (ZSC), Guangdong Province, South China, were extracted from the national geochemical database. Estimated the average value of air-absorbed dose rate is 139.4 nGy⁻¹ in the granite area and 73.7 nGy⁻¹ in the sedimentary area, respectively. The level of air-absorbed dose rate is closely related with the surface lithology. Estimated mean air-absorbed dose rate approximates to the measured average value by a portable plastic scintillator dosimeter in Zhuhai City, where bordered with ZSC. The results show that the pre-evaluation of ionizing radiation level using regional geochemical data is feasible.

The Study of Environmental Contamination and Public Health in the Vicinity of the Uranium Legacy Sites in the Tajik Republic

Natalya Shandala^a, Vladimir Seregin^a, Aleksandr Tukov^a, Sergey Kiselev^a, Vladimir Shlygin^a, Aleksandr Pozhidaev^b, Mirzoshokir Hojion^c

^aSRC - Burnasyan Federal Medical Biophysical Center, Moscow, Russia

^bFederal Center for Nuclear and Radiation Safety, Moscow, Russia

^cFSE, Tajikredmet, Chkalovsk, Tajikistan

Abstract. The Inter-State Target Programme “Reclamation of areas of the EurAsEC countries affected by uranium mining activities” envisages reclamation of the uranium legacy site located in Istiklol city (Taboshar). The work within the first stage included the comprehensive assessment of doses to the public living around the legacy sites in comparison with the background areas, and assessment of the public health based on the medical statistics data. The public doses were assessed due to the contribution of some components of natural exposure: external gamma radiation exposure, internal exposure due to radionuclide intake via drinking water and foods and inhalation of the radon progenies. The results of comparative analysis of the malignant neoplasms incidence of the public in the vicinity of tailings and background areas have been obtained; the malignant neoplasms incidence of the population has been analyzed. High uranium concentrations have been revealed in drinking and household waters. Recommendations have been developed how to improve the public health during reclamation operations, through both the public dose reducing and enhancing the social health monitoring system, and activities on early diagnostics of malignant neoplasms incidence.

The Study of Environmental Contamination and the Public Health in the Vicinity of Uranium Legacy Sites in the Kyrgyz Republic

Natalia Shandala^a, Vladimir Seregin^a, Aleksandr Tukov^a, Sergey Kiselev^a, Aleksey Titov^a, Sergey Akhromeev^a, Aleksandr Pozhidaev^b, Gulnura Abasova^c, Aleksander Samoylov^a

^aSRC - Burnasyan Federal Medical Biophysical Center, Moscow, Russia

^bFederal Center for Nuclear and Radiation Safety, Moscow, Russia

^cMinistry of Emergency Situations, Bishkek, Kyrgyzstan

Abstract. The Inter-State Target Programme “Reclamation of areas of the EurAsEC countries affected by uranium mining activities” envisages reclamation of two uranium legacy sites in Kyrgyzstan: Min-Kush and Kaji-Say. The work within the first stage included the comprehensive assessment of doses to the public living around the legacy sites in comparison with the background areas, and assessment of the public health based on the medical statistics data. The public doses were assessed due to the contribution of some components of natural exposure: external gamma radiation exposure, internal exposure due to radionuclide intake via drinking water and foods and inhalation of the radon progenies. The results of comparative analysis of the malignant neoplasms incidence of the public in the vicinity of tailings and background areas have been obtained; the malignant neoplasms incidence of the population has been analyzed. Inhalation of radon progenies makes the main contribution to annual effective dose to the public. Recommendations have been developed how to improve the public health during reclamation operations, through both the public dose reducing and enhancing the social health monitoring system, and activities on early diagnostics of malignant neoplasms incidence.

Estimation of Natural Ionizing Radiation Levels Based on the Data of Gamma-Ray Spectrometry and Regional Geochemical Data in Zhuhai City Urban, China

Nanping Wang, Ling Zheng, Xingming Chu, Ting Li, Hongtao Liu, Xiaohong Meng

China University of Geosciences, Beijing, China

Abstract. This paper presents a method of estimating the absorbed dose rates at 1 m height above the ground due to natural radioactivity nuclides of ^{238}U and ^{232}Th series and ^{40}K , which were estimated base on the data extracted from gamma-ray spectrometry and 1:200000 regional geochemistry database in Zhuhai City Urban (ZCU), Guangdong Province, Southern China. The calculated average value of radioactivity specific concentration of ^{238}U , ^{232}Th and ^{40}K from regional geochemical data in ZCU is 85.61 ± 35.66 , 204.46 ± 88.54 and 681.60 ± 330.14 respectively, and ranges from 29.64 to 229.71Bq/kg, 64.55 to 397.88Bq/kg and 127.81 to 1361.55Bq/kg, respectively. The research results show that natural radionuclides' radioactivity concentrations in the granite areas are higher than that in the Quaternary sediments areas. ^{238}U , ^{232}Th , ^{40}K radioactivity concentration are general high values in the Wugui mountain areas, where covered by Yanshan period biotite granite, and developing of Nanping - Tang Jia fractures. The average and highest value of absorbed dose in air are 191.47 ± 83.72 and 403.22 nGy/h respectively. The average and highest value of outdoor annual effective dose are 0.23 ± 0.10 mSv/y and 0.49 mSv/y. Therefore, based on the contents of radionuclides from stream sediment geochemical database, the radionuclide activity concentration observed using gamma-ray spectrometry, the terrestrial gamma-ray dose rate at 1 m height above the ground can be calculated. Moreover, the anomaly distribution in study areas can be delineated. This is a rapid, effective, feasible method for radiation level estimation. The research was supported by National Natural Science Foundation of China (No. 41474107 and 41274133).

Evaluation of Radioactivity Concentrations in Some Bottled Drinking Water Produced in Nigeria and Associated Radiological Risk to Consumers

Oladele Ajayi, Ademola Abokede

Federal University of Technology, Akure. Ondo State, Nigeria

Abstract. Thirty brands of commercialized bottled drinking-water commonly consumed in Nigeria were investigated for natural radioactivity content. The technique of gamma spectroscopy, by using high-purity germanium (HPGe) detector, was employed to determine activity concentrations of ^{40}K , ^{226}Ra and ^{228}Ra . The activity concentration values ranged from $0.06 \pm 0.02 \text{ Bq l}^{-1}$ for ^{226}Ra to $23.72 \pm 10.36 \text{ Bq l}^{-1}$ for ^{40}K , which accounted for most of the activity. The measured activity concentrations of ^{226}Ra and ^{228}Ra were used with their ingested dose conversion factors to estimate annual effective doses for age groups 0 – 1y, 1 – 2y, 2 – 7y, 7 – 12y, 12 – 17y and >17y due to the consumption of the waters. Estimated annual effective doses ranged from 0.87 to 37.16, 0.22 to 9.26, 0.20 to 6.44, 0.21 to 8.76, 0.53 to 21.57 and 0.09 to 3.71 mSv y^{-1} , for the age groups respectively. Most of the water samples gave annual effective doses that exceeded the average worldwide ingestion exposure dose value from uranium and thorium series reported by the United Nations Scientific Committee on Effects of Atomic Radiation (UNSCEAR). Clearly there is need for taking remedial measures to reduce radium in these bottled drinking-waters.

Radiological Hazard Assessment of Natural Radionuclides in Soils of Some Oil-Producing Areas in Imo State, Nigeria

Oladele Ajayi, Chidiebere Dike

Federal University of Technology, Akure. Ondo State, Nigeria

Abstract. The activity concentrations of natural radionuclides ^{226}Ra , ^{232}Th and ^{40}K were measured in soil core samples collected from eight (8) locations with untapped crude oil deposits and two (2) oilfields where crude oil exploration and exploitation are on-going in Imo State, Nigeria. Measurement was carried out using high purity germanium (HpGe) detector. The measured activity concentrations were used to assess the radiological hazard to humans due to the radiation emitted from the radionuclides. In areas with untapped crude oil deposits, the mean values of the absorbed dose rates (D), annual effective dose equivalent (AEDE), radium equivalent activity (Ra_{eq}), annual gonadal dose equivalent (AGED), external hazard index (H_{ex}), internal hazard index (H_{in}), representative gamma index (I_{γ}) and excess lifetime cancer risk (ECLR) are 11.40 nGy h⁻¹, 13.98 μSv y⁻¹, 23.39 Bq kg⁻¹, 82.41 mSv y⁻¹, 0.06, 0.08, 0.18, and 0.05 respectively. In areas where crude oil exploration is on-going, the mean values of D, AEDE, Ra_{eq} , AGED, H_{ex} , H_{in} , I_{γ} and ECLR are 29.42 nGy h⁻¹, 59.53 μSv y⁻¹, 59.60 Bq kg⁻¹, 206.69 mSv y⁻¹, 0.16, 0.20, 0.46 and 0.21 respectively for workers that spend up to 8 hours per day at the oilfields. For workers that spend up to 10 hours per day on the field, the mean values of the AEDE and ECLR are 75.76 μSv y⁻¹ and 0.27 respectively. Although, all the calculated radiation hazard indices are lower than the permissible limits set by the International Commission on Radiological Protection (ICRP), the values are higher in areas where crude oil explorations are on-going than areas with untapped crude oil deposits. This shows that oil and gas exploration activities have impacted adversely on the radiological status of the environment of the study area.

Radionuclide Concentrations in Edible Mushrooms Consumed in South-Western Nigeria and Radiation Dose Due to their Consumption

Oladele Ajayi, Olusola Omotoso

Federal University of Technology, Akure. Ondo State, Nigeria

Abstract. The exposure of humans to naturally-occurring radionuclides through food gives rise to radiation dose which depends on the location, diet and lifestyle. The naturally-occurring radionuclides present in soil are transferred to foodstuff through plant nutrient uptake from the soil. In order to estimate the radiation dose due to consumption of common edible mushroom, the activity concentration of ^{40}K , ^{232}Th and ^{238}U were determined in 37 mushroom samples belonging to 14 species. Samples were analysed using gamma ray spectrometry technique employing NaI(Tl) detector. Activity concentration ranges were 69.42 to 1939.56 Bq kg⁻¹ for ^{40}K (dry weight), 6.02 to 19.94 Bq kg⁻¹ for ^{232}Th (dry weight) and 9.01 to 29.75 Bq kg⁻¹ (dry weight) for ^{238}U . The geometric mean concentrations were 511.11, 12.87 and 17.00 Bq kg⁻¹ (dry weight) for ^{40}K , ^{232}Th and ^{238}U respectively. The results, along with food consumption data, were used to calculate the annual intake of these radionuclides per person through the mushrooms. The mean annual effective dose equivalent of the radionuclides from the consumption of the mushrooms was estimated to be 0.33 $\mu\text{Sv y}^{-1}$. This is about 30% of the limit recommended by International Commission on Radiological Protection (ICRP) for radionuclide intake from food.

Vertical Migration of Some Natural Radionuclides in Soils of Some Oil-Producing Areas in Imo State, Nigeria

Oladele Ajayi, Chidiebere Dike

Federal University of Technology, Akure. Ondo State, Nigeria

Abstract. The vertical distributions of the natural radionuclides ^{226}Ra , ^{232}Th and ^{40}K were investigated in soil core samples collected from 8 locations with untapped crude oil deposits and 2 oilfields where crude oil exploration is on-going in Imo State, Nigeria. Soil core samples were taken up to 30 cm depth and were sliced into 5 cm sections. Measurement was done using high purity germanium (HpGe) detector. Results revealed that the mean activity concentration of ^{226}Ra was highest at the 15 – 20 cm layer and lowest at 10 – 15 cm layer; that of ^{232}Th was highest at the 10 – 15 cm layer and lowest at 5 – 10 cm layer while the mean activity concentration of ^{40}K was highest at the 25 – 30 cm layer and lowest at 5 – 10 cm layer. Results of statistical analysis show that the vertical distributions of the natural radionuclides in the study area, to a large extent, do not follow particular trend. The activity concentrations of the radionuclides in areas where crude oil exploration is on-going are higher than those of areas with untapped crude oil deposits. Hence, crude oil exploration must have caused an increase in the activity concentrations of natural radionuclides in the areas where crude oil exploration is on-going.

Assessment of Radionuclide Concentrations in Some Cereals and Tea Products Available in Nigeria

Olufunmilayo Alatise, Irete Okeyode, Christianah Adebisin

Federal University of Agriculture, Department of Physics, Abeokuta, Ogun State, Nigeria

Abstract. Foodstuffs may contain radionuclides from natural and man-made sources. It is estimated that at least one-eighth of the mean annual effective dose due to radionuclides from natural sources is from food consumption. Cereals and teas are important components of Nigerian diet, so it is of particular concern to estimate the possible radiological hazards that may be incurred through their consumption. This study investigates the presence of ^{226}Ra , ^{232}Th , ^{40}K and ^{137}Cs in the cereals products commonly available in Nigeria. Fifteen cereal samples and ten tea samples were purchased from different markets in Nigeria. The samples were homogenized and weighed into 1 litre Marinelli beakers. The beakers were then left for a period of 4 weeks to attain secular equilibrium between parent radionuclides and their decay products. The samples were later analyzed in the gamma-ray spectrometer comprising high-purity germanium (HPGe) detector. Activity concentrations of ^{226}Ra , ^{232}Th , ^{40}K were evaluated and the associated hazard indices were calculated. ^{226}Ra , ^{232}Th , ^{40}K were detected in all the samples but ^{137}Cs was below detection limit in all the samples analyzed. The ranges of concentrations (Bqkg^{-1}) of ^{226}Ra , ^{232}Th , ^{40}K in cereal samples are 0.18 to 2.95, 0.23 to 4.62, and 10.54 to 36.78, respectively. The associated hazard indices for cereals range from 0.0065 to 0.0368 while the calculated mean annual effective doses in the cereals range from 0.0681mSvy^{-1} to 0.1890mSvy^{-1} for age groups ranging from <1y to >17y. The highest effective dose was for age group 12-17y, and the lowest was for age group 1-2y. The annual effective dose values are below the limit of 1mSvy^{-1} for the general public as recommended by International Commission on Radiological Protection (ICRP). The annual effective doses and hazard indices obtained in this study do not present any radiological concern for consumers of the cereals.

Radioactivity Levels in Samples of Detergent Powder available in Local Markets of South-western Nigeria

Olufunmilayo Alatise, Thomas Olaniyan

Federal University of Agriculture, Abeokuta, Ogun, Nigeria

Abstract. This study focuses on the evaluation of the natural radioactivity levels in ten samples of the detergent powders that are available in South-Western Nigerian markets. We have determined the specific activities of U-238, Th-232 and K-40 using gamma-spectroscopy (High Purity Germanium) and calculation of radiation hazard indices. The results of the activities of radionuclides (^{238}U , ^{232}Th , ^{40}K) for detergent powders samples, are found that the ^{238}U specific activities were varied from $(1.465 \pm 0.220) \text{ BqKg}^{-1}$ to $(8.871 \pm 1.331) \text{ BqKg}^{-1}$, while the ^{232}Th specific activities were varied from $(1.347 \pm 0.202) \text{ BqKg}^{-1}$ to $(10.579 \pm 1.587) \text{ BqKg}^{-1}$ and ^{40}K were varied from $(98.432 \pm 14.765) \text{ BqKg}^{-1}$ to (323.154 ± 48.473) . These values are always lower those of raw materials, what is explained by the conservation of radioactive materials throughout the manufacturing process. The radium equivalent activity R_{eq} and the external hazard index Hex dose due to natural radioactivity estimated below the regulatory standard recommended which are $(370 \text{ BqKg}^{-1}$ and 1) according to OECD 1979 and ICRP 2000, allows us to show that detergent powders samples products are not contaminated by radioactivity, are healthy and do not have harmful radiological impact on the consumer.

Polonium-210 Concentration in Cuban Tobacco Products and their Contribution to the Annual Effective Dose by Inhalation of Cigarette Smoke

Osvaldo Brígido-Flores, Orlando Fabelo-Bonet, Adelmo Montalván-Estrada

Radiation Protection Unit, Environmental Engineering Centre of Camagüey, Camagüey, Cuba

Abstract. Cigarette smoking is one of the pathways that might contribute significantly to the increase in the radiation dose reaching man, due to the relatively large concentrations of polonium-210 found in tobacco leaves. The results of ^{210}Po determination on the 11 most frequently smoked brands of cigarettes and cigars which constitute over 75% of the total cigarette consumption in Cuba are presented and discussed. Moreover, the polonium content in cigarette smoke was estimated on the basis of its activity in cigarettes, ash, fresh filters and post-smoking filters. ^{210}Po was determined by gas flow proportional detector after spontaneous deposition of ^{210}Po on a high copper-content disk. The annual committed equivalent dose for lungs and the annual effective dose for smokers between 12-17 years old and for adults were calculated on the basis of the ^{210}Po inhalation through cigarette smoke. The results showed concentrations ranging from 9.3 to 14.4 mBq per cigarette with a mean value of $11.8 \pm 0.6 \text{ mBq.Cig}^{-1}$. The results of this work indicate that Cuban smokers who smoke one pack (20 cigarettes) per day inhale from 62 to 98 mBq.d^{-1} of ^{210}Po and smokers between 12-17 years old who consume 10 cigarettes daily inhale from 30-50 mBq.d^{-1} . The average committed equivalent dose for lungs is estimated to be 466 ± 36 and $780 \pm 60 \text{ } \mu\text{Sv.year}^{-1}$ for young and adult smokers, respectively and annual committed effective dose is calculated to be 60 ± 5 and $100 \pm 8 \text{ } \mu\text{Sv}$ for these two groups of smokers, respectively.

Cancer Risk from Radon in Drinking Water in South-western Nigeria

Olatunde Michael Oni^a, Adetola Olive-Adelodun^a, Emmanuel Abiodun Oni^b

^aLadoke Akintola University of Technology, Ogbomoso, Oyo State, Nigeria

^bOduduwa University, Ipetumodu, Osun State, Nigeria

Abstract. Radon, mostly radon-222, is responsible for the largest percentage of internal exposure to radiation from natural sources. Being a water - soluble gas, it is found in appreciable concentration in all water samples available for human use. For over two decades, groundwater has been the dominant source of water for consumption and domestic use in Nigeria. Without prior treatment, groundwater may serve as a radiation source of concern if the concentration of radon in such water is high. A total of 250 water samples from boreholes, hand-dug wells, as well as those which have undergone treatment processes, were collected from areas of average and elevated background radiation levels in some cities and towns in Southwestern Nigeria. Measurement of radon concentration in the water samples was carried out using RAD7, thus leading to the estimation of the cancer risk by radon ingestion from drinking water. The result revealed a steady trend of variation in the concentration of radon-222 in the water samples. Highest concentration (112.00 Bq.L^{-1}) was found in water from borehole sources. Tap water (from surface water source) was measured to have the least (0.15 Bq.L^{-1}). Significant proportion of the water samples from underground sources has radon concentration above the limit specified for areas without radon monitoring policies. A risk estimate due to radon ingestion from drinking water has shown an annual increase of about 300 times as a result of ground water consumption in Southwestern Nigeria.

Radiological Impact Assessment within the Context of the Environmental Impact Assessment Process Associated with the Proposed South African Nuclear Power Programme; Challenges Associated with a Multiagency and Regulatory Overlap Environment

Paul Fitzsimons, Elisabeth Nortje

GIBB (Pty) Ltd, Johannesburg, South Africa

Abstract. South Africa is proposing to embark on the development of a large nuclear power generation programme and has over the last few years been conducting Environmental Impact Assessments for proposed nuclear reactors on potential sites. The Environmental Impact Assessment regulatory regime is independent and separate from but overlaps with the regulatory regime for nuclear licensing and radiological protection. There is thus a degree of duplication in the legislation applying to authorisation of a nuclear installation in that radiological issues are required to be addressed by both the National Environmental Management Act (NEMA) (Act No. 107 of 1998) and the National Nuclear Regulator (NNR) Act (Act No. 47 of 1999). Both regimes therefore potentially envelop radiological impact in an environmental protection context. As yet there has been no nuclear licence application associated with this programme. The paper will describe the proposed nuclear power programme, the associated regulatory regimes, some of the conflicts and challenges posed, and the resultant accommodations made within the Environmental Impact Assessment process to realise the most technically robust outcome.

Integrating the Radiation Protection System for Human and Non-Human Biota: How to do it in Practice

Diego Telleria, Peter Johnston

International Atomic Energy Agency, Division of Radiation, Transport and Waste Safety, Vienna, Austria

Abstract. In 2005 the IAEA initiated the Plan of Activities on the Radiation Protection of the Environment to work with International Organizations and Member States towards enhancing international standards and guidance for the control of radiological impacts to people and the environment. Until then, protection of the environment was based on the assumption that compliance with standards for human protection would ensure that other species are not put at risk; this assumption was being challenged by the international community. IAEA standards considering a new perspective were started in 2006 with the Fundamental Safety Principles and continued with the IAEA Basic Safety Standards on Radiation Protection and the Safety of Radiation Sources. In these standards, the radiation protection objectives for non-human species were related to higher organization levels as populations, communities and ecosystems, rather than on the protection of individuals as it is the case for humans; the need to consider protection of humans and other species in an integrated manner was also recognized. The IAEA followed the recommendations of the ICRP and proposed an assessment methodology similar to that applied for demonstrating compliance of doses to humans with predefined criteria. The method entails the use of a set of reference animals and plants (RAPs) that relates to various species and ecosystems. Radiation exposure levels can be estimated and compared to criteria identified, below which no or only very limited adverse effects to biota are expected. The integration of the protection of humans and other species was approached by assuming the linkage of the exposure scenarios between humans and flora and fauna. This resulted in a practical methodology which can be implemented with basically the same resources as those used to demonstrate protection of humans; the approach is verifiable by similar environmental monitoring in the relevant media. The IAEA established different ways to consider protection of biota for different exposure situations. For planned exposure situations, the results of the estimation of exposures to RAPs are compared to reference levels, and this could imply the need of control of the source. For existing and emergency situations, the control of those exposures is limited or impossible and the results of the assessments should be considered as an aspect in the optimization process, together with others, like social and economic factors. The paper presents the methodology developed by the IAEA and its implementation in currently prepared IAEA Safety Guides and in guidance developed for the London Convention on the Prevention of Marine Pollution by Dumping of Wastes and Other Matter and for the OSPAR Convention for the Protection of the Marine Environment of the North-East Atlantic.

A Map of Moscow Geogenic Radon Potential

Peter Miklyaev^a, Tatyana Petrova^c, Albert Marennyy^b, Andrey Tsapalov^b, Sergey Kiselev^d

^aSergeevs Institute of Environmental Geoscience, Moscow, Russia

^bResearch and Technical Center of Radiation-Chemical Safety and Hygiene, FMBA, Moscow, Russia

^cMoscow State University, radiochemistry department, Moscow, Russia

^dSRC Burnasyan Federal Medical Biophysical centre, FMBA, Moscow, Russia

Abstract. We have selected a categorial GRP (geogenic radon potential) indicator as an end-state variable of our work. This indicator is generally similar to the categorial RI radon index used in the European countries. However, as input parameters, values of radon flow rate (RFT) from the soil surface and radium activity concentration in soils forming the territory of the city to a depth of 20 meters are used to assess GRP. Assessment of the geogenic radon potential level (category) of the specific territory depending on its determining parameters (low, medium, high), is based on the following: The average RFT at the building sites, in mBq/(m²s): ≤ 150 and >150 ; the highest radium activity concentration in the soil depth of up to 20 meters, in Bq/kg): low: <40 , medium: 40-100, high: >100 . As a basis for the GRP mapping, the cadastral division of Moscow is accepted. Such approach is suitable for designing and building companies, which are the main commercial consumers of information on geogenic radon potential of the Russian areas. The GRP map for Moscow territory is based on statistical results of engineering studies of more than 1000 building sites. According to the received data, 51 cadastral quarters have been identified, where GRP assessment was high. Within 172 cadastral quarters, GRP was medium. The rest part of the city (1354 cadastral quarters) is specified by low GRP.

Outdoor Radon Levels in China

Qifan WU, Ziqiang Pan, Senlin Liu

Dept. of Engineering Physics of Tsinghua University, Beijing, China

Abstract. Several regional and nation-wide indoor radon concentration surveys in China have been carried out since 1980s (PAN Ziqiang, 2011). Although the earliest measurement of radon in atmosphere was made in 1928 (WANG Ganchang,1928), few projects of the outdoor radon concentration survey in China have been completed. Data from previous surveys, the average value of the outdoor radon concentration is 14 Bq/m^3 (PAN Ziqiang, 2011). These data were based on a variety of measurements. A nation-wide survey of outdoor radon concentration was conducted to evaluate the environmental outdoor radon level in 2014. In this survey, Cr-39 detectors were used, and distributed in 33 provincial cities in China, 7 Cr-39 detectors for each city, four detectors of them placed in urban areas, two in the suburb and the rest one detector returned to detect the background from transportation. The detectors were placed in three months period and six months period for measurement precision improvement respectively, then retrieved collectively and etched. The Background of detectors were evaluated less than 30 tracks/m^2 , or the outdoor radon concentration equivalent exposure for 3 months is less than 3.6 Bq/m^3 , or 5 Bq/m^3 including additional background from transportation. The outdoor mean radon concentration in China was $13.4 \pm 7.2 \text{ Bq/m}^3$, ranging from 3.0 Bq/m^3 to 30.0 Bq/m^3 in 2014. Considering admissible error, the result was almost the same as the value of 14 Bq/m^3 , reported previously (Pan Ziqiang, 2011), although some values in the cities such as Fuzhou and Lasha were quite different (Pan Ziqiang, 2003, T. lida and Y. lkebe, 1996). Based on the sixth nationwide population census in 2010, urban population is 665,575,306(49.68%). However, most of the data in this survey were from city areas. Therefore, more measurement locations should be considered in rural areas. And as the result, Outdoor radon level in China will be lower in some extend. The authors would like to acknowledge the Ministry of Environment Protection for the financial support, and the 33 provincial environment radiation monitoring units for their contributions. Finally, we also thank Mr. Zhou Weihai for his technical support.

A Platform for Assessment of Doses to the Public from Routine Discharges of Radionuclides to the Environment from Nuclear Installations

Rodolfo Avila^a, Robert Broed^a, Erik Johansson^a, Vladimir Maderich^b, Roman Bezhenar^b

^aFacilia, Stockholm, Sweden

^bUkrainian Centre of Environmental and Water Projects, Kiev, Ukraine

Abstract. In this presentation we provide an introduction to a platform for assessment of doses to the public from routine discharges to the environment from nuclear installations. The platform consists of a software package implemented in the commercial software Ecolego (www.ecolego.facilia.se). The main advantage of the platform are: Flexibility – it can be easily adapted to different sites and source terms, Transparency – all models and parameters are transparent to users, State of the art models - can be easily modified and extended by users as knowledge and models improve. The platform has three main components: 1) a simulator – that allows integrating models and performing deterministic and probabilistic simulations, as well as sensitivity analyses, 2) a model library – includes models of transport of radionuclides in the atmosphere and the sea, radioecological and dose assessment models and 3) a parameter database which includes a system for quality control of the parameter values used in the models. The atmospheric dispersion of radionuclides can be done using any external model, which can be easily integrated in the platform or with one of the simple atmospheric models included in the model library, such as the screening models used in the IAEA SR 19. The radionuclide transport in the sea can be modelled using the Poseidon model, which can be called from the platform or with a simpler box model included in the library. The platform includes radioecological models for the following types of environments: crop lands, pasture lands, garden plots, forests, fruit lands, lakes, rivers, marine basins. Models for calculation of doses by all potential exposure pathways are included. The parameter database has default values for all model parameters, including ICRP dose coefficients and values of radioecological parameters (like Concentration Ratios and Distribution Coefficients) recommended by the IAEA. Examples of application of the platform in the PRED0 project will be presented. This project was dedicated to the assessment of doses from routine discharges from all existing Swedish nuclear installations.

Radon In-Air Assessments within Selected Wine Cellars in the Western Cape (South Africa) and its Associated Effective Radiation Exposure Dose

Ryno Botha^{a,b}, Robert Lindsay^a, Richard Newman^b, Peane Maleka^c

^aUniversity of the Western Cape, Western Cape, South Africa

^bStellenbosch University, Stellenbosch, South Africa

^ciThemba-Labs, National Research Foundation, Somerset West, South Africa

Abstract. Measurements were made for radon (^{222}Rn) in-air activity concentration within nine selected active wine cellars in four wine districts of the Western Cape (South Africa) to determine the associated radiation exposure risks during two measurement series (F1 and F2). The radon in-air levels ranged from $12 \pm 7 \text{ Bq/m}^3$ to $820 \pm 40 \text{ Bq/m}^3$ within the nine wine cellars. During the first measurement series (F1); a general overview of average radon in-air levels were surveyed. Eight of the nine wine cellars (exclude the wine cellar with elevated radon levels) had an average radon in-air activity concentration of $45 \pm 8 \text{ Bq/m}^3$, which originates from the radon within the atmosphere. During the second measurement series (F2); extensive radon and thoron in-air levels measurements were performed within the one wine cellar (w-6) with the elevated radon in-air levels ($820 \pm 40 \text{ Bq/m}^3$) detected during the first measurement series (F1). The mean radon in-air activity (E-PERM detectors) values ranged from $386 \pm 24 \text{ Bq/m}^3$ to $510 \pm 30 \text{ Bq/m}^3$ measured at different locations within this wine cellar (F2). The continuous radon and thoron in-air activity concentrations ranged respectively from $70 \pm 22 \text{ Bq/m}^3$ to $732 \pm 70 \text{ Bq/m}^3$ (^{222}Rn) and below the lower level of detection to $1520 \pm 190 \text{ Bq/m}^3$ (^{220}Rn) for the two detectors (RAD-7). In the Paarl wine district, geological factors such as permeable granite structures (containing ^{226}Ra) was the primary cause for elevated radon in-air levels. Activity concentration measurements (HPGe-detector) of the granite yielded a concentration ^{226}Ra : $93 \pm 11 \text{ Bq/kg}$ and ^{232}Th : $245 \pm 26 \text{ Bq/kg}$. The inhalation ionization radiation exposure risk due to radon in-air and its daughter products within wine cellars expressed as an effective annual dose ranged from $0.03 \pm 0.01 \text{ mSv}$ to $2.1 \pm 0.1 \text{ mSv}$. In general most of the wine cellars pose negligible associated health risk due to ionization radiation exposure from the inhalation of radon and its daughter products.

Environmental Thoron: Monitoring, Techniques and Dose Conversion

Rakesh Chand Ramola

Hemwati Nandan Bahuguna Garhwal University, Tehri Garhwal, India

Abstract. It is an established fact that exposure of high radon is one of the causative factors of human lung cancer. The presence of thoron, ^{220}Rn , was often neglected because it was considered that the quantity of thoron in the environment is less than that of radon. However, recent studies have shown that the dose due to exposure to ^{220}Rn and its progeny can equal or several times exceed that of ^{222}Rn and its progeny. The results of thoron and its progeny measurements in the houses of normal and high background radiation areas (HBRA) of India using both active and passive techniques in different types of houses are presented here. A comparison between the results obtained with various techniques is presented in this paper. The effectiveness of various thoron and progeny measurement techniques and their usefulness in estimating the dose to general public are discussed in details.

Influence of Release Height on Radioactive Gas Effluent in Short-term for Nuclear Power Plant in China

Ruiping Guo^a, Chunlin Yang^b, Chunming Zhang^a

^aNuclear and Radiation Safety Center, Beijing, China

^bHenan Institute of Science and Technology, Xinxiang, China

Abstract. The environmental dangers of radioactive gas effluent were always focused in the review of nuclear power plant when design. In this paper, it was demonstrated that the atmosphere dispersion characters of radioactive gas effluents in short-term for Nuclear power plant in China when accidents happened in nuclear power plant. In order to study the atmosphere dispersion of radioactive gas effluent, the PAVAN model was selected to simulate the relative concentration of radioactive material. Also, the effect of release height on atmosphere dispersion factor in different time scale was discussed. The result showed that the atmosphere dispersion factor in short-term would in decrease with the release height increase. Diffused by the atmosphere, the concentration of radioactive gas effluent would obviously decrease with time. For different time scales, the relative difference of atmosphere dispersion factor in the EAB and LPZ boundaries presented obvious variation with wind direction. The characters of atmosphere dispersion factor of radioactive gas effluents in short-term in nuclear power plant were discussed when assumed designed accident happened. Moreover, it was explored that the role of release height and wind direction in influencing atmosphere dispersion of radioactive gas effluents. We ran the PAVAN model for 1000 times and selected the release height as the variable to simulate the atmosphere dispersion factor in short-term (2 hours, 8 hours, 24 hours, 4 days and 30 days) and analysed that the effect of release height on radioactive gas effluent. This study will be helpful for us to master the regular pattern of discharge of radioactive material into atmosphere and will supply the theory support for the emergency response for nuclear power plant in China.

Synergistic Effect of Caffeine and Melatonin against Radiation Induced Damage in C57BL/6 Mice at Sub Lethal Radiation Dose

Ritu Kushwaha, Dhruv K Nishad, Aseem Bhatnagar

Institute of Nuclear Medicine and Allied Sciences, Delhi, India

Abstract. The present study was undertaken to enhance the radioprotective efficacy of melatonin by using combination of melatonin and caffeine. C57BL/6 male mice (n= 24) were randomly divided into four groups: control, radiation (2Gy), melatonin (50mg/kg body wt.)+ radiation (2Gy), melatonin and caffeine (50 & 30 mg/kg body wt respectively)+ radiation (2Gy). Control mice were sham irradiated, radiation grouped mice received 2 Gy of gamma radiation, melatonin +radiation grouped mice received 50mg/kg body wt. of melatonin intra-peritoneally 30 min prior to 2 Gy of gamma radiation, melatonin and caffeine + radiation grouped mice received 50 mg/kg body wt. of melatonin in combination with 30mg/kg body wt. of caffeine 30 min prior to 2Gy of gamma radiation. All the mice were sacrificed 24 hr post irradiation and liver and blood was collected. The anti-genotoxic action of melatonin and combination of melatonin and caffeine was studied by measuring chromosomal aberrations and DNA damage (comet assay). Irradiation induced damage to cellular DNA as evident from increase in chromosomal aberrations and comet parameters like tail DNA%, tail moment, tail length and olive tail moment in the radiation control group. Melatonin administration significantly reduced chromosomal aberrations and DNA damage as evident from the results. Treatment of caffeine in combination with melatonin showed profound reduction in chromosomal aberrations and DNA damage in liver and bone marrow cells when compared with melatonin + radiation group ($p<0.05$). This study suggests that melatonin in combination with caffeine can effectively reduce the effects of radiation (2Gy) in liver and bone marrow cells of C57BL/6 mice.

Radiation Protection Calculations for both ingestion of ^{226}Ra and ^{228}Ra in Reservoir and Spring Water from Central Region of Cameroon

Rose Lydie Marie^a, Oum Keltoum Hakam^b, Abdel Majid Choukri^b

^aNational Radiation Protection Agency, Yaounde, Cameroon

^bFaculty of Sciences, University of Ibn Tofail, Kenitra, Morocco

Abstract. The preliminary results of ^{226}Ra and ^{228}Ra activities obtained for reservoir and springs water samples collected in 2010 in Cameroon's central region covered Ngoaekelle, Minboman, Etoudi and Njougolo, are given in this work. Water samples were collected during the dry and the rainy season. The average concentrations of radium's isotopes were estimated from measurement of mean specific activity using both well calibrated Canberra NaI(Tl) and HPGe detector systems. Assuming an individual daily consumption of 2.5 litres of water, the annual effective dose received by an adult as a result of ingestion of this drinking water is respectively 1.86 mSv for reservoir water, and 0.67 mSv for spring water. According to ICRP recommendations, the maximum effective dose for public exposure is 1 mSv/y; springs water do not present any risk for public health but, there is a need for monitoring the reservoir water quality.

Gamma-emitting Radionuclides Analysis in Water Samples from Two Mines in South Africa

Raymond Njinga

North-West University, North West, South Africa

Abstract. The gross alpha and gross beta activity in five water samples from within and the surrounding of two mines in South Africa were measured as a screening technique to give first order estimates of total activity concentrations. In the first mine, the gross alpha and gross beta activity in the treated underground water (sample A1005) were 1150 ± 130 mBq/L and 871 ± 113 mBq/L respectively while for the fissure water (sample B1006) were 563 ± 104 mBq/L and 518 ± 106 mBq/L respectively. The second face of water samples were obtained based on the local activities around the mine. The gross alpha and gross beta activity in the three water samples obtained were 15200 ± 1300 mBq/L and 12700 ± 800 mBq/L for sample A1004, 10100 ± 800 mBq/L and 11900 ± 700 mBq/L for sample Z1004 and 12000 ± 1000 mBq/L and 11900 ± 700 mBq/L for sample Z1005 respectively. From the above results, the activity concentration in the five water samples were analyzed for the radionuclides; ^{238}U , ^{234}U , ^{230}Th , ^{226}Ra , ^{210}Po , ^{235}U , ^{237}Th , ^{223}Ra , ^{232}Th , ^{228}Th , and ^{224}Ra in the uranium and thorium series using alpha spectrometry based on the ISO/IEC Standard 17025 methods. The dose rate in $\mu\text{Sv/yr}$ were evaluated for the age group > 1 yr to > 17 yr according to the guidelines in Nuclear regulator licensing guide LG-1032 and the conversion factors used were obtained from the published IAEA safety Series 115.

Setting Up a Continuous Monitor for Controls the Temporal Variability of ^{222}Rn in the Atmosphere and Groundwater of the Tadla Basin, Morocco

Radouan Saadi^a, Hamid Marah^b, Oum Keltoum Hakam^b

^aNational Center for Energy Sciences and Nuclear Techniques (CNESTEN), Rabat, Morocco

^bPolymers, radiation and environment laboratory, Ibn Tofail University, Kenitra, Morocco

Abstract. Radon-222, naturally occurring radioactive gas, the inhalation of radon and its progeny is a potential health risk to humans. In fact, radon can accumulate in confined spaces such as buildings, or infiltrate to water, is responsible for one third of the total radiation exposure of the general population to radiation. The main difficulty is related to the variability of radon exposure in the national territory. Therefore, it is very important to find a rapid way to delineate the geological regions with high radon concentration and emanation. In this work, the use of a simple, robust method and portable technique (RAD7) for measuring moderately high levels of ^{222}Rn in air, natural waters such as coastal water, groundwater and rivers, is investigated. This technique with a high sensitivity is used for the first time in Morocco to survey radon in the atmosphere and for monitoring spatial distribution of radon in natural waters in some areas which are rich in phosphate. In this context, we inspected the parameters influencing the results by performing several laboratory test and we attempted to apply this air-water radon equilibrium technique to the analysis of radon in grab samples. The experiments are attempted in the laboratory of Water and Climate Unite of the National Center for Nuclear Energy, Science and Technology. This will enable a rapid in situ assessment of moderate levels of ^{222}Rn activity in various types of samples (air, surface and ground water) in Tadla basin. The system analyses ^{222}Rn from a constant stream of water passing through an air-water exchanger that distributes radon from the running flow of water to a closed air loop. The air stream is fed to a commercial radon-in-air monitor, which determines the concentration of ^{222}Rn by collection and measurement of the α -emitting daughters, ^{214}Po and ^{218}Po , via a charged semiconductor detector. Since the distribution of radon at equilibrium between the air and water phases is governed by a well-known temperature dependence, the radon concentration in the water is easily calculated. Tests conducted in the laboratory have shown good correlation between the water temperature and the radon concentration. We note that the low humidity in the measuring chamber increase the sensitivity. As well the system allows monitoring of radon in the atmosphere, an activity is determined inside the laboratory of about 0.326 ± 0.058 pCi/L. A measurement of certain points in the Tadla region provides a vision of space distribution radon in natural waters, likewise the results found are below the regulatory limits.

KEYWORDS: ^{222}Rn ; RAD7; continuous monitor; waters; radiation; surveillance.

Radon-thoron Discriminative Measurements and Corresponding Dosimetry in the Thorium Bearing Region of Lolodorf, Cameroon

Saidou^{a,b}, Shinji Tokonami^c, Mirosław Janik^d

^aNuclear Technology Section, Institute of Geological and Mining Research, Yaounde, Centre, Cameroon

^bNuclear Physics Laboratory, Faculty of Science, University of Yaounde I, Yaounde, Centre, Cameroon

^cInstitute of Radiation Emergency Medicine, Hirosaki University, Hirosaki, Aomori, Japan

^dRegulatory Science Research Program, National Institute of Radiological Sciences, Inage, Chiba, Japan

Abstract. Discriminative RADUET detectors were deployed in 90 houses of the high natural radiation areas of the thorium bearing region of Lolodorf in Southwestern Cameroon. Radon and thoron concentrations were determined using Image-J and Microscope Methods for track evaluation. Radon and thoron concentrations follow lognormal distributions and ranged respectively from 27 ± 26 to 937 ± 5 Bq m⁻³ and from 48 ± 40 to 700 ± 128 Bq m⁻³. The arithmetic means of radon and thoron concentrations were found to be 92 ± 3 Bq m⁻³ and 260 ± 13 Bq m⁻³. Less than 2% of houses have indoor radon above the reference level of 300 Bq m⁻³ and 30 % of houses have thoron concentrations above 300 Bq m⁻³. Gamma doses indoors range between 0.26- 9.5 mSv yr⁻¹ with the mean value of 1.1 mSv yr⁻¹. Inhalation doses due to radon and thoron range respectively between 0.6- 17.7 mSv yr⁻¹ and 0.2- 3 mSv yr⁻¹ with the mean values of 1.4 mSv yr⁻¹ and 1 mSv yr⁻¹. The contribution of indoor thoron to the total inhalation dose ranges between 15%- 78.5% with the mean value of 47%. Thus thoron cannot be neglected when assessing radiation dose.

A New Facility for Assuring the Measurements Traceability in the Environment Dosimetry

Sorin Bercea, Aurelia Celarel, Constantin Cenusă, Elena Iliescu, Ioan Cenusă

“Horia Hulubei” National Institute for R&D in Physics and Nuclear Engineering (IFIN-HH), Magurele, Romania

Abstract. The correct measurement in the environmental dosimetry strongly depend the calibration of the field instruments. The importance of the calibration for the instruments dedicated to the radiological measurements in the environment in Europe is proved by including in the EMRP Program of a R&D Project regarding the “Metrology for radiological early warning network in Europe” In this project, Task 3.3 is dedicated to the “Installation of a new underground low-dose rate calibration facility. This task will be accomplished by an international cooperation (IFIN- HH/Romania, CEA/France, CMI/Czech Republic, ENEA/Italy, PTB/Germany). In accordance with the aim of this task, IFIN-HH established a new irradiation facility in the Slanic-Prahova salt mine and allow the calibration of the dosimeters in the range of the natural environment radiation (30 nSv/h – 300 nSv/h) in a collimated photon field. Because of a rock overburdened of about 150 m, secondary cosmic radiation is largely suppressed, in this new underground laboratory. The mean value of the rate of the dose equivalent in the area where the facility is located is of 2 nSv/h; this value is very adequate to the environment dosimetry; the measuring range of these instruments should cover the usual range of H^* in environment, i.e. 30 nSv/h – 300 nSv/h. The paper presents the irradiation bench and the results of measurements performed in the collimated gamma beam produced by the ^{137}Cs source, as well as the development to be achieved by using other radioactive sources.

Bioaccumulation Factor of the Heavy Metal in Marine Organism from the Korean Coast

Seokwon Choi, Heungjun Cho, Daeji Kim, Jungseok Chae

Korea Institute of Nuclear Safety, Daejeon, Republic of Korea

Abstract. The concentrations and bioaccumulation factor of 14 heavy metals in marine organisms at the neighbouring sea of Korea were measured and investigated, respectively. The 162 seawater samples, 189 fish samples, 13 Cephalopods and 12 Crustaceans were measured the concentrations of heavy metals. The bioaccumulation factors in 162 sampling locations were analyzed in concentration of seawater and marine organisms. The concentrations of heavy metal in seawater increased in the order of $\text{Mn} < \text{Cd} < \text{Co} < \text{Cr} < \text{Pb} < \text{Ni} < \text{Cu} < \text{Zn} < \text{Mo} < \text{P} < \text{Fe} < \text{Rb} < \text{Sr} < \text{Na}$. Metal concentrations were highest in Crustaceans, except for P and lowest in the squid muscle of all the fish species, except for Cu. Highest concentrations of Na ($6300 \text{ mg}\cdot\text{kg}^{-1}$), P ($4600 \text{ mg}\cdot\text{kg}^{-1}$), Fe ($200 \text{ mg}\cdot\text{kg}^{-1}$) and Sr ($71 \text{ mg}\cdot\text{kg}^{-1}$) were measured in shrimp, respectively. The concentrations of muscle in fishes showed strikingly high Na ($1500 \text{ mg}\cdot\text{kg}^{-1}$), P ($3200 \text{ mg}\cdot\text{kg}^{-1}$), Sr ($21 \text{ mg}\cdot\text{kg}^{-1}$) and Fe ($23 \text{ mg}\cdot\text{kg}^{-1}$). The concentrations of muscle in Cephalopods showed Na ($640 \text{ mg}\cdot\text{kg}^{-1}$), P ($110 \text{ mg}\cdot\text{kg}^{-1}$), Fe ($5.9 \text{ mg}\cdot\text{kg}^{-1}$) and Sr ($4.9 \text{ mg}\cdot\text{kg}^{-1}$). The results indicated that the concentration of metals in the Cephalopods was higher than that in the fish and Crustaceans. The mean bioaccumulation factor of the heavy metal except for Zn, Pb, Mn, Cd, Ni and Fe were similar to the recommended value from IAEA (2004), were not similar to the value reported from KAERI(1989).

In-situ Measurements of Radon Levels in Water, Soil and Exhalation Rate using Continuous Active Radon Detector

Sanjeev Kumar

^aPunjabi University College, Ghanaur, Patiala, Punjab, India

^bGuru Nanak Dev University, Amritsar, Amritsar, Punjab, India

Abstract. The radon concentration levels in water and soil-gas from some locations from areas of Punjab, India have been measured on in-situ basis. Continuous active radon detector (Alpha- Guard, Model - PQ 2000 PRO, Genitron instruments, Germany) is used for this purpose. Exhalation rate measurements have also been carried out at these places, using closed- circuit technique. The radon concentration in soil and water varied from 1.9 – 16.4 and 5.01 – 11.6kBqm⁻³, respectively. The exhalation rate (ER_n) ranged between 7.48 –35.88 mBqm⁻² s⁻¹ with an average value of 18.17 mBqm⁻² s⁻¹. Annual dose rates have also been calculated for water radon concentration. The minimum to maximum values of dose rates were found to be 13.42 – 31.08 μSv/y. The recorded values of radon concentration in water are within the recommended safe limit of 11 Bq l⁻¹ recommended by US Environment Protection Agency. All measurements were made in similar climatic and environmental conditions to ensure minimal variation in metrological parameters.

Exposure to External Gamma Radiation Emitted from Soil of the High Background Radiation Areas of Ramsar Reduces Bacterial Susceptibility to Antibiotics

SMJ Mortazavi^a, Samira Zerei^b, Mohammad Taheri^c, Saeed Tajbakhsh^b, S Ranjbar^a, F Momeni^a, Samaneh Masoumi^a, Leila Ansari^a, SAR Mortazavi^a, Masoud Haghani^a, S Taeb^a

^aShiraz University of Medical Sciences, Shiraz, Iran

^bBushehr University of Medical Sciences, Bushehr, Iran

^cKerman University of Medical Sciences, Kerman, Iran

Abstract. Over the past several years our laboratories have investigated different aspects of the challenging issue of the alterations in bacterial susceptibility to antibiotics induced by physical stresses. This study is an attempt to explore the bacterial susceptibility to antibiotics in samples of *Salmonella enterica* subsp. *enterica* serovar Typhimurium (*Salmonella* Typhimurium), *Staphylococcus aureus*, and *Klebsiella pneumoniae* after exposure to gamma radiation emitted from the soil samples of the high background radiation areas of Ramsar. Standard Kirby-Bauer test which evaluates the size of the zone of inhibition as an indicator of the susceptibility of different bacteria to antibiotics was used in this study. The maximum alteration of the diameter of inhibition zone was found for *Klebsiella pneumoniae* when tested for Ciprofloxacin (CP) antibiotic. In this case, the diameter of no growth zone in non-irradiated control samples of *Klebsiella pneumoniae* was 20.33 ± 0.58 mm, while it was 14.67 ± 0.58 mm in irradiated samples. On the other hand, the minimum changes in the diameter of inhibition zone were found for *Salmonella* Typhimurium and *Staphylococcus aureus* when these bacteria were tested for Nitrofurantoin (FM) and Cefalexin (CN), respectively. As in this experiment, gamma rays were capable of making some antibiotic-resistant bacteria susceptible, it can be hypothesized that short term exposure of these bacteria to high levels of natural background radiation cannot induce adaptive phenomena to help them better cope with lethal effects of antibiotics. On the other hand, the increased susceptibility to antibiotics observed in this study may have important clinical applications.

Discharge of Gaseous Radioactive Waste in FDG Synthesis: Clearance Levels and Licensing in Italy

Sandro Sandri^a, Maurizio Guarracino^a, Ruggero Cifani^b

^aItalian National Agency for New Technologies, Energy and Sustainable Economic Development (ENEA), Frascati, Rome, Italy

^bIstituto Tecnico Industriale Statale Antonio Meucci, Rome, Italy

Abstract. The production of 2-[F-18]fluoro-2-deoxy-D-glucose (FDG) usually is done in a cleanroom whose internal conditions are: temperature $22^{\circ}\text{C} \pm 2$, relative humidity $< 60\%$, and overpressure of 10 Pa respect to adjacent rooms. Ceilings are sealed to prevent ingress of air bearing particles. Floor is non-porous, slip-resistant, abrasion-resistant, and conductive. Inside the cleanroom component preparation, synthesis and filling are carried out in separate areas: a laminar air flow work station for component preparation, two airtight hot cells for synthesis, and an airtight dispensing hot cell for filling. The air extracted from these systems pass through a high efficiency absolute filter (99.97%), and activated carbon. The gas released in the environment at the main stack is bearing F-18 waste and is subject to specific preliminary licensing in the design phase and to active measurements during the operations. Production of FDG is done using an automatic synthesizer that is a closed system where the evacuation is performed via a cooling trap with liquid nitrogen, so the volatile radioactive substances are partially trapped. The radioactive exhaust gas is usually collected with high efficiency into suitable bags used for delaying the discharge and permitting the radioactive decay. Sometime the exhaust gas is compressed in a compression system for the delayed discharge. In Italy Regulatory Authorities require that the potential F-18 release in the environment during the normal synthesis process has to be assessed during the design of the facility. The released amount has to be used as radioactive source term to assess the (annual) dose to the most exposed individual in the specific situation. The assessment can be done using computer codes, or deterministic analyses, or making reference to the existing experimental data. In the present work the specific licensing requirement in Italy are presented and discussed and some examples of real assessments of the dose to the population are shown. The study points out that, in many situations, the F-18 that could be released, in agreement with the Italian regulation, is much more than that usually released at very active radio-pharmacies.

External Evaluation of the Amounts of Exposures and Intern to the Telluric Radiations Gamma, in the South-East of Gabon

Sylvere Yannick Loemba Mouandza^{a,c}, Alain-Brice Moubissi^a, Germain Hubert Ben-Bolie^b, Patrice Ele Abiama^b, Bouchra Ramzi^c, Mohammed Zaryah^c

^aUniversité des Sciences (USTM) et Techniques de Masuku; Faculty of Sciences, Department of physics, Franceville, Haut-Ogooué, Gabon

^bLaboratory of Nuclear Physics of the University of Yaounde I, Yaounde, Cameroon

^cCentre National d'Energie et des Sciences et Techniques Nucléaire(CNESTEN), Rabat, Morocco

Abstract. The area of Mounana in Gabon is a strongly uranium-bearing area. It was during many years (1961-1999) prone to industrial uranium exploitation; with its famous layer of Oklo (natural reactor of fission). The primordial radionuclides that are uranium 238, thorium 232, potassium 40 and their descendants are always present in the grounds, the rocks and in much of building materials. The gamma radiations emitted by these radionuclides constitute the telluric radiation which involves an external exposure of the organism; and the gases such as radon and the thoron constitute an internal exposure to the organism. Objectives and Methodology: Mounana in Gabon, we have to determine by gamma spectrometry the concentrations of following natural radionuclides: ²²⁶Ra, ²³²Th and ⁴⁰K, in samples of rocks, soil and vegetables collected in this area. This was done in order to evaluate the external amount of exposure received by the populations and to estimate the indices of external risks of radiation and to evaluate the internal amount of exposure inhaled by the populations. However, thirty (30) samples were collected in Mounana, they have been conditioned and are being analyzed in progress in Centre National d'Energie et des Sciences des Techniques Nucléaire in Rabat from Morocco. We used a HpGe detector coupled with a software Genie 2000 for the gamma spectrometry and count channel for the alpha-beta total. The procedure consisted in tracing the spectra of these radionuclides coming from soil and rock collected samples; these spectra gave us information necessary for the calculation of the activity of these radionuclides. For the water samples; we use the other technology. Some results will be presented in a poster to the IRPA conference.

Challenges in Managing Exposures due to Natural Radiation Sources

Tony Colgan, Trevor Boal

International Atomic Energy Agency, Vienna International Centre, Vienna, Austria

Abstract. While regulatory bodies often focus their resources on controlling artificial sources of radiation, most of our exposure is due natural radiation sources. There is a growing recognition that some natural radiation sources can and should be controlled, applying the principle of optimization and using a graded approach, as appropriate. While these issues are being addressed in many countries and some progress has been made, much more remains to be done to harmonize national and international approaches. This paper describes three areas where challenges arise in managing such exposures. Exposure of the public due to radon indoors has been studied for many years and the epidemiological evidence of an increased risk down to concentrations routinely found in many homes is well established. Nevertheless, there are some concerns about the ability to undertake representative measurements, the cost-effectiveness of programs to reduce radon concentrations in existing buildings and the communication of risk. Radon can also be an important source of radiation exposure of workers in certain workplaces and in many NORM industries. Where such industries are regulated, exposure due to radon is managed as a planned exposure situation and dose limits apply. On the other hand, in many workplaces occupational exposure is managed as an existing exposure situation using reference levels. The approach to managing exposure due to radon in workplaces and NORM industries is still developing and many challenges remain to be resolved. In relation to consumer products, an issue of recent concern relates to negative ion bands to which thorium-232 has been intentionally added. In line with the IAEA safety standards, such consumer products should firstly be justified and then meet the criteria for exemption before being authorized by the regulatory body in the country of manufacture. As such items can easily be sold over the internet and may be difficult to identify, importing countries may find it difficult to prevent their sale to and use by the public. This suggests the need for greater harmonization in the approach to justification and the acceptance in one country of a justification decision made in another.

Radioactivity in Some Leafy Vegetables in Roodepoort South Africa

Thulani Dlamini, Victor Tshivhase, Manny Mathuthu

North-West University, Mmbatho, North West Province, South Africa

Abstract. The Witwatersrand has been mined for more than a century. It is the world's largest gold and uranium mining basin with the extraction, from more than 120 mines, of 43 500 tons of gold in one century and 73 000 tons of uranium between 1953 and 1995. The basin covers an area of 1600 km², and led to a legacy of some 400 km² of mine tailings dams (270 tailings dams and 380 MRDs) containing 6 billion tons of pyrite tailings and 430 000 tons low-grade uranium. It is estimated that 6000 km² of soils are significantly impacted by gold mining on the Witwatersrand Basin alone. There is definitely contamination of the nearby environment from the NORM nuclides and this study looked at the leafy vegetables grown and consumed in one of these nearby environments. Thirty leafy vegetable samples were collected from home gardens and from small local markets selling locally produced leafy vegetables. Thirty samples were collected in total, 10 samples each of spinach, cabbages and lettuce. Samples were taken to the laboratory and prepared for gamma analysis to measure the activity of the NORM nuclides. Canberra Model GCW 2021 HPGe Well detector, with 20% relative efficiency and a resolution of FWHM @ 122keV < 1.2 keV and FWHM @ 1332keV < 2.1 keV, was used for measurement. Genie 2000 and DSA 1000 digital spectrum analyser accompanied the detector for spectra acquisition and analysis. ²⁴¹Am, ⁵⁷Co, ¹³⁷Cs, ⁵⁴Mn and ⁶⁰Co were used for energy calibration. For peak efficiency calibration, a ground vegetable sample of leafy vegetables obtained from the supermarket was prepared in the same way as samples but it was not sealed. The matrix was then spiked with measured standards of ⁶⁰Co and ¹³³Ba and the efficiency at each measured peak was plotted as a function of energy. Corrections for coincidence summing were done for some of the peaks. The preliminary results of the study show an elevated activity of ²³⁸U and its daughter nuclides in the leafy vegetables and normal ⁴⁰K and ²³²Th concentration. Calculated dose show an ingestion dose below the dose constraint of 250 μSv/a set by the NNR (South Africa). Only half of the samples have been analyzed so far.

Determination of Natural Radioactivity in the North East Beach Sands of Madagascar

Tiana Harimalala Randriamora

INSTN-MADAGASCAR, Antananarivo, Analamanga, Madagascar

Faculty of Sciences, University of Antananarivo, Antananarivo, Analamanga, Madagascar

Abstract. Exploration and exploitation of radioactive ores (ilmenite and zircon) are considered as the main source of exposure to ionizing radiation of the population living in the coast of Analanjanorofo Region (Fénérive-Est and Soanierana Ivongo Districts). Radioactivity measurements were performed. The distribution of natural radionuclide gamma-emitters (^{238}U , ^{232}Th and ^{40}K) and their respective annual effective dose rates were determined for sand, water and air sampled along and around the coast of the region. The radiation emitted from the natural radioactivity containing in the environmental samples was determined by using a gamma spectrometry equipment and Radon meter (SARAD). Exposure dose rates at 1 m above the ground were measured along and in the villages around the exploitation sites by using a Dosimeter Graetz X5 DE, equipped of Geiger Müller Counter. Results were compared with the reference values provided by IAEA (BSS 115) and UNSCEAR 2000.

KEYWORDS: *coastal sands; ^{238}U , ^{232}Th and ^{40}K concentrations; annual effective dose rate; gamma spectrometry; Geiger Müller counter.*

Availability and Reliability of Meteorological Data for Atmospheric Dispersion Models

Tamas Pázmándi, Sándor Deme, Lilla Hoffmann, Péter Szántó

Hungarian Academy of Sciences Centre for Energy Research, Budapest, Hungary

Abstract. Atmospheric dispersion calculations are widely used in the nuclear industry, not only for environmental impact assessment of normal operation and safety analysis for DBC (design basis conditions) or DEC (design extension conditions), but also for decision support systems for nuclear emergency response. Appropriate information about the source term and adequate meteorological data are essential for these calculations. Different methods and numerical models can be used for the different purposes, and also various input data are applicable for the calculations. Assuming that the source term is known, meteorological data are necessary to specify radioactivity distribution in the environment and to provide adequate dose consequences for areas affected by the emission. The most important meteorological data for activity dispersion calculations are wind speed and wind direction, precipitation, atmospheric stability and height of atmospheric boundary layers. These meteorological data may originate from local measurements or from numerical weather prediction data. These databases have different spatial and time resolution, accuracy and also credibility of the data varies. Data available in different databases, reliability of the data and their consequences on the results of dose calculations will be presented; advantages and disadvantages of these data will be discussed.

A Study on Adsorption of the Radioactive Noble Gases in the Atmosphere by a Portable Sampling System

Wanno Lee, Young-Yong Ji, Young-Hyun Cho, Sando Choi, Jiyoung Park, Geen-sik Choi, Hyunchel Kim, Jong-Myong Lim

Korea Atomic Energy Research Institute, Daejeon, Republic of Korea

Abstract. Measurements of radioactive Kr-85 and Xe-133 in atmosphere are very important for detecting clandestine plutonium production and underground nuclear test. Additionally, the radioactive krypton can be used as a tracer of research for the climate change. Noble gases monitoring such as Kr-85 and Xe-133 could detect remotely on-going reprocessing activities and nuclear explosion as well as accidents when an atmospheric transport model is simultaneously used. In this study, a portable noble gas sampling device based on the BfS-IAR system (Bundersamt für Strahlenschutz-Institute of Atmospheric Radioactivity) is improved for the mobile collection such as ship or vehicle. Sampling method during movement and device structure will be introduced and discussed. In order to evaluate the adsorption capability for the Krypton and Xenon in the atmosphere, 10 m³ air volumes are collected by the change of a sampling time from one day to six days. The adsorption volumes of the Krypton and Xenon were also compared to the values by a commercial BfS-IAR system. Finally the activities of Kr-85 and Xe-133 in ground level are measured.

Animal-to-water Concentration Ratios of Various Elements in Marine Ecosystems around two Korean Nuclear Sites

Yong-Ho Choi, Kwang-Muk Lim, In Jun, Byung-Ho Kim, Dong-Kwon Keum

Korea Atomic Energy Research Institute, Yuseong, Daejeon, Republic of Korea

Abstract. Concentration ratios (CRs) defined as the ratio of the radionuclide concentration in the fresh whole body of a wildlife species to that in the environmental medium are a key parameter in estimating the internal radiation doses to wildlife. The generic CR values of the IAEA are to be used when site-specific data are unavailable. This is because CR values can vary greatly with the environmental conditions and with the wildlife species even within the same group. In preparation for the anticipated future regulation on wildlife exposure to ionizing radiations in Korea, this study was conducted as a part of a 5-year research planned to establish Korean data files of CR values. Marine areas within about 5 km radii of the Gyeongju (GJ) and Younggwang (YG) nuclear sites were investigated. Through samplings at different times in 2012, 16 fish species and three mollusc species were collected around the GJ site, whereas ten fish species and two crustacean species were collected around the YG site. Fish and crustaceans were caught using fishing nets, which were laid at depths of several meters. Molluscs were caught near the seashores by a traditional female diver. The samples of the associated water were collected near the animal-catching locations using a Van Dorn sampler. The elemental concentrations were measured using an ICP-AES and an ICP-MS. A total of 22 elements were analysed. Isotopes are well-established analogies to one another for their behaviour in equilibrium. For fish, the CR values of Na and Mg were lower than 1 in all cases but the opposite was true for the others except Li, Ni, Th and U. Zn showed mostly the highest values, followed by Mn, Al, Cu, Fe or Cr in general. The highest fish value was 2.4×10^4 , which occurred in Zn of silver whiting in the GJ area. Similarly, the CR values of Al, Fe, Mn, Cr, Cu, Zn and Pb were generally higher than those of the others in molluscs, for which the Na, Mg and Li values were also mostly lower than 1. In crustaceans, the Cu values were the highest, ranging from 6.1×10^2 to 8.8×10^3 , whereas the Na or Li values were the lowest, ranging from 1.6×10^{-1} to 8.8×10^{-1} . Almost all of the CR values of Cs were in the range of 10-200. In many cases, there are considerable differences between the values obtained and the corresponding IAEA values, indicating the importance of using site-specific data. Further studies need to be conducted for filling data gaps and improving the CR data files.

Review of Approaches based on ^{210}Po and other Daughters of ^{222}Rn for Retrospective Estimate of Radon Concentration

Yazdan Salimi^a, Mohammad Reza Kardan^{b,h}, Mohammad Reza Deevband^a, Dariush Askari^c, Jalal Ordoni^c, Mohammad Hossein Jamshidi^d, Hamed Dehghani^e, Fatemeh Ramrodi^g, Hamid Behrozi^f

^aDepartment of Physics & Medical Engineering, Faculty of Medicine, Shahid Beheshti University of Medical Sciences, Tehran, Iran

^bNuclear Safety and Radiation Protection Group, Nuclear Sciences and Technology Research Institute, Tehran, Iran

^cDepartment of Radiology, Faculty Paramedical Sciences, Shahid Beheshti University of Medical Sciences, Tehran, Iran

^dDepartment of Medical Physics, Faculty of Medicine, Jundishapur University of Medical Sciences, Ahvaz, Iran

^eDepartment of Biomedical Engineering and Physics, Faculty of Medicine, Tehran, Iran

^fDepartment of Radiologic Technology, Faculty of Paramedicine, Jundishapur University of Medical Sciences, Ahvaz, Iran

^gDepartment of Radiology, Faculty Paramedical Sciences, Zahedan University of Medical Sciences, Zahedan, Iran

^hIranian Nuclear Regulatory Authority, Tehran, Iran

Abstract. Radon, a naturally occurring radioactive gas in the decay series of Uranium238 is ubiquitous in indoor environment. The main sources of ^{222}Rn to the air are soil and rock. It is a major natural radiation source of human exposure to ionizing radiation (half of it). At present radon is considered the second most probable cause of lung cancer after smoking. Measurement Radon concentration just at this time is not sufficient for calculation of someone's total exposure and estimating the risk. But retrospective methods can present the long-term exposure of people lived in a place. Many novel retrospective approaches were defined from 1944. All of them tried to find a correlation between a measurable quantity in present and the past concentration of radon. In this study we reviewed retrospective methods based on detection of implanted radon alpha emitter daughters on easily accessible surfaces like CDs or glass. It has been proved that alpha activity on glass exposed to ^{210}Po has a linear correlation to the total radon exposure. Some of radon progeny on glass surface will embed in the glass by alpha recoil process. Because of the long half-life of ^{210}Pb (22.3 y), the glass acts as a memory for the airborne radon activity over several decades. This activity can be measured by means of polycarbonate dosimeters like Kodak LR-115 and CR-39, Or by optically stimulating luminescent (OSL). There are approaches to remove background activity effect due to potassium40 on the surface: 1- using two CR-39 dosimeters on the top and back of the glass 2- using a separate LR115 and CR39 because of their sensitivity to different energies of alpha, 3- Using two CR-39s, with an absorber layer and without it. The sensitivity of method was reported concentration of $1\text{Bq}/\text{m}^2$ for six month measuring. In non-smoking environment correlation factors from 0.75 to 0.99 were reported. But this system is will fail in smoking environments. The material if base of CD and DVDs is polycarbonate, commercially named Makrofol. CD method is based on radon absorption ability of Makrofol. After chemical and electronical etching alpha tracks in depth of 60 to 80 micrometres will become countable. Number of these tracks is related to integrated concentration of radon in the past. Radon concentrations even less than currently proposed WHO reference levels can be identified with CDs stored less than a year; precision of 10% was reported for this method.

A Simple Method for Measurement of Radon in Groundwater

Yunyun Wu, Hongxing Cui, Bing Shang, Jianxiang Liu

National Institute for Radiological Protection (NIRP), Chinese Center for Disease Control and Prevention, Beijing, China

Abstract. Radon-in-water activity concentrations are conventionally detected by means of liquid scintillation counting (LSC) and Lucas cells. Although ^{222}Rn in water may be measured reliably by these classical methods, it requires cumbersome handwork and a relatively long time for radioactive equilibration. Moreover, the complex instrumental setup is inconvenient on field sites. Therefore, a simple method was developed for the continuous monitoring of ^{222}Rn using a radon-in-air monitor coupled to an air-water exchanger. Laboratory and field experiments were carried out in order to evaluate the applicability of the experimental set-up for analysis of radon in water samples. A sample bottle with aerator is connected to a radon monitor RTM2200 (SARAD GmbH, Germany) in a closed air-loop mode. The system determines ^{222}Rn in continuously circulating air in fast mode, which is in equilibrium with a constant stream of water passing through an air-water exchanger. The measurement system is portable and simple, and no desiccant is required. The experiment to explore the dependence of the radon-in-water/radon-in-air equilibration time on flow rate of air pump and water sample volume were carried out. It showed that the radon-in-water/radon-in-air equilibration time closely depends on the flow rate of internal air pump in monitor; for example, equilibration takes only about 5 min at a flow rate of 0.65 l/min. However, the water sample volume had no effect on the equilibrium time between water and air phase. The system is calibrated with ^{226}Ra -standard solution. As expected, it produces accurate results for measurements of radon in water. The detection limit for radon-in-water for the system in this work is about 0.268 Bq/L at a temperature of 25 °C at a 5 min counting cycle. In order to test the applicability of the RTM2200H₂O for on-site analysis of groundwater samples, drinking water samples were taken in public water supply and wells from several sites in Beijing, China. The results achieved with RTM2200H₂O and RADH₂O for radon activity concentrations in groundwater are in very good agreement. Main advantage of the developed experimental set-up compared with the RADH₂O, is that our system no desiccant is required. Hence, it is more convenient and suitable for extensive radon in water surveys or on-site measurements of radon.

Application of Non-equilibrium Adsorption Model in the Migration of Radionuclides

Zhu Jun

China Institute for Radiation Protection, TaiYuan, ShanXi, China

Abstract. The influence of the shallow stratum disposal of the low and medium radioactive waste on the environment, the key is to consider the migration of radionuclides in the groundwater environment, and its movement is the result of a series of complex process of physical, chemical, microbiological and so on. In the course of its development, it is coupled with advection-dispersion, molecular diffusion, adsorption and decay process. Adsorption accounted for a large proportion in the factors affecting migration, is mainly divided into equilibrium adsorption and non-equilibrium adsorption. Equilibrium adsorption models were applied to the premise that solute in porous media can quickly reach the adsorption-desorption equilibrium or is a long enough time for adsorption phase and dissolved phase to achieve a balance. However, when the contact time is short and the adsorption is not fast enough, we find that the equilibrium adsorption models is not always a good description for the adsorption. Such as the breakthrough curve is not symmetric and smearing, colloidal attachment-divorced, flow only in the fractured movement, non-fracture zone restricted phenomena. The main reason for the above problems is that the different forms of adsorption and the different forms of flow in solid media. Based on the above reasons, the radionuclide migration model is gradually developed to the non-equilibrium adsorption model.

Environmental Impact Assessment of the NPP Krško for Period of 5 years

Zeljka Knezevic^a, Zeljko Grahek^a, Borut Breznik^b

^aRudjer Boskovic Institute, Zagreb, Croatia

^bNuclear Power Plant Krsko, Krsko, Slovenia

Abstract. External radiation from different radionuclides naturally present in the environment or released from man-made sources or events is an important component of the exposure to human populations. Nuclear power plant (NPP) Krško (PWR type) is located close to densely populated areas with over one million inhabitants including Zagreb city. Under normal operating conditions NPP release small amounts of radiation (radioactive isotopes) into the environment. Therefore radiological environmental monitoring programs at nuclear power plants are required in accordance with the regulations. Objectives of program include: identification, measurement and evaluation of existing radionuclides in the environs of the facility and fluctuations in radioactivity levels which may occur; evaluation of the measurements to determine the impact of operations on the local radiation environment, collection of data to refine transport models and verification that radioactive material containment systems are functioning to minimize environmental releases to levels that are as low as reasonably achievable (ALARA). Implicit in these objectives are the requirements to trend and assess radiation exposure rates and radioactivity concentrations in the environment that may contribute to radiation exposures to the public. Therefore main aim of this work is to show impact of nuclear power plant Krško on the environment and public. For this purpose the following environmental pathways and sample analyses are investigated: liquid discharge from NPP, bottom sediment, fish, river water, drinking or potable water, ground water, and ambient dose equivalent using passive solid state dosimeters (thermoluminescent and radiophotoluminescent dosimeters (TLDs and RPLs). Results of long term measurements of ³H, ⁹⁰Sr, gamma emitting radionuclides and ambient dose equivalent will be presented. On the base of these results, contribution by each pathway to the individual and cumulative dose will be assessed.

**The Proceedings of the 14th International Congress of the International Radiation
Protection Association
Volume 4 of 5**

Area 8: Transport / Sealed Source Management

Validation Testing of Canberra-Obayashi Mobile type TruckScan Pre- production Unit

Atsuo Suzuki^{a*}, Frazier L. Bronson^b, Masaru Noda^c, Naoya Takada^c, Keizo Yamasaki^c

^aCanberra Japan KK, Asakusabashi Bldg, 4-19-8, Asakusabashi, Taito-ku, Tokyo, 111-0053

^bCanberra Industries Inc., 800 Research Parkway, Meriden, Connecticut, 06450

^cObayashi Co., Shinagawa Intercity Tower B, 2-15-2, Konan, Minato-ku, Tokyo 108-8502

Abstract. Canberra Industries, Inc. [CI] has developed and validated a new truck monitoring system ‘TruckScan’ for Interim Storage Facilities [ISF] in Japan. There is an estimated 28 million cubic meters of soil and vegetation from the decontamination efforts around Fukushima. This material is in 1 cubic meter flexible containers called Super Sacks [SS]. These SSs will be transported to ISF by trucks. The SSs will be separated according to Total Cs level [<3000 , >3000 but <8000 , <8000 , >8000 but $<100,000$, $>100,000$ Bq/kg]. Some TruckScan units will be at the entrance of ISF to measure the incoming trucks. But to allow more flexibility in future deployments, CI and CJKK (Canberra Japan KK) designed the unit to allow it to be quickly deployed to the Temporary Storage areas or other areas where the trucks are loaded. The pre-production version of the TruckScan has been deployed by CI and Obayashi Corporation for validation testing, at a temporary site near to the Fukushima NPP and the future location of the ISF. The TruckScan has eight LED-stabilized 3x3” NaI detectors, each in a lead shield with a collimated view of the truck; four detectors on each side of the truck, at about 1.1 meter from the truck, spaced at equal distances. These NaI detectors and collimators were calibrated by In Situ Object Counting System (ISOCS) mathematical efficiency calculation tool. An advanced version of the software [SuperISOCS] computes the efficiency of each individual sack on each truck dynamically as part of the assay. The truck stops in-between the two sets of detectors for the [typical] 15 second measurement period. The special software performs gamma spectroscopy on each of the 8 spectra, and then decodes the results to determine the activity in each of the 6-7 [typically] SSs using a Maximum Entropy Analysis Method. The information about the truck, the SS loading pattern, weight and fill height of each sack is entered in the field on a Tablet PC using software developed by Obayashi corporation, and sent to TruckScan operation PC. Validation testing was done by using 70 SSs in different loading patterns. Each of these SSs was measured with an ISOCS Ge system to determine the “true” activity. The results of the TruckScan assay indicate good accuracy for the wide range of conditions. The results of these validation tests show that the unit has a combined standard deviation for SS at 8000 Bq/kg at less than 20%, which was the predicted performance. In addition to these, more important merits of TruckScan are to reduce the radiation dose of workers, cost for measurement and to improve throughput.

KEYWORDS: *decontamination waste; Fukushima; flexible container; fast Cs measurement; radiation dose reduction.*

1 INTRODUCTION

After Fukushima NPP accident, five years has passed. The decontamination of the land has made considerable progress. As a result, there are a large number flexible container bags, commonly called SuperSacks [SS], in Temporary Storage Area [TSA]. The SSs contain radioactive waste, mainly soil and vegetation. The primary radionuclides remaining today are Cs-137 and Cs-134. These SSs are nominally 1.1m diameter by 1m tall, and typically weigh between 0.5 and 1.5 metric tons. Also some broken SSs are repacked to 1.3m diameter SSs, weighing between 1.5 and 2.0 metric tons. Starting in 2015, these SSs were transported as a test case to several Temporary Interim Storage Facilities [Temporary ISF] near Fukushima Daiichi NPP, called Pilot Transportation Campaign. Ten ton trucks are used for this transportation campaign, each containing typically 6-7 for SSs, or 4-5 of the large SSs.

* Presenting author, e-mail: atsuo.suzuki@canberra.com

The authorities are now considering where and how to measure radioactivity of SSs. CI and Obayashi Corporation have developed a system called Mobile TruckScan (MTSCAN). This system is able to measure multiple SSs loaded onto trucks of typically 10ton capacity, and accurately report the activity of each individual SS, with typically a 10-20second assay time. The system can also accommodate smaller 2ton and larger 20ton trucks. The system is relatively compact, and therefore easy to move and setup at a different location. MTSCAN is expected to measure the SSs after they are loaded onto trucks at the TSA, and at the entrance of the ISF.

This document reports the testing results from the large-scale demonstration campaign of the pre-production unit of the MTSCAN conducted in the fall of 2015.

2 THE RESULTS OF VALIDATION TESTING

2.1 Mobile Type TruckScan Components

2.1.1 Hardware and Software

Figure 1 is an illustration of MTSCAN. It consists of eight LED-stabilized 3x3" NaI detectors, each in a lead shield with a collimated view of the truck. Two detectors are on each lift unit, which can adjust the detector height for various sizes of trucks, or lower them for easy transport. Four detectors are on each side of the truck, at about 1.1m from the truck side wall, equally spaced at approximately 1.3m. These NaI detectors and collimators were calibrated by the ISOCS mathematical efficiency calculation tool. The efficiency of each detector was calculated quickly at every measurement by Super ISOCS. The truck stops in-between the two sets of detectors for the short measurement period – typically 10-20s for 8000Bq/kg SSs and higher, 30 seconds for 3000Bq/kg SSs. The special software performs gamma spectroscopy on each of the 8 spectra, and then decodes the results to determine the activity in each of the [typically 6 or 7] SSs using a Maximum Entropy Analysis Method.

Figure 1: Image of the Mobile Type TruckScan.



2.1.2 Shield

The MTSCAN is designed to be installed outdoors and in an elevated Cs background area, as shown in Figure 2. For typical applications, such as in this case, the around MTSCAN area needs preparation. This can be done by removing contaminated soil or adding steel plates in between the detectors and adding shielding behind the detectors. For this test, the shielding was created with SSs of clean soil. The background (BG) of the Cs-134+137 peak area needs to decrease to approximately 1-2 cps.

In this validation test location, the BG level was 1 $\mu\text{Sv/h}$, which for Cs-134+137 peak area was about 38 cps without shielding. After setting of 24mm steel plate and 3 layers of uncontaminated SSs, the BG level decreased to about 4 cps without truck at the counting area. When an empty truck entered at the counting area, BG level decreased to about 1.4 cps. For this geometry, 1 cps represents approximately 300 Bq/kg for a typical soil SS, and 2100 Bq/kg for a vegetation SS. Based upon this validation test, we recommend increasing the steel plate to about 50mm steel plate, or removing the contaminated soil between the detectors.

Figure 2: Shielding for validation test.



2.2 Validation Test Procedure

Four types of decontamination waste were prepared. Low contaminated level soil (10 sacks), high contaminated level soil (41 sacks), very high contaminated filtration residue of waste water (2 sacks) and decontaminated vegetation (16 sacks) were prepared. The Cs concentrations are approximately 4000, 10,000, 200,000 and 1500Bq/kg, respectively.

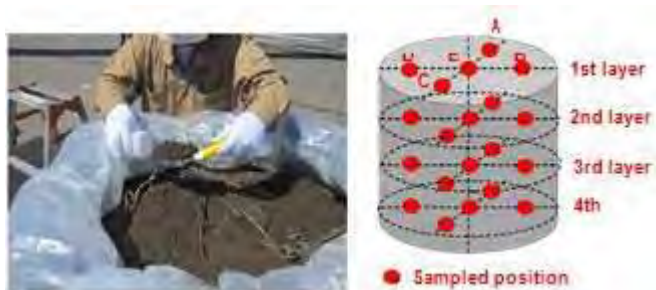
Each of these SS test sacks was measured with Ge in- situ system (Fig.3). Each SS was counted 4 times from the side, each count at 90 degrees from the previous measurement. The concentration of each sample was determined by the average of the 4 measurement results. As further confirmation, 2 SS were evaluated by extracting samples which were then measured with a Ge detector (Fig.4). Each sample was about 1kg. Samples were taken from 20 different positions to evaluate the degree of homogeneity. The average of the 20 samples was then used to confirm the accuracy of the in-situ measurement result.

Figure 3: The measurement of SS with Ge in- situ system.



The MTSCAN analysis method was validated by using these calibrated test sacks and loading them in various patterns, at various distributions or concentration levels, on both 4 ton and 10 ton trucks. These MTSCAN results were compared with in-situ Ge system measurement results.

Figure 4: Sampling situation, positions and containers.



2.3 Validation Test Result

2.3.1 Results (In-situ Ge System and Sampling Measurement)

Table 1 lists the results of each measurement of the 51 soil sacks. Columns 5 and 6 show the measurement results and uncertainty (1sd) of 4 90-degree measurements of each SS. The counting time for each measurement was 5 minutes. The results of low level SSs (S41 - S50) were from 2590 - 6110 Bq/kg. Middle level SSs (S01 - S40, and S51) were 10700 - 24400 Bq/kg. Average standard deviation of 4 90-degree measurements is 6.0% in 51 SSs. This value was used as the non-uniformity component for the MTSCAN TMU (Total Measurement Uncertainty).

Column 7 and 8 of Table 1 show the measurement results and uncertainty (1sd) of sampling measurements. The results from sampling of S15 and S45 were $15000 \pm 9.6\%$ and $4520 \pm 38.4\%$, respectively. The results from the 4 90-degree in-situ Ge measurements were $13500 \pm 3.9\%$ and $4130 \pm 18.5\%$, respectively. These measurements are statistically consistent with each other, with the ± 1 sd ranges overlapping. These results also show the advantage of in-situ measurements as used in the Ge measurements here and in the MTSCAN – the larger viewed area of the in-situ measurement gives a much lower uncertainty for non-homogeneous materials.

Table 2 lists the results of each measurement of the sludge from the filtration of waste water. There were only 2 of these sacks. The Ge in-situ results and uncertainty (1sd) were 166,000 and 219,000 Bq/kg, 13% and 5.5%, respectively.

Table 3 lists the in-situ Ge results of each of the 16 vegetation sacks. These sack activities were 330 - 4030 Bq/kg. The average standard deviation from the 4 90-degree measurement was 10.2%, larger than the 6% average sd from the soil sacks. The cause of the larger sd of the vegetation SSs likely from the contaminated soil that was also present in the vegetation SSs.

Table 1: Results of total Cs concentration of soil sacks. Unit:Bq/kg

Sample Name	Num. of measurement	MTSCAN		In-situ Ge		Sampled method		Density (g/cc)	Ratio MTSCAN/Ge
		Ave.	1sigma %	Ave.	1sigma %	Ave.	1sigma %		
S01	12	10,800	7.6%	11,500	9.4%			1.57	0.94
S02	7	13,400	9.1%	14,200	3.5%			1.12	0.94
S03	5	14,000	8.0%	13,200	5.8%			1.35	1.06
S04	7	17,600	12.0%	17,400	5.8%			1.24	1.01
S05	5	17,200	8.7%	16,000	2.3%			1.31	1.08
S06	3	12,800	10.3%	13,400	4.0%			1.26	0.95
S07	3	16,200	11.1%	17,000	3.5%			1.13	0.95
S08	2	14,500	14.2%	14,700	6.5%			1.31	0.99
S09	8	14,000	17.8%	13,900	12.3%			1.65	1.01
S10	3	17,500	6.1%	17,500	4.7%			1.30	1.00
S11	3	16,400	5.6%	15,600	4.1%			1.23	1.05
S12	1	10,500		10,700	4.3%			1.48	0.98
S13	1	13,300		13,100	5.3%			1.43	1.01
S14	2	12,600	6.5%	14,300	5.7%			1.39	0.88
S15	13	13,400	6.2%	13,500	3.9%	15100	9.6%	1.45	0.99
S16	2	15,500	4.9%	12,800	3.8%			1.45	1.21
S17				11,000	4.7%			1.36	
S18	2	10,800	12.2%	11,100	3.9%			1.49	0.98
S19	2	10,700	0.7%	10,900	5.9%			1.58	0.98
S20	10	11,700	8.5%	11,800	3.0%			1.56	0.99
S21	2	11,200	8.2%	10,900	6.9%			1.32	1.03
S22				12,900	3.6%			1.47	
S23	2	12,100	8.1%	11,700	4.5%			1.57	1.03
S24	2	11,000	4.0%	11,900	3.8%			1.68	0.92
S25	10	12,300	17.2%	12,200	7.6%			1.48	1.01
S26	3	14,900	2.9%	14,500	4.8%			1.48	1.03
S27	9	13,000	10.5%	13,500	8.6%			1.39	0.96
S28	1	13,700		14,700	5.2%			1.25	0.93
S29	1	14,900		11,800	5.2%			1.42	1.26
S30	10	12,900	11.3%	13,000	11.8%			1.31	0.99
S31	10	10,900	16.2%	10,700	10.5%			1.44	1.02
S32	10	13,000	7.2%	12,200	17.0%			1.41	1.06
S33	2	14,600	15.9%	14,700	7.8%			1.43	0.99
S34	1	15,100		15,200	4.0%			1.51	1.00
S35	1	15,200		14,800	7.8%			1.30	1.03
S36	1	16,100		15,400	2.7%			1.39	1.05
S37	2	15,900	28.5%	16,100	1.4%			1.33	0.99
S38	2	15,600	2.9%	15,800	1.5%			1.30	0.99
S39	1	16,300		13,900	5.4%			1.40	1.18
S40	2	19,500	16.3%	15,600	5.8%			1.53	1.25
S41	2	4,230	28.3%	4,270	4.7%			1.80	0.99
S42	1	4,140		3,520	4.4%			1.81	1.18
S43				2,590	7.0%			1.59	
S44	8	5,970	17.7%	5,700	13.1%			1.52	1.05
S45	10	4,730	23.1%	4,130	18.5%	4,520	38.4%	1.53	1.14
S46	11	5,050	22.2%	4,640	2.9%			1.55	1.09
S47	3	4,550	34.4%	5,290	7.3%			1.50	0.86
S48	4	5,950	25.6%	6,110	4.9%			1.62	0.97
S49	1	3,430		3,940	6.9%			1.38	0.87
S50	2	4,620		4,860	4.0%			1.39	0.95
S51	2	25,900	32.4%	24,400	2.8%			1.46	1.06
Total	207								
Average			12.9%		6.0%			1.44	1.02
TMU 1 sigma									14.8%

Table 2: Results of total Cs concentration of filtration residue of waste water. Unit:Bq/kg

Sample Name	Num. of measurement	MTSCAN		In-situ Ge		Density (g/cc)	Ratio MTSCAN/Ge
		Ave.	1sigma %	Ave.	1sigma %		
H01	7	170000	4.0%	166000	13%	1.08	1.02
H02	4	189000	5.6%	218000	5.5%	1.03	0.87
Total	11		4.6%		9.4%	1.05	0.95

Table 3: Results of total Cs concentration of vegetation sacks. Unit:Bq/kg

Sample Name	Num. of measurement	Num. of detectable	MTSCAN		In-situ Ge		Density (g/cc)	Ratio MTSCAN/Ge
			Ave.	1sigma %	Ave.	1sigma %		
F01	6	6	3,930	26.9%	2,910	4.8%	0.28	1.35
F02	9	2	2,760	9.3%	1,150	9.6%	0.29	2.40
F03	5	4	3,210	30.7%	3,560	15.2%	0.28	0.90
F04	5	3	3,220	28.1%	2,680	17.5%	0.36	1.20
F05	9	2	2,890	18.7%	380	21.1%	0.28	7.61
F06	4	1	3,780		1,690	7.1%	0.28	2.24
F07	3	2	2,930	16.4%	330	15.2%	0.32	8.88
F08	6	2	3,530	26.4%	540	13.0%	0.27	6.54
F09					3,030	18.8%	0.30	
F10					3,320	7.8%	0.30	
F11	5	0	ND		730	6.8%	0.30	
F12	1	1	2,570		1,660	3.0%	0.31	1.55
F13	5	0	ND		3,280	4.3%	0.27	
F14	5	0	ND		940	4.3%	0.27	
F15	5	0	ND		520	5.8%	0.30	
F16	2	2	4,910	9.7%	4,030	2.7%	0.14	1.22
Total	70	25				10.2%	0.28	

2.3.2 Results (MTSCAN Measurement)

Columns 3 and 4 in Table 1 show the measurement results and 1sd in each soil SS with MTSCAN. The last column shows the Ratio - MTSCAN results divided by in-situ Ge results. The average Ratio is 1.02 and 1sd of 14.8%. These results indicate MTSCAN can accurately measure the activity over this wide range of activities and loading patterns.

Columns 4 and 5 in Table 3 show the measurement results and 1sd in each Vegetation SS with MTSCAN. Column 3 shows the number of times that the sack activity was above the MDA. These sacks were at quite low levels and for many of the measurements they were loaded next to soil sacks with considerably more activity. About two thirds of the vegetation SS measurements were less than MDA. Although a proper statistical analysis cannot be done, a cursory look at those 4 sacks that were detected >80% of the time shows an average Ratio of 1.25 and 1sd of 27%. The elevated ratio is due to the elevated background in the area.

Column 7 of Table 2 shows the Ratio of the MTSCAN to the Ge in-situ values for those two sacks. The average ratio is 0.95 and both results are in good statistical agreement with the Ge values.

2.3.3 Analysis of Data (MTSCAN Measurement)

In this section, more detailed analyses are shown about the performance of the MTSCAN under various measurement conditions.

2.3.3.1 Analysis of Various Loading Patterns

SSs were measured in various loading patterns. Fig. 5 shows the various loading patterns with 10t and 4t trucks. Fig. 6 shows the measurement of both 4t and 10t trucks. Table 4 shows the statistical results of 10t and 4t trucks. The average Ratio and measurement uncertainty are very close to each other. This indicates there is no difference in capabilities between using 10t truck and 4t truck.

Figure 5: Various loading pattern of 10t (Blue) and 4t truck

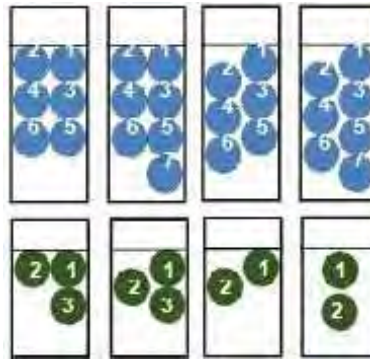


Table 4: The statistical results of 10t and 4t truck.

Truck type	Num. of measurement	Measurement		Ratio	
		1sd %	MTSCAN/Ge	1sd %	
10 ton	207	12.9%	1.02	14.8%	
4 ton	15	11.0%	1.02	13.4%	

Figure 6: Measuring situation of 10t and 4t truck.



2.3.3.2 Analysis of Measuring Different Face of each SS

If the radioactivity in the SS is not unevenly distributed, the uncertainty in the MTSCAN results will be worse than a homogeneous sack, since the MTSCAN only looks at one side of the SS. To evaluate this component of uncertainty, 12 different SSs were measured in MTSCAN 4 different times, each time with a different face of the SS pointed toward the detector, as shown in Figure 7. The ‘FACE’ measurement value is the comparison between the MTSCAN results to each of the individual 90-degree ISOCS-Ge results. The ‘MEAN measurement’ value is compared to the mean of the 4 90-degree Ge results. Figure 8 shows these data graphically and demonstrates visually that there is no difference between the two data sets. Table 5 shows that the average MTSCAN/Ge ratio is 1.03 for both sets of data. And since the uncertainties are similar, the sack non-homogeneity is a small component of the TMU.

Figure 7: Measurement of different face of each SS

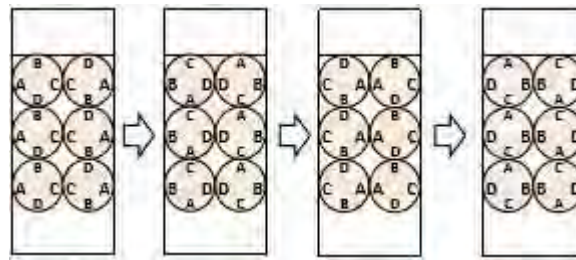


Figure 8: The correlation between each FACE and MEAN measurement.

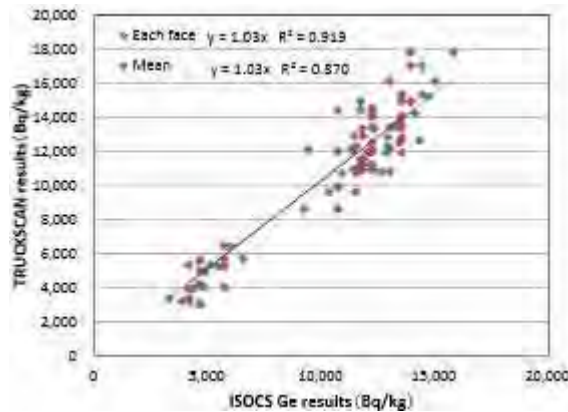


Table 5: The ratio of MEAN and FACE

Truck type	MTSCAN/Ge	Ratio	
			1sd %
MEAN	1.03		15.5%
FACE	1.03		12.2%

2.3.3.3 *Mixing Extremely High and Low Activity SSs*

The MTSCAN can measure 10 SSs on the same truck, but if there are some very high activity SSs on the truck, those low activity SSs near the high activity SSs will be more difficult to measure accurately. Fig.9 show the loading patterns designed to test for this effect. While the results of the high activity sacks were quite consistent with other results in terms of percent uncertainty, those same high activity sacks made the uncertainty of the low activity sacks very large. The conclusion is that if a MTSCAN truck assay shows the presence of these very high activity SSs, then those high level ones should be removed, and the remaining items assayed again.

Figure 9: Loading patterns combining high and low activity SSs

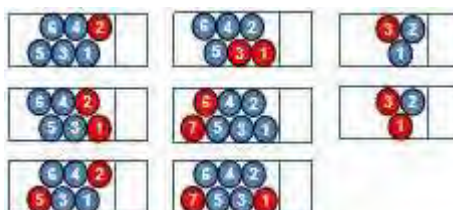


Figure 10: The situation of MTSCAN transportation.

2.3.3.4 Portability of MTSCAN

The MTSCAN is built from several small units for easy transportation. There are 4 measurement units and 1 operations room. Fig.10 shows the MTSCAN being moved from one location to a different location. The only connection from the operation room to the measurement unit is one LAN cable to each detector. AC power is also required at each measurement unit for the detector elevation lift. The weight of a measurement unit is about 1500kg. The MTSCAN was demonstrated to be removed and prepared for operation in about 4 hours.

2.4 Estimated Total Measurement Uncertainty (TMU)

The measurement accuracy of MTSCAN is very important. The TMU of traditional manual methods of single sack activity measurements in Japan is estimated to be more than 20%. The target performance of MTSCAN TMU is less than 20% for 8000 Bq/kg SSs. Table 6 shows estimated uncertainty for different elements of MTSCAN. These uncertainty contributions are listed at the 1sigma level, both as a percentage and as an uncertainty on the activity concentration for an 8000 Bq/kg assay result. Finally, all of the listed uncertainty contributors are added in quadrature to estimate the TMU. Certain items were identified as key contributors to the TMU. Improvements have been developed and are in the process of being implemented and tested. Values are listed for those from the original calculations, and for those from the planned improvements. We estimate that the TMU will be 19%. The TMU from the actual measurements was only 15%, because many of the variables in real operations were carefully controlled in those tests.

Table 6: Total Measurement Uncertainty contribution by component (750mm fill height condition)

Contributing Factor to the Total Measurement Uncertainty	1sd condition	1sd TMU contribution, original estimate	Validation testing result
Matrix layering	Validation testing data	4%	4%
Different matrix material	Idem	2%	2%
Matrix density inhomogeneity	Idem	2%	2%
Different material per sack	Idem	3%	3%
Heterogeneous source distribution	Idem	5%	5%
Bed height	±100mm	6.5%	Controlled suitably
Sidewall height	±25mm	1.5%	Idem
Sidewall thickness	13 – 23mm	18%	Idem
(with planned improvement)	(New modeling)	(2.4%)	
Sack fill height	±125mm	17%	Idem
(with planned improvement)	(±25mm) Validation	(4%)	
Sack diameter and positioning	testing data (New	5-25%	Idem
(with planned improvement)	Modeling)	(6.5%)	
Sack weight	±5% difference	0.25%	Idem
Vehicle location – fwd / bkw/d	±100mm	4.3%	Idem
Vehicle location – left / right	±100mm	8.2%	Idem
Different concentrations per sack	8000±5000 Bq/kg	10%	Idem
Counting statistics	8000 Bq/kg condition	4.8%	Idem
Combined TMU at 8000 Bq/kg (With planned improvements)		34% (2700 Bq/kg) (19%) (1550 Bq/kg)	15% (1200 Bq/kg)

2.5 Throughput

Throughput of MTSCAN production version is estimated to be about 600 tons per hour. This assumes 45 seconds to measure the truck and get a new truck in position, and trucks holding 7 SSs of 1 ton each. The current pre-production version takes about 90-120 for the measurement and truck exchange, with a throughput of about 250 tons per hour.

2.6 Reducing Operational Cost and Worker Radiation Dose

Now the concentration of SS is measured by a ‘Simple Method’ in Japan - a survey meter with a collimator (Fig.11). This method needs two workers near to each SS, increasing the workers radiation exposure. On the other hand, MTSCAN needs only one operator, and the operator does not need to be close to the SS. MTSCAN can reduce workers labor cost and exposure dose. According to the estimation from the Validation test, the total cost of MTSCAN per SS is about 140 JPY and that of Simple method is about 2100 JPY. This shows the MTSCAN can reduce total cost to about 1/93 in the entire ISF working period. In addition to this, MTSCAN can reduce the number of workers to 1/17 and the total exposure dose to 1/7 of that in case using the Simple method.

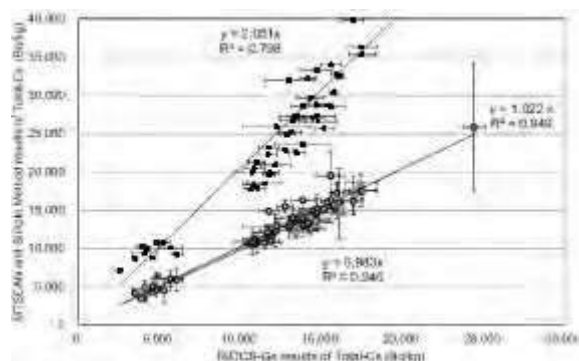
Figure 11: The situation of Simple Method



2.7 Accuracy of MTSCAN as compared to the ‘Simple Method’

The measurement result by the ‘Simple Method’ is typically 2x higher than the correct value, due to the influence of nearby SSs. Fig.12 shows both the results of the Simple Method and MTSCAN for both 4t and 10t trucks. The correlation factors between MTSCAN and the Ge in-situ results are ‘ $y=1.022x$, $R^2=0.949$ ’ for 10t trucks and ‘ $y=0.983x$, $R^2=0.945$ ’ for 4t trucks. This shows very good accuracy, and shows no bias as a function of activity. Whereas the correlation factor of between Simple Method and Ge in-situ is ‘ $y=2.051x$, $R^2=0.798$ ’. This means that Simple Method has about 2 times bias and much worse uncertainty than MTSCAN.

If some extremely high contaminated [$>100,000$ Bq/kg] SSs happen to be in the truck during the MTSCAN measurements onto the truck bed, the accuracy the low level sack results from MTSCAN are worse. To avoid this situation, if some very high SSs are detected, these SSs should be removed and remainder should be measured again.

Figure 12: The results of Simple Method and MTSCAN in comparison with ISOCS-Ge.

3 CONCLUSION

MTSCAN has a better accuracy and throughput than Simple Method, and no bias. For the measurement uncertainty, MTSCAN has equal or better than single sack measurement system. In addition to this, MTSCAN can reduce the total cost and total exposure dose of workers drastically in comparison with the Simple method and traditional/latest method in Japan.

The production version of MTSCAN will offer reduced measurement uncertainty by controlling TMU components suitably and higher throughput by more efficient software coding.

4 ACKNOWLEDGEMENTS

This research was planned by Obayashi Corporation and adopted as ‘Decontamination and volume reduction of decontamination waste technical proof project’ by the Ministry of Environment (MOE). Obayashi Corporation and Canberra Japan KK received financial support of MOE.

5 REFERENCES

- [1] A. SUZUKI, F. BRONSON, M. NODA, et. al., 2015. Validation Testing of Canberra-Obayashi TruckScan Calculation Method, Proceedings of Waste Management WM2015 Conference, Phoenix, AZ, March 15.
- [2] B. M. Young, A. Patil, M. Vicuna, et al., 2016. Performance of Canberra TruckScan Waste Assay Measurement System, Proceedings of Waste Management WM2016 Conference, Phoenix, AZ, March 8.
- [3] R. VENKATARAMAN, F. BRONSON, V. ATRASHKEVICH, et. al., 1999. Validation of InSitu Object Counting System (ISOCS) Mathematical Efficiency Calibration Software, Nuclear Instruments and Methods in Physics Research (A), 422.
- [4] M. REGINATTO, P. SHELBELL, and K. M. MILLER, 1996. An application of the maximum entropy method for assessments of residual radioactivity at contaminated sites,” IEEE Trans. Nucl. Sci. 43.

Regulatory actions in the case of a radioactive source stuck in an oil well

Marcela G. Ermacora*, Claudia Chiliutti, Valeria Amado, Horacio Lee Gonzáles, Hugo Vicens

Nuclear Regulatory Authority, Av. del Libertador 8250, C1429BNP Buenos Aires, Argentina

Abstract. Radioactive sources, and in some cases radiation generators, are widely used in the petroleum industry as tools for the purposes of well characterization. The radioactive sources used in this activity imply certain unique hazards, thus strict protocols must be followed, regulatory control is essential and a solid safety culture must be promoted. The mobile nature of these tools and risk associated with their transport through difficult access locations are important issues to be considered. There are approximately 9 000 well logging sources in the world and hundreds of such sources have been lost down-hole and cemented in place over the years. At present, 228 radioactive sources are used for this purpose in Argentina. The radioactive sources are under the control of the Nuclear Regulatory Authority and 5 have been cemented since 2002. This paper describes the regulatory framework in Argentina with regard to well logging sources and the compliance with these regulations will ensure their safe use. The paper also describes a particular event in which a tool containing radioactive sources got stuck in an oil well. Doses of members of the public which may be associated with the possible dispersion of the material in the radioactive source for loss of tightness, as well as radiological consequences, were evaluated using conservative scenarios. Based on these results and considering the location of the radioactive sources, the sequential actions made and the regulatory decisions taken are described. As a conclusion, all the steps were analyzed and they were consistent with the practices recommended at an international level for similar cases.

KEYWORDS: *radioactive sources; regulatory control; well-logging; doses; hazards; petroleum industry.*

1 INTRODUCTION

Well logging allows operators to record the geological layers properties such as permeability, porosity and conductivity as a function of depth. Thus the location and quality of the hydrocarbons present in the area are characterized, facilitating their exploitation. There are different types of well logging: electrical, radioactive, sonic, induction, and others. In particular, in well logging using radioactive sources a source is introduced into the well to study the interaction of radiation with the ground (gamma-gamma and neutron-gamma well logging). The gamma-gamma logging measures the overall density of the lithological formations traversed by the borehole. The well logging probes contain a gamma radiation source in the form of a metal sealed capsule and separate detectors shielded with respect to the source. Usually the radioisotope ^{137}Cs is used as source (661.6 keV gamma energy and 30.17 years radioactive half-life $-T_{1/2}$). The neutron logging determines the amount of hydrogen present, being a humidity indicator; it can also be used as an indicator of gas existence [1,2]. In this case, the sources most commonly used are those of ^{241}Am (Be) ($T_{1/2}$ of the ^{241}Am : 4.32×10^2 years). ^3H (neutron generators) and ^{252}Cf are also used. In all cases they are sealed sources.

This practice is regulated in Argentina by the Nuclear Regulatory Authority (ARN) through the Regulatory Standard A.R. 7.9.2 Rev.0 [3], in which the requirements that must be met to carry out the operations are established.

During use, the source is extracted from its shielding quickly and is placed in a tool set that then descends to the bottom of the well to obtain profiles. During logging tasks, the supporting tool of sealed radioactive sources could get stuck at a certain depth without a viable alternative for recovery. In this case, it is necessary to implement actions to minimize radiological risk for release of radioactive material into the groundwater, because of the natural degradation of shielding or by the accidental destruction due to an unexpected collision with another tool.

* Presenting author, e-mail: mermacora@arn.gob.ar

This paper describes the regulatory framework in Argentina with regard to well logging sources and also describes the regulatory decisions taken for a particular event in which a tool containing radioactive sources got stuck in an oil well, based on the results of a simplified assessment of doses of members of the public associated with the possible dispersion of the radioactive material.

2 THE REGULATION AND CONTROL IN ARGENTINA

Law No. 24,804 [4], called the National Nuclear Activity Act, enacted on April 2, 1997, and its Regulatory Decree 1390/98, provides that the National State will establish nuclear policy and perform the functions of regulation and control by the Nuclear Regulatory Authority (ARN). Among other things, this Act gives the ARN the competition to dictate regulatory standards on radiation safety and transport of radioactive material; grant, suspend and revoke licenses and permits; and conduct inspections and regulatory assessments.

In the particular case of well logging, the requirements that must be met in radiation safety in this field of application are set out in the Standard AR 7.9.2 Revision 0 "Operation of radiation sources for industrial applications." Other related standards in force are: AR 7.11.2 Revision 0 "Individual permits for operators of radiation sources for industrial applications", AR 10.16.1 Revision 3 "Transport of Radioactive Material" and AR 10.1.1 Revision 3 "Basic Radiation Safety Standard"[5,6,7].

In addition, in case of non-compliance with current legislation, the "Sanctions Regime for Classes II and III Facilities, Non-routine Practices and Transport of Radioactive Materials" applies, in force since August 31st, 2002 by resolution of the ARN Board of Directors No. 32/02. [8]

In the case of Standard AR 7.9.2, it establishes general criteria and specific criteria for the operation. It also establishes requirements regarding individual monitoring, controls associated with the maintenance and repair of all equipment, and for documentation, records and reports to be sent to the ARN.

2.1 Operating licenses

Service providers hired by companies awarded oil exploration areas must have an operating license to enable them for the purpose of well logging. They must have a person responsible for the radiation safety of the installation and comply with the Standard AR 7.9.2. These licensees have authorized bases whose deposits must meet the building requirements associated with the safe storage of radioactive sources, authorized persons with individual permit in force and elements of radiation protection such as radiation detectors, shielding and personal dosimetry of whole body and limbs for the staff involved.

Transport of radioactive sources and tools from the base to the location of usage is done by means of vehicles that must comply with the standard of transport of radioactive materials and the general regulations for the transport of dangerous goods by road.

There are currently 6 companies in Argentina conducting oil well logging, totalling 19 bases and 228 radioactive sources. These bases are mainly distributed in the southern region of the country.

Table 1: Distribution of oil bases and personnel authorized by province

Province	Amount of bases	Authorized personnel
Chubut	5	91
Salta	1	1
Santa Cruz	4	32
Neuquén	7	70
Mendoza	2	23

2.2 Individual permits

The enabling individual permits for this type of practice are valid for five years and holders must comply with the requirements of Standard AR 7.11.2 Rev. 0, which are detailed as follows: be over 21 years of age, have completed secondary education and a course of radiation protection, which is valid for three years. These courses are held in institutions with educational programs and teachers approved by the regulatory body. Refresher training in radiation safety is compulsory for permit renewal.

Currently there are 217 people with an enabling individual permit for the "Use of Sealed Sources in Oil Well Logging."

2.3 Regulatory actions in case of radioactive sources stuck in operation well

When this type of incident occurs, the sources may be stuck at depths of hundreds / thousands of meters from the wellhead. In these cases, the operator must inform the regulatory authority of the incident and implement specific procedures for this type of event approved in the mandatory documentation without delay. Then a report must be produced detailing step by step and day-to-day the tasks to rescue the sources and the result of effluent sludge monitoring to ensure that the integrity of the sources is maintained.

The detailed report of activities should specify the activities of string release by pumping drilling pipe, pipelines milling, pipelines recovery tasks in case of string cutting, fishing and washing activities, in addition to monitoring data, etc.. If recovery attempts are unsuccessful and the operator decides to make the final on-site disposal of the sources ("technical abandonment"), authorization from the regulatory authority must be sought by presenting an environmental impact assessment associated with this decision.

Once the evaluation of the documentation submitted by the licensee is done, ARN conducts its independent evaluation, and if applicable, authorizes the final on-site disposal of the assembly tool/sources.

This procedure is carried out jointly between the licensee and the oil exploring company (the contractor). The final on site disposal of the tool consists of placing a cement plug approximately 60 m long and a metal wedge as described in the figure ('Fig. 1'), to deflect any eventual reuse of this drilling. This process requires prior preparation of the well, a permanent check of pressures to prevent collapse and the installation of a hydraulic circuit for injecting cement. Once the well is cemented the licensee must record the exact location and depth of the top of the cement plug, place a plaque on the surface of the wellhead and vertical coordinates indicating: vertical location of the sources, the text "CAUTION DO NOT RE-DRILL THIS WELL", the radioactive symbol identifying the presence of the sources and the date of the final disposal. In addition, the plaque should include the identifying code of the well, the contractor company and the depth of the disposed source. ('Fig. 2', 'Fig.3').

Figure 1: Diagram of a well with a stuck tool

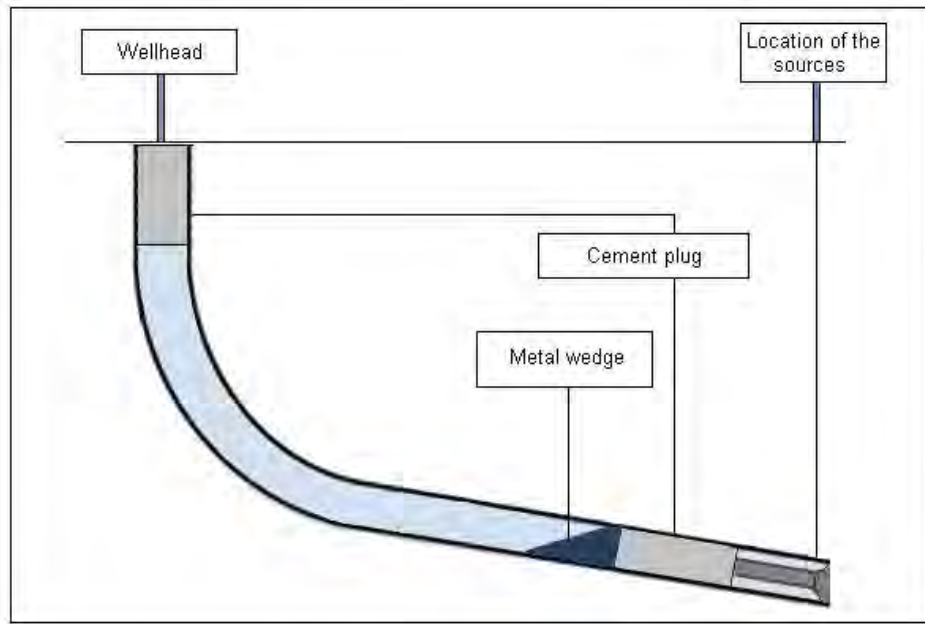


Figure 2: Sign on the wellhead [9]



Figure 3: Sign on the location of the sources [9]



During operations, measurements are made at the wellhead to verify conditions of radiation safety. Both the contractor and the licensee must preserve the records associated with the disposal of sources.

ARN performs on-site inspections to verify that the corresponding signs have been placed, in addition to making measurements and taking soil and/or sludge samples in the wellhead which are then analyzed in its own laboratories. Once the tasks are completed the licensee, together with the contractor must submit a final report to the ARN. In the case of planning a new intervention to drill a lateral branch details must be submitted. This must include the path and anti-collision analysis to ensure that the new path is at a considerable distance from where the tool is immobilized.

3 EVALUATION OF A CASE OF RADIOACTIVE SOURCES STUCK IN WELL OPERATION

3.1 Description of the event

On May 23rd, 2014, a supporting tool of sealed radioactive sources got stuck at a depth of 578 m in an oil well of an oil field located in the province of Neuquén. Four sources were involved: three of ¹³⁷Cs of 3.5 kBq, 3.1 kBq and 66 GBq, respectively, and one of ²⁵²Cf of 163 MBq.

Unable to retrieve the tool, authorization was requested to immobilize it and seal the access to it by covering it with a cement plug of 61 m in thickness.

3.2 Evaluation of the potential consequences of the dispersion of radionuclides associated with the event

The radiological consequences of the possible dispersion of the material contained in the radioactive sources by loss of tightness were assessed by conservative scenarios.

In this work the dose that would be received by a member of the adult public due to ingestion of water contaminated with ¹³⁷Cs and ²⁵²Cf, from a well located in the direction of groundwater flow was estimated. While there are no specific hydrogeologic records of the zone, studies conducted in the eastern region of Neuquén province allowed an estimation that the aquifer was developed in permeable sands approximately 250 m above the stuck sources [10]. However, for this evaluation, it was conservatively assumed that the aquifer for human consumption was in direct contact with the sources at about 580 m depth and total deterioration of the sources and the consequent passage of the radioactive contents into the aquifer was assumed, after one year.

The evaluation was performed by applying the Dispersion of Radionuclides in Aquifers model [11]. This model was developed in the Environmental Studies Division of the Radiation and Nuclear Safety Department of the National Atomic Energy Commission (CNEA), by D. E. Rives in 1992 [11]. In particular, No. 24 version corresponding to motion and time evolution of the concentration of a radioactive element dissolved in water in a saturated medium was used. This solved numerically, in discretized form, by computational modeling, the equation of solute transport in saturated porous media in three dimensions [12]. It takes into account hydrodynamic dispersion, advection, radioactive decay and the entry and exit of radionuclides in the region of interest.

In order to perform modeling, a region of interest of 300 m in length by 10 m in width and 6 m in depth was chosen and was represented by 18,000 nodes 1 m³ each. It was assumed that the initial activity of ¹³⁷Cs (6.6×10^{10} Bq) and ²⁵²Cf (1.6×10^8 Bq) is uniformly distributed on a node (volume of 1 m³) located at one end of the region. In addition it was assumed that the release occurs at regular intervals of 1 day at a constant value, and that the total radioactive content enters the aquifer after a year. The duration of the simulation was taken equal to 800 years.

A groundwater uniform flow speed equal to 50 meters per annum, and in longitudinal direction was considered. This value is within the typical range and coinciding with previous applications [11].

Delay coefficients in sand for ^{137}Cs and ^{252}Cf were estimated based on the delay equation [11]. For this purpose, the distribution coefficient in sand for Cs and Cf, and the density and porosity referenced [13] were used.

In addition, the longitudinal and transverse dispersivity are within the parameters required by the model. The estimates in this paper were made considering typical values and coinciding with previous applications [11,14].

From the activity concentration, the maximum annual dose that an adult would receive due to the ingestion of water from the aquifer [15,16] was estimated.

3.3 Results

Since the objective of the analysis was to estimate the order of magnitude of the doses to the public for the migration scenario and taking into account that very conservative assumptions were adopted, it was considered that the doses would not be excessively overestimated beyond the distance of 60 meters from the location of the sources.

Consequently, the concentration of maximum annual activity due to ^{137}Cs , at that distance, obtained by the model was equal to 5×10^{-4} Bq/l and would be reached after 470 years; while for ^{252}Cf , the activity concentration was 2×10^{-37} Bq/l and would be reached 148 years later.

For these reasons, the maximum annual effective dose that would be received by an adult consuming water at that point was:

$$\begin{aligned} &5 \times 10^{-6} \text{ mSv/a, due to } ^{137}\text{Cs} \\ &1 \times 10^{-38} \text{ mSv/a, due to } ^{252}\text{Cf} \end{aligned}$$

In this work the dependence of the results with the choice of parameters that characterize the aquifer was not studied. Moreover, there are conditions imposed on the choice of spatial and temporal discretization intervals so that no instabilities in the calculation are produced. It is expected that a variation of relevant parameters of the model involves no significant differences in the results.

4 CONCLUSION

In Argentina five tools have been disposed in oil wells since 2002. Currently the oil industry has increased so it can be expected that by increasing the amount of oil drilling could increase the amount of tools stuck that could not be recovered.

Moreover, the protocols applied in the case evaluated are consistent with the practices internationally recommended for similar cases and there are approximately 9,000 radioactive sources intended for well logging in the world [17], and hundreds of them have been stuck and later cemented in depth to proceed to a safe disposal.

This paper has presented a simplified evaluation of the maximum annual effective dose that a person would receive due to the consumption of water from the aquifer, contaminated by the loss of tightness of three sources of ^{137}Cs and one source of ^{252}Cf . The scenario presented and the assumptions made were very conservative, i.e. allowed to estimate maximized values of the expected activities and of the doses involved. Based on the proposed scenario, the result implies that the doses involved are well below the recommended values for members of the public [7]. Furthermore, the concentrations obtained from ^{137}Cs and ^{252}Cf , at a point at 60 m from the sources, are lower than the reference values for water consumption (10 Bq/l and 1 Bq/l, respectively) [18].

5 REFERENCES

- [1] OIEA, 2011. Guía para autorización e inspección: Perfilaje de pozos, OIEA-RLA/9/064-ATS 1.
- [2] ARNR, 2014. Norma UY121: Perfilaje de pozos petroleros. Autoridad Regulatoria Nacional en Radioprotección, Uruguay.
- [3] ARN, 2006. Operación de fuentes de radiación para aplicaciones industriales. Norma AR 7.9.2 Revisión 0. Autoridad Regulatoria Nuclear, Buenos Aires, Argentina.
- [4] “Ley Nacional de la Actividad Nuclear” Ley N° 24.804, 1997. Boletín Oficial de la República Argentina, Buenos Aires, Argentina.
- [5] ARN, 2006. Permisos individuales para operadores de fuentes de radiación para aplicaciones industriales. Norma AR 7.11.2 Revisión 0. Autoridad Regulatoria Nuclear, Buenos Aires, Argentina.
- [6] ARN, 2016. Transporte de materiales radiactivos. Norma AR 10.16.1 Revisión 3. Autoridad Regulatoria Nuclear, Buenos Aires, Argentina.
- [7] ARN, 2001. Norma Básica de Seguridad Radiológica. Norma AR 10.1.1 Revisión 3. Autoridad Regulatoria Nuclear, Buenos Aires, Argentina.
- [8] ARN, 2002. Régimen de Sanciones para Instalaciones Clases II y III, Prácticas No Rutinarias y Transporte de Materiales Radiactivos. Autoridad Regulatoria Nuclear, Buenos Aires, Argentina.
- [9] Chiliutti, C. A., Poletti, M., Calabria, M., et al., 2015. Acción regulatoria en caso de aprisionamiento de fuentes radiactivas en operaciones de perfilaje, X Congreso Regional Latinoamericano IRPA, Buenos Aires, 12 al 17 de abril.
- [10] Laurencena, P. y Kruse, E., 2008. Caracterización de acuíferos profundos en un sector de la cuenca neuquina. IX Congreso Latinoamericano de Hidrología Subterránea, Quito, Ecuador.
- [11] Rives, D. E., 1999. Manual del usuario del Modelo de Dispersión de Radionucleidos en Acuíferos Freáticos, ARN PI-5/99, Buenos Aires, Argentina.
- [12] Jacob Bear, 1972. Dynamics of fluids in porous media. American Elsevier Publishing Company, Inc, New York, Estados Unidos.
- [13] Environmental Assessment Division Argonne National Laboratory, 2001. User’s Manual for RESRAD versión 6. ANL/EAD-4.
- [14] Gelhar, L. W., C. Welty and K. R. Rehfeldt, 1992. A critical review of data on field-scale dispersion in aquifers, Water Resources Research. Vol 28, N° 7, pp. 1955-1974.
- [15] Alvarez, D.E., Czerniczyniec, M.A. Amado, V.A., Curti, A.R., y Lee Gonzáles, H.M., 2015. Verificación del control de las descargas de efluentes radioactivos al ambiente, X Congreso Regional Latinoamericano IRPA, Buenos Aires, 12 al 17 de abril, 2015.
- [16] ARN, 2003. Factores dosimétricos para irradiación externa y contaminación interna, y niveles de intervención para alimentos, Guía Regulatoria AR 1 Revisión. Autoridad Regulatoria Nuclear, Buenos Aires, Argentina.
- [17] Badruzzaman, A., Barnes, S., Bair, F., et al., 2009. Radioactive Sources in Petroleum Industry: Applications, Concerns and Alternatives. SPE Asia Pacific Health, Safety, Security and Environment Conference and Exhibition, Jakarta, Indonesia, 4–6 August.
- [18] OMS, 2006. Guías para la calidad del agua potable, Primer Apéndice a la Tercera Edición, Volumen 1, Recomendaciones. Organización Mundial de la Salud, Ginebra.

Safety and security of sealed sources during transportation to remote area in Egypt

M A M Gomaa*

International Radiation Protection Association, Egypt

Abstract. In the present study, several fields of nuclear security and safety related to transport of radioactive materials shall be reviewed. Peaceful uses of atomic energy in medical, industrial, agriculture and other fields depends not only on production of isotopes But also on its transport from production site to storage sites and from storage sites to work sites, Some countries produce its isotopes other countries do not produce it. Hence these countries import it from abroad; hence these countries import and re-export it. This is done by air, sea and by road, this necessities implementation of safety and security requirements during transport of radioactive sources. IAEA issued transport documents and IAEA update it following latest ICRP recommendations. In the present work experience gained during transport of radioactive sources to remote sites in Egypt shall be reviewed.

1 INTRODUCTION

International organizations such as International Atomic Energy Agency (IAEA), International Maritime Organization (IMO) , International Air Transport Association(IATA) and others issue Regulations related to transportation of radioactive material. These organizations regulations are based upon International Commission for Radiological protection of ICRP for 1977, 1990 and 2007, hence IAEA regulations are updated. Following latest ICRP recommendations of 2007 and IAEA GSR part-3, exposure situation during transportation to remote or nearby area is recognized as Planning Exposure Situation(1-7). In case of abnormal events during transportation, exposure situation is recognized as emergency exposure situation.

2 TRANSPORTATION OF SEALED SOURCES TO REMOTE AREAS IN EGYPT

Transportation of sealed sources in Egypt is the same as in every country; they follow IAEA safe transportation of radioactive materials. In Egypt there is more than 3000 radioactive isotopes sites licensed by the Egyptian Nuclear and regulatory Authority (ENRRA). Nearly 10% of these sites act as storage facilities for unsealed radioactive sources. Other sites (nearly 90%) these are storage facilities for sealed radioactive sources. Although Egypt has facilities to produce radioactive sources such as cyclotron and two research reactors, limited number of radioisotopes is currently produced at the second nuclear research reactor EY-RR-2. Majority of radioactive sources in use in Egypt are imported from abroad. Radioactive sources are delivered by air or by sea. Furthermore, passage of ships caring radioactive materials on board crossing Suez Canal from both sides under supervision of ENRRA taking all necessary protection and security.

Surface transport routes may be classified as route from ports to storage sites as the first route and the other route from storage site to working area as the second routes

2.1 Routes from Ports

The first route of transportation is from Cairo Airport or Sea shore ports such as Alexandria, Port Saied and Suez, or from Marine Ports to the storage sites. Consequently surface transportation routes vary according to the location of the storage site.

Examples of transport first routes to remote areas was from Cairo airport to Marsi Matrough , it is 500 Km north west of Egypt . Other route to remote area was accompanying radioactive sources from

*mangomaa@gmail.com, C/O Atomic Energy Authority, Cairo, Egypt

Cairo Airport to Marsi Alam , it is 800 Km South East of Egypt. Furthermore, remote route was from Cairo Airport to Oases, it was 800 Km West South of Egypt . Egyptian regulation imply that radioactive sources are exported back to country of origin for final disposal or for recharging the radioactive sources as in the case of Ir-192 or inspection or for Co-60 in use for radiotherapy purposes or for industrial irradiation facilities.

In several circumstances, unused and spent radioactive sealed sources are collected by the Egyptian Waste Disposal Unit (EWDU) of the Egyptian Atomic Energy Authority (EAEA) upon the request of the owner of these sources. So transportation route is from the storage sites to (EWDU), EWDU is located 35 Km east of Cairo.

2.2 Routes to working sites

The second transportation route is to move the radioactive sources to working sites. There are two types of working sites, the standing type and the moving routes type.

For the standing type radioactive sealed sources are placed at specific location as in the case of petroleum refining units. In Egypt most refineries are located few Km west of Alexandria. Furthermore several refineries are located at petroleum companies located at the coast of Gulf of Suez. So these sources are transported from the storage site to fixed locations. During repair of the units, radioactive sources are returned back to company storage site.

On rare occasions, transportation of very high activity sealed radioactive sources are transported by night from Cairo Airport to EAEA Gamma ray Irradiation Facilities (GIF) , Cairo GIF is 20 Km from Cairo Airport and Alexandria GIF is 20 Km from Alexandria city center.

Since year 2000, several Co-60 radiotherapy facilities are in use Egypt, not only in Cairo but also at Main Egyptian cities from Alexandria to Aswan, hence, transportation of these sources for long distances up to 1200 Km from Cairo Airport.

For the moving type radioactive sources are routinely moved from the storage site to the working site as in case of inspection of welding pipes where it moves daily to site and return back.

For certain circumstances, there are several (secondary) storage sites for the same company. For example, for one company there are 4 secondary storage sites at Cairo, Marsi Matrouh, Port Saied and at Assuit.

3 RADIATION PROTECTION OF RADIOACTIVE SEALED SOURCES

After Meet Half accident in Egypt , Ministry of Health issued ministerial order no 202 for year 2000 , in which the responsibility of transport of radioactive material is the sole responsibility of the qualified radiation protection expert or radiation protection officer of the facility . In 2010 the Egyptian new ionizing radiation legislation was issued. The law number 7(2010) and transport of radioactive material is an important part in the legislation. Furthermore, in 2011 the executive regulation is issued.

4 SECURITY OF SEALED RADIOACTIVE SEALED SOURCES

In Egypt several organizations are involved in the security of radioactive sources, mainly ENRRA play important role in issuing approval documents dealing with import and export of radioactive sources, It also issue approval for transport of radioactive sources. ENRRA inform Civil Protection and Armed Forces about the movement of radioactive sources from Cairo Airport to the companies' storage sites. Usually, radioactive sources transport car are followed by Civil Protection Cars. In

remote area, Armed Forces cars follow the transport of radioactive.

5 CASE STUDIES OF PERSONNEL EXPERIENCE GAINED DURING TRANSPORTATION OF RADIOACTIVE SOURCES

5.1 Case One

In June 2000, Ir-192 missing radioactive source was located at Meet Halfa 20 km North of Cairo. At night Ir-192 source was transported to EAEA storage site – 35 Km East of Cairo. National Security and safety organizations were involved, necessary measures were implemented. The Ir-192 source was unshielded and its activity in June 2000 was 185 GBq (50 Ci).

5.2 Case Two

Transport of several gamma rays and neutron sources from Cairo Airport to Alexandria free zone, then to Marsi Matrough. Two years later these sources were exported abroad. Safety and security measures were implemented.

5.3 Case Three

Sea Transport of contaminated valves and pipes from Petroleum marine site to company on shore storage site. In some situations radioactive sources are transported by helicopters from storage sources to marine fields.

5.4 Case Four

In single occasion, 167 radioactive sources were transported from Cairo Airport to Petroleum Company at Red Sea.

5.5 Case Five

Several Cs-137 radioactive sources were in use at various petroleum field as Sensor with others to estimate on line for the estimation of the rate of production of gas, oil and water. Recently, these Cs-137 (T_{1/2} 30 years) sources are replaced by Ba-133 (T_{1/2} 10.51 years)

6 REFERENCES

- [1] IAEA, FAO, ILO, et al., 2014. Radiation Protection and Safety of Radiation Sources: International Basic Safety Standards. IAEA Safety Standards Series No. GSR Part 3. International Atomic Energy Agency, Vienna.
- [2] ICRP, 2007. The 2007 Recommendations of the International Commission on Radiological Protection. ICRP Publication 103. Ann. ICRP 37(2–4).
- [3] IAEA, Regulations for the Safe Transport of Radioactive Material - 2012 Edition, Series No. SSR-6, International Atomic Energy Agency, Vienna.
- [4] Advisory Material for the IAEA Regulations for the Safe Transport of Radioactive Material, Series No. SSG-26, 2014. International Atomic Energy Agency, Vienna.
- [5] Schedules of Provisions of the IAEA Regulations for the Safe Transport of Radioactive Material, Series No SSG-33,2015, International Atomic Energy Agency, Vienna.
- [6] Planning and Preparing for Emergency Response to Transport Accidents Involving Radioactive Material, Series No. TS-G-1.2 (ST-3), 2002, International Atomic Energy Agency, Vienna.
- [7] Radiation Protection Programs for the Transport of Radioactive Material, Series No. TS-G-1.3, 2007. International Atomic Energy Agency, Vienna.

Orphan sources search and secure in Republic of Serbia – planning, implementation and current status

Milan Vujovic^{a*}, Maja Eremic-Savkovic^a, Ivana Avramovic^a, Vedrana Vuletic^a, Sladan Velinov^a

^aSerbian Radiation Protection and Nuclear Safety Agency, Masarikova 5/XV, 11000 Belgrade, Republic of Serbia

Abstract. This paper describes planning phase, administrative and physical search and all actions on implementation of orphan sources search and secure activities in Republic of Serbia. From historical data, types of sources produced and used in Republic of Serbia are generally known but number and locations of many of them are not. Most of those sources without proper control are used in radioactive lightning rods and ionizing smoke detectors. These types of sources are not listed in current inventory and location of many of them is still uncertain. For these types of sources systematic searches have not been undertaken up to beginning of 2014. At the end of 2013 planning phase was conducted by drafting Orphan sources search and secure Programme for Republic of Serbia. Radioactive lightning rods were recognized by this programme as orphan sources with highest threat risk and decision was made to immediately start with their removal and secure storage. Administrative search started from the beginning of 2014 and by the mid 2015 last phase of administrative search was finished. This search gave current number and location of radioactive lightning rods that are not under regulatory control. Since the end of administrative search implementation of physical search and dismantling has started. Ongoing activities have main goal to properly dismantle and securely storage all radioactive lightning rods.

1 HISTORICAL OVERVIEW

Use of sources of ionizing radiation in Serbia started before Second World War and it was based on use of sources in medicine. Use of sealed radioactive sources on much higher scale started in Vinca institute of Nuclear Sciences from the end of 1947. Main source of radiation used at that time was radium and its daughter nuclides and neutron sources based on them [1].

Manufacture of sealed radioactive sources in Republic of Serbia started in early 1960s when the RA research reactor started with operation and lasted until 1984. Radioactive sources for, industrial, medical and research applications were produced in Vinca institute of Nuclear Sciences (at that time called Boris Kidric Institute of Nuclear Sciences). In period of operation of the RA research reactor, 20 different radionuclides were produced for industrial and medical purposes [2].

Particular problem in Republic of Serbia is a large number of radioactive lightning rods that were installed on many industrial, public and residential buildings. At that time, installation of radioactive lightning rods as a part of lightning protection system was common solution. Production of sealed radioactive sources for lightning rods started in 1968. At first Co-60 sources were produced, and they were replaced with Eu-152/Eu-154 during the 1970's. These sources were then placed in three different types of radioactive lightning rods assembled by three different companies in Republic of Serbia (former Yugoslavia). The appearance of these three types of lightning rods is given in figure 1. Such sources, if not properly secured, may pose hazard to population.

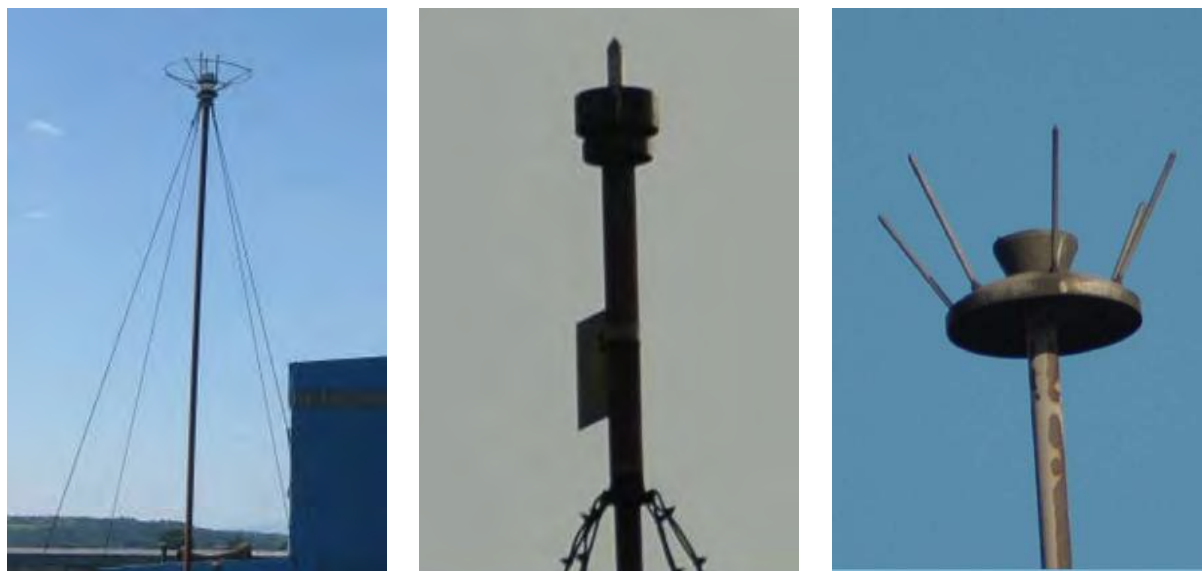
Also, a large number of unregistered ionizing smoke detectors, installed in industrial and public buildings pose another problem. Ionizing smoke detectors were produced by several companies and radionuclides used in these devices – Ra-226 and Am-241 were imported.

Following the recommendation of the ICRP and the IAEA from the 1981, the installation of radioactive lightning rods was forbidden by the Law on radiation protection and on special safety measures in application of nuclear energy (“Official gazette of SFR Yugoslavia” no. 62/84) from

* Presenting author, e-mail: vujovic@srbatom.gov.rs

1984. Installation of ionizing smoke detectors with gaseous daughter nuclides was forbidden by the Law on Radiation Protection and on Nuclear Safety (“Official gazette of Republic of Serbia” no. 36/09). Large number of sealed radioactive sources of these two types is currently under regulatory control but many of them are still not.

Figure 1: The appearance of these three types of lightning rods assembled in Republic of Serbia



From historical data, types of sources produced and used in Republic of Serbia are generally known but current number and locations of some of them are not. Most of those sealed radioactive sources without proper control are sources from radioactive lightning rods and ionizing smoke detectors. For these types of sealed radioactive sources systematic searches have not been undertaken up to beginning of 2014. There is a high confidence that most of dangerous sources (IAEA category 1, 2 and 3) in Republic of Serbia are registered and controlled.

In addition to lightning rods and ionizing smoke detectors, sealed radioactive sources were also used in industrial, medical and educational purposes and there is possibility that some of these sources became orphaned. Reasons for sources to become orphan in Republic of Serbia are mostly of financial nature. Many companies that used sources in previous decades are now bankrupt or defunct. Radioactive sources can also be unintentionally imported with the shipments of scrap metal.

2 LEGAL AND REGULATORY FRAMEWORK

Matters relating to ionizing radiation protection, nuclear safety and radioactive waste management in Republic of Serbia are regulated by the Law on Ionizing Radiation Protection and on Nuclear Safety (“Official Gazette of Republic of Serbia” no. 36/09 and 93/12). In accordance with this Law, series of subordinate regulations which regulate the matter from this field more closely were adopted during the 2011 and at the beginning of 2012. Pursuing to the Law on Ionizing Radiation Protection and on Nuclear Safety (“Official Gazette of Republic of Serbia” no. 36/09 and 93/12) Serbian Radiation Protection and nuclear Safety Agency was established in December 2009 and became operational by the end of 2010. Responsibilities of the Serbian Radiation Protection and nuclear Safety Agency related to search and secure of orphan sources are issuing Regulations defined by the Law, licencing and authorization and maintaining the relevant databases.

Regulatory infrastructure in Republic of Serbia is divided between Serbian Radiation Protection and Nuclear Safety Agency and two ministries responsible for inspections. Serbian Radiation Protection and Nuclear Safety Agency is established in accordance with the Law on radiation protection and on nuclear safety (“Official gazette of Republic of Serbia” no. 36/09) for the purpose of providing quality

and efficient implementation of radiation protection and nuclear safety measures, while performing radiation practices and nuclear activities as an independent regulatory body, performing public competencies in line with this Law. Inspection over the implementation of radiation protection measures is being carried out by the Ministry competent for radiation protection through its inspectors for radiation protection. Inspection over the implementation of nuclear safety measures is being carried out by the Ministry competent for nuclear safety and radioactive waste management through its inspectors for nuclear safety and radioactive waste management.

When found, all orphan sources can be, securely stored in Secure storage for sealed radioactive sources which is operated by Public Company “Nuclear Facilities of Serbia”. Public Company “Nuclear Facilities of Serbia” was established in 2009 for the purpose of carrying out the management of nuclear facilities and radioactive management facilities. Activities are ongoing on establishing source conditioning facilities for source categories 3, 4 and 5.

3 REASONS FOR LOSS OF CONTROL OF SEALED RADIOACTIVE SOURCES IN REPUBLIC OF SERBIA

Loss of control of sealed radioactive sources in Republic of Serbia occurred either inadvertently or intentionally and many sources simply became orphaned because of neglect. Several times during previous decades sources used for weld inspections were simply lost by construction companies after being used to check welds on construction sites. Some of these sources ended in hands of people from public who found them accidentally. Intentional attempts to remove a source from regulatory control were mostly not to obtain the source itself but to scrap valuable of metals used for containers or as shielding. In some cases sources were intentionally orphaned by their owners in order to avoid expenses of source keeping and licensing. As it was already stated in the text, many companies that used sources in previous decades are now bankrupt or defunct and in some cases their properties were sold sometimes together with all equipment including sealed radioactive sources. In many cases no information about sealed radioactive sources or even on their existence were transferred to new owners. Another problem are companies that due to loss of educated staff are not aware of possession of sealed radioactive sources. All of such sources belong to so called “historic legacy” due to non-existence of proper regulatory control at one or more points during or after their use.

If we summarize causes of loss of control of sealed radioactive sources in Republic of Serbia they include:

- Lack of, or inadequate, security during storage, transport and use;
- Human error;
- Deliberate avoidance of regulatory requirements;
- Abandonment;
- Theft;
- Loss of corporate knowledge, due to lack of activities in which source is used and loss of key personnel;
- Bankruptcy;
- Decommissioning of plant and facilities;
- Change in ownership of equipment or plant, especially moving from public to private ownership;
- Defunct owner;
- Inhibitions to legal storage or disposal, such as high costs of storage.

In Republic of Serbia many orphan sources are found in scrap metal. These sources are in many cases dismantled lightning rods and smoke detectors that accidentally get into scrap metal.

In all cases until now, when orphan source was found, people who found the source and people who performed recovery of the source have not received doses that would pose significant radiation risk.

4 ORPHAN SOURCE SEARCH AND SECURE PROGRAMME

As first activity related to orphan source search and secure, draft of Orphan source search and secure Programme was prepared. Draft Programme was reviewed and updated during expert mission organized by the IAEA in December 2013. Purpose of this Programme is that, when implemented, will bring orphan sealed radioactive sources that currently pose a risk to the public and the environment, under appropriate regulatory control and also make proper arrangements for any future orphan source search and secure campaign. It was recognized that sealed radioactive sources that are not under regulatory control can result in a number of undesirable consequences including human health impacts, socio-psychological impacts, political and economic impacts, as well as environmental impacts. This Programme gives necessary measures and actions in order to provide an appropriate level of control over sealed radioactive sources currently not under control. This Programme also states the likelihood and magnitude of the radioactive source control problem in Republic of Serbia and the priorities necessary to address the identified problems. It will provide for direct available resources to be allocated appropriately to ensure that control is first regained over those sources presenting the highest risks.

Objective of the Programme is to establish systematic process to search for and to recover orphan sealed radioactive sources and to gain full control of radioactive sources on territory of Republic of Serbia.

The Programme recognizes radioactive lightning rods and ionizing smoke detectors as the most common sealed radioactive sources that became orphaned and as sealed radioactive sources with highest probability to become orphaned in near future until they all are dismantled.

The Programme is planned to be implemented through several phases:

- Administrative search which deals with gathering of information,
- Planning stage,
- Physical search which deals with identification of the sources on the field and
- Recovery of the sources

Following completion of the programme it is expected that sealed radioactive sources that are now orphaned will be recovered and trained and equipped teams will be available to respond in situations which might happen in the future.

5 PREVIOUS ACTIVITIES RELATED TO DISMANTLING OF RADIOACTIVE LIGHTNING RODS

During previous decades, since installation of radioactive lightning rods was forbidden by the Law several campaigns were conducted in order to remove part of radioactive lightning rods from buildings. Large scale actions were done in several major cities and radioactive lightning rods were removed from apartment buildings and some public institutions. These campaigns were organized by cities and in some cases did not cover all city parts and only radioactive lightning rods known to the local institutions were covered. Radioactive lightning rods installed on industrial buildings were left to their owners to fund their removal. These campaigns significantly reduced number of radioactive lightning rods but majority of them was still left installed on buildings.

6 ADMINISTRATIVE SEARCH

In an administrative search, information is gathered without the use of radiation detection equipment or visual searches for sources that are known or suspected to be lost, missing or stolen [3, 4]. Two key aspects of administrative search are determining the most useful source of information and determining the best method of collecting the information from that source.

Implementation of Orphan source search and secure programme started in January 2014 by conducting administrative search for radioactive lightning rods. It was decided to start with search for radioactive lightning rods as they were recognized as the highest threat. Administrative search was conducted by staff of Serbian Radiation Protection and Nuclear Safety Agency.

First task was to collect data from legal entities which installed, maintained and dismantled radioactive lightning rods in previous decades. Beside this, information on dismantled radioactive lightning rods which are stored as radioactive waste was also obtained. All acquired data on radioactive lightning rods was entered into a database. These data included municipality, settlement, name of legal entity which possess radioactive lightning rod, address, data about source such as radionuclide and activity on date of installation and short description of exact location within owner's premises (is it on roof or on pole, description of building or exact spot on location relative to other buildings etc.).

Second task was to send official letters to all municipalities in Republic of Serbia. In these letters, Serbian Radiation Protection and Nuclear Safety Agency requested from all municipalities to check whether they have any information or document related to radioactive lightning rods. It was also advised that municipalities try to check through their own inspection mechanisms if there were any radioactive lightning rods on their area. Response from the municipalities gave information on numerous radioactive lightning rods that were dismantled in the previous years as well as information on legal entities that do not exist anymore or that are now part of other legal entities. During this activity information was obtained that some of the radioactive lightning rods now belong to natural persons due to restitution of property confiscated after the Second World War.

Activities done during the administrative search attracted positive media attention. This resulted in several newspapers articles and television broadcasts about radioactive lightning rods and need for their removal and replacement. In this way awareness was raised and people even called to report of noticed radioactive lightning rods.

Outcome of administrative search was database in which data about radioactive lightning rods was entered as described. This database was used as base for planning and conducting physical search which is described in following chapter. Total number of entries (presumed radioactive lightning rods) listed in this database was 3429. There was no proven information on current status for 2264 lightning rods, and for 1165 written proof of dismantling existed. Activities on physical search took nearly one year mostly due to time needed for typing all data received in hard copy and for actions taken by municipalities.

After administrative search is completed planning of physical search should be performed [3, 4]. Planning stage shall start after legal entity is engaged for implementation of this Programme. Planning involves prioritization based on evaluation of radiation risk and on likely locations. During planning stage physical search and recovery team(s) will be formed and their needs for training will be recognized and training will be, if necessary, performed during planning stage. Also, need for instrumentation and equipment have to be recognized in planning stage and adequate instrumentation and equipment have to be provided. Internal procedures should be developed and approved by the Serbian Radiation Protection and Nuclear Safety Agency during planning stage. Format of records that need to be produced shall be established and arrangement with waste management organization has to be in place.

7 PHYSICAL SEARCH

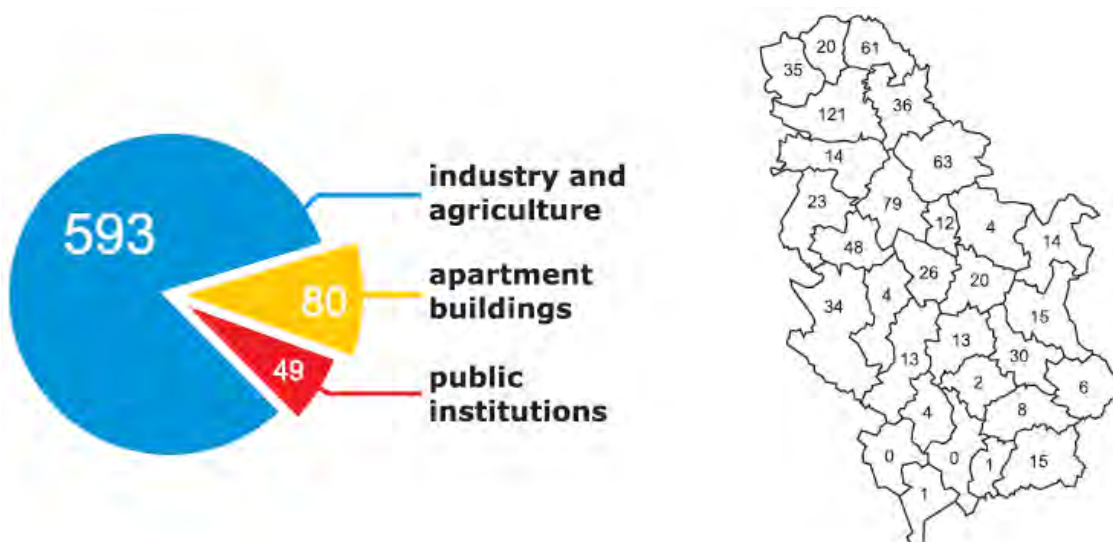
A physical search involves a search team of one or more persons that goes to physically locate sealed radioactive sources both visually and using radiation detectors [3, 4]. Generally, a physical search is conducted following an administrative search but, in certain circumstances, a physical search may start at the same time as, or even before, an administrative search. Because search teams may encounter radioactive sources, radiation protection measures for these individuals are needed.

Physical search started in 2015 and it was conducted by Inspectors for radiation protection. At the beginning of physical search, decision was made to make only visual search for radioactive lightning rod constructions due to lack of measuring equipment and staff. Locations for inspections were taken from database made during administrative search. Physical search took most of year 2015 and all locations listed in database were checked. Positions, status and ownership of all radioactive lightning rods from database were investigated. Status of dismantled lightning rods was confirmed by obtaining proofs of dismantling from owners.

Legal entities, in whose possession constructions of radioactive lightning rods were found, were requested to immediately check the condition of the source, report the source to Serbian Radiation Protection and Nuclear Safety Agency and to start with the procedure and preparations for proper dismantling of the radioactive lightning rods. If any of the radioactive lightning rods is leaning to a side or is damaged thus presenting threat, immediate action was made by the inspector who engaged authorized legal entity to dismantle it.

Outcome of physical search were inspection report and update of database prepared during administrative search. Total number of radioactive lightning rods whose locations were confirmed during physical search was 722. Particular issue are radioactive lightning rods whose owner is bankrupt or defunct and total number of such radioactive lightning rods is still not exactly known due to not clear status of some of the legal entities. Results of physical search have shown that 593 lightning rods are still on or next to industrial and agricultural buildings, 80 are still on apartment buildings and 49 are on buildings of public institutions. Locations with radioactive lightning rods are present in nearly all districts of Republic of Serbia. Number of radioactive lightning rods by type of their owner and their distribution in districts of Republic of Serbia is shown on figure 2. Discrepancy between presumed and confirmed number of locations with radioactive lightning rods was due to proving that some of the radioactive lightning rods were dismantled, confirming that some of the entries were doubled due to change of the owner and illegal dismantling of some of the sources by unauthorized legal entities.

Figure 2: Number of radioactive lightning rods by type of their owner and their distribution in districts of Republic of Serbia



8 RECOVERY OF THE SOURCES FROM RADIOACTIVE LIGHTNING RODS

After inspection report on physical search was completed first actions to dismantle and recover sources were planned and done. As first activity on recovery of the sources from radioactive lightning rods Serbian Radiation Protection and Nuclear Safety Agency allocated funds from its own resources

to dismantle seven lightning rods that were on public institutions (e.g. retirement homes, kindergartens etc.). Public call was made to select legal entity which will dismantle these seven sources from lightning rods, properly store them at radioactive waste storage and put new lightning protection. That way no building from which radioactive lightning rod was dismantled was left unprotected. Beside these seven radioactive lightning rods, dismantlement of around 40 radioactive lightning rods in 2015 was financed by their owners.

Selected legal entity completed these activities in 3 months and delivered report to Serbian Radiation Protection and Nuclear Safety Agency.

Final result of this, action on recovery of sources is that part of the sealed radioactive sources from radioactive lightning rods on public institutions is dismantled and that mechanisms for selection and engagement of legal entities for dismantling are set. Beside this, legal entity which performed dismantling activities confirmed its operating procedures for dismantling of radioactive lightning rods, transport of sealed radioactive sources and performing radiation protection measurement during these activities.

9 CURRENT STATUS AND PLANNED ACTIVITIES

After finishing administrative and physical search for radioactive lightning rods and first activities on recovering some of them as described in previous section there is now clear information on number and locations of sealed radioactive sources from radioactive lightning rods. Based on this information future actions are planned in order to dismantle and properly storage all sealed radioactive sources from radioactive lightning rods.

Owners of the most of radioactive lightning rods are currently known and part of them is reported to the Serbian Radiation Protection and Nuclear Safety Agency. These sources, thus, should not be considered as orphaned but their removal has to be performed. Some of the sources whose owner is bankrupt or defunct, or which are on buildings with shared ownership are current priority for dismantling and mechanisms for funding of their removal are considered.

In previous months another activities on administrative search for sources used in medical, industrial and veterinary practices are ongoing. Lists of all medical and veterinary institutions were obtained through national chamber of commerce and plan is to officially request from them any information on current and previous use of sealed radioactive sources. A lot more effort is needed for search in the field of industrial applications since in previous decades as well as now there are several industry fields in which sources are used with large number of companies that used these sources now bankrupt, defunct or privatized or simply changed field of work which all are possible causes for sources to become orphaned. This search will be based on similar way as it was done for radioactive lightning rods and information will be obtained from legal entities that import, install and maintain equipment with sealed radioactive sources.

10 CONCLUSION

First activities taken in order to put orphaned sealed radioactive sources under regulatory control have shown that prepared Orphan Source Search and Secure Programme covers all necessary steps from search for the source until its storage. Performed administrative and physical search shown that lack of information and staff can pose potential problem. Preparedness of legal entities involved in securing, dismantling, transportation and storage of sealed radioactive sources to act was also confirmed. All of this shows that legal entities in Republic of Serbia involved in search and secure of orphan sources are prepared for future planned searches as well as for acting in case of accidental finding of orphan source.

11 ACKNOWLEDGMENTS

The authors would like to express their gratitude to International Atomic Energy Agency and management team of interregional project INT/9/182 for support in presentation of this paper.

12 REFERENCES

- [1] Vinca Institute of Nuclear Sciences, 2000, 50 years of Vinca Institute (1948-1998), (in Serbian), Serbian State Publisher of Textbooks, Belgrade.
- [2] Sotic O., 1984, Research Reactor RA, potentials and perspectives (in Serbian). Retrieved 2016-05-05 from http://www.iaea.org/inis/collection/NCLCollectionStore/_Public/38/065/38065404.pdf
- [3] IAEA, 2011, National Strategy for Regaining Control over Orphan Sources and Improving Control over Vulnerable Sources. IAEA Specific Safety Guide No. SSG-19, International Atomic Energy Agency, Vienna.
- [4] IAEA, 2004, Strengthening control over radioactive sources in authorized use and regaining control over orphan sources. IAEA TECDOC No. 1388, International Atomic Energy Agency, Vienna.

The worldwide problem of Disused Sealed Radioactive Sources (DSRS) and what should be done to alleviate the situation.

Robin George Heard*

Rob Heard Consulting, Unit 5 - Addstone, 510 Atterbury Road, Pretoria, Republic of South Africa.

Abstract. Sealed radioactive sources (SRS) provide great benefit to humanity through their utilization in agriculture, industry, medicine, research and education, and the vast majority are used in well-controlled environments. None-the-less, control has been lost over a small fraction of those sources resulting in accidents of which some had serious – even fatal – consequences. Indeed, accidents and incidents involving radioactive sources and in particular disused sealed radioactive sources (DSRS) indicate that the existing regime for the control of sources needs improvement. Additionally, today's global security environment requires more determined efforts to properly control radioactive sources. Consequently, the current regimes must be strengthened in order to ensure control over sources that are outside of regulatory control (orphan sources), as well as for sources that are vulnerable to loss, misuse, theft, or malicious use. Besides improving the existing situation, appropriate norms and standards at the national and international levels must continue to be developed to ensure the long-term sustainability of control over radioactive sources. In order to improve the existing situation, concerted national and international efforts are needed and, to some degree, are being implemented to strengthen the safety and security of sources in use, as well as to improve the control of disused sources located at numerous facilities throughout the world. More efforts must also be made to identify, recover, and bring into control orphan sources.

KEYWORDS: *Sealed Radioactive Sources, Disused Sealed Radioactive Sources, Borehole Disposal, Return to Supplier, Repatriation of Sources.*

1 INTRODUCTION

The IAEA and other international bodies have been trying to improve the control of sealed radioactive sources almost since these sources were first produced. As the production and use of sources has increased, so too has the amount of disused sources. Accidents and incidents involving radioactive sources indicate that the existing regime for the control of sources needs improvement. Additionally, today's global security environment requires more determined efforts to properly control radioactive sources. Consequently, the current international and national regimes must be strengthened in order to ensure control over sources that are outside of regulatory control (orphan sources), as well as for sources that are vulnerable to loss, misuse, theft, or malicious use. Besides improving the existing situation, appropriate norms and standards at the national and international levels must continue to be developed to ensure the long-term sustainability of control over radioactive sources. Once sources become disused, the national authorities in countries usually are responsible for the control of these DSRS. The detail of whom and how this is done varies from country to country but in general the governments accept responsibility for exercising control. In order to do this, a documented policy and strategy for the management of DSRS should be put in place where end-points should be identified for each type and category of source. These end-points could be the export of sources from the country, indefinite storage (not recommended) or disposal in a borehole or in other types of repository. A number of options exist and these end-points should be consistent with the national needs and regulatory regimes in individual countries.

Presenting author, email: rheard2000@yahoo.com

2 ACCIDENTS AND INCIDENTS

Despite their predominantly small physical size, sources contain very high concentrations of radioactivity. Industrial and medical sources are typically in the GBq to PBq range. The radiation emitted from the sources is usually intense, requiring reliable encapsulation for operational use and heavily shielded containers for storage. Owing to their small physical size, they are easily lost or misplaced if not properly managed. This is a particular problem when items of industrial or medical equipment containing sources become obsolete and are replaced, or simply scrapped, or when the sources weaken and need to be replaced. In all these circumstances, the sources are said to be 'disused'. Poor management practices in many parts of the world have meant that disused sources have been found stored in exposed and unprotected locations and are consequently sometimes in poor condition, perhaps even leaking. There have been accidents and incidents recorded in the last 40 years involving fatalities as a result of sources being used in an inappropriate manner and being inadvertently mishandled by the public [1].

When a source is exposed, both people and the surrounding environment can be affected. Injuries from unprotected exposure to a radiation source can be devastating, both for the immediate victims and the community at large. Most countries that use radiation sources have regulations in place to control their use, and the sources themselves have protective shielding to prevent exposures, but accidents continue to happen. The causes for these accidents, while complex, more often than not involve someone finding a source that was lost, or worse, one that was not properly controlled. This is generally the exception rather than the rule as many thousands of sources are safely used throughout the world on a daily basis.

National regulations and international standards governing the manufacture and use of sealed radioactive sources (SRS) ensure that the source is safe when used as intended. In fact, prior to a major accident involving a sealed source in Goiania, Brazil in 1987 [2], it was widely believed that these regimes were effective in ensuring safety.

The Goiania accident, caused by a ruptured ^{137}Cs source (50.9 TBq (1375 Ci)) from an abandoned and later dismantled teletherapy device, resulting in our fatal exposures, 28 cases of radiation burns, significant environmental contamination in the affected area, and large-scale socio-economic disruption, was the first of several accidents in the 1980s to 1990s that challenged the view that regulations and management systems of that time were effective to ensure safety. The IAEA has issued a series of reports on these accidents and lessons learned from them [3], [4], [5], [6].

The IAEA publication [7] although published a long time ago in 2001 details many sources that were lost at sea with the vast majority coming from the oil industry. The highest activity sources lost include Radioisotope Thermoelectrical Generators (RTG). One of these was a soviet built RTG with an activity at the time of the loss (20 August 1987) of 12.95 PBq (350 kCi). To illustrate the dangers of sources, contrast this with nuclear submarine K-219 [3] which was lost at sea the previous year (October 1986). The total activity reported in reference [7] for both reactors was 9.25 PBq.

A recent well publicized accident occurred in May 2010 in New Delhi, India where a self-shielded irradiator was sold to a junk dealer who sold off some of the parts and dismantled others. Some of the source pencils were sawn open and the slugs of ^{60}Co were scattered around. One person died as a result of keeping one of the slugs in his wallet.

The IAEA has as yet not compiled a report on the Indian accident but the similarities between the Indian accident and the one at Samut Prakarn are obvious. It is clear from all these reports and from many other references that accidents and incidents involving sources are still of concern even though much work has done on improving the control over sources.

3 ORPHAN SOURCES

Radioactive sources that are not under regulatory control can result in a number of undesirable consequences including human health impacts, socio-psychological impacts, political and economic impacts, as well as environmental impacts. Disused sources represent the largest pool of vulnerable and potential orphan sources. History has shown that many accidents involving orphan sources come about because sources that are no longer in use are eventually forgotten, with subsequent loss of control years later.

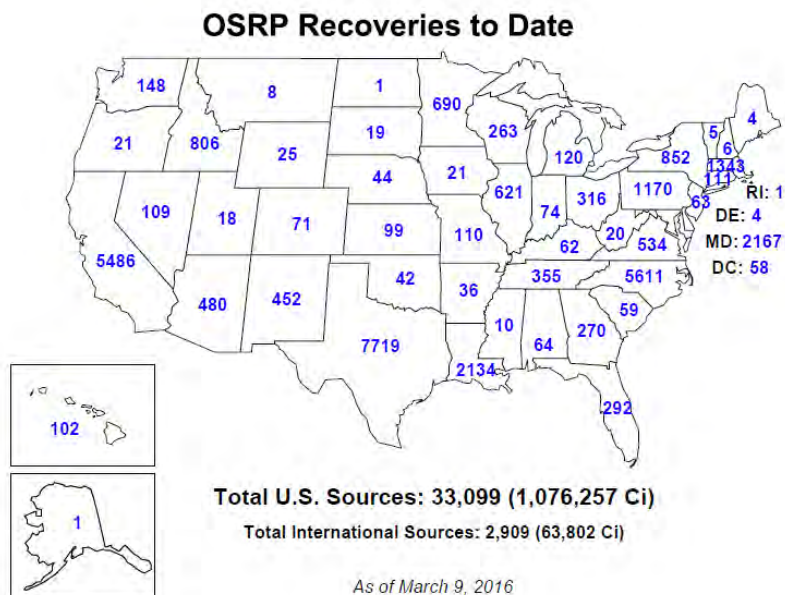
To this end, it is beneficial from both a safety and security viewpoint for all disused sources to be identified and to undergo proper disposition. One of the difficulties is that sources do not usually become disused abruptly but, instead, their frequency of use decreases slowly over a period of time. In addition, licensees are discouraged from proper disposition of disused sources by the cost involved, by the bureaucracy of doing so, or by the lack of an available disposal option. The regulatory regimes in many countries and also the transport regulations are becoming ever more stringent and it is sometimes impossible for a country with limited resources and expertise to repatriate disused sources to the country of origin. This often means that these sources are candidates for becoming orphaned.

Regional and national campaigns to improve the overall control of radioactive sources have been found useful in significantly reducing the numbers of disused sources that can potentially become orphaned, or to dispose of these sources properly. The IAEA has developed strategies [8] that can be used by countries to regain control over orphan sources and assists its member states by funding the development of a verified inventory and also by training people to go out on search and secure missions. Provision of suitable searching equipment also forms part of this assistance.

4 IDENTIFYING THE WEAK LINKS

Unfortunately, an international inventory of sources does not exist. Therefore the weak links in the management of sources in general and DSRS in particular are not that easy to identify. As a general rule, one can say that the richer countries with greater resources have a better chance of keeping their sources under good control. This is of course constrained by the fact that these countries have many more sources than the less wealthy countries. Even the most advanced economies have sources that go out of control. To illustrate the point of large inventories, the Off Site Recovery Project (OSRP) of the United States (US) has recovered 33,099 disused sources up to 9 March 2016. The work started in 1999. This is many more sources than the entire inventory of most of the countries in the world. See Figure 1 below from the OSRP web site.

Figure 1: OSRP recoveries to date.



Typically, most developing countries have inventories of a few hundred and this figure may go as high as a few thousand. Many developing states have limited infrastructure to deal with DSRS and this includes the lack of suitable premises to store the DSRS for extended periods. In order to safely and securely store sources one needs qualified staff, equipment, management systems, regulatory control, and sufficient funding. The IAEA and its major donors are trying to improve the sustainability of the national systems for control of sources in many countries. A holistic approach is followed with emphasis on improving the legislative and regulatory environment, consolidating and conditioning the DSRS and removing the DSRS from user premises to more suitable locations. These efforts are often not sustainable as the root causes of the lack of control are not identified and dealt with. These root causes could include poor economic growth, political instability, poor education systems, poor safety and security culture and weak regulatory infrastructures. The author has often visited countries where safety and security has been previously upgraded by either the IAEA or its donor States but has not been maintained due to the root causes mentioned above.

Unfortunately, loss of control over sources is still happening due mostly to political turmoil, conflict, economic weakness and poor governance. The conflict areas of Syria, Libya and Nigeria to name but a few are examples where sources are or will become vulnerable. The IAEA glossary definition of vulnerable is “A radioactive source for which the control is inadequate to provide assurance of long term safety and security, such that it could relatively easily be acquired by unauthorized persons” [9]. When the war was at its height in Iraq, the neighboring countries were receiving many more illicit sources than was usual. Obviously the sources could not be returned and these countries were obliged to take over control of them. One of weak links in the control of sources is clearly found in areas where it is impossible to exercise good control over sources due to the above-mentioned reasons.

5 FRAMEWORK FOR IMPROVING MANAGEMENT OF DSRS

Given the premise that better resourced countries are better able to sustain the control over their sources, what happens to sources when countries do not have the necessary resources to adequately manage their inventories? Two end-points come to mind namely, removal of the sources from the country or disposing of these in the country itself. These end-points should be formally identified by putting in place a Policy and Strategy for the management of radioactive sources in a country. Once the alternatives are identified, the necessary resources should be put in place to attain the outcomes identified in the Strategy.

Without adequate resources in place, storage cannot be regarded as sustainable in the long term. This is when the Borehole Disposal System (BDS) becomes attractive as an end-point in the life cycle of sealed radioactive sources (SRS). The alternative is to remove the DSRS from the country and either repatriate them to the country of origin or send them to another country for re-use or re-cycling. This option has been pursued on a number of occasions on a case by case basis.

5.1 Removal of sources from countries

The IAEA has returned 17 drums of Pu and Am sources from Brazil back to the United States. This was done by loading the drums on a ship carrying spent research reactor fuel as Pu sources cannot be flown into the United States. High activity sources have also been repatriated back to Canada, Russia, the US and France. Some sources have been returned to India.

This has only been done on a limited scale because of the high cost and difficulties encountered in the transport of the sources. Another factor is the charges associated with the long term storage and disposal in the supplier countries. Most developed countries charge a substantial amount of money to receive disused sources back into their countries. These charges are intended to cover the costs of management of the long term storage and also the “disposal” charges when these may realise. Some developed countries have limited disposal capability for disused sources but others have not as yet opened up this route for their sources.

The US has commercial disposal routes open to only 14 States. Only EnergySolutions in Barnwell, South Carolina, and American Ecology in Richland, Washington, can dispose of commercial A, B, and C sealed sources [10]. These facts may have recently changed since the reference was written. The report [10] emphasizes the US concern over lack of disposal facilities for sources in the US and a quote from the report indicates their concern. “Due to the potential public health, safety, and national security concerns of lost or stolen sealed sources, the sealed source community—including sealed source manufacturers, distributors, and users, Federal, State, and local officials, and those involved in the radioactive waste storage and disposal industry—**encourages sealed source users to permanently dispose of sources that are no longer in use and cannot be recycled.**” [10].

It is clear that strengthening the regulations for long term storage will have a limited impact on sustainability, but reducing the number of sources in storage will reduce the number of storage locations, thereby decreasing the number of attractive targets for those who seek to illegitimately procure a sealed source for malicious purposes. The difficulty and cost of removing sources from developing countries is a barrier that can be overcome and the risks associated with these sources can be decreased but not removed entirely when the sources are moved to a supplier country. Unless the supplier country has a disposal route open, the risk posed by a source will never reduce to zero.

5.2 Disposal as an end-point

Storage has been up to now the only option for dealing with DSRS in most countries. In the past some shorter-lived sources have been disposed of in shallow land trenches but most of the higher activity sources are not amenable to this disposal route. The advantage of storing DSRS is that full control is maintained and this allows possible better solutions in the future. The main disadvantage of long-term storage is that resources must be put aside to maintain control for a long time. This in some countries as mentioned above is not sustainable. Disposal therefore becomes the most sustainable option for the control of DSRS in countries where resources are limited. This improves the safety and reduces the threat of malicious use to zero.

The BDS is currently being implemented in three countries – Philippines, Malaysia and Ghana. A good description of the development of the concept as well as the history of this development can be found in [11]. A number of technical advances have been recently completed by the IAEA and these include:-

- Altering the Mobile Hot Cell (MHC) to allow disposal of high activity sources in a borehole.
- Designing and manufacturing a Mobile Tool Kit (MTC) to assist the IAEA Member States in conditioning and disposing of lower activity sources in a borehole. Figure 2 shows the transfer cask that is part of this MTC.

Given the advances that have recently been made, the BDS is now being implemented and very soon one of the three countries mentioned above will have disposed of DSRS into a borehole. Hopefully this will be the start of many more Borehole Disposal Projects. Figure 3 shows management options for DSRS and the emphasis is on disposal as a solution to the many challenges in maintaining better control over sources in countries with limited resources. The economics of disposal in a borehole have been looked at and the costs of disposal are clearly far less expensive than the costs of removal of sources from a country. A typical project to remove a single teletherapy (Cat 1 or 2) source from a country can cost between US\$ 100 000 to US\$ 200 000 or more. If all the categories of sources in a country are disposed in a borehole this is much less expensive than removing them all from the country.

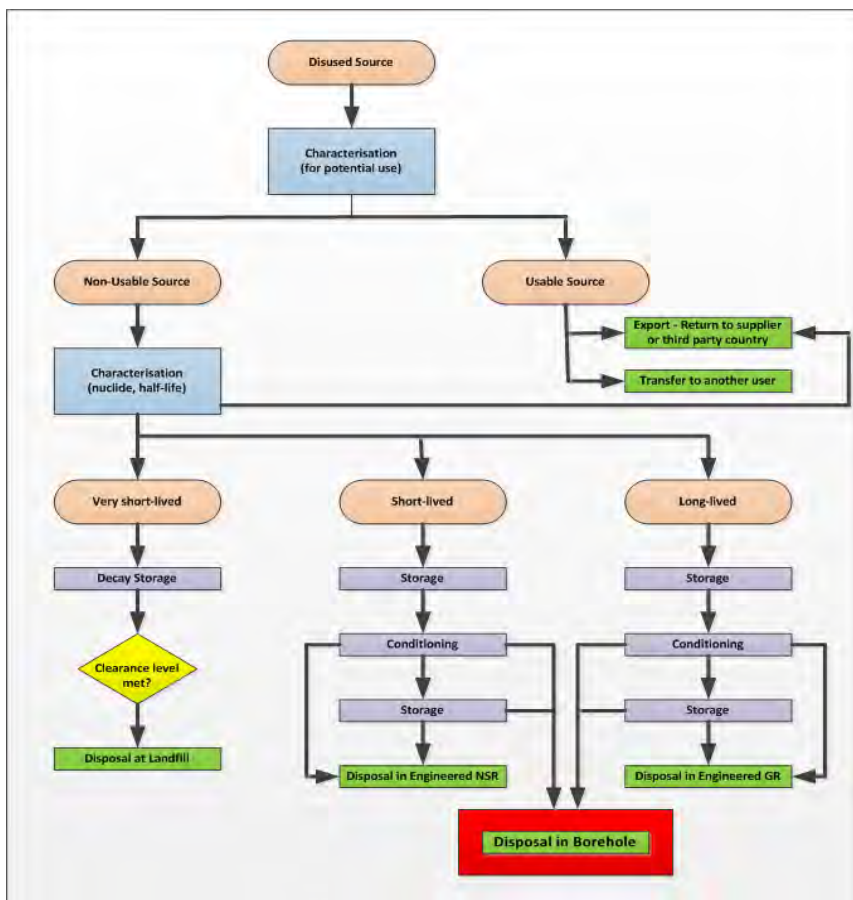
5.3 Security of the BDS

Recently, the Canadian government has donated money to the IAEA to assist some of the Member States mentioned above in implementing the BDS to dramatically improve the security of the DSRS in these countries. The reduction in the threat of malicious use by disposing of sources in developing countries is obvious. The IAEA is currently developing a Security Series document on security aspects of the BDS.

Figure 2: Newly manufactured transfer Cask showing position of the borehole. Photo courtesy of Mr Janos Balla.



Figure 3: Framework for managing DSRS.



6 CONCLUSION

Sustainability of the control over radioactive sources and in particular DSRS cannot be guaranteed worldwide due to various factors including weak economies, political instability, warfare, poor safety and security culture and weak regulatory infrastructures in many poorly resourced countries. As removal of the sources from these countries is very expensive, disposal becomes the only viable option. Recent advances in the technologies for the BDS have allowed three BDS projects to go ahead in the Philippines, Malaysia and Ghana. There are other countries interested in moving forward with borehole disposal and this should considerably improve the safety and security of DSRS that are currently being stored in these countries.

7 REFERENCES

- [1] IAEA, 1998. Lessons Learned from Accidents in Industrial Radiography. Safety Reports Series No. 7, International Atomic Energy Agency, Vienna.
- [2] IAEA, 1988. The Radiological Accident in Goiania. International Atomic Energy Agency, Vienna.
- [3] IAEA, 2000, Radiological Accident in Istanbul. IAEA, International Atomic Energy Agency, Vienna .
- [4] IAEA, 2000. Radiological Accident in Lilo. International Atomic Energy Agency, Vienna.
- [5] IAEA, 2000. The Radiological Accident in Yanango. International Atomic Energy Agency, Vienna.
- [6] IAEA, 2002. The Radiological Accident in Samut Prakarn. International Atomic Energy Agency, Vienna.
- [7] IAEA, 2001. Inventory of accidents and losses at sea involving radioactive material. TECDOC 1242, International Atomic Energy Agency, Vienna.
- [8] IAEA, 2011. National Strategy for Regaining Control over Orphan Sources and Improving Control over Vulnerable Sources. Specific Safety Guide No. SSG-17, International Atomic Energy Agency, Vienna.
- [9] IAEA, 2007. IAEA Safety Glossary, terminology used in Nuclear Safety and Radiation Protection. International Atomic Energy Agency, Vienna.
- [10] US DEPARTMENT OF HOMELAND SECURITY 2009. Sealed Source Disposal and National Security – Problem Statement and Solution Set. Deliverable (part 1) of the removal and disposition of disused sources focus group of the radioisotopes sub-council of the Nuclear Government and Sector Coordinating Councils. Washington DC.
- [11] Van Blerk, J.J. 2011. The BOSS Concept: Long-Term Solution for the Management of Disused Sealed Radioactive Sources (DSRS). Unpublished report commissioned by the IAEA. Vienna.

Assessment of the radiological consequences of accidents in vehicle transportation of radioactive material in the area of Bologna

Sara Vichi^a, Sara Baldazzi^a, Angelo Infantino^b, Gianfranco Cicoria^c, Giulia Lucconi^c, Domiziano Mostacci^a, Mario Marengo^c

^aNuclear Engineering Laboratory of Montecuccolino, Industrial Engineering Department, University of Bologna, Bologna, Italy.

^bCERN - EN/EA, CH-1211 Geneva 23, Switzerland.

^cMedical Physics Department, "S. Orsola-Malpighi" Hospital, Bologna, Italy.

Abstract. Radiopharmaceuticals represent more than 90 % of radioactive material packages transported within in EU Member States. This work is intended to collect statistical information on transportation of radioactive materials in the area of Bologna (Italy) and to evaluate the potential radiological risk for population in case of an accident; data were used to create a model for risk assessment as a basis for the definition of an emergency protocol. An investigation of the transportation of radioactive materials in the area of Bologna was performed collecting data spanning on authorized carriers, consignees, itineraries, type of package transported (excepted package, type A package, type B package), radioactive content in each package (radionuclide, physical form, activity), population density, vehicle density and accident rate. Risk assessment was performed using RADTRAN (Sandia National Laboratories) and INTERTRAN2. Scenarios of accident have been studied in detail using HotSpot (NARAC, Lawrence Livermore Laboratory). A scenario involving a vehicle carrying a mixture of packages of ⁹⁹Mo (generators for ^{99m}Tc), ¹³¹I (capsules for thyroid therapy) and ¹²⁵I (kits for in vitro RIA tests) is expected to produce a maximum total effective dose in the range of 4 – 6 x10⁻⁷ Sv. In general, the variety of scenarios studied for accidents in vehicle transportation or radiopharmaceuticals for medical in the geographical area considered, showed a very low risk for representative persons of the population, inferior to the criteria of radiological relevance. The collected information and results allowed the implementation of a database to perform risk assessment in the transportation of radioactive material in the area of Bologna, with reasonable and realistic assumptions.

KEYWORDS: *transportation of radioactive material; risk assessment; atmospheric release.*

1 INTRODUCTION

Road transport of radioactive material is regulated in Italy by the Ministerial Decree of January 3, 2007, containing the translation in Italian of the European Agreement of International Carriage of Dangerous Goods by Road (ADR). The national technical regulatory framework is based on the IAEA "Regulations for the Safe Transport of Radioactive Material".

This work aims to study the entity of transport of radioactive substances in a specific local area, central to the national transport network. In particular, a risk assessment and accident patterns, including in urban areas, have been developed with regard to the frequent transport of radiopharmaceuticals, delivered to hospitals.

2 MATERIALS AND METHODS

2.1 Transport risk assessment

Risk assessment in the transportation of radioactive sources was made using INTERTRAN2, a computer code system developed by AMC Konsult (Bromma, Sweden) in the scope of an IAEA Coordinated Research Program, and based on RADTRAN, a program for analyzing the risks and consequences of transporting radioactive materials developed by Sandia National Laboratories. In order to provide meaningful results, modelling as much as possible realistic accidental situations, a detailed investigation on transportation of radioactive materials in the area of Bologna was conducted.

Data on authorized carriers, consignees, itineraries, type of package transported (excepted, type A/B) and radioactive content of each package (radionuclide, physical form, activity) were collected.

The more frequent pathways and their territorial context in terms of population density, vehicles density and accident rate were considered and grouped, for the input in INTETTRAN2, into six different itinerary type: Highway A1, A13, A14, freeway, urban streets, suburban streets. In Table 1 for each itinerary type the main features are reported. [1,2]

Table 1: Territorial context

Itinerary Type	Population density (persons/km ²)	Vehicles density (Vehicles/hr)	Accidents rate (Accidents/vehicle*km*Year)
Highway A1	169	4.21E+03	4.04E-08
Highway A13	284.6	2.39E+03	5.24E-08
Highway A14	732.5	3.49E+03	7.98E-08
Freeway	1212	3.32E+03	1.75E-07
Urban area	2728	8.10E+02	1.35E-07
Suburban area	712	8.10E+02	2.24E-07

A statistical study of collected data using event tree analysis was conducted, for the definition of most significant situations to be analysed in order to obtain realistic case studies.

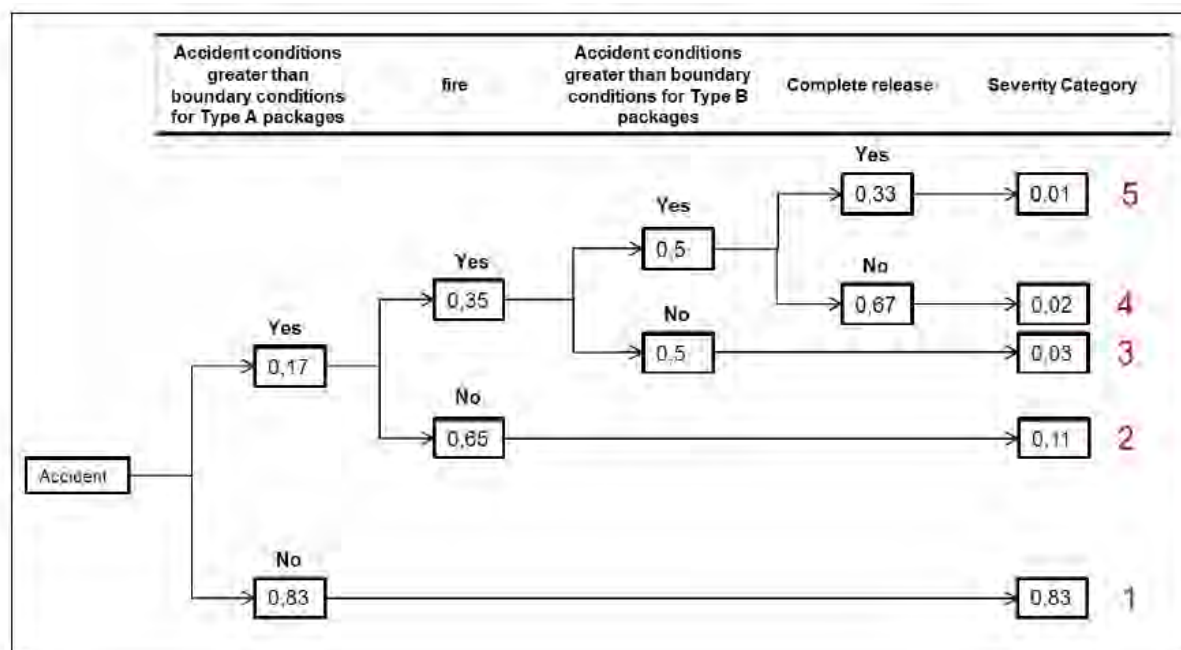
To take into account the different levels of danger of an accident, severity categories were defined; the probability that an accident belonged to a defined severity category (severity fraction) was assessed depending on the type of Area (Table 2). [3,4,5]

Table 2: Definition of Severity categories and Severity Fractions

Severity Category	Description	Severity Fraction		
		Urban Area	Suburban Area	Rural Area
1	Accident conditions lower than boundary conditions imposed by the regulations for Type A packages.	0,83	0,71	0,63
2	Accident conditions greater than boundary conditions for Type A packages but lower than boundary conditions imposed for Type B packages not involving fire.	0,11	0,16	0,18
3	Accident conditions greater than boundary conditions for Type A packages but lower than boundary conditions imposed for Type B packages involving fire.	0,04	0,07	0,09
4	Accident conditions greater than boundary conditions for Type B package but that do not result in the complete release of radioactive contents.	0,02	0,04	0,06
5	Accident conditions greater than boundary conditions for Type B package but that result in the complete release of the radioactive contents.	0,01	0,02	0,04

For the assignation of severity fraction for each zone a Log-Normal distribution were assumed. In Figure 1 the event tree for the evaluation of severity fractions in Urban areas is reported [6].

Figure 1: Event tree analysis for the definition of severity fractions



For each severity category, the package response was defined in terms of release of radioactive material.

Packages were divided in physical-chemical group on the basis of physical properties (i.e., whether the material is a monolithic solid, divided solid as powders of various types, liquid, or gas) and of chemical properties (such as melting point or oxidation state) of radioactive content that might affect dispersion or toxicity in potential accidents (Table 3). [3,4,5,6,7,8]

Table 3: Fraction of radioactive material released for each physical-chemical group in case of an accident occurring in a particular severity category

Physical-chemical group	Sev 1	Sev 2	Sev 3	Sev 4	Sev 5
Excepted package – liquid or gas	1	1	1	1	1
Excepted package - solid	0	0,5	1	1	1
Type A package – liquid or gas	0	1	1	1	1
¹³¹ I therapy capsule	0	0,25	0,5	1	1
Generators	0	0	0,25	0,75	1
Type A package - solid	0	0	0,25	0,5	1
Special Form	0	0	0,1	0,25	1
Type B package	0	0	0	0,1	1

2.2 Accidents involving fire

Scenarios of accident involving fire were studied in detail using HotSpot, a set of software tools developed by The Department of Energy (DOE, United States) for the estimation of radiation effects associated with the atmospheric release of radioactive materials.

In particular, the following scenarios were analysed:

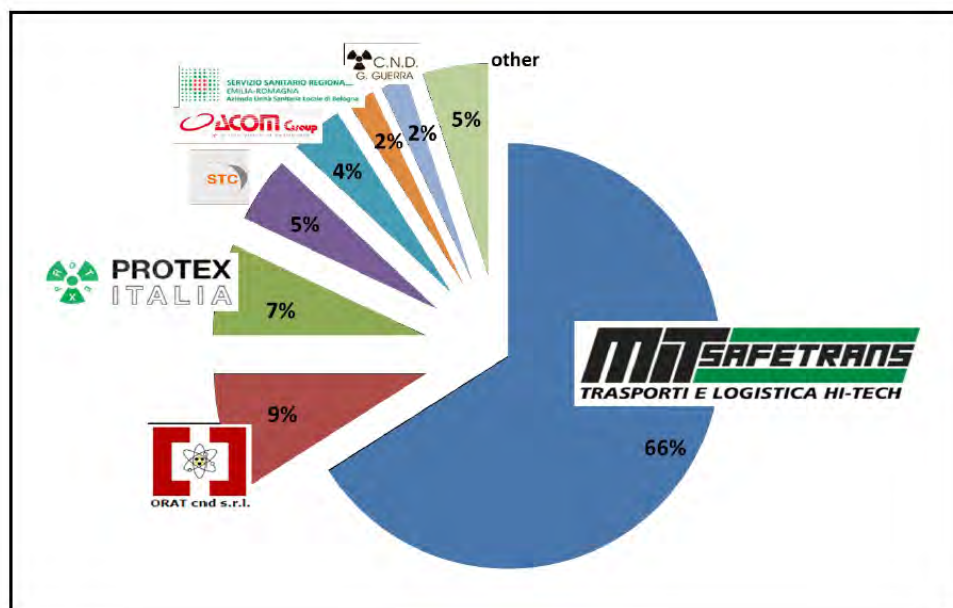
- Vehicles carrying Packages of capsules of ¹³¹I, Vials of ¹⁸F, ⁹⁰Y, ²²³Ra, Generators ⁹⁹Mo/^{99m}Tc and ⁶⁸Ge/⁶⁸Ga;
- 3 different type of vehicle, each with an Equivalent Fuel Volume of 55 gal, 90 gal, 180 gal;
- Different fire durations (from 10 to 120 minutes);
- Different meteorological conditions.

3 RESULTS

3.1 Statistical analysis of radioactive sources transport in Bologna

Our study for the Province of Bologna confirm that the company MITSafetrans, the Italian leader in the transportation of radioactive materials, is the most important carrier in our area, managing more than 66% of shipments, mainly type A packages (Figure 2). As regards transportation of radioactive waste the most important authorized carrier is Protex. Other companies like Orat or STC are involved in the transportation of iridium and selenium-based gamma ray sources for non-destructive controls. [9,10]

Figure 2: Authorized consignors



In the area of Bologna facilities involved in transportation of radioactive materials are mainly Hospitals. In Table 4 a summary of typical packages transported during the year 2014 to the S.Orsola-Malpighi Hospital is reported [11].

Table 4: Main Packages transported to the S.Orsola-Malpighi Hospital

Nuclide	Package Type	Activity (Bq)	n ^o of packages in a year
⁵¹ Cr	A	7,09E+07	10
⁶⁸ Ge	A	1,85E+09	4
¹²³ I	A	6,52E+08	97
¹²⁵ I	E	9,25E+08	122
¹³¹ I	A	2,17E+10	240
¹¹¹ In	A	1,61E+08	1
¹⁹² Ir	A	4,52E+11	11
⁹⁹ Mo	A	1,14E+11	292
⁹⁰ Y	A	6,53E+09	24

3.2 Results of the risk assessment

More than 200 different scenarios were studied. In the following only most significant scenarios are described.

In Table 5 results obtained with INTERTRAN2 for the assessment of risk associated with single packages are reported, risk was expressed in terms of collective dose (person Sv).

Table 5: INTERTRAN2 evaluation of risk associated with single packages

Nuclide	Activity (Bq)	Risk (person Sv)			
		Highway	Suburban road	Freeway	Urban road
⁹⁹ Mo	2.25E+11	3.72E-15	9.91E-13	1.32E-12	6.66E-13
¹³¹ I	2.92E+10	1.29E-14	3.78E-12	5.02E-12	2.85E-12
¹²⁵ I	9.25E+08	5.17E-16	1.56E-13	2.08E-13	1.20E-13
¹²³ I	8.91E+08	7.1E-16	2.2E-13	2.92E-13	1.8E-13
⁹⁰ Y	5.52E+10	3.61E-16	9.35E-14	1.24E-13	6.25E-14
¹⁷⁷ Lu	1.47E+11	1.28E-12	3.97E-10	5.28E-10	3.25E-10
¹¹¹ In	5.78E+08	1.76E-15	5.44E-13	7.23E-13	4.45E-13
¹⁹² Ir	4.52E+11	6.61E-13	1.58E-10	2.11E-10	1.07E-10

Afterwards realistic scenarios of accident, with more than one package, were analysed. In Table 6 Risk associated with the most frequent transportations in Bologna are reported.

Table 6: Risk associated with the most frequent transportations in Bologna

Starting point	Consignees	packages	Risk (person Sv)
Milan	MITsafetrans storage (Quarto Inferiore) Policlinico S. Orsola-Malpighi	5 packages (p.) of ¹²³ I, 10 p. of ¹³¹ I, 5 p. of ¹²⁵ I, 1 p. of ⁹⁹ Mo	5.05E-10
Milan	MITsafetrans storage (Quarto Inferiore) Policlinico S. Orsola-Malpighi Ospedale Bellaria	8 p. of ¹³¹ I, 4 p. of ⁹⁹ Mo	4.59E-10
Milan	Policlinico S.Orsola-Malpighi	8 p. of ¹³¹ I, 6 p. of ¹²⁵ I, 2 p. of ⁹⁹ Mo	5.26E-10
Milan	MITsafetrans storage (Quarto Inferiore) Policlinico S. Orsola-Malpighi Istituto Ortopedico Rizzoli	2 p. of ¹²³ I, 8 p. of ¹³¹ I, 7 p. of ¹²⁵ I, 1 p. of ⁹⁹ Mo	4.39E-10

On the basis of these results, it has been possible to estimate the average risk for single transport in case of an accident associated with main consignees in the area of Bologna (Figure 3).

Figure 3: Average risk for single transport in case of an accident associated with main consignees in the area of Bologna; number of transports in 2011/2012 for each consignee and radioactive material transported.



3.3 Release in case of fire

An excerpt of the main results obtained using HotSpot is given in the following Tables. In particular, Table 7 gives the results of the estimation of radiation effects associated with an accident involving fire, in the case of singles packages. Table 8 instead refers to a more realistic scenario, with transportation of a variety of radioactive packages in the same vehicle.

Table 7: Radiological consequences associated with the atmospheric release of radioactive materials following an accident involving fire. Data calculated using Hotspot. Case of single package.

Nuclide	Activity (Bq)	Fire Duration (min)	Maximum Dose Distance (km)	Maximum TEDE (Total Effective Dose Equivalent) (Sv)
^{131}I	3.7E+09	10	9	3.09E-09
		30	2.8	1.54E-08
		60	1.3	5.16E-08
^{90}Y	3.7E+09	10	8.9	1.18E-13
		30	2.8	5.98E-13
		60	1.3	2.00E-12
^{18}F	7.4E+09	10	4.7	2.19E-14
		30	1.6	1.45E-09
		60	0.82	4.82E-09
$^{99}\text{Mo}/^{99m}\text{Tc}$	6.8E+10 of ^{99}Mo and 6.0E+10 of ^{99m}Tc	10	7.8	2.97E-02
		30	2.7	1.64E-11
		60	1.2	5.53E-11
$^{68}\text{Ge}/^{68}\text{Ga}$	1.85E+09	10	4	4.65E-13
		30	1.4	3.24E-12
		60	0.79	1.10E-11
^{223}Ra	5.0E+07	10	5.3	1.38E-09
		30	1.6	8.25E-09
		60	0.84	2.68E-08

Table 8: Radiological consequences associated with the most frequent transportations in Bologna, calculated using Hotspot. Realistic case of multi-package transport.

Starting point	Consignees	packages	Maximum TED in case of fire (Sv)
Milan	MITsafetrans storage (Quarto Inferiore)	5 packages (p.) of ^{123}I , 10 p. of ^{131}I , 5 p. of ^{125}I , 1 p. of ^{99}Mo	5.50E-7
	Policlinico S. Orsola-Malpighi		
Milan	MITsafetrans storage (Quarto Inferiore)	8 p. of ^{131}I , 4 p. of ^{99}Mo	5.49E-7
	Policlinico S. Orsola-Malpighi		
Milan	Ospedale Bellaria	8 p. of ^{131}I , 6 p. of ^{125}I , 2 p. of ^{99}Mo	4.81E-7
	Policlinico S. Orsola-Malpighi		
Milan	MITsafetrans storage (Quarto Inferiore)	2 p. of ^{123}I , 8 p. of ^{131}I , 7 p. of ^{125}I , 1 p. of ^{99}Mo	4.47E-7
	Policlinico S. Orsola-Malpighi		
	Istituto Ortopedico Rizzoli		

4 CONCLUSIONS

This work is the first systematic and detailed analysis of the impact of this type of radiological accidents in the Bologna area. As expected, radiopharmaceuticals and other sources for medical use are by far the most transported radioactive sources. Our study shows that each individual transport of radiopharmaceuticals in the area of Bologna has a very small impact, well below the "no radiological relevance criteria". Not less than 20 major accidents per year, including fire, would be necessary in order to challenge a criteria of 10 $\mu\text{Sv}/\text{year}$.

The model developed, based on widely diffused and validated codes, as INTERTRAN2 and HotSpot, can be extended to other scenarios or applied to different geographic areas.

5 REFERENCES

- [1] <http://www.istat.it>
- [2] Localizzazione degli incidenti stradali, Automobile Club d'Italia e Sistema Statistico Nazionale, a cura della Direzione Studi e Ricerche ACI, Roma – Novembre 2013.
- [3] Regulation for the safe transport of Radioactive Material, 2009 Edition, Safety Requirements N°. TS-R-1, IAEA Safety Standards.
- [4] *J-P Degrange (CEA), A-M Ericsson (AMC konsult AB), C. Jarnry, T.F Kempe (AMC Konsult AB), S. Neuhauser (Sandia National Laboratories), H. Wilkinson (AEA Technology)*. Advisory Material for the INTERTRAN2 computer program.
- [5] International Atomic Energy Agency (IAEA), 2003. Input data for quantifying risks associated with the transport of radioactive material, Final report of a co-ordinated research project 1996-2000.
- [6] IAEA-TECDOC-1346, March 2003. Input data for quantifying risks associated with the transport of radioactive material. Final report of a co-ordinated research project 1996-2000.
- [7] *Harvey, M.P., Jones, A.L.*, 2012. Radiological Consequence Resulting from Accidents and Incidents Involving the Transport of Radioactive Materials in the UK – 2011 Review. Report HPA-CRCE-037 part of "Radiation: HPA-CRCE scientific and technical report series".
- [8] *McClure, J.D., Yoshimura, H.R., Fagan, H.F, Thomas, T.*, 1997. Radioactive Material (RAM) Transportation Accident And Incident Experience In The U.S.A. (1971-1997). In: 12. international conference on packaging and transportation of radioactive materials; Paris (France); 10-15 May 1998; SAND--97-2909C; CONF-980507.
- [9] <http://www.regione.emilia-romagna.it>
- [10] <http://www.isprambiente.gov.it>
- [11] *Vichi, S., Cicoria, G., Pancaldi D., Infantino A., Po, C., Mostacci D., Marengo M.* Transportation of radioactive material for Nuclear Medicine: risk assessment in the area of Bologna. Eur J Nucl Med Mol.

Actions for Spent Radioactive Sources Removal

Teresa Ortiz*, Elena Alcaide

Radiological Protection Technical Unit, C/Emilio Vargas, 7, 28043, Madrid, Spain

Abstract. Radioactive waste is produced in regulated medical, industrial, and research and teaching facilities, besides that generated at nuclear power plants. This radioactive waste includes spent sources that may also occur in non-regulated facilities. One important group of non-regulated facilities is metal industry companies, who are signatories to a protocol on the radiation monitoring of metallic materials and a protocol for radiological monitoring of containers in ports, part of a global initiative. Spent sources may also appear in industries, research centres, educational institutions and other locations, from past practices which never gained authorisation. Because of this, a specific search and recovery campaign for orphan sources was carried out between 2007 and 2009. During the years of implementation covered by this paper, more than 8,000 sources were verified for removal, most of them from regulated facilities. The campaign for orphan sources handled over 450 sources, of which more than 250 were orphan sources. This paper describes the actions which have been underway for several years to recover these spent sources, and their outcomes.

KEYWORDS: *radiological protection; orphan sources.*

1 INTRODUCTION

Spain's National Radioactive Waste Company (ENRESA) is responsible for the management of radioactive waste generated throughout the country. These radioactive wastes are produced in nuclear facilities and regulated radioactive installations for medical, industrial, research and teaching purposes. Radioactive waste includes spent radioactive sources that may appear in both regulated and unregulated facilities.

Removal of spent sources from regulated facilities is easier because of the availability of documentation for the source, specifying the isotope and activity. Recovery actions are more complex, however, when sources are located in older installations that have never been authorised, in regulated installations for past practices, in other places such as metal industry plants, or when they result from the radiological monitoring of containers and vehicles at ports or waste dumps.

The preferred choice for the management of spent sources is their return to the supplier. This option is not always possible, however, especially when the supplier is unknown, is no longer in business, or has insufficient financial resources. In these cases, ENRESA collects the sources and either stores them or disposes of them, depending on their radiological characteristics.

Preparation for the removal of spent sources is carried out by ENRESA's Radiological Protection Technical Unit, which collects the necessary data and carries out any necessary conditioning of the sources for transportation.

This paper describes all activities carried out for the removal of spent radioactive sources from both regulated and unregulated facilities. It also describes the campaign for recovery of orphan sources carried out between 2007 and 2009.

*Presenting author, e-mail: torr@enresa.es

2 RECOVERY PROCEDURES FOR SPENT SOURCES

For the removal of any radioactive source, it is essential to have adequate information on the isotope, activity and date, as well as the serial number and other information, such as that relating to transport, e.g. the Special Form Certificate. The procedures that the Technical Unit follows to obtain the necessary information and prepare the source for transport are described below.

2.1 Characterisation of Spent Sources

When the source does not have a Source Certificate detailing its activity or the equipment is not labelled with the necessary data (isotope, activity and date) this information must be obtained for the purposes of transport. If the activity is sufficiently low, the source is extracted from the shielding and measurements are taken to determine the activity from the dose rate at different distances and a spectrum is obtained using portable spectrometry equipment. If the activity is high, it is estimated using mathematical models that simulate the shielding and external dose rate measurements.

2.2 Disassembly of Equipment Containing Sources

In some cases, it is necessary to disassemble the equipment in situ and remove the source, with or without its shielding, so that it can be transported in an appropriate container which complies with regulations governing the transport of radioactive material. In general, the source is disassembled and transported in its original shielding (Fig.1), although additional shielding is sometimes used. Only alpha-emitting sources are removed from their shielding.

Figure 1: Disassembly of a cobalt therapy head



2.3 Conditioning of Sources

Conditioning of sources includes all the tasks necessary to prepare the source for transport, packaging and storage/disposal. These operations include the partial cutting of the shielding, the placement of additional shielding, when the source is not in a safe position and the operating mechanism is not working, removing the source from the device or its container to place it in another container (Fig. 2 and Fig. 3), either to meet transport requirements or because the owner wishes to keep it.

On several occasions, rods have been cut from TROLEX gauges for measuring soil density and moisture levels, to enable them to be inserted into the transport package. To ensure that cutting is carried out correctly, without damaging the source, digital radiography is used to determine the position of the source.

Figure 2: Separation of Cs-137 and Am-241 sources



Figure 3: B(U) package for Am-241 sources



When the dose rate of the source, device or its container exceeds 10 mSv/h, additional shielding must be used in order to comply with transport regulations.

3 ACTIVITIES UNDERTAKEN

As mentioned above, spent sources can be recovered from both regulated and unregulated facilities. Removals from regulated facilities are carried out in line with the facility's operating permit. At unregulated facilities, removals must be carried out on the basis of a specific authorisation issued by the Ministry of Industry, following approval from the Nuclear Safety Council (CSN), called a Transfer Resolution. Most sources come from regulated facilities.

3.1 Removal of Sources from Radioactive Installations and Unregulated Facilities

Since 1993, ENRESA has removed more than six thousand radioactive sources, varying widely in activity. Most of them have been low or intermediate activity sources. The number of sources removed is lower than the number of sources inspected by the Technical Unit, because cases involving the same isotope and low unit activity (verification sources, etc.), are considered a single source for the purposes of removal.

High activity sources that have been removed since 1998 include 49 disused teletherapy unit heads, the majority with Co-60 sources (although three had Cs-137 sources), and two research irradiators, one with a Cs-137 source and the other Co-60.

Relevant sources removed from radioactive installations and unregulated facilities include:

Figure 4: Disassembly of one of the sources



- Almagrera Mines (Huelva, 2004): a confiscation by the Ministry of Industry of radioactive sources from a bankrupt coal mine. Thirteen Cs-137 sources were removed with levels of activity between 3.7 GBq and 55.5 GBq, with dose rates between 0.12 and 0.2 mSv/h with the shutter closed, as well as one Cm-244 source with an activity of 3.7 GBq and a dose rate of 0.2 mSv/h, which had to be disassembled from the device. Seven of the sources were in a bunker and the others had to be disassembled (Fig. 4).

Figure 5: Location of the sources



- Alfique Mines (Granada, 2014): this involved a Transfer Resolution for sources which had belonged to a mine being readied for re-opening and were located by the new owner. There were five level gauges with Co-60 sources, four of 1.11 GBq and one of 3.7 GBq in 1969, so the dose rates were very low. The devices were outside, in wooden boxes (Fig. 5).

Figure 6: Devices in transport packages



- Gammagraphy company (Guarnizo and Arrigorraia, 2015): this was a confiscation by the Basque Government at a radioactive installation of 10 gammagraphy devices with Ir-192 sources which were already decayed, but with depleted uranium shielding (Fig. 6).

All these inspection and removal activities are still ongoing and without incident.

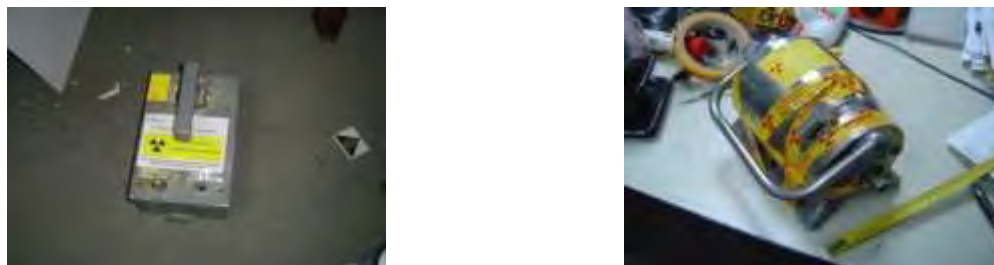
In addition to these ongoing recovery actions for sources, a campaign was launched in Spain for seizure of Ra-226 used for medical purposes. This campaign lasted three decades and resulted in the seizure of thousands of sources, totalling 600 GBq of activity. At the same time, the dismantling and removal of all radioactive lightning rods has been undertaken throughout the country. In total, more than 22,000 units have been removed. These are ongoing tasks, and a few dozen are removed each year.

3.2 Campaign for Recovery of Orphan Sources

On the basis of Royal Decree 229/2006, transposing European Council Directive 2003/122 on the control of high-activity sources and orphan sources, ENRESA was assigned to carry out a campaign for the recovery of orphan sources. This campaign was conducted in accordance with the requirements of the Ministry of Industry and with guidance from the Nuclear Safety Council. It was conducted between 2007 and 2009.

As part of this campaign, the Technical Unit was responsible for the characterisation, disassembly and conditioning of the sources. The sources were located through requests for information sent out to the different sectors which were likely to have them, such as industries, hospitals, research centres, universities, educational institutions, suppliers etc., either by direct contact or through professional associations. The relevant official agencies and ministries were also contacted.

Figure 7: Equipments located during the campaign for recovery of orphan sources



461 radioactive sources were removed as a result of this campaign, of which 200 were below the exemption level and 261 were actual orphan sources. The activity of the orphan sources was 165 GBq and the exempt sources amounted to 638 MBq. The isotopes identified were those generally found in sources used in industry and research, including Cs-137, Ra-226 and Sr-90. Other radioactive materials were also recovered, including unsealed sources (13 units), depleted uranium shielding (15 units), luminous signs with H-3 (56 units), valves (7 units) and uranium salts and natural uranium. The sources were located in industries, government agencies, healthcare facilities and research facilities. The number of sources and distribution by isotope is shown in Table 1.

Table 1: Number of orphan sources located and distribution by isotope

Isotope	Number of orphan sources	Percentage
Cs-137	104	40 %
Ra-226	46	18 %
Sr-90	26	10 %
Ni-63	19	7 %
Po-210	11	4 %
Pb-210	9	3 %
Various	7	3 %
Am-241	6	2 %
Co-60	6	2 %
H-3	6	2 %
Kr-85	6	2 %
Am-241/Be	5	2 %
Ra-226/Be	3	1 %
Tl-204	3	1 %
Ba-133	2	1 %
Co-57	2	1 %
Total	261	100%

3.3 Detection Protocols for Radioactive Material

3.3.1 Protocol for Radiological Monitoring of Metallic Materials

The Protocol for Radiological Monitoring of Metallic Materials was signed in November 1999. The parties involved were ministries, agencies, steel companies, scrap metal merchants and trade unions. Facilities belonging to signatories to the Protocol must have systems to detect the presence of any type of radioactivity in scrap metal. Radiation portal monitors are the most commonly used, through which the lorry, carrying the scrap metal, passes.

In the period 1998-2015 the signatory companies, of which there are over 150, detected more than 1000 cases.

These detections may involve more than one radioactive material. Items located include: radioactive sources, with or without shielding; consumer products containing radioactive material (smoke detectors, lightning rods, alloys containing thorium, articles with luminous paint with Ra-226, etc.); items with naturally occurring radioactive material (NORM); and parts with artificial radioactive material (Co-60, Cs-137, depleted uranium, etc.). These parts include pipes, sheet metal, valves, compacted parts, etc.

3,870 items of various types were located during this period, of which 331 have been classified as radioactive sources. Of the remaining items, the majority (59%) contained natural radioactive material. Of the sources recovered, 62% were Ra-226, generally of low activity, originating from past activities, while 9.95% of the activity corresponds to sources with artificial isotopes.

Recovered parts with activity higher than the reference level are managed as radioactive waste for disposal at ENRESA's El Cabril facility in Córdoba. Much of the time, conditioning is necessary to enable their removal in appropriate packages. In these cases, the parts are cut to fit the package. In addition, in order to reduce the volume of radioactive waste, where possible, the part is cut and separated from any soils containing naturally occurring radioactive material (NORM). Once complete, the metal component of the part is checked for the absence of radioactive material. This metal part can be incorporated into the process.

3.3.2 MEGAPORT Protocol

The MEGAPORT Protocol is a United States initiative which aims to deter, detect and intercept illicit trafficking of nuclear and radioactive materials in the global shipping trade. This requires inspecting the largest number of containers possible, both for export and import, with minimal impact on trade flows. Through this protocol, Spanish ports have installed radiation portal monitors for containers at the ports' entrances and exits. There are also spectroscopic portals for identifying the isotope.

Under this protocol, some containers have been returned to their country of origin and some materials and sources have been recovered by means of Transfer Resolutions. The last detection at the port of Valencia involved the conditioning and removal of four Cs-137 sources of 6.14 GBq each.

4 CONCLUSIONS

- In Spain, various actions have been carried out for the recovery of disused sources, both in radioactive installations and unregulated facilities;
- With the exception of incidents involving accidental melting/breakage of sources in the metal industry, there have been no incidents involving orphan sources;
- The Ministry of Industry has established the mechanism of Transfer Resolutions so that ENRESA can remove all radioactive material that is recovered;
- Existing protocols ensure early detection of uncontrolled radioactive material.

Leak Radiation Assessment of Scanner HCV-Mobile, THSCAN Scanner And Scanner HCP-Portal

Tahiry Razakarimanana*, H.A. Razafindramiandra, Raelina Andriambololona, J.L.R. "Zafimanjato, R.D. Randriantsizafy

Institut National des Sciences et Techniques Nucléaires (INSTN-Madagascar), PO Box 4279, Antananarivo, Madagascar.

Abstract. Madagascar is among the big islands in the world with 5000 km border length. The increase of illicit trafficking at the border leads the Malagasy Government through INSTN-Madagascar, Custom Department and GasyNet Company to take an interest in the priority to monitor the borders, in spite of detection equipment lack. The technology using X- Rays is increasingly used for border control. GasyNet Company has introduced three types of high technologies detection equipments to avoid the illicit import and export of undeclared goods including radioactive materials. Two types of detection equipments has been used at boundary, they are the Heimann Cargo Vision-Mobile (HCV mobile and HCV-Portal), and one X- rays THSCAN detection scanner at the railway station. These X-Rays detection equipments are used for the control of container content at four ports and one railway station. Following this situation, the radiation protection plays a very important role to protect the workers and the public against the harmful effect of ionizing radiation [1]. This work has been done to optimize the radiation safety and to avoid unnecessary exposure to ionizing radiation from X-Ray scanners. The use of portable detectors to measure the leaks radiation and the respect of the three means of protection (time, distance and screen) is the most effective means to protect the Customs Officer in the use of X-Ray scanners. The results showed the existence of an adequate radiation protection program taking into account the dose assessment carried out around the workplace. All dose rates values measured in the controlled and supervised areas have not exceeded the regulatory limits for workers and the public [2].

KEYWORDS: X Rays, HCV-Mobile, HCV- portal and, THSCAN, leakage radiation.

1 INTRODUCTION

GasyNet Company has introduced three types of high technologies detection equipments to avoid the illicit import and export of undeclared goods including radioactive materials. Following this situation, the radiation protection plays a very important role to protect the workers and the public against the harmful effect of ionizing radiation [1]. This work has been done to optimize the radiation safety and to avoid unnecessary exposure to ionizing radiation from X-Ray scanners [3]. This work is the evaluation of leaks radiation on HCV-Mobile scanners, scanner THSCAN and HCV-Portal against the harmful effects of ionizing radiation.

2 MATERIALS AND METHODS

This work is to check the leakage radiation around the facility within the controlled area located outside. Madagascar has five types of X-ray scanner (three-HCV Mobile, HCV-Portal scanner at the border, and THSCAN scanner to the railway station). The description of X-ray scanners are the following:

2.1 scanners HCV-Mobile [5]

The scanners HCV-Mobile are mobile truck type, have tow brand (ATEGO 2528 Smith Heimann, AXOR 2533 Smiths Heimann) and serial number are Mobile 515, Mobile 542 and 850 553. The location of these trucks are secured by metal barriers. The HCV-Mobile scanner is characterized by a maximum energy various between 2, 5 MeV and 3, 8 MeV, penetrating a steel with a thickness of 270 mm, an inspection rate of 25 vehicles per hours, the scanning height 0,4 m to 4,65 m. This X-ray equipment can be used with a maximum power of 44 kilowatts.

* Presenting author, e-mail: tahirlangori@yahoo.fr

2.2 Scanner THSCAN

Another company NUTECH limited also provides X-Ray inspection equipment called THSCAN scanner, it is a mobile railway of THSCAN MB 1215 HS Relocatable vehicle inspection brand. The GasyNet Company holds in this possession a serial number of scanner -050050 TFND it installed in a concrete shed. The THSCAN scanner are characterized by a maximum energy of 6 MeV, penetrating a steel with a thickness of 300 mm, an inspection rate of 15 vehicles per hours, this scanner has a dimension of the tunnel width 3600 mm; height 4600 mm.

2.3 Scanner HCVP [6]

The HCVP X-Ray inspection system optimizes security checks at ports crossings by inspecting trucks, containers and vehicles for threats such as explosives, narcotics, weapons of mass destruction and contraband, as well as manifest verification; reducing the need for timely manual inspections. HCVP meets the most demanding security requirements that control has the energy level of the accelerator delivering 4 MeV to 6 MeV with serial number 2607, penetrating steel with a thickness of 300mm, and inspect up to 100 vehicles per hour.

3 MEASUREMENT

The study was performed in X-Ray units of five scanner containers of five cities, in Madagascar. The measurements were made in the sites within the controlled area located outside the scanners security zone. During the measurements session, we used the doses rate meters with gamma detection equipment Thermo FH 40 GL 10. Among the three HCV mobile scanners, we take only in consideration one HCV Mobile as the dose rate measurements, because the number of container inspection depend the number of container to be inspected. So, we cannot carry out the measurements for the two other scanners

The result of dose rate measurements in the area A, B, C, D, E, F, G, and H are shown in the table 1.

Table 1: Doses rate ($\mu\text{Sv.h}^{-1}$) around the sites outside the scanners security

Sites	HCV-Mobile ($\mu\text{Sv.h}^{-1}$)	THSCAN ($\mu\text{Sv.h}^{-1}$)	HCV-Portal ($\mu\text{Sv.h}^{-1}$)
A At the entrance of Truck	0,12	0,38	0,21
B At the exit of truck	0,18	0,38	0,18
C Opposite side of beam	0,28	0,18	0,13
D Beam direction	0,42	0,20	0,16
E Driver Cabin	0,13	-	4 Scan start 60 During the scan
F Image operator Cabin	0,09	0,10	0,05
G System operator cabin	0,09	0,10	0,06

The area measurement in the facility site is in the following images:

Figure 1: The facility site of HCV-Mobile and THSCAN scanners

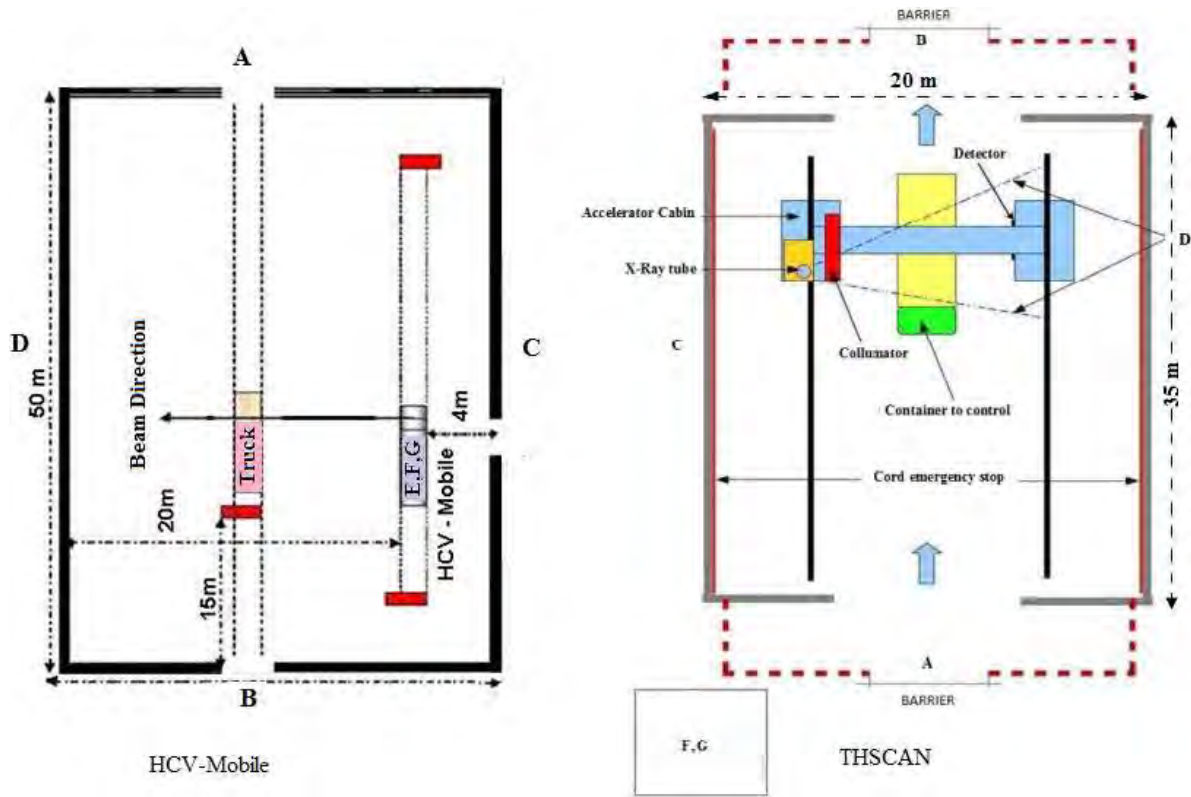
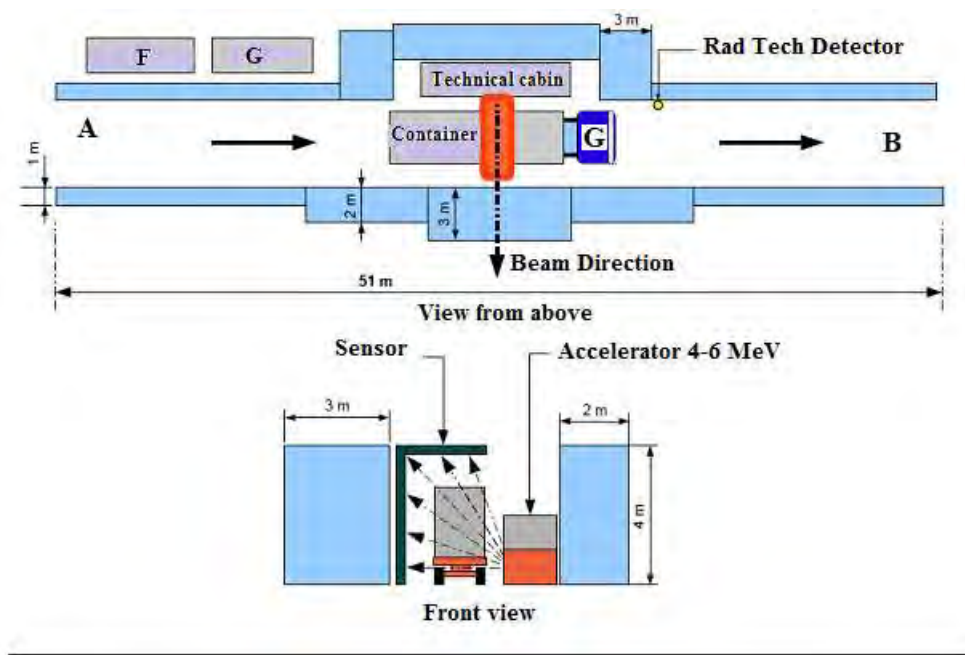


Figure 2: The facility site of HCV-P



4 DISCUSSIONS

4.1 Case of HCV M scanner

According to the above table, the dose rate value in the beam direction is more high than the value obtained at the entrance, at the exit of truck and at the opposite beam direction, because the radiation intensity is very high in spite of presence of the truck carrying the container.

The measured dose rate with container around the secured area (facility) or the controlled area respects the radiation protection standard, so the steel container can reduce the ionizing radiation. The measured dose rate does not depend on the volume of the container, but they depend only on the goods inside the container.

4.2 Case of THSCAN scanner

The dose rates values in the control room (F, G) are almost at the detection limit of dose rate meters ($<0.07 \text{ mSv. h}^{-1}$ and 0.2 mSv. h^{-1}) in comparison with the values at the entrance, at the exit of the truck, at the beam direction and the opposite side of the beam direction, these values are low because the barrier is made of concrete, which is an effective means to protect workers and the public against the harmful effects of ionizing radiation emitted by the scanner and the procedure of security facility respect the radiation protection standard.

4.3 Cases of HCV P scanner

The measured dose rates around the safety area are all below regulatory limits, except that in the cabin driver of the truck carrying the container, even at the start and during the scan because the radiation intensity arrived directly on the driver without protection, so the driver must wear TLD personal dosimeter and a lead apron. The safety facility area is delimited by concrete walls, providing sufficient protection for site workers and the public, the safety system of the installation is satisfactory. During the scan a container with radioactive materials inside, the message "DANGER" by the dose rate meter in the cabin was found and the four emergency lights and siren stop automatically the system. After several minutes, they take up and the pictures of the suspected goods are marked in yellow. This means that the scanner HCVP provided with a RAD CHECK detector detects the presence of radioactive materials within the container. This is not the case for the THSCAN and HCVM.

4.4 Commons case of three scanners

In the case of three scanners, the measurements have been performed by the passage of a truck container. All measured dose rates values in all places around the scanner is small compared to the prescribed standards for the safety system of the facility, the delimitation of areas has been well respected and safety procedures before the X-ray emission have been respected and applied by customs agents and GasyNet team.

5 CONCLUSIONS

This work aims to assess the radiation during the inspection of containers with the use of HCV M, HCV P and THSCAN X-Rays systems. The measurement of the dose rate has been done around these X-Ray inspection systems of containers and the secured area of the facility at the control containers containing goods, the assessment of the protection system against radiation was performed.

The values of dose rate are below the regulatory standard in radiation protection: So we can say that the protection of workers and members of the public around these three scanners is assured.

However, the radiation protection system for Gasynet Company should be reinforced following the ICRP recommendation and the ALARA principle [4], in particular the wearing of TLD personal dosimeters and use of portable dosimeter during investigation and inspection of goods.

Therefore, the safety of workers with industrial scanner is not ensured when the control and safety procedure and are not respected.

In radiation protection, the absolute requirement is to use gamma detection equipment to assess the exposure level received by workers.

6 REFERENCES

- [1] AGENCE INTERNATIONALE DE L'ENERGIE ATOMIQUE, « *collection sécurité* » N°115, AIEA Vienne1997.
- [2] AGENCE INTERNATIONALE DE L'ENERGIE ATOMIQUE « *Cours postuniversitaire de radioprotection Volume 2* », Collection cours de formation N°5, AIEA Vienne1995.
- [3] COURS REGIONAL SUPERIEUR DE FORMATION SUR LA SURETE RADIOLOGIQUE ET CONTROLE DES SOURCES DE RAYONNEMENT, « *les détecteurs*», Faculté des Sciences, Rabat-Maroc en 2006.
- [4] FORMATION SUPERIEURE REGIONALE EN RADIOPROTECTIO ET SURETE DES SOURCE DE RAYONNEMENT IONISANT « *Principe généraux et notions fondamentales* » 11 octobre 2010- 4 Mars 2011 au Rabat MAROC.
- [5] HCV-Mobile, www.smithsdetection.com
- [6] HCV-P, www.smithsdetection.com/locations

Occupational exposure in the transport of radioactive materials in Cuba

Zayda Haydeé Amador Balbona*, Miguel Antonio Soria Guevara

Centre of Isotopes, Ave. Monumental y carretera La Rada, Km 31/2, San José de Las Lajas, Mayabeque, Cuba.

Abstract. The Centre of Isotopes (CENTIS) is the main consignor and carrier of radioactive material in Cuba. The purpose of this paper is to assess the occupational exposure from the operations related with the transport of radioactive materials. Data belong to the period 1996-2015 are processed. The effective annual doses (E) and collective doses (S) distributions are analyzed. The equivalent doses to hands of the main driver and distributor have been controlled since 2009. ALARA principle is implemented and maintained for all activities. Type A packages with the CENTIS' products are designed taking into account international applicable regulations and using a qualitative method for reaching ALARA principle in the selection of the second containment. During all years with the exception of three cases, workers have not received E higher than 50 % of the dose constrain adopted (5 mSv y^{-1}). Also the average value of Hp(0.007) for 7 years is 1.2 mSv. It has not been reported any incident in about 3000 road shipments carried out. The segregation measures and the achievement of the international requirements for the design of our type A packages are the most effective ways to obtain the optimization of occupational exposure.

KEYWORDS: *Occupational exposure; radiation safety; transport of radioactive materials; type A package; design.*

1 INTRODUCTION

CENTIS is located about 30 Km to the southeast of Havana city. Up today, there are about eighteen years of experiences in the transport of radioactive materials. There is a prevalence of excepted and type A packages in about 250 shipping by year. A Radiation Protection Programme (RPP) was implemented to cover the functions of CENTIS like designer, manufacturer, consignor and carrier of radioactive packages. This is intended to establish and document in a systematic and structured way the framework of control applied to satisfy the radiation protection requirements and provisions established in the transport regulations [1-4]. The purpose of this paper is to show the behavior of the occupational exposure of the transport related worker and analyze this.

2 METHODS

The annual effective doses in 18y period covering 1996-2015 are measured using a credited individual dosimetry. Film dosimetry was used only for the five first years in this period. Since 2001 workers has been monitored with TLD and Hp(10) is an estimate of the effective dose (E) [5]. Dosimeters were issued on a thirdly or monthly basis and the recording levels considered were 0.20 and 0.10 mSv, respectively. The overall uncertainty reported is lower than 20 %. In order to take into account the distribution of the occupational exposure for transport related operations, mean effective doses, maximum and minimum values of E were calculated.

The collective effective dose (collective dose) was also determined, following the expressions mentioned in ICRP Publication 103 [6-7]. For the purposes of this work, monitored workers are people to whom a dosimeter was issued. It is analyzed the relation of annual average collective dose (average S) of these workers and S for the period of study.

*Presenting author, e-mail:zabalbona@centis.edu.cu

The equivalent dose to hands ($H_p(0.07)$) for the main driver and distributor are controlled with

TLD since 2009 by a requirement of the Cuban Regulatory Body.

3 RESULTS AND DISCUSSION

3.1 Dose Assessment and Optimization

The maximum and minimum values of E per year are shown in Table 1. Maximum dose is about 5.71 mSv and minimum dose is 0 mSv (dose lower than the minimum limit of detection). The first value was registered for a driver in 2003. He cannot explain us the cause of this behavior and during all of transport related operations this deviation does not present again. In this table also are presented the collective doses (S).

In the Figures 1 and 2 is showed its relation with the number of monitored workers (MW) and the maximum effective dose (E_{max}). The increase of personnel implies the same behavior of S, but reduces E. In spite of this, in 2003 the increment of effective doses contributed to the highest value of S (about 10 man-mSv⁻¹). It should be observed in the Figure1 that an appreciable reduction of individual exposures determines the decreasing of E after this year.

Figure 3 shows the annual averaged values of E. The highest values registered in 1998, 2000, 2002-2003, 2010 and 2012-2013 and 2015 are due to the increase of the number of packages with category III-YELLOW and TI in consignments. In the other hand, the annual effective dose constraint adopted for the practice is 5 mSv.

With the exception of one case, workers have not received a dose higher than 50% of this until 2014. In spite of this, in 2015 two workers (a driver and distributor) received an E more than 2.5 mSv (about 2.7 mSv).

The average value of $H_p(0.007)$ for the last seven years is 1.2 mSv and the maximum value for this dosimetric magnitude is 3.22 mSv.

Table 1: Maximum and minimum annual individual effective dose and collective dose for transport related workers.

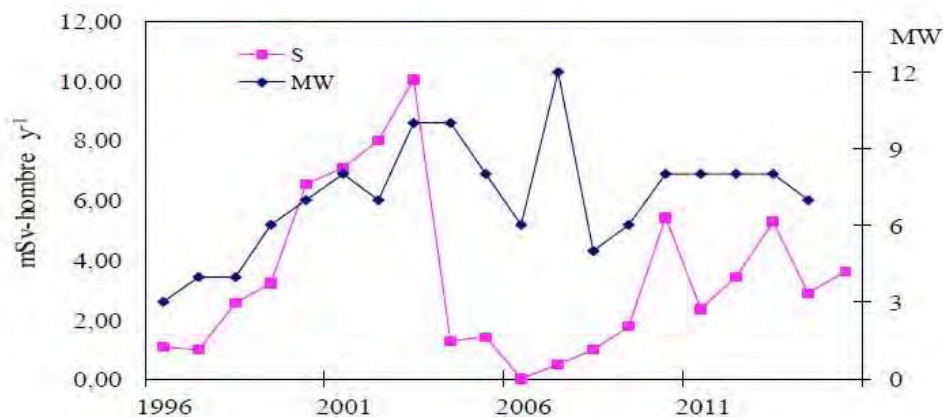
Year	E_{max} (mSv)	E_{min} (mSv)	S (man-mSv y ⁻¹)
1996	0.86	0	1.06
1997	0.55	0	0.97
1998	1.37	0	2.54
1999	1.06	0	3.2
2000	1.88	0.1	6.53
2001	1.57	0.24	7.05
2002	2.88	0	7.98
2003	5.71	0.11	10.06
2004	0.82	0	1.26
2005	0.49	0	1.42
2006	0	0	0
2007	0.28	0	0.48
2008	0.53	0.1	0.99
2009	1.04	0.26	1.76
2010	1.35	0.26	5.42
2011	0.88	0	2.32
2012	2.07	0	3.39
2013	2.76	0	5.27
2014	1.72	0	2.89
2015	2.71	0.13	3.61

You can see in the Table 2 the maximum and minimum values of Transport Index (TI) of received packages with ^{131}I and with ^{99}Mo , and their total activity by year. The highest registered TI is 7 and belongs to a package with ^{131}I that has been received in 1999. Nevertheless, there are packages with ^{99}Mo with the larger TI. Mean annual activities of ^{131}I and ^{99}Mo are 7.84 TBq and 47.3 TBq, respectively.

Maximum activities are registered in 2014 and 2012, respectively. The annual increase of activity of ^{131}I is presented in 1998, 2001, 2004, 2007 and 2009-2014. The beginning of the generator of Technetium production in 2003, determine the increase of transported activity of ^{99}Mo . Its annual variations since 2003 show the highest increase (44.2 TBq) in 2012.

The maximum TI of its radioactive package was registered in 2002. This radioisotope has been received in type B(U) and type A packages since 2008, but in the last two years only in B(U). As it is known, the use of the first type of package contributes to reduce the occupational exposure, but the increase of productions implies the same behavior of S, as it can see in Figure 1. The increase of individual exposures has determined the value of S in the last 2 years.

Figure 1: Collective dose (S) vs. number of monitored workers (MW) by year.



3.2 Segregation Measures

The dispatch staff segregates consignments when loading the packages on to the vehicle. This segregation is commensurate with the type and category of packages [8]. This means all packages, especially the high TI packages, are placed at the rear of the goods compartment. The storage area is about 10 m from an on-site workshop. The personnel of this workshop are regarded by CENTIS as members of the public.

There is a maximum of 2 h of exposure for these by week due to the stored packages. This represents an exposure of 100 h per year. Therefore, the maximum total TI number at this distance would be limited to 100, corresponding to an annual dose of 1 mSv. This is the maximum total TI anticipated for present operations. However, the concrete storeroom walls, which are 25 cm thick, provide a dose rate reduction factor of 100 [4], and therefore annual doses are anticipated to be of the order of 10 μSv .

3.3 Design and Test of CENTIS' Type A Packages

Components of type A packages of six manufacturers are studied and absolute frequencies of their use of are obtained. Considering [1-4] and ALARA principle, a qualitative method of optimization is applied to select the second containment system. The test methods for demonstrating their ability to withstand normal conditions of transport for liquid and solid contents [1-3] are carried out in the CENTIS' facilities.

Dose rate in contact and the TI for each package are calculated using the software Microshield Version 5.0.3 [9] for the date of dispatch. In these assessments are taking into account the radioactive decay; cylindrical source in contact with packaging; point source for 1m from this; materials of shielding; maximum activity by product for the date of manufacturing and reference distances for all external surfaces of package.

Table 3 presents the radiological issues for all designed packages. Their radioactive content determines these are 69 packages as a total. In the other hand, there has been necessary to change the packaging of the Technetium generators twice again due to changing its supplier and we need calculated their values of TI for these packages. Nevertheless for packages with others radionuclides was changed the twice barrier (cover with easy opening element). In the Figure 5 it is shown the package number A13 modified.

Figure 2: Collective dose (S) vs. maximum Effective Dose (Emax) by year.

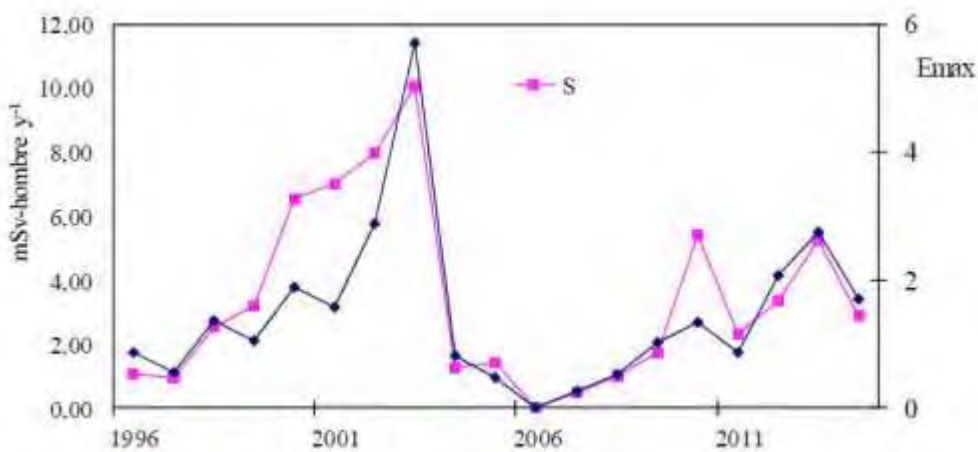


Figure 3: Mean effective doses for monitored workers.

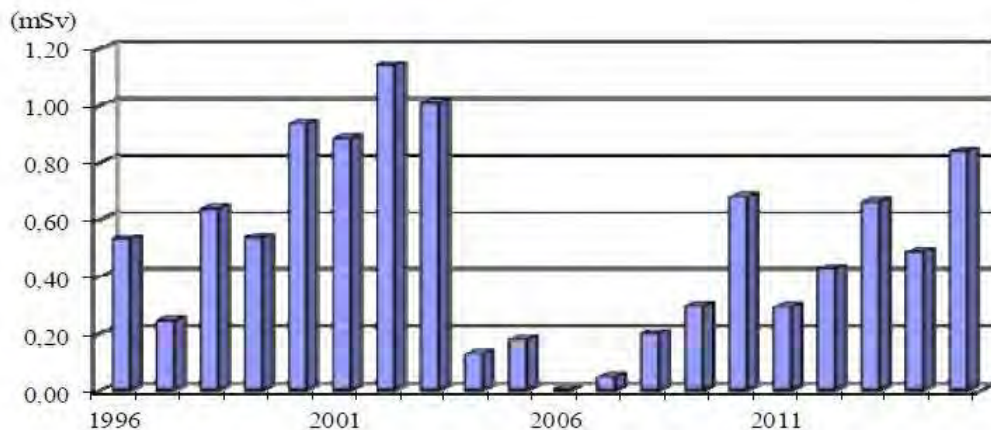
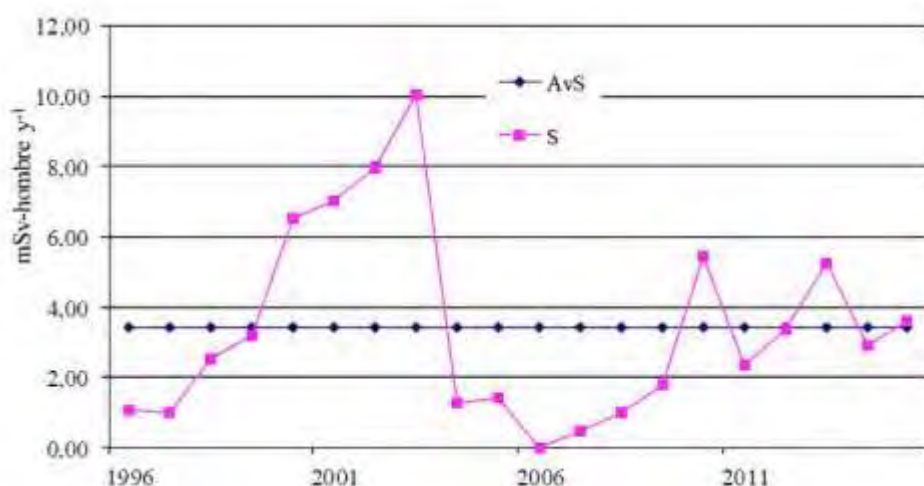


Figure 4: Annual collective dose (S) vs. average S for the studied period.**Table 2:** Maximum and minimum TI and total received activity by year of radioisotopes with larger contribution to E.

Year	Maximum TI ¹³¹ I	Minimum TI ¹³¹ I	Activity ¹³¹ I (Bq y ⁻¹)	Maximum TI ⁹⁹ Mo	Minimum TI ⁹⁹ Mo	Activity ⁹⁹ Mo (Bq y ⁻¹)
1996	--	--	--	2.5	--	3.20E+11
1997	1.7	0.5	7.33E+11	2.5	--	5.92E+11
1998	0.9	0.1	4.90E+12	2.5	1.3	5.39E+11
1999	7.0	0.4	4.87E+12	3.1	0.6	6.60E+11
2000	4.0	0.3	4.84E+12	3.1	0.6	5.35E+11
2001	1.0	0.2	4.88E+12	3.1	0.2	1.38E+12
2002	2.4	0.2	4.60E+12	4.1	1.9	1.59E+12
2003	2.9	0.6	3.94E+12	3.5	0.9	1.49E+13
2004	1.7	0.1	4.71E+12	3.3	0.2	2.73E+13
2005	1.4	0.1	4.08E+12	3.3	0.2	2.77E+13
2006	1.7	0.1	3.28E+12	3.6	1.5	2.29E+13
2007	1.3	0.1	4.91E+12	3.4	1.4	2.52E+13
2008	2.1	0.1	4.33E+12	3.4	0.1	2.32E+13
2009	2.9	0.1	5.76E+12	3.1	0.1	4.01E+13
2010	1.5	0.1	7.09E+12	3.0	1.6	3.19E+13
2011	3.0	0.1	1.05E+13	3.2	1.8	3.19E+13
2012	0.5	0.2	1.54E+13	3.1	0.4	4.42E+14
2013	0.5	0.2	1.86E+13	3.0	0.3	6.79E+13
2014	0.5	0.1	2.13E+13	0.6	0.2	6.77E+13
2015	0.5	0.1	2.02E+13	1.0	0.4	1.19E+14

Table 3: Issues of the designed radioactive packages at CENTIS.

Name of the packaging design	Radionuclide	Activity (Bq)	Category	Maximum TI
A01/A02, A06/ A07	^{131}I	1.85E+09	III	0.7
A01/A06	^{131}I	3.70E+09	III	0.9
		5.55E+09		1.4
		7.40E+09		1.8
		9.25E+09		2.4
		7.40E+07	II	0.2
		1.48E+08		0.5
A03/A08	^{131}I	2.22E+08		0.7
		2.96E+08		1
		3.70E+08		1.2
A10	^{131}I	7.40E+09	III	2.1
		3.70E+09	III	0.3
		5.55E+09		0.4
A12/A13	^{131}I	7.40E+09		0.5
		9.25E+09		0.7
		1.11E+10		0.9
		1.48E+10		1.2
Excepted	^{125}I	3.70E+05	---	---
Excepted	^{32}P	2.00E+07	---	---
A03/A08	^{32}P	3.70E+08	I	0
		7.40E+08		
A03/A08	^{90}Y	1.11E+09	I	0
A02/A07	^{188}Re	1.11E+09	II	0.2
GBTec02	$^{99}\text{Mo}/^{99m}\text{Tc}$	5.99E+09	II	0.3
		7.99E+09	III	0.4
		2.00E+10	III	1.1
		3.00E+10	III	1.6
		3.70E+10	III	2.1
		7.40E+10	III	3.3
MET01/ MET02	^{131}I	7.40E+08	III	1
A02/A07	^{131}I	7.40E+08	III	0.5
MET01/ MET02	^{32}P	7.40E+08	I	0
A03/A08	^{32}P	7.40E+08	I	0
MET01/ MET02	^{99m}Tc	7.40E+09	II	0
A05/A09	^{99m}Tc	7.40E+09	I	0
MET01/ MET02	^{188}Re	1.85E+09	III	1.3
A02/A07	^{188}Re	7.40E+09	III	1.1
MET01/ MET02	^{125}I	3.70E+08	II	0.5
A03/A08	^{125}I	3.70E+08	I	0

Figure 5: Modified package A13.

4 CONCLUSIONS

Analyzing data from radiological surveillance of workers of CENTIS for operations related with transport of radioactive materials we can appreciate during all years, with the exception of three cases, that they have not received E higher than 50% of the dose constrain adopted (5 mSv^{-1}). The equivalent doses to hands registered during last seven years are very low and smaller than 4 mSv.

In spite of the increasing activity and amount of radioactive packages and TI by expedition, there are no registered radiological occurrences.

The segregation measures and the achievement of the international applied requirements for the design of our type A packages are the most effective ways for reaching ALARA principle.

5 REFERENCES

- [1] Cuban Nuclear Regulatory Authority, Regulations for the Safe Transport of Radioactive Material, Resolution No. 121, Havana, (2000).
- [2] International Atomic Energy Agency, Regulations for the Safe Transport of Radioactive Material, Specific Safety Requirements, N° SSR-6, Vienna (2013).
- [3] International Atomic Energy Agency, Radiation Protection Programmes for the Transport of Radioactive Material, Safety Guide No. TS-G-1.3, Vienna, (2011).
- [4] International Atomic Energy Agency, Planning and Preparing for Emergency Response to Transport Accident Involving Radioactive Material, Safety Guide, No. TS-G-1.2 (ST-3), IAEA, Vienna, (2009).
- [5] Christensen, P., Julius, H. W. and Marshall, T. O., Technical recommendations for monitoring individuals occupationally exposed to external radiation. Radiation Protection 73, DG XI, EUR-14852 (Luxembourg: European Commission), (1994).
- [6] International Commission on Radiological Protection. Recommendations of the International Commission on Radiological Protection. Publication 103. Ann. ICRP 37 (1–332) Elsevier, (2007).
- [7] European Commission, Food and Agriculture Organization of the United Nations, International Atomic Energy Agency, International Labour Organization, OECD Nuclear Energy Agency, Pan American Health Organization, United Nations Environment Programme, World Health Organization, Radiation Protection and Safety of Radiation Sources: International Basic Safety Standards, General Safety Requirements, IAEA Safety Standards Series No. GSR Part 3, Vienna (2014).
- [8] Centre of Isotopes, Radiation Protection Department, Manual of Radiological Safety for Transport of Radioactive Material, DSR.DOC.012, Havana, (2015).
- [9] Afti Company, Grove Engineering, Microshield Version 5.0.3, (1998).

Safety Assessment for Incident-Free Pilot Transportation of Decontamination Radioactive Waste Resulting from the Fukushima Nuclear Power Plant Accident

Min Jun Kim, A Ra Go, Kwang Pyo Kim *

Department of Nuclear Engineering, Kyung Hee University, Gyeonggi-do, Republic of Korea

Recently, radioactive waste from remediation of contaminated soil caused by the Fukushima nuclear power plant accident was transported from temporary storage sites to an interim storage facility as pilot test. Transportation planning for the decontamination radioactive waste will be developed based on the pilot transportation experience. It is required to perform radiological safety assessment for the pilot transportation. The objective of this study was to assess radiation doses to the public and crew workers from the incident free pilot transportation. External dose rates around a transportation vehicle were calculated using MCNP code to confirm that the transportation satisfies the decontamination waste transfer guideline. Collective doses and maximally exposed individual dosed to the public and effective dosed to crew workers were calculated using RADTRAN. Two transportation routes, Asakawa-machi to Okuma-machi and Iwaki-shi to Okuma-machi were considered. Dose influencing factors, including decontamination waste properties, transportation route characteristics, and exposure conditions for each transportation route were collected and used for the dose assessments. Maximum radioactivity concentration in the decontamination waste was calculated to be 660 kBq/kg to satisfy the MOE guideline. The collective doses to the public per shipment were 1.8×10^{-3} person-mSv for the Asakawa route and 2.2×10^{-4} person-mSv for the Iwaki route. Maximally exposed individual doses to the public were 9.6×10^{-7} mSv for the Asakawa route and 2.7×10^{-5} mSv for the Iwaki route. Total effective doses to crew workers were 0.026 mSv for the Asakawa route assuming 5 shipments per worker and 1.07 mSv for the Iwaki route assuming 45 shipments per worker. The radiation dose levels to the public and workers evaluated in this study were much smaller than the annual dose limits of the general public and radiation workers. This study results can be used to develop transportation plan and guideline for decontamination waste transportation. In addition, the radiological safety assessment procedure can be used for emergency preparedness purpose.

KEYWORDS: *Fukushima nuclear power plant accident; radioactivity contamination in soil; decontamination waste; interim storage facility; transportation; safety assessment.*

1. INTRODUCTION

Radioactive materials were dispersed in the atmosphere and deposited onto the terrestrial environment following the Fukushima nuclear power plant (NPP) accident. Japan government has continued to remediate the contaminated areas. Remediation activities generated large volume of decontamination waste and they were estimated approximately 22 million m³ [1]. According to the decontamination plan formulated by the Ministry of the Environment (MOE) of Japan, decontamination waste generated from remediation in Fukushima Prefecture have been stored at temporary storage sites (TSS) [2]. Within the Special Decontamination Area (SDA) where Japan government has the responsibility of formulating and effecting remediation plans, approximately 4.6 million m³ of decontamination waste has been stored in about 250 TSS [3].

In September 2014, the governor of Fukushima accepted construction of interim storage facilities (ISF) in Okuma-machi and Futaba-machi to ensure safety and provide complete control over the decontamination waste until a disposal site would be available [1]. Since March 2015, pilot transportation of decontamination waste from TSS to a ISF had been implemented for about one year in order to confirm safe and secure transportation [1, 4]. By the pilot transportation, approximately 45,000 m³ of decontamination waste was transported from 43 TSS during the period [5]. MOE is preparing for future transportations through implementation and review of the pilot transportation.

Radiological safety assessments for radioactive material transportation have been reported in literature. The US Department of Energy (DOE) developed safety assessment tools such as RADTRAN and

* Presenting author, e-mail: kpkim@khu.ac.kr

RISKIND [6]. Vieru study evaluated safety and risk for transportation of radioactive materials [7]. Weiner assessed radiological risk resulting from transportation of low level radioactive waste (LLW) and natural occurring radioactive material (NORM) under incident-free condition [8]. Argonne National Laboratory (ANL) reported transportation impact assessment for shipment of uranium hexafluoride (UF_6) cylinders [9]. MOE assessed radiation dose to the public from a decontamination waste transportation [10].

For the radiological safety assessment of decontamination waste transportation, it is required to assess radiation doses to the public and workers. A radiological safety assessment for the transportation was performed by Japan MOE [10]. However it was preliminary evaluation for transportation planning. Therefore, MOE suggested that radiation dose assessment to pedestrians and workers should be performed during the decontamination waste transportation. The objective of the present study was to assess radiological safety for the transportation of decontamination waste resulting from the Fukushima NPP accident. We calculated radiation doses to the public and crew workers due to the pilot transportation of the waste. External dose rates around a transportation vehicle were evaluated using a radiation transport code. Radiation doses to the public and workers were calculated using a safety assessment tool for radioactive waste transportation. This study was limited to incident-free transportation.

2. MATERIALS AND METHODS

2.1 Evaluation of external dose rates around a transportation vehicle

According to the decontamination waste transfer guideline by MOE, the maximum external dose rate should not exceed 100 μ Sv/h at 1 m from the back and sides of the vehicle and 20 μ Sv/h at 1 m from the front side of the vehicle. External dose rates around a transportation vehicle were evaluated to confirm that the transportation satisfies the MOE guideline. The radiation dose rates were evaluated by changing radioactivity concentration in decontamination waste from 3 kBq/kg to 1,000 kBq/kg.

Input parameters for the dose rate evaluation were collected by literature review and used for the evaluation. Decontamination waste made up more than 75% of contaminated soil [12]. Therefore, decontamination waste was assumed to be contaminated soil. Mass density and elemental compositions of the contaminated soil were referred to soil type 1 in International Commission on Radiation Units and measurement (ICRU) publication 53 [13]. The soil properties for radiation dose assessment are summarized in Table 1. In most cases, waterproof sandbag or flexible container was used for package of decontamination waste in TSS. Diameters and heights of the sandbag and container were about 1.1 m (Figure 1-a). The sandbag or container was used to prevent dispersion, outflow, and leakage of the waste and thus having no radiation shielding effect [11]. The ratio of radioactivity concentrations between ^{134}Cs and ^{137}Cs in decontamination waste was assumed 1 to 3 by considering decay time after the Fukushima NPP accident. Transportation vehicle was assumed 10 ton truck which can load 7 decontamination waste packages (Figures 1-b and 1-c).

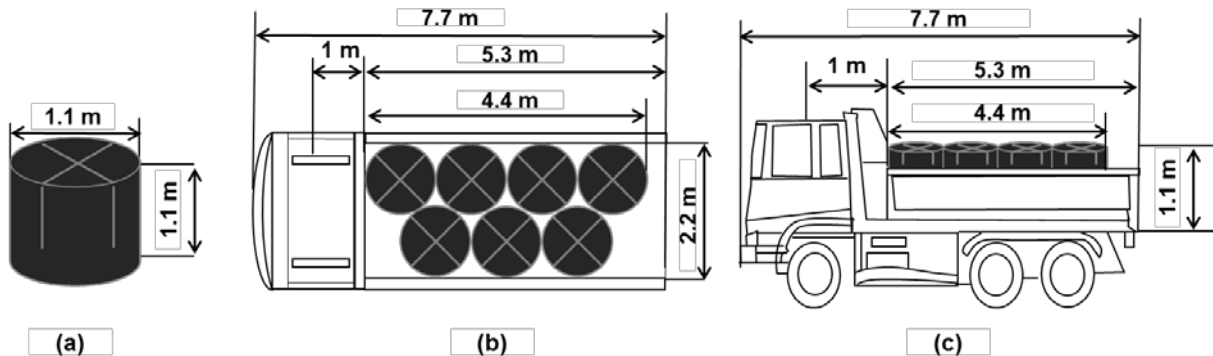
Table 1: Soil properties for radiation dose assessment to the public and crew workers.

Property		Value
Density (g/cm^3)		2.0
	H	2.20
	O	57.5
Elemental Composition (%)	Al	8.5
	Si	26.2
	Fe	5.60

External dose rate was calculated using Monte Carlo N-Particle (MCNP) code by simulating the contaminated soil and exposure condition. The external dose rates were calculated at side and front positions of a transportation vehicle, 1 m from the vehicle surface at the center line position of side

surface (P-1) and at the center line position of front surface (P-2). Dose conversion coefficients in International Commission on Radiological Protection (ICRP) publication 74 were used for dose calculation [14].

Figure 1: Geometrical dimensions of decontamination waste packages and transportation vehicle.



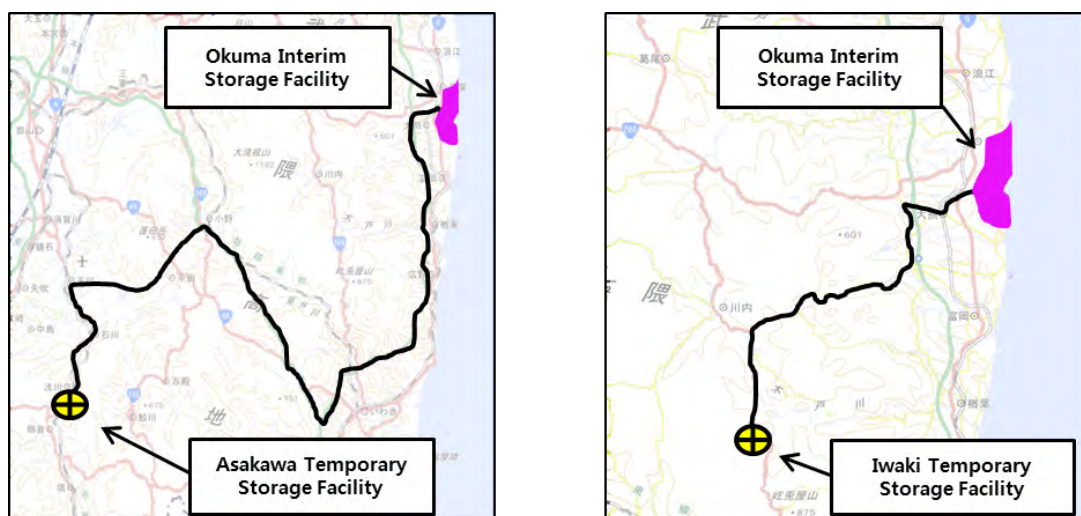
2.2 Assessment of radiation dose to the public and workers

Radiation dose to the public and crew workers were assessed. For the public exposure, collective doses and maximally exposed individual doses were calculated. For worker exposure, effective dose for each link and route was calculated. In addition, cumulative dose for each route was calculated considering multiple transportations. RADTRAN 6.0 code was used to calculate the radiation doses from incident free transportation. Radiation dose resulting from the waste transportation depended on transportation route characteristics and exposure conditions. Therefore, such data were collected and used for the dose assessment.

Transportation route characteristics

Two transportation routes, Asakawa-machi to Okuma-machi and Iwaki-shi to Okuma-machi were considered (Figure 3). Each route was subdivided into 3 links by road type or region. Asakawa route was subdivided into Asakawa TSS - Tamakawa IC (link 1), Tamakawa IC - Tomioka IC (link 2), and Tomioka IC - Okuma ISF (link 3) by road type. Iwaki route was subdivided into Iwaki TSS - Kawauchi cho (link 4), Kawauchi cho - Nogami cho (link 5), and Nogami cho - Okuma ISF (link 6) by region.

Figure 3: Transportation routes for decontamination waste: Asakawa-Okuma route (left) and Iwaki-Okuma route (right).



Road type and route length information were abstracted from Ministry of Land, Infrastructure, Transport and Tourism (MLIT). Road type of link 2 was freeway and road type of the others was non-freeway. Population density and vehicle density for each link were abstracted from Statistics Bureau in Ministry of Internal Affairs and Communication (MIC) and traffic information from Fukushima Prefecture. The volumes of decontamination waste transported through Asakawa and Iwaki routes were about 100 m³ and 1,000 m³, respectively [15, 16]. Numbers of shipments were 15 for Asakawa route and 143 for Iwaki route. Average numbers of shipments per worker were 5 for Asakawa route and 45 for Iwaki route.

Table 2. Transportation route information, which influence radiation doses to the public and crew workers.

Route	Link	Detail route	Road Type	Route length (km)	Vehicle density (vehicle/hr)	Population density (person/km ²)	Number of shipments (Average per worker)
Asakawa - Okuma	Link 1	Askawa TSS - Tamkawa IC	Non-Freeway	21.2	758	181.8	15 (5 per worker)
	Link 2	Tamakawa IC - Tomioka IC	Freeway	108.0	72.5	93.8	
	Link 3	Tomioka IC - Okuma ISF	Non-Freeway	36.7	- ^(a)	- ^(a)	
Iwaki - Okuma	Link 4	Iwaki TSS - Kawauchi cho	Non-Freeway	16.4	47.5	106.4	143 (45 per worker)
	Link 5	Kawauchi cho - Nogami cho	Non-Freeway	20.4	40.3	13.9	
	Link 6	Nogami cho - Okuma ISF	Non-Freeway	10.0	- ^(a)	- ^(a)	

^(a) Areas where it is anticipated that residents will not be able to return for a long time

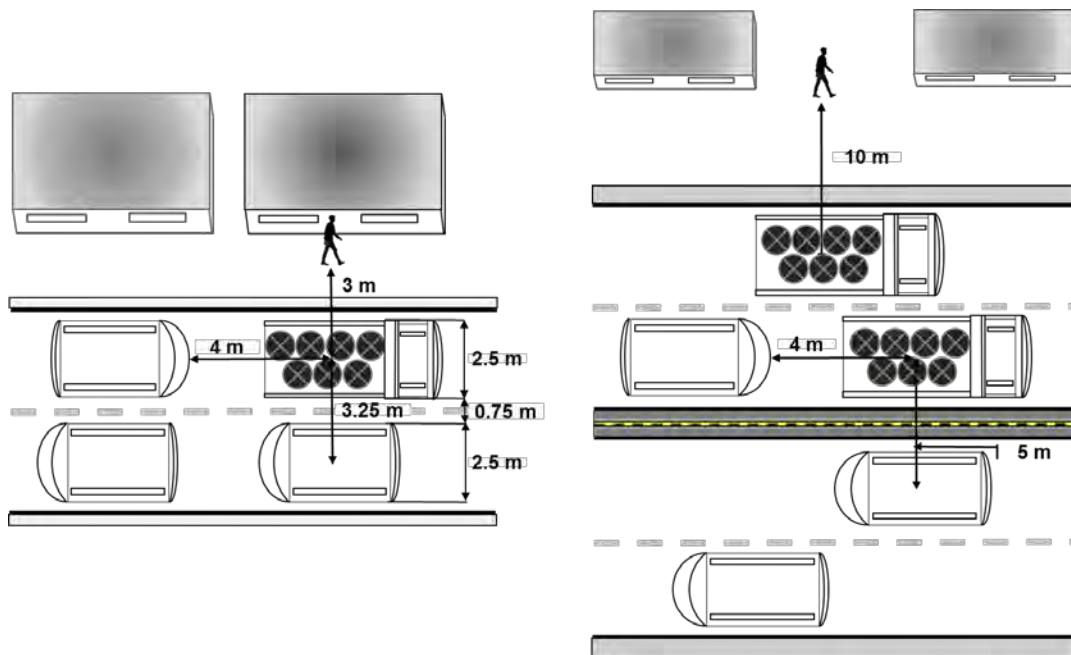
Assessment of radiation doses to the public and workers

The public members around the transportation routes were subdivided into whom along the route (off-link) and sharing the route (on-link). Off-link population were all persons living or working each side of the transportation route. On-link population were persons in all vehicles sharing the transportation routes and this group included persons traveling in the same or opposite directions as the shipment, as well as persons in vehicles passing the shipment. Ratio of pedestrians to residential population in off-link was assumed to be 1 to 3. The shielding factor was set as 0.4 considering wooden house in Japan.

Figure 2 shows exposure condition for the public during transportation on non-freeway and freeway. Exposure conditions for non-freeway and freeway were assumed based on H22 road information [12]. For non-freeway, it was assumed that minimum distance between side surface of vehicle and residents along the street was 3 m. In addition, minimum distance between vehicles travelled in the same direction was 4 m and minimum distance between vehicles travelled in the opposite direction was 3.25 m. For freeway, minimum distance between side surface of vehicle and residents along the street was 10 m considering the shoulder and width of street. In addition, minimum distance between vehicles travelled in the same direction was 4 m and minimum distance between vehicles travelled in the opposite direction was 5 m considering a median strip and width of road. Average speeds of vehicle in non-freeway and freeway were assumed to be 30 km/h and 70 km/h, respectively.

Radiation doses to crew workers were assessed. It was assumed that the crew worked alone and didn't work in shift. Exposure condition of the crew workers was the same with the public exposure condition mentioned previously. Radiation dose per one shipment was evaluated by link and route. In addition, the cumulative dose for each route was calculated by considering average number of shipments per crew worker.

Figure 2: Exposure conditions for the public during transportation on non-freeway (left) and freeway (right).



3. RESULTS AND DISCUSSION

3.1 Radiation dose rates around a transportation vehicle

Table 3 shows external dose rates at 1 m distance from transportation vehicle surface. Assuming 3 kBq/kg of waste radioactivity concentration in waste, dose rates were 0.17 $\mu\text{Sv/h}$ at the center line position of side surface and 0.09 $\mu\text{Sv/h}$ at the center line position of front surface. Increasing the radioactivity concentrations in the decontamination waste up to 1000 kBq/kg, the dose rates increased up to 56 $\mu\text{Sv/h}$ at the side position and 29 $\mu\text{Sv/h}$ at the front position. The study results were about 37-60% lower than MOE's preliminary results [10]. MOE assumed that the vehicle container was fully filled with decontamination waste, and thus overestimating radiation source and resulting radiation doses. In reality, seven decontamination waste packages were loaded on a vehicle for the transportation. This study evaluated dose rates from the vehicle with 7 waste packages to simulate realistic condition (Figures 1 and 2).

Table 3: External dose rate around a transportation vehicle by radioactivity concentration in decontamination waste.

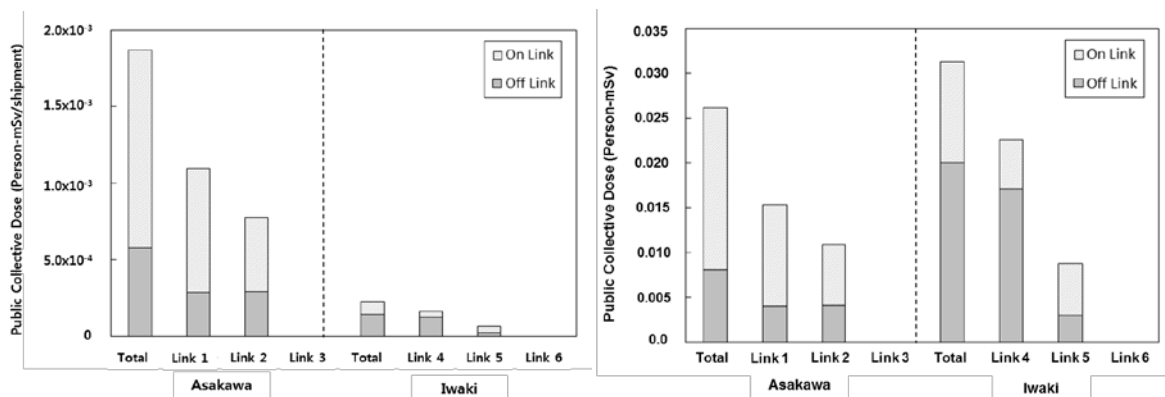
Radioactivity concentration in decontamination waste (kBq/kg)	External dose rate ($\mu\text{Sv/h}$)			
	P-1 (Side position)		P-2 (Front position)	
	This study	MOE	This study	MOE
3	0.17	0.27	0.09	0.20
8	0.45	0.72	0.23	0.53
30	1.7	2.7	0.87	2.0
150	8.3	13	4.4	10
500	28	44	15	33
1,000	56	89	29	66

Maximum radioactivity concentration in the decontamination waste was estimated to be about 660 kBq/kg to satisfy the MOE guideline (less than 100 $\mu\text{Sv/h}$ at the back and sides and 20 $\mu\text{Sv/h}$ at front side of the vehicle). For the radioactivity concentration, dose rates were 37 $\mu\text{Sv/h}$ at the side position and 20 $\mu\text{Sv/h}$ at the front position. No radiation shielding effect was considered for the dose rate calculation. Special transportation container with proper radiation shielding may need to be developed and used to transport decontamination waste concentrated more than the maximum concentration value above.

3.2 Radiation doses to the public

Figure 4 shows collective dose to the public from incident free transportation. The collective dose per shipment was the highest for link 1 (1.1×10^{-3} person-mSv per shipment). The difference in collective dose could be attributed to transportation time (determined by route length and vehicle speed), population density, and road type. Transportation time of link 2 was 2.2 times higher than link 1 by route length and road type. However, population density of link 1 was 2 times higher than link 2 and the distance between road and residents along the street of link 1 (non-freeway) was closer than link 2 (freeway). Therefore collective dose for link 1 was the highest for the Asakawa route. Although route length and vehicle density of link 4 was similar to link 5, population density of link 4 was 10 times higher than link 5. Therefore, collective dose for link 4 was the highest for the Iwaki route. For links 3 and 6, it was assumed that residents would not be able to return for a long time. Therefore, collective doses for the links were not calculated. The collective doses per shipment were 1.8×10^{-3} person-mSv for the Asakawa route and 2.2×10^{-4} person-mSv for the Iwaki route.

Figure 4: Collective doses to the public resulting from incident free transportation: Radiation doses per shipment (left) and cumulative doses from multiple transportations (right). For the cumulative dose calculations, total number of shipments for each route was considered.



Collective doses for off-link population in the Asakawa route were 4.0×10^{-3} person-mSv (26%) in link 1 and 4.0×10^{-3} person-mSv (38%) in link 2. In case of the Iwaki route, collective doses for off-link population were 1.7×10^{-2} person-mSv (76%) in link 4 and 2.9×10^{-3} person-mSv (34%) in link 5. Collective dose for off-link depended on transportation time, population density, and exposure condition of off-link population. Link 4 occupied the highest proportion of collective dose for off-link because population density relative to vehicle density was much higher than the other links.

The cumulative dose varied depending on number of shipments as well as radiation dose per shipment. The cumulative doses were calculated by considering total number of shipments for each route, 15 times for the Asakawa route and 143 times for the Iwaki route. The cumulative dose was higher for the Iwaki route due to the larger number of shipments. The cumulative doses were 0.026 mSv for the Asakawa route and 0.031 mSv for the Iwaki route.

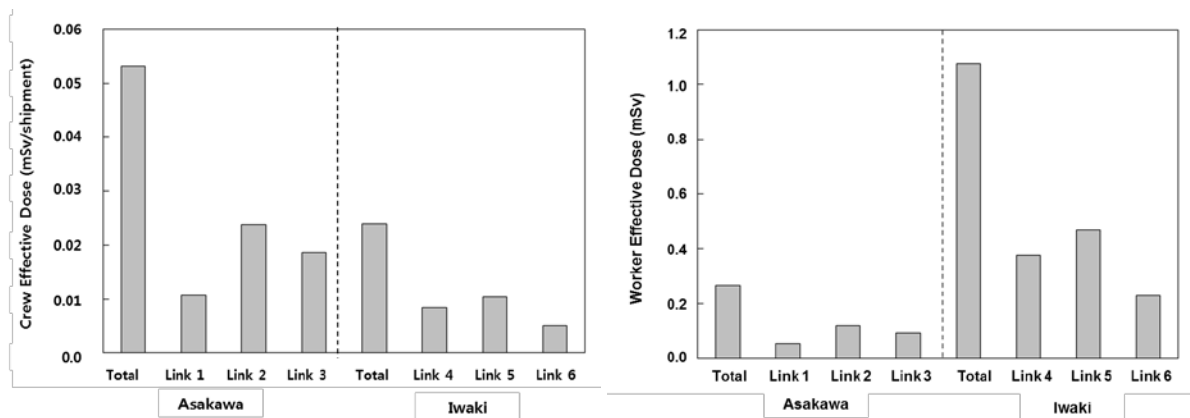
Maximally exposed individual doses to the public were 9.6×10^{-7} mSv and 2.7×10^{-5} mSv at 3 m distance from the vehicle for the Asakawa route and the Iwaki route, respectively. The dose levels were much smaller than the annual dose limit of the general public.

3.3 Radiation doses to the crew workers

Figure 5 shows effective dose to crew workers from incident free transportation. Radiation doses to crew workers per shipment were the highest for link 2 (0.024 mSv per shipment) and the lowest for link 6 (0.005 mSv per shipment). The difference in effective doses to workers could be attributed to route length and vehicle speed, and therefore transportation time. Transportation time of link 2 was about 1.5 hours which was the longest time for the Asakawa route. In case of the Iwaki route, transportation time of link 5 was about 0.7 hour which was the longest time for the route. Radiation doses per shipment were 0.053 mSv for the Asakawa route and 0.024 mSv for Iwaki route.

The cumulative doses were calculated by considering average number of shipments for each route. Total effective doses were 0.026 mSv and 1.07 mSv for the Asakawa route and the Iwaki route, respectively. The dose levels were much smaller than the annual dose limit of radiation workers.

Figure 5: Effective dose to crew workers resulting from incident free transportation: Radiation dose per shipment (left) and cumulative dose from multiple transportations (right). For the cumulative dose calculations, average number of shipments per crew worker was considered for each route.



4. CONCLUSION

Radiological safety assessment for pilot transportation of decontamination waste caused by the Fukushima NPP accident was performed. Radiation doses to the public and crew workers resulting from the transportation were assessed by transportation route. Decontamination waste properties, transportation route characteristics, and exposure conditions for each route were considered for the dose assessment.

External dose rates around a transportation vehicle were proportional to radioactivity concentrations in decontamination waste. Assuming 660 kBq/kg of radioactivity concentration in waste, the external dose rates were 37 μ Sv/h at the side position and 20 μ Sv/h at the front position. The collective doses to the public per shipment were 1.8×10^{-3} person-mSv for the Asakawa route and 2.2×10^{-4} person-mSv for the Iwaki route. Maximally exposed individual doses to the public were 9.6×10^{-7} mSv for the Asakawa route and 2.7×10^{-5} mSv for the Iwaki route. Total effective doses to crew workers were 0.026 mSv for the Asakawa route and 1.07 mSv for the Iwaki route.

Maximum radioactivity concentration in the decontamination waste without shielding effect of the waste package was 660 kBq/kg to satisfy the MOE guideline. Special transportation container with proper radiation shielding may need to be developed and used to transport the waste concentrated more than maximum value. The dose levels to the public and workers were evaluated much smaller than the annual dose limits of the general public and radiation workers. Therefore, it can be concluded that radiological safety was acquired for this incident-free transportation. Further study for radiological safety assessment is necessary by considering potential incidents during waste

transportation. This study results can be used to develop transportation plan and guideline for decontamination waste transportation. In addition, the safety assessment procedure can be used for emergency preparedness purpose.

5. ACKNOWLEDGEMENTS

This study is supported by Grant 20141510101630 from the Energy Technology Development Project of Korea.

6. REFERENCES

- [1] MOE. (2016). Progress on Off-site Cleanup and Interim Storage in Japan. Retrieved 2016-05-02 from: http://josen.env.go.jp/en/pdf/progressseet_progress_on_cleanup_efforts.pdf.
- [2] MOE. (2011). Basic Principles of the Act on Special Measure Concerning the handling of Environment Pollution by Radioactive Materials Discharged from the Nuclear Power Station Accident Associated with the Tohoku District-Off the Pacific Ocean Earthquake that Occurred on March 11, 2011.
- [3] MOE. (2016). Storage Status of Removed Soil in temporary storage sites within Special Decontamination Area. Retrieved 2016-04-22 from: http://josen.env.go.jp/area/provisional_yard/number.html.
- [4] MOE, 2014. Basic plan for transportation of removed soil to interim storage facility (in Japanese).
- [5] MOE. (2016). Status of Pilot Transportation in H27. Retrieved 2016-02-01 from: <http://josen.env.go.jp/chukanchozou/situation/h27>.
- [6] DOE, 2002. A Resource Handbook on DOE Transportation Risk Assessment. DOE/EM/NTP/HB-01. New Mexico.
- [7] Vieru, G. 2014. The Safety of Transport of Radioactive Materials in Romania, RAMTRANS, London. 14(1), pp. 15-27.
- [8] Weiner, R.F., 1998. Incremental Risks of Transporting NARM to the LLW Disposal Facility at Hanford. Sandia National Laboratories. New Mexico.
- [9] ANL, 2001. Transportation Impact Assessment for Shipment of Uranium Hexafluoride Cylinders from the East Tennessee Technology Park to the Portsmouth and Paducah Gaseous Diffusion Plants. ANL/EAD/TM-112. Illinois.
- [10] MOE, 2015. Implementation plan for transportation of removed soil to interim storage facility in H26~H27 (in Japanese).
- [11] MOE, 2013. Decontamination Guidelines 2nd Edition; Guidelines Pertaining to the Collection and Transfer of the Removed Soil. Part 3.
- [12] MOE. (2015). Storage Status of Removed Soil within Intensive Contamination Survey Area. Retrieved 2015-12-01 from: http://josen.env.go.jp/en/pdf/progressseet_progress_on_cleanup_efforts.pdf.
- [13] ICRU, 1994. Gamma-Ray Spectrometry in the Environment. ICRU Publication 53.
- [14] ICRP, 1996. Conversion Coefficients for use in Radiological Protection against External Radiation. Ann. ICRP 26(3-4).
- [15] MOE. (2015). Planning for transportation of contaminated soil from Asakawa-machi. Retrieved 2015-09-10 from: http://josen.env.go.jp/chukanchozou/pdf/moving_soil_plan_asakawa_each.pdf.
- [16] MOE. (2015). Planning for transportation of contaminated soil from Iwaki-shi. Retrieved 2015-09-10 from: http://josen.env.go.jp/chukanchozou/pdf/moving_soil_plan_iwaki_each.pdf.

Operation of Radiation Source Location Tracking System

BokHyoung Lee, CheolHong Um, KiWon Jang, DaeHyung Cho

Korea Institute of Nuclear Safety, Daejeon, Republic of Korea

Abstract. To strengthen the security management of sealed radiation source, South Korea has been operating Radiation Source Location Tracking System (RADLOT) since 2006. The main purpose of the system operation is to monitor locations and using status of mobile sealed sources which have higher possibilities of missing and over exposure incidents or accidents and to response earlier on those caseworks. The system had been developed and installed during 2004 and 2005. It has started with about 1,000 mobile terminals to monitor locations of industrial radiography irradiators with some limitations on system application and circumstance. Korea Institute of Nuclear Safety (KINS) has upgraded shapes and performances of mobile terminals and the central control system. Still there are tasks to be improved, such as connection to regulatory, performance, etc. In this paper, there will be a looking back on last 10 years system operation including errors and improvements were made, and a sharing of some idea on expectations and suggestions for the radiation source security. In addition, the status of ROK-VIETNAM-IAEA PILOT PROJECT REGARDING ESTABLISHMENT OF RADLOT SYSTEM IN VIETNAM will be shared.

Designing a Physical Protection System for the 444 TBq Co-60 Irradiation Facility at the Centre for Applied Radiation Science and Technology, Mafikeng, South Africa

Cyrus Cyril Arwui^{a,b}, Victor Tshivhase^a

^aNorth-West University, Mafikeng Campus, Mafikeng, North-West Province, South Africa

^bGhana Atomic Energy Commission, Accra, Greater Accra Region, Ghana

Abstract. This study designed a physical protection system (PPS) for the ⁶⁰Co irradiation facility at the Centre for Applied Radiation Science and Technology of the North-West University (Mafikeng Campus), South Africa. The design of the PPS also covered the whole Centre as a whole in terms of security. The designed PPS was analysed and evaluated quantitatively by the use of Estimate Adversary Sequence Interruption (EASI) code for effectiveness of the PPS. These evaluation was done to calculate the Probability of interruption (PI) of a potential adversary attack scenario along a specific path since EASI can only consider a pathway at a time. Due to the limitation of the EASI code which can only consider a pathway at a time, a new code is in the developmental stages to evaluate the PPS for multiple pathways. PI values shows the extent to which the security system is effective. Results obtained from this study using the EASI code indicated low values of PI for the existing protection system and high values of PI for the upgraded protection system that was designed. The values of PI increased from 0 to a range of 0.46 (46%) to 0.78 (78%) which strengthens the overall security.

IAEA Approach to Cradle to Grave Control and Management of Disused Sealed Radioactive Sources

Monika Kinker, Gerard Bruno, Hilare Mansoux

International Atomic Energy Agency, Vienna, Austria

Abstract. Radioactive sources are used throughout the world, and they bring many benefits and advantages to humankind. Yet radioactive sources may pose potentially harmful threats to people and the environment if under poor control and poor management. Once sealed sources become disused (e.g. once they cannot accomplish their intended purpose due to radioactive decay) and if they are not then managed safely and securely, they may leak, become abandoned or lost, or stolen or misused by unauthorized persons, potentially causing radiation incidents or accidents. A comprehensive and holistic approach to the cradle to grave management of radioactive sources is needed in order to protect the public and the environment from potential ionizing radiation hazards associated with sources. The IAEA defines a 'disused source' as "a radioactive source that is no longer used, and is not intended to be used, for the practice for which an authorization has been granted". Best practice and IAEA guidance indicates that users should identify appropriate routes for the management and disposal of disused sealed radioactive sources (DSRS) before they acquire and use radioactive sources. For low level and short-lived DSRS, the use of a near surface disposal option may be possible. However, high activity and long-lived sources, even after reaching the end of their useful life may need to be disposed of in geological disposal facilities when recycling or export options do not exist. For those countries without the competence or human or financial resources to develop mined geological facilities, a valid option to dispose of relatively small amounts of DSRS declared as waste in a cost effective manner could be disposal in specially engineered boreholes whose safety has to be demonstrated. The International Atomic Energy Agency (IAEA) fosters international cooperation between countries and encourages the development of a harmonized "cradle to grave" approach to managing sources consistent with international legal instruments, IAEA safety standards, and international good practices. This "cradle to grave" approach, which is set out in this presentation, requires the development of a national policy and implementing strategy, an adequate legal and regulatory framework, and adequate resources and infrastructure that cover the entire lifecycle, from production and use of radioactive sources to disposal. Regulatory framework, and adequate resources and infrastructure that cover the entire lifecycle, from production and use of radioactive sources to disposal.

Safety Case of The Libyan Central Radioactive Waste Storage Facility

Husam Shames, Usama Elghawi

Libyan Atomic Energy Establishment, Tripoli, Libya

Abstract. A valuable amount of Disused Sealed Radioactive Sources (DSRS) and Orphan Sources are wide spread throughout Libya and needed to be categorized, collected, transported, conditioned and stored. The potential awful effects of DSRS and Orphan Sources on human health and the environment in the country made the need for a National Storage facility of Radioactive Waste (RW) a vital issue. The only Radioactive Waste Management (RWM) facility in Libya is a repository belongs to Tajura Nuclear Research Centre (TNRC). This facility used to receive RW resulting from the operation of the reactor and from the production of radioisotopes, pharmaceuticals and other RW in the centre. Currently, It is also used for the temporarily storage of DSRS and Orphan Sources coming from outside the centre. This facility does not fit with the Libyan policy and strategy for RWM, furthermore, wasn't designed to host DSRS and Orphan Sources. The Libyan Atomic Energy Establishment (LAEE) is the authorized body to deal with the aspects related to the use of peaceful application of nuclear energy in Libya. Regarding LAEE efforts to improve RWM system in Libya; a draft for a Libyan Nuclear Law has been prepared, a Radioactive Waste Management Division has been created, Policy and Strategy of RWM has been developed, a national project of Orphan Sources Management and a project of Central Radioactive Waste Storage Facility has been launched. Although, The current stage of the storage facility project is the design phase, safety case with safety assessment for the facility has been developed. The objective of The safety case is to insure the fulfilling of the regulatory requirements and the satisfaction of the public and the decision makers, moreover, to clearly address the real protection level of the facility during its design, operation, shutdown and decommissioning. These goals cannot be achieved without reporting in full details all the safety aspects of the facility including supporting safety assessment. The aim of the safety assessment is investigating and measuring the radiological impact of the facility on the human health and the environment. This paper will address recent developments has been done on RWM system in Libya regarding DSRS and Orphan Sources, after that, will introduce the project of the Libyan Central Radioactive Waste Storage Facility and summarize its safety case.

Safety and Radiation Protection Requirements for Cargo and Containers Inspection Services in Brazil

Josilto Aquino^a, Alfredo Ferreira Filho^b, Marcello Nicola^a

^aNational Nuclear Energy Commission (CNEN), Rio de Janeiro, Brazil

^bInstituto de Radioproteção e Dosimetria (IRD), Rio de Janeiro, Brazil

Abstract. This paper deals with the safety requirements and radiation protection required for the operation of inspection facilities and cargo containers in Brazil. It includes administrative requirements, authorization to operate, notifications, responsibilities, operators training, individual monitoring, radiation protection equipment, ionizing radiation generating equipment, conduct of operations, monitoring of areas, emergency and physical protection program.

Radiation Protection in Radioactive Material Transport

Li Guoqiang, Zhuang Dajie, Wang Xuexin, Sun Hongchao, Wang Renze, Zhang Jiangang

China Institute for Radiation Protection, Taiyuan, Shan'xi, China

Abstract. Regulation requirements on radiation protection in radioactive material transport are introduced in China. Code for estimate radiation consequence for both workers and public during transport normal conditions and accident conditions is introduced in this paper also. Radiation level of several kinds material and impact to workers and public during transport are concluded.

Practical Application Illustrating Excellence in the Safety and Security of Industrial Radiography Sources Employed at the Eskom, Generation Power Stations

Marc Maree

Eskom, Cape Town/Western cape, South Africa

Abstract. Eskom Holdings SOC Ltd (Eskom) generates 95% of the electricity in South Africa via a coal-fired power stations, gas/liquid fuel turbines, hydroelectric power plants, pumped stored schemes, a nuclear power plant and wind turbines. Eskom has a total nominal capacity of approximately 42 GW. A total of 13 coal-fired power stations produces 85% of the Eskom electricity supply. In order to ensure plant reliability, Eskom employs a stringent weld inspection programme which results in high volume industrial radiography work at the coal-fired power stations. Industrial radiography activities involve application of Category 2 radioactive sources to obtain clear photographic images of welds and/or defective metallic plant for inspection and evaluation purposes. The radiation protection programme employed at the Eskom coal-fired power stations is aligned to International safety principles, recommendations and requirements to maintain public and occupational exposures as low as reasonably achievable (ALARA) during planned exposure situations, emergency exposure situations and existing exposure situations. This presentation provides information about practical applications and practices employed in radiation protection at the Eskom, Generation Power Stations in accordance with the Eskom Radiation Protection and the Safety of Radiation Sources Policy (Eskom RP Policy). The Eskom RP Policy sets out principles and overarching rules which are aligned with the Nuclear Energy Policy for the Republic of South Africa which states that: "In pursuing a national nuclear energy programme there shall be full commitment to ensure that nuclear and radiation safety receives the highest priority to provide for the protection of persons, property and the environment". The presentation addresses practical application illustrating excellence in the safety and security of industrial radiography sources employed at the Eskom, Generation Power Stations relating to: Radiation Protection Rules, Radiation Protection Training, Safety and Security of radiation sources and Emergency Preparedness and Response.

Safe Transport of Radioactive Material in Argentina

**María Soledad Rodríguez Roldán, Alejandro Fernández, Emiliano Juanena,
Christian Elechosa**

Autoridad Regulatoria Nuclear, Buenos Aires, Argentina

Abstract. The current paper aims to present an overview of the main activities related to the safe transport of radioactive material in Argentina. The implementation of national regulatory standards in this field will be detailed as well as the control tasks performed by the Nuclear Regulatory Authority. Additionally, the domestic experience in the design, development and manufacture of packages and special form radioactive material will be described.

Spent fuel elements transfer between the Units I and II of the Atucha Nuclear Power Plant in Argentina

María Soledad Rodríguez Roldán, Alejandro Fernández, Emiliano Juanena, Christian Elechosa

Autoridad Regulatoria Nuclear, Buenos Aires, Argentina

Abstract. Since the operator point of view, Nucleoeléctrica Argentina Sociedad Anónima (NA-SA), the spent fuel elements (SFE) transfer operation from the Unit I to the Unit II in the Atucha Nuclear Power Plant, is the only achievable strategy that will allow the Unit I to reach their design end of life. The transfer technical specifications are: 620 SFE to be transfer (Natural Uranium, 25 years old); on site operation; started date after Competent Authority (ARN) permission. In this case, the Argentine Standard AR 10.16.1 'Transport of radioactive material' does not apply because the transfer operation involve radioactive material moved within an establishment that is subject to appropriate safety regulations in force and where the movement does not involve public roads or railways. However, for the ARN, the operator must fulfill some aspects of the national Standards. This paper aims to describe the adaptation of some specific paragraphs of the Standard AR 10.16.1 that the operator shall apply.

Challenges in Managing Radiation Safety Program at a Biotech Facility

Rao Goriparthi

Genentech, SSF/CA, USA

Abstract. Genentech is a biotech facility with an emphasis on research and development of drugs. We have radiation users that use extremely low activities of radioactivity and we have some who use extremely high activities. We train receiving staff to process radioactive packages. These are employees with very low scientific knowledge. We receive packages that contain two curies (74.0 GBq) of F-18 and at times receiving staff are uncomfortable in handling these high activity packages. Hence, we radiation safety staff processes these and delivers to respective labs. I'm curious to know if other institutes process similarly or provide additional training to receiving so that they are completely comfortable. We also receive Ge/Ga generators that contain more than 30.0 curies (1110 GBq) which are considered high activity packages. My goal is to have all radioactive packages processed by receiving. It makes lot easier to have receiving processes these packages as they also transport some of our radioactive packages within Genentech campus where there are some public roads. Anytime, we transport hazmats on public roads, we need to make sure we are in full compliance with DOT regulations.

Intermediate Nuclear Waste Return December 2015

Steven Dimitrovski

Australian Nuclear Science & Technology Organisation, Sydney, NSW, Australia

Abstract. In the 1990's the Australian Government entered into agreement with the French Government to reprocess spent nuclear fuel used by Australia's HIFAR research reactor. The repatriation project was the culmination of years of planning by State and Federal agencies to ensure Australia safely met its international obligations to deal with the by-products of its nuclear program. On December 5th 2015, a shipment of repatriated nuclear intermediate level waste arrived in Australia from France and was safely transported by road from the port to the Australian Nuclear Science and Technology Organisation facility (ANSTO) in Sydney. The reprocessed waste, safely immobilised into a durable vitrified glass form, was transported in a specially designed TN-81 type B(u) cask which comprised of 20 stainless steel canisters. In addition, six drums of technological wastes in cemented form (waste generated from the reprocessing process) were also received contained within a DV-78 ISO container. Radiation Protection staff from ANSTO were involved in taking various radiological measurements (including dose rates & contamination clearance checks on the TN-81, DV-78, transport trailers, trucks, ship and heavy lifting equipment) and to provide advice and radiation monitoring to all personnel involved in the scope of the work. Radiation levels at contact with the TN-81 cask were very low and the project was successfully completed with no contamination above normal background levels found and dose received by individuals minimal. The TN-81 and DV-78 are now safely stored in a purpose built facility at ANSTO and will remain there until a National Radioactive Waste management facility is designed, constructed and commissioned for operation in Australia.

Strategies to Improve the Safety Culture in the Field of Industrial Radiography in Peru

Susana Gonzales

Instituto Peruano de Energia Nuclear, Lima, Peru

Abstract. The main lesson learned from the Yanango accident (1999) was the strengthening of the legal framework. However in the last three years, 02 serious accidents in industrial radiography had occurred: Chilca (January 16, 2012) and Ventanilla (February 14, 2014). Due to the severity of the lesions of the affected workers - one in each case - the support of the IAEA was requested. Peru has initiated actions to foster the safety and security in industrial radiography, working mainly with the end users on the issue of risk perception and safety culture in sustained way. IPEN is the national authority in Peru to control and enforce the law and apply the regulations. It also applies sanctions when the regulations are not fulfilled. The root causes were similar in both accidents. Neither the operators nor the radiological protection officers did follow the proper radiation safety procedures, despite the fact that they had operating licenses issued by the regulatory body, that means, “to know but not to do”. To face this problem, an action plan with scope to end users has been implemented. First of all, the records of companies and personnel working in the field of industrial radiography were updated, theoretical courses and practical training were performed with the IAEA support, the hours of practice were increased in the radiation protection courses. A poster called “zero accidents in industrial radiography”, was given to each occupationally exposed worker, to put it in a visible place in their place of work. A photo of the workers and the managers of the company beside the poster was the visible indicator that they had placed it properly. Also, brochures about radiation protection were massively distributed. The testimony of the irradiated workers and their families had been the greatest impact they have received. Currently, a monitoring program - directed mainly to operators and radiation protection officers - has been established, obtaining good results. Also includes engagement with management on developing the Culture within the facility or institution. This paper shows the experience to implement the national action plan in the field of industrial radiography. The difficulties and the responses are shared as a model of strengthening of the safety culture.

Detection of Orphan Industrial Neutron and Americium Sources in Metal Scrap Cargo

Michael Iwatschenko-Borho

Thermo Fisher Scientific Messtechnik GmbH, Erlangen, Germany

Abstract. In recent years several incidents have been reported, where orphan Am-241 sources, inadvertently included in scrap metal, were melted in the furnaces of a steel plant. Despite the fact that the steel remains largely uncontaminated in such melts (due to its physical properties most of the Am-241 activity ends up in the slag and dust), the cost of clean-up and disposal are significant. Unlike other industrial sources (Co-60, Cs-137, Ir-192, Eu-152) and naturally occurring radioactive materials (NORM), Am-241 predominantly emits low energy gamma radiation below 100 keV (mainly 59 keV). The emission rate of penetrating higher energy gamma radiation is very low (in the order of E-5), so that even high activity sources can remain undetected by conventional systems based on gamma detectors. In order to address this gap in the detection capabilities of conventional industrial gate monitors, Thermo Fisher Scientific Messtechnik GmbH, Erlangen, Germany has developed a highly sensitive neutron detector system which can be integrated into existing Thermo Fisher gate monitors or can be operated as stand-alone parallel installation. The design of the system was led by the observation that any Am-241 source emits in addition a certain amount of neutron radiation. These high energy neutrons are produced in the AmOxide source matrix by nuclear alpha,n reaction. Compared to gamma radiation, these neutron particles are highly penetrating and therefore much less attenuated by the shielding of the source and the surrounding scrap material. In addition to the surprisingly good detection capability for high activity Am-241 sources, these systems obviously provide excellent protection against neutron sources (AmBe, Cf-252, Pu-238, Pu-240, Cm isotopes) which are in common use in industry, including low activity portable devices which may be deeply buried in dense scrap material and remain undetected by conventional gate monitors. For facilities with low throughput of material, a portable device using the same detector technology is available too.

KEYWORDS: *orphan sources; Am-241; scrap metal; portal monitor; melting; steel plant; scrap yard; neutron detection.*

**The Proceedings of the 14th International Congress of the International Radiation
Protection Association
Volume 4 of 5**

Area 9: Non-Ionising Radiation

Evaluation of bone density importance in pediatric MR only treatment planning

Banafsheh Zeinali-Rafsanjani^{a,b*}, Reza Faghihi^{c,d}, Mahdi Saeedi-Moghadam^a,
Reza Jalli^a

^a Medical imaging research center, Shiraz University of medical sciences, Shiraz, Iran

^b Nuclear medicine and molecular imaging research center, Shiraz university of medical sciences, Shiraz, Iran

^c Nuclear engineering department, school of mechanical engineering, Shiraz University, Shiraz, Iran

^d Radiation research center, school of mechanical engineering, Shiraz University, Shiraz, Iran

Abstract. In order to reduce the patient dose and more precise target definition for pediatric radiation therapy, MR only treatment planning is useful. One of the important steps in this method is bone segmentation and assigning a suitable bulk electron density to bone tissue. Bone in children between 0-14 years old is progressively developing so its mineral density content is changing during these ages. The objective of this study is to assess that if assigning a same bulk electron density to bone tissues of the children with different ages can have a significant effect in dose distribution or not? CT images of children between 0 to 19 years old were used. Skull bones were segmented and the CT numbers extracted and converted to density. MCNPX version 2.5 was used to model inhomogeneous phantoms. A slab of $5 \times 5 \times 0.5$ cm³ skull bone (With various electron densities related to different ages) on a slab of $5 \times 5 \times 10$ cm³ brain was modeled as inhomogeneous phantoms. Percentage depth dose (PDD) was calculated for kilovoltage and Megavoltage photons and 12 MeV electron therapy beams in these phantoms in order to compare the differences of dose distribution due to differences in bone density. The study revealed that there was not a significant difference (<2%) between PDDs in photon and electron therapy in phantoms with different bone electron densities so that when MR only treatment planning use for pediatric radiotherapy planning, bulk density method is accurate enough for treatment of brain or underneath area of bone. But it should be considered that, if the target of radiation therapy is bone, this method may cause a little error in dose calculation especially in superficial and electron therapy, so that voxel based methods are more reliable for these treatments.

KEYWORDS: *bone development; pediatric radiotherapy; MR only treatment planning.*

1 INTRODUCTION

Nowadays magnetic resonance imaging (MRI) has a significant role in radiotherapy treatment planning. This modality has lots of advantages for this application in comparison to computed tomography (CT) although it cannot provide electron density information [1-5]. One of the methods which can help to overcome this problem is segmentation of tissues and assigning a bulk density to each segment.

Bone in children between 0-14 years old is progressively developing so its mineral density content is changing during these ages. Because of this development it is expected that the electron density of bone, changes in children with different ages. Despite of this variation a same electron density for these children uses in MR treatment planning. The objective of this study is to assess that whether assigning a same bulk electron density to bone tissues of the children with different ages can have a significant effect in dose distribution or not? In order to examine the effect of electron density of bone, first of all CT number of bones should be extracted from CT images. Then these numbers

* Presenting author, e-mail: b.zeinali.r@gmail.com

should be converted to electron density. Different electron densities should assign to bony areas in treatment planning codes to check its effect on dose in different depths.

2 MATERIALS AND METHODS

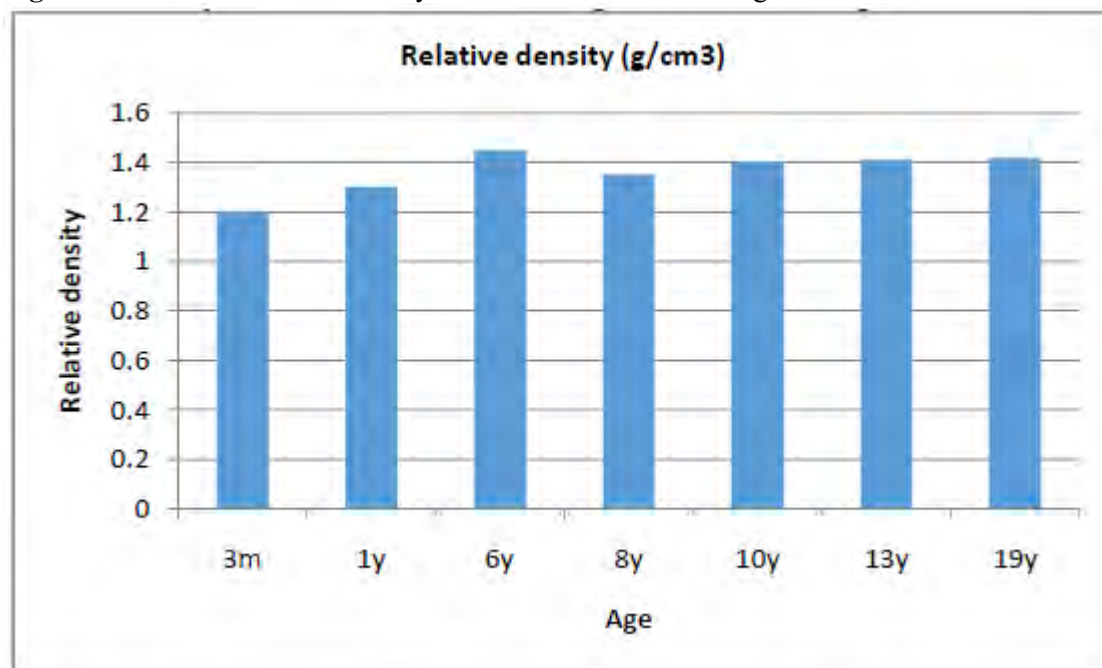
Skull CT images of children between 0 to 19 years old were used. Skull bones were segmented and the CT numbers extracted and converted to density using CTCREAT ramp which is used in PEGS4 cross section data file.

MCNPX version 2.5 was used in this study for treatment planning. A slab of $5 \times 5 \times 0.5 \text{ cm}^3$ skull bone (With various electron densities related to different ages) on a slab of $5 \times 5 \times 10 \text{ cm}^3$ brain was modeled as inhomogeneous phantoms. Percentage depth dose (PDD) was calculated for kilovoltage (120 kV), Megavoltage photons (6 MeV) and 12 MeV electron therapy beams in these phantoms in order to compare the differences of dose distribution due to differences in bone density. Mesh tally type 3 were used to calculate the dose distribution in the phantom.

3 RESULTS

Extracted electron density of children with different ages was shown in figure 1.

Figure 1: Extracted electron density of children with different ages.



The results of percentage depth dose in 120 kVp and 6 MeV x-ray and 12 MeV electron therapy in children with different ages demonstrated in figures 2, 3 and 4.

Figure 2: The results of percentage depth dose in kilovoltage (120 kVp) treatment of children with variable electron density.

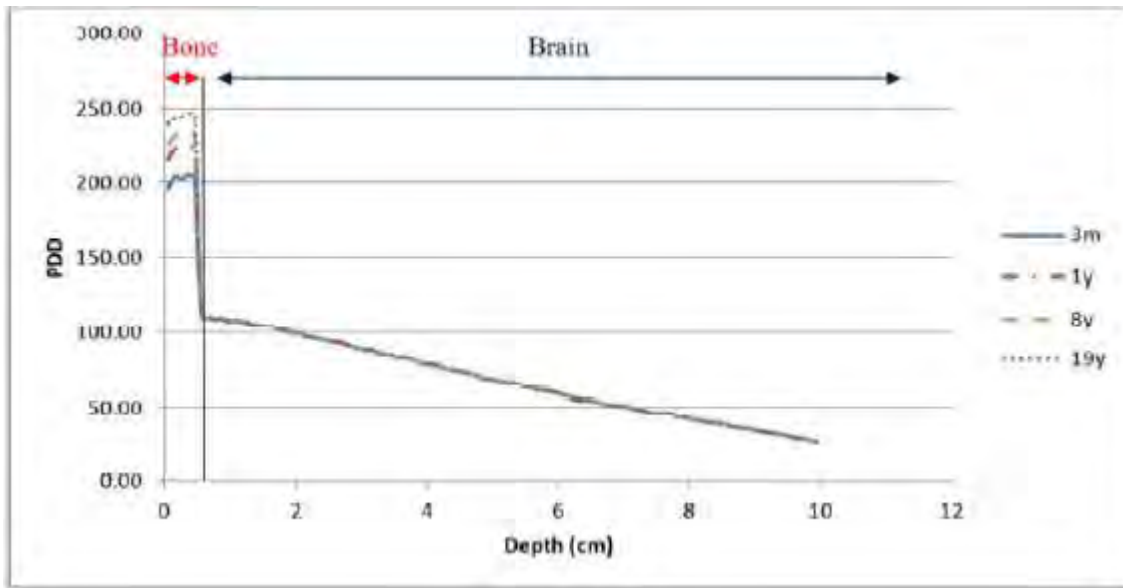


Figure 3: The results of percentage depth dose in Megavoltage (6 MeV) treatment of children with variable electron density.

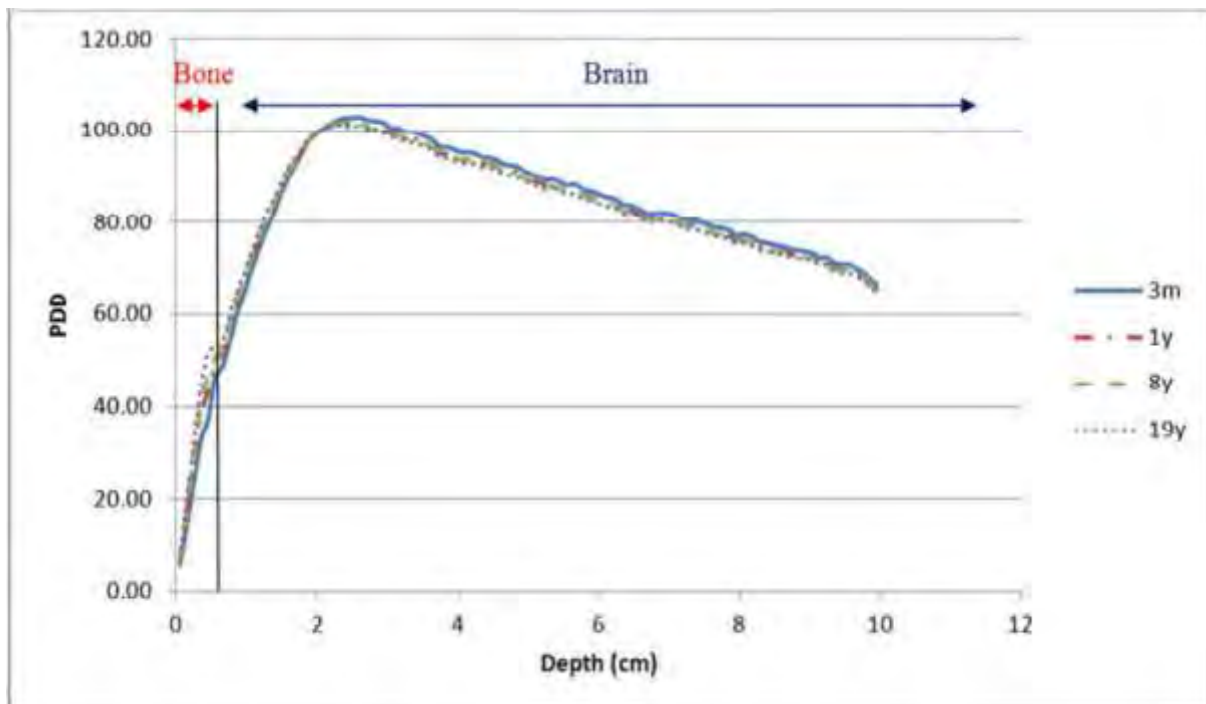
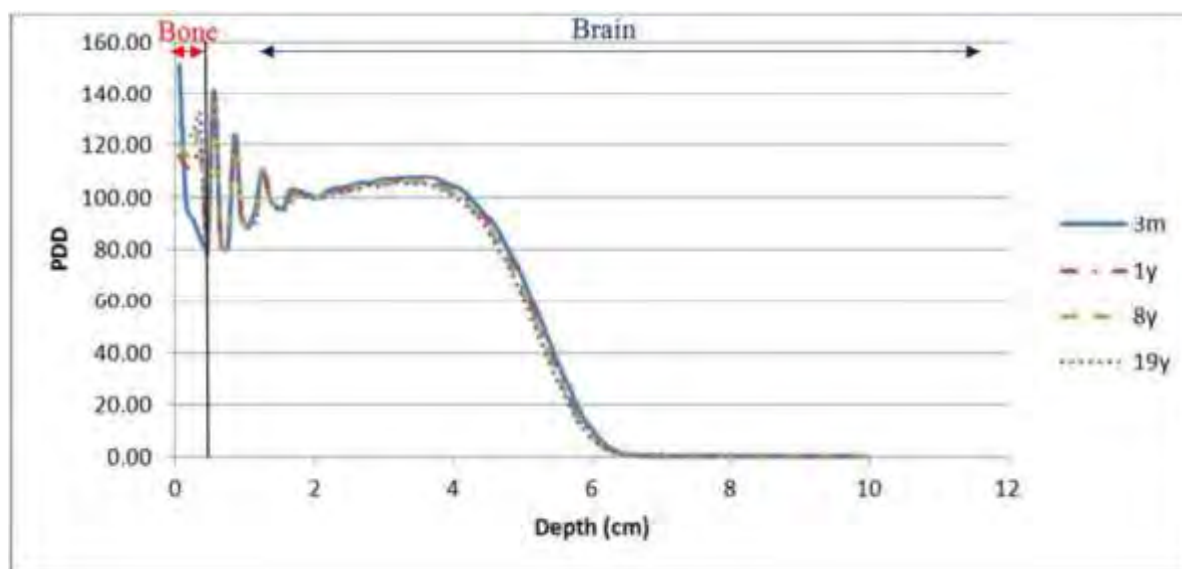


Figure 4: The results of percentage depth dose in electron therapy (12 MeV) of children with variable electron density.



4 DISCUSSION AND CONCLUSION

According to figure 1 bone electron density of children less than 19 years old is a little changing. Figure 2 demonstrated that this change in kilovoltage therapy don't have a significant effect on the radiation dose in the areas beneath bony structures but photoelectric effect in bony parts result in dose variation. Figure 3 illustrated that in megavoltage therapy the difference in bone electron density don't have any remarkable effect on dose in bony or soft tissue structures. Figure 3 showed that in electron therapy the differences of bone electron density can cause some variations in absorbed dose of bone. The study revealed that there was not a significant difference (<2%) between PDDs in photon and electron therapy in phantoms with different bone electron densities so that when MR only treatment planning use for pediatric radiotherapy planning, bulk density method is accurate enough for treatment of brain or underneath area of bone. But it should be considered that, if the target of radiation therapy is bone, this method may cause a little error in dose calculation especially in superficial and electron therapy, so that voxel based methods are more reliable for these treatments.

5 REFERENCES

- [1] C. M. Rank, N. Hunemohr, A. M. Nagel, M. C. Rothke, O. Jakel, and S. Greulich, "MRI-based simulation of treatment plans for ion radiotherapy in the brain region," *Radiother Oncol*, vol. 109, pp. 414-8, Dec 2013.
- [2] P. Metcalfe, G. P. Liney, L. Holloway, A. Walker, M. Barton, G. P. Delaney, *et al.*, "The potential for an enhanced role for MRI in radiation-therapy treatment planning," *Technol Cancer Res Treat*, vol. 12, pp. 429-46, Oct 2013.
- [3] T. Stanescu, J. Hans-Sonke, P. Stavrev, and B. G. Fallone, "3T MR-based treatment planning for radiotherapy of brain lesions," *Radiol Oncol*, vol. 40, pp. 125-32, 2006.
- [4] M. Koshy, M. Pentaleri, S. Paryani, C. Anderson, J. Cesaretti, A. Deshmukh, *et al.*, "The Role of MRI in Radiation Therapy Planning," F. R. O. G. MRI Center of North Florida, Ed., ed. Jacksonville, Florida.
- [5] T. Boettger, T. Nyholm, M. Karlsson, C. Nunna, and J. C. Celi, "Radiation therapy planning and simulation with magnetic resonance images " *Medical Imaging* 2008.

Simulation of heat distribution in a phantom for a Philips Sonalleve MRgHIFU unit

Barbara Caccia^a, Silvia Pozzi^a, David Bianchini^b, Francesco Marcocci^b, Enrico Menghi^b, Marcello Benassi^b

^aIstituto Superiore di Sanità, Roma, Italy

^bIstituto Scientifico Romagnolo per lo Studio e la Cura dei Tumori (IRCCS-IRST), Meldola, Italy

Abstract. Magnetic Resonance guided High Intensity Focused Ultrasound (MRgHIFU) is being investigated for routine clinical practices with the aim of enabling thermal ablation of both benign and malignant tumour lesions, and bone metastasis. MRgHIFU treatment is based on the power of a focused ultrasound beam to locally heat biological tissues over a necrotic level with minimal impact on the surrounding tissues. The aim of this work was the commissioning of a computational tool, based on Kuznetsov, Zabolotskaya and Khokhlov equation (KZK) and Bioheat Transfer Equation (BHTE) solution, to predict the heat deposition in a multilayer phantom mimicking bone and soft tissues. Numerical simulation of heat propagation in different biological tissues provides useful information to better understand the limitations and safety concerns of performing MRgHIFU treatments. A mathematical model of the Philips Sonalleve MRgHIFU unit installed at IRST - IRCCS (Istituto Scientifico Romagnolo per lo Studio e la Cura dei Tumori) in Meldola (Italy) was performed. To evaluate the behavior of the ultrasound beam in presence of bone, a multilayer model has been implemented to simulate different materials between the ultrasound transducer and the target region. The results obtained with the mathematical model were compared with the experimental temperature measurements on a phantom.

Extrapolation techniques for evaluation of 24 hours average electromagnetic field emitted by Radio Base Station installations: spectrum analyzer measurements of LTE and UMTS signals

Elisa Nava^a, Stefano Mossetti^a, Daniela de Bartolo^a, Ivan Veronese^{b,c}, Marie Claire Cantone^{c,d}, Cristina Cosenza^b

^aARPA Lombardia, Via Rosellini 17, 20100 Milano, Italy

^bDipartimento di Fisica, Università degli Studi di Milano, Via Celoria 16, 20133 Milano, Italy

^cIstituto Nazionale di Fisica Nucleare, Sezione di Milano, Via Celoria 16, 20133 Milano, Italy

^dDipartimento di Scienze Biomediche, Chirurgiche ed Odontoiatriche, Università degli Studi di Milano, Via Pascal 36, 20133 Milano, Italy

Abstract. In Italy reference level for public protection from electromagnetic fields exposure for frequencies 0.1MHz to 3 GHz is 6 V/m. With the continuous development of all the mobile telephone networks (four in Italy), it is nowadays possible, in densely built-up areas, to find values exceeding that law level. The legislation changed recently: the reference value was not changed, but it must now be evaluated as the 24 hours average value instead of the former highest 6 minutes in a day (Decreto Legge, n. 179 del 18 ottobre 2012, coordinato con la Legge di conversione del 17 dicembre 2012, n. 221). With the implementation of the long-term evolution technique (LTE - 4G), in 2013 the technical guide “CEI 211-7/E” was published. It introduces extrapolation techniques that enable to obtain the 24 hours average value from short-term selective measurements. In this work we present measurements performed to identify technical critical aspects in these extrapolation techniques. We focused also finding a good balance between statistically significant values and logistic managements. As in control activity the signal trend in situ is not known, the minimum measurement time that allows to acquire a sufficiently stabilized signal has been investigated. The distance, the relative positions of the pointing direction of the antennas and the measurement point and the resulting fading and reflection effects were considered. We performed selective measurements of UMTS and LTE signals for more than 24 hours, with a vector signal analyzer. Measurements were repeated several times in some months and for different mobile companies. Outcome presented in this paper allowed us to evaluate the reliability of the extrapolation results obtained and to have a starting point in order to define operating procedures.

KEYWORDS: *electromagnetic fields; measurements guideline; Spectrum RF Field analyser; limit compliance; environmental exposure – legislation.*

Radiation Protection Dosimetry (2017), Vol. 173, No.1-3, pp. 43–48

doi:10.1093/rpd/ncw337

Managing Non-Ionizing Radiation through International Basic Safety Standards

Jacques Abramowicz^{a,g}, Efthymios Karabetos^b, Sigurdur Magnusson^c, Rudiger Matthes^h, Mirjana Moser^j, Shengli Niu^f, John O'hagan^{d,i}, Rick Tinker^e, Emilie Van Deventer^k

^aWayne State University, Detroit, MI, USA

^bGreek Atomic Energy Commission, Athens, Greece

^cIcelandic Radiation Safety Authority, Reykjavik, Iceland

^dPublic Health England, Chilton, Oxfordshire, UK

^eAustralian Radiation Protection and Nuclear Safety Agency, Yallambie, Victoria, Australia

^fInternational Labour Organization, Geneva, Switzerland

^gWorld Federation for Ultrasound in Medicine and Biology, Laurel, MD, USA

^hIndependent, Munich, Germany

ⁱInternational Commission on Illumination, Vienna, Austria

^jMirjana Moser Consulting, Bern, Switzerland

^kWorld Health Organization, Geneva, Switzerland

Abstract. The International Basic Safety Standards (BSS) for protection against ionizing radiation and for the safety of radiation sources reflect an international consensus on what constitutes a high level of safety for protecting people and the environment from harmful effects of ionizing radiation. These standards establish an integrated and consistent set of safety requirements which are governed by the objective and principles of the safety fundamentals. These requirements provide a regulatory framework that can be used by national regulatory bodies and other relevant national authorities as a reference for their own national regulations. The latest BSS, published in 2014, embody the consensus and efforts of eight international organizations, under the IAEA leadership. Currently, there is no such common, coherent and overarching standard for health protection against non-ionizing radiation. Fragmentary and inconsistent national standards give rise to public concern, and sometimes to barriers to trade and technical developments. Health-based standards being one of the core functions of WHO, it is planned to develop BSS for the protection of human health against non-ionizing radiation (including the general public, workers and patients). The non-ionizing radiation spectrum includes electromagnetic, optical and acoustic radiation (infrasound and ultrasound). This activity is motivated by the interest of Member States for harmonized standards and their application within an international protection framework. Such a framework would reduce the burden on states to produce their own legislation, and would help address existing gaps (e.g., unregulated applications for non-medical purposes). Based on positive feedback from WHO Member States, WHO held bilateral meetings with several relevant UN agencies and organised a Consultancy meeting with stakeholders. A Core Group of experts has been convened to chart this new activity.

Designing a Laser Lab, Errors and Solutions

Ken Barat

Laser Safety Solutions, Maricopa, AZ, USA

Abstract. Every researcher looks forward to designing their own laser laboratory. But in doing so there is a potential for a number of common mistakes to occur. Some are from a lack of homework others from a lack of awareness of building codes and others not recognizing that construction project managers do not always understand what researchers are asking for. This presentation demonstrates a number of lessons learned as well as solutions to new lab design problems. The solutions cover institutional requirements the user may not be aware of, a checklist to follow and some innovative product choices one once again may not have considered. This is all based on over 20 years of laser research observations by the author.

Threshold Dose Estimation for Short Delay Onset of Cataract after In Vivo exposure to Ultraviolet Radiation, a General Strategy for Threshold Estimation for Continuous Dose Response Functions

Per Söderberg^{a,b}, Konstantin Galichanin^b, Nooshin Talebizadeh^b, Zhaohua Yu^b

^aInternational Commission on Non-Ionizing Radiation Protection, Munich, Germany

^bGullstrand lab, Ophthalmology, Dept. of Neuroscience, Uppsala University, Uppsala, Sweden

Abstract. Introduction: Short delay onset of cataract after in vivo exposure to ultraviolet radiation (UVR) expresses a continuous dose-response relationship. There is currently limited possibilities to estimate a statistically meaningful threshold dose for continuous dose-response relationships associated with toxic agents. We propose that a confidence interval for Maximum Tolerable Dose-2.3:16 (MTD_{2.3:16}) is used for estimation of threshold dose for toxicity. Methods: An algorithm was developed for estimation of a statistically defined threshold for toxic dose in small samples expressing a continuous dose-response relationship, MTD- Alpha:Beta. The algorithm is based on an assumption of some linear relationship between the dose and the toxic response, a selected upper level of response considered, the cut off for non-toxic response defined by a probability Alpha that a response that exceeds the cut off is non-toxic, and a probability Beta that the response at the estimated toxic dose exceeds the cut off level for non-toxic response. Results: It can be shown that if experimental small sample data is fitted with linear regression, and Alpha is set 2.5 % and Beta to 16 %, the MTD-2.3:16 is simply the square root of the ratio between the residual standard deviation and the inclination coefficient. An analytical strategy to express the confidence interval for MTD-2.3:16 was developed. In cataract after in vivo exposure to UVR, intensity of induced forward light scattering increases linearly. The MTD-2.3:16 strategy was used to estimate a threshold for cataract development after in vivo exposure to ultraviolet radiation. Conclusion: A statistically defined threshold dose, MTD-2.3:16, can be estimated as a confidence interval from a small sample experiment. At the estimated threshold dose there is a 16 % probability that the response exceeds a level found in only 2.3 % of a population that was not exposed to the toxic agent. The MTD-2.3:16 has been used to estimate a confidence interval for the threshold dose for in vivo UVR induced cataract.

Effects of Early Life Exposure to RF Fields

Kerry Broom, Jutta Jarvinen, Darren Addison, Zenon Sienkiewicz

Public Health England, Didcot, Oxfordshire, UK

Abstract. Despite much research, there are still gaps in knowledge about the health effects of low level exposure to radiofrequency (RF) fields associated with mobile phones. This study is investigating the effects of exposure to RF fields used by 4G mobile phones on brain function and behaviour in C57BL mice. Animals have been exposed to controlled intensities of RF fields (whole body specific energy absorption rate of 0, 0.5 or 1 W/kg) from the later stages of pregnancy through to weaning; other animals have been exposed to 0.5 Gy of X-rays on gestational day 18 as a positive control. Following exposures, natural behaviour relating to long-term exploration, locomotion and activity patterns are being investigated, and cognitive behaviour measured using a water maze. Brain tissues are being examined using immunohistochemistry for synaptophysin, NeuN, and GFAP, and the expression of genes associated with learning in the hippocampus and cortex. All assessments are conducted blind and exposure status will be revealed once all data have been collected. Results will be presented. This research will help to fill a gap in knowledge about 4G mobile phone technologies, and should be informative of possible risks to human health. Commissioned and funded by the Department of Health Policy Research Programme (England) (Early Life Exposure to Radiofrequency Fields, PRP X01-01-01).